SUSTAINABLE DECOLORIZATION OF REACTIVE AND ACID DYE WASTEWATER USING PHOTO-FENTON OXIDATION BOTH WITH AND WITHOUT BIODEGRADATION: LABORATORY AND FIELD STUDIES

By

Marissa R. Jablonski

A Dissertation Proposal Submitted in

Fulfillment of the

Requirements for the Degree of

Doctor of Philosophy

In Engineering

at

The University of Wisconsin-Milwaukee

May 2015

ABSTRACT

SUSTAINABLE DECOLORIZATION OF REACTIVE AND ACID DYE WASTEWATER USING PHOTO-FENTON OXIDATION BOTH WITH AND WITHOUT BIODEGRADATION: LABORATORY AND FIELD STUDIES

By

Marissa R. Jablonski

The University of Wisconsin-Milwaukee, 2015

Under the Supervision of Dr. John R. Reisel

Photo-Fenton oxidation is an advanced oxidation process (AOP) used to degrade low-concentration textile dye wastewater using expensive chemicals. The technique has shown promise in laboratory-scale projects, but has not been scaled up sustainably to function for industry. Aerobic biodegradation is a common biological treatment method used in large-scale textile industrial applications that generates large amounts of hazardous biological waste. This waste is often left open to the elements and subsequently leaches into natural waterways or onto land. This is the first study of its kind to combine the two to treat cottage-scale industry-grade textile wastewater with a dye concentration of 5 g/L and then scale up the sustainable photo-Fenton oxidation for a demonstration project in India. The need to provide rural textile communities with an effective and low-cost method to clean dye wastewater is enormous because of their lack of funds and influence in the industry; they have very little control over their

environmental health and often no choice in the location of the disposal of their wastewater often dumping close to water systems. This dissertation details methods on constructing and testing a sustainable decolorization unit that includes a reactor and filter to treat 50 and 100-liter batches of textile dye wastewater for dyers in rural Bangalore, India using photo-Fenton oxidation and sand and carbon (and sometimes cotton) filtration testing whether biodegradation is also necessary as a secondary treatment. The reactor and filter is constructed of recycled rusty metal, sand, cotton fabric, and wood charcoal found locally and inexpensively. All chemicals used in the reaction are readily available in the form of sheet metal, pharmacy grade hydrogen peroxide, and household acid. Once wastewater is decontaminated it may be reused in industry or released to recharge groundwater. Test results include UV-visible spectrometry to determine color removal, COD levels to determine the removal of organics, GC/MS to quantify and qualify organics removed, ICP to quantify and qualify metal ions removal, and sludge volume production.

© Copyright by Marissa R. Jablonski, 2015
All Rights Reserved

TABLE OF CONTENTS

LIST OF FIGURES x

LIST OF TABLES xiv

LIST OF ABBREVIATIONS xix

LIST OF SYMBOLS xxi

ACKNOWLEDGMENTS xxii

EPIGRAPH xxv

CHAPTER 1 – INTRODUCTION 1

1.1 Background 1
1.2 Contents of Dissertation 5

CHAPTER 2 – THEORY AND LITERATURE REVIEW 7

2.1 Dyeing Silk: Process and Effluent 7
2.1.1 History of Silk Production 7
2.1.2 Dyeing Silk: Silk Composition 10
2.1.3 General Synthetic Dyes Effluent 11
2.1.3.1 Reactive Dyes 12
2.1.3.2 Acid Dyes 13
2.2 Advanced Oxidation Processes as Treatment for Textile Dye Effluent 16
2.2.1 Fenton Process 18
2.2.2 Photo-Fenton Oxidation 19
2.2.2.1 Oxidation Time 22
2.2.2.2 pH 24
2.2.2.3 Hydrogen Peroxide 25
2.2.2.4 Iron 27
2.2.2.5 Dye Concentration 28
2.2.2.6 Temperature 29
2.2.2.7 UV Light 30
2.2.2.8 Hydroxyl Radicals 30
2.2.2.9 Photo-Fenton Oxidation Summary 33
2.2.3 Photo-Fenton Oxidation Coupled with Biodegradation 34
2.3 Sustainable Containers and Materials for Oxidation 36
2.3.1 Container 36
2.3.2 Iron Scrap as Iron Source 47
2.4 Pilot Projects 49
2.5 Summary 51

CHAPTER 3 – EXPERIMENTAL APPARATUS AND METHODOLOGY 53

3.1 Introduction 53
3.2 Experimental Overview 53
3.3 Container 54
3.3.1 Laboratory-Scale Study 54
3.3.2 Field Study 55
3.3.3 Options for Sustainable Reactor 55
3.3.3.1 Rusty Iron 56
3.3.3.2 Plastic Bottles 57
3.3.3.3 Fused Plastic Bags 59
3.3.3.4 Concrete 60
3.3.3.5 Wood 61
3.4 Variables in photo-Fenton Oxidation 62
3.4.1 UV Light Source 63
3.4.2 Dye 63
3.4.2.1 Reactive Dyes 64
3.4.2.2 Acid Dyes 66
3.4.3 Soap and Soda 68
3.4.4 Water 72
3.4.5 Hydrochloric Acid 72
3.4.6 Hydrogen Peroxide 73
3.4.7 Iron 74
3.4.8 Time 76
3.4.9 Sand Filter 77
3.4.10 Carbon Filter 78
3.5 Methods of Analysis 79
3.5.1 UV-visible Spectroscopy 81
3.5.2 COD 82
3.5.3 SPME-GC/MS 83
3.5.4 ICP-AES 84
3.5.5 Total Iron 86
3.5.6 SEM 87
3.5.7 Respirometric Analysis 89
3.6 Summary 91

CHAPTER 4 – REACTIVE DYE PHOTO-FENTON OXIDATION RESULTS AND DISCUSSION 92

4.1 Introduction 92
4.2 UV-visible Spectroscopy Results 93
4.2.1 Rate Reaction 93
4.2.2 Partial and Full Oxidation Results 95
4.2.2.1 Reactive Red 120 95
4.2.2.2 Reactive Yellow 81 97

4.2.2.3 Reactive Blue 4 100
4.3 COD Results 101
4.3.1 Reactive Red 120 102
4.3.2 Reactive Yellow 81 104
4.3.3 Reactive Blue 4 107
4.3.4 Sludge Production 110
4.3.5 Solar Irradiance and Temperature 111
4.4 GC/MS Results 112
4.4.1 Reactive Red 120 113
4.4.2 Reactive Yellow 81 116
4.4.3 Reactive Blue 4 118
4.5 ICP Results 120
4.5.1. Reactive Red 120 121
4.5.2 Reactive Yellow 81 123
4.5.3 Reactive Blue 4 125
4.6 Respirometric Results 127
4.6.1 Reactive Red 120 127
4.6.2 Reactive Yellow 81 128
4.6.3 Reactive Blue 4 129
4.6.4 Statistical Analysis 130
4.7 Discussion of Results 131
4.8 Summary 142

CHAPTER 5 – ACID DYE PHOTO-FENTON OXIDATION RESULTS AND DISCUSSION 145

5.1 Introduction 145
5.2 UV-visible Spectroscopy Results 146
5.2.1 Rate Reaction 146
5.2.2 Partial and Full Oxidation Results 149
5.2.2.1 Acid Fast Red 149
5.2.2.2 Acid Golden Yellow 151
5.2.2.3 Acid Ananda Blue 152
5.3 COD Results 154
5.3.1 Acid Fast Red 155
5.3.2 Acid Golden Yellow 157
5.3.3 Acid Ananda Blue 159
5.3.4 Sludge Production 161
5.3.5 Solar Irradiance and Temperature 162
5.4 GC/MS Results 163
5.4.1 Acid Fast Red 164
5.4.2 Acid Golden Yellow 166
5.4.3 Acid Ananda Blue 167
5.5 ICP Results 168
5.5.1 Acid Fast Red 170
5.5.2 Acid Golden Yellow 172

5.5.3 Acid Ananda Blue 174
5.6 Respirometric Results 176
5.6.1 Acid Fast Red 177
5.6.2 Acid Golden Yellow 178
5.6.3 Acid Ananda Blue 179
5.6.4 Statistical Analysis 180
5.7 Discussion of Results 180
5.8 Summary 191

CHAPTER 6 – ACID DYE WITH SOAP AND SODA PHOTO-FENTON OXIDATION RESULTS AND DISCUSSION 193

6.1 Introduction 193
6.2 UV-visible Spectrometry Results 195
6.2.1 Partial and Full Oxidation Results 195
6.2.1.1 Acid Fast Red with Soap and Soda 195
6.2.1.2 Acid Golden Yellow with Soap and Soda 197
6.2.1.3 Acid Ananda Blue with Soap and Soda 198
6.2.1.4 Field Samples Green and Maroon 200
6.3 COD Results 201
6.3.1 Acid Fast Red with Soap and Soda 201
6.3.2 Acid Golden Yellow with Soap and Soda 203
6.3.3 Acid Ananda Blue with Soap and Soda 205
6.3.4 Field Samples Green and Maroon 207
6.3.5 Sludge Production 208
6.3.6 Solar Irradiance and Temperature 209
6.4 GC/MS Results 210
6.4.1 Acid Fast Red with Soap and Soda 211
6.4.2 Acid Golden Yellow with Soap and Soda 212
6.4.3 Acid Ananda Blue with Soap and Soda 213
6.4.4 Field Studies Green and Maroon 216
6.5 ICP Results 216
6.5.1 Acid Fast Red with Soap and Soda 218
6.5.2 Acid Golden Yellow with Soap and Soda 220
6.5.3 Acid Ananda Blue with Soap and Soda 221
6.5.4 Field Samples Green and Maroon 223
6.6 Respirometric Results 224
6.6.1 Acid Fast Red with Soap and Soda 224
6.6.2 Acid Golden Yellow with Soap and Soda 225
6.6.3 Acid Ananda Blue with Soap and Soda 226
6.6.4 Field Samples Green and Maroon 226
6.7 Discussion of Results 227
6.8 Summary 237

CHAPTER 7 – DEMONSTRATION PROJECT: SUSTAINABLE PHOTO-FENTON OXIDATION OF COTTAGE-SCALE SILK DYE WASTEWATER IN KARNATAKA, INDIA 240

7.1 Introduction 240
7.2 Background and Set-up 240
7.2.1 Cottage-Scale Dye Industry Questionnaire 243
7.3 Apparatus and Methodology 246
7.4 Results 247
7.4.1 Karnataka State Pollution Control Board Standards 254
7.5 Discussion of Results 255
7.6 Estimated Cost of Treatment in Mobile Unit 259
7.7 Recommendations for continuation of project and construction of 150-liter pilot project June 2015 261
7.8 Summary 262

CHAPTER 8 – CONCLUSIONS AND FUTURE WORK 263

8.1 Conclusions 263
8.2 Recommendations for Future Work 266

LIST OF REFERENCES 269

APPENDICES 278
Appendix A – UV-visible Spectrometry Tables 278
Appendix B – COD Tables 300
Appendix C – GC/MS Graphs 312
Appendix D – ICP Tables 366
Appendix E – Oxygen Uptake Graphs 376
Appendix F – FTIR Graphs 394
Appendix G – Educational Brochure: Sustainable photo-Fenton Oxidation and Slow Sand Filtration of Textile Dye Wastewater 405
Appendix H – Educational Brochure: Making a Rusty Iron Reactor to be used for photo-Fenton Oxidation of Textile Dye Wastewater 412
Appendix I – Educational Brochure: Making a Slow Sand Filter to be used after photo-Fenton Oxidation of Textile Dye Wastewater 414

CURRICULUM VITA 419

LIST OF FIGURES

Figure 2.1: Lifecycle of mulberry silkworm (*Bombyx mori L*) (Datta and Nanavaty, 2005) 10

Figure 2.2: Reactive Dye molecule with 5 major groups labeled: Reactive group (R), Leaving group (X), Chromophoric group (C), Bridging group (B), and Solubilizing group (S) (Uddin and Hossain, 2010) 13

Figure 2.3: Possible degradation pathway for C.I. Reactive Organge 16 proposed by Bilgi and Demir (2005) 24

Figure 3.1: Photo of rusty metal reactor made in India to hold between 50 and 100 liters of industry grade dye effluent at a cottage-scale dye industry 57

Figure 3.2: Photo of recycled plastic bottle reactor 58

Figure 3.3: Photo of recycled plastic bag reactor 60

Figure 3.4: Photo of plywood reactor in preliminary design stages including baffles and scrap metal in the form of rusty bicycle parts 62

Figure 3.5 Reactive Red 120 chemical composition (Santa Cruz Biotechnology, 2014) 65

Figure 3.6 Reactive Yellow 81 (Procion Yellow H-E3G) chemical composition (World Dye Variety, 2012) 65

Figure 3.7: Reactive Blue 4 chemical composition (MP Biomedicals, 2014) 66

Figure 3.8: Azobenzene type Acid Dye is the typical acid red dye that would include the Acid Fast Red dye used in this study (Essential Chemical Industry Online a., 2013) 67

Figure 3.9: Triphenylmethane type Acid Dye is the typical acid yellow dye that would include the Acid Golden Yellow dye used in this study (Sigma Aldrich b, 2014) 67

Figure 3.10: Anthraquinone type Acid Dye is the typical acid blue dye that would include the Acid Ananda Blue dye used in this study (Sigma Aldrich a, 2014) 68

Figure 3.11: Picture of 501 Bar Soap 70

Figure 3.12: Simple soap chemical composition as an anionic detergent including a hydrophobic group and a hydrophilic group (Essential Chemical Industry Online b, 2013) 71

Figure 3.13: Bicarbonate powder chemical structure (Chemical Education Digital Library) 71

Figure 3.14: Picture of locally available bicarbonate powder used in this study .. 72

Figure 3.15: Open dumping site showing old yogurt containers used for scrap iron for study 75

Figure 3.16: Scrap metal cut from the yogurt container. This is a medium-sized piece, the size was halved for low, and doubled for high iron surface area 76

Figure 3.17: (A) SEM of Iron Rust from India Fe 1.5K, (B) map of composition of surface of scrap iron S (red), Fe (green), Al (blue), C (teal) 88

Figure 4.1: UV-visible spectra for t_0, partial oxidation, and full oxidation of the three Reactive Dye colors using (A) high iron, (B) medium iron, and (C) low iron 95

Figure 4.2: Reactive Red 120 UV-visible spectra of the diluted control C1 compared to (A) R1H-R6H, (B) R1M-R6M, and (C) R1L-R6L 97

Figure 4.3: Reactive Yellow 81 UV-visible spectra of the diluted control C1 for Reactive Yellow 81 compared to (A) R1H-R6H, (B) R1M-R6M, and (C) R1L-R6L 99

Figure 4.4: Reactive Blue 4 UV-visible spectra of the diluted control C1 for Reactive Blue 4 compared to (A) R1H-R6H, (B) R1M-R6M, and (C) R1L-R6L 101

Figure 4.5: COD results comparing Reactive Red 120 USA and India samples C1 to (A) R1H-R6H, (B) R1M-R6M, and (C) R1L-R6L 104

Figure 4.6: COD results comparing Reactive Yellow 81 USA and India samples C1 to (A) R1H-R6H, (B) R1M-R6M, and (C) R1L-R6L 107

Figure 4.7: COD results comparing Reactive Blue 4 USA and India samples C1 to (A) R1H-R6H, (B) R1M-R6M, and (C) R1L-R6L 110

Figure 5.1: UV-visible spectra for A4, A7, and A10 of (A) Acid Fast Red, (B) Acid Golden Yellow, and (C) Acid Ananda Blue 148

Figure 5.2: Acid Fast Red UV-visible spectra of the diluted control C1 compared to (A) A1-A3, (B) A4-A6, (C) A7-A9, and (D) A10-A12 150

Figure 5.3: Acid Golden Yellow UV-visible spectra of the diluted control C1 for Acid Golden Yellow compared to (A) A1-A3, (B) A4-A6, (C) A7-A9, and (D) A10-A12 152

Figure 5.4: Acid Ananda Blue UV-visible spectra of the diluted control C1 for Acid Ananda Blue compared to (A) A1-A3, (B) A4-A6, (C) A7-A9, and (D) A10-A12 154

Figure 5.5: COD results comparing Acid Fast Red samples C1 to (A) A1-A12 in India, and (B) A1-A12 in the USA 157

Figure 5.6: COD results comparing Acid Golden Yellow samples C1 to (A) A1-A12 in India, and (B) A1-A12 in the USA 159

Figure 5.7: COD results comparing Acid Ananda Blue samples C1 to (A) A1-A12 in India, and (B) A1-A12 in the USA 161

Figure 6.2: Acid Fast Red with Soap and Soda UV-visible spectra of the diluted control C1 compared to (A) S1-S3 and (B) S4-S6 196

Figure 6.3: Acid Golden Yellow with Soap and Soda UV-visible spectra of the diluted control C1 compared to (A) S1-S3 and (B) S4-S6 198

Figure 6.4: Acid Ananda Blue with Soap and Soda UV-visible spectra of the diluted control C1 compared to (A) S1-S3 and (B) S4-S6 199

Figure 6.5: Field Samples UV-visible spectra of the control C1 compared to F1-F3 (A) Green and (B) Maroon 200

Figure 6.6: COD results comparing Acid Fast Red with Soap and Soda USA and India samples C1 to S1-S6 203

Figure 6.7: COD results comparing Acid Golden Yellow with Soap and Soda USA and India samples C1 to S1-S6 205

Figure 6.8: COD results comparing Acid Ananda Blue with Soap and Soda USA and India samples C1 to S1-S6 207

Figure 6.9: COD results comparing Field Samples Green and Maroon F1-F3 in India 208

Figure 7.1: Questionnaire completed for of each cottage-scale dyer visited 246

LIST OF TABLES

Table 2.1: Container and Material Results Overview 47

Table 3.1: Low carbon steel properties (Ashby, 2009) 56

Table 3.2: PET properties (Ashby, 2009) 58

Table 3.3: PE properties (Ashby, 2009) 59

Table 3.4: Concrete properties 61

Table 3.5: Plywood properties (Ashby, 2009) 62

Table 3.6: Amount of 6% hydrogen peroxide used with various dye colors, types, and amounts of rusty iron 74

Table 3.7: Partial and full oxidation times for Reactive Dyes 77

Table 3.8: Partial and full oxidation times for Acid Dyes 77

Table 3.9: Partial and full oxidation times for Acid Dyes with Soap and Soda 77

Table 3.10: India's permissible effluent standards for wastewater in Dye and Dye Intermediate Industries for disposal in surface waters (Hasan, 2014) 79

Table 3.11: Global permissible drinking water standards comparing USEPA, CPCB, BIS, and, WHO (Kumar and Puri, 2012; Hasan, 2014; Paul *et al.*, 2012) 80

Table 3.12: Peak absorbance wavelengths for the tested dyes and their designated responsible chemical 82

Table 4.1: Abbreviations of sample names for Reactive dyes 93

Table 4.2: Abbreviations of control names 93

Table 4.3: COD overview comparing C1-C5 to R1H-R6H, R1M-R6M, and R1L-R6L for Reactive Red 120 in India and the USA 103

Table 4.4: COD overview of Reactive Yellow 81 comparing C1-C5 to R1H-R6H, R1M-R6M, and R1L-R6L in India and the USA 106

Table 4.5: COD overview of Reactive Blue 4 comparing C1-C5 to R1H-R6H, R1M-R6M, and R1L-R6L in India and the USA 109

Table 4.6: Percent sludge produced per 1-liter laboratory study during full oxidation in India according to color and surface area of iron..... 111

Table 4.7: GC/MS overview of Reactive Red 120 comparing C1-C5 to R1H-R6H, R1M-R6M, and R1L-R6L..... 114

Table 4.8: GC/MS overview of Reactive Yellow 81 comparing C1-C5 to R1H-R6H, R1M-R6M, and R1L-R6L 117

Table 4.9: GC/MS overview of Reactive Blue 4 comparing C1-C5 to R1H-R6H, R1M-R6M, and R1L-R6L..... 119

Table 4.10: Calculated oxygen uptake for Reactive Red 120 according to low, medium, or high iron and non-filtered or sand filtered sample results 128

Table 4.11: Calculated oxygen uptake for Reactive Yellow 81 according to low, medium, or high iron and non-filtered or sand filtered sample results 129

Table 4.12: Calculated oxygen uptake for Reactive Blue 4 according to low, medium, or high iron and non-filtered or sand filtered sample results..... 130

Table 4.13: Analysis of Variance (3-way ANOVA) for partially oxidized samples. Variables for reactive dye are color (red, yellow, blue), iron surface area (low, medium, high), and filtration method (no filter, sand filter) 131

Table 4.14: Hazardous effects of the definable chemicals that remain in solution listed according to the Globally Harmonized System of Classification and Labeling of Chemicals (GHS) 142

Table 5.1: Abbreviations of sample names for acid dyes 146

Table 5.2: COD overview of Acid Fast Red comparing C1-C5 to A1-A12 in India and the USA..... 157

Table 5.3: COD of Acid Golden Yellow comparing C1-C5 to A1-A12 in India and the USA..... 159

Table 5.4: COD overview of Acid Ananda Blue comparing C1-C5 to A1-A12 in India and the USA..... 161

Table 5.5: Percent sludge produced per 1-liter laboratory study during full oxidation in India according to color 162

Table 5.6: GC/MS overview of Acid Fast Red comparing C1-C5 to A1-A12 ... 165

Table 5.7: GC/MS overview of Acid Golden Yellow comparing C1-C5 to A1-A12 ... 167

Table 5.8: GC/MS overview of Acid Ananda Blue comparing C1-C5 to A1-A12 ... 168

Table 5.9: Calculated oxygen uptake for Acid Fast Red according to partial oxidation time 1, 2, 3 and non-filtered or sand filtered sample results ... 177

Table 5.10: Calculated oxygen uptake for Acid Golden Yellow according to partial oxidation time 1, 2, 3 and non-filtered or sand filtered sample results ... 178

Table 5.11: Calculated oxygen uptake for Acid Ananda Blue according to partial oxidation time 1, 2, 3 and non-filtered or sand filtered sample results ... 179

Table 5.12: Analysis of Variance (3-way ANOVA) for partially oxidized samples. Variables for acid dye are time (partial 1, partial 2, partial 3), color (red, yellow, blue), and filtration method (no filter, sand filter) ... 180

Table 5.14: Hazardous effects of the definable chemicals that remain in solution after photo-Fenton oxidation of acid dyes listed according to the Globally Harmonized System of Classification and Labeling of Chemicals (GHS) ... 190

Table 6.1: Abbreviations of sample names for acid dyes with soap and soda ... 194

Table 6.2: COD overview of Acid Fast Red with Soap and Soda comparing C1-C5 to S1-S6 in India and the USA ... 202

Table 6.3: COD of Acid Golden Yellow with Soap and Soda comparing C1-C5 to S1-S6 in India and the USA ... 204

Table 6.4: COD of Acid Ananda Blue with Soap and Soda comparing C1-C5 to S1-S6 in India and the USA ... 206

Table 6.5: COD of Field Samples Green and Maroon comparing C1 to F1-F3 in India ... 208

Table 6.6: GC/MS overview of Acid Fast Red with Soap and Soda comparing C1-C5 to S1-S6 ... 212

Table 6.7: GC/MS overview of Acid Golden Yellow with Soap and Soda comparing C1-C5 to S1-S6 213

Table 6.8: GC/MS overview of Acid Ananda Blue with Soap and Soda comparing C1-C5 to S1-S6 214

Table 6.9: GC/MS overview of Field Samples Green and Maroon comparing C1 to F1-F3 216

Table 6.10: ICP results for photo-Fenton oxidized Field Samples Green and Maroon samples F1-F3 compared with C1 224

Table 6.11: Calculated oxygen uptake for Acid Fast Red with Soap and Soda according to partial oxidation time and non-filtered or sand filtered sample results 225

Table 6.12: Calculated oxygen uptake for Acid Golden Yellow with Soap and Soda according to partial oxidation time and non-filtered or sand filtered sample results 225

Table 6.13: Calculated oxygen uptake for Acid Ananda Blue with Soap and Soda according to partial oxidation time and non-filtered or sand filtered sample results 226

Table 6.14: Calculated oxygen uptake for Field Samples Green and Maroon according to partial oxidation time and non-filtered or sand filtered sample results 227

Table 6.15: Hazardous effects of the definable chemicals that remain in solution after photo-Fenton oxidation of acid dyes with soap and soda listed according to the Globally Harmonized System of Classification and Labeling of Chemicals (GHS) 237

Table 7.1: Parameters of sustainable photo-Fenton oxidation trials 248

Table 7.2: Results of sustainable photo-Fenton oxidation of Trial 1 249

Table 7.3: Results of sustainable photo-Fenton oxidation of Trial 2 249

Table 7.4: Results of sustainable photo-Fenton oxidation of Trial 3 250

Table 7.5: Results of sustainable photo-Fenton oxidation of Trial 4 251

Table 7.6: Results of sustainable photo-Fenton oxidation of Trial 5 251

Table 7.7: Results of sustainable photo-Fenton oxidation of Trial 6 252

Table 7.8: Results of sustainable photo-Fenton oxidation of Trial 7 252

Table 7.9: Results of sustainable photo-Fenton oxidation of Trial 8 253

Table 7.10: Parameters of sustainable photo-Fenton oxidation tested..... 254

Table 7.11: Results of sustainable photo-Fenton oxidation of Swan Silk Limited effluent 254

Table 7.13: Peak location and identification of respective organic molecule (Jozwiak *et al*., 2007) 258

Table 7.14: Materials and services costs for initial set-up of 50-liter sustainable photo-Fenton oxidation treatment unit 260

Table 7.15: Materials costs for 50-liter sustainable photo-Fenton oxidation treatment process 260

LIST OF ABBREVIATIONS

ANOVA Analysis of Variance

AOP Advanced Oxidation Process

BET Brunauer-Emmett-Teller

BIS Bureau of Indian Standards

BOD Biological Oxygen Demand

CAS Chemical Abstracts Service

COD Chemical Oxygen Demand

CETP Common Effluent Treatment Plant

CPCB Central Pollution Control Board

CSIR- NEERI The Council of Scientific and Industrial Research - National Environmental Engineering Research Institute

DI De-Ionized

EDTA Ethylenediaminetetraacetic Acid

EDX Energy Dispersive X-ray Spectrometry

EPA Environmental Protection Agency

FTIR Fourier Transform Infrared Spectroscopy

GC/MS Gas Chromatography and Mass Spectrometry

GHS Globally Harmonized System of Classification and Labeling of Chemicals

IBR Immobilized Biomass Reactor

ICP Inductively Coupled Plasma Atomic Emission Spectroscopy

ICMR Indian Council of Medical Research

ISI Indian Standard Institution

KSPCB Karnataka State Pollution Control Board

MLSS Mixed Liquor Suspended Solids

OD Optical Density

PAH Polycyclic Aromatic Hydrocarbon

PDMS/DVB Polydimethylsiloxane/Divinylbenzene

PE plastic bags

PET plastic bottles

SEM Scanning Electron Microscopy

SPME Solid Phase Micro-Extraction

TDS Total Dissolved Solids

TOC Total Organic Carbon

TSS Total Suspended Solids

UWM University of Wisconsin-Milwaukee

UV Ultra Violet

WHO World Health Organization

LIST OF SYMBOLS

H_2O_2 Hydrogen Peroxide

*OH or OH* Hydroxyl Radical

hv UV light

uv UV light

CO_2 Carbon dioxide

Fe^{2+} Ferrous iron

Fe^{3+} Ferric iron

OH^{-} Hydroxide

H_2O Water

H^{+} Hydronium ion

$[Fe(OH)]^{2+}$ Iron hydroxide

HO_2^{*} Hydroperoxyl radical or Perhydroxyl radical

R Organic chemical

R^{+} Charged organic contaminant

RH Acidified organic chemical

ROH Hydrolyzed organic chemical

H_2 Hydrogen gas

Fe^{0} Zero-valent iron

$FeOOH^{2+}$ Iron oxide

$[Fe(OH)]^{2+}$ Iron hydroxide

CO_2 Carbon Dioxide

O_2 Oxygen gas

ACKNOWLEDGMENTS

A great many people have helped me on this journey. This work has become a major part of my personal and professional life and many of the people that I have connected with for the last five and a half years have had a major influence on me. Sometimes their impact was in helping me realize that I was not alone, and that I will never be alone no matter where I go. But there are some people that I would like to specifically thank because they have been vital to this project's success.

Thank you Dr. John Reisel for believing in this study and in me. I appreciate your patience, honesty, and calmness, and found your advice invaluable. I knew that a Ph.D. interested me but only if it included sustainable development engineering. Thank you for saying yes and for helping this project grow from the ground up.

Thank you Dr. Hemant Purohit, HOD of Environmental Genomics Division, for your great feedback, ideas, and space in your lab—I hope to always keep our collaboration open. Thank you Director of CSIR-NEERI for allowing me to visit and complete a large amount of fieldwork at NEERI.

Thank you Committee for reading this dissertation, asking pertinent questions that helped me grow in this field, and for allowing sustainable community-driven engineering into my Ph.D. program.

Thank you Karnataka State Pollution Control Board for taking time away from your busy schedule to listen to my proposal, for finding me a dyer to complete the demonstration project, and for holding me to a high standard thus improving this work. I will continue this work after graduation so I am sure I will be seeing you again.

Thank you Banu Prakash for the tour of the Chintamani Sericulture Cooperative and the many industries that complete the system. Without you I could not have begun this work or furthered my connections in the industry.

Thank you Asifa Qureshi for continually reminding me of the importance of publishing, always asking me important questions, and requiring that I know how to best explain my studies to people from all different backgrounds. I realize that it must have been difficult to share your office with me during four and a half summers—but I really treasure the memories of work and stories that we have shared.

Thank you Heidi Ranicke for your ever-persistent help with wet lab work and your steadfast editing. You are intelligent, and I hope that you realize how much you helped in the completion of this task.

Thank you Dr. Satya for helping me connect with people in Bangalore and for pushing me to defend and publish this important work. And thank you Reddappa for sacrificing your time to help me find acid, peroxide, and to make my first rusty metal box in the K.R. Market.

Thank you to the Director, Mr. K.S. Radhusa, and Dye Manager, Mr. Prakash Mangalagatti, of Swan Silk Ltd. for opening your business and helping me during June and July of 2014 giving complete support for space, work assistance, and all chemical needs. All of your staff were incredibly gracious and supportive. I would also like to thank Babu and Narasimhamurti for their patience with my poor Hindi and my insistence to help—you both added substantially to the feasibility of the future implementation of a pilot project, giving real practical advice about this system's protocol.

Thank you GE Healthcare, specifically Bill Berezowitz for introducing me to Mahesh Kapri in Bangalore, and thank you Mahesh for connecting me with Pramod Galagali, and Pramod for initiating meetings with the KSPCB as well as giving me valuable advice and input into my proposals, presentations, and work. I am grateful that we have connected because of this project. You have influenced my life by showing me that there are good people who are working to better the world.

Thank you MATC's Chemical Technology Department for giving me lab space and letting me use your GC/MS, ICP, and UV-visible Spectrophotometer and for all of the chemical advice in the study.

Thank you PEO for awarding me the Scholar Award and for consistently showing interest in my studies. And a special thanks to Chapter AW for the personal support.

Thank you Betty Warras for your wisdom and guidance through graduate school. Thank you Michelle Schoenecker for your valuable advice helping me write grants—your exceptional skill was paramount to our success.

Thank you Mike Hoffmann for reminding me that everything happens when it must. I'll never forget your excitement when I told you that I had an awful day writing when no words had come and you exclaimed, "Great! That means you're about to explode with productivity!" Your talent and outlook amaze and inspire me.

Thank you Mom and Dad. Mom for helping me realize we need to push ourselves and live our own lives. If we are not happy with our choices then we should change the path. You showed me engineering by introducing me to people. And you taught me to be a strong woman. Dad, I know you are proud of me and always have been. I remember you telling me years ago that I had arrived and I have never forgotten it. I'm sorry for choosing to work on projects far away from home—but I'm excited for your first trip to India or Baltimore.

Thank you Jessica, Chuck, Addison, and Eli for believing in me and buying that Congratulations card before I even passed the Qualifying Exam.

Thank you Grandma for always being proud of me, praying to St. Jude, and believing that I can do anything. Sorry I couldn't finish in time, but I know in your mind, I was already a doctor.

Thank you Shirley Grade for always being on my side and in my corner and for the mind breaks and inspiration.

Thank you Alana for sharing W349 with me, spending many long nights deciphering engineering and life, and for helping create Magic 7 that got me through the Qualifying and you through the GRE.

Thank you Abhay and Manisha for including me in your family and for the many meals and terrific conversations and the endless support, encouragement, and generosity.

Thank you labmates at NEERI, Nagpur. You are an incredible group—despite changing over the years you are all supportive, intelligent, and nice. A special thanks to Shraddha for being there for me in the lab with my many questions, and to Sampada for knowing what to say to get me to continue writing.

Thank you to all of my friends for believing in me and grounding me. Thanks for all of your words of encouragement. You have stayed with me despite the distance between us. I could not have done this without any of you.

“What you do makes a difference,
and you have to decide what kind of difference you want to make.”

—Jane Goodall

CHAPTER 1: INTRODUCTION

1.1 Background

Clothing is an essential part of daily human life worldwide, but rarely is thought given to how clothing is actually made. Before fabric is sewn into sweaters, silk blouses, and denim jeans, the fabric must be dyed. Looking at the tags in clothing lines available in the most developed countries worldwide, it can be deduced that the clothing manufacturing process is often outsourced to developing countries, where it is frequently located in rural communities where the heavy pollution caused from the industry is not readily seen but still is damaging to the environment. For example, the operation of dyeing silk saris in Bangalore, India most often occurs in small communities that are then crippled with environmental problems due to the high levels of chemicals in the dyes. The fundamental problem is that once the fabrics are dyed, the dye waste is discharged back into the community's water source or thrown directly onto the ground where it can seep into the groundwater that feeds the local water systems. Many of the residents in these communities are very poor and are forced to use contaminated water for their daily needs.

Dye effluent has very complex chemical structures that can cause irreparable harm to ecosystems. Yet the total discharge is more than 10,000,000 kg/year because of high demand, thus making a huge impact on the Earth (Daud and Hameed, 2010). Acid and Reactive red dyes are types of azo dyes which have been banned in many countries of the world, but they continue to be used in some countries in great quantities. According to Daud *et al.* (2010), azo dyes are dyes that have one or more double nitrogen bonds in

their chemical structure bonded to aromatic rings; this is one of the most difficult synthetic linkages to break. Daud *et al.* (2010) also mention that Fenton's reagent was discovered a century ago and its use of hydroxyl radicals shows great promise in breaking these environmentally-destructive bonds; however, the use of iron as a catalyst in reaction tends to create additional unpredicted pollutants in solution. Hsing *et al*. (2007) add that it is very difficult to remove azo dyes from solution, but that the reaction that forms hydroxyl radicals allows 85% of Chemical Oxygen Demand (COD) and color to be removed in 20-40 minutes.

Reactive and Acid Dyes are also used frequently in the silk dyeing industry. Reactive Dyes are used for 32% of all dye operations. In these operations, only 70% of the dye is absorbed during a dye job, leaving 30% to enter the waste stream (Aplin and Waite, 2000). Reactive Dyes are frequently used for dyeing silk because they have a very high stability that sustains their color once the textile is washed. Considering that the homespun silk industry in rural Bangalore currently uses no treatment for their dye wastewater prior to discharging it into streams or onto land, the typical textile wastewater entering the groundwater of the area contains a pH ranging between 7-9, Biological Oxygen Demand (BOD) 80-6000 mg/l, COD 150-12000 mg/l, Total Suspended Solids (TSS) 15-8000 mg/l, Total Dissolved Solids (TDS) 2900-3100 mg/l, chloride levels between 1000-1600, total Kjeldahl Nitrogen from 70-80 mg/l, and color from 50-2500 color units (Al-Kdasi *et al*, 2004).

To help alleviate this problem, it is proposed to test two methods to clean contaminated

dye wastewater using very affordable materials that can be easily found in and around the homes of the dyers. The two forms of treatment to be studied here are sustainable photo-Fenton oxidation with sand and carbon filtration and sustainable photo-Fenton oxidation with sand filtration coupled with biodegradation. Both techniques have been shown to be affordable, efficient methods of decolorizing dye wastewater using acid, hydrogen peroxide, iron scrap, and sunlight (Tantak and Chaudhari, 2006; Lodha and Chaudhari, 2007; Chamarro *et al*., 2001; Rodriguez *et al.*, 2002; dos Santos *et al.*, 2007), but this work is the first of its kind (1) to use a 5 g/l dye concentration equivalent to effluent from cottage-scale textile dye industries, and (2) to use sand filtration to bring the pH back to neutral and to separate the sludge formed from the oxidation process from the aqueous solution.

Preliminary testing of the effectiveness of sustainable photo-Fenton oxidation, with specific attention paid to creating a system that is readily transferrable to rural communities in developing nations, was performed at the University of Wisconsin-Milwaukee. The use of sustainable photo-Fenton oxidation coupled with biodegradation was studied in collaboration with the National Environmental Engineering Research Institute in Nagpur, India. When the systems are ready for field use, a functioning treatment unit will be installed and studied at a cottage-scale textile dyer in rural Bangalore, India.

India is the second-largest global producer of silk, employing over one million peasant families, where the majority of silk dyeing is accomplished in peasant homes within

small villages (Datta and Nanavatty, 2005). In 2010, a rural village in Karnataka was identified as a typical community containing small-scale silk dyeing businesses owned and operated by local families. In addition, families in this village had expressed great interest in finding a system that would allow them to economically treat the dye wastewater. To meet their needs, this project was developed in order to create a mobile wastewater treatment unit that uses sustainable photo-Fenton oxidation with sand and carbon filtration to remove the color and the most dangerous chemicals from dye wastewater. The project would concentrate the waste into a sludge that would be safer for disposal or for reuse, and leave the water clear to reuse in future dye batches. The impact of the project does not end in this one rural village. There are approximately 150 silk dyers in central Bangalore that are currently using no wastewater treatment and many other small communities of cottage-scale silk dyers surrounding the city. One of these locations will be used for the development of a pilot project and educational program, with growth open to the rest of the world.

As the system is designed to help poor communities in developing countries, it is important that it be able to be constructed from readily available, inexpensive, or scrap materials. For the study in rural India, the demonstration-scale unit was made of rusty sheet metal for one dyer in June 2014. The rusty sheet metal was chosen after completing a feasibility study of containers made of iron, scrap wood, concrete, and plastic bags or bottles. The system uses technology that has shown to be promising in the laboratory, where more expensive materials were used. Once the demonstration project has been modified to be as successful as its laboratory counterparts, the system will be

easily replicable to a larger-scale pilot project in June 2015, and then be transferred to other rural dyeing communities throughout the world, including Morocco, Mexico, and Turkey. Therefore, this study has the potential to offer an affordable treatment option to the thousands of dyers in the world who are currently using no decolorization method because of lack of funds. With this new technology and education of how it works, people will be able to clean their dye effluent before discarding it to the environment which will reduce soil and ground water pollution. Alternatively, they will be able to reuse the water in future dye batches thus decreasing their overall water consumption.

1.2 Contents of Dissertation

This dissertation will cover the sustainable photo-Fenton oxidation of Reactive, Acid, and Acid with Soap and Soda dyes comparing red, yellow, and blue color both on a 1-liter laboratory scale and a 50 to 100-liter scale in the field. Chapter 2 contains a discussion of the theory of the work and a literature review of previous studies covering the dyeing process, photo-Fenton oxidation, photo-Fenton oxidation coupled with biodegradation, and sustainable containers and materials used for oxidation. Chapter 3 contains details of the experimental apparatus and methodology including the experimental procedure, the rusty metal container, variables in photo-Fenton oxidation (including UV radiation, dye, soap and soda, water, acid, hydrogen peroxide, iron, time, filtration), and methods of analysis (including UV-visible spectrometry, COD, GC/MS, ICP, total iron, SEM, respirometric analysis). Chapter 4 describes the Reactive Dye photo-Fenton oxidation laboratory-scale results for Reactive Red 120, Reactive Yellow 81, and Reactive Blue 4 using high (645 cm^2), medium (323 cm^2), and low (161 cm^2) surface area of scrap iron

after partial and full oxidation followed by no filtration, sand filtration, and sand and carbon filtration. Chapter 5 contains a similar discussion of the Acid Dye photo-Fenton oxidation laboratory-scale results for Acid Fast Red, Acid Golden Yellow, and Acid Ananda Blue using 645 cm^2 surface area of scrap iron after three partial oxidation times and full oxidation followed by no filtration, sand filtration, and sand and carbon filtration. Chapter 6 contains the results of the Acid Dye photo-Fenton oxidation for Acid Fast Red with Soap and Soda, Acid Golden Yellow with Soap and Soda, and Acid Ananda Blue with Soap and Soda using 645 cm^2 surface area of scrap iron after partial and full oxidation followed by no filtration, sand filtration, and sand and carbon filtration. Chapter 7 presents a review of the 50 to 100-liter sustainable demonstration photo-Fenton oxidation reactor project constructed in Karnataka, India detailing the results and discussing recommendations for continuation of the project and construction of 150-liter pilot project in June 2015. Chapter 8 reports the conclusions from the work and includes a discussion on how to expand this work in the future.

CHAPTER 2: THEORY AND LITERATURE REVIEW

2.1 Dyeing Silk: Process and Effluent

2.1.1 History of Silk Production

Documentation of sericulture dates back to approximately 2500 B.C. when stories of Chinese Queen Hsi-Ling-Shih discovering silk worms in her gardens eating mulberry and her accidently dropping their cocoons into a hot water bath, which resulted in silk yarn being produced (Datta and Nanavaty, 2005). However, it is also debated that the domestication of silk worms originated at the base of the Himilaya Mountains (Datta and Nanavaty, 2005). After its discovery, the extremely elegant fabric was highly protected—anyone caught smuggling any part of the mulberry seeds or silkworm eggs out of the Chinese empire was penalized by death (Datta and Nanavaty, 2005). Finally global trade was in full swing by the 6th century A.D.; thus silk also became globally produced and can now be found on all corners of Earth (Datta and Nanavaty, 2005). Although silk production is only 0.2 % of the total textile industry, silk is still a highly coveted textile for auspicious occasions such as weddings and elegant home furnishings and fashion (Datta and Nanavaty, 2005). Silk sales in the USA increased the most during World War I when women replaced men in work environments, which required them to wear silk stockings, and silk sales saw the largest decrease in this market around the time of World War II when nylon and rayon replaced silk in many markets (Datta and Nanavaty, 2005).

Silk production in India occurs in over 60,000 villages and focuses 90% of its production in the southern states of Karnataka, Andhra Pradesh, and Tamil Nadu, with the remaining 10% in the northern states of West Bengal and Kashmir. The silk industry through India gives jobs to an estimated 6-8 million residents, more than one million of these people being peasant families in scattered villages (Datta and Nanavaty, 2005). Karnataka State has the highest production of silk within India and focuses their production on multivoltine silk. They have also constructed a Central Silk Board and Central Sericulture Research and Training Institutes and cooperatives that help farmers, rearers, dyers, and weavers to get high quality raw materials and to sell their final products to each other and the public (Datta and Nanavaty, 2005).

The silk production process can be broken into the different life-cycle stages of the silk worm where each stage can be separated by different farms. Figure 2.1 shows the life cycle of the mulberry silkworm and breaks it into the many growth stages of the worm starting with the egg, different growth stages of the instar, the ripe silkworm, spinning, pupation that creates the cocoon, and finally the hatching to create more eggs (Datta and Nanavaty, 2005). To share the work of silk production in a community, farmers split the rearing according to their mulberry crop thus buying young worms and selling the older ones or buying the older ones and selling the cocoons to market. Almost all farmers in the silk cooperatives also grow mulberry to keep more than one form of possible income on their farm in case of emergency.

There are many different kinds of silk due to the different species of worm and also the different food they digest. Wild silk is known as tussah while cultivated silk is known as mulberry. However, all silk is a natural protein fiber that is extruded from two glands on the silk worm and it has a small content of sulphur (Uddin and Hossain, 2010). The silk is secreted as a viscous fluid made of fibroin comprising the fiber and sericin which is the gum surrounding the fiber. The complete composition of silk is fibroin (75% composition), and sericin (23%), while the remaining is fat and wax, and 0.5% is mineral salts (Uddin and Hossain, 2010). The silk industry in Karnataka with its cooperative programs buying and trading mulberry, worms, cocoons, and silk at auction is all completed with visual inspection and therefore does not break their silk quality into several grades, but either acceptable or not. In the interest of increasing income, India is starting to test their silk for evenness, cleanliness, neatness, size deviation, winding breaks, tenacity, elongation, cohesion, and conditioned weight adapted to come up with data and grades of their silk according to ISA standards (Datta and Nanavaty, 2005).

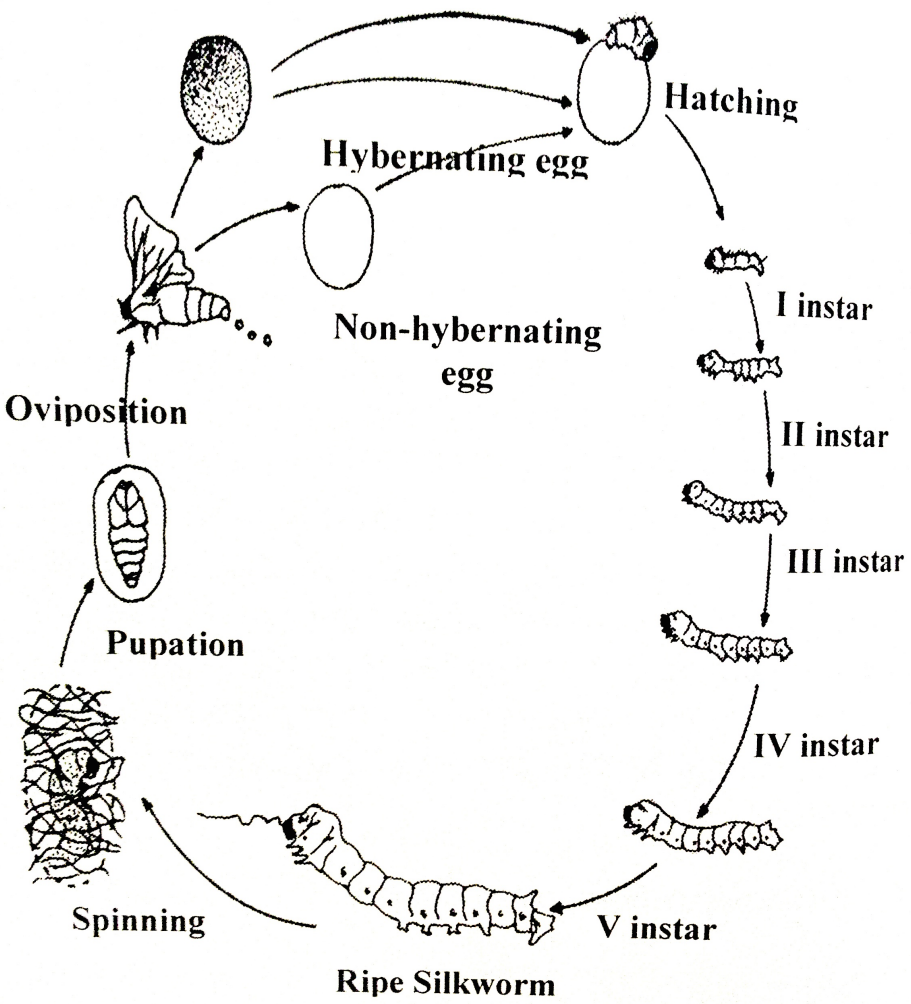

Figure 2.1: Lifecycle of mulberry silkworm (*Bombyx mori L*) (Datta and Nanavaty, 2005).

2.1.2 Dyeing Silk: Silk Composition

Silk is a natural fiber, but since it is the cocoon of a worm it is protein-based fiber. Dyeing a silk fiber depends on its ability to react with the chemical composition of the dye. Specifically for silk, free amino and carboxyl groups are needed, as are phenolic groups with accessible hydroxyl groups. Silk has a slightly cationic character with an isoelectric point above 5.0, therefore silk can absorb anionic dyes that include Acid Dyes,

Metal Complex Dyes, Reactive Dyes, and selected Direct Dyes (Uddin and Hossain, 2010).

2.1.3 General Synthetic Dyes Effluent

Synthetic dyes and their extreme variability are one of the world's major industrial pollutants that disrupt water health (Modirshahla *et al.*, 2007). Approximately 30 million tons of textiles are produced every year around the globe—this requires 0.7 million tons of dye (Lin *et al.*, 2008). Approximately 70% of that dye produced lies within the azo group which is banned in some areas of the world; the azo group was banned in the EU in 2003, and is being considered for banning in Australia. However, it is still used in many places (Bavas, 2014; CBI, 2012). Textile industrial wastewater typically contains a pH ranging from 7-9, Biological Oxygen Demand (BOD) 80-6000 mg/l, Chemical Oxygen Demand (COD) 150-12000 mg/l, Total Suspended Solids (TSS) 15-8000 mg/l, Total Dissolved Solids (TDS) 2900-3100 mg/l, chloride levels between 1000-1600, total Kjeldahl Nitrogen from 70-80 mg/l, color from 50-2500 color units, as well as heat (Al-Kdasi *et al.*, 2004). Of the 10,000 dyes available, 40 of them are biodegradable; 280,000 tonnes of residual color is discharged into wastewater every year worldwide (Al-Kdasi *et al.*, 2004; Aplin and Waite, 2000; Tantak and Chaudhari, 2006; Lodha and Chaudhari, 2007). Liu *et al.* (2007) agree that textile and dye industry effluent is very high is suspended solids, COD, BOD, heat, acidity, basicity, and color. They add that most pollutants are manageable in a Common Effluent Treatment Plant (CETP) using typical methods, however, color needs more attention because of its intensity and its residual effect on the natural environment.

2.1.3.1 Reactive Dyes

Reactive Dyes are used for 32% of dye jobs. Only 70% of the dye is being absorbed during a dye job, leaving 30% to enter the waste stream (Aplin and Waite, 2000). One of the main causes of the high levels of dye in the waste stream is due to the hydrolysis process that must occur at the end of the Reactive Dye process. This hydrolysis process renders the dye left in solution unusable (Aplin and Waite, 2000). Specifically a typical end of use Reactive Dye bath will contain 0.6 g/L unfixed dye, 40-80 g/L sodium chloride or sodium sulfate, and small quantities of other additives at a pH of 11 and 50 °C (Aplin and Waite, 2000). Aplin and Waite (2000) showed that sodium chloride greatly inhibited the Fenton and photo-Fenton oxidation processes.

Reactive Dyes are a popular choice for dyeing silk because upon completion of the process, the color becomes chemically bonded to the fiber in such a way that the dye is a part of the fiber. The reactive group of the dye covalently bonds with the neucleophilic group on the silk (Uddin and Hossain, 2010). This covalent bond is the strongest known molecular attraction and therefore creates a very strong color fastness and is popular to the consumer since the color will only go when the fiber itself degrades (Uddin and Hossain, 2010).

All Reactive Dye molecules have 5 major groups: Reactive group (R), Leaving group (X), Chromophoric group (C), Bridging group (B), and Solubilizing group (S). These are labeled in Figure 2.2 from Uddin and Hossain (2010) below:

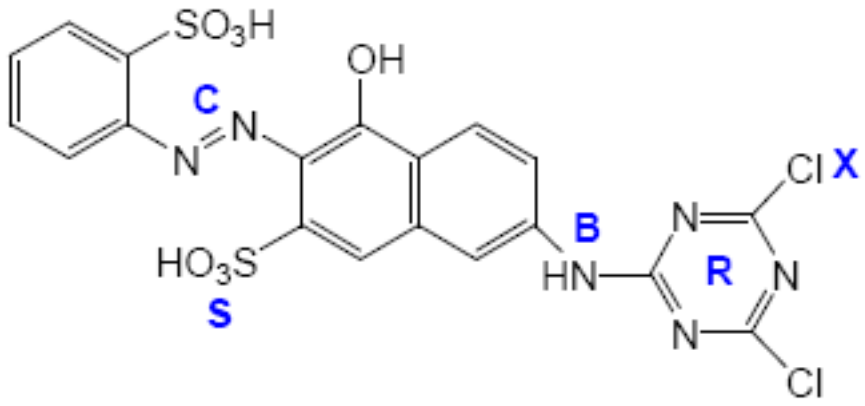

Figure 2.2: Reactive Dye molecule with 5 major groups labeled: Reactive group (R), Leaving group (X), Chromophoric group (C), Bridging group (B), and Solubilizing group (S) (Uddin and Hossain, 2010).

The fixation of Reactive Dyes take place in three stages: the dye is adsorbed from dye bath to the fiber, the dye diffuses to the center of the fiber, and finally is fixed onto the fibroin of the fiber via the covalent bonding taking place because of the protonation of the fibroin creating sites for very strong binding (Uddin and Hossain, 2010).

2.1.3.2 Acid Dyes

Acid Dyes received their name because they were originally used in acidic solutions such as mineral or organic acids. In fact, as detailed by Uddin and Hossain (2010), the color of Acid Dyes is anionic and originates from the sodium salts from sulfuric acids or sometimes carboxylic acids. Since they are anionic they bond with cationic sites on fibers; in the case of silk, the fiber absorbs acids making cationic sites by substituting ammonium ions in the fiber and protonating the fiber's amino group. The chemical equations for this exchange between Acid Dyes and silk are as follows in Reactions (2.1) and (2.2):

$$Fiber - NH_2(s) + H^+(aq) + HSO_4^-(aq) \rightarrow Fiber - NH_3^+HSO_4^-(s) \quad (2.1)$$

$$Fiber - NH_3^+HSO_4^-(s) + Dye - SO_3^-(aq) \rightarrow Fiber - NH_3^+Dye - SO_3^-(s) + HSO_4^-(aq) \quad (2.2)$$

(Uddin and Hossain, 2010).

Acid Dyes are also commonly used to dye silk, wool, acrylics, and polyamide fibers making them very common in textile effluents across the globe (Alaton and Teksoy, 2005). Often the red spectrum of Acid Dyes contains azo bonds; azo dyes still contribute approximately 70% of all used dyes (Idel-aouad *et al.*, 2011). In fact, half of the world's production of synthetic textile dyes are azo dyes classified as such because of the presence of at least one double nitrogen bond (-N=N-) in its chemical composition (Fu *et al*., 2010; Lin *et al.*, 2008). Lin *et al.* (2008) state that 70% of all dyes used are azo dyes. Because of their dangerous azo linkage, their discharge into the environment, including sometimes drinking water, releases hydrolyzed dye and carcinogenic metabolites into water sources causing major human health problems and even inhibit benthic photosynthesis (Idel-aouad *et al.*, 2011; Lin *et al.*, 2008). Lin *et al.* (2008) and Modirshahla *et al.* (2007) add that biological treatment is also inhibited due to the fact that the high pollutant content of the effluent kills the bacteria or fungi to be used in the activated sludge and thus resistant to general CETP treatment. Hydrolysis occurs when dyes are dissolved in water and creates one or more compounds; for example, when the water molecule is broken into negative hydroxyl ions and positive hydrogen ions that also create positive hydronium ions. The dissolution of dyes in water also creates alkaline solution and can increase with high temperature, high pH, and longer dyeing time.

Oxidation of dye effluent can mineralize pollutants into carbon dioxide and water, however care must be taken to fully oxidize in order to prevent the formation of chemical intermediates (Zheng *et al.*, 2007).

To be more specific, there are five major groups for Acid Dyes: sulphonated azo dyes, anthraquinone, triphenylmethane, xanthenes, and sulphonated copper phthalocyanine. Simply put, the sulphonated azo dyes comprise the majority of Acid Dyes and contain either single or double azo bonds; these dyes include colors such as yellow, red, violet, and brown. The double-bonded sulphonated azo dyes can also be navy blue or black. Anthraquinone Acid Dyes range in color spectroscopically from green to violet and keep their color very well. Triphenylmethane Acid Dyes include green and blue colors. Xanthene Acid Dyes include reds and violets, and sulphonated copper phthalocyanine Acid Dyes create bright turquoise colors also with good light fastness (Uddin and Hossain, 2010).

Another way to classify Acid Dyes is through their behavior, which can be broken into four major groups: level dyeing/equalizing Acid Dyes, fast Acid Dyes, milling Acid Dyes, or super-milling Acid Dyes (Uddin and Hossain, 2010). The three Acid Dyes compared in these studies are Acid Fast Red which can be characterized in the fast Acid Dyes class and also in the azobenzene group (which can change to a sulphonated azo dye when SO_3Na is attached), Acid Golden Yellow in the milling class and triphenylmethane group, and Acid Ananda Blue in the leveling class and the anthraquinone group. General drawings of the different groups of Acid Dyes studied here can be found in Chapter 3

section 3.4.2.2. Acid Dye drawings, however, are not specific to dyes used in the study because exact chemical composition of locally available dyes are unavailable and could only be generalized and assumed to also include some impurities.

2.2 Advanced Oxidation Processes for Textile Dye Effluent

Advanced oxidation processes (AOPs) offer chemical treatment methods that surpass conventional biological wastewater treatment processes because they react with many different pollutants by changing the chemical structure of pollutants with hydroxyl radicals which have a strong oxidation potential of 2.80 volts (Bauer and Fallmann, 1997; Chacon *et al.*, 2006; Kang *et al.*, 2000; He and Lei, 2004; Kumar and Ameta, 2013; Alaton and Teksoy, 2005). The main goal of a chemical oxidation process is to produce enough hydroxyl radicals to oxidize any and all organic pollutants present. Researchers agree that measuring COD levels is a valid way to determine decreasing organic levels. A useful way of enumerating a high level of non-biodegradable organic matter present, specifically dyes, is to calculate whether the BOD to COD ratio of a sample is less than 0.1 (Al-Kdasi *et al.*, 2004; Rodriguez *et al.*, 2002; Tantak and Chaudhari, 2006). Oxidation of organic pollutants occurs when hydroxyl radicals attaches to and mineralizes pollutants into carbon dioxide, water, and inorganic salts such as chloride, and various acids including sulfuric, hydrochloric, and nitric (Chacon *et al.*, 2006; Ruppert *et al.*, 1992). Another efficient way to analyze the level of mineralization or organic carbon present is to measure Total Organic Carbon (TOC) levels (Ruppert *et al.*, 1992).

Because of its recalcitrant nature and its toxic aromatic intermediate contamination, dye effluent is known to be untreatable in its raw form using typical aerobic wastewater treatment methods including adsorption, coagulation, and precipitation (Alaton and Teksoy, 2005; Behnajady *et al.*, 2007; Chang *et al*., 2009; Modirshahla *et al.* (2007)). But all research agrees that dye wastewater must be treated before discharging to terrestrial or aqueous environments because of its extreme chemical composition. Alaton and Teksoy (2005) and Modirshahla *et al.* (2007) describe the hydroxyl radical as being almost indiscriminate in its nature to react and breakdown pollutants in aqueous acidic solutions. Liu *et al.* (2012) describe the hydroxyl radical as a very strong undiscriminating oxidant that has been documented to degrade polycyclic aromatic hydrocarbons (PAHs), phenols, dyes, and pesticides, among many other organic pollutants. Hydroxyl radicals have such a strong reaction potential that they can be extremely useful in wastewater treatment; however, they must be generated continuously in order for full oxidation to take place. Hydroxyl radicals react with organic matter to create intermediates and if the hydroxyl radicals are continuously generated in situ then the oxidation reactions continue until only harmless species such as carbon dioxide and water are left in solution (Khataee *et al*., 2009).

Fenton processes are general AOPs that are convenient treatment methods because they create oxygen and water from the hydrogen peroxide oxidant in use while also creating hydroxyl radicals, which are one of the most powerful oxidation agents available (Liu *et al.*, 2007). The photo-Fenton oxidation process is an accelerated version of the Fenton process that uses ultraviolet (UV) light to increase the production of hydroxyl radicals.

Here the comparison is made between sustainable photo-Fenton oxidation as a complete dye wastewater treatment and sustainable photo-Fenton oxidation as a partial treatment followed by biodegradation.

2.2.1 Fenton Process

The Fenton process relies on hydrogen peroxide to degrade pollutants in the presence of iron that is in the form of ferrous ions to create hydroxyl radicals that react with pollutants (Liu *el al.*, 2012). Liu *et al.* (2012) and Modirshahla *et al.* (2007) state that the presence of UV light enhances the formation of hydroxyl radicals and is thus called photo-Fenton oxidation; however, the Fenton process is able to function at a slower rate. The low toxicity of zero-valent iron is a benefit to using the Fenton process as an AOP for dye wastewater treatment because it requires no further treatment before discharge (Fu *et al.*, 2010). Basically, using the reaction with iron naturally reduces ferric ions to ferrous as can be seen in the following chemical Reactions (2.3) and (2.4) (Fu *et al.*, 2010):

$$Fe^0 + 2H^+ \rightarrow Fe^{2+} + H_2 \qquad (2.3)$$

$$2Fe^{3+} + Fe^0 \rightarrow 3Fe^{2+} \qquad (2.4)$$

Ferrous and ferric ions can easily be used in the Fenton process to oxidize many pollutants in aqueous solutions. The chemical reactions describing the full Fenton process are as follows in Reactions (2.5) through (2.13) (Behnajady *et al.,* 2007):

$$H_2O_2 + Fe^{2+} \rightarrow {}^{*}OH + {}^{-}OH + Fe^{3+} \qquad (2.5)$$

$${}^{*}OH + Fe^{2+} \rightarrow {}^{-}OH + Fe^{3+} \qquad (2.6)$$

$$^{*}OH + organics \rightarrow products \quad (2.7)$$

$$^{*}OH + H_2O_2 \rightarrow H_2O + HO_2^{*} \quad (2.8)$$

$$^{*}OH + {}^{*}OH \rightarrow H_2O_2 \quad (2.9)$$

$$H_2O_2 + Fe^{3+} \leftrightarrow H^{+} + FeOOH^{2+} \quad (2.10)$$

$$FeOOH^{2+} \rightarrow HO_2^{*} + Fe^{2+} \quad (2.11)$$

$$HO_2^{*} + Fe^{2+} \rightarrow HO_2^{-} + Fe^{3+} \quad (2.12)$$

$$HO_2^{*} + Fe^{3+} \rightarrow O_2 + Fe^{2+} + H^{+} \quad (2.13)$$

There is debate whether the process follows first or second order kinetics (Behnajady *et al.*, 2007). The reaction creating radicals to oxidize the solution and ultimately the pollutants can be seen, as is the formation of oxygen, iron, and hydrogen ions. Arslan-Alaton *et al*. (2008) concur that Fenton's reagent and the above reactions can remove all color in solution along with a large portion of COD; however, they also mention that care should be taken to decrease the toxicity of the remaining intermediates in solution that can inhibit further biological treatment and pollute natural environments.

2.2.2 Photo-Fenton Oxidation

As the primary technique for the wastewater treatment in this study, a sustainable photo-Fenton oxidation process is to be used. Photo-Fenton oxidation is an AOP that is typically employed using relatively expensive materials as compared with biodegradation (Liu *et al.*, 2012). To improve its utility for poor communities, the technique is modified to be sustainable by including iron chemical substitutes in the form of rusty scrap metal,

sunlight, household hydrochloric acid, and 6% hydrogen peroxide. Modirshahla *et al.* (2007) suggest that the system is dependent on initial dye concentration, iron, and hydrogen peroxide and also suggest a pH of 3.

The photo-Fenton reaction can be seen in Reactions (2.14-2.17) (Bauer and Fallmann, 1997). Reactions (2.14) and (2.15) are the Fenton-like reactions when there is no UV reacting where ferric iron is acting as the catalyst to decompose hydrogen peroxide into hydroperoxyl radical and hydroxyl radicals that are the oxidizing agents in solution to attack the pollutants (Khataee *et al*., 2009). Reaction (2.17) can replace Reaction (2.16) at low pH because of the natural tendency for ferric ions in a hexaquo complex to dissociate at acidic pH from 2-4 and create more hydroxyl radicals (Bauer and Fallmann, 1997; He and Lei, 2004).

$$Fe^{2+} + H_2O_2 \rightarrow Fe^{3+} + OH^- + OH^* \qquad (2.14)$$

$$Fe^{3+} + H_2O_2 \rightarrow Fe^{2+} + HO_2^* + H^+ \qquad (2.15)$$

$$Fe^{3+} + H_2O + h\nu \rightarrow Fe^{2+} + H^+ + OH^* \qquad (2.16)$$

$$\left[Fe(OH)\right]^{2+} + h\nu \rightarrow Fe^{2+} + OH^* \qquad (2.17)$$

Reaction (2.18) is called the Fenton reaction and works with or without UV light but is very sensitive to the amount of hydrogen peroxide. In fact, the more hydrogen peroxide initially used, the less ferrous iron is needed. Sahunin *et al.* (2004) and Kang *et al.* (2000) agree that the Fenton reaction, photolysis of hydrogen peroxide, and the photo-reduction of ferric ions are responsible for the production of hydroxyl radicals. Chacon *et al.* (2006) and Modirshahla *et al.* (2007) add that the use and production of ferrous iron

is cyclical. Sahunin *et al.* (2004), Kang *et al.* (2000), and Hai *et al.* (2007) break the process into similar chemical reactions. Reaction (2.19) is where the photolysis of hydrogen peroxide occurs and forms two hydroxyl radicals that will then react with organic contaminants (Sahunin *et al.*, 2004; Al-Kdasi *et al.*, 2004). This works most efficiently under acidic conditions. Reaction (2.20) is where the photo-reduction of ferrous iron occurs completely independent of pH. Reaction (2.21) describes the catalyzed decomposition of hydrogen peroxide by ferric iron that is dependent on hydrogen peroxide and the UV present (Hsueh *et al.*, 2004; Ruppert *et al.*, 1992; Sahunin *et al.*, 2004). Since this is happening concurrently and cyclically, all of the ferrous iron ions that are regenerated in Reaction (2.21) go through a chemical change in Reaction (2.18) and are transformed into hydroxyl radicals (Ruppert *et al.*, 1992). The rate of Reaction (2.18) is 2650 times that of Reaction (2.21) (Sahunin *et al.*, 2004).

$$H_2O_2 + Fe^{2+} \rightarrow HO^* + Fe^{3+} + OH^- \qquad (2.18)$$

$$H_2O_2 + uv \rightarrow 2HO^* \qquad (2.19)$$

$$Fe^{3+} + H_2O + uv \rightarrow HO^* + Fe^{2+} + H^+ \qquad (2.20)$$

$$Fe^{3+} + H_2O_2 + uv \rightarrow HO_2 + Fe^{2+} + H^+ \qquad (2.21)$$

Hsueh *et al.* (2004) and Vermilyea and Voelker (2009) agree that iron ions and hydrogen peroxide can be naturally occurring in open waters and that when sunlight reacts with the two naturally occurring chemicals, the Fenton process may be the dominant producer of hydroxyl radicals in open waters at an acidic pH. Zheng *et al.* (2007) add that the homogeneous reaction between hydrogen peroxide and UV light is one of the most important reactions in the production of hydroxyl radicals as can be seen by the

continuation of Reaction (2.19) in the following overview of the entire photo-Fenton oxidation process in Reactions (2.22), (2.23), and (2.24).

$$H_2O_2 + hv \rightarrow 2\,{}^{*}OH \tag{2.22}$$

$${}^{*}OH + dye \rightarrow dye\,\mathrm{int}ermediates \tag{2.23}$$

$${}^{*}OH + dye\,\mathrm{int}ermediates \rightarrow CO_2 + H_2O + \mathrm{min}erilzationproduct \tag{2.24}$$

Sahunin *et al.* (2004) illustrate the chemical decomposition of organic pollutants in Reactions (2.25-2.27):

$$HO + RH \rightarrow H_2O + R \tag{2.25}$$

$$R + Fe^{3+} \rightarrow R^{+} + Fe^{2+} \tag{2.26}$$

$$R^{+} + H_2O \rightarrow ROH + H^{+} \tag{2.27}$$

2.2.2.1 Oxidation Time

Sahunin *et al.* (2004) and Kang *et al.* (2000) break the photo-Fenton oxidation process into three stages of decolorization: (1) five minutes of fast color removal using hydrogen peroxide and ferrous iron, (2) 25 minutes of slow color removal using hydrogen peroxide and UV light, (3) color resurgence caused by the photo-reduction of ferric ions used. Once hydrogen peroxide is used, ferrous iron concentration increases to 90% of its theoretical amount causing the resurgence of color (Ruppert *et al.*, 1992). Due to these reactions and proven by experimental trials, it can be concluded that a higher initial concentration of ferrous iron increases COD removal, while a higher initial level of UV light increases color removal in the first five minutes and increases overall TOC

degradation rate (Ruppert *et al.*, 1992; Sahunin *et al.*, 2004). Ruppert *et al.* (1992) state further that TOC degradation occurs once the hydrogen peroxide is consumed, unless higher levels of oxygen are present thereby replenishing hydrogen peroxide and allowing TOC to degrade in its presence.

The visible spectrum peaks degrade faster. Lucas and Peres (2006) agree and see the chromophore of their studied azo dye degrade in the first 2-5 minutes followed by the slower decomposition of the remaining intermediates. They describe the first stage as involving a reaction between ferrous iron and hydrogen peroxide at $K=76\ M^{-1}s^{-1}$. Whereas the second stage targets the aromatic peaks at the lower wavelengths mentioned above, as ferric iron reacts with hydrogen peroxide. Lucas and Peres (2006), discuss that ferric iron production occurs much slower, takes 1-30 minutes, and degrades only about 44% of the aromatic peaks, 28% being degraded during the first minute. The aromatics left in solution and degraded during the second stage require UV spectra analysis compared with the visible spectra analysis required for the first stage. As expected, the visible peaks that represent the color and chromophores in the chemical composition of the Reactive Dyes tested here decrease considerably after partial and full treatment, most often to negligible levels revealing the agreement that the chromophore chemical bond is broken first leaving much more difficult to degrade organic amines in solution.

Bilgi and Demir (2005) also found that kinetically the rate of oxidation of azo dyes is four times faster than degradation of benzene and naphthalene rings with a possible chemical degradation pathway described in Figure 2.3.

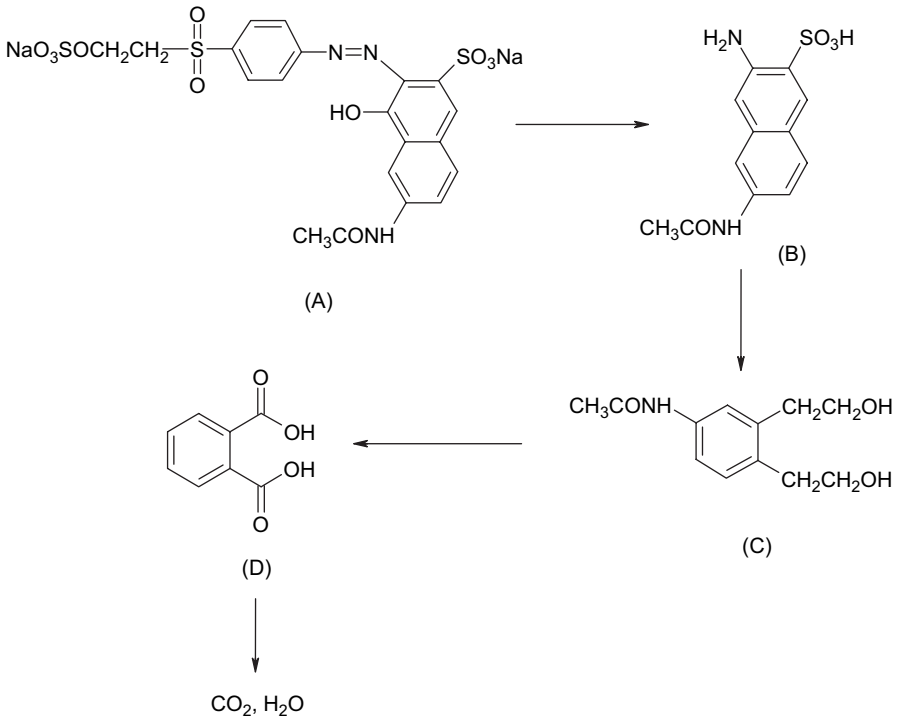

Figure 2.3: Possible degradation pathway for C.I. Reactive Organge 16 proposed by Bilgi and Demir (2005).

2.2.2.2 pH

The first step is to acidify the dye solution. Acidity controls the production of hydroxyl radicals—the reason the pH should be below 4 is that higher levels the hydrogen peroxide have a tendency to form ferric hydroxide with the ferrous catalyst available for photo-Fenton oxidation and this will decrease the free hydroxyl radicals available in solution for oxidation (Sun *et al.*, 2007; Papic *et al.*, 2009). This is why the pH of all of the previously described degradation work uses a pH between 2.5 to 3.0. Papic *et al.* (2009), add that using a pH above 9 produces ferric hydroxo complexes including $[Fe(OH)_4]^-$. Mineralization efficiency is greatest when the redox potential is highest; using a pH of 3 for the reaction is optimal because the stability of hydrogen peroxide and iron is greater

below a pH of 3.5 thus creating these optimal conditions for degradation of organic dye compounds (Papic *et al.*, 2009).

It was seen that the pH rises during the photo-Fenton oxidation reaction. Sun *et al.* (2007) explain that this is due to the formation of acids during the mineralization process, whereas the pH decrease during mineralization may occur because of the consumption of hydrogen ions by the hydrogen peroxide in solution. According to Sun *et al.* (2007), the reaction of hydrogen ion consumption looks like Reaction (2.28) where the kinetic rate constant of reaction time is $k_3=10^7\text{-}10^{10}\ M^{-1}s^{-1}$.

$$^{*}OH + RH \rightarrow H_2O + R^{*} \qquad (2.28)$$

Behnajady *et al.* (2007) constructed a kinetics model that describes real applications of decolorization reactions. They agree that 97.4% degradation of dye occurs at pH 3 whereas only 6.1% degradation occurs at pH 7. Their model uses Equation (2.1) where the slope, b, and the intercept, m, can be used to calculate the details of degradation.

$$\frac{C}{C_0} = 1 - \frac{t}{m + bt} \rightarrow \frac{t}{1 - \frac{C}{C_0}} = m + bt \qquad (2.1)$$

2.2.2.3 Hydrogen Peroxide

There are optimal pH levels (acid quantities), hydrogen peroxide quantities, and iron surface area for the photo-Fenton oxidation process to be efficient and successful in degrading chemical dyes from solution. Scavenging of the hydroxyl radicals by the overabundance of any of these chemicals can take the hydroxyl radicals out of solution

and cause them to react with elements other than the targeted dyes; this can be due to many chemical reactions during the photo-Fenton oxidation process and can be difficult to prevent. According to Lucas and Peres (2006), the optimal concentration of hydrogen peroxide is $7.3x10^{-4}$ M because above this scavenging of hydroxyl radicals takes place according to the Reaction (2.29).

$$HO_2^* + HO^* \rightarrow H_2O + O_2 \qquad (2.29)$$

Sun *et al*. (2009) concur that $1.0x10^{-2}$ M hydrogen peroxide creates 92.5% decolorization using $3.5x10^{-5}$ M ferrous iron. Considering that the over-addition of hydrogen peroxide creates water and oxygen rather than degrading organics in solution, and hydrogen peroxide is one of the chemicals that adds to the cost of the treatment of dye wastewater, its quantity should be minimized. In this study hydrogen peroxide volume varied with color and type of dye, however using 6% hydrogen peroxide ranged from 100 mL to 500 mL per 1-liter of laboratory-scale dye solution. When using 50% hydrogen peroxide for the demonstration scaled project described in Chapter 7, 1.2 liters were used for 50 liters of dye solution.

One of the benefits of using hydrogen peroxide is that its chemical composition allows it to be naturally soluble in water. Therefore, hydrogen peroxide requires no chemical separation once the oxidation treatment is complete (Bauer and Fallmann, 1997). Despite the fact that Fenton alone can catalyze the hydrogen peroxide oxidation at a wider pH range of 4-8, Fenton alone cannot mineralize more than 50% of organic pollutants into carbon dioxide due to the inherent properties of organic carbon (Hai *et al.*, 2007; Chacon

et al., 2006). Kang *et al.* (2000) add that the Fenton process or the hydrogen peroxide/UV process separately have proven successful in color removal from dye industry wastewater. Al-Kdasi *et al.* (2004) add that the hydrogen peroxide/UV process is not successful at higher pH levels due to the tendency of hydrogen peroxide to decompose into dioxygen and water. Chacon *et al.* (2006) add that one of the largest disadvantages of using the Fenton process without hydrogen peroxide or UV is the slower degradation rate and the high production of iron sludge. In fact, Alaton and Teksoy (2005) add that it is best to use the optimal molar ratio between iron or hydrogen peroxide for the pollutants in question. This is to ensure that the hydroxyl radicals stay available to attack the dye instead of scavenging other things in solution. The molar ratios and chemical reactions according to Alaton and Teksoy (2005) are displayed in Reactions (2.30) and (2.31).

$$Fe^{2+} + {}^{*}OH \rightarrow Fe^{3+} + OH^{-} \quad (k_{20°C}=3.0x10^{8}\ M^{-1}\ x^{-1}) \qquad (2.30)$$

$$H_2O_2 + {}^{*}OH \rightarrow H_2O + HO_2^{*} \quad (k_{20°C}=2.7x10^{7}\ M^{-1}\ x^{-1}) \qquad (2.31)$$

2.2.2.4 Iron

Iron concentration in solution is another interference that can and will scavenge hydroxyl radicals away from degrading their targeted dye molecules. Sun *et al.* (2007) found that high concentration of iron decreased degradation rates because of Reaction (2.32) with a kinetic rate constant reaction time of $k_{10}=4.3x10^{8}\ M^{-1}s^{-1}$.

$$^{*}OH + Fe^{2+} \rightarrow Fe^{3+} + OH^{-} \qquad (2.32)$$

Lucas and Peres (2006) agree that iron causes scavenging of hydroxyl radicals away from the targeted dye in solution and optimize iron centration as $1.5x10^{-4}$ M. Here the iron was calculated according to surface area rather than molarity in order to make the treatment process applicable the cottage-scale dye industries throughout the world. In the case of the demonstration project described in Chapter 7, the actual reactor was built of rusty metal to optimize cost over available iron for the sustainable photo-Fenton oxidation process, knowing that this may offer far too many iron ions to the reaction and therefore also create unruly scavenging of the hydroxyl radicals.

Another version of the photo-Fenton oxidation process involves the use of ferrioxalate as the source for the iron catalyst as described by Zheng *et al.* (2007). Because of hydrogen peroxide's low molar extinction coefficient, it is only able to absorb UV light radiation up to a wavelength of 400 nm thus limiting the reaction efficiency of the photo-Fenton oxidation process (Zheng *et al.*, 2007). The addition of ferrioxalate to the solution helped in expanding the absorption spectrum thus increasing the oxidation efficiency by three times, but also adding to the load of the system and thus is not always considered appropriate for use. Zheng *et al.* (2007) expand that with complete mineralization of pollutants the carbon may combine with oxygen increasing the carbon dioxide output having less impact on the danger of a high carbon load.

2.2.2.5 Dye Concentration

Lucas and Peres (2006) also mention that lower dye concentrations take shorter time to react. Sun *et al.* (2007), use 10-100 mg/L to keep their reaction period short. Fu *et al.*

(2010) describe the competition between hydrogen peroxide and dye for hydroxyl radicals in solution. They describe that the lower dye concentration allows for the hydroxyl radicals in solution to give attention to both the hydrogen peroxide and dye thus creating a higher degradation rate constant and the higher color removal efficiency using 100 mg/L dye in comparison to 300 mg/L. Considering that this study was created with the intention of studying a possible future dye industry wastewater treatment option, the dye concentration used is equivalent to that which is used by the cottage industries for which it is intended to help. This high dye concentration prevents UV light from penetrating the colored solution and slows the photo-Fenton oxidation process.

2.2.2.6 Temperature

Temperature is also mentioned as a possible limiting factor for degradation of dye industry effluent. Sun *et al.* (2007) found the optimal temperature range between 15 ˚C and 45 ˚C with an increase in temperature leading to an increase in reaction rate between hydrogen peroxide and iron. Fu *et al.* (2010) mention the Arrhenius equation as an explanation as to the importance of temperature for the photo-Fenton oxidation process efficiency to increase as can be seen in Equation (2.2).

$$\ln k = -\frac{Ea}{RT} + \ln A_0 \qquad (2.2)$$

In this work, temperature was not a controlled variable, but was recorded in order to provide additional information for interpreting results. It was not chosen as a controlled variable because it is impractical for cottage-scale industries to perform such controls when using the process outdoors.

2.2.2.7 UV Light

Chacon *et al.* (2006) explain that once the optimum UV power is used, solar energy generates hydroxyl radicals. According to Bauer and Fallmann (1997), hydrogen peroxide alone does not absorb light of a wavelength greater than 300 nm, and UV inefficiently produces hydroxyl radicals with a low wavelength (250 nm). Studies that use UV/visible lamps overwhelmingly use 253 to 650 nm wavelength to agree with the aforementioned theory (Georgiou *et al*., 2004; Muruganandham and Swaminathan, 2006; Arslan and Balcioglu, 2001; Chacon *et al.*, 2006). To refine the parameters needed for successful operation, solar irradiance must be measured; however, natural sunlight has been shown to be effective at times (Hai *et al.*, 2007; Chacon *et al.*, 2006; Bauer and Fallmann, 1997).

2.2.2.8 Hydroxyl Radicals

García-Montaño *et al.* (2008) along with many other authors describe hydroxyl radicals as the main oxidizing species who complete the photo-Fenton oxidation process. They add that since hydroxyl radicals are strong electrophilic oxidants, they always attack on an electron-rich site which is located near the nitrogen atom or near the amino groups. As described in a previous section, all azo dyes contain a minimum of two atoms of nitrogen that are double bonded together; this is a perfect site for the hydroxyl radical to attack since it is an electron-rich site. As is also described, the photo-Fenton oxidation process happens in stages, the first of which is fast decolorization. This fast decolorization suggests that the primary attack by the hydroxyl radical is on the

chromophores at the center of the dye molecule (García-Montaño *et al.*, 2008). This attack cleaves the molecule into 3 parts—2 naphthalene rings and a central body.

García-Montaño *et al.* (2008) believe there can be places the hydroxyl radical may attack. The first is the carbon-nitrogen bond between the azo group and the naphthalene ring. The reactions for creating nitrogen gas are shown in Reactions (2.33) and (2.34).

$$R_1 - N = N - HO^* \rightarrow R_1 - N = N - N^\bullet + R_2 - OH \qquad (2.33)$$

$$R_1 - N = N^* \rightarrow R_1^* + N\Xi N \qquad (2.34)$$

The second option proposed by García-Montaño *et al.* (2008) is that the primary attack is made to the chromophores double bond thus forming aromatic amines. The hydroxyl radicals continue to attack thus forming amino groups and finally ammonium ions. The secondary hydroxyl radical attack is on the amino group between the naphthalene or benzene rings—this forms the primary amine that is linked to the triazine ring. The first showing of the presence of carboxylic acids is in Reaction (2.35).

$$\left[Fe(III)LCOO\right]^{2+} \xrightarrow{h\nu} Fe(II) + CO_2 + L^\bullet \qquad (2.35)$$

With stoichiometric oxidation, inorganic ions are shown to appear in Reactions (2.36) and (2.37) during the oxidation of Procion Red HH-E7B and Cibacron Red FN-R, respectively (García-Montaño *et al.*, 2008).

$$C_{52}H_{34}O_{26}S_8Cl_2N_{14} + 76.5O_2 \rightarrow 52CO_2 + 14NO_3^- + 8SO_4^{2-} + 2Cl^- + 32H^+ + H_2O \qquad (2.36)$$

$$C_{29}H_{19}O_{13}S_4ClFN_7 + 41.5O_2 \rightarrow 29CO_2 + 7NO_3^- + 4SO_4^{2-} + Cl^- + F^- + 17H^+ + H_2O \qquad (2.37)$$

García-Montaño *et al.* (2008) also describe that hydroxylation of these naphthalene and benzene rings form short chain carboxylic acids (formic, acetic, oxalic, maleic) as can be seen in some of the GC/MS results in this study. These short chain carboxylic acids are easily biodegraded, although triazine is very difficult to mineralize by AOPs (García-Montaño *et al.*, 2008) and it is a slow process to transform and oxidize ammonium.

Jozwiak *et al*. (2007) agree that the degradation process occurs in steps. The first step is to rupture the azo double nitrogen bond and the metal oxygen bond. These bond breakages form various amines and nitro aromatic compounds depending on the dye in question. Through continued oxidation, linear acids and aldehydes are formed from the aromatic ring opening from the attack of the hydroxyl radical. Gutowska *et al.* (2007) almost completely agree with Jozwiak *et al*. (2007) in that the first step is the degradation of the double nitrogen bond followed by splitting of the nitrogen bond which forms a mono or multi substituted benzene and naphthalene compound ending with opening the aromatic rings to form alcohols, aldehydes, carboxylic acids, and finally carbon dioxide and water as can be seen in all of the GC/MS results of this study.

Amines have been shown as poisonous towards the natural environment and systems; Pinheiro *et al.* (2004) also discuss the threat they pose with bioaccumulation in the natural environment and eco-systems. They discuss the severity that chemicals, such as dyes, containing azo double nitrogen bonds have on the environment and their strength of resisting certain treatment and decolorization methods such as biodegradation.

Pielesz *et al.* (2002) detail the biochemistry of the cleavage of azo bonds analyzing what eases their degradation. They describe the energy around the double nitrogen bond as a protective coating surrounding the azo group preventing its cleavage. An example of the molecules breaking this azo bond and reducing the molecule is when NH_2 and OH bond to the azo group allowing the bonds to break, releasing aromatic amines into solution (Pielesz *et al.,* 2002). Pielesz *et al.* (2002) also mention that the addition of hydrogen bonds to the two nitrogen atoms in the azo bond allows degradation and is created by electron donations in the ortho-position of the azo bond. They add that for Disperse Yellow 7 dye, making the dye less alkali-resistant by bonding an OH group in the para-position to the azo bond allows for easier degradation. This may be a similar explanation as to how the azo group on the dyes studied here was chemically enhanced to allow for degradation of those double bonded nitrogen azo bonds.

2.2.2.9 Photo-Fenton Oxidation Summary

The photo-Fenton oxidation process is a very simple and inexpensive AOP that uses hydrogen peroxide, ferrous iron, and UV to create hydroxyl radicals (Bauer and Fallmann, 1997). Research has found that adding UV power to the Fenton reaction can expedite the degradation of many organic pollutants. The Fenton process that is completed in the dark can produce one single hydroxyl radical, whereas the photo-Fenton oxidation process under UV light can produce countless hydroxyl radicals (Ruppert *et al.*, 1992). Chacon *et al.* (2006) and Hai *et al.* (2007) state that the photo-Fenton oxidation process using solar power could solve many problems with sludge disposal, claiming that the process creates no sludge, and that the process helps overcome economic barriers due

to the decrease in electricity costs; photo-Fenton oxidation is very efficient and cost effective due to the homolysis of hydrogen peroxide with UV yielding hydroxyl radicals as seen in Reaction (2.38) (Bauer and Fallmann, 1997).

$$H_2O_2 + uv \rightarrow 2OH^* \qquad (2.38)$$

Due to cost constraints of small-scale dyeing units, the research focus here will be to minimize hydrogen peroxide, iron chemical use, and UV lamps, all of which will be replaced with sustainable materials when possible. Specifically 6% hydrogen peroxide is typically available at global pharmacies, rusty steel scrap provides an accessible source of iron, and natural solar power contains the UV light that will be utilized to degrade the Reactive Dye bath. The system under development is the first to utilize readily available chemicals, sunlight, and a recycled container.

2.2.3 Photo-Fenton Oxidation Coupled with Biodegradation

AOPs are reported to degrade color well but are often found to create toxic aromatic amines in the process. To combat this reality biodegradation can be used after partial oxidation has occurred from the photo-Fenton oxidation process. According to Tantak and Chaundhari (2006), allowing the Fenton oxidation process to completely decolorize a dye sample also allows aromatic amines to be partially cleaved thus preparing them for complete degradation using bacterial sludge. Liu *et al.* (2012) agree that the photo-Fenton oxidation process can be used as a primary treatment to partially degrade aromatic compounds after which biodegradation can be used to complete the treatment before discharging to the environment since bacteria can easily consume the partially

oxidized organics. In Tantak and Chaundhari's study (2006) the Fenton oxidation is used on a dye solution of 50 mg/L concentration using ferrous sulphate $FeSO_4 \cdot 7H_2O$, 50% w/w hydrogen peroxide at pH 3. After the oxidation is complete, the pH is raised to 7 and the colorless supernatant is fed into the bioreactor. The bioreactor is prepared using seed material from cow dung with dextrose as a carbon source. Each reactor was created in a 1-liter beaker with initial Mixed Liquor Suspended Solids (MLSS) 1% slurry. The reactor is acclimated with tap water and 0.4 g dextrose for 74 days adding half of the reactor's volume in seed material every other day. After acclimation, half of the volume is replaced with AOP effluent and left for treatment for 96 hours. Lodha and Chaudhari (2007) ran a very similar experiment keeping MLSS in the reactors at approximately 3000 mg/l.

Lodha and Chaudhari (2007) explain that they optimized the hydrogen peroxide dose according to a dye concentration 50 mg/L, pH 3, and the iron dose of 20 mg/L and found that optimal hydrogen peroxide concentration varies from 25-150 mg/L but that 50 mg/L was enough for all dyes tested to decolorize. Overall, the higher concentration of hydrogen peroxide the more decolorization until the 50 mg/L believed to be the threshold after which hydroxyl radicals did not cleave any more than already accomplished by the 50 mg/L including partial breaking of aromatic amine rings (Lodha and Chaudhari, 2007).

Lodha and Chaudhari (2007) tested optimal ferrous iron dose for decolorization varying the iron standards from 5 to 50 mg/L. Just as with the hydrogen peroxide dosing,

decolorization increased as the concentration of iron increased, but rate of decolorization leveled off at 15 mg/L, although 35 mg/L is the maximum ferrous iron concentration until the plateau effect took place (Lodha and Chaudhari, 2007). The reason to optimize at a lower concentration of 15 mg/L is to minimize sludge production since there is a direct relationship between sludge production and iron present; also iron left in solution acts as a mild oxidant and can inhibit biological growth during biodegradation processes (Lodha and Chaudhari, 2007).

2.3 Sustainable Containers and Materials for Oxidation

2.3.1 Container

An integral part of this work is to create a container that is sustainable by being made of components readily accessible to the end-users. Before creating such a container, it is important to note previous efforts to create containers in which the sustainable photo-Fenton oxidation process will work. In addition, it is important to find the materials that will be used in the process, so that the materials can be readily acquired in developing countries. Therefore, the previous efforts involving types of iron and hydrogen peroxide concentrations are reviewed below and results are summarized in Table 2.1.

Bauer and Fallmann (1997) built a reactor of Duran glass instead of quartz glass to ease the UV penetration. This was mostly done to save money when buying the UV lamps. The reactor was made of two cylinders inside of each other, 0.4 m tall, 0.009 m thick with inner diameters of 0.2 m and 0.25 m. The wastewater to be treated was pumped into the space between the two cylinders. UV lamps were placed inside the inner cylinder and

outside of the outer one. Bauer and Fallmann (1997) also built a reactor basin of window glass with volume 0.6 m x 0.7 m x 0.6 m using 0.006 m thick glass to use solar UV light for treatment. The solar energy was measured to be 50-200 W/m^2 when the container was in shadow, and 650-850 W/m^2 in direct sun. The methods for treatment were as follows: wastewater was acidified to pH 2.8-3.0 with sulfuric acid, stirred with magnetic stirrers with initial concentrations of TOC of 72 ppm, iron of $2.5x10^{-4}$ M, and hydrogen peroxide of $1x10^{-2}$ M. Bauer and Fallmann (1997) increased initial concentrations of iron and hydrogen peroxide with higher initial concentrations of TOC. Some things that Bauer and Fallmann (1997) noticed regarding their experimental efficiency is that once the hydrogen peroxide was consumed, hydroxyl radicals were no longer being produced and the oxidation reaction stopped. In fact, Bauer and Fallmann (1997) specifically ran one of their experiments using wastewater from a dyehouse, and found it to be the slowest set of oxidation experiments due to the dark color of the wastewater absorbing the majority of the UV rays which prevented it from reacting with the iron, hydrogen peroxide, and the organic pollutants. Bauer and Fallmann (1997) allowed the UV lamp experiments to run for five hours and documented their results including a note at 30 minutes when TOC degradation ended, while color continued to bleach, 60% mineralization at 2.5 hours, and at 3 hours 100% color was removed, after which TOC re-commenced to degrade until the hydrogen peroxide was gone. TOC was 60% degraded after 4 hours, after which time 1/3 the original amount of hydrogen peroxide was added to the solution and 83% degraded after 5 hours. Their solar radiation undocumented experiment results and the results of the experiments using UV lamps agreed well, but the reduced light completes the reaction, but at a slower pace. Similar TOC reduction

tendencies occurred with solar radiation displaying quicker degradation in the beginning. It may be worth noting that the photo-Fenton method of TOC degradation is considered to follow first-order kinetics.

A very positive aspect of the photo-Fenton oxidation process is that the energy costs may be negated due to solar energy and manual power used instead of pumps or process controls. It can also be hypothesized that enlarging the system to fit an industrial-sized plant will be more cost effective than a process including ozone or titanium dioxide because of its faster reaction time requiring a smaller reactor (Bauer and Fallmann, 1997). Bauer and Fallmann (1997) claim the cost of chemicals in 1997 to be as follows: \$1.16/kg for 35% hydrogen peroxide, \$0.655/kg for 95% sulfuric acid, \$0.45/kg for $FeSO_4 \cdot 7H_2O$. It is obvious that hydrogen peroxide is the most expensive material in the photo-Fenton oxidation process and should be minimized as best as possible. Bauer and Fallmann (1997) also mention that cost reduction can be expected by a factor of 100 due to price breaks for larger scale buying.

Sahunin *et al.* (2004) used a batch reactor to run the photo-Fenton oxidation reaction. They ran their experiments at room temperature (30 °C) and changed the pH level, UV power, ferrous iron dosage, and hydrogen peroxide dosage to see what effects the changes had on COD and color removal. Their batch reactor was made of a large glass jar that held 1-liter of wastewater. The jar was placed in a box 0.68 m x 0.68 m x 0.78 m and was surrounded by eight 15-W UV lamps of a wavelength of 365 nm. Initial concentration of hydrogen peroxide was 100 mg/L and of ferrous iron was 20 mg/L. The

solution was stirred to ensure homogeneity and allowed to react for 60 minutes under UV lamps using 60 W of power. Once the hour was complete, 12M sodium hydroxide was added to the solution to terminate the reaction by raising the pH to 11 and then readjusted to 4. The results were documented with the idea that degradation was broken into three stages. With initial pH of 1-3, 20-38% of COD was removed in the first 5-10 minutes, and with initial pH of 3-5, 78-83% of color was removed in the first 5 minutes. Experiments were also completed using initial pH of 7; however, the higher pH decomposed hydrogen peroxide to water and oxygen gas more readily and therefore generated hydroxyl radicals at a much slower rate and degraded the organic pollutants at a less than optimal rate (Sahunin *et al.*, 2004). Results presented by Sahunin *et al.* (2004) conclude that 3 is the optimal pH for simultaneous COD and color removal.

Sahunin *et al.* (2004) also studied the impact of different initial concentrations of ferrous iron using constant hydrogen peroxide concentrations (100 mg/l), UV power (60 W), and pH of 3. They have concluded that ferrous iron concentrations have very little to do with color removal, but greatly impact COD removal due to ferrous iron's vital role in the chemical reaction to create hydroxyl radicals in the Fenton reaction (Sahunin *et al.*, 2004). The optimum ferrous iron dosage to ensure simultaneous degradation of color up to 87% and COD up to 41% was found to be 80 mg/L (Sahunin *et al.*, 2004). They also tested the effect of UV light keeping ferrous iron concentration constant at 80 mg/L and hydrogen peroxide concentration constant at 100 mg/L with a constant pH of 3 and found that there was a slight increase in color removal with an increase in UV power, but no change in COD removal. An optimal power of 60 W was found to best balance removal

efficiency and power usage, removing 41% COD and 87% color (Sahunin *et al.*, 2004). Due to the higher cost of hydrogen peroxide compared with all other chemicals used in the photo-Fenton oxidation process, Sahunin *et al.* (2004) also used hydrogen peroxide as the variable to test the critical amount needed to obtain optimal results. From a range of 100-300 mg/L, 200 mg/L hydrogen peroxide degraded 52% of COD, and 87-91% color. Overall, Sahunin *et al.* (2004) concluded that the optimum conditions to obtain the highest COD (52%) and color removal (90%) were 80 mg/L ferrous iron, 200 mg/L hydrogen peroxide, 60 W UV power, pH of 3, and 5-10 minutes of operating time.

Chacon *et al.* (2006) built a reactor using eight Pyrex glass tubes one meter long with internal diameter of 0.025 m placed in a short box with a surface area of 0.8 m^2. The collection surface was tilted towards the sun at the appropriate local latitude of 19°. The pH was kept at a constant 5, while the ferrous iron concentration was studied at $7.16x10^{-5}$ M, $1.07x10^{-4}$ M, and $1.43x10^{-4}$ M, and hydrogen peroxide concentration was either $5.2x10^{-3}$ M or $7.8x10^{-3}$ M. The ferrous iron was added to the covered 200mg/L synthetic sample and mixed for 10 minutes. The hydrogen peroxide was then added and the reactor was uncovered. After 30 minutes of reaction, more hydrogen peroxide was added. Depending on the solar intensity, the wavelength reaching the reaction ranged from 280-2800 nm (tested with a Li-Cor pyranometer), while the photo-Fenton oxidation process only used wavelengths between 300-650 nm. Chacon *et al.* (2006) concluded that larger concentrations of ferrous iron expedited the color removal reactions. In fact, using $7.16x10^{-5}$ M ferrous iron and $5.2x10^{-3}$ M hydrogen peroxide, they found 75% color reduction in 100 kJ/L and 85% color reduction using 150 kJ/L. That increased to 90%

color removal using only 83 kJ/L when ferrous iron increased to $1.07x10^{-4}$ M and hydrogen peroxide stayed constant. Increasing hydrogen peroxide was also found to increase reaction rates in a similar way. 85% color removal was observed using only 80 kJ/L with $7.16x10^{-5}$ M ferrous iron and $7.8x10^{-3}$ M hydrogen peroxide. When seeking to use the least kJ/L possible, 70% color removal was observed using only 25 kJ/L with $1.43x10^{-4}$ M ferrous iron and $5.2x10^{-3}$ M hydrogen peroxide. It should be noted that ferrous iron levels are linked to waste sludge production and hydrogen peroxide is expensive.

Kang *et al.* (2000) mention that past results of dye industry wastewater decolorization and COD removal has proven the photo-Fenton oxidation process's ability to treat high dye concentrations in manufacturing wastewater. They specifically test hydrogen peroxide concentration, ferrous iron concentration, irradiation time, UV intensity, pH, and COD initial concentrations. Kang *et al.* (2000) add polyvinyl alcohol to their synthetic sample of Reactive Dye to create desirable COD and color concentrations. They create a sample that is approximately 60% COD and 40% color and also add salts to create an accurate sample. Kang *et al.* (2000) use a batch photo-reactor made of annular quartz with a 0.095 m inside diameter, and 0.35 m tall with a volume capacity of 2.2 liters. Sixteen UV low-pressure mercury lamps (8 W each) surround the annular quartz reactor and emit 254 nm of wavelength. The hydrogen peroxide and ferrous sulfate was added to the reactor and stirred until homogeneity was reached, after which sodium hydroxide, sulfuric acid was added to adjust the pH to 4. Upon completion of the experiment, the pH was raised to 11 in order to terminate the experiment and then

lowered to 4. Kang *et al.* (2000) concluded that COD and color are both attacked by hydroxyl radicals in the beginning of the oxidation process but that over the entire duration of the process, COD removal has very little to do with the presence of hydroxyl radicals, whereas color removal is completely dependent on hydroxyl radical formation and its rate of formation. They have concluded from these findings that despite the presence of high COD, color removal is possible as long as hydroxyl radicals are being produced. Due to the link between hydroxyl radical production and acidic conditions, Kang *et al.* (2000) reiterate that the photo-Fenton oxidation process described above has shown to degrade color in dye manufacturing wastewater when the pH is 3.5.

Kang *et al.* (2000) also focused a portion of their research on color resurgence and found that it related to the presence of ferrous iron. In preliminary studies, it was found that during the first five minutes of reaction, COD reduced 21%, and color 70%; after 30 minutes, COD reduced 36%, and color 93%; and after 60 minutes, COD was still down 36%, while color had increased again but was overall down 85%. Testing the impact of pH on this, Kang *et al.* (2000) shows that lower pH removes color at a faster rate than neutral pH, but given 60 minutes, the color of a lower pH solution has resurged to the same level as that in a neutral pH solution that has no resurgence. Due to the goal of creating a fast process with little color resurgence, the optimal pH is considered between 3-5 where the hydroxyl radical formation is basically the same. Color resurgence was found to be completely related to the presence of ferrous iron (Kang *et al.*, 2000). In fact, the photo-production of ferric iron to ferrous iron is logically responsible for the color resurgence (Kang *et al.*, 2000).

Kang *et al.* (2000) using 20 mg/L ferrous iron with 150 mg/L hydrogen peroxide found 61% color removal after five minutes and 94% removal after 30 minutes. They then kept hydrogen peroxide concentration constant at 100 mg/L and varied ferrous iron concentration from 0 to 40 mg/L increasing by a factor of 10 and resulting in 27, 56, 70, 72, and 83% respectively after five minutes rationalizing that the increase in ferrous iron ions allows more hydroxyl radicals to get produced. The color reduction caused by the ferrous iron concentration increase was described by Kang *et al.* (2000) as a pseudo-first order reaction with an increase in significance from 0.081 to 0.187 per minute respectively. As previously described, the majority of hydrogen peroxide is consumed during the first stage of the oxidation process (the first five minutes) and is later decomposed through the UV photolysis process. The hydrogen peroxide concentration has shown to impact overall color removal, whereas ferrous iron concentration is responsible for the speed of the reaction (Kang *et al.*, 2000). UV power was also studied to measure its impact on color removal. It was shown that higher UV power speeds the rate of color removal; however, increased time can make up the difference (Kang *et al.*, 2000). Overall, the most efficient concentrations were: 100 mg/L hydrogen peroxide, 20 mg/L ferrous iron, pH of 4, and UV power 64 W but should take into account iron sludge disposal (which should not occur when solar UV used) and costs of acidifying the solution (Kang *et al.*, 2000).

Arslan and Balcioglu (2001) claim that the photo-Fenton oxidation process is economically infeasible because dye-manufacturing waste contains such high pollution levels requiring high oxidant and UV doses as well as reaction times. Arslan and

Balcioglu (2001) use a UV-C reactor with a 2.5 liter capacity which is a type of annular photo batch reactor surrounded by 25-W low pressure mercury lamps 0.45 m long and 0.025 m diameter giving off 254 nm in wavelength (I_0 of $2.02x10^{-5}$ dm^3/s) with a quartz sleeve of 0.45 m. Tests were carried out for an hour with a mixing rate of 250 cm^3 per minute using raw wastewater with pH of 11. Considering that the optical density of raw wastewater is very high, one of the major limitations of this particular experiment was the poor UV penetration creating competition of hydrogen peroxide and UV light (Arslan and Balcioglu, 2001). Because of this, high concentrations of hydrogen peroxide were used, specifically 1700 mg/L or 50 mM. Decolorization was 4-23 times faster than COD or TOC removal (Arslan and Balcioglu, 2001). After 1 hour, COD removal was 27% and TOC removal 50%. The sample was not sensitive to direct UV-C photolysis because only a mild discoloration of the sample could be noticed. In fact, pre-ozonation was required for any major change (Arslan and Balcioglu, 2001). It was concluded that this type of oxidation should be done as the last stage on an industrial plant if it's to be done at all (Arslan and Balcioglu, 2001).

He and Lei (2004) focus more of their research on the intermediates formed during the degradation processes and the role they play with the kinetics of the overall oxidation. They used an annular photo batch reactor with a volume of one liter, filling it to only 0.3 liter with wastewater and surrounded by mercury medium pressure lamps using a quartz filter. The wastewater solution is re-circulated by a pump. The pH was adjusted with sulfuric acid. Minimal results are available but they conclude that the combination of

high initial iron and hydrogen peroxide concentrations with a low pH is more likely to create a complex oxidation process.

Experiments by Al-Kdasi *et al.* (2004) determined that high amounts of light was wasted due to absorption by organic molecules and scattered by suspended solids present in the wastewater. The higher concentration of dye in the wastewater may interfere when light is needed for the AOP. Al-Kdasi *et al.* (2004) found an inverse relationship between UV/hydrogen peroxide degradation efficiency and wastewater dye concentration. Overall, their test results proved that increasing the UV light intensity will increase the rate of dye degradation with more than 90% gone using 82 W/m^2, as well as 82% of TOC removal in two hours, with no dependency on temperature as a factor in the degradation of color of synthetic textile wastewater (Al-Kdasi *et al.*, 2004).

Ruppert *et al.* (1992) use a three-necked flask to run their photochemical wastewater treatment process. They have a gas inlet and a thermostat to measure the temperature. The flask contains a Duran window that allows 3300 mm^2 of light through. Dark Fenton experiments were found to degrade no TOC although all ferrous iron was completely oxidized to ferric iron, whereas UV light continued to degrade even after hydrogen peroxide was gone, described completely by Equation (2.21) (Ruppert *et al.*, 1992).

The fluidized bed reactor described by the U.S. Patent number 6,143,182 does not use UV power to degrade wastewater but utilizes the crystallization of ferric iron on the particulate bed matter to reduce sludge production (Huang *et al.*, 2000). There are

benefits to this type of reactor including its ability to remove heavy metals simply by changing the bed matter to a carbonate or bicarbonate and running the solution at a high pH (Huang *et al.*, 2000). The fluidized bed also allows for heavy contained mixing thereby removing higher COD as compared to other systems (Huang *et al.*, 2000). Hai *et al.* (2007) agree that fluidized bed reactors have proven to efficiently utilize and manage resources like light, temperature, and chemical-compound interaction.

Hsueh *et al.* (2004) used a 3000 mL reactor at room temperature with a pH ranging from 1.5 to 6.5 focusing on low iron concentrations degrading azo dyes. Hsueh *et al.* (2004) agree that the optimum pH is 3.0 and add that either ferrous iron or ferric iron are sufficient to degrade the dye.

Aplin and Waite (2000) used a water-jacketed reactor with a quartz window for UV light penetration. They used 1.0 g/L dye and 0.1 mM Fe, 1.0 mM hydrogen peroxide, and 200 W lamp at room temperature. Their results agree with others and found that the reaction rate was extremely slow at a high pH of 8, and most efficiently with pH of 3. Also noted is that using an initial pH of 4-6 the solution naturally dropped pH to 2-4. This natural drop occurred during the first five minutes and corresponded with very rapid degradation as mentioned by Sahunin *et al.* (2004) and Kang *et al.* (2000). Aplin and Waite (2000) did note a high inhibition of degradation, 10% and 45%, due to the presence of sodium chloride, 1 g/L and 3 g/L respectively, not mentioned by other authors. They described the cause to be due to the chemical reactions forming $FeCl^{2+}$ and $FeCl_2^{+}$ and the inability of the other chemical reactions to reduce these chemicals to ferrous iron.

Table 2.1: Container and Material Results Overview

Author	UV Source	Container Material	Container Size	Iron Conc.	H2O2 Conc.	Time	Color Removal	Other
Bauer and Fallmann (1997)	UV lamps	Duran Glass	0.4m tall, 0.009m thick	2.5x10-4 M	1x10-2 M	3 hours	100%	60% TOC
Sahunin *et al.* (2004)	8 15-W UV lamps	Batch reactor, glass jar	1 L	20 mg/L	100 mg/L	1 hour	87%	41% COD
Chacon *et al.* (2006)	Sun	8 Pyrex glass tubes	1 m long	1.07x10-4 M	5.2x10-3 M	NA	90%	NA
Kang *et al.* (1999)	64-W UV lamps	Batch reactor, annular quartz	2.2 L	20 mg/L	100 mg/L	30 min	94%	NA
Arslan and Balcioglu (2001)	25-W UV lamps	Batch reactor, quartz	2.5 L	NA	1700 mg/L	1 hour	4-23X faster than COD or TOC removal	27% COD, 50% TOC

2.3.2 Iron Scrap as Iron Source

Another modification to the typical photo-Fenton oxidation process is using iron scrap to replace iron salt, which reduces the process costs and can help expand the impact of this work reaching cottage-scale dyers as a low-cost, more sustainable dye treatment option. Modirshahla *et al.,* (2007) agree that the abundance and nontoxicity of iron makes Fenton oxidation processes very accessible for all.

Zhang *et al.* (2009) used a stock solution of Acid Orange 7 at 200 mg/L with iron metal powder (analytical grade, 200 mesh) rather than iron salts. Iron powder addition was 0.5 g/L and the pH was 3. The idea behind this chemical replacement was to avoid the addition of counter ions into the solution that theoretically would disturb the aquatic system since iron powder is zero-valent. Using the iron powder helped degrade 4-chlorophenol in solution, which is a typically difficult dye intermediate to degrade.

Two other publications were found that use alternatives to iron salt. For these steel scrap was the option as the catalyst for the photo-Fenton oxidation process used in this study, however, differences in methodology occur. The steel scrap was collected from saw scrap, washed and dried. This means that surface area of the scrap is not easily measured topically because of its three-dimensional quality. Ganesan *et al.* (2014) use the Brunauer-Emmett-Teller (BET) theory as a method to characterize their steel scrap and found the BET surface area 0.5192 m^2/g of iron with an iron content of 45.91% by weight and carbon 41.39% by weight. Ganesan and Thanasekaran (2011) varied their iron content from 0.5 to 2.0 g/L BET surface area of steel scrap with the same SEM findings of iron and carbon percent by weight and find the larger iron BET quantity decreases the photo-Fenton oxidation efficiency, most likely due to hydroxyl radical scavenging of the ferric to ferrous ions. Both of these studies also use a pH of 3 similar to Zhang *et al.* (2009). Steel scrap shavings create a plethora of iron sludge that is very difficult to manage. Specifically, cleaning the iron after each photo-Fenton oxidation reaction in the field is difficult and time-consuming.

Lin *et al.* (2008) used cast iron alloy, where the main composition elements are iron and carbon, to create a battery within the solution. This form of degradation using cast iron rather than iron salt degraded Acid Red 14 at 50 mg/L using Chinese cast iron by a first-order rate constant of 7.50×10^{-2} min^{-1} while using cast iron available in the USA 2.58×10^{-1} min^{-1}. In this example iron acts as the anode and carbon as the cathode. Just is seen in the current study under discussion, Lin *et al.* (2008) found iron oxides/hydroxides as well as dye degradation products covering the cast iron during the photo-Fenton

oxidation process. Lin *et al.* (2008), however, assume that this inhibits the oxidation and degradation process, however, it was seen by the current study that photo-Fenton oxidation continues despite this sludge formation.

2.4 Pilot Projects

There have been a handful of descriptions of pilot-scale photo-Fenton oxidation treatment plants published in the last seven years. The Oller *et al.* (2007) demonstration plant for the solar photo-Fenton/biological treatment of saline non-biodegradable industry wastewater includes two parts: the solar photo-Fenton reactor and the aerobic biological system. The solar reactor consists of a 3000-liter buffer tank, a centrifugal pump and a 10 m^2 solar collector field. The collector field is made up of 3 rows with 15 modules per row. These modules are glass absorber tubes set on an aluminum frame which is tilted to account for the sun's changing position. The aerobic biological system consists of a 5000-liter neutralization tank, a 2000-liter conditioner tank and a 1000-liter immobilized biomass reactor (IBR). During the photo-Fenton experiments, the wastewater pH was adjusted to 2.3-2.5 and a non-biodegradable compound, iron salt and hydrogen peroxide were added. The mixture was homogenized between each addition and the Fenton reaction was occurring during the whole process. The partially oxidized wastewater was then introduced to the biological system. It was first neutralized with sodium hydroxide in the neutralization tank and with further pH changes to pH 6.8-7.5 in the conditioner tank so the iron would settle and be removed. Lastly the sample would enter the IBR where it would be discharged if the sample had reached a stationary state after conditioning.

The Conte *et al.* (2012) 35-liter pilot plant system used a batch recycling system consisting of a high-flow-rate centrifugal pump, a storage tank and a solar reactor. The solution was preheated in a lower chamber, heated again in an upper chamber, and then used the UV and infrared radiation captured by the solar reactor in Argentina to degrade the pollutants in the solution. Results stated that almost complete degradation was obtained in 60 minutes using this method.

In Farias *et al.* (2010) pilot plant, the water solution enters a lower channel where it is preheated and then circulated to an upper channel where it is exposed to the radiation that is obtained from the solar panels to degrade the pollutants. The solution is recirculated from a reservoir tank through the system by a centrifugal pump. The solar panel was first covered to block radiation while the solution in the storage tank was adjusted to the correct pH level and treated with the desired amounts of acid. The cover was then removed from the solar rector to allow for the radiation to treat the sample.

Lucas *et al.* (2009) describe their solar pilot plant installed in Almeria, Spain consisting of solar panels tilted 37 degrees to simulate the same energy reaching the panels regardless of the sun's location. At the beginning of the process, the pH of the sample is adjusted and iron salt is added. The mixture is homogenized all while the solar panels are covered to block collection. Once the sample is homogenized, the collectors are uncovered and the sample is cycled through the system to react with the radiation. The system is able to treat up to 40 liters of wastewater

García-Montaño *et al.* (2008) detailed their 35-liter pilot plant, located in Almeria, Spain, that included three solar collectors (1.03 m^2 each), a storage tank, and a recirculation tank. The collectors were covered to block radiation collection while the mixture was adjusted to the desired pH (2.8-3.0) and homogenized with iron salt and hydrogen peroxide. The collectors were then uncovered and the radiation collected reacted with the sample circling through the system at the specific interval. Inconsistencies in the pilot system included UV light collection that differed at different times and types of days (ideal conditions being a sunny day at noon), and temperatures varying between 25-48 ˚C.

2.5 Summary

In summary, the literature review details the history of silk, silk production, and dyeing the protein-based fiber, as well as the environmental problems caused by the disposal of the untreated effluent. The literature review then goes on to describe photo-Fenton oxidation and photo-Fenton oxidation coupled with biodegradation and previously described varieties of the processes as detailed by other authors. The photo-Fenton oxidation process includes variables such as acidity, iron, hydrogen peroxide volume, dye concentration, UV light, temperature, and oxidation time. In order for this study to be carried out to benefit small-scale textile dye industries, the photo-Fenton oxidation process must be made low-cost. For this reason, the literature review describes viable options for a sustainable container, iron scrap as a possible replacement of iron salt in the chemical oxidation process, and lastly pilot projects of larger volume reactions. All

of this literature review has led to the design of a sustainable photo-Fenton oxidation and sand/carbon filtration system using sustainable, locally available materials.

CHAPTER 3 – EXPERIMENTAL APPARATUS AND METHODOLOGY

3.1 Introduction

The goal of this work is to study the effectiveness of a mobile oxidation unit in a lab and in the field for use in developing countries to decolorize industrial-grade dye wastewater for cottage-scale dyeing operations that currently use no effluent treatment. The system should decrease levels of all organics contained in the resulting solution to levels suitable for reuse in the dye industry. In this chapter, the apparatus and methodology used to study the viability and success of sustainable photo-Fenton oxidation alone and coupled with biodegradation is described.

3.2 Experimental Overview

The laboratory-scale treatment process encompasses eight stages. The dye wastewater is (1) created in a 1-liter pot (or 50 to 100 liters in the case of field studies), (2) acidified to pH 2.5-3.0 with hydrochloric acid, (3) stirred and infused with pharmacy-grade 6% hydrogen peroxide, (4) poured into the mobile photo-Fenton oxidation reactor that contains multiple pieces of rusty metal on its base (or is made of rusty metal in the case of field studies), (5) is left open to the sun for one hour, (6) poured through a sand filter to separate the iron/dye sludge from solution, (7) poured through activated carbon (or wood charcoal in the case of field studies) to absorb any remaining organics, and (8) tested for color change, temperature, acidity (pH), and concentrations of COD, any other organic material present, metals and ions, and biodegradability. See Appendix G for the

educational brochure prepared as part of this project on the sustainable photo-Fenton oxidation and filtration of textile effluent protocol.

There are eight main variables to be tested throughout the study: (1) decolorization of different colors of dye (red, yellow, and blue) at a concentration of 5 g/L, (2) decolorization of different dyes (Reactive or Acid or Acid with Soap and Soda), (3) container size (1-liter laboratory-scale and 50-100 liter demonstration-scale), (4) angle of incoming natural UV sunlight (India or USA), (5) volume of hydrogen peroxide (optimized according to color), (6) quantity of rusty iron (high, medium, or low), (7) time of oxidation (partial or full), and (8) filtration (none, sand, sand and carbon) affect on treated water quality. All water samples were tested for color using a UV-visible scanning spectrophotometer, broad organic chemical levels through COD, specific identification of organic chemicals and metals present using Gas Chromatography and Mass Spectrometry (GC/MS) and Inductively Coupled Plasma Atomic Emission Spectroscopy (ICP), acidity using a pH meter, and biodegradability using respirometric analysis.

3.3 Container

3.3.1 Laboratory-Scale Study

The reactor in the laboratory-scale experiments in India and the USA used a 44 cm diameter plastic tub that holds one-liter of wastewater at a maximum depth of 2.5 cm.

3.3.2 Field Study

Figure 3.1 shows the reactor built in India. The demonstration unit holds approximately 50-100 liters, with a similar shallow depth of 2.5-6 cm holding the wastewater for a longer two-hour treatment and leads to a slow sand and carbon filter to collect any solids from the clean water.

3.3.3 Options for Sustainable Reactor

There are five main options for building a large-scale reactor made of sustainable materials in India: rusty metal, plastic bottles (PET), fused plastic bags (PE), concrete, or wood covered in resin. Tables defining material properties of these options are as follows: Table 3.1 for rusty iron, Table 3.2 for PET, Table 3.3 for PE, Table 3.4 for concrete, and Table 3.5 for wood.

The reactor is ideally made of readily available refuse locally available for the dyers. In some areas there is a vast quantity of plastic bottles and bags available as refuse found in ditches. The biggest downfall with using plastic is that, although it relieves the environment of waste, the resulting containers are prone to leaking and difficult to prepare to hold large quantities of liquids as they often fold onto themselves. Wood is sturdier and easier to work with in a construction sense; however, the wood should be treated with a resin to eliminate the possibility of leakage or absorption, and wood is fairly expensive and difficult to find in India. Concrete is another option but renders the container immobile due to weight. Rusty metal sheets can be found in local metal markets and is less expensive because rusty metal is considered a low quality material.

Thicker sheets last longer and cost more. It was found that a thickness of 0.8 mm degraded 0.5-2% per 1-liter run for 1-hour experiments. Percent iron rust created is considerably higher when iron surface area is limited and low. This means that during the photo-Fenton oxidation process with high iron, the degradation of iron is minimal and therefore leaves the container in good condition for a 50-200 batches. Although this is a conservative estimate and requires field studies for a more accurate analysis. Finding someone to fold the sheet into a shallow container and weld the corners making it leak proof is also locally available and inexpensive.

3.3.3.1 Rusty Iron

The properties of low carbon steel from Ashby (2009) are listed in Table 3.1 and Figure 3.1 is a photo of the rusty metal container made in India to hold 50 to 100 liters of industry grade dye wastewater. See Appendix H for the educational brochure prepared in this project detailing methods to make a rusty iron reactor to hold 50-100 liters of dye effluent in India.

Table 3.1: Low carbon steel properties (Ashby, 2009).

Property	Low range	High range	Unit
Density	7800	7900	kg/m^3
Price	0.79	0.90	USD/kg
Melting Point	1480	1530	°C
Maximum service temperature	350	400	°C
Thermal conductivity	49	54	W/m.K
Thermal expansion coefficient	11.5	13	µstrain/°C
Annual world production	$1.1x10^9$	$1.2x10^9$	tonne/yr
CO_2 footprint, primary production	2.2	2.8	kg/kg
Water usage	23	69	l/kg
Eco-indicator	79	87	millipoints/kg

Figure 3.1: Photo of rusty metal reactor made in India to hold between 50 and 100 liters of industry grade dye effluent at a cottage-scale dye industry.

3.3.3.2 Plastic Bottles

The reactor can be made of used plastic soda bottles. Plastic bottles are made of Polyethylene terephthalate (PET), also known as plastic #1. The chemical composition of PET is: $(CO - C_6H_4) - Co - O - (CH_2)_2 - O)_n$. The properties of the plastic from Ashby (2009) are listed in Table 3.2. Figure 3.2 is a photo of a recycled plastic bottle reactor.

Due to the strength of the already-molded plastic, reshaping is a challenge; however, with some manipulation, each bottle can be cut into rectangular pieces and sewn together using a regular household (non-industrial) sewing machine. The curve of the plastic should be taken into account when sewing to make sure that the ends of the resulting reactors open up to the sun and the sides stay erect. All seams should be coated with silicone or Shoe Goo. Shoe Goo is a sealer made of toluene and petroleum distillates. It is flammable, has a density of 0.899 kg/l, has a VOC of 486 g/l, has a viscosity of

170,000 cps, and cures in approximately 24-48 hours. Once cured, Shoe Goo has excellent resistance to water, dilute acids, and dilute bases, and has a dielectric strength of 400 V/mil, tensile strength of 2,671,664.4 kg/m^2, elongation of 900%, and a service temperature of -40 to 60 °C (Eclectic Products, 2012). Using an extra material adds to the unsustainability of the unit; however, it may be necessary to use the extra material in order to create a leak-free reactor.

Table 3.2: PET properties (Ashby, 2009).

Property	Low range	High range	Unit
Density	1290	1400	kg/m^3
Price	1.63	1.79	USD/kg
Tensile Strength	48.3	72.4	MPa
Melting Point	212	265	°C
Maximum service temperature	66.9	86.9	°C
Thermal conductivity	0.138	0.151	W/m.K
Thermal expansion coefficient	115	119	µstrain/°C
CO_2 footprint, primary production	2.21	2.45	kg/kg
Water usage	14.7	44.2	l/kg
Eco-indicator	360	400	millipoints/kg

Figure 3.2: Photo of recycled plastic bottle reactor.

3.3.3.3 Fused Plastic Bags

The reactor can be made of used plastic bags fused together in layers of approximately six. Plastic bags are made of Polyethylene (PE), also known as plastic #2 or #4. The chemical composition of PE is: $(-CH_2 - CH_2 -)_n$. The properties of the plastic from Ashby (2009) are listed in Table 3.3. Figure 3.3 is a picture of a recycled plastic bag reactor.

Fusing plastic bags takes time and energy and must be done using a hot pressing iron holding six layers of plastic bags between two sheets of wax paper to provide enough heat to fuse the plastic but not so much that the plastic melts creating holes in the reactor. Each piece can then be sewn together using a regular household (non-industrial) sewing machine. All seams should be coated with silicone or Shoe Goo as described in 3.3.1.2 for the construction of the PET reactor.

Table 3.3: PE properties (Ashby, 2009).

Property	Low range	High range	Unit
Density	939	960	kg/m^3
Price	1.85	2	USD/kg
Tensile Strength	21	45	MPa
Melting Point	125	132	°C
Maximum service temperature	90	110	°C
Thermal conductivity	0.4	0.44	W/m.K
Thermal expansion coefficient	126	198	µstrain/°C
Annual world production	$68x10^6$	$69x10^6$	tonne/yr
CO_2 footprint, primary production	2	2.2	kg/kg
Water usage	38	1.1e2	l/kg
Eco-indicator	310	350	millipoints/kg

Figure 3.3: Photo of recycled plastic bag reactor.

3.3.3.4 Concrete

The reactor can also be made of concrete. Concrete is composed of 6:1:2:4 of Water:Portland cement:Fine aggregate:Coarse aggregate. The properties of the plastic from Ashby (2009) are listed in Table 3.4.

A concrete tank will require preplanning and the use of forms and it will become a permanent part of the dye removal process. For example, it may take on the form of an extension of the workroom but exposed to the sun. A reactor made of concrete would not be considered a mobile-unit.

Table 3.4: Concrete properties.

Property	Low range	High range	Unit
Density	2300	2600	kg/m^3
Price	0.041	0.062	USD/kg
Melting Point	972	1230	°C
Maximum service temperature	480	510	°C
Thermal conductivity	0.8	2.4	W/m.K
Thermal expansion coefficient	6	13	µstrain/°C
Annual world production	$15x10^9$	$15.5x10^9$	tonne/yr
CO_2 footprint, primary production	0.13	0.15	kg/kg
Water usage	1.7	5.1	l/kg
Eco-indicator	3.6	4	millipoints/kg

3.3.3.5 Wood

The reactor can be made of particleboard or plywood or some other type of readily available wood. Plywood specifically is made of cellulose/hemicellulose/lignin/12%H2O/adhesive. The properties of plywood from Ashby (2009) are listed in Table 3.5. Figure 3.4 is a picture of a plywood reactor in preliminary design stages including baffles and scrap metal in the form of rusty bicycle parts on its base.

Wood is a material that is easily manipulated to construct things like a reactor. The wood will be coated with a sustainable resin made by Entropy Resins called Super Sap CLR Epoxy. Super Sap is sourced from paper pulp, biofuels, and pine industries. Entropy Resins uses sap in their epoxies as a replacement for petrochemicals to form elastic adhesives. Super Sap has a decomposition temperature greater than 200°C, a flashpoint over 200°C and has no solubility in water (Entropy Resins, 2011). The resin coating will prevent dyestuff from seeping through the pores of the wood and exiting the reactor prior to full oxidation. A coating of resin or epoxy makes this choice of reactor less affordable and less applicable to developing world needs, creating a cost that may be unattainable to

most small-scale industries; however, the strength of the reactor will allow for a longer lifespan than the more delicate plastic and more mobile than concrete.

Table 3.5: Plywood properties (Ashby, 2009).

Property	Low range	High range	Unit
Density	700	800	kg/m^3
Price	1.04	2.07	USD/kg
Tensile Strength	10	44	MPa
Maximum service temperature	100	130	°C
Thermal conductivity	0.3	0.5	W/m.K
Thermal expansion coefficient	6	8	µstrain/°C
CO_2 footprint, primary production	0.73	0.77	kg/kg
Water usage	500	1000	l/kg
Eco-indicator	37	41	millipoints/kg

Figure 3.4: Photo of plywood reactor in preliminary design stages including baffles and scrap metal in the form of rusty bicycle parts.

3.4 Variables in photo-Fenton Oxidation

Variables that affect the photo-Fenton oxidation process include the UV light source (sunlight angle in India or the USA), type of dye at 5 g/L concentration (Reactive Dye, Acid Dye, and Acid Dye with Soap and Soda), color of dye (red, yellow, or blue), water

source for mixing dyes, acid used to bring pH to 2.5-3.0 (here hydrochloric acid is used), hydrogen peroxide volume added as the main oxidizing agent, surface area of rusty iron pieces as the chemical catalyst (high iron of 645 cm^2, medium iron of 323 cm^2, low iron of 161 cm^2), time (partial or full oxidation), and filtration (none, sand, or sand and carbon).

3.4.1 UV Light Source

Photo-Fenton research at UWM used direct sunlight during the summer months and at CSIR-NEERI Nagpur sunlight was also used. Solar radiation was measured using CEM's DT-1307 Solar Power Meter measuring up to 1999 W/m^2 or 634 BTU/ft^2*hr (CEM Instruments, 2012). Milwaukee also has a website that measures solar irradiance and posts (Curtronics, 2013). Preliminary studies showed that a metal halide bulb was also able to act as the UV source for the photo-Fenton oxidation process. However, since this study focuses on low-cost options for cottage-scale industries throughout developing communities, electricity is not a feasible option for the future and metal halide bulbs were not further studied.

3.4.2 Dye

Typical cottage-scale dyers use a mixture of 12-14 g/L Acid Dyes with 1 square of soap per 10 liter solution (approximately 31 g soap) and 10 g/L soda to make between 80 and 150 liters of dyestuff. Considering that dyeing is followed by rinsing, dilution of the highly concentrated dye water is certain, as is a lower dye concentration per batch in a double-sized batch. Samples here were taken at 5 g/L because there are 1-2 rinses that

take place that dilute the dye effluent by approximately 60%. This study considers both Reactive Dyes and Acid Dyes. Reactive Dyes were used as the literature indicated that they were the leading silk dye used by industry (Aplin and Waite, 2000). Acid Dyes were used because they were found to be heavily-used in cottage-scale operations. It was also found that Acid Dye with Soap and Soda is most frequently used, and so is included as a third dye solution in this study.

3.4.2.1 Reactive Dyes

This study compares three Reactive Dyes: Red 120, Yellow 81, and Blue 4. These were chosen because of their wide use in industry, ease of procurement, and ability to compare with other dye oxidation studies. The Reactive Red 120 linear chemical formula is $C_{44}H_{24}Cl_2N_{14}O_{20}S_6Na_6$ and has a molecular weight of 1469.98 g/gmol and CAS number 61951-82-4 with a color wavelength tested at 535 nm. The chemical structure can be seen in Figure 3.5. The Reactive Yellow 81 (also known as Procion Yellow H-E3G) linear chemical formula is $C_{52}H_{34}Cl_2N_{18}Na_6O_{20}S_6$ and has a molecular weight of 1632.18 g/gmol and CAS number 59112-78-6 with a documented maximum wavelength of 270 nm and second at 356 nm. The chemical structure can be seen in Figure 3.6. The Reactive Blue 4 linear chemical formula is $C_{23}H_{14}Cl_2N_6O_8S_2$ and has a molecular weight of 637.43 g/gmol and CAS number 13324-20-4 with a documented maximum wavelength at 595 nm. The chemical structure can be seen in Figure 3.7.

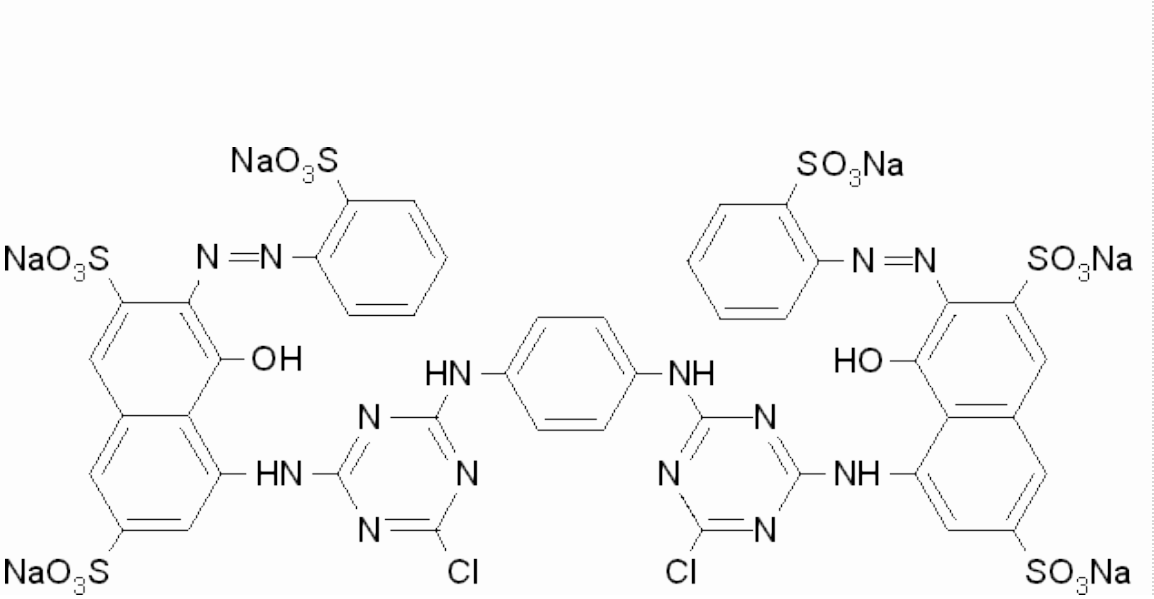

Figure 3.5 Reactive Red 120 chemical composition (Santa Cruz Biotechnology, 2014).

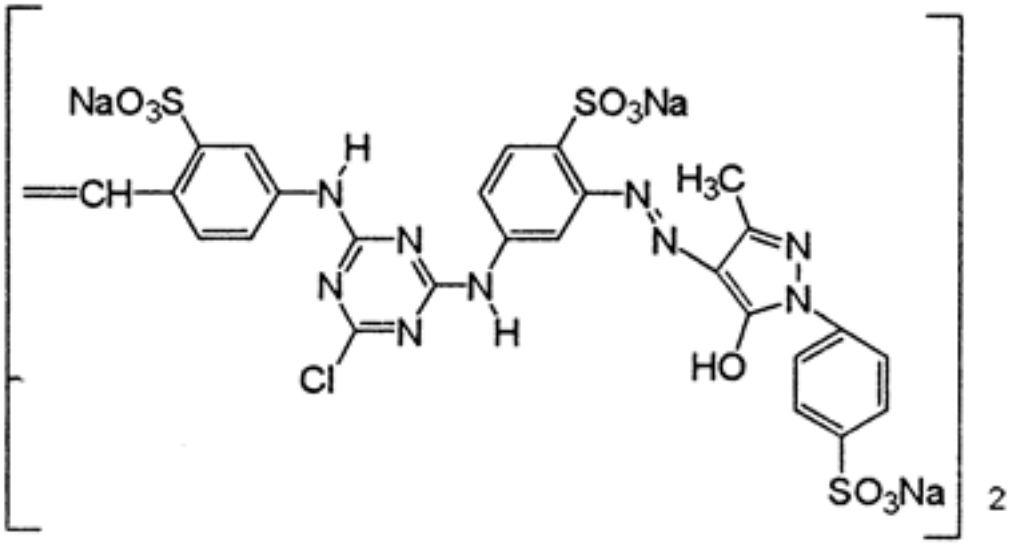

Figure 3.6 Reactive Yellow 81 (Procion Yellow H-E3G) chemical composition (World Dye Variety, 2012).

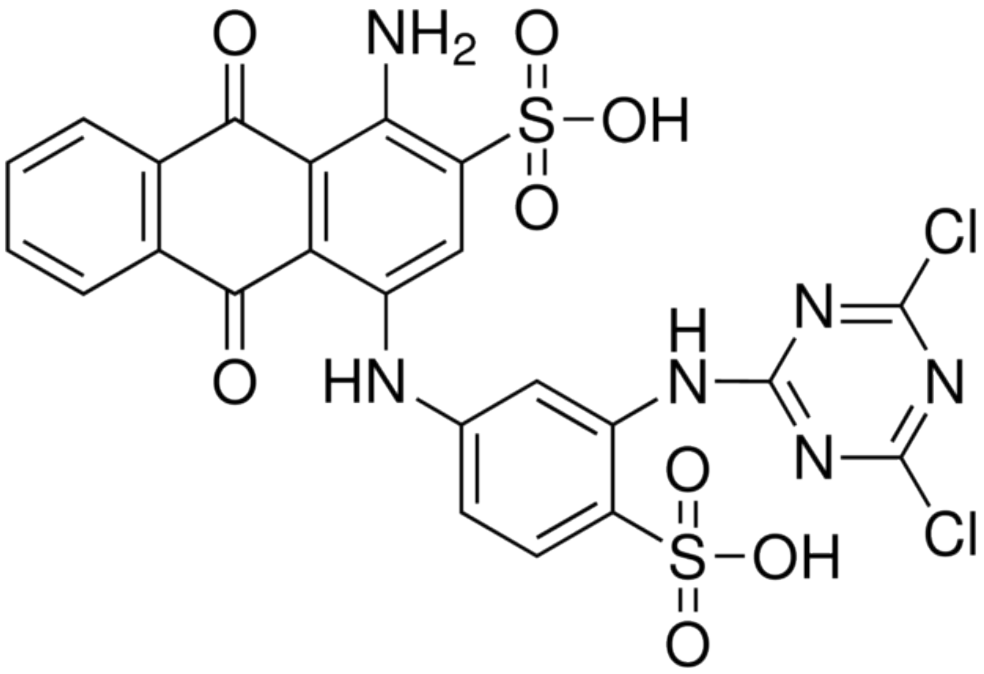

Figure 3.7: Reactive Blue 4 chemical composition (MP Biomedicals, 2014).

3.4.2.2 Acid Dyes

This study compares three Acid Dyes: Fast Red, Golden Yellow, and Ananda Blue. These were chosen because of their use in cottage-scale operations, low quality, low cost, and ease of procurement. Since these are industry dyes purchased from local dye markets, the true chemical formula, molecular weight, and CAS number is not available. A general chemical formula is described assuming that the low-quality grade dye available to cottage-scale dyers will also contain some impurities. Acid Fast Red maximum wavelength tested at 505 nm. The basic chemical structure of an Azobenzene type red dye where the Acid Fast Red can be characterized can be seen in Figure 3.8. Acid Golden Yellow maximum wavelength tested at 399 nm. The basic chemical structure of an Triphenylmethane type yellow dye where the Acid Golden Yellow can be characterized can be seen in Figure 3.9 with CAS Number 519-73-3,

linear formula of $(C_6H_5)_3CH$, molecular weight of 244.33 (Sigma Aldrich b, 2014). Acid Ananda Blue maximum wavelength tested at 637 nm. The basic chemical structure of an Anthraquinone type blue dye where the Acid Ananda Blue can be characterized can be seen in Figure 3.10.

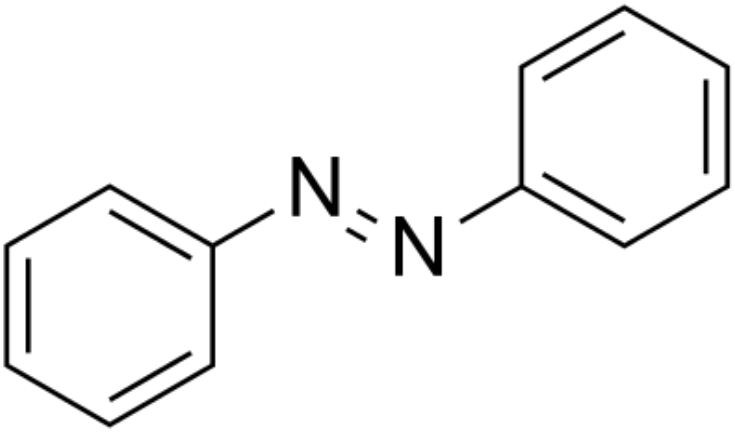

Figure 3.8: Azobenzene type Acid Dye is the typical acid red dye that would include the Acid Fast Red dye used in this study (Essential Chemical Industry Online a., 2013).

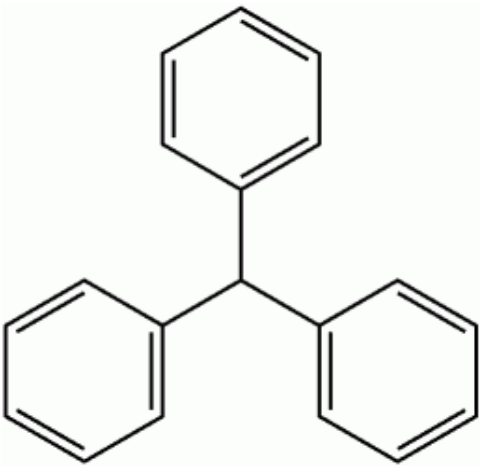

Figure 3.9: Triphenylmethane type Acid Dye is the typical acid yellow dye that would include the Acid Golden Yellow dye used in this study (Sigma Aldrich b, 2014).

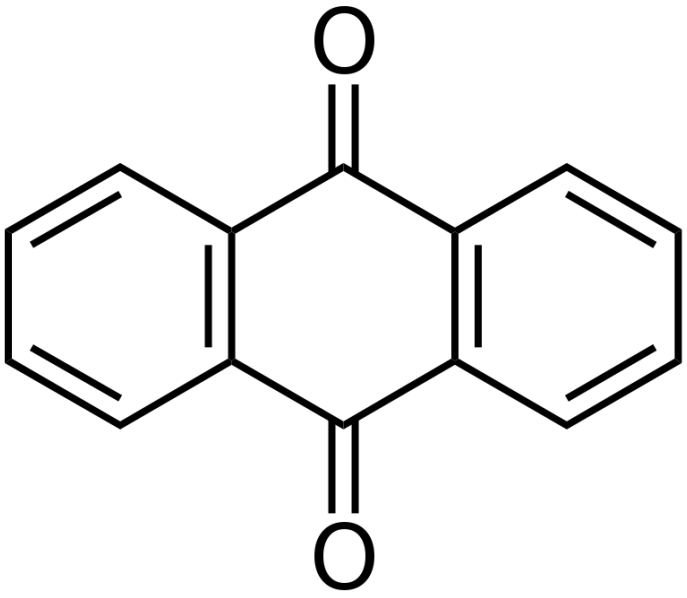

Figure 3.10: Anthraquinone type Acid Dye is the typical acid blue dye that would include the Acid Ananda Blue dye used in this study (Sigma Aldrich a, 2014).

3.4.3 Soap and Soda

Soap and soda are used in the silk industry to wash the gum off of the raw silk before it is dyed and woven into cloth. In medium and large-scale dye operations, the soap and soda bath are separated from the dye bath in order to optimize and decrease the quantity of dye required for a color match; the dye is absorbed into the silk yarn more than the yarn absorbs the water solution and therefore more time and less dye can be traded for darker colored fabric. For cottage-scale operations, the soap and soda are first boiled in solution and then dye is added directly in after which the yarn is washed and dyed at one time. This decreases the amount of water used in the industry and also the number of pots needed to dye a batch of yarn, both limiting factor in a cottage-scale operation. This also decreases the ability of the dye to enter the pores of the fiber thus requiring more dye in the original solution and then also greatly increasing the concentration of dye in the

industrial effluent. Although effluent of medium and large-scale operations is mixed before treatment, because they are originally separated, the color content of the final effluent is more than 100 times lower concentration than the cottage-scale dyer. This is a major issue that is not currently being addressed by the Indian State Pollution Control Boards because they are not able to track the cottage-scale dye industries because of the fact that they are located in homes hidden within villages very far off of the beaten path. Cottage-scale industries used approximately 31 g of soap per 10-liter dye and soda at a concentration of 10g/L for batches between 80 and 150 liters.

Soap is a low quality surfactant that is used by cottage-scale dye industries. In fact when the supplies were purchased from a local supplier, a higher quality soap, 501 Bar Soap, was offered by the vender. 501 Bar Soap is a name-brand soap used in some silk dye industries. Figure 3.11 is a picture of the 501 soap weighing approximately 250 g with each of its 8 equal parts weighing approximately 31 g. 501 Bar Soap ingredients are: sodium tallowater and or sodium palmate, water, sodium cocater and or sodium palm kernelate, glycerin, sodium chloride, fragrance, coconut acid and or palm kernel acid and or tallow acid and or palm acid and or tetrasodium EDTA (Austoria *et al.*, 2010). Local soap venders also sell a nameless soap that accomplishes the same task, although it does not offer the promises of 501 Bar Soap that includes whiteners and its ingredients are not available. 501 Bar Soap has been found to have a very high irritation level for human skin increasing dryness and wrinkling compared with 17 other typical Indian soaps (Austoria *et al.*, 2010). This study uses the nameless and low quality soap purchased from a local soap vender, although both versions were seen being used in industry.

Figure 3.12 shows the chemical structure of an anionic detergent including a hydrophobic group and a hydrophilic group (Essential Chemical Industry Online b, 2013) displaying a version of the simple soap used in this study.

Soda is a bicarbonate powder that also washes the silk in preparation for the dye to enter the silk. Figure 3.13 shows the chemical structure of soda. Figure 3.14 is a photo of the bicarbonate powder as it is used in cottage-scale silk dyeing operations.

Figure 3.11: Picture of 501 Bar Soap.

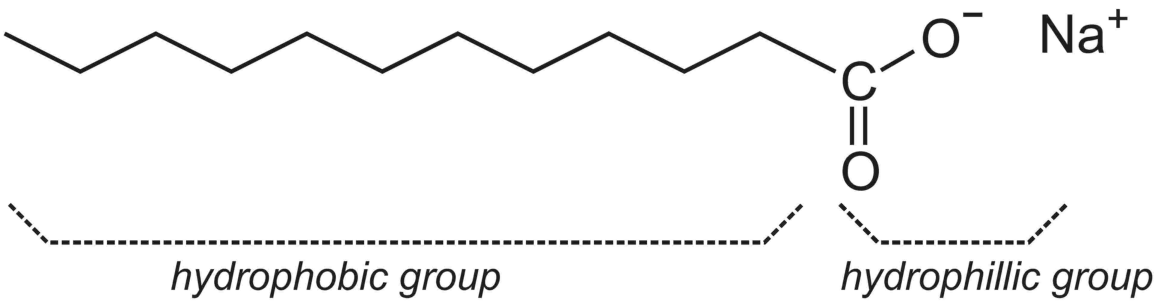

Figure 3.12: Simple soap chemical composition as an anionic detergent including a hydrophobic group and a hydrophilic group (Essential Chemical Industry Online b, 2013).

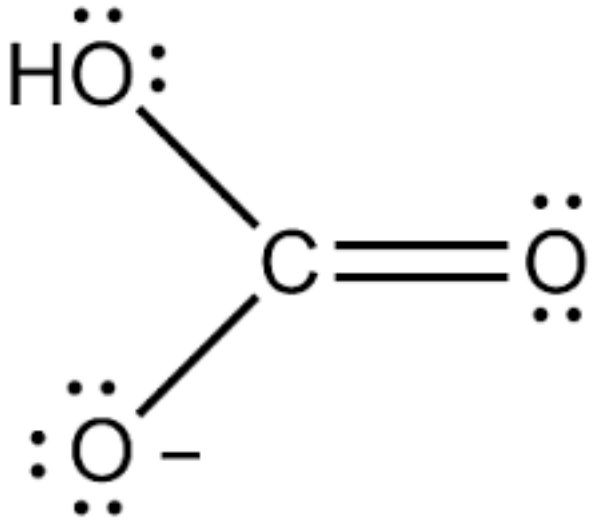

Figure 3.13: Bicarbonate powder chemical structure (Chemical Education Digital Library).

Figure 3.14: Picture of locally available bicarbonate powder used in this study.

3.4.4 Water

Tap water was used to dissolve all dyes. Water quality varies throughout the globe. The difference between the water quality in the USA and India and within India whether it is in a rural community or a city alters dye samples with enough variability that results may differ greatly.

3.4.5 Hydrochloric Acid

Hydrochloric acid of approximately 1M is a toilet bowl cleaner throughout India and is the most readily available of all acids. For this reason it was chosen as the acidifier to bring the dye solution to pH 2.5-3.0. It is understood that hydrochloric acid can react

with the oxidation chemicals and the dye intermediates thus producing some unwanted byproducts such as chlorides. Sodium levels are often high in dye solutions. Because of the strong attraction between chloride and sodium ions, sodium chloride is easily formed. Sodium chloride is very soluble in water and will remain in solution even after filtration. Other acids can be added instead of hydrochloric acid such as sulfuric acid, nitric acid, or acetic acid. Typically acetic acid is not used to bring pH to 2.5 because it is required in great volume to do this. Sulfuric and nitric acid usage will also create byproducts in solution that are more dangerous to effluent than chloride. In the case of sulfuric acid, sulfates will be produced, and in the case of nitric acid, nitrates. Sulfuric acid, however, is available at much higher concentrations resulting in the need for less volume of acid per batch. Sodium sulfate is not as soluble in water as sodium chloride which may result in its capture during filtration keeping sodium out of the treated effluent; for this, further study is required. Nitrates in water are dangerous to human health and can create holes in the hearts of fetuses and because of this are known as the source of blue baby syndrome causing babies to be born with blue bodies. Chloride levels from hydrochloric acid are high; however, of the possible byproducts after acidification for photo-Fenton oxidation are the least obtrusive effluent.

3.4.6 Hydrogen Peroxide

Hydrogen peroxide is the chosen oxidizer in the photo-Fenton process. In these laboratory experiments a 6% solution, which is a 1.76 M solution, was used. In industry 50% solution is available and was used in the field studies. The amounts of 6% hydrogen peroxide vary with changes in dye color and type as listed in Table 3.6.

Table 3.6: Amount of 6% hydrogen peroxide used with various dye colors, types, and amounts of rusty iron.

Dye Type	Dye Color	Iron Quantity	6% Hydrogen Peroxide Quantity (mL)
Reactive	Red	Low	250
Reactive	Red	Medium	150
Reactive	Red	High	100
Reactive	Yellow	Low	250
Reactive	Yellow	Medium	150
Reactive	Yellow	High	100
Reactive	Blue	Low	500
Reactive	Blue	Medium	300
Reactive	Blue	High	200
Acid	Red	High	200
Acid	Yellow	High	200
Acid	Blue	High	200

3.4.7 Iron

Rusty metal sheets were cut from the sides of old yogurt containers found in an open dumping site in India, where half of the studies were performed. Figure 3.15 displays the yogurt containers used as the scrap iron in this study. Scanning Electron Microscopy (SEM) of the rusty metal found that the majority of the rust was iron-based; however, because of the fact that the metal was found in the field rather than purchased as laboratory grade, some impurities are to be expected. Figure 3.17 compares the SEM images captured and analyzed for surface composition of the rusty metal. This work is intended to function for small-scale cottage industry silk dyers, and since this is the case, the materials used were as found in the field.

In this study low, medium, and high iron surface areas were compared for Reactive Dye oxidation. Low iron surface area is 161 cm^2, medium iron surface area is 323 cm^2, and high iron surface area is 645 cm^2. The medium iron surface area piece is shown in Figure 3.16. However, after realizing that less time and less hydrogen peroxide were needed

with higher iron, and realizing that chemical costs and time are limiting factors for the use of technologies for small-scale silk dyers throughout rural India, the studies involving Acid Dye and Acid Dye with Soap and Soda used only high surface areas of iron. Furthermore, the studies involving Acid Dye also increased the partial oxidation time studies.

Figure 3.15: Open dumping site showing old yogurt containers used for scrap iron for study.

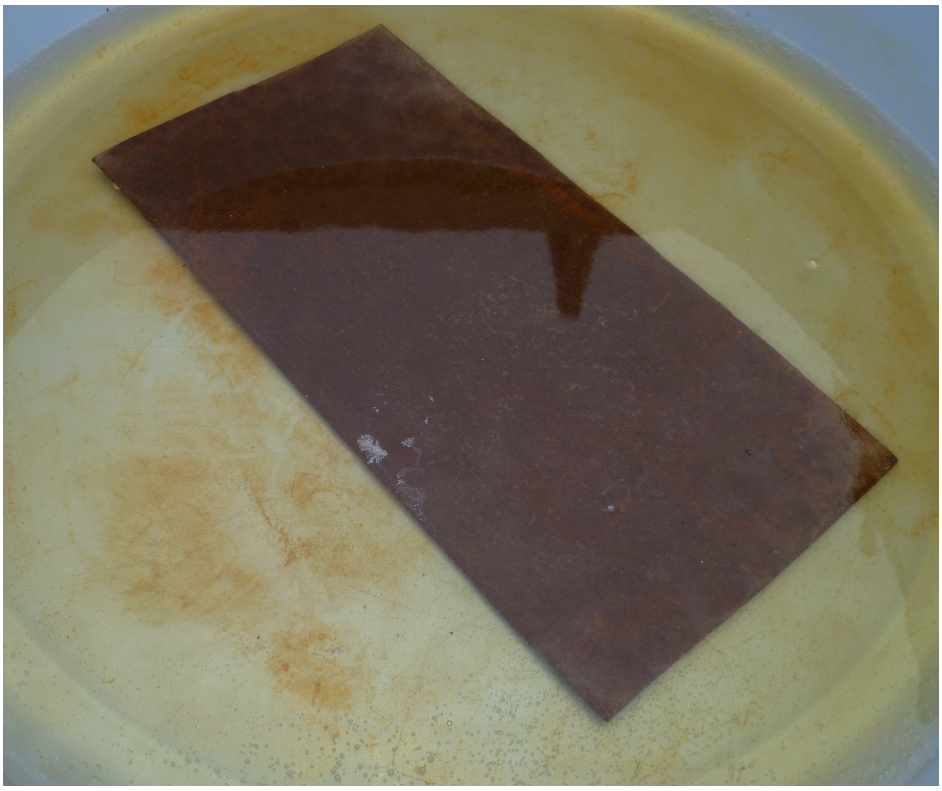

Figure 3.16: Scrap metal cut from the yogurt container. This is a medium-sized piece, the size was halved for low, and doubled for high iron surface area.

3.4.8 Time

Optimization of time experiments were completed by taking a 5 mL sample every 5 minutes during oxidation, adding 1 drop of 0.1M sodium hydroxide to raise the pH above neutral (9 for Reactive Red 120, 9.37 for Reactive Yellow 81, and 8.86 for Reactive Blue 4) in order to stop the photo-Fenton oxidation reaction. The undiluted samples were then analyzed using UV-visible spectrometry to find the time when the color became partially degraded by watching the peak height of the color and any organics left in solution decrease with increased oxidation time. Full oxidation time was chosen when all peaks on the spectral analysis decreased to zero. Partial oxidation time was chosen when the peaks on the spectral analysis were visibly separated from each other and could each be identified as an individual chemical peak. Acid Dye studies included three partial

oxidation times in order to analyze the difference that time makes on oxidation of Acid Dyes. The second and third partial oxidation times were chosen five or ten minutes before the first, depending on the length of time from t_0.

The lengths of the time studies for each scenario for Reactive Dyes are shown in Table 3.7, for Acid Dyes in Table 3.8, and for Acid Dyes with Soap and Soda in Table 3.9.

Table 3.7: Partial and full oxidation times for Reactive Dyes.

Dye	Iron Quantity	t_0 (min.)	$t_{partial}$ (min.)	t_{Full} (min.)
Reactive Red 120	High	0	40	60
Reactive Red 120	Medium	0	55	75
Reactive Red 120	Low	0	75	135
Reactive Yellow 81	High	0	35	70
Reactive Yellow 81	Medium	0	85	155
Reactive Yellow 81	Low	0	75	135
Reactive Blue 4	High	0	100	125
Reactive Blue 4	Medium	0	155	180
Reactive Blue 4	Low	0	180	220

Table 3.8: Partial and full oxidation times for Acid Dyes.

Dye	t_0 (min.)	$t_{Partial1}$ (min.)	$t_{Partial2}$ (min.)	$t_{Partial3}$ (min.)	t_{Full} (min.)
Acid Fast Red	0	45	35	25	60
Acid Golden Yellow	0	25	20	15	60
Acid Ananda Blue	0	60	50	40	80

Table 3.9: Partial and full oxidation times for Acid Dyes with Soap and Soda.

Dye	t_0 (min.)	$t_{Partial}$ (min.)	t_{Full} (min.)
Acid Fast Red with Soap and Soda	0	5	25
Acid Golden Yellow with Soap and Soda	0	10	25
Acid Ananda Blue with Soap and Soda	0	30	50

3.4.9 Sand Filter

The sand filter for the 1-liter experiments displayed here were made of readily-available construction sand from the area and required approximately 0.5 m depth of sand with a diameter of 40 cm. In the case of the laboratory experiments in the United States, the

fully oxidized sample was first filtered, followed by the partially oxidized sample; after this, the sand was changed. In the case of the Acid Dye experiment, the fully oxidized sample was filtered followed by the longest partially oxidized sample, the next longest, and then the shortest oxidized sample after which the sand was changed. The reason for this is because un-oxidized dye color permanently dyes the sand in the filter and cannot be removed without using excessive amounts of water. Again, the purpose of this work is to benefit cottage-scale silk dyers and therefore it is necessary to optimize the system performance while keeping the cost as low as possible. Knowing that the cost of water is rising with global water shortages, it is important to find the minimum amount of time needed to obtain clear effluent samples after sand filtration and also ease the use of the technology for dyers.

3.4.10 Carbon Filter

Activated carbon was used after sand filtration with the hopes of adsorbing any residual color or chemical intermediate in solution after oxidation and sand filtration. In the field, it may be possible to use wood charcoal instead of more expensive activated carbon; however, further studies are required to determine the feasibility of wood charcoal.
The carbon filter was rinsed twice between filtration of different samples.
See Appendix I for the educational brochure developed as part of this work on how to make a slow sand and carbon filter for the treatment of 50-100 liters of dye effluent using readily available materials in India.

3.5 Methods of Analysis

Tests for color change included UV-visible spectra scans from 190-1100 nm to find peaks of color intensity. Tests to find quantity of organic chemicals in solution were completed by testing COD. To qualitatively analyze the organic chemicals left in solution after oxidation and filtration, GC/MS was performed. ICP was used to analyze metals left in solution and their quantity. To see whether all of that which is left in solution would be biodegradable in a Common Effluent Treatment Plant (CETP) using biodegradation, respirometric analysis was performed. Levels of pollutants found were compared to India's permissible limits for dye and dye intermediate industries' effluent disposal into surface waters as shown in Table 3.10.

Table 3.10: India's permissible effluent standards for wastewater in Dye and Dye Intermediate Industries for disposal in surface waters (Hasan, 2014).

Parameter	Disposal in Surface Water	Unit
pH	6.0-8.5	
Suspended Solids	100	mg/L
COD	250	mg/L
Colour (Hazen Units)	400	mg/L
Hg	0.0	mg/L
Total Chromium	2.0	mg/L
Copper	2.0	mg/L
Zinc	5.0	mg/L
Nickel	3.0	mg/L
Lead	0.1	mg/L
Manganese	2.0	mg/L
Cadmium	0.2	mg/L
Chloride	1000.0	mg/L
Sb+As+Pb+Cr+Co+Cu+Mn+Ni+V+Cd+Th+Hg	1.5	mg/Nm3

Table 3.11: Global permissible drinking water standards comparing US EPA, CPCB, BIS, ISI, ICMR, and WHO (Kumar and Puri, 2012; Hasan, 2014; Paul *et al.*, 2012).

Essential Characteristics of Drinking Water:		**US Environmental Protection Agency (EPA)**	**Central Pollution Control Board (CPCB)**	**Bureau of Indian Standards (BIS) & Indian Standard Institution (ISI)**		**Central Public Health & Environmental Engineering Organization as Recommended by the World Health Organization**		**Indian Council of Medical Research (ICMR)**
Substance or Characteristic	**Unit of Measure**			**Requirement (Desirable Limit)**	**Permissible Limit in absence of Alternate Source**	**Acceptable**	**Cause for Rejection**	
Colour Hazen Units, Max	Hazen Units			5	25	5	25	
pH Value		6.5 to 8.5		6.5 to 8.5	6.5 to 8.5	7.0 to 8.5	<6.5 or >9.2	
Phenolic Compounds (as C6H5OH)	mg/L			0.001	0.002	0.001	0.0002	
Calcium (as Ca)	mg/L	-	200	75	200	75	200	200
Magnesium (as Mg)	mg/L	-	100	30		50	150	-
Iron (as Fe)	mg/L		1	0.3	1.0	0.1	1	1
Sodium	mg/L	20						
Manganese (as Mn)	mg/L			0.10	0.3	0.1	0.5	
Arsenic (as As)	mg/L	0.05	No Relaxation	0.05	0.05	0.01	0.05	0.05
Cadmium (as Cd)	mg/L	0.005	No Relaxation	0.01	0.01	0.005	0.01	0.01
Lead (as Pb)	mg/L	-	No Relaxation	0.05-0.1	0.05	0.05	0.05	0.05
Chromium (as Cr6+)	mg/L	0.1	No Relaxation	0.05	0.05	0.05	0.05	-
Aluminum (as Al)	mg/L			0.03	0.2	0	0.2	
Boron	mg/L			1	5			
Chlorides (as Cl)	mg/L	250	1000	250	1000	200	1000	1000
Copper (as Cu)	mg/L	1.3	1.5	0.05	1.5	0.1-1	1.5	1.5
Fluoride (as F)	mg/L	4	1.5	0.6-1.9	1.5	1	1.5	1.5
Mercury (as Hg)	mg/L	0.002	No Relaxation	0.001	0.001	0.001	0.001	0.001
Selenium (as Se)	mg/L	0.05	No Relaxation	0.01	0.01	0.01	0.01	-

Zinc (as Zn)	mg/L	-	15	5	15	5	15	0.1
Alkalinity	mg/L		600	200	600	200	600	
Cyanide (as CN)	mg/L			0.05	0.05	0.05	0.05	
Residual Free Chlorine	mg/L			0.2	--	0.2	>1.0	
Total Dissolved Solids			2000					
Dissolved Solids	mg/L			500	2000	500	2000	
Total Hardness (as CaCO3)	mg/L	-	600	300	600	500		600
Nitrate (as NO3)	mg/L	-	100	45	100	45	45	100
Sulfate (as SO4)	mg/L	-	400	150-200	400	200	400	400
Turbidity	NTU	-	10	5	10	1	10	25
Odour				Unobjectio nable	Unobjectio nable	Unobjecti onable	Unobject ionable	
Taste				Agreeable	Agreeable	Unobjecti onable	Unobject ionable	
Anionic Detergents (as MBAS)	mg/L			0.2	1.0	0.2	1	
Polynuclear aromatic hydro carbons (as PAH)	g/L			--	--	0.2	0.2	
Mineral Oil	mg/L			0.01	0.03	0	0	
Pesticides	mg/L			Absent	0.001	Absent	NA	

3.5.1 UV-visible Spectrometry

Color change was monitored using UV-visible spectrophotometer (HP 8453 Agilent) scanning absorbance between 190-1100 wavelengths in 10 mm quartz cuvettes. Experiments on each dye yielded peak absorbance at particular wavelengths. These wavelengths can be found in Table 3.12.

Table 3.12: Peak absorbance wavelengths for the tested dyes and their designated responsible chemical.

Dye	**Phenol:** 209 nm, 269 nm, (He and Lei, 2004)	**Benzene:** 235 nm, (Bilgi and Demir, 2005); 226 nm, (Sun *et al.,* 2007); 230 nm, (Feng *et al.*, 2000); 260 nm, (Jozwiak *et al*., 2007)	**Naphthalene:** 315 nm, (Bilgi and Demir, 2005); 318 nm, (Sun *et al.,* 2007)	**Color Wavelenths (nm)**	**Unknown Peaks Found**
Reactive Red 120	206	237		536	291, 371, 512
Reactive Yellow 81	206	229, 243		268, 352	410, 520
Reactive Blue 4	206	230, 258		597	369, 520
Acid Fast Red	206, 214		318	505	289, 330, 610
Acid Golden Yellow	203	255		399	350
Acid Ananda Blue	206	257	313	637	340, 411
Acid Fast Red with Soap and Soda	203, 214		317	505	280
Acid Golden Yellow with Soap and Soda	195, 205	248		403	360
Acid Ananda Blue with Soap and Soda	196, 205	259	311	638	360, 411

3.5.2 Chemical Oxygen Demand (COD)

COD is an indirect measurement of the amount of organic compounds present in a solution. Very specifically, COD is the mass of oxygen that is being consumed per liter of solution (Boyles, 1997). The main reason for testing COD and not Total Organic Carbon (TOC) is referenced by Dhuale and Mahajani (1999) who explain that TOC analysis is not as thorough of a test as COD since it omits certain contributions to organics such as H, S, Cl when oxygen is present in the molecule. The Karnataka State Pollution Control Board, the environmental protection agency for the Indian State of Karnataka allows effluent with less than or equal to 250 mg/L COD to be released into the natural environment without further treatment. In this study, COD was measured colorimetrically using a Hach Meter 890. Samples were digested at 148˚C for 120

minutes with one sample of DI water as a control. The digested samples were then measured at 600 nm colorimetrically with the control as zero to measure the color change relative to water.

3.5.3 Solid-phase Micro Extraction Coupled with Gas Chromatography / Mass Spectrometry (SPME-GC/MS)

The samples were extracted using Solid Phase Micro-Extraction (SPME) with a 65-um Polydimethylsiloxane/Divinylbenzene (PDMS/DVB), Stableflex 24Ga fiber assembly (Supelco) controlled by a manual Micro-Extractor holder immersed in each sample for a minimum of 50 minutes. A 65 µm PDMS/DVB partially polar fiber is typically used for amines and nitro-aromatic compounds with molecular weights between 50-300. Since the oxidation of dyes typically results in the formation of amines, this fiber was chosen.

After the extraction was complete, the fiber was injected into the GC/MS (GC System Hewlett Packard, HP 6890 Series, MS Agilent Technologies Mass Selective Detector 5973 Network) column HP-5MS (Crosslinked 5% PH ME Siloxane) 30 m x 0.25 mm, 0.25 µm film thickness (Hewlett Packard Special Performance Capillary Column). The injector volume maximum is 1.0 µl with an inlet heat of 250 °C with a pressure of 7.60 psi with a total flow of 103 mL/min and split ratio of 100:1 and flow of 99.5 mL/min and an average velocity of 36 cm/sec. Helium was used as the carrier gas at a flow-rate of 103 mL/min at a pressure of 7.60 psi. The oven was set for an initial hold at 50 °C for 5 minutes, followed by a ramp of 10 °C per minute until a temperature of 160°C was reached. Then, there was a hold for 2 minutes, followed by a ramp of 5 °C per minute

until 235 °C was reached. This was followed by a hold for 17 minutes for a total run-time of 50 minute. The maximum temperature of the column is 300 °C. The detector heat was set at 150 °C, hydrogen gas flow set at 40 mL per minute and air at 450 mL per minute. Analysis of samples was completed by the attached mass spectrometer connected with NBS75K.L library.

3.5.4 Inductively Coupled Plasma – Atomic Emission Spectrometry (ICP-AES)

ICP-AES was used for the determination of metals and ions in order to quantify and qualify the levels of metal ions left in solution after the following tests: (1) photo-Fenton oxidation, (2) photo-Fenton oxidation followed by sand filtration, and (3) photo-Fenton oxidation followed by sand and carbon filtration (both fully and partially oxidized). The measured spectral element lines were divided into five groups:

Group 1: Cadmium 2 ppm (wavelength 226.5 nm), Manganese 2 ppm (wavelength 257.61 nm), Lead 10 ppm (wavelength 220.35 nm), Zinc 5 ppm (wavelength 213.86 nm);

Group 2: Cobalt 2 ppm (wavelength 228.62 nm), Copper 2 ppm (wavelength 324.75 nm), Iron 100 ppm (wavelength 259.94 nm);

Group 3: Arsenic 10 ppm (wavelength 193.7 nm), Molybdenum 10 ppm (wavelength 202.03 nm), Tin 5 ppm (wavelength 283.9 nm);

Group 4: Aluminum 10 ppm (wavelength 308.2 nm), Calcium 50 ppm (wavelength 317.93 nm), Chromium 5 ppm (wavelength 267.72 nm), Sodium 50 ppm (wavelength 589 nm), Nickel 5 ppm (wavelength 231.6 nm);

Group 5: Silver 5 ppm (wavelength 328.07 nm), Magnesium 50 ppm (wavelength 279.08 nm), Antimony 10 ppm (wavelength 206.83 nm).

According to Skoog and Holler, (2007), Argon gas reacts with charged particles in an electromagnetic field creating a high temperature plasma of up to 10,000 K. The sample is changed into a mist and injected inside the plasma flame. The sample then breaks down into the various molecules and their respective atoms. At this time, electrons are lost from the molecules and recombine with the plasma, giving off radiation at the wavelengths of the elements involved. Once the light is separated into its different wavelengths/colors, the light intensity is measured and compared to intensities of known concentrations of elements and computed by interpolation (Skoog and Holler, 2007). The intensity quantified is proportional to the amount of the element in the solution and each element matches a specific calibrated wavelength (Basic Overview of ICP-AES, 2000).

The test methods followed in this study were similar to Bobu *et al.* (2008), Muthuvel and Swaminatham (2008), and Dash *et al.* (2011). Under the standard methods for the examination of water and wastewater (Eaton, *et al.*, 1995) all results were determined in filtered and acidified samples and the flowing stream of Argon gas was ionized by applied radio frequency field ~27.1 MHz.

The Instrument Parameters of ICP were as follows:

Power 1.00 kW

Plasma runs at 15 L/min

Nebulizer pressure 200 kPa

Argon flow 1.5 L/min

Viewing Height 10 mm

Pump Rate 15 rpm

Spectrometer Atomic Emission Spectroscopy, photo-diode array

Dwell Time 30 seconds

3.5.5 Total Iron

Iron pieces were characterized according to surface area. This differs from other studies that use scrap metal that measured iron quantity by volume or weight (Ganesan and Thanasekaran, 2011; Ganesan *et al.*, 2014; Lin *et al.*, 2008; Zhang *et al.*, 2009). Characterization by surface area was done because it is believed that the iron that acts as a catalyst in the photo-Fenton oxidation reaction acts at the interface between UV light and iron. For 1-liter solutions, low iron was 165 cm^2, medium iron was 323 cm^2, and high iron was 645 cm^2.

Sludge that is produced during the photo-Fenton oxidation process includes both organic dye and inorganic iron. ICP-AES measured quantities of iron in control samples and treated samples. For the Indian samples, iron and dye sludge was quantified volumetrically. Volumetrically, the 1-liter solution was poured into a volumetric cylinder and allowed to settle overnight. A measurement was then taken of the foam that rose to the top as well as the sludge that settled to the bottom of the solution. In order to try to find the mass of the sludge that was composed of dye as opposed to that composed of

iron, a total solids test was completed. A 10-ml sample was filtered onto filter paper and then dried and weighed and compared with an oven-baked filter paper in order to quantify the total solids in solution and compare them with the inorganic solids after baking at 500 ˚C for 30 minutes and then weighed.

3.5.6 Scanning Electron Microscopy (SEM)

SEM was used to measure surface content of iron pieces to ensure that the ferrous ions in the rust was in fact working as the catalyst for the photo-Fenton oxidation process and to see if there were any other impurities in solution affecting the oxidation process.

SEM can be described as a focused beam of electrons that scans the surface of a sample in a raster scan pattern. As the electrons interact with the atoms of the sample, signals are given off in the form of back scattered and secondary electrons. These signals are detected and amplified and an image is created by mapping the different intensities (Skoog and Holler, 2007).

In more detail, an electron source (usually tungsten) excites the electrons of a beam to energy up to 30 keV. A magnetic condenser and objective lens system is used to reduce the spot size to a diameter of 2-10 nm so that it is a focused beam when it reaches the specimen. The beam scans the surface of the sample using two pairs of electromagnetic coils located within the objective lens. One pair deflects the beam in the x-direction and the other deflects the beam in the y-direction. Scanning is controlled by applying an electrical signal to one of the coils and varying the signal as a function of time. This

moves the electron beam in a straight line across the sample and returns it to the original position. The signal is then applied to the y coil to deflect the beam in the y-direction slightly before moving in another line across the x-direction. There are two image monitors used: one is used at a scan rate of 50 frames per second to appear as an image, and the other is for photographic reading, usually 1 frame in 50 to 100 seconds for high resolution (Skoog and Holler, 2007).

These studies used Energy Dispersive X-ray Spectrometry (EDX) 15mm with a detector distance of 1.5 mm for elements analysis and found and mapped Fe, Cl, S, Al, Fe, O, C elements. The SEM of the iron rust from India at 1.5K is displayed in Figure 3.17 along with a composition map displaying S, Fe, Al, and C with the vast majority of the surface as iron.

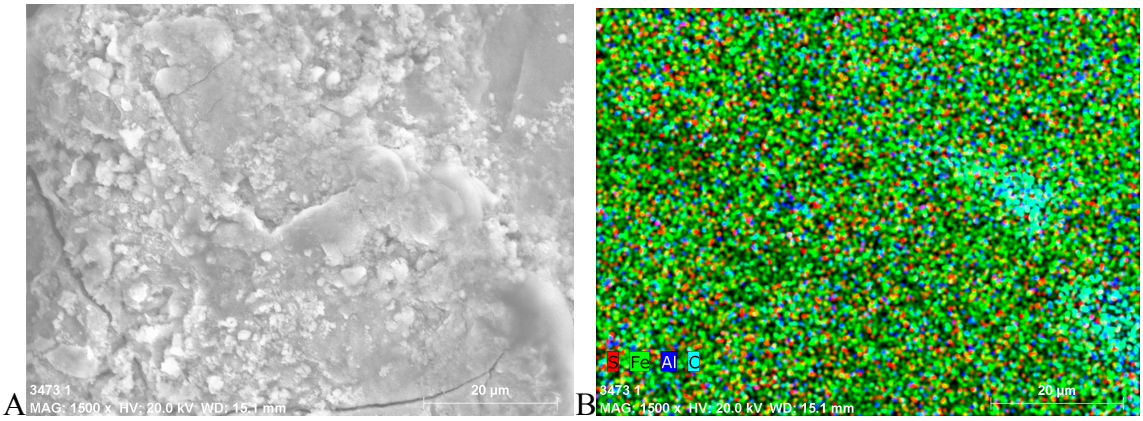

Figure 3.17: (A) SEM of Iron Rust from India Fe 1.5K, (B) map of composition of surface of scrap iron S (red), Fe (green), Al (blue), C (teal).

3.5.7 Respirometric Analysis

Respirometric analysis was carried out to study whether the the chemicals remaining in the treated samples could be biodegraded at a CETP. For that reason sludge from a local CETP in India was used as the substrate for respirometric analysis. This allowed for the determination of whether the sludge from a CETP can uptake oxygen in the presence of the contaminants left in the photo-Fenton oxidized samples. Respirometric analysis was only completed for partially oxidized samples since the COD of the fully oxidized samples were found to be below the effluent limit and too low to act as food for any bacterial activity. If the bacteria are able to consume the pollutant they are given, they will, and in return they will release oxygen which can be measured in the digital oxygen system (model 10, Rank Brothers, Bottisham UK) instrument. All oxygen uptake experiments were done in triplicate; an average value of the three tests is shown here.

After the digital oxygen system was initiated using phosphate buffer, the next step is to measure the oxygen being released by the bacteria when there is no pollutant in the phosphate buffer substrate—this is called endogenous activity. After 180 seconds, the substrate is added and the readings are recorded as exogenous activity. In order to calculate oxygen uptake by a bacterial sludge in an oxidized solution the first step is to subtract the exogenous activity from the endogenous activity. Next, that answer should be multiplied by mg of 100% solubility of oxygen (8.53 mg); this will give mg oxygen L^{-1} min^{-1}. Next it should be considered that 32 g of oxygen are in one liter to figure out moles in solution (thus multiplying by 1000 mL L^{-1} and dividing by 32000 mg oxygen) to calculate mMols oxygen $minute^{-1}$. Finally there is 1 OD of substrate per mL in 3 mL

solution. This is 3 OD cell weight meaning 0.33 mg dry weight of sludge. To figure out how much 0.33 mg cells is consumed, divide by that number to come up with nmol oxygen minute^{-1} mg dry weight cells^{-1}. If this number is positive, it means that the bacteria is able, hypothetically, to consume the substrate; if the number is negative, the substrate is not being utilized by the sludge bacteria.

The biological variable was treated as dependent and was analyzed using three-way analysis of variance (Andonian *et al*, 2011), to determine the main effects and the interaction effects due to three factors. For Reactive Dyes, the factors were color (red, yellow, or blue), iron quantity (low, medium, or high), and filtration method (no filter or sand filter). For Acid Dyes, the factors were color (red, yellow, or blue), partial oxidation time (1, 2, or 3), and filtration method (no filter or sand filter). For each combination of factors, the dependent variable data was available in triplicate, resulting into a balanced factorial design. If Y_{ijk} denotes the dependent variable, then the three-way ANOVA complete model would be given by Equation 3.1 where, m is the overall mean, α represent effect due to i^{th} history (i=1,2,3), β gives the effect due to j^{th} pre-treatment (j = 1,2,3,4) and g provides the effect due to kth substrate.

$$Y_{ijk} = m + \alpha_i + \beta_j + g_k + (\alpha\beta)_{ij} + (\beta g)_{jk} + (\alpha g)_{ik} + (\alpha\beta g)_{ijk} + e_{ijk} \qquad (3.1)$$

The model also includes all the possible two-way interaction and the three-way interaction. The e is the error component, which is distributed $N(0, s^2)$. The ANOVA was

performed with this full model separately for all the three variables similar to Narde *et al.* (2004).

3.6 Summary

In this chapter the experimental procedures used in this study were described. In review, Reactive, Acid, and Acid with Soap and Soda dyes of either red, yellow, or blue, at 5 g/L were chosen because they imitate cottage-scale silk dyeing operations. The container (reactor) for the 1-liter laboratory studies was a simple, readily available plastic tub holding rusty metal sheet iron at the bottom for the reaction to occur. The container for the field studies was made of scrap rusty metal and held 50 to 100-liters for the demonstration project. The rusty metal is a replacement for the iron salt required for the photo-Fenton oxidation process to occur. The angle of natural UV light from the sun differed between the two testing sites location in India and the USA. Hydrochloric acid was used to lower the pH to 2.5. Hydrogen peroxide is used as the oxidizing agent and the quantity varied according to color and dye type. 6% hydrogen peroxide was used for laboratory studies, and 50% hydrogen peroxide was used for field studies. Partial and full oxidation times were compared and varied according to dye color and type. Sand and carbon filtration were used (with an added cotton filter for the demonstration project) to separate sludge from the oxidized solution. All samples were tested for color removal (UV-visible spectrometry), organics removal (COD), organics identification (GC/MS), metals present (ICP), acidity (pH), and biodegradability (respirometric analysis).

CHAPTER 4 – REACTIVE DYE

PHOTO-FENTON OXIDATION RESULTS AND DISCUSSION

4.1 Introduction

Reactive dye was chosen for this study because of its wide use in silk dyeing industries throughout the world. Its chemical composition varies greatly by color and is detailed in Chapter 3. Reactive Red 120, Reactive Yellow 81, and Reactive Blue 4 were specifically used in this study. The laboratory-scale study detailed here used 5 g/L dye mixed in 1-liter tap water which was then acidified to pH 2.5 using hydrochloric acid. Next, hydrogen peroxide was added as an oxidizing agent, and the resulting mixture was poured over rusty scrap iron to a depth of 2.5 cm. The mixture was then left in the sun (in India or the USA) for the appropriate time for full or partial photo-Fenton oxidation to occur. Tests were performed with three levels of iron surface area (high: 645 cm^2; medium: 323 cm^2; low: 161 cm^2). Samples were then tested after experiencing three filtration methods (none, sand, sand and carbon). For ease of documentation, the abbreviations listed in Table 4.1 are used for notation of the different sample types and Table 4.2 for notation of the control samples. Methodology of the experimental procedures is detailed in Chapter 3.

Complete analysis of all samples was completed using UV-visible spectrometry, COD, GC/MS, and ICP. The purpose of this was to determine the organic and inorganic contaminants left in solution. In addition, respirometric analysis was completed to predict the biodegradability of the contaminants left in solution.

Table 4.1: Abbreviations of sample names for Reactive dyes.

Oxidation Time (Full or Partial)	Filtration Type	Iron Surface Area (High, Medium, Low)	Abbreviation
Full	None	High	R1H
Full	Sand	High	R2H
Full	Sand and Carbon	High	R3H
Partial	None	High	R4H
Partial	Sand	High	R5H
Partial	Sand and Carbon	High	R6H
Full	None	Medium	R1M
Full	Sand	Medium	R2M
Full	Sand and Carbon	Medium	R3M
Partial	None	Medium	R4M
Partial	Sand	Medium	R5M
Partial	Sand and Carbon	Medium	R6M
Full	None	Low	R1L
Full	Sand	Low	R2L
Full	Sand and Carbon	Low	R3L
Partial	None	Low	R4L
Partial	Sand	Low	R5L
Partial	Sand and Carbon	Low	R6L

Note: If iron surface area is not taken into account, the notation R1*-R6* will be used.

Table 4.2: Abbreviations of control names

Oxidation Time (t_0 or t_F Full)	Added Chemicals (None, HCl, HCl and H_2O_2)	Abbreviation
t_0	None	C1
t_0	HCl	C2
t_0	HCl and H_2O_2	C3
t_F Full	HCl	C4
t_F Full	HCl and H_2O_2	C5

4.2 UV-visible Spectrometry Results

4.2.1 Rate Reaction

UV-visible spectrometry was used as an analysis method to determine the optimal time for partial and full oxidation for Reactive Dyes using photo-Fenton oxidation after optimizing hydrogen peroxide quantity (detailed in Chapter 3). Undiluted C1, R1H, and R4H spectra of Reactive Red 120, Reactive Yellow 81, and Reactive Blue 4 are presented in Figure 4.1 to display the unmodified spectra peak heights for t_0, partial, and full oxidation clearly. Figure 4.1 (A) displays C1, R1H, and R4H spectra of the three

Reactive Dye colors, Fig. 4.1 (B) displays C1, R1M, and R4M spectra of the three Reactive Dye colors, and Fig. 4.1 (C) displays C1, R1L, and R4L spectra of the three Reactive Dye colors. Generally, UV and visible peaks for t_0 are beyond the 4.0 maximum of Fig. 4.1 thus denoting the need for decolorization and degradation. Partial oxidation visible peaks have decreased to within the 4.0 scale and display clear peaks that can be described as individual organic chemicals. Full oxidation samples displayed peaks at a lower UV range and no peaks in the visible range meaning that full oxidation time was chosen when complete decolorization had occurred. Table 3.7 lists the partial and full oxidation times chosen from Fig. 4.1 for the three Reactive Dye colors using different iron surface areas. The actual control peak heights C1-C5 are calculated from dilutions in Table A.1 for Reactive Red 120, A.3 for Reactive Yellow 81, and A.5 for Reactive Blue 4 in Appendix A.

A

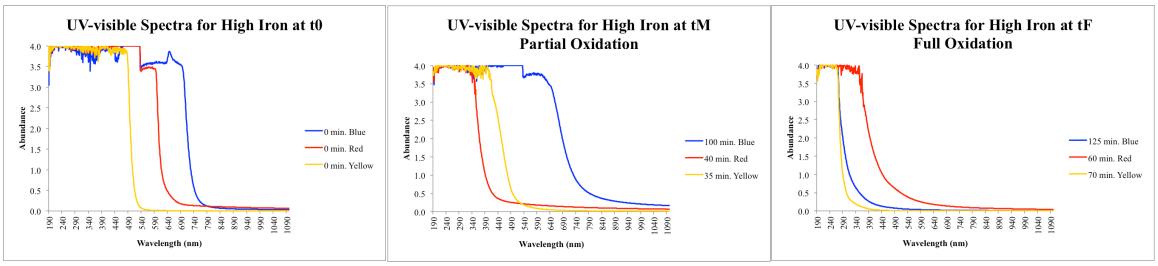

B

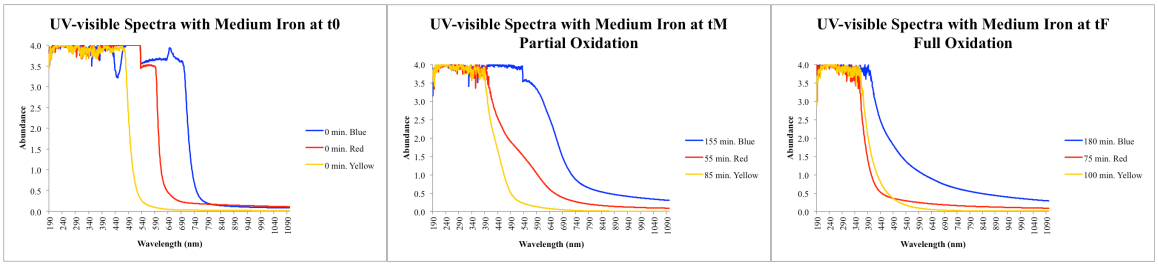

C

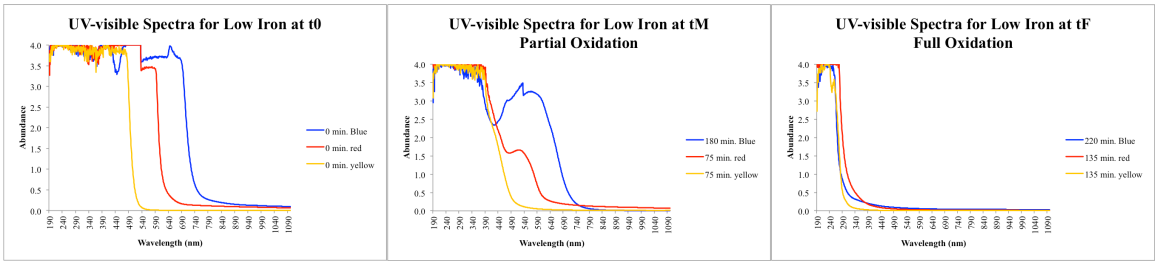

Figure 4.1: UV-visible spectra for t_0, partial oxidation, and full oxidation of the three Reactive Dye colors using (A) high iron, (B) medium iron, and (C) low iron.

4.2.2 Partial and Full Oxidation Results

4.2.2.1 Reactive Red 120

Table 3.12 lists the wavelengths of the peaks found in the UV-visible spectra for Reactive Red 120. Figure A.1 in Appendix A displays diluted samples of the Reactive Red 120 controls C1-C5. Table A.1 in Appendix A displays calculated actual peak heights for C1-C5 from dilutions. Table A.2 in Appendix A displays peaks for Reactive Red 120 R1H-R6H, R1M-R6M, and R1L-R6L. The results can be viewed in Fig. 4.2 which compares (A) R1H-R6H, (B) R1M-R6M, and (C) R1L-R6L to the diluted control peak

C1. Peaks found at 206 nm were only present after acid and hydrogen peroxide were added to solution (C2-C5). Peaks at 237 nm, 291 nm, 371 nm, 512 nm, and 536 nm were also visible in C1.

In general and despite treatment, the peak at 206 nm stayed much higher than the other pollutants in solution. The contaminants displaying UV peaks at 206 nm, 237 nm, 291 nm, 371 nm were reduced most by full oxidation. Sand and carbon filtration following oxidation greatly decreased the height of the peaks by physically removing the organics out of solution. The greatest impact of iron on peak degradation occurred for medium iron.

The contaminants displaying visible peaks at 512 nm and 536 nm degraded more by partial oxidation than by full oxidation consistently for all iron levels. However, sand and carbon filtration following full oxidation was more effective at removing the chemicals responsible for peaks at 512 nm and 536 nm (thus making full oxidation followed by sand alone or sand and carbon the most effective treatment). The medium iron level was still the most effective for removal of these organics. As with the UV wavelength peaks, generally sand filtration accomplished more than the carbon filter due to physical capturing of the solids created by the photo-Fenton oxidation process and physically removed them from solution, although carbon filtration did no harm to the process.

A

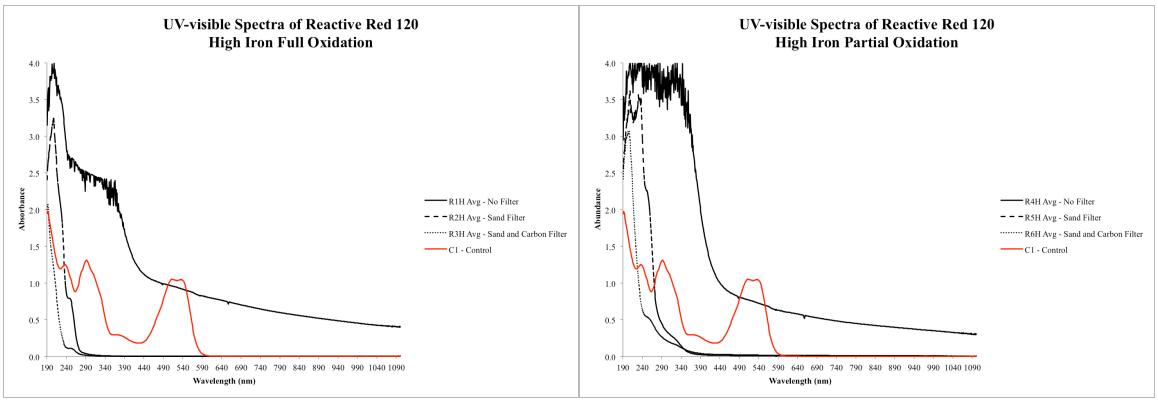

B

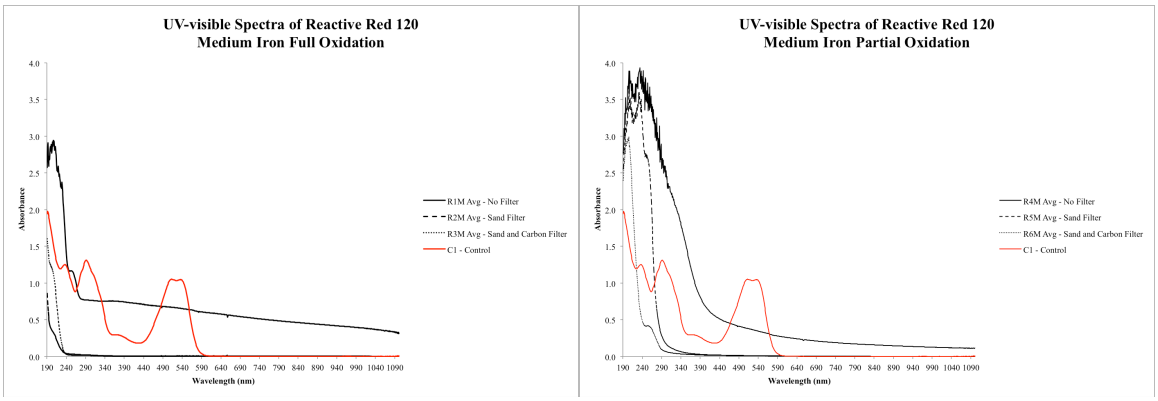

C

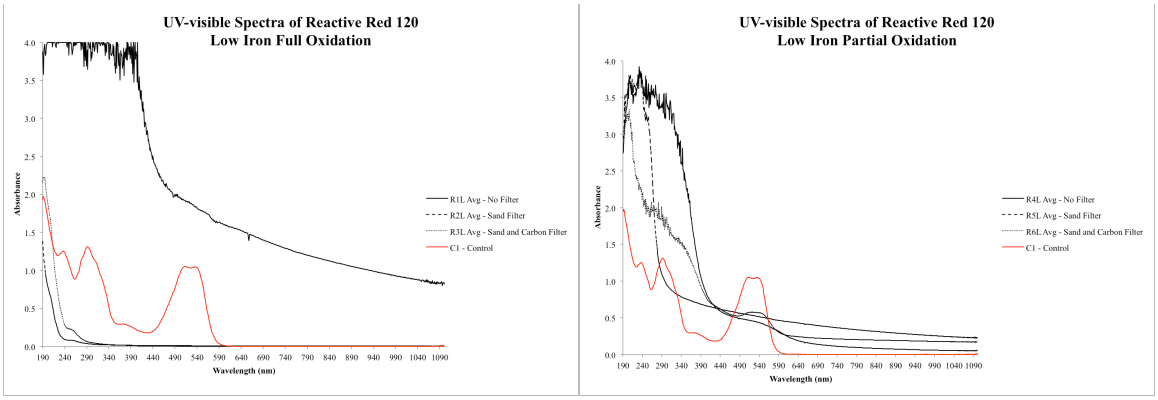

Figure 4.2: Reactive Red 120 UV-visible spectra of the diluted control C1 compared to (A) R1H-R6H, (B) R1M-R6M, and (C) R1L-R6L.

4.2.2.2 Reactive Yellow 81

Table 3.12 lists the peaks found in UV-visible spectra for Reactive Yellow 81. Figure A.2 in Appendix A displays diluted samples of the Reactive Yellow 81 controls C1-C5.

Table A.3 in Appendix A lists calculated actual peak heights for C1-C5 from dilutions. Table A.4 in Appendix A displays peaks for Reactive Yellow 81 R1H-R6H, R1M-R6M, and R1L-R6L. These results can also be viewed in Fig. 4.3 which compares the UV-visible spectra of the diluted control C1 for Reactive Yellow 81 to (A) R1H-R6H, (B) R1M-R6M, and (C) R1L-R6L. Peaks for Reactive Yellow 81 were found at 206 nm, 229 nm, 243 nm, and 520 nm in C2-C5 only after acid and hydrogen peroxide were added to solution. Peaks at 268 nm, 352 nm, and 410 nm were also found in C1.

Just as with Reactive Red 120, the peak at 206 nm remained after treatment. In addition, the peak at 229 nm stayed much higher than the other peaks despite treatment. The contaminants that displayed UV peaks at 206 nm, 229 nm, 243 nm, 268 nm were reduced the most from full oxidation compared to partial oxidation. Sand and carbon filtration following oxidation greatly decreased the heights of the peaks by physically removing the organics out of solution. In general medium iron had the greatest impact on the degradation of these peaks.

The contaminants displaying peaks at 352 nm, and 410 nm exhibited behavior similar to both the UV and visible peaks of Reactive Red 120. Partial oxidation decreased peak height to below full oxidation samples; however, sand and carbon filtration raised the levels again. Full oxidation followed by sand and carbon decreased the levels to near negligible. Medium iron gave the lowest numbers, however the same samples using low and high iron were similar.

The contaminants displaying a visible peak at 520 nm was reduced most from full oxidation followed by sand and carbon filtration. Unlike all other dyes tested, low iron levels removed pollutants from the treated Reactive Yellow 81 solution the most, closely followed by medium and then high iron.

A

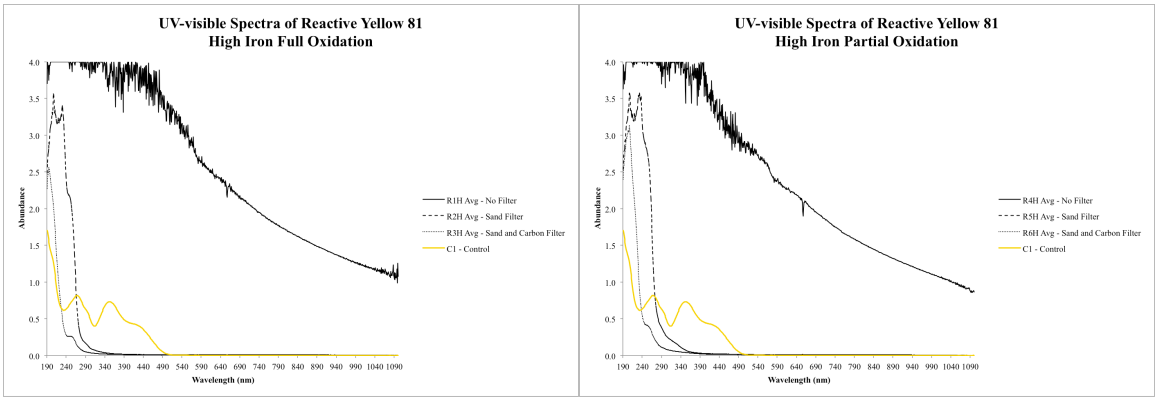

B

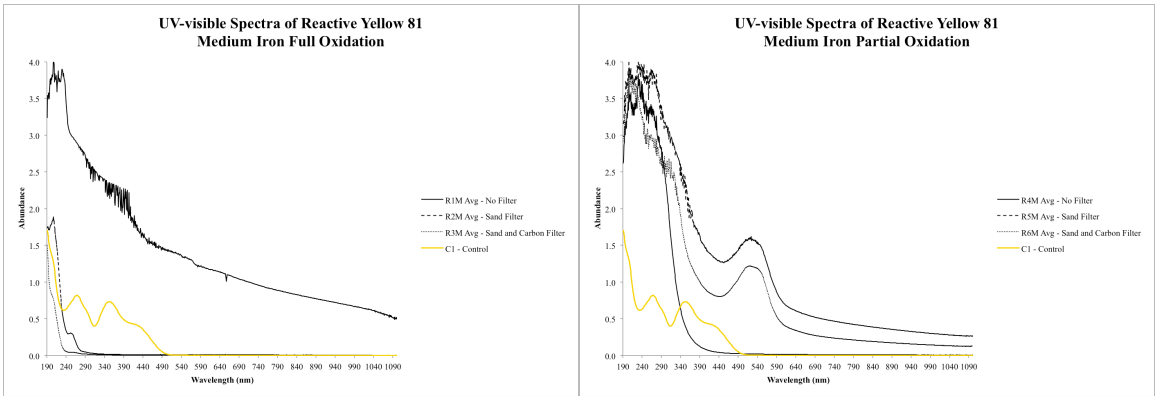

C

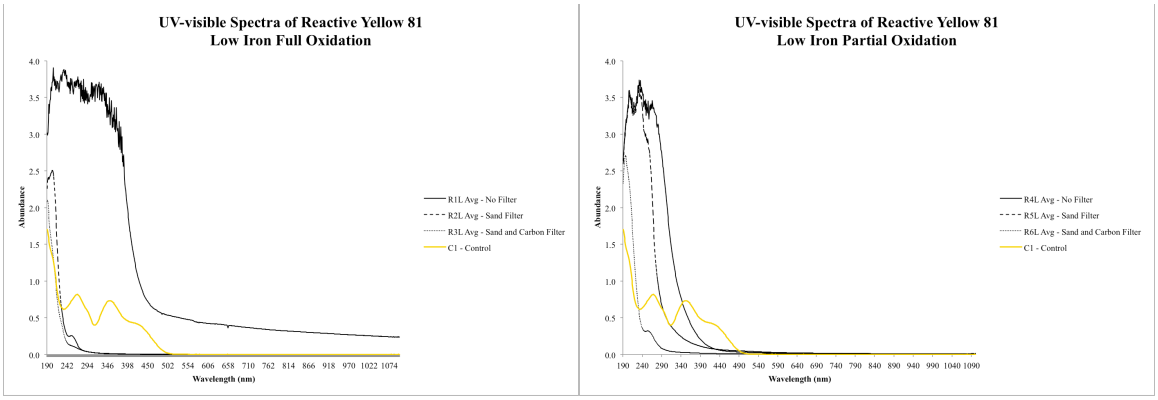

Figure 4.3: Reactive Yellow 81 UV-visible spectra of the diluted control C1 for Reactive Yellow 81 compared to (A) R1H-R6H, (B) R1M-R6M, and (C) R1L-R6L.

4.2.2.3 Reactive Blue 4

Table 3.12 lists the peaks found in UV-visible spectra for Reactive Blue 4. Figure A.3 in Appendix A displays diluted samples of the Reactive Blue 4 controls C1-C5. Table A.5 in Appendix A displays calculated actual peak heights for C1-C5 from dilutions. Table A.6 in Appendix A displays peaks for Reactive Blue 4 R1H-R6H, R1M-R6M, and R1L-R6L. These results can also be viewed in Fig. 4.4 which compares the UV-visible spectra of the diluted control C1 for Reactive Blue 4 to (A) R1H-R6H, (B) R1M-R6M, and (C) R1L-R6L. Peaks for Reactive Blue 4 were found at 206 nm, and 520 nm only after acid and hydrogen peroxide were added to solution (C2-C5), while peaks at 230 nm, 258 nm, 369 nm, and 597 nm were also found in C1.

Just as with Reactive Red 120 and Reactive Yellow 81, the UV peaks at 206 nm, 230 nm, 258 nm remained much higher than the visible peaks despite treatment. Degradation of the contaminants displaying these UV peaks occurred most after full oxidation using high iron followed by sand and carbon filtration.

The contaminants displaying peaks at 369 nm, 520 nm, and 597 nm presented a mixture of results. The greatest degradation was still with high iron, followed closely by low iron and medium iron.

A

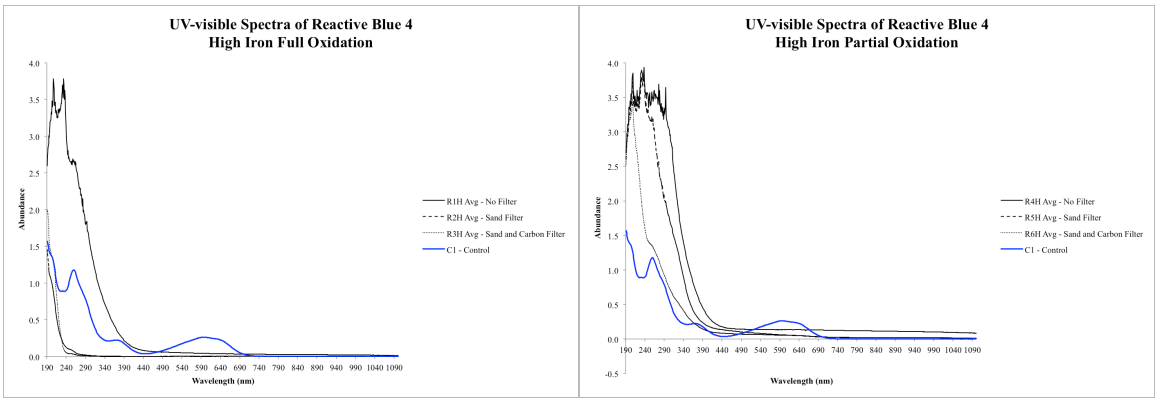

B

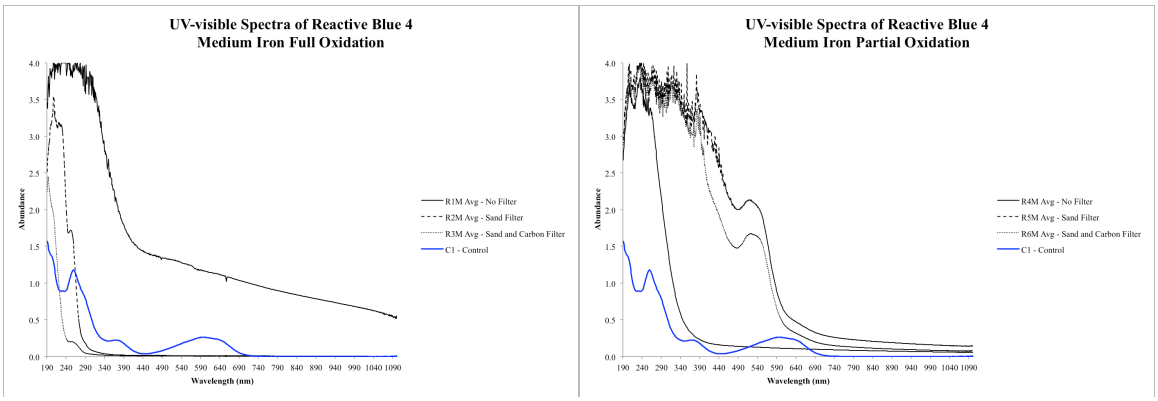

C

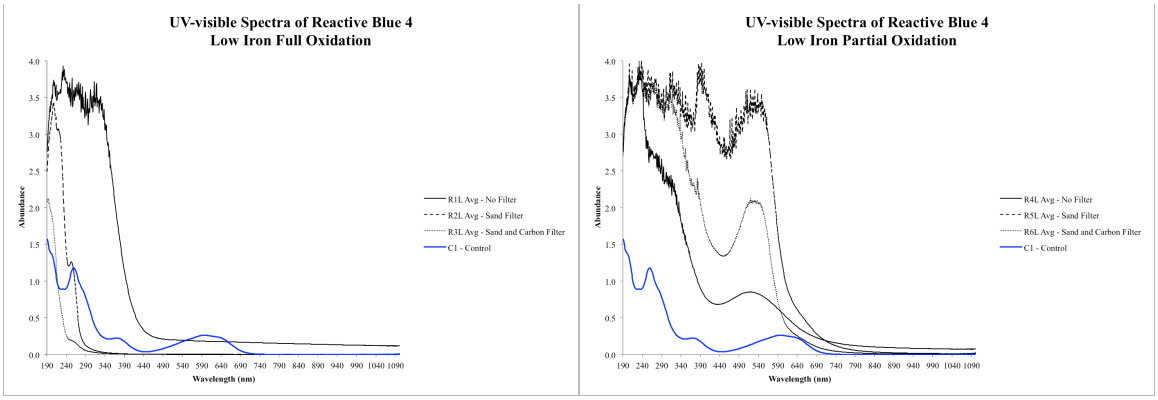

Figure 4.4: Reactive Blue 4 UV-visible spectra of the diluted control C1 for Reactive Blue 4 compared to (A) R1H-R6H, (B) R1M-R6M, and (C) R1L-R6L.

4.3 COD Results

COD was used to analyze organic levels in solution. COD levels showed great variability, even when comparing similar samples. This is because the high level of dye

used in this study has an exceptional level of organic material. Photo-Fenton oxidation also forms sludge in solution that is comprised of dye and rust from the iron catalyst. For this reason COD levels that dropped below the Karnataka State Pollution Control Board's (KSPCB) allowable 250 ppm are particularly noted. In the analysis of the data, it is important to also consider ambient temperature, sunlight, and pH during the experiment in order to capture the effects of these variables on the COD reduction caused by the photo-Fenton oxidation process. Chapter 2 contains a discussion of a connection between temperature, sunlight, and COD reduction in dye effluent for studies conducted with dyes at lower concentrations; it is uncertain whether there will be such connections for the photo-Fenton oxidation of the 5 g/L dye effluent.

4.3.1 Reactive Red 120

COD results for Reactive Red 120 as it relates to temperature, pH, iron, and sunlight can be viewed in Table B.1 in Appendix B. Table 4.3 presents an overview of the average results in India and the USA comparing C1-C5 to R1H-R6H, R1M-R6M, and R1L-R6L. Figure 4.5 depicts the general decrease of COD from C1 to R4*, R1*, R5*, R6*, R2*, R3* for the respective surface areas of iron in solution.

The control samples had COD levels that ranged between 2392 and 7320 ppm. Full oxidation using medium iron followed by sand filtration lowered COD levels the most and this agrees with the UV-visible spectrometry results. COD decreased well below the permissible effluent levels using full oxidation followed by filtration despite iron surface area. From highest to lowest, the COD value trends, regardless of iron

differences, are R4*, R1*, R5*, R6*, R2*, R3*. The fully oxidized samples produced more sludge than the partially oxidized samples. Sludge kept the COD higher than permissible effluent levels; however, after physical removal of the sludge using sand and carbon filtration the COD lowered close to negligible. Since partial oxidation does not fully precipitate the organics out of solution (and thus creates less sludge), the sand and carbon filtration cannot fully separate them from the water base which results in a higher COD. The low iron sample in India did not exactly follow the same trend since full oxidation brought the COD to permissible effluent levels and much lower than the partially oxidized sand and carbon filtered samples.

Table 4.3: COD overview comparing C1-C5 to R1H-R6H, R1M-R6M, and R1L-R6L for Reactive Red 120 in India and the USA.

Reactive Red 120	Avg. COD India using High Iron	Avg. COD USA using High Iron	Avg. COD India using Medium Iron	Avg. COD USA using Medium Iron	Avg. COD India using Low Iron	Avg. COD USA using Low Iron
C1	2388	3000	3084	3000	2334	3000
C2	NA	2594	NA	2594	NA	2594
C3	NA	6920	NA	6920	NA	6920
C4	NA	2392	NA	2392	NA	2392
C5	NA	7320	NA	7320	NA	7320
R1H	558	700	750	140.4	288	1530
R2H	16	25.5	55	0	0	0
R3H	98	3	74	0	0	1
R4H	627	9780	1209	850	3822	8820
R5H	670	136	302	0.01	924	480
R6H	NA	103.5	88	0.025	756	451.5

A

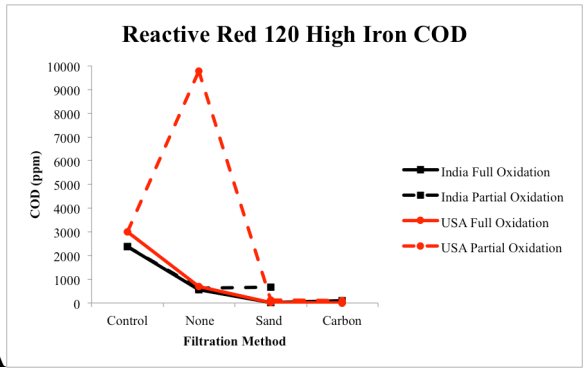

B

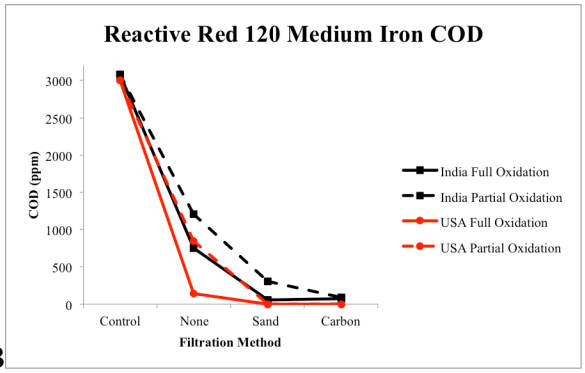

C

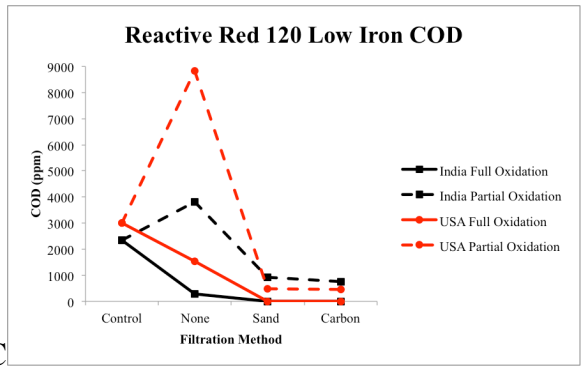

Figure 4.5: COD results comparing Reactive Red 120 USA and India samples C1 to (A) R1H-R6H, (B) R1M-R6M, and (C) R1L-R6L.

4.3.2 Reactive Yellow 81

COD results for Reactive Yellow 81 as it relates to temperature, pH, iron, and sunlight can be viewed in Table B.2 in Appendix B. An overview of the average results in India and the USA comparing C1-C5 to R1H-R6H, R1M-R6M, and R1L-R6L is presented in Table 4.4. Figure 4.6 depicts the general decrease of COD from C1 to R4*, R1*, R5*,

R6*, R2*, R3* for the respective surface areas of iron in solution.

The control samples had COD levels that ranged between 2070 and 9760 ppm. Full oxidation using medium iron followed by sand filtration lowered the COD levels the most; this matches the UV-visible spectrometry results. When full oxidation followed by filtration was used, COD decreased well below the allowable effluent levels for all iron surface area levels. From highest to lowest, the COD value trends, despite iron differences, were the same as Reactive Red 120: R4*, R1*, R5*, R6*, R2*, R3*. The trend is independent of iron level and the location of the study. Note, while the trends are consistent, the individual numbers can differ greatly between repeated experiment samples.

The fully oxidized sample produced sludge that kept the COD higher than permissible effluent levels. However, after physical removal of these organics, the sand and carbon filtered samples brought COD close to negligible. Since partial oxidation does not fully precipitate the organics out of solution, the sand and carbon filtration cannot fully separate them from the water base, resulting in a higher COD measurement. The high iron sample in India did not follow this same trend—the fully oxidized and filtered sample had higher COD than the partially oxidized and filtered sample.

Table 4.4: COD overview of Reactive Yellow 81 comparing C1-C5 to R1H-R6H, R1M-R6M, and R1L-R6L in India and the USA.

Reactive Yellow 81	Avg. COD India using High Iron	Avg. COD USA using High Iron	Avg. COD India using Medium Iron	Avg. COD USA using Medium Iron	Avg. COD India using Low Iron	Avg. COD USA using Low Iron
C1	1794	5540	2070	5540	2328	5540
C2	NA	3700	NA	3700	NA	3700
C3	NA	8180	NA	8180	NA	8180
C4	NA	4000	NA	4000	NA	4000
C5	NA	9760	NA	9760	NA	9760
R1H	270	513	399	121.2	246	550
R2H	139	33.5	62	0.015	28	0
R3H	101	13	32	0.04	8	1
R4H	768	9240	600	1400	954	4380
R5H	0	84.5	142	0.35	108	187
R6H	NA	33.5	112	0.07	50	105.5

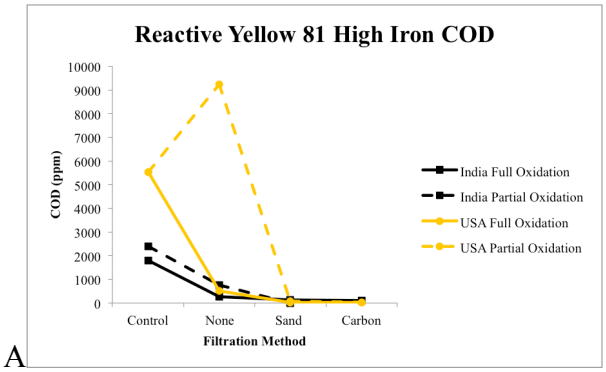

A

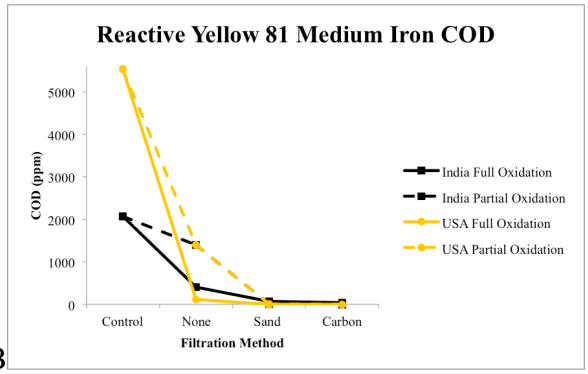

B

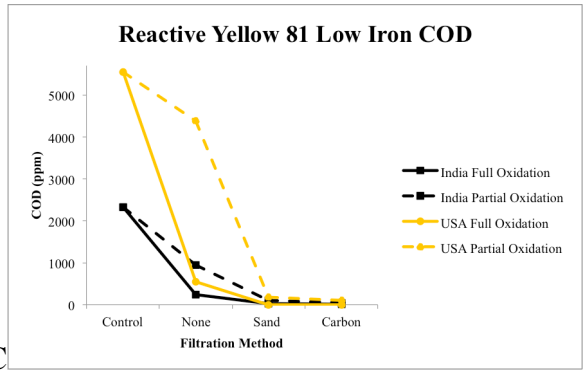

C

Figure 4.6: COD results comparing Reactive Yellow 81 USA and India samples C1 to (A) R1H-R6H, (B) R1M-R6M, and (C) R1L-R6L.

4.3.3 Reactive Blue 4

COD results for Reactive Blue 4 as it relates to temperature, pH, iron, and sunlight can be viewed in Table B.3 in Appendix B and an overview of the average results in India and the USA in Table 4.5 comparing C1-C5 to R1H-R6H, R1M-R6M, and R1L-R6L. Figure 4.7 depicts the general decrease of COD from C1 to R4*, R1*, R5*, R6*, R2*, R3* for

the respective surface areas of iron in solution.

The control samples had COD levels that ranged between 2262 and 7240 ppm. Full oxidation using medium iron followed by sand filtration lowered COD levels the most. This agrees with the UV-visible spectrometry results. COD decreased well below the allowable effluent levels using full oxidation followed by filtration, independent of the iron surface area. From highest to lowest, the COD value trends were the same as Reactive Red 120 and Reactive Yellow 81: R4*, R1*, R5*, R6*, R2*, R3*. The trend is consistent for different iron surface area levels and for the location of the study.

The fully oxidized sample produced sludge that kept the COD higher than allowable effluent levels. However, the sand and carbon filtered samples brought COD close to negligible as the organics were physically removed. Since partial oxidation does not fully precipitate the organics out of solution, the sand and carbon filtration cannot fully separate them from the water base, resulting in a higher COD measurement. The high iron sample in India did not follow this same trend—the fully oxidized and filtered sample had higher COD than the partially oxidized and filtered sample.

Table 4.5: COD overview of Reactive Blue 4 comparing C1-C5 to R1H-R6H, R1M-R6M, and R1L-R6L in India and the USA.

Reactive Blue 4	Avg. COD India using High Iron	Avg. COD USA using High Iron	Avg. COD India using Medium Iron	Avg. COD USA using Medium Iron	Avg. COD India using Low Iron	Avg. COD USA using Low Iron
C1	4590	2360	4170	2360	3396	2360
C2	NA	2700	NA	2700	NA	2700
C3	NA	5620	NA	5620	NA	5620
C4	NA	2262	NA	2262	NA	2262
C5	NA	7240	NA	7240	NA	7240
R1H	1404	116	282	162	228	4560
R2H	39	8.5	219	0	62	78
R3H	24	0.5	32	0	30	10.5
R4H	1497	6720	1416	210	1536	13980
R5H	82	280	216	0.72	3855	3000
R6H	NA	88	124	0.24	190	975

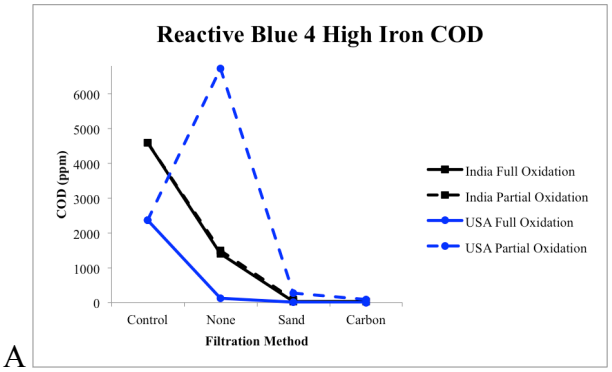

A

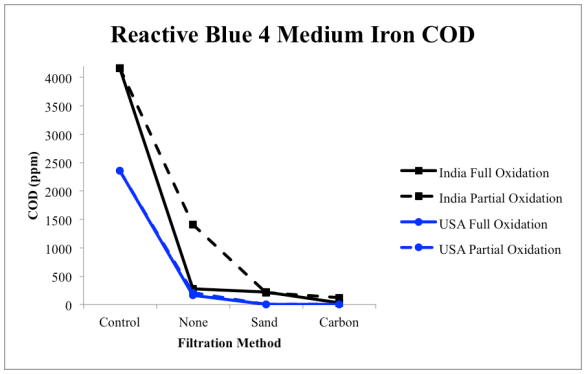

B

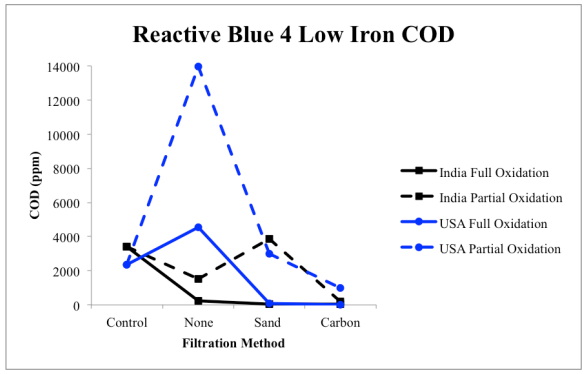

C

Figure 4.7: COD results comparing Reactive Blue 4 USA and India samples C1 to (A) R1H-R6H, (B) R1M-R6M, and (C) R1L-R6L.

4.3.4 Sludge Production

Sludge production was notable during the photo-Fenton oxidation process with more sludge being produced for longer duration experiments. Sludge volume was quantified during the India studies and volumes are listed in Table B.1 for Reactive Red 120, Table B.2 for Reactive Yellow 81, and Table B.3 for Reactive Blue 4 in Appendix B. Percent

volume sludge per 1-liter laboratory tests are listed in Table 4.6 for each dye color after full oxidation. High iron surface area produced the least amount of sludge, followed by low iron, and then medium iron. Sludge was removed from solution using filtration. Therefore, the presence of sludge in non-filtered samples can greatly impact the overall COD level. During an interview with a medium-scale dyer in India, it was learned that sludge production created from biodegradation (customary method of dye effluent treatment in medium and large-scale textile plants) of their wastewater, was approximately 15% of total solution. Percentage sludge production using sustainable photo-Fenton oxidation was much less.

Table 4.6: Percent sludge produced per 1-liter laboratory study during full oxidation in India according to color and surface area of iron.

Dye Color	High Iron	Medium Iron	Low Iron
Reactive Red 120	0.971%	6.74%	6.45%
Reactive Yellow 81	0.962%	7.33%	4.33%
Reactive Blue 4	3.33%	7.96%	5.43%

4.3.5 Solar Irradiance and Temperature

Generally, the solar irradiance in the USA tests was higher than solar irradiance in the India tests since studies in India were completed as the rainy season was beginning. The solar irradiance in India was between 81-485 W/m^2 and in the USA between 383-720 W/m^2. Meanwhile, the USA tests were completed at lower ambient temperatures than the India tests, due to the time of year the studies were performed. The temperatures in India ranged from 25.6-28.9 ºC and in the USA 0.41-23.9 ºC. Decolorization and degradation occurred for both test sites, indicating that the process can work for a wide range of temperatures and solar irradiances. COD levels varied more as a result of time

and filtration rather than solar irradiance and temperature. The COD levels that resulted from the extreme ends of solar irradiance or temperature were mid-range COD results. It is therefore concluded that while UV irradiance and temperature are important parts of the chemical reaction, without which the reaction could not take place, they are not key factors in the success of the study. The tests were successful despite the lack of direct sunlight in partly cloudy or partly sunny conditions as long as there was daylight. This is important for eventual field implementation of the process, as both solar irradiance and temperature are variables that cannot be easily controlled in practice.

4.4 GC/MS Results

GC/MS analysis was used to measure and identify chemical intermediates found in solution before and after oxidation. To qualify, chemical peaks detected by the GC must reach a minimum of 10,000 abundance (based on electrical signal passed through sample) and match the MS library with 80% or more accuracy. In order to verify the quantification of abundance of organics found in solution, a 95% pure sample of Tolylene, 2,4-diisocyanate (also called Benzene, 2,4-diisocyanato-1-methyl) was tested using the same GC/MS methods listed in Chapter 3. This aromatic and cyanate chemical was chosen because of its abundance in the reactive dye solution after treatment. Figure C.46 in Appendix C displays the GC/MS graph of this control. The 95% pure sample absorbed onto the Solid Phase Micro Extraction (SPME) fiber was found to have an abundance of Benzene, 2,4-diisocyanato-1-methyl at 1,800,000; 2H-Benzimidazol-2-one, 1,3-dihydro-5-methyl at 100,000; Bis(2-ethylhexyl) phthalate at 95,000; Squalene at 50,000; 2-Propenoic acid, 3-(4-methoxyphenyl)-, 2-ethylhexyl ester

at 40,000; and Dodecanoic Acid, Ethyl Ester at 28,000. The presence of Benzene, 2,4-diisocyanato-1-methyl at 1,800,000 abundance in the pure sample verifies the accuracy of finding a lesser abundance in treated samples tested using the same SPME and GC/MS methodology. The presence of the other organics in the control sample reinforce that the control sample was only 95% pure. The level of Benzene, 2,4-diisocyanato-1-methyl in the 95% pure sample can be described by either fraction of mass or fraction of ions. GC/MS displays the fraction of mass in its measured level of abundance, here reaching 85% of the total chemicals found; however, the sample is labeled 95% pure based on the fraction of ions in solution.

4.4.1 Reactive Red 120

Table C.1 in Appendix C lists all of the GC/MS results as they relate to C1-C5, R1H-R6H, R1M-R6M, and R1L-R6L for Reactive Red 120 including when complete degradation had occurred (which resulted in no noticeable peaks). Table 4.7 contains an overview of GC/MS results of all chemicals found in C1-C5, R1H-R6H, R1M-R6M, and R1L-R6L for Reactive Red 120 and what type of compound each result is and their responsible functional groups. Reactive Red 120 had various organic compounds left in solution after treatment: aromatic and alcohol combined compounds to a total abundance of 177,700; aromatic and cyanate combined compounds at 127,000 abundance; aromatic and ether combined compounds at 68,000 abundance; and aromatic and aldehyde combined compounds at 49,000 abundance. Figures C.1, C.2, C.3, C.4, and C.5 in Appendix C display GC/MS peaks for C1, C2, C3, C4, and C5 respectively for Reactive Red 120.

C1 had the most detectable organic chemicals found in solution. Regarding treated samples, fully oxidized samples degraded more than partially oxidized samples. Medium iron samples had the least amount of organics as found from GC/MS analysis. India had many more organics in solution than USA samples. Full oxidation using medium iron followed by sand filtration in the USA revealed the least amount of chemicals (carbon samples were not tested if sand filtered samples found no chemicals).

Table 4.7: GC/MS overview of Reactive Red 120 comparing C1-C5 to R1H-R6H, R1M-R6M, and R1L-R6L.

Code	Country	Chemical Name	Abundance	Type of Compound	Functional Group
C1	USA	Benzene, (1-butylheptyl)	66500	Aromatic	Phenyl
C1	USA	Benzene, (1-butyloctyl)	76500	Aromatic	Phenyl
C1	USA	Benzene, (1-butylnonyl)	72000	Aromatic	Phenyl
C1	USA	Benzene, (1-ethyldecyl)	58000	Aromatic	Phenyl
C1	USA	Benzene, (1-ethylnonyl)	57000	Aromatic	Phenyl
C1	USA	Benzene, (1-ethylnonyl)	80000	Aromatic	Phenyl
C1	USA	Benzene, (1-ethyloctyl)	26500	Aromatic	Phenyl
C1	USA	Benzene, (1-methyldecyl)	72500	Aromatic	Phenyl
C1	USA	Benzene, (1-methylunecyl)	76000	Aromatic	Phenyl
C1	USA	Benzene, (1-pentylheptyl)	84000	Aromatic	Phenyl
C1	USA	Benzene, (1-pentyloctyl)	84000	Aromatic	Phenyl
C1	USA	Benzene, (1-propyldecyl)	60500	Aromatic	Phenyl
C1	USA	Benzene , (1-propylnonyl)	63000	Aromatic	Phenyl
C1	USA	Benzene, (1-propyloctyl)	69000	Aromatic	Phenyl
C1	USA	Cyclopentasiloxane, decamethyl	65000	Organic	Silica
C1	USA	Cyclotetrasiloxane, octamethyl	64000	Organic	Silica
C1	USA	Eicosane	41000	Alkane	Hydrocarbon
C1	USA	Heneicosane	51000	Alkane	Hydrocarbon
C1	USA	Heptadecane	52000	Alkane	Hydrocarbon
C1	USA	Hexadecane	25000	Alkane	Hydrocarbon
C1	USA	Phenol, bis(1,1-dimethylethyl)	55000	Aromatic, Alcohol	Phenyl, Hydroxy
C1	USA	Phosphoric acid tributyl ester	66000	Alkane	Hydrocarbon
C2	USA	Benzaldehyde, 4-methyl	59000	Aromatic, Aldehyde	Phenyl, Carbonyl
C2	USA	1,3-Benzenediamine, 4-methyl	89000	Aromatic, Amine	Phenyl, Amino
C2	USA	Benzene, 2,4-diisocyanato-1-methyl	135000	Aromatic, Cyanate	Phenyl, Cyanate
C2	USA	2H-Benzimidazol-2-one, 1,3-dihydro-5-methyl	67500	Aromatic, Ketone, Amine	Phenyl, Carbonyl, Amino

C3	USA	Benzaldehyde, 3-methyl	38000	Aromatic, Aldehyde	Phenyl, Carbonyl
C3	USA	Cyclotetrasiloxane, octamethyl	23000	Organic	Silica
C4	USA	Benzaldehyde, 2-methyl-	75000	Aromatic, Aldehyde	Phenyl, Carbonyl
C4	USA	Benzene, 2,4-diisocyanato-1-methyl	60000	Aromatic, Cyanate	Phenyl, Cyanate
C4	USA	Benzene, 2,4-diisocyanato-1-methyl	51000	Aromatic, Cyanate	Phenyl, Cyanate
R1L	USA2	Benzene, 2,4-diisocyanato-1-methyl	58000	Aromatic, Cyanate	Phenyl, Cyanate
R2H	India	Benzene, 1-methoxy-4-(1-propenyl)-Anethole	20000	Aromatic, Ether	Phenyl, Alkoxy
R2H	India	Butylated Hydroxytoluene	30000	Aromatic, Alcohol	Phenyl, Hydroxy
R2M	India	Phenol, 2,4-bis(1,1-dimethylethyl)	11700	Aromatic, Alcohol	Phenyl, Hydroxy
R2L	India	Phenol, 2,4-bis(1,1-dimethylethyl)	36000	Aromatic, Alcohol	Phenyl, Hydroxy
R3H	India	Benzene, 1-methoxy-4-(1-propenyl)-Anethole	23000	Aromatic, Ether	Phenyl, Alkoxy
R3H	India	Butylated Hydroxytoluene	25000	Aromatic, Alcohol	Phenyl, Hydroxy
R4H	India	Benzene, 2,4-diisocyanato-1-methyl	14000	Aromatic, Cyanate	Phenyl, Cyanate
R4L	USA2	Benzene, 2,4-diisocyanato-1-methyl	40000-70000	Aromatic, Cyanate	Phenyl, Cyanate
R5H	USA2	Benzaldehyde, 2-methyl-	49000	Aromatic, Aldehyde	Phenyl, Carbonyl
R5H	India	Benzene, 1-methoxy-4-(1-propenyl)-Anethole	25000	Aromatic, Ether	Phenyl, Alkoxy
R5H	India	Butylated Hydroxytoluene	25000	Aromatic, Alcohol	Phenyl, Hydroxy
R6H	India	Phenol, 2,4-bis(1,1-dimethylethyl)	80000	Aromatic, Alcohol	Phenyl, Hydroxy

4.4.2 Reactive Yellow 81

Table C.2 in Appendix C lists all of the GC/MS results as they relate to C1-C5, R1H-R6H, R1M-R6M, and R1L-R6L for Reactive Yellow 81 including when complete degradation had occurred (which resulted in no noticeable peaks). Table 4.8 contains an overview of GC/MS results of all chemicals found in C1-C5, R1H-R6H, R1M-R6M, and R1L-R6L for Reactive Yellow 81 and what type of compound each result is and their responsible functional groups. Reactive Yellow 81 had various organic compounds left in solution after treatment: aromatic and alcohol combined compounds left in solution to a total abundance of 261,000; aromatic and cyanate combined compounds at 119,500 abundance; aromatic and aldehyde combined compounds at 22,000 abundance; aromatic, ketone, and amine combined compounds at 20,000 abundance; aromatic, azine, and chloride combined compounds at 20,000 abundance; and aromatic, chloride, and imino combined compounds at 15,500 abundance. Figures C.6, C.7, C.8, C.9, and C.10 in Appendix C display GC/MS peaks for C1, C2, C3, C4, and C5 respectively for Reactive Yellow 81.

C1 had the most detectable organic chemicals found in solution. Regarding treated samples, partially oxidized samples degraded more than fully oxidized samples. Low iron samples had the least amount of organics as indicated by GC/MS measurements. India had many more organics in solution than USA samples. Medium iron oxidized samples in the USA returned no organics in solution.

Table 4.8: GC/MS overview of Reactive Yellow 81 comparing C1-C5 to R1H-R6H, R1M-R6M, and R1L-R6L.

Code	Country	Chemical Name	Abundance	Type of Compound	Functional Group
C1	USA	Benzene, 2,4-diisocyanato-1-methyl	185000	Aromatic, Cyanate	Phenyl, Cyanate
C1	USA	Benzene, 2,4-diisocyanato-1-methyl	35000	Aromatic, Cyanate	Phenyl, Cyanate
C1	USA	5-methyl-2-(N-ethyl-p-chlorophenyl amino)-2-thiazoline	75000	Aromatic	Phenyl
C1	USA	5-methyl-2-(N-ethyl-p-chlorophenyl amino)-2-thiazoline	375000	Aromatic	Phenyl
C1	USA	5-methyl-2-(N-ethyl-p-chlorophenyl amino)-2-thiazoline	360000	Aromatic	Phenyl
C2	USA	Benzene, 2,4-diisocyanato-1-methyl	44000	Aromatic, Cyanate	Phenyl, Cyanate
C3	USA	Benzaldehyde, 3-methyl	49000	Aromatic, Aldehyde	Phenyl, Carbonyl
C3	USA	2-Heptanone, 4-methyl	19000	Ketone	Carbonyl
C4	USA	Benzene, 2,4-diisocyanato-1-methyl	36000	Aromatic, Cyanate	Phenyl, Cyanate
C4	USA	Benzene, 2,4-diisocyanato-1-methyl	35500	Aromatic, Cyanate	Phenyl, Cyanate
R1H	USA2	Picloxydine	15500	Aromatic, Chloride, Imino	Phenyl, Chloride, Imino
R2H	USA1	Benzaldehyde, 4-methyl-	22000	Aromatic, Aldehyde	Phenyl, Carbonyl
R2H	India	Benzene, 2,4-diisocyanato-1-methyl	10000	Aromatic, Cyanate	Phenyl, Cyanate
R2M	India	Phenol, 2,4-bis(1,1-dimethylethyl)	115000	Aromatic, Alcohol	Phenyl, Hydroxy
R2M	India	1,3,5-Triazin-2-amine, 4,6-dichloro-	20000	Azine, Amine, Chloride	Azine, Amino, Chloride
R3H	India	Benzene, 2,4-diisocyanato-1-methyl	20000	Aromatic, Cyanate	Phenyl, Cyanate
R3H	India	2H-Benzimidazol-2-one, 1,3-dihydro-5-methyl-	20000	Aromatic, Ketone, Amine	Phenyl, Carbonyl, Amino
R3M	India	Phenol, 2,4-bis(1,1-dimethylethyl)	115000	Aromatic, Alcohol	Phenyl, Hydroxy
R4H	India	Benzene, 2,4-diisocyanato-1-methyl	18000	Aromatic, Cyanate	Phenyl, Cyanate
R4H	India	Benzene, 2,4-diisocyanato-1-methyl	20000	Aromatic, Cyanate	Phenyl, Cyanate
R4L	USA2	Benzene, 2,4-diisocyanato-1-methyl	20000	Aromatic, Cyanate	Phenyl, Cyanate
R5H	India	Benzene, 2,4-diisocyanato-1-methyl	20000	Aromatic, Cyanate	Phenyl, Cyanate
R5L	India	Phenol, 2,4-bis(1,1-dimethylethyl)	31000	Aromatic, Alcohol	Phenyl, Hydroxy
R6H	India	Benzene, 2,4-diisocyanato-1-methyl	11500	Aromatic, Cyanate	Phenyl, Cyanate

4.4.3 Reactive Blue 4

Table C.3 in Appendix C lists all of the GC/MS results as they relate to C1-C5, R1H-R6H, R1M-R6M, and R1L-R6L for Reactive Blue 4 including when complete degradation had occurred (which resulted in no noticeable peaks). Table 4.9 contains an overview of GC/MS results of all chemicals found in C1-C5, R1H-R6H, R1M-R6M, and R1L-R6L for Reactive Blue 4 and what type of compound each result is and their responsible functional groups. Reactive Blue 4 had various organic compounds left in solution after treatment: azine, amine, and chloride combined compounds left in solution to a total abundance of 782,000; aromatic and aldehyde combined compounds at 110,000 abundance; aromatic, chloride, and alcohol combined compounds at 27,400 abundance; aromatic and alcohol at 62,000 abundance; and aromatic and cyanate combined compounds at 19,000 abundance. Figures C.11, C.12, C.13, C.14, and C.15 in Appendix C display GC/MS peaks for C1, C2, C3, C4, and C5 respectively for Reactive Blue 4.

Unlike Reactive Red 120 and Reactive Yellow 81, C4 for Reactive Blue 4 had the most detectable organic chemicals found in solution. This means that after acidifying the solution and leaving it to react with neither oxidant nor iron catalyst in the sun, more organic compounds were found in solution. Regarding treated samples, fully oxidized samples degraded more than partially oxidized samples. Just as Reactive Yellow 81 samples, low iron samples had slightly less chemicals in solution than medium iron. USA had many more organics than India samples. Medium iron oxidized samples in India returned no organics in solution.

Table 4.9: GC/MS overview of Reactive Blue 4 comparing C1-C5 to R1H-R6H, R1M-R6M, and R1L-R6L.

Code	Country	Chemical Name	Abundance	Type of Compound	Functional Group
C2	USA	1-Hexanol, 3,5,5-trimethyl	60000	Alkane, Alcohol	Hydrocarbon, Hydroxy
C2	USA	1-Hexanol, 3,5,5-trimethyl	19000	Alkane, Alcohol	Hydrocarbon, Hydroxy
C3	USA	4H-3,1-Benzaxazin-4-diisocyanato-1-methyl	91000	Aromatic, Ketone	Phenyl, Carbonyl
C3	USA	1,3,5-Triazin-2-amine, 4,6-dichloro	22500	Azine, Amine, Chloride	Azine, Amino, Chloride
C4	USA	Benzene, 2,4-diisocyanato-1-methyl	28500	Aromatic, Cyanate	Phenyl, Cyanate
C4	USA	Benzene, 2,4-diisocyanato-1-methyl	21000	Aromatic, Cyanate	Phenyl, Cyanate
C4	USA	1-Hexanol, 3,5,5-trimethyl	32000	Alkane, Alcohol	Hydrocarbon, Hydroxy
R1H	USA1	1,3,5-Triazin-2-amine, 4,6-dichloro	150000	Azine, Amine, Chloride	Azine, Amino, Chloride
R1H	USA2	1,3,5-Triazin-2-amine, 4,6-dichloro	200000	Azine, Amine, Chloride	Azine, Amino, Chloride
R1M	USA1	1,3,5-Triazin-2-amine, 4,6-dichloro	180000	Azine, Amine, Chloride	Azine, Amino, Chloride
R1L	USA2	1,3,5-Triazin-2-amine, 4,6-dichloro	15000	Azine, Amine, Chloride	Azine, Amino, Chloride
R4H	India	Benzaldehyde, 3-methyl-	50000	Aromatic, Aldehyde	Phenyl, Carbonyl
R4H	India	Benzaldehyde, 3,4-dimethyl	60000	Aromatic, Aldehyde	Phenyl, Carbonyl
R4H	India	Phenol, 2,4-bis(1,1-dimethylethyl)	35000	Aromatic, Alcohol	Phenyl, Hydroxy
R4H	USA2	1,3,5-Triazin-2-amine, 4,6-dichloro	22500	Azine, Amine, Chloride	Azine, Amino, Chloride
R4H	India	1,3,5-Triazin-2-amine, 4,6-dichloro	90000	Azine, Amine, Chloride	Azine, Amino, Chloride
R4H	USA1	1,3,5-Triazin-2-amine, 4,6-dichloro	53500	Azine, Amine, Chloride	Azine, Amino, Chloride
R4M	USA1	1,3,5-Triazin-2-amine, 4,6-dichloro	39000	Azine, Amine, Chloride	Azine, Amino, Chloride
R4M	USA2	1,3,5-Triazin-2-amine, 4,6-dichloro	11000	Azine, Amine, Chloride	Azine, Amino, Chloride
R4L	USA2	1,3,5-Triazin-2-amine, 4,6-dichloro	21000	Azine, Amine, Chloride	Azine, Amino, Chloride
R5L	USA2	Benzene, 2,4-diisocyanato-1-methyl	19000	Aromatic, Cyanate	Phenyl, Cyanate
R5H	India	Phenol, 2,4-bis(1,1-dimethylethyl)	27000	Aromatic, Alcohol	Phenyl, Hydroxy
R5L	USA1	Phenol, 2-chloro	16800	Aromatic, Chloride, Alcohol	Phenyl, Chloride, Hydroxy
R5M	USA2	Phenol, 2-chloro	10600	Aromatic, Chloride, Alcohol	Phenyl, Chloride, Hydroxy

4.5 ICP Results

ICP testing was used to determine metals left in solution. Although 18 metals were measured, only four were found regularly at high levels: calcium, iron, magnesium, and sodium. Their levels were measured for all samples from C1-C5, R1H-R6H, R1M-R6M, and R1L-R6L to track when levels decreased below permissible limits. Arsenic, cadmium, lead, and manganese were occasionally found above permissible limits and it is noted when this occurred. Data were taken for all of the samples, including both the India and USA tests. Table 3.10 displays India's permissible effluent standards for wastewater in Dye and Dye Intermediate Industries for disposal in surface waters. India effluent standards do not list calcium, iron, magnesium, and sodium in their effluent regulations; therefore levels of these metals were compared to drinking water standards shown in Table 3.11. Permissible calcium levels are limited to 75-200 mg/L because calcium causes water hardness between 40-100 mg/L. Permissible magnesium levels are limited to 30-150 mg/L because at 500 mg/L the taste of the water is affected. Permissible iron levels are limited to 0.1-1.0 mg/L because at 0.3 mg/L the taste and aesthetics of the water is affected. Permissible sodium levels are limited to 20 mg/L because at 250 mg/L the taste and aesthetics of the water is affected and can alter natural biological activity. Natural waters have sodium levels between 5-50 mg/L. Permissible manganese levels are limited to 0.1-0.5 mg/L but at 0.05 mg/L the taste and aesthetics of the water is affected. Permissible arsenic levels are 0.01-0.05 mg/L because at 0.05 mg/L arsenic affects human health. Permissible cadmium levels are 0.005-0.01 mg/L but at 0.005 mg/L cadmium is toxic to humans. Permissible lead levels are 0.05-0.1 mg/L

because lead causes irreversible neurological damage to humans, especially children (Sengupta, *et al.*, 2008).

The general trend of these ions in solution was an increase of calcium and magnesium after sand filtration. Iron had the opposite trend, as it increased during the oxidation process and decreased to an almost negligible amount after sand filtration. This was a result of the physical capturing of the iron/dye sludge formed in solution during the oxidation process. Sodium increased or remained stable during oxidation and decreased after sand and carbon filtration. Note, the levels of increase or decrease do not fit a mathematical trend because of the variability in chemical composition of the wastewater at such a high dye concentration. In addition, there is little control as to the sand's contents in India since it was construction sand that had been stored outside open to nature prior to use. Because of the difference in quantitative results between India and the USA, trends are described instead. These trends often match despite these numerical differences. In the case of Reactive Dyes, trends are also described according to the varying iron surface areas described in this study.

4.5.1 Reactive Red 120

Reactive Red 120 ICP results are found in Table D.1 in Appendix D. Other than calcium, magnesium, iron, and sodium, for Reactive Red 120 ICP results, manganese was present occasionally in the India samples, but only after sand or carbon filtration was performed. The USA samples did, at times, contain manganese, lead, and arsenic at lower levels than the India samples, and typically after no filtration. Calcium controls ranged from 20 to

37 ppm with the highest level in C1, magnesium ranged from 7 to 14 ppm with the highest level in C1, iron from 0.1 to 4 ppm with the highest level in C4-C5, and sodium from 580 to 1100 ppm with the highest level in C4.

Calcium and magnesium content in solution changed as iron surface area and location of test changed. For high iron, India fully oxidized samples had more metals than partially oxidized samples; USA fully oxidized samples had fewer metals than partially oxidized samples. All of these samples increased with filtration. For medium iron, partially oxidized samples had more metals than fully oxidized samples. All of these samples increased with filtration except for USA samples R2M-R3M having the opposite result. For low iron, fully oxidized samples had more metals than partially oxidized samples. All of these samples increased with filtration except USA samples R2M-R3M. All ICP results were within the drinking water permissible limits: 200 mg/L for calcium, 150 mg/L for magnesium. Many samples were below the permissible drinking water limit of 75 mg/L calcium including R4H-R6H in India, R1H-R4H in the USA, all R1M-R4M, R2L-R6L in India, and R2L-R4L in the USA. Many samples were below the permissible drinking water limit of 50 mg/L magnesium including R2H-R6H in India and R1H-R6H in the USA, R1M-R6M in India and R1M-R4M in the USA, and R2L-R6L in India and R1L-R6L in the USA.

Iron content in solution changed as iron surface area and location of test changed. Longer oxidation time resulted in higher iron metal content for non-filtered samples; filtration resulted in lower iron content especially after full oxidation (except India

samples R5L-R6L). Medium, low, and high iron surface area resulted in less metal in solution respectively for all samples. One exception is for India samples R5L-R6L having a larger metal content than R4L. R2H, R3H, R2M, R3M, R2L, and R3L are below the permissible limits. R6H, and R6M are also below the permissible limits, although 3-10 times higher than the fully oxidized equivalents.

For sodium, none of the samples decreased to below permissible limits except R6H in India, and R2M and R3M in the USA. R2H-R3H, R2M-R3M, and R2L-R3L (except R2H and R3H in India) are lower than R5H-R6H, R5M-R6M, and R5L-R6L. Generally, the more filtration, the more sodium was removed from solution. Low, medium, and high iron surface area resulted in less metal in solution respectively for all samples.

Most India filtered samples found a level of manganese in solution (except R2H, R2L-R3L), and arsenic was also found in R3H. For USA samples, arsenic, lead, and manganese were found in varying levels in R1H, R4H, R1M, R1L, R3L, and R5L.

4.5.2 Reactive Yellow 81

Reactive Yellow 81 ICP results are found in Table D.2 in Appendix D. Other than calcium, magnesium, iron, and sodium, manganese showed occasionally and only after sand or carbon filtration in India, whereas manganese, lead, and arsenic appeared in USA samples at lower levels but more often after no filtration. Similarly to Reactive Red 120 calcium controls ranged from 21 to 39 ppm with the highest level in C1, magnesium

ranged from 6 to 14 ppm with the highest level in C1, iron from 0 to 4 ppm with the highest level in C5, and sodium from 634 to 1140 ppm with the highest level in C2.

Calcium and magnesium content in solution changed as iron surface area and location of test changed. For high iron, India fully oxidized samples had more metals than partially oxidized samples; USA fully oxidized samples had fewer metals than partially oxidized samples. All of these samples increased with filtration. For medium iron, partially oxidized samples had more metals than fully oxidized samples. All of these samples increased with filtration except for calcium having the opposite result for USA samples R2M-R3M. For low iron, fully oxidized samples had more metals than partially oxidized samples. All of these samples increased with filtration except USA samples R2M-R3M. All ICP results were within the drinking water permissible limits: 200 mg/L for calcium, 150 mg/L for magnesium. Many samples were below the permissible drinking water limit of 75 mg/L calcium including R4H-R6H in India, R4H in the USA, all R1M-R4M and R4L-R6L samples, and R1L-R3L in the USA. Many samples were below the permissible drinking water limit of 50 mg/L magnesium including USA samples R2H, R5H, and R5M-R6M.

For iron, generally, the longer oxidation time followed by more filtration resulted in lower iron levels. Longer oxidation time resulted in higher iron metal content for non-filtered samples; filtration resulted in lower iron content especially after full oxidation (except R6M in India, and R6L). Medium, low, and high iron surface area resulted in less metal in solution for USA samples respectively, and low, high, medium for India

samples. R2H-R3H, R2M-R3M in the USA, R2L-R3L, R5H-R6H in the USA, R5M in India, and R5L are below the permissible limits.

For sodium, none of the samples decreased to below permissible limits except R3M which narrowly achieves permissibility in the USA. Generally the more filtration the more sodium was removed from solution. R2H-R3H, R2M-R3M, and R2L-R3L, (except R2H-R3H in India) were lower than R5H-R6H, R5M-R6M, and R5L-R6L. Medium, low, and high iron surface area in the USA resulted in less metal in solution respectively for all samples.

Most India filtered samples found a level of manganese in solution (except R3H, R5H, R3L). For USA samples, arsenic, cadmium, and manganese were found in varying levels in R1H, R3H-R5H, R1M, R4M, R1L-R2L, R5L-R6L.

4.5.3 Reactive Blue 4

The results for the ICP testing are found in Table D.3 in Appendix D. Other than calcium, magnesium, iron, and sodium, in India cadmium in R4H, and lead in R6L and manganese in all R2*, R3*, R5*, and R6* samples with the exception of R3M, and R2L (with one appearance in a non-filtered sample R4H). In the USA samples, cadmium and manganese were present in the non-filtered samples R1H, R1M, R1L. Arsenic was found in R4H, and R4L, and with manganese in R5L. Calcium controls ranged from 25.9 to 44.2 ppm with highest level in C5, magnesium ranged from 6.9 to 12.7 ppm with highest level in C1, iron from 0 to 4.7 ppm with highest level in C5, and sodium from 789.1 to

1402.9 ppm with the highest level in C1.

Calcium and magnesium content in solution changed as iron surface area and location of test changed. For high iron, India fully oxidized samples had more metals than partially oxidized samples; USA fully oxidized samples had less metals than partially oxidized samples. All of these samples increased with filtration except for magnesium R2H-R3H. For medium iron, partially oxidized samples had more metals than fully oxidized samples, although for magnesium this was only slightly. All of these samples increased with filtration. For low iron, fully oxidized samples had more metals than partially oxidized samples. All of these samples increased with filtration. All ICP results were below the drinking water impermissible limits: 200 mg/L for calcium, 150 mg/L for magnesium. Many samples were below the permissible drinking water limit of 75 mg/L calcium including R4H-R6H in India, R1H-R4H in the USA, R1M, R3M-R4M in India, and R1M, R3M-R4M in the USA, all R4L-R5L samples, and R1L, R4L-R6L in the USA. All samples were below the permissible drinking water limit of 50 mg/L magnesium.

For iron, generally, the longer oxidation time followed by more filtration resulted in lower iron levels. Longer oxidation time resulted in higher iron metal content for non-filtered samples; filtration resulted in lower iron content especially after full oxidation. High, low, and medium iron surface area resulted in less metal in solution for India samples, and medium, high, low for the USA samples respectively. R2H-R3H, R2M-R3M in the USA, R3M in India, R2L-R3L in India, R2L in the USA, R5H-R6H in the USA, and R6L in India were below the permissible limits.

For sodium, none of the samples decreased to below permissible limits except R2H in the USA. Generally the more filtration the more sodium was removed from solution. R2H-R3H and R2M-R3M (except R2H-R3H, R2M, in India) were lower than R5H-R6H and R5M-R6M with an exception with low iron samples. High, medium, and low iron surface area in the USA resulted in less metal in solution respectively.

Most India filtered samples found a level of manganese in solution (except R3M, and R2L), arsenic was also found in R6L, and cadmium in R4H. For USA samples, arsenic, cadmium, and manganese were found in varying levels in R1H, R4H, R1M, R1L, R4L-R5L.

4.6 Respirometric Results

Respirometric analysis was conducted for partially oxidized India samples of differing colors (red, yellow, blue), with different amounts of iron (low, medium, high), and that used different filtration methods (no filter, sand filter). Fully oxidized samples' COD values were too low to biodegrade further so respirometric analysis was only completed for partially oxidized samples.

4.6.1 Reactive Red 120

Oxygen uptake results can be viewed in Figure E.1 in Appendix E and compare three trials of endogenous and exogenous data describing the oxygen uptake of R4H, R4M, R4L or R5H, R5M, R5L for Reactive Red 120.

The results of the calculated oxygen uptake based on the data in Figure E.1 in Appendix E are presented in Table 4.10 for Reactive Red 120. As can be seen for the samples with low iron surface area, oxygen uptake was found to be 0.00 nMol min^{-1} mg^{-1} for both R4L and R5L. This means that filtration had little effect on the sample, but partial oxidation for 75 minutes using an iron surface area of 161 cm^2 was not enough to leave the sample biodegradable for Common Effluent Treatment Plant (CETP) sludge. For the medium iron group, R4M had an oxygen uptake of 40.6 nMol min^{-1} mg^{-1} and 75.4 nMol min^{-1} mg^{-1} for R5M; therefore being oxidized for the same 55 minutes was enough for the partially oxidized sample to create biodegradability by CETP sludge, although almost double the amount for the filtered sample. The group with high amount of iron was found to have zero theoretical biodegradability by CETP sludge for R5H and very low oxygen uptake of 3.84 nMol min^{-1} mg^{-1} for R4H.

Table 4.10: Calculated oxygen uptake for Reactive Red 120 according to low, medium, or high iron and non-filtered or sand filtered sample results.

Sample	Iron Amount	No Filter/Filter	Oxygen Uptake (nmol/min/mg)
R4H	High	No Filter	3.84
R5H	High	Sand Filter	0.00
R4M	Medium	No Filter	40.6
R5M	Medium	Sand Filter	75.4
R4L	Low	No Filter	0.00
R5L	Low	Sand Filter	0.00

4.6.2 Reactive Yellow 81

Oxygen uptake results can be viewed in Figure E.2 in Appendix E and compare three trials of endogenous and exogenous data describing the oxygen uptake of R4H, R4M, R4L or R5H, R5M, R5L for Reactive Yellow 81.

The results of the calculated oxygen uptake based on the data in Figure E.2 in Appendix E are presented in Table 4.11 for Reactive Yellow 81 with low iron surface area, oxygen uptake was found to be 0.00 nMol min^{-1} mg^{-1} for R4L, and 101 nMol min^{-1} mg^{-1} for R5L. This means that filtration had a 100 times effect on the sample, and partial oxidation after 75 minutes using low surface area iron followed by sand filtration was enough to leave the sample biodegradable for CETP sludge. For the medium iron group R4M had an oxygen uptake of 365 nMol min^{-1} mg^{-1} and 2.33 nMol min^{-1} mg^{-1} for R5M. Being oxidized for the same 85 minutes was enough for the partially oxidized sample to create biodegradability by CETP sludge, whereas the filtered sample had an extremely low oxygen uptake of 2.33 nMol min^{-1} mg^{-1}. The group with high amount of iron was found to have very low theoretical biodegradability by CETP sludge with or without filtration at 1.58 nMol min^{-1} mg^{-1} for R4H and 0.00 nMol min^{-1} mg^{-1} for R5H.

Table 4.11: Calculated oxygen uptake for Reactive Yellow 81 according to low, medium, or high iron and non-filtered or sand filtered sample results.

Sample	Iron Amount	No Filter/Filter	O2 Uptake (nmol/min/mg)
R4H	High	No Filter	1.58
R5H	High	Sand Filter	0.00
R4M	Medium	No Filter	365
R5M	Medium	Sand Filter	2.33
R4L	Low	No Filter	0.00
R5L	Low	Sand Filter	101

4.6.3 Reactive Blue 4

Oxygen uptake results can be viewed in Figure E.3 in Appendix E and compare three trials of endogenous and exogenous data describing the oxygen uptake of R4H, R4M, R4L or R5H, R5M, R5L for Reactive Blue 4.

The results of the calculated oxygen uptake based on the data in Figure E.3 in Appendix E are presented in Table 4.12 for Reactive Blue 4 with low iron surface area, oxygen uptake was found to be 0.00 nMol min^{-1} mg^{-1} for R4L, and 0.00 nMol min^{-1} mg^{-1} for R5L. This means that filtration had little effect on the sample, but partial oxidation for 100 minutes using low surface area iron was not enough to leave the sample biodegradable for CETP sludge. For the medium iron group R4M had an oxygen uptake of 7.36 nMol min^{-1} mg^{-1} and 620 nMol min^{-1} mg^{-1} for R5M. Being oxidized for the same 155 minutes was enough for the partially oxidized sample to barely create biodegradability by CETP sludge, whereas the filtered sample had an extremely high oxygen uptake almost 100 times that of non-filtered. The group with high amount of iron was found to have no theoretical biodegradability by CETP sludge with or without filtration. Overall oxygen uptake results for reactive dyes show the greatest promise for biodegradability created after medium iron usage with or without filtration.

Table 4.12: Calculated oxygen uptake for Reactive Blue 4 according to low, medium, or high iron and non-filtered or sand filtered sample results.

Sample	Iron Amount	No Filter/Filter	O2 Uptake (nmol/min/mg)
R4H	High	No Filter	0.00
R5H	High	Sand Filter	0.00
R4M	Medium	No Filter	7.36
R5M	Medium	Sand Filter	620
R4L	Low	No Filter	0.00
R5L	Low	Sand Filter	0.00

4.6.4 Statistical Analysis

Three-way ANOVA was completed to statistically analyze the interaction between three different variables (color, iron surface area, filtration method) for the reactive dye experiments and how they affected respirometric analysis of the partially oxidized

samples. Table 4.13 reveals that none of the three factors show a statistically significant effect on oxygen uptake ($P > 0.05$). Also, the interaction effect was insignificant. While the numbers of tests performed were too low to be statistically significant with regards to variables like iron surface area, the results do indicate that the process is beneficial, and there are indications that certain combinations are potentially better than others. For instance, medium iron tends to lead to oxygen uptake, indicating that pollutants are being consumed, while that is seen less with other iron surface areas.

Table 4.13: Analysis of Variance (3-way ANOVA) for partially oxidized samples. Variables for reactive dye are color (red, yellow, blue), iron surface area (low, medium, high), and filtration method (no filter, sand filter).

	Df	Sum	Sq Mean	Sq F	value Pr(>F)
Dye(D)	2	21430	10715	0.265	0.780
Iron(I)	2	135007	67503	1.671	0.297
Filter(F)	1	4653	4653	0.115	0.751
D:I	4	43871	10968	0.272	0.883
D:F	2	78815	39408	0.976	0.452
I:F	2	8824	4412	0.109	0.899
Resid	4	161572	40393		

4.7 Discussion of Results

The purpose of the studied photo-Fenton oxidation procedure is to completely degrade organic compounds from a Reactive Dye solution and to bring inorganics to the permissible drinking water level. The level of degradation achieved through various combinations of experimental variables was described above. UV-visible spectrometry can be compared with published data to describe which organics were left after treatment. The COD results can be used to show the total organic load remaining and whether it agrees with the UV-visible spectrometry results. The GC/MS analysis can be used to identify the organics and their respective quantities. The ICP results can be used to

describe the inorganic metal ions left in solution. The respirometric analysis allows for the determination of whether the remaining solution is theoretically biodegradable. Finally, the combined results can be used to identify an experimental procedure that will achieve the most effective treatment of the dye effluent in a cost-effective and sustainable manner.

Before recommendations can be made, it is important to understand the actual activities cottage-scale silk dyers perform. By mimicking the cottage-scale silk dyers' wastewater in laboratory-scale studies, the intent was to augment dyers' processes with a low-cost treatment option. For this reason, the following experimental methodology was chosen: (1) Reactive Dyes at 5 g/L concentration were mixed with household hydrochloric acid; (2) pharmacy-grade hydrogen peroxide was poured into the solution in containers holding rusty metal from old yogurt containers; (3) natural sunlight at ambient temperature was employed; (4) following treatment, sand and carbon filtration of the dye effluent was used. This process was developed to be low-cost and readily available. Since the work was not completed using laboratory-grade supplies, some contamination was expected to be found in the results in the form of outliers in the analysis. That being said, organic and inorganic chemicals found before (in the controls), during (after partial oxidation and followed by filtration), and after (after full oxidation, and followed by filtration) the sustainable photo-Fenton oxidation process, agreed with the literature as described in Chapter 2. And since this study has a practical application because of the need for low-cost decolorization and dye wastewater treatment, the goal of the results is to prioritize the importance of certain variables over others in order to create a viable treatment unit to

be used by small-scale silk dyers worldwide. The overall intention is to make sure that the color degrades and the chemical composition oxidizes to a simpler form before reusing the treated water for a second batch of dye, or before disposing of it as is normally done.

The variables used for the sustainable photo-Fenton process (including dye color, dye concentration, hydrochloric acid, hydrogen peroxide, iron surface area, solar irradiation, temperature, oxidation time, filtration method) all contribute to the degradation of the chemical dyes in solution. Each variable impacts the outcome of the sustainable photo-Fenton oxidation experiments detailed here. However, the importance of each variable differed from what was expected and previously documented by other research (see Chapter 2). Not all variables were tested in these studies—most were kept constant for all experiments. Time, iron surface area, and filtration were tested for each color to measure their impact on the photo-Fenton oxidation process. Dye concentration, acidification using hydrochloric acid, and the quantity of hydrogen peroxide were held constant, and will impact the photo-Fenton oxidation process. Solar irradiation and temperature are also variables that impact photo-Fenton oxidation, but were not controlled in this work. The values of these were recorded, and so it was possible to determine if they significantly impacted the results.

Dye concentration was constant for all tests at 5 g/L, which is similar to that in the small-scale industry. Acidification with hydrochloric acid did not use a specific volume per solution, but instead always brought solution pH to 2.5. Each dye color required a

different volume of 6% hydrogen peroxide, as was decided according to the optimization tests, but then the volume was not altered within each color set. In the case of temperature and solar irradiation, location is noted as India or USA. It is evident that temperature variation is less important than solar irradiation variation. Temperature did not seem to impact oxidation provided that the sample remained above the freezing temperature. UV light is incredibly important for the reaction to take place, but direct sunlight is not necessary. Each location varies greatly for temperature and solar irradiation, but since the process worked in both places their various levels do not prevent the chemical reaction from taking place.

The results here do not compare dye color but rather test the degradation of three colors that are typically used in the field. Knowing that red, yellow, and blue can form all colors in the rainbow, if their separate degradation using sustainable photo-Fenton oxidation is successful, their mixture, although slightly more complicated, should also be able to be oxidized. High COD levels were found in control samples due to the high concentration of dye in solution. UV-visible spectra of the control samples also reach well beyond the graph maximum thus denoting very high organic levels in solution. The high concentration of dye also offered great variation in the measured COD and GC/MS degradation results before filtration. Through UV-visible spectrometry, GC/MS, and COD, it was found that full oxidation followed by sand filtration (or sand and carbon filtration) lowered the amount of organics in solution to near negligible in many cases. The hazard quality of the chemicals remaining in solution is listed according to the Globally Harmonized System of Classification and Labeling of Chemicals (GHS) where

each chemical receives an H label for being hazardous followed by a number. 200 level labels distinguish they are physically hazardous, 300 level labels are hazardous to health, and 400 level labels are hazardous to the environment.

Bilgi and Demir (2005) state that while sulphonated azo dyes cannot be analyzed using GC/MS because they are non-volatile, their degradation products and intermediates can be detected; this was also the case in this study. The most prevalent intermediate found using GC/MS analysis differed for each Reactive Dye. The different chemical groups present their respective hazard as listed in Table 4.14. Reactive Red 120 was found to contain mostly aromatics. After oxidation aromatics connected to cyanates decreased, but aromatics and alcohols increased and aromatics and ethers were found where they were not previously (although many organics degraded completely during oxidation as well). Aromatics pose a threat to human health and the natural environment because they are combustible, cause skin and serious eye irritation, and may cause respiratory irritation. Reactive Yellow 81 was found to contain mostly aromatics linked with cyanates that decreased by more than half during oxidation. Aromatics and cyanates combined cause skin and serious eye irritation, are fatal if inhaled, may cause breathing difficulties or respiratory irritation. Reactive Blue 4 was found to contain mostly alkanes connected to alcohols which degraded completely during oxidation, aromatics linked with cyanates which decreased by half during oxidation, and azine, amine, and chloride functional groups which increased during oxidation. Compounds that contain azine, amine, and chloride functional groups also cause skin and serious eye irritation, are toxic

if swallowed, may cause respiratory irritation, and can cause long-lasting harm to aquatic life.

The biodegradability of these organics found in solution was measured using respirometric analysis. The oxygen uptake measured during this procedure showed positive activity only in approximately one-third of the samples. Considering that the UV-visible spectrometry peaks, COD levels, and GC/MS peaks showed aromatics and other functional groups left in solution, it can be concluded that the quantity of pollutants in solution were very low and may not be sufficient for the CETP sludge to react in a short time.

Since full oxidation followed by filtration left the least amount of organics in solution, it can be concluded that longer photo-Fenton oxidation time allows for the chemical reaction to separate more of the dissolved dye from the water in solution. More reaction time resulted in more sludge created by the separation of dye and iron rust from the aqueous solution. The creation of sludge occurs due to the chemical reaction between hydrochloric acid, iron, UV light, and hydrogen peroxide that frees hydroxyl radicals to attack the pollutants. Dye and rust sludge is easily removed from solution but is also easily remixed into solution. This explains why the organic level of the non-filtered fully oxidized samples, in some cases, was found to be comparable or higher than the non-filtered partially oxidized samples. The fully oxidized sample may have contained re-dissolved pollutants while the partially oxidized sample still contained dissolved chemicals. Although care was taken to not mix the settled non-filtered sample before

testing, this inadvertent mixing can explain any unexpected spikes in COD or peak height of UV-visible spectra. This also explains why the filtration of the sludge out of the fully oxidized sample resulted in lower organics than filtering the partially oxidized sample which still contained dissolved pollutants.

Iron/dye sludge is very fine and dissolution of sludge particulates is possible. This is a concern and should be studied further. Field studies detailed in Chapter 7 describe two methods that prevent the dissolution of the organic sludge content (that upon dissolution would be un-filterable and render the filtered-water colored) and prevent the inorganic content from clogging the sand filter. The first is to remove the organic sludge that is present in the form of foam from the top of solution before filtration but after photo-Fenton oxidation has taken place. Future studies should create a method that more efficiently utilizes labor time for removing the sludge foam. A third type of filtration in the form of cotton fabric located just before the sand filter is suggested to prevent the inorganic iron rust from clogging the sand. The cotton fabric is more easily washed as compared to the sand and is a finer filter to capture the particulates preventing their reentrance into solution. Future studies should detail a method of separating iron and dye from the sludge. Preliminary work has begun to dissolve the dye from the iron in the sludge thus proving that in fact there are separate organic and inorganic elements within the sludge. It would help decrease costs of photo-Fenton oxidation treatment if iron can be reused; and it would decrease costs for dyers if dye, depending on the extent of its oxidation, can be extracted and reused in future batches.

Using hydrochloric acid results in increased levels of chloride and sodium as measured using ICP. Chapter 3 describes the strong attraction between chloride and sodium ions; and also describes that sodium chloride is very soluble in water which makes it un-filterable through sand or carbon. The ICP results agree with this conclusion. Other photo-Fenton oxidation studies detailed in Chapter 2 use sulfuric acid preventing these high levels, but producing high levels of sulfates in their effluent. Future studies should investigate ways of removing sodium and chloride from treated effluent or compare the results from other acids and their impact on treated water quality.

Iron metal ions that are added to solution during the photo-Fenton oxidation process, via the iron scrap catalyst, are completely removed from solution after filtration. Calcium and magnesium increased during the filtration process but most often stayed below the permissible limits, especially for fully oxidized samples. Cadmium, lead, arsenic, and manganese ions are noted if they are above the permissible limits for drinking water which is rarely the case, and they most often decrease to permissible levels after full treatment. All of these ions, and especially lead, are often the ingredients in chemical dyes to give them their vibrant color. As discussed in the results, calcium, magnesium, and iron decreased to permissible levels after full oxidation followed by sand and carbon filtration most successfully using medium iron, although the other iron surface areas were still adequate. Although the sodium in solution decreased substantially after full oxidation followed by filtration, treatment rarely brought the sample to below drinking water permissible limit of 20 mg/L. Further sodium removal will be needed for the success of future studies.

The impact that iron surface area had on the photo-Fenton oxidation process was tested in these experiments as it varied from low (161 cm^2), medium (323 cm^2), and high (645 cm^2) surface area under 2.5 cm of solution above the iron. Iron rust was used in the sustainable photo-Fenton oxidation process in place of the laboratory-grade chemical iron (II) ferrous salt. Medium iron surface area caused the most degradation of dye solution resulting in the least pollutants remaining in solution after degradation. Most photo-Fenton oxidation studies, as detailed in Chapter 2, describe optimal iron salt concentrations in mg/L iron to solution volume. This study uses scrap iron according to how its surface reacts when it is struck by UV radiation after it passes through the dye effluent. There are few previous studies that utilize scrap iron in their research and they quantify iron ion production according to iron weight. These studies utilized iron scrap in the form of shavings which have very high and immeasurable surface area. The role of iron as a catalyst in the photo-Fenton oxidation chemical reaction is detailed in Chapter 2. The amount of iron must be high enough for free iron ions to react in the photo-Fenton oxidation process in order to oxidize the pollutants, but not so high that there are extra ions in solution attracting hydroxyl radicals away from the chemical dye pollutant towards the iron. For that reason, it is not surprising that medium iron resulted in the lowest remaining organics in solution. High and low iron, however, often did not differ much from the medium iron results, although low iron differed less frequently. It can be concluded that despite possible scavenging, it is more beneficial for the degradation process that more iron be present, thus enabling the oxidation to occur, as compared to less iron, which may prevent it from starting. Any iron in solution after degradation is in the form of sludge and is easily filterable thus decreasing iron levels to negligible proven

through the ICP results. It was found that higher surface areas of iron resulted in shorter full oxidation times. This information can be used to future studies to utilize rusty metal containers for pilot-scale treatment unit construction.

Combining the UV-visible spectra data, COD levels, and the GC/MS labels gives specific detail regarding which organics remain in solution after sustainable photo-Fenton oxidation. The first thing worth mentioning is that UV-visible spectra peaks cannot be simply defined or labeled since a peak at a certain wavelength can be present for many different compounds depending on the color of that compound. Table 3.12, in Chapter 3, lists the labels for the peaks found in Reactive Red 120, Reactive Yellow 81, and Reactive Blue 4 samples according to past studies detailed in Chapter 2. There are similarities between many peaks found in the UV spectra that may be categorized according to other studies. Visible peaks that are responsible for the color in the dye are already well labeled by previous studies. Many UV and visible peaks remain unlabeled. GC/MS results assist in the labeling, but do not match the location of a UV-visible spectra peak to a specific organic. The UV peaks found in the spectra show high-level peaks as well, thus concluding that the solution contains a variety of organics at different abundances.

A confirmation that the photo-Fenton oxidation reaction is changing the chemical composition of solution can be seen by the presence of different peaks in the UV-visible spectrometry results with oxidation. As can be seen in the analysis of the control samples, UV peaks other than those shown in the control sample C1 were evident after

the addition of acid and oxidant. He and Lei (2004) also discuss the presence of new peaks coming on the UV-visible spectra after oxidation.

UV peaks degrade much slower than visible peaks. The peak at 206 nm found for all three Reactive Dyes in this study is at the approximate location of phenol as described by He and Lei (2004) as listed in Table 3.12. Although this cannot be completely confirmed, many organics containing the same phenyl ring were identified by GC/MS as described in Tables 4.4, 4.5, and 4.6. The peak at 206 nm is by far the highest of the peaks present in the controls even after partial and full oxidation and sand and carbon filtration. This is expected because it is difficult to degrade the phenyl or benzene ring.

Visible peaks degrade very quickly. Chapter 2 reveals the theory that the chromophores located in the chemical composition of dyes degrade very quickly. The peaks responsible for dye color in this study also degrade quickly and are completely degraded after full oxidation. Other visible peaks that have not been clearly identified as coming from the color composition also fully degrade; this identification is beyond the scope of this study.

Table 4.14: Hazardous effects of the definable chemicals that remain in solution listed according to the Globally Harmonized System of Classification and Labeling of Chemicals (GHS).

Type of Compound	Hazard Statements
Alkane	Varies on Compound: (1)Not a hazardous substance or mixture; (2) H304 May be fatal if swallowed and enters airways; (3) H315 Causes skin irritation; (4) H302 + H332 Harmful if swallowed or if inhaled. H315 Causes skin irritation. H351 Suspected of causing cancer. H401 Toxic to aquatic life.
Alkane & Alcohol	H315 Causes skin irritation. H319 Causes serious eye irritation. H373 May cause damage to organs through prolonged or repeated exposure if swallowed. H411 Toxic to aquatic life with long lasting effects.
Aromatic	H227 Combustible liquid H315 Causes skin irritation. H319 Causes serious eye irritation. H335 May cause respiratory irritation.
Aromatic & Alcohol	H410 Very toxic to aquatic life with long lasting effects
Aromatic & Chloride & Alcohol	H227 Combustible liquid. H315 Causes skin irritation. H319 Causes serious eye irritation. H335 May cause respiratory irritation.
Aromatic & Cyanate	H315 Causes skin irritation. H317 May cause an allergic skin reaction. H319 Causes serious eye irritation. H330 Fatal if inhaled. H334 May cause allergy or asthma symptoms or breathing difficulties if inhaled. H335 May cause respiratory irritation.
Azine, Amine, Chloride	H315 Causes skin irritation. H301 Toxic if swallowed. H319 Causes serious eye irritation. H335 May cause respiratory irritation. H413 May cause long lasting harmful effects to aquatic life.
Butylated Hydroxytoluene	H410 Very toxic to aquatic life with long lasting effects
Organic	H226 Flammable liquid and vapour. H361 Suspected of damaging fertility or the unborn child. H413 May cause long lasting harmful effects to aquatic life.

4.8 Summary

In summary, laboratory-scale research using sustainable photo-Fenton oxidation to degrade 5 g/L Reactive Dyes using pharmacy-grade 6% hydrogen peroxide, household hydrochloric acid, scrap iron sheets, and sunlight is best done with medium iron surface area (323 cm^2) as the iron catalyst using full oxidation time followed by sand and carbon filtration to remove sludge.

There are many variables in the photo-Fenton oxidation process that impact the success of dye degradation. These include chemical composition of dyes, concentration of dye, acidified pH of solution, quantity of hydrogen peroxide used, solar irradiation, oxidation time, iron surface area, and filtration method. This study uses a cottage-scale industry dye concentration that is higher than any previous photo-Fenton oxidation study. This study also compares data taken in different locations whose solar irradiation varies greatly. Despite these differences from previous studies, complete color degradation occurred, as other organic and inorganic chemicals in solution also decreased to below permissible effluent levels. Degradation benefited from longer oxidation time, although using iron with a greater surface area resulted in less time required for full oxidation. High sodium and chloride levels after full treatment are a concern because of the choice to use readily available hydrochloric acid to acidify the solution.

Overall, the sustainable photo-Fenton oxidation process using scrap metal as the iron catalyst coupled with sand and carbon filtration shows great promise for the decolorization and chemical degradation of Reactive Red 120, Reactive Yellow 81, and Reactive Blue 4. The process may not need biodegradation after complete oxidation and filtration, as little additional benefit is seen with biodegradation. Future studies should focus on the remaining treated effluent after filtration including ways to lower sodium and chloride levels as well as how to separate and reuse iron and dye present in solid sludge that settles out of solution or is captured by sand filtration.

When considering that a cottage-scale dyer uses a very high concentration of dye in their dye batch, there is an opportunity for education and system improvement. Speaking with a medium-scale silk dyer in India, it was discovered that small process changes can decrease the impacts that dye effluent has on the environment. However, there are many rationales that interplay and cause a dyer to apply the methodology s/he uses. This work's focus was engineering an option for the current methodology of a cottage-scale silk dyer in rural Bangalore. It is worth mentioning here that there is a need for discussion and upgrading of the current small-scale dyer methodology in order to preserve and protect the natural environment. Despite treatment of the high concentration of dye wastewater, starting with a high level of chemical in an industry results in a high level of chemical waste. This project has successfully contained and modified the chemical waste to a form that is less dangerous and more manageable. However, using a lower concentration of dye or using natural dyes would lessen the impact of the dyeing process on the natural environment.

CHAPTER 5 – ACID DYE PHOTO-FENTON OXIDATION RESULTS AND DISCUSSION

5.1 Introduction

Acid Dye was chosen for this study because of its wide use in the cottage-scale silk dyeing industry in Karnataka, India. Its chemical composition varies greatly by color and is detailed in Chapter 3. Acid Fast Red, Acid Golden Yellow, and Acid Ananda Blue were specifically used in this study. Sustainable photo-Fenton oxidation with filtration was used to treat acid dyes in a manner similar to the oxidation of Reactive Dyes discussed in Chapter 4.

The laboratory-scale study detailed here used 5 g/L dye mixed in 1-liter tap water which was then acidified to pH 2.5 with hydrochloric acid. Next, hydrogen peroxide was added as an oxidizing agent, and the resulting mixture was poured over 645 cm^2 of rusty scrap iron to a depth of 2.5 cm. The mixture was then left in the sun (in India or the USA) for the appropriate time for full or partial photo-Fenton oxidation to occur. Acid Dye partial oxidation times were found via visual observation because separation of acid dyes from water is very noticeable and easy to detect. Samples were then tested using UV-visible spectrometry to validate chosen times and their respective decolorized peaks. Three partial oxidation times were chosen—the first one is just before dye sank to the bottom of solution, and the other two were chosen by subtracting five or ten minutes depending on how much time elapsed from the beginning of the test.. Samples were then tested after experiencing three filtration methods (none, sand, sand and carbon). For ease

of documentation, the abbreviations listed in Table 5.1 are used for notation of the different sample types and Table 4.2 for notation of the control samples. Methodology of the experimental procedures is detailed in Chapter 3.

In addition to the UV-visible spectrometry described above, COD, GC/MS, and ICP analysis was also performed on the samples. The purpose of this was to determine the organic and inorganic contaminants left in solution. In addition, respirometric analysis was completed to predict the biodegradability of the contaminants left in solution.

Table 5.1: Abbreviations of sample names for acid dyes.

Dye Type	Oxidation Time (Full or Partial)	Filtration Type (None, Sand, Sand and Carbon)	Abbreviation
Acid	Full	None	A1
Acid	Full	Sand	A2
Acid	Full	Sand and Carbon	A3
Acid	Partial 1	None	A4
Acid	Partial 1	Sand	A5
Acid	Partial 1	Sand and Carbon	A6
Acid	Partial 2	None	A7
Acid	Partial 2	Sand	A8
Acid	Partial 2	Sand and Carbon	A9
Acid	Partial 3	None	A10
Acid	Partial 3	Sand	A11
Acid	Partial 3	Sand and Carbon	A12

5.2 UV-visible Spectrometry Results

5.2.1 Rate Reaction

UV-visible spectrometry was used as an analysis method to determine the optimal time for partial and full oxidation for Acid Dyes using photo-Fenton oxidation after optimizing hydrogen peroxide quantity (detailed in Chapter 3). Undiluted A4, A7, and A10 spectra of Acid Fast Red, Acid Golden Yellow, and Acid Ananda Blue are presented in Figure

5.1 to display the unmodified spectra peak heights for the three chosen partial oxidation times. As seen in Figure 5.1, the magnitudes of the peaks are clearly decreasing with increasing oxidation time.

The Acid Golden Yellow A7 sample has the highest peak in Figure 5.1 (B) and is an anomaly to the results; this can be explained by the separation of dye from solution re-mixing during spectral analysis. Another explanation for the unexpected peak increase is due to the fact that the partial oxidation times are very low and within 5 minutes of each other.

Generally, UV and visible peaks for t_0 (as shown in the graphs of the diluted control samples in Figure A.4 in Appendix A) are beyond the 4.0 maximum of the graph when calculated from dilutions. This denotes the need for decolorization and degradation. Partial oxidation visible peaks have decreased to within the 4.0 scale and display clear peaks that can be described as individual organic chemicals. Full oxidation samples displayed lower UV peaks and no visible peaks meaning that full oxidation time was chosen when complete decolorization had occurred (not shown). Table 3.7 lists the partial and full oxidation times chosen from Figure 5.1 for the three Acid Dye colors. The actual control peak heights C1-C5 are calculated from dilutions in Table A.7 for Acid Fast Red, A.9 for Acid Golden Yellow, and A.11 for Acid Ananda Blue in Appendix A.

A

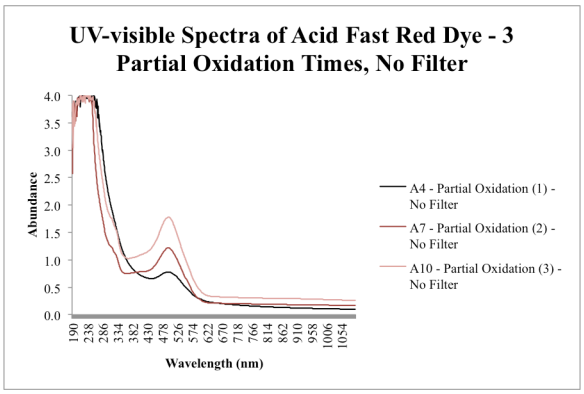

B

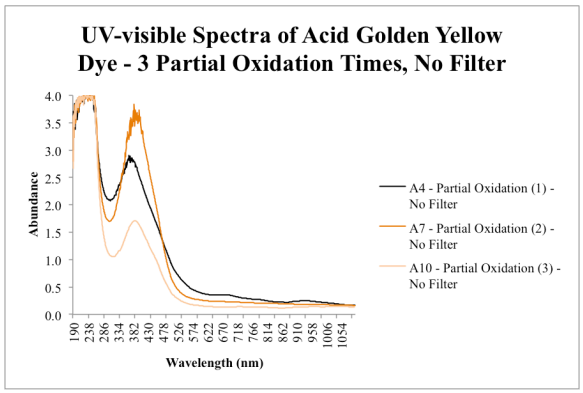

C

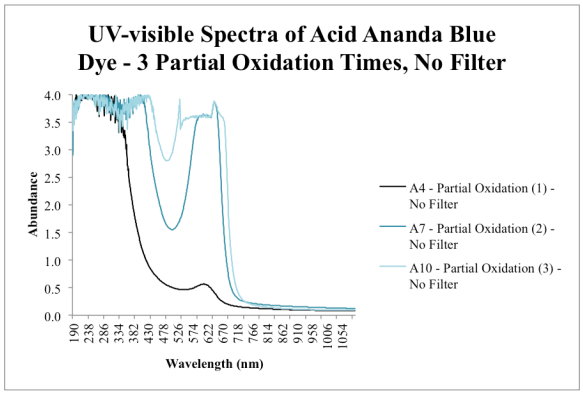

Figure 5.1: UV-visible spectra for A4, A7, and A10 of (A) Acid Fast Red, (B) Acid Golden Yellow, and (C) Acid Ananda Blue.

5.2.2 Partial and Full Oxidation Results

5.2.2.1 Acid Fast Red

Table 3.12 lists the wavelengths of the peaks found in the UV-visible spectra for Acid Fast Red. Figure A.4 in Appendix A displays diluted samples of the Acid Fast Red controls C1-C5. Table A.7 in Appendix A displays calculated actual peak heights for C1-C5 from dilutions. Table A.8 in Appendix A displays peaks for Acid Fast Red A1-A12. The results can be viewed in Figure 5.2 which compares (A) A1-A3, (B) A4-A6, (C) A7-A9, (D) A10-A12 to the diluted control peak C1. Peaks found at 206 and 610 nm were only present after acid and hydrogen peroxide were added to solution (C2-C5). Peaks at 214, 289, 318, 330, and 505 nm were also visible in C1.

In general and despite treatment, peaks at 206 nm and 214 nm stayed much higher than the other pollutants in solution. The contaminants displaying UV peaks at 206 nm, 237 nm, 291 nm, 371 nm were reduced most by full oxidation followed predictably by the longest partial oxidation time (1), (2), and then (3). Sand and carbon filtration following oxidation greatly decreased the height of the peaks by physically removing the organics out of solution. Occasionally there was a larger peak shown after carbon filtration than after sand filtration. Specifically the peak at 214 nm rose after carbon filtration of the fully oxidized sample as compared with the sand filtered sample; this was unexpected. The result is likely a result of an inability to completely clean the carbon filter between filtration.

The visible peaks at 505 and 610 nm decreased at a faster rate than the UV peaks but followed the same trends – decreasing more with longer oxidation time. Sand and carbon filtration following full oxidation was more effective at removing the chemicals responsible for peaks at 505 nm and 610 nm (thus making full oxidation followed by sand alone or sand and carbon filtration the most effective treatment). As with the UV wavelength peaks, generally sand filtration accomplished more than the carbon filtration due to the physical capture of the solids created by the photo-Fenton oxidation process and the physical removal of them from solution. It should be noted that carbon filtration did no harm to the process.

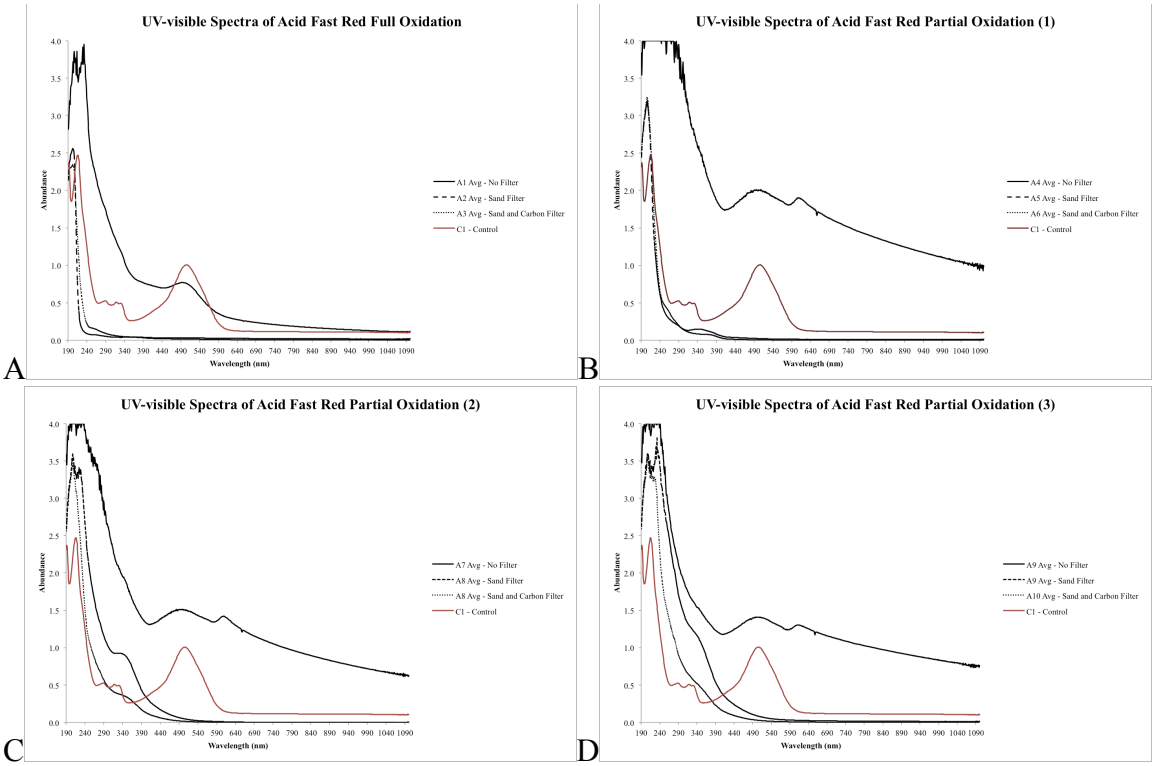

Figure 5.2: Acid Fast Red UV-visible spectra of the diluted control C1 compared to (A) A1-A3, (B) A4-A6, (C) A7-A9, and (D) A10-A12.

5.2.2.2 Acid Golden Yellow

Table 3.12 lists the wavelengths of the peaks found in the UV-visible spectra for Acid Golden Yellow. Figure A.5 in Appendix A displays diluted samples of the Acid Golden Yellow controls C1-C5. Table A.9 in Appendix A displays calculated actual peak heights for C1-C5 from dilutions. Table A.10 in Appendix A displays peaks for Acid Golden Yellow A1-A12. The results can be viewed in Figure 5.3 which compares (A) A1-A3, (B) A4-A6, (C) A7-A9, and (D) A10-A12 to the diluted control peak C1. Peaks found at 203 nm and 350 nm were only present after acid and hydrogen peroxide were added to solution (C2-C5). Peaks at 255 nm and 399 nm were also visible in C1.

In general and despite treatment, the peak at 203 nm stayed much higher than the other pollutants in solution. The contaminants displaying UV peaks at 203 nm, 255 nm, 350 nm, and 399 nm were reduced most by full oxidation followed predictably by the longest partial oxidation time (1), (2), and then (3). Sand and carbon filtration following oxidation greatly decreased the height of the peaks by physically removing the organics out of solution. Occasionally there is a larger peak shown after carbon filtration than after sand filtration, specifically the peaks at 203 nm after full oxidation, partial oxidation (1) and (3); 255 nm after full oxidation and partial oxidation (1); 350 nm after full oxidation and partial oxidation (1); 399 nm after full oxidation and partial oxidation (1). This is likely again due to the inability to completely clean the carbon filter between filtration. There are no visible peaks for Acid Golden Yellow. The longer wavelength at 399 nm is on the cusp between UV and visible but in this case acts similarly to the other UV peaks despite it being the lowest of the four peaks.

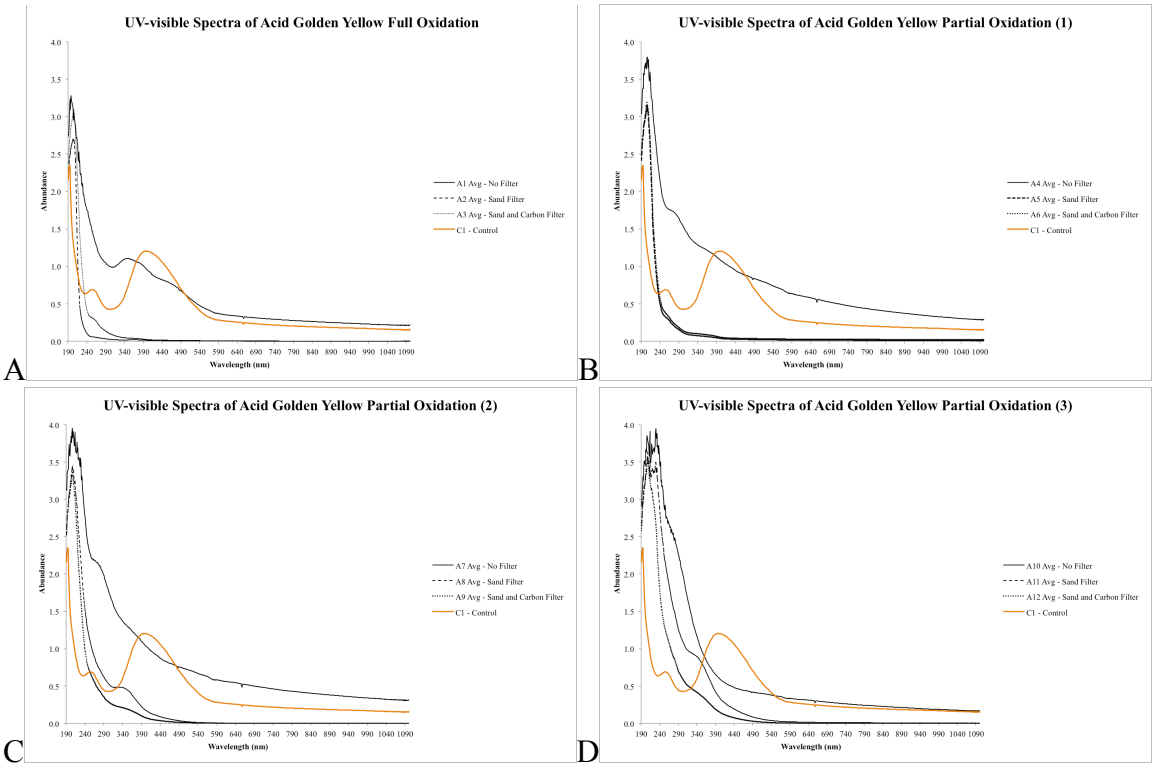

Figure 5.3: Acid Golden Yellow UV-visible spectra of the diluted control C1 for Acid Golden Yellow compared to (A) A1-A3, (B) A4-A6, (C) A7-A9, and (D) A10-A12.

5.2.2.3 Acid Ananda Blue

Table 3.12 lists the wavelengths of the peaks found in the UV-visible spectra for Acid Ananda Blue. Figure A.6 in Appendix A displays diluted samples of the Acid Ananda Blue controls C1-C5. Table A.11 in Appendix A displays calculated actual peak heights for C1-C5 from dilutions. Table A.12 in Appendix A displays peaks for Acid Ananda Blue A1-A12. The results can be viewed in Figure 5.4 which compares (A) A1-A3, (B) A4-A6, (C) A7-A9, and (D) A10-A12 to the diluted control peak C1. Peaks found at 206 nm and 340 nm were only present after acid and hydrogen peroxide were added to solution (C2-C5). Peaks at 257 nm, 313 nm, 411 nm, and 637 nm were also visible in C1.

In general and despite treatment, the peak at 206 nm stayed much higher than the other pollutants in solution. The contaminants displaying UV peaks at 206 nm, 257 nm, 313 nm, and 340 nm were reduced most by partial oxidation differing the magnitude of degradation and order of oxidation most frequently by partial oxidation (1) or (2). Sand and carbon filtration, however, following oxidation greatly decreased the height of the peaks by physically removing the organics out of solution showing decreasing peaks with increasing time. Following full oxidation, there was a larger peak shown after carbon filtration than after sand filtration.

The visible peaks at 411 and 637 nm decreased at a faster rate than UV peaks and follow the expected trends decreasing more with longer oxidation time. Sand and carbon filtration following full oxidation was more effective at removing the chemicals responsible for peaks at 411 nm and 637 nm (thus making full oxidation followed by sand alone or sand and carbon the most effective treatment). As with the UV wavelength peaks, generally sand filtration accomplished more than the carbon filtration due to physical capturing of the solids created by the photo-Fenton oxidation process and physically removing them from solution. Again, carbon filtration did no harm to the process.

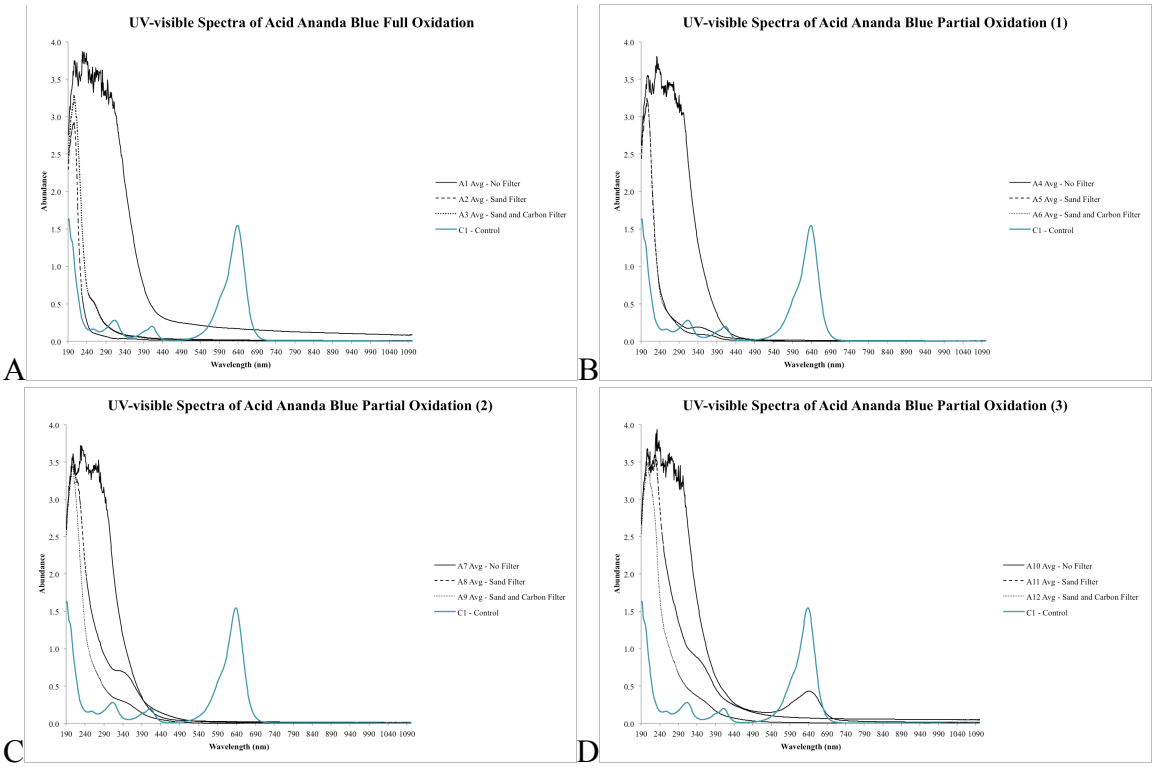

Figure 5.4: Acid Ananda Blue UV-visible spectra of the diluted control C1 for Acid Ananda Blue compared to (A) A1-A3, (B) A4-A6, (C) A7-A9, and (D) A10-A12.

5.3 COD Results

COD is used to analyze organic levels in solution. COD levels showed great variability, even when comparing similar samples. This is because the high level of dye used in this study has an exceptional level of organic material. Photo-Fenton oxidation also forms sludge in solution that is comprised of dye and rust from the iron catalyst. For this reason COD levels that dropped below the Karnataka State Pollution Control Board's (KSPCB) allowable 250 ppm are particularly noted. The general trend expected for oxidized samples from high COD to low is: A10, A7, A4, A1, A11, A8, A5, A12, A9, A6, A2, A3. Variability is expected within the partially oxidized samples regarding their order of decreased COD with filtration and time because of the very low partial

oxidation (3) times. The fully oxidized sample produces sludge that can keep the COD higher than permissible effluent levels; however, after physical removal of these organics, the sand and carbon filtered samples after full oxidation often brings COD close to negligible (neither type of filtration is worst). Since partial oxidation does not fully precipitate the organics out of solution, with the shortest partial oxidation times precipitating the least organics, the sand and carbon filtration cannot fully separate them from the water base thus resulting in a higher COD. In the analysis of the data, it is important to also consider ambient temperature, sunlight, and pH during the experiment in order to capture the effects of these variables on the COD reduction caused by the photo-Fenton oxidation process. Chapter 2 contains a discussion of a connection between temperature, sunlight, and COD reduction in dye effluent for studies conducted with dyes at lower concentrations; it is uncertain whether there will be such connections for the photo-Fenton oxidation of the 5 g/L dye effluent.

5.3.1 Acid Fast Red

COD results for Acid Fast Red as it relates to temperature, pH, iron, and sunlight can be viewed in Table B.4 in Appendix B. Table 5.2 presents an overview of the average results in India and the USA comparing C1-C5 to A1-A12. Figure 5.5 depicts the decrease of COD.

The control samples had COD levels that ranged between 865 and 6880 ppm. For India, sample COD in decreasing order was as follows: C1, A10, A7, A11, A4, A8, A12, A6, A1, A2, A3, A9, A5. For the USA, sample COD in decreasing order was as follows:

A10, C1, A7, A1, A11, A4, A8, A12, A9, A5, A6, A3, A2. Although the order of decrease was not exactly the same, it was similar. For both locations the unfiltered samples A10, A7, and A4 were above the permissible effluent levels. A10 and C1 were very close to each other, meaning that partial oxidation (3) alone (with no filtration) did very little to the sample in respect to decreasing the COD from the control sample level. A7, A11, and A4 followed closely and in that order meaning that A11, despite being filtered through sand, did not differ from A7 or even A4 non-filtered samples. Note that the A7 and A4 non-filtered samples still had a COD above the permissible effluent level. A8 and A12 came next for both locations with varying order and were near the allowable COD limit meaning that the A8 sand filtered sample was equivalent to the A12 carbon filtered sample. All samples remaining were below permissible limits and followed the basic trend that longer oxidation time followed by filtration decreased COD levels the most.

Table 5.2: COD overview of Acid Fast Red comparing C1-C5 to A1-A12 in India and the USA.

Acid Fast Red	COD India	Avg. COD USA
C1	1614	1762
C2	NA	1586
C3	NA	5900
C4	NA	865
C5	NA	6880
A1	108	480
A2	58	14
A3	na	18.5
A4	474	280
A5	0	89.5
A6	214	88
A7	1308	1530
A8	322	234
A9	16	161
A10	1506	2540
A11	828	358
A12	250	229

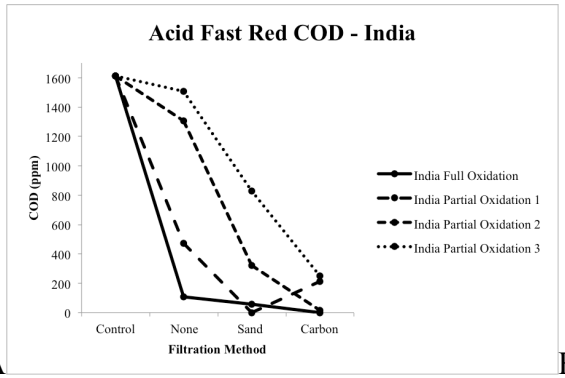

A

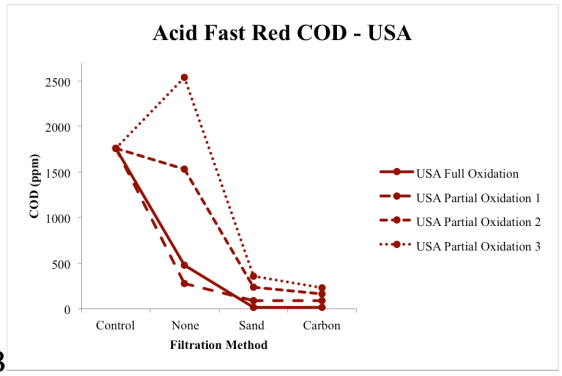

B

Figure 5.5: COD results comparing Acid Fast Red samples C1 to (A) A1-A12 in India, and (B) A1-A12 in the USA.

5.3.2 Acid Golden Yellow

COD results for Acid Golden Yellow as it relates to temperature, pH, iron, and sunlight can be viewed in Table B.5 in Appendix B. Table 5.3 presents an overview of the

average results in India and the USA comparing C1-C5 to A1-A12. Figure 5.6 depicts the decrease of COD.

The control samples had COD levels that ranged between 182 and 6220 ppm. For India, sample COD in decreasing order was as follows: A10, C1, A11, A12, A8, A9, A6, A1, A5, A3, A2, A7, A4. For the USA, sample COD in decreasing order was as follows: A10, A4, A7, C1, A1, A11, A5, A2, A12, A8, A6, A3, A9. Although the order of decrease was not exactly the same, it was similar. For the USA, unfiltered samples A10, A7, and A4 were above the permissible effluent levels and above C1, meaning partial oxidation, no matter the time (with no filtration) did very little to the sample with respect to decreasing the COD from the control sample level. For India samples, A10 and C1 were very close to each other, indicating that partial oxidation (3) alone (with no filtration) did not decrease COD levels from the control. For both locations all samples other than those mentioned above, fell below the permissible limits. Sustainable photo-Fenton oxidation followed by filtration, no matter the time of oxidation, decreased COD of 5 g/l Acid Golden Yellow to below permissible limits. USA samples followed the general trend that longer oxidation time followed by filtration decreased COD levels the most.

Table 5.3: COD of Acid Golden Yellow comparing C1-C5 to A1-A12 in India and the USA.

Acid Golden Yellow	COD India	Avg. COD USA
C1	618	730
C2	NA	482
C3	NA	6120
C4	NA	182
C5	NA	6220
A1	216	60
A2	68	18
A3	NA	26
A4	1086	0
A5	120	68
A6	2	84
A7	900	0
A8	24	132
A9	0	122
A10	1584	3840
A11	172	252
A12	26	196

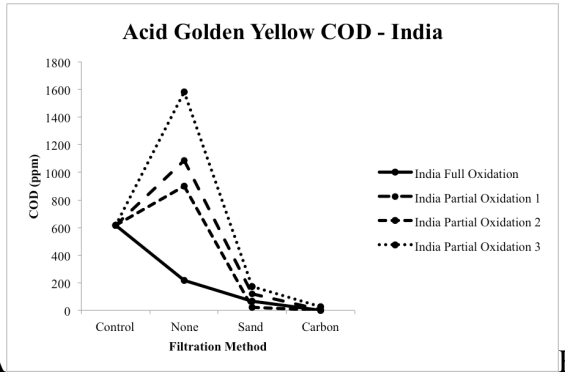

A

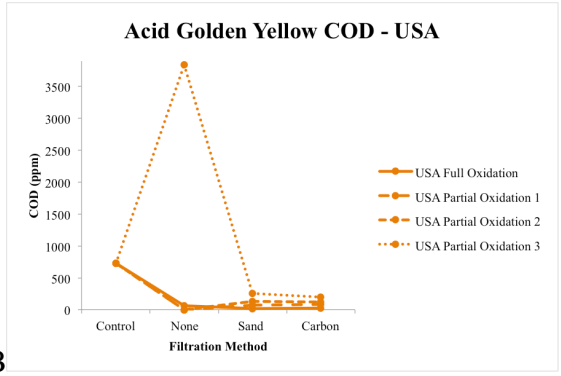

B

Figure 5.6: COD results comparing Acid Golden Yellow samples C1 to (A) A1-A12 in India, and (B) A1-A12 in the USA.

5.3.3 Acid Ananda Blue

COD results for Acid Ananda Blue as it relates to temperature, pH, iron, and sunlight can be viewed in Table B.6 in Appendix B. Table 5.4 presents an overview of the average

results in India and the USA comparing C1-C5 to A1-A12. Figure 5.7 depicts the general decrease of COD.

The control samples had COD levels that ranged between 1728 and 6720 ppm. For India, sample COD in decreasing order was as follows: C1, A11, A7, A4, A9, A10, A1, A12, A8, A5, A6, A3, A2. For the USA, sample COD in decreasing order was as follows: A10, C1, A7, A4, A11, A8, A12, A9, A5, A6, A3, A1, A2. Although the order of decrease was not exactly the same, it was similar. For both locations the unfiltered samples A10, A7, and A4 were above the permissible effluent levels, meaning partial oxidation, no matter the time (with no filtration) did not decrease the COD sufficiently. In the USA samples, sustainable photo-Fenton oxidation followed by filtration, no matter the time of oxidation, decreased COD of 5 g/l Acid Ananda Blue very quickly to below permissible limits. USA samples followed the general trend that longer oxidation time followed by filtration decreased COD levels the most.

Table 5.4: COD overview of Acid Ananda Blue comparing C1-C5 to A1-A12 in India and the USA.

Acid Ananda Blue	COD India	Avg. COD USA
C1	1728	2402
C2	NA	2544
C3	NA	6720
C4	NA	2666
C5	NA	5980
A1	258	50
A2	4	22.5
A3	na	66
A4	756	760
A5	50	93.5
A6	12	85.5
A7	1188	1750
A8	92	166
A9	528	136
A10	398	3850
A11	1440	208
A12	114	162

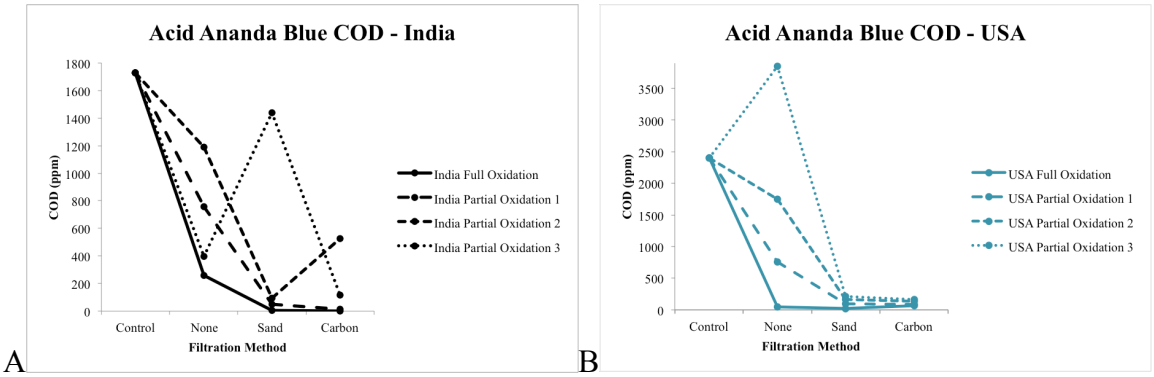

A B

Figure 5.7: COD results comparing Acid Ananda Blue samples C1 to (A) A1-A12 in India, and (B) A1-A12 in the USA.

5.3.4 Sludge Production

Sludge production was notable during the photo-Fenton oxidation process with more sludge being produced during longer duration experiments. Sludge volume was

quantified during the India studies and volumes are listed in Table B.4 for Acid Fast Red, Table B.5 for Acid Golden Yellow, and Table B.6 for Acid Ananda Blue in Appendix B. Percent volume sludge per 1-liter laboratory tests are listed in Table 5.5 for each dye color after full oxidation. Sludge is removed from solution using filtration. Therefore, the presence of sludge in non-filtered samples can greatly impact the overall COD level. During an interview with a medium-scale dyer in India, it was learned that sludge production created from biodegradation (customary method of dye wastewater treatment in medium and large-scale textile plants) of their wastewater, was approximately 15% of total solution. Percentage sludge production using sustainable photo-Fenton oxidation is much less.

Table 5.5: Percent sludge produced per 1-liter laboratory study during full oxidation in India according to color.

Dye Color	% Sludge
Acid Fast Red	7
Acid Golden Yellow	9
Acid Ananda Blue	1

5.3.5 Solar Irradiance and Temperature

Generally, the solar irradiance in the USA tests was higher than solar irradiance in the India tests since studies in India were completed as the rainy season was beginning. The solar irradiance in India was between 101-631 W/m^2 and in the USA between 410-856 W/m^2. Meanwhile, the USA tests were completed at lower ambient temperatures than the India tests, due to the time of year the studies were performed. The temperatures in India ranged from 25-27.8 ºC and in the USA 3.1-14.4 ºC. Decolorization and degradation occurred for both test sites, indicating that the process can work for a wide

range of temperatures and solar irradiances. COD levels varied more as a result of time and filtration rather than solar irradiance and temperature. The COD levels that resulted from the extreme ends of solar irradiance or temperature were mid-range COD results. It is therefore concluded that while UV irradiance is needed for the reaction to occur, and the temperature must be above the freezing temperature UV irradiance and temperature are not key factors in producing a successful process. The tests were successful despite the lack of direct sunlight in partly cloudy or partly sunny conditions as long as there was daylight. This is important for eventual field implementation of the process, as both solar irradiance and temperature are variables that cannot be easily controlled in practice.

5.4 GC/MS Results

GC/MS analysis was used to measure and identify chemical intermediates found in solution before and after oxidation. To qualify, chemical peaks detected by the GC must reach a minimum of 10,000 abundance (based on electrical signal passed through sample) and match the MS library with 80% or more accuracy. In order to verify the quantification of abundance of organics found in solution, a 95% pure sample of Tolylene, 2,4-diisocyanate (also called Benzene, 2,4-diisocyanato-1-methyl) was tested using the same GC/MS methods listed in Chapter 3. This aromatic and cyanate chemical was chosen because of its abundance in the reactive dye solution after treatment. Figure C.46 in Appendix C displays the GC/MS graph of this control. The 95% pure sample absorbed onto the Solid Phase Micro Extraction (SPME) fiber was found to have an abundance of Benzene, 2,4-diisocyanato-1-methyl at 1,800,000; 2H-

Benzimidazol-2-one, 1,3-dihydro-5-methyl at 100,000; Bis(2-ethylhexyl) phthalate at 95,000; Squalene at 50,000; 2-Propenoic acid, 3-(4-methoxyphenyl)-, 2-ethylhexyl ester at 40,000; and Dodecanoic Acid, Ethyl Ester at 28,000. The presence of Benzene, 2,4-diisocyanato-1-methyl at 1,800,000 abundance in the pure sample verifies the accuracy of finding a lesser abundance in treated samples tested using the same SPME and GC/MS methodology. The presence of the other organics in the control sample reinforce that the control sample was only 95% pure. The level of Benzene, 2,4-diisocyanato-1-methyl in the 95% pure sample can be described by either fraction of mass or fraction of ions. GC/MS displays the fraction of mass in its measured level of abundance, here reaching 85% of the total chemicals found; however, the sample is labeled 95% pure based on the fraction of ions in solution.

5.4.1 Acid Fast Red

Table C.4 in Appendix C lists all of the GC/MS results as they relate to C1-C5 and A1-A12 for Acid Fast Red including when complete degradation had occurred (which resulted in no noticeable peaks). Table 5.6 contains an overview of GC/MS results of all chemicals found in C1-C5 and A1-A12 for Acid Fast Red and what type of compound each result is and their responsible functional groups. Acid Fast Red had various organic compounds left in solution after treatment: aromatic compounds at 110,000 abundance; aromatic and alcohol combined compounds at 18,000 abundance; and aromatic and aldehyde combined compounds at 16,000 abundance. Figures C.16, C.17, C.18, C.19, and C.20 in Appendix C display GC/MS peaks for C1, C2, C3, C4, and C5 respectively for Acid Fast Red.

C2 had the most detectable organic chemicals found in solution. Regarding treated samples, fully oxidized samples degraded more than partially oxidized samples. A1, A8, and A11 were the only samples where organics were detected after treatment. This means that full oxidation followed by filtration provided the greatest reduction in organics, although the longer partial oxidation times were also sufficient compared to the shorter partial oxidation times. USA samples had more organics than India samples. The results also show that benzene and naphthalene derivatives were the most prevalent in solution and the most difficult to degrade completely as seen by their presence in the treated samples.

Table 5.6: GC/MS overview of Acid Fast Red comparing C1-C5 to A1-A12.

Code	Country	Chemical Name	Abundance	Type of Compound	Functional Group
C1	USA	Benzaldehyde, 4-methyl	35000	Aromatic, Aldehyde	Phenyl & Carbonyl
C1	India	2-Naphthalenol	47000	Aromatic, Alcohol	(Naphth)Phenyl, Hydroxy
C1	USA	2-Naphthalenol	375000	Aromatic, Alcohol	(Naphth)Phenyl, Hydroxy
C2	USA	Benzaldehyde, 3-methyl	50000	Aromatic, Aldehyde	Phenyl, Carbonyl
C2	USA	[1,1'-Binaphthalene]-2,2'-diol	25000	Aromatic, Alcohol	Phenyl, Hydroxy
C2	USA	2-Naphthalenol, 1-bromo	70000	Aromatic, Alcohol, Bromide	Phenyl, Hydroxy, Bromide
C2	USA	2-Naphthalenol	1060000	Aromatic, Alcohol	(Naphth)Phenyl, Hydroxy
C3	USA	2-Naphthalenol, 1-bromo	17000	Aromatic, Alcohol, Bromide	Phenyl, Hydroxy, Bromide
C3	USA	2-Naphthalenol	33000	Aromatic, Alcohol	(Naphth)Phenyl, Hydroxy
C4	USA	2-Naphthalenol	120000	Aromatic, Alcohol	(Naphth)Phenyl, Hydroxy
C5	USA	1,4-Naphthalenedione	170000	Aromatic, Ketone	Phenyl, Carbonyl
A1	USA2	2-Naphthalenol	18000	Aromatic, Alcohol	(Naphth)Phenyl, Hydroxy
A8	USA2	Benzaldehyde	16000	Aromatic, Aldehyde	Phenyl, Carbonyl
A11	USA2	Benzenemethanamine, N-ethyl-	110000	Aromatic	Phenyl Group

5.4.2 Acid Golden Yellow

Table C.5 in Appendix C lists all of the GC/MS results as they relate to C1-C5 and A1-A12 for Acid Golden Yellow including when complete degradation had occurred (which resulted in no noticeable peaks). Table 5.7 contains an overview of GC/MS results of all chemicals found in C1-C5 and A1-A12 for Acid Golden Yellow and the types of compounds and their responsible functional groups. Acid Golden Yellow had various organic compounds left in solution after treatment: aromatic and aldehyde combined compounds at 20,500 abundance. Figures C.21, C.22, C.23, C.24, and C.25 in Appendix C display GC/MS peaks for C1, C2, C3, C4, and C5 respectively for Acid Golden Yellow.

C5 had the most detectable organic chemicals found in solution. Regarding treated samples, fully oxidized samples degraded more than partially oxidized samples. A5 was the only sample where organics were detected after treatment. Although Acid Golden Yellow oxidized samples had the least organics in solution compared to the other acid dyes, full oxidation followed by filtration still provided the most reduction in organics. USA samples had more organics than India samples. The results also show that benzene derivatives were the most prevalent in solution and the most difficult to degrade completely as seen by their presence in the treated sample.

Table 5.7: GC/MS overview of Acid Golden Yellow comparing C1-C5 to A1-A12.

Code	Country	Chemical Name	Abundance	Type of Compound	Functional Group
C2	USA	Benzaldehyde, 3-methyl	24500	Aromatic, Aldehyde	Phenyl, Carbonyl
C2	USA	Phenol	20750	Aromatic, Alcohol	Phenyl, Hydroxyl
C5	USA	Benzene, ethoxy	127000	Aromatic compound	Phenyl
C5	USA	Cyclohexasiloxane, dodecamethyl	15500	Organic	Silica
C5	USA	Parachlorophenol	65000	Alcohol, Electrophile	Hydroxyl, Halogen
A5	USA2	Benzaldehyde, 4-methyl-	20500	Aromatic, Aldehyde	Phenyl, Carbonyl

5.4.3 Acid Ananda Blue

Table C.6 in Appendix C lists all of the GC/MS results as they relate to C1-C5 and A1-A12 for Acid Ananda Blue including when complete degradation had occurred (which resulted in no noticeable peaks). Table 5.8 contains an overview of GC/MS results of all chemicals found in C1-C5 and A1-A12 for Acid Ananda Blue and what type of compound each result is and their responsible functional groups. Acid Ananda Blue had various organic compounds left in solution after treatment: aromatic compounds at 420,000 abundance; aromatic and aldehyde combined compounds at 20,000 abundance; and aromatic and alcohol combined compounds at 10,750 abundance. Figures C.26, C.27, C.28, C.29, and C.30 in Appendix C display GC/MS peaks for C1, C2, C3, C4, and C5 respectively for Acid Ananda Blue.

C3 had the most detectable organic chemicals found in solution. Regarding treated samples, fully oxidized samples degraded more than partially oxidized samples. A11 was the only sample where organics were detected after treatment. This means that full oxidation followed by filtration provided the greatest reduction in organics, although the longer partial oxidation times were also sufficient compared to the shorter partial

oxidation times. USA samples had more organics than India samples. The results also show that benzene derivatives were the most prevalent in solution and the most difficult to degrade completely as seen by their presence in the treated sample.

Table 5.8: GC/MS overview of Acid Ananda Blue comparing C1-C5 to A1-A12.

Code	Country	Chemical Name	Abundance	Type of Compound	Functional Group
C2	USA	Benzaldehyde	310000	Aromatic, Aldehyde	Phenyl, Carbonyl
C2	USA	Benzenemethanamine, N-ethyl-N-phenyl	20000	Aromatic	Phenyl
C2	USA	2-Propenal, 3-phenyl	35000	Aromatic, Aldehyde	Phenyl, Carbonyl
C3	USA	Benzaldehyde	760000	Aromatic, Aldehyde	Phenyl, Carbonyl
C3	USA	Benzaldehyde, 2-hydroxy	280000	Aromatic, Aldehyde	Phenyl, Carbonyl
C3	USA	Phenol	40000	Aromatic, Alcohol	Phenyl, Hydroxy
C4	USA	Benzaldehyde	255000	Aromatic, Aldehyde	Phenyl, Carbonyl
C4	USA	Benzenemethanamine, N-ethyl-N-phenyl	30000	Aromatic	Phenyl
C4	USA	2-Propenal, 3-phenyl	40000	Aromatic, Aldehyde	Phenyl, Carbonyl
C5	USA	Benzaldehyde	170000	Aromatic, Aldehyde	Phenyl, Carbonyl
C5	USA	Benzaldehyde, 2-hydroxy	140000	Aromatic, Aldehyde	Phenyl, Carbonyl
C5	USA	Phenol	22000	Aromatic, Alcohol	Phenyl, Hydroxy
A11	USA2	Benzaldehyde	20000	Aromatic, Aldehyde	Phenyl, Carbonyl
A11	USA2	Benzenemethanamine, N-ethyl-	420000	Aromatic	Phenyl
A11	India	Phenol, bis(1,1-dimethylethyl)-	10750	Aromatic, Alcohol	Phenyl, Hydroxy

5.5 ICP Results

ICP testing was used to determine metals left in solution. Although 18 metals were measured, only four were found regularly at high levels: calcium, iron, magnesium, and sodium. Their levels were measured for all samples from C1-C5 and A1-A12 to track when levels decreased below permissible levels. Arsenic, cadmium, lead, and manganese were occasionally found above permissible limits and it is noted when this occurred. Data were taken for all of the samples, including both the India and USA tests. Table

3.10 displays India's permissible effluent standards for wastewater in Dye and Dye Intermediate Industries for disposal in surface waters. India effluent standards do not list calcium, iron, magnesium, or sodium standards in their effluent regulations; therefore levels were compared to drinking water standards shown in Table 3.11. Permissible calcium levels are limited to 75-200 mg/L because calcium causes water hardness between 40-100 mg/L. Permissible magnesium levels are limited to 30-150 mg/L because at 500 mg/L the taste of the water is affected. Permissible iron levels are limited to 0.1-1.0 mg/L because at 0.3 mg/L the taste and aesthetics of the water is affected. Permissible sodium levels are limited to 20 mg/L because at 250 mg/L the taste and aesthetics of the water is affected and can alter natural biological activity. Natural waters have sodium levels between 5-50 mg/L. Permissible manganese levels are limited to 0.1-0.5 mg/L but at 0.05 mg/L the taste and aesthetics of the water is affected. Permissible arsenic levels are 0.01-0.05 mg/L because at 0.05 mg/L arsenic affects human health. Permissible cadmium levels are 0.005-0.01 mg/L but at 0.005 mg/L cadmium is toxic to humans. Permissible lead levels are 0.05-0.1 mg/L because lead causes irreversible neurological damage to humans, especially children (Sengupta, *et al.*, 2008).

The general trend of these ions in solution was an increase of calcium and magnesium after sand filtration. Iron had the opposite trend, as it increased during the oxidation process (increasing more with longer oxidation time) and decreased to an almost negligible amount after sand filtration. This was a result of the physical capturing of the iron/dye sludge formed in solution during the oxidation process. Sodium increased or remained stable during oxidation and decreased after sand and carbon filtration. Note,

the levels of increase or decrease do not fit a mathematical trend because of the variability in chemical composition of the wastewater at such a high dye concentration. In addition, there is little control as to the sand's contents in India since it was construction sand that had been stored outside open to nature prior to use. Because of the difference in quantitative results between India and the USA, trends are described instead. These trends often match despite these numerical differences.

5.5.1 Acid Fast Red

Acid Fast Red ICP results are found in Table D.4 in Appendix D. Other than calcium, magnesium, iron, and sodium, for Acid Fast Red ICP results, manganese and arsenic were present occasionally and only after sand or carbon filtration in India, whereas manganese, arsenic, cadmium, and chromium shown in USA samples at lower levels than in India but more often after no filtration. Calcium controls ranged from 24.6 to 72.4 ppm with the highest level in C5, magnesium ranged from 1.7 to 17.9 ppm with the highest level in C5, iron from 0 to 1 ppm with the highest level in C5, and sodium from 947 to 1720 ppm with the highest level in C1.

Calcium and magnesium content in solution changed as the location of the study changed. For calcium, the USA samples were higher than the India samples. A1 in the USA had approximately half that of A4, A7, or A10. Sand filtration brought these numbers remarkably high, at times more than 100 percent higher than the India sample equivalents. India fully oxidized samples followed the same trend increasing after sand filtration and decreasing after carbon filtration. The largest increase was in the partial

oxidation (1) sand filtered samples for both India and USA samples. The smallest increase was after full oxidation. The partial oxidation (3) samples increased the least among the other partial oxidation times. The non-filtered USA samples and all of the India samples were below the drinking water permissible limits.

Magnesium did not follow such clear trends as calcium. It was expected that samples would increase after sand filtration; however this was only the case with samples in India. In the USA, A1 was the lowest of the non-filtered samples, just as with calcium, tripled for A4 and A7, and only doubled for A10. The sand filtration of each sample decreased magnesium levels to negligible except with A11. Carbon filtration only impacted A3. India samples differed in that they all increased after sand filtration by more than two times, and slightly decreased after carbon filtration. All magnesium levels stayed very low and were well below the permissible drinking water limit.

Iron content in solution changed as the location of the study changed. Before filtration, USA samples had the highest iron in A4 and the lowest in A10, and A1 was in between the two and was equivalent to A7. The iron levels of all of the sand filtered samples decreased to negligible and stayed there after carbon filtration except A2. The iron levels in the India samples increased with less time (A1 India has no sample), and the filtration efficacy decreased as time decreased. The only exception to this was after full oxidation (A2 and A3). All A3, A5-A6 samples, and A8-A9, A11-A12 USA samples were below the permissible drinking water limit.

Of the metals found in solution, sodium had very similar numbers in both India and USA samples. Filtration greatly decreased sodium levels and had the greatest impact after longer filtration times. The only samples found to be below permissible drinking water limits were A2-A3 in the USA.

Most India filtered samples found a level of manganese in solution including A2-A3, A8, A11-A12, while only A1 in the USA. Arsenic was also found in A6, A9, and A12 in India, while it was found in A2-4, A7, A10-A11 in the USA. Cadmium was only found in USA samples A4, A10-A11, while chromium in USA samples A5-A6.

5.5.2 Acid Golden Yellow

Acid Golden Yellow ICP results are found in Table D.5 in Appendix D. Other than the consistent presence of calcium, magnesium, iron, and sodium, manganese is present occasionally (and only after sand or carbon filtration) in India, whereas manganese, arsenic, cadmium, lead, and chromium are present in USA samples occasionally (when it is present it is after no filtration). Calcium controls ranged from 32.2 to 58.5 ppm with the highest level in C4, magnesium ranged from 5.9 to 14.7 ppm with the highest level in C5, iron from 0.2 to 1.2 ppm with the highest level in C5, and sodium from 1380 to 2080 ppm with the highest level in C4.

Calcium content in solution changed as the location of the study changed. For calcium, the USA samples were higher than the India samples. A1 in the USA had approximately four times that of A4, A7, or A10. Sand filtration brought all of these numbers

remarkably higher, at times more than 20 times higher than the India sample equivalents. India fully oxidized samples followed the same trend increasing after sand filtration and decreasing after carbon filtration. The largest increase was in the partial oxidation (1) sand filtered samples for both India and USA samples. The smallest increase was after full oxidation (A1 has no India sample). The partial oxidation (3) samples increased the least among the other partial oxidation times, and slightly decreased in the India sample. The non-filtered partially oxidized USA samples and all of the India samples were below the drinking water permissible limits.

The impact that location had on the magnesium content of solution is not as clear since all of the samples have concentrations that are very low and well below the permissible drinking water limit. It was expected that samples would increase after sand filtration, however this was only the case with samples in India. In the USA samples, A10 was the lowest of the non-filtered samples, just as with calcium. The sand filtration of each sample lowered magnesium levels to negligible except with A11. Carbon filtration changed very little only increasing A3. India samples differed in that they all stayed much more steady. Filtration often resulted in no change, but since all levels were very low, little impact was needed.

Iron content in solution changed as the location of the study changed. Before filtration, USA samples had the highest iron in A4 and the lowest in A10, and A1 is by far the highest at three times A4. All sand filtered samples' iron levels decreased to negligible and remain there after carbon filtration. The iron in the India samples increased with

more time (A1 India has no sample) and the filtration efficacy decreased as time decreased. The only exception to this was after full oxidation (A2 and A3). All A3, A5-A6, A9, A12 samples, A8, and A11 USA samples were below the permissible drinking water limit.

Of the metals found in solution, sodium had very similar numbers in both India and USA samples. Filtration greatly decreased sodium levels and most profoundly after longer filtration times, although India samples A8-A9 and A11-A12 surprisingly reacted oppositely. No samples were found to decrease below permissible drinking water limits.

Most India filtered samples found a level of manganese in solution including A2-A3, A5-A6, A11, while only A1, A4, and A7 in the USA. Arsenic was only found in the USA in A6, A2, A9, A11, and A12. Cadmium was only found in USA samples A4-A6, A9, A11-A12, while chromium was found in USA sample A4.

5.5.3 Acid Ananda Blue

Acid Ananda Blue ICP results are found in Table D.6 in Appendix D. Other than calcium, magnesium, iron, and sodium, for Acid Ananda Blue results, manganese and arsenic were present occasionally and only after sand or carbon filtration in India, whereas manganese, arsenic, cadmium, lead, and chromium were present in USA samples and most often after no filtration. Calcium controls ranged from 22.4 to 41.8 ppm with the highest level in C4, magnesium ranged from 5.7 to 15.3 ppm with the

highest level in C4, iron from 1.6 to 3.7 ppm with the highest level in C4, and sodium from 819 to 1260 ppm with the highest level in C4.

Calcium content of solution changed as the location of the study changed. For calcium, the USA samples were higher than the India samples. A1 in the USA had approximately double that of A4 and A7, and triple of A10. Sand filtration brought all of these numbers remarkably high, at times more than 50 times higher than the India sample equivalents. The India fully oxidized samples followed the same trend increasing after sand filtration and decreasing after carbon filtration. The largest increase was in the partial oxidation (1) sand filtered samples for both India and USA samples. The smallest increase was after full oxidation (A1 has no India sample). The partial oxidation (3) samples increased the least among the other partial oxidation times. The non-filtered partially oxidized USA samples and all of the India samples (except A5 and A8) were below the drinking water permissible limits.

Regarding the impact that location had on the magnesium content of solution was not as clear since all of the samples are very low and well below the permissible drinking water limit. It was expected that samples would increase after sand filtration; however, this was only the case with samples in India. In the USA samples, filtration caused all samples to decrease to negligible levels. A10 was the lowest of the non-filtered samples and A1 was highest, just as with calcium.

Iron content of solution changed as the location of the study changed. Before filtration, USA samples decreased with shorter oxidation times with the highest iron in A1 and the lowest in A10. A1 is by far the highest at five times the levels seen in A4. Most sand filtered samples' iron levels decreased to negligible and remained at those levels after carbon filtration. Only A11-A12 in India were slightly above permissible drinking water levels. The iron content of the India samples increased with more time (A1 India had no sample) and the filtration efficacy decreased as time decreased. All A2-A3, A5-A6, A8, and A9 and A11-A12 USA samples are below the permissible drinking water limit.

Of the metals found in solution, sodium had very similar numbers in both India and USA samples. Filtration greatly decreased sodium levels and most profoundly after longer filtration times. No samples were found to lower below permissible drinking water limits.

Most India filtered samples found a level of manganese in solution including A2-A3, A5, A8-A9, A11-A12 while only A1 in the USA. Arsenic was only found in India sample A9 and USA sample A1-A3, A6, A9-A12. Cadmium was only found in USA samples A1, A3-A7, A10, A12, while chromium in USA samples A3, A5-A6, and lead in USA sample A4-A5, A7, A10.

5.6 Respirometric Results

Respirometric analysis was conducted for partially oxidized India samples of different times (partial 1, partial 2, partial 3), of differing colors (red, yellow, blue), and that used

different filtration methods (no filter, sand filter). Fully oxidized samples' COD values were too low to biodegrade further so respirometric analysis was only completed for partially oxidized samples.

5.6.1 Acid Fast Red

Oxygen uptake results can be viewed in Figure E.4 in Appendix E which compare three trials of endogenous and exogeneous data describing the oxygen uptake of A4, A7, A10 or A5, A8, A11 for Acid Fast Red.

The results of the calculated oxygen uptake based on the data in Figure E.4 in Appendix E are presented in Table 5.9 for Acid Fast Red. As can be seen for the samples oxygen uptake was found to be 22.0 nMol min^{-1} mg^{-1} for A4, and 56.8 nMol min^{-1} mg^{-1} for A5. This means that the filtered sample after 45 minutes had more biodegradability than the one not filtered, although the one not filtered still had theoretical biodegradability by CETP sludge. For A7 oxygen uptake was found to be 68.1 nMol min^{-1} mg^{-1} and 0.0 nMol min^{-1} mg^{-1} for A8. Being oxidized for 35 minutes was enough for the partially oxidized (2) sample creating biodegradability by CETP sludge. A10 and A11 were found to have zero theoretical biodegradability by CETP sludge whether it was or was not filtered.

Table 5.9: Calculated oxygen uptake for Acid Fast Red according to partial oxidation time 1, 2, 3 and non-filtered or sand filtered sample results.

Sample Name	Color	Time	No Filter / Filter	O2 Uptake Value (nMol/min/mg)
A4	Acid Fast Red	Partial Oxidation (1)	No Filter	22.0
A5	Acid Fast Red	Partial Oxidation (1)	Sand Filter	56.8
A7	Acid Fast Red	Partial Oxidation (2)	No Filter	68.1
A8	Acid Fast Red	Partial Oxidation (2)	Sand Filter	0.00
A10	Acid Fast Red	Partial Oxidation (3)	No Filter	0.00
A11	Acid Fast Red	Partial Oxidation (3)	Sand Filter	0.00

5.6.2 Acid Golden Yellow

Oxygen uptake results can be viewed in Figure E.5 in Appendix E which compare three trials of endogenous and exogeneous data describing the oxygen uptake of A4, A7, A10 or A5, A8, A11 for Acid Golden Yellow.

The results of the calculated oxygen uptake based on the data in Figure E.5 in Appendix E are presented in Table 5.10 for Acid Golden Yellow. As can be seen for the samples oxygen uptake was found to be 0.00 nMol min^{-1} mg^{-1} for A4, and 22.7 nMol min^{-1} mg^{-1} for A5. This means that only the filtered sample after 25 minutes had biodegradability compared with the one not filtered. For A7 oxygen uptake was found to be 27.8 nMol min^{-1} mg^{-1} and 0.00 nMol min^{-1} mg^{-1} for A8. Being oxidized for 20 minutes was enough for the partially oxidized (2) sample to create biodegradability by CETP sludge. For A10 oxygen uptake was found to be 0.00 nMol min^{-1} mg^{-1} and 113 nMol min^{-1} mg^{-1} for A11. In this case the 15 minutes of partial oxidation followed by sand filtration created the most biodegradability by CETP sludge in this group of Acid Golden Yellow dye.

Table 5.10: Calculated oxygen uptake for Acid Golden Yellow according to partial oxidation time 1, 2, 3 and non-filtered or sand filtered sample results.

Sample Name	Color	Time	No Filter / Filter	O2 Uptake Value (nMol/min/mg)
A4	Acid Golden Yellow	Partial Oxidation (1)	No Filter	0.00
A5	Acid Golden Yellow	Partial Oxidation (1)	Sand Filter	22.7
A7	Acid Golden Yellow	Partial Oxidation (2)	No Filter	27.8
A8	Acid Golden Yellow	Partial Oxidation (2)	Sand Filter	0.00
A10	Acid Golden Yellow	Partial Oxidation (3)	No Filter	0.00
A11	Acid Golden Yellow	Partial Oxidation (3)	Sand Filter	113

5.6.3 Acid Ananda Blue

Oxygen uptake results can be viewed in Figure E.6 in Appendix E which compare three trials of endogenous and exogeneous data describing the oxygen uptake of A4, A7, A10 or A5, A8, A11 for Acid Ananda Blue.

The results of the calculated oxygen uptake based on the data in Figure E.6 in Appendix E are presented in Table 5.11 for Acid Ananda Blue. As can be seen for the samples oxygen uptake was found to be 6.87 nMol min^{-1} mg^{-1} for A4, and 22.0 nMol min^{-1} mg^{-1} for A5. This means that the filtered sample had more than 3 times the biodegradability by CETP sludge after 60 minutes of oxidation compared with the one not filtered. For A7 oxygen uptake was found to be 14.4 nMol min^{-1} mg^{-1} and 23.5 nMol min^{-1} mg^{-1} for A8. Being oxidized for 50 minutes was enough for the partially oxidized (2) sample to create half of the biodegradability by CETP sludge created after partial oxidation followed by sand filtration. For A10 oxygen uptake was found to be 47.7 nMol min^{-1} mg^{-1} and 0.00 nMol min^{-1} mg^{-1} for A11. In this case the 40 minutes of partial oxidation created the most biodegradability by CETP sludge in this group of Acid Ananda Blue dye.

Table 5.11: Calculated oxygen uptake for Acid Ananda Blue according to partial oxidation time 1, 2, 3 and non-filtered or sand filtered sample results.

Sample Name	Color	Time	No Filter / Filter	O2 Uptake Value (nMol/min/mg)
A4	Acid Ananda Blue	Partial Oxidation (1)	No Filter	6.87
A5	Acid Ananda Blue	Partial Oxidation (1)	Sand Filter	22.0
A7	Acid Ananda Blue	Partial Oxidation (2)	No Filter	14.4
A8	Acid Ananda Blue	Partial Oxidation (2)	Sand Filter	23.5
A10	Acid Ananda Blue	Partial Oxidation (3)	No Filter	46.7
A11	Acid Ananda Blue	Partial Oxidation (3)	Sand Filter	0.00

5.6.4 Statistical Analysis

Three-way ANOVA was completed to statistically analyze the interaction between three different variables (time, color, filtration method) for the acid dye experiments and how they affected respirometric analysis of the partially oxidized samples. Table 5.12 reveals that none of the three factors show a statistically significant effect on oxygen uptake ($P > 0.05$). Also, the interaction effect was insignificant. While the numbers of tests performed were too low to be statistically significant with regards to variables like iron surface area, the results do indicate that the process is beneficial, and there are indications that certain combinations are potentially better than others. For instance, shorter oxidation times with no filtration resulted in the highest biodegradability by CETP sludge.

Table 5.12: Analysis of Variance (3-way ANOVA) for partially oxidized samples. Variables for acid dye are time (partial 1, partial 2, partial 3), color (red, yellow, blue), and filtration method (no filter, sand filter).

	Df	Sum	Sq Mean	Sq F	value Pr(>F)
Dye(D)	2	215	107	0.069	0.935
Iron(I)	2	85.0	42.5	0.027	0.973
Filter(F)	1	150	150	0.096	0.773
D:I	4	4390	1100	0.700	0.631
D:F	2	2060	1030	0.656	0.567
I:F	2	2720	1360	0.867	0.487
Resid	4	6270	1570		

5.7 Discussion of Results

The purpose of the studied photo-Fenton oxidation procedure is to completely degrade organic compounds from an acid dye solution and to bring inorganics to the permissible drinking water level. The level of degradation achieved through various combinations of experimental variables was described above. UV-visible spectrometry can be compared

with published data to describe which organics were left after treatment. The COD results can be used to show the total organic load remaining and whether it agrees with the UV-visible spectrometry results. The GC/MS analysis can be used to identify the organics and their respective quantities. The ICP results can be used to describe the inorganic metal ions left in solution. The respirometric analysis allows for the determination of whether the remaining solution is theoretically biodegradable. Finally, the combined results can be used to identify an experimental procedure that will achieve the most effective treatment of the dye effluent in a cost-effective and sustainable manner.

Before recommendations can be made, it is important to understand the actual activities cottage-scale silk dyers perform. By mimicking the cottage-scale silk dyers' wastewater in laboratory-scale studies, the intent was to augment dyers' processes with a low-cost treatment option. For this reason, the following experimental methodology was chosen. (1) Acid dyes at 5 g/L concentration were mixed with household hydrochloric acid; (2) pharmacy-grade hydrogen peroxide was poured into the solution in containers holding rusty metal from old yogurt containers; (3) natural sunlight at ambient temperature were employed; (4) following treatment, sand and carbon filtration of the dye effluent was used. This process was developed to be low-cost and readily available. Since the work was not completed using laboratory-grade supplies, some contamination was expected to be found in the results in the form of outliers in the analysis. That being said, organic and inorganic chemicals found before (in the controls), during (after partial oxidation and followed by filtration), and after (after full oxidation, and followed by filtration) the

sustainable photo-Fenton oxidation process, agreed with the literature as described in Chapter 2. And since this study has a practical application because of the need for low-cost decolorization and dye wastewater treatment, the goal of the results is to prioritize the importance of certain variables over others in order to create a viable treatment unit to be used by small-scale silk dyers worldwide. The overall intention is to make sure that the color degrades and the chemical composition oxidizes to a simpler form before reusing the treated water for a second batch of dye, or before disposing of it as is normally done.

The variables used for the sustainable photo-Fenton process (including dye color, dye concentration, hydrochloric acid, hydrogen peroxide, iron surface area, solar irradiation, temperature, oxidation time, filtration method) all contribute to the degradation of the chemical dyes in solution. Each variable impacts the outcome of the sustainable photo-Fenton oxidation experiments detailed here. However, the importance of each variable differed from what was expected and previously documented by other research (see Chapter 2). Not all variables were tested in these studies—most were kept constant for all experiments. Time and filtration were tested for each color to measure their impact on the photo-Fenton oxidation process. Dye concentration, iron surface area, acidification using hydrochloric acid, and the quantity of hydrogen peroxide were held constant, and will impact the photo-Fenton oxidation process. Solar irradiation and temperature are also variables that impact photo-Fenton oxidation, but were not controlled in this work. The values of these were recorded, and so it was possible to determine if they significantly impacted the results.

Dye concentration was constant for all tests at 5 g/L, which is similar to that in the small-scale industry. Acidification with hydrochloric acid did not use a specific volume per solution, but instead always brought solution pH to 2.5. Each dye color required a different volume of 6% hydrogen peroxide, as was decided according to the optimization tests, but then the volume was not altered within each color set. In the case of temperature and solar irradiation, location is noted as India or USA. It was evident that temperature variation is less important than solar irradiation variation. Temperature did not seem to impact oxidation provided that the sample remained above the freezing temperature. UV light is incredibly important for the reaction to take place, but direct sunlight is not necessary. Each location varies greatly for temperature and solar irradiation, but since the process worked in both places their various levels do not prevent the chemical reaction from taking place.

The results here do not compare dye color but rather test the degradation of three colors that are typically used in the field. Knowing that red, yellow, and blue can form all colors in the rainbow, if their separate degradation using sustainable photo-Fenton oxidation is successful, their mixture, although slightly more complicated, should also be able to be oxidized. High COD levels are found in control samples due to the high concentration of dye in solution. UV-visible spectra of the control samples also reach well beyond the graph maximum thus denoting very high organic levels in solution. The high concentration of dye also offered great variation in the measured COD and GC/MS degradation results before filtration. Through UV-visible spectrometry, GC/MS, and COD, it is found that full oxidation followed by sand filtration (or sand and carbon

filtration) lowers the amount of organics in solution to near negligible in many cases. The hazard quality of the chemicals remaining in solution are listed according to the Globally Harmonized System of Classification and Labeling of Chemicals (GHS) where each chemical receives an H label for being hazardous followed by a number. 200 level labels distinguish they are physically hazardous, 300 level labels are hazardous to health, and 400 level labels are hazardous to the environment.

Bilgi and Demir (2005) state that while sulphonated azo dyes cannot be analyzed using GC/MS because they are non-volatile, their degradation products and intermediates can be detected, as can other types of dyes such as the non-azo ones tested here; this was also the case in this study. The most prevalent intermediate found using GC/MS analysis differed for each Acid Dye. The different chemical groups present their respective hazard as listed in Table 5.14. Acid Fast Red was found to contain mostly aromatics. After oxidation aromatics connected to alcohols and aromatics connected to aldehydes decrease, but general aromatics are found where they were not in the controls (although many organics present degraded completely during oxidation including aromatics/alcohols/bromides and aromatics/ketones). The aromatics here are harmful if swallowed or if they come in contact with skin. Acid Golden Yellow was found to contain mostly aromatics linked with aldehydes that decrease during oxidation. Aromatics and aldehydes combined are combustible, harmful if swallowed, and cause skin, eye, and possibly respiratory irritation. Acid Ananda Blue was found to contain mostly aromatics although it also contains aromatics connected to aldehydes and aromatics connected with alcohols. The compounds that contain aromatic and alcohol

functional groups here are harmful if swallowed, causes serious eye irritation, and are very toxic to aquatic life.

The biodegradability of these organics found in solution was measured using respirometric analysis. The oxygen uptake measure during this procedure showed positive activity in approximately two-thirds of the samples. Considering that the UV-visible spectrometry peaks, COD levels, and GC/MS peaks show aromatics and other functional groups left in solution, it can be concluded that the quantity of pollutants in solution are very low and may not be sufficient for the CETP sludge to react in a short time.

Since full oxidation followed by filtration left the least amount of organics in solution, it can be concluded that longer photo-Fenton oxidation time allows for the chemical reaction to separate more of the dissolved dye from the water in solution. More reaction time results in more sludge created by the separation of dye and iron rust from the aqueous solution. The creation of sludge occurs due to the chemical reaction between hydrochloric acid, iron, UV light, and hydrogen peroxide that frees hydroxyl radicals to attack the pollutants. Dye and rust sludge is easily removed from solution but is also easily remixed into solution. This explains why the organic level of the non-filtered fully oxidized samples, in some cases, can be comparable or higher than the non-filtered partially oxidized samples. The fully oxidized sample may have contained re-dissolved pollutants while the partially oxidized sample still contained dissolved chemicals. Although care was taken to not mix the settled non-filtered sample before testing, this

inadvertent mixing can explain any unexpected spikes in COD or peak height of UV-visible spectra. This also explains why the filtration of the sludge out of the fully oxidized sample results in lower organics than filtering the partially oxidized sample which still contains dissolved pollutants.

Iron/dye sludge is very fine and dissolution of sludge particulates is possible. This is a concern and should be studied further. Field studies detailed in Chapter 7 describe two methods that prevent the dissolution of the organic sludge content (that upon dissolution would be un-filterable and render the filtered-water colored) and prevent the inorganic content from clogging the sand filter. The first is to remove the organic sludge that is present in the form of foam from the top of solution before filtration but after photo-Fenton oxidation has taken place. Future studies should create a method that more efficiently utilizes labor time for removing the sludge foam. A third type of filtration in the form of cotton fabric located just before the sand filter is suggested to prevent the inorganic iron rust from clogging the sand. The cotton fabric is more easily washed as compared to the sand and is a finer filter to capture the particulates preventing their reentrance into solution. Future studies should detail a method of separating iron and dye from the sludge. Preliminary work has begun to dissolve the dye from the iron in the sludge thus proving that in fact there are separate organic and inorganic elements within the sludge. It would help decrease costs of photo-Fenton oxidation treatment if iron can be reused; and it would decrease costs for dyers if dye, depending on the extent of its oxidation, can be extracted and reused in future batches.

Using hydrochloric acid results in increased levels of chloride and sodium as measured using ICP. Chapter 3 describes the strong attraction between chloride and sodium ions; and also describes that sodium chloride is very soluble in water which makes it un-filterable through sand or carbon. The ICP results agree with this conclusion. Other photo-Fenton oxidation studies detailed in Chapter 2 use sulfuric acid preventing these high levels, but producing high levels of sulfates in their effluent. Future studies should investigate ways of removing sodium and chloride from treated effluent or compare the results from other acids and their impact on treated water quality.

Iron metal ions that are added to solution during the photo-Fenton oxidation process, via the iron scrap catalyst, are completely removed from solution after filtration. Calcium and magnesium increased during the filtration process but most often stayed below the permissible limits, especially for fully oxidized samples. Cadmium, lead, arsenic, and manganese ions are noted if they are above the permissible limits for drinking water which is sometimes the case, and they most often decrease to permissible levels after full treatment. All of these ions, and especially lead, are often the ingredients in chemical dyes to give them their vibrant color. As discussed in the results, calcium, magnesium, and iron decrease to permissible levels after full oxidation followed by sand and carbon filtration most successfully. Although the sodium in solution decreased substantially after full oxidation followed by filtration, treatment rarely brought the sample to below drinking water permissible limit of 20 mg/L. Further sodium removal will be needed for the success of future studies.

The impact that iron surface area (rather than dissolved iron (II) ferrous salt) has on the photo-Fenton oxidation process is tested in these experiments as 645 cm^2 surface area under 2.5 cm of solution above the iron. Iron rust is used in the sustainable photo-Fenton oxidation process in place of the laboratory-grade chemical iron (II) ferrous salt. Most photo-Fenton oxidation studies, as detailed in Chapter 2, describe optimal iron salt concentrations in mg/L iron to solution volume. This study uses scrap iron according to how its surface reacts when it is struck by UV radiation after it passes through the dye effluent. There are few previous studies that utilize scrap iron in their research and they quantify iron ion production according to iron weight. These studies utilized iron scrap in the form of shavings which have very high and immeasurable surface area. The role of iron as a catalyst in the photo-Fenton oxidation chemical reaction is detailed in Chapter 2. The amount of iron must be high enough for free iron ions to react in the photo-Fenton oxidation process in order to oxidize the pollutants, but not so high that there are extra ions in solution attracting hydroxyl radicals away from the chemical dye pollutant towards the iron. It can be concluded that despite possible scavenging, it is more beneficial for the degradation process that more iron be present, thus enabling the oxidation to occur, as compared to less iron, which may prevent it from starting. Any iron in solution after degradation is in the form of sludge and is easily filterable thus decreasing iron levels to negligible proven through the ICP results. It was found that higher surface areas of iron resulted in lower full oxidation times. This information can be used for future studies to utilize rusty metal containers for pilot-scale treatment unit construction.

Combining the UV-visible spectra data, COD levels, and the GC/MS labels gives specific detail regarding which organics remain in solution after sustainable photo-Fenton oxidation. The first thing worth mentioning is that UV-visible spectra peaks cannot be simply defined or labeled since a peak at a certain wavelength can be present for many different compounds depending on the color of that compound. Table 3.12, in Chapter 3, lists the labels for the peaks found in Acid Fast Red, Acid Golden Yellow, and Acid Ananda Blue samples according to past studies detailed in Chapter 2. There are similarities between many peaks found in the UV spectra that may be categorized according to other studies. Visible peaks that are responsible for the color in the dye are already well labeled by previous studies. Many UV and visible peaks remain unlabeled. GC/MS results assist in the labeling, but do not match the location of a UV-visible spectra peak to a specific organic. The UV peaks found in the spectra show high-level peaks as well, thus concluding that the solution contains a variety of organics at different abundances.

A confirmation that the photo-Fenton oxidation reaction is changing the chemical composition of solution can be seen by the presence of different peaks in the UV-visible spectrometry results with oxidation. As can be seen in the analysis of the control samples, UV peaks other than those shown in the control sample C1 were evident after the addition of acid and oxidant. He and Lei (2004) also discuss the presence of new peaks coming on the UV-visible spectra after oxidation.

UV peaks degrade much slower than visible peaks. The peak at 206 nm (or very close to it) found for all three Acid Dyes in this study is at the approximate location of phenol as described by He and Lei (2004) as listed in Table 3.12. Although this cannot be completely confirmed, many organics containing the same phenyl ring were identified by GC/MS as described in Tables 5.6, 5.7, and 5.8. The peak at 206 nm is by far the highest of the peaks present in the controls even after partial and full oxidation and sand and carbon filtration. This is expected because it is difficult to degrade the phenyl or benzene ring.

Visible peaks degrade very quickly. Chapter 2 reveals the theory that the chromophores located in the chemical composition of dyes degrade very quickly. The peaks responsible for dye color in this study also degrade quickly and are completely degraded after full oxidation. Other visible peaks that have not been clearly identified as coming from the color composition also fully degrade; this identification is beyond the scope of this study.

Table 5.14: Hazardous effects of the definable chemicals that remain in solution after photo-Fenton oxidation of acid dyes listed according to the Globally Harmonized System of Classification and Labeling of Chemicals (GHS).

Type of Compound	Hazard Statement
Aromatic	H302 + H312 Harmful if swallowed or in contact with skin
Aromatic & Aldehyde	H227 Combustible liquid. H302 Harmful if swallowed. H315 Causes skin irritation. H319 Causes serious eye irritation. H335 May cause respiratory irritation.
Aromatic & Alcohol	H302 + H332 Harmful if swallowed or if inhaled. H319 Causes serious eye irritation. H400 Very toxic to aquatic life.

5.8 Summary

In summary, laboratory-scale research using sustainable photo-Fenton oxidation to degrade 5 g/L Acid Dyes using pharmacy-grade 6% hydrogen peroxide, household hydrochloric acid, scrap iron sheets, and sunlight is best done using full oxidation time followed by sand and carbon filtration to remove sludge.

There are many variables in the photo-Fenton oxidation process that impact the success of dye degradation. These include chemical composition of dyes, concentration of dye, acidified pH of solution, quantity of hydrogen peroxide used, solar irradiation, oxidation time, iron surface area, and filtration method. This study uses a cottage-scale industry dye concentration that is higher than any previous photo-Fenton oxidation study. This study also compares data taken in different locations whose solar irradiation varies greatly. Despite these differences from previous studies, complete color degradation occurred, as other organic and inorganic chemicals in solution also decreased to below permissible effluent levels. Degradation benefited from longer oxidation time and using iron with a greater surface area requires less time for full oxidation. High sodium and chloride levels after full treatment are a concern because of the choice to use readily available hydrochloric acid to acidify the solution.

Overall, the sustainable photo-Fenton oxidation process using scrap metal as the iron catalyst coupled with sand and carbon filtration shows great promise for the decolorization and chemical degradation of Acid Fast Red, Acid Golden Yellow, and Acid Ananda Blue. The process may not need biodegradation after complete oxidation

and filtration, as little additional benefit is seen with biodegradation. Future studies should focus on the remaining treated effluent after filtration including ways to lower sodium and chloride levels as well as how to separate and reuse iron and dye present in solid sludge that settles out of solution or is captured by sand filtration.

When considering that a cottage-scale dyer uses a very high concentration of dye in their dye batch, there is an opportunity for education and system improvement. Speaking with a medium-scale silk dyer in India, it was discovered that small process changes can decrease the impacts that dye effluent has on the environment. However, there are many rationales that interplay and cause a dyer to apply the methodology s/he uses. This work's focus was engineering an option for the current methodology of a cottage-scale silk dyer in rural Bangalore. It is worth mentioning here that there is a need for discussion and upgrading of the current small-scale dyer methodology in order to preserve and protect the natural environment. Despite treatment of the high concentration of dye wastewater, starting with a high level of chemical in an industry results in a high level of chemical waste. This project has successfully contained and modified the chemical waste to a form that is less dangerous and more manageable. However, using a lower concentration of dye or using natural dyes would lessen the impact of the dyeing process on the natural environment.

CHAPTER 6 – ACID DYE WITH SOAP AND SODA PHOTO-FENTON OXIDATION RESULTS AND DISCUSSION

6.1 Introduction

Acid Dye with Soap and Soda was chosen for this study because it is commonly used in cottage-scale silk dyeing industries in Karnataka, India. Its chemical composition varies greatly by color and is detailed in Chapter 3. Acid Fast Red with Soap and Soda, Acid Golden Yellow with Soap and Soda, and Acid Ananda Blue with Soap and Soda were specifically used in this study. Field Samples taken from a small-scale silk dyer just outside of Bangalore, Karnataka, India and were also tested. These are labeled Field Sample Green and Field Sample Maroon and also contain soap and soda; these samples are representative of industrial silk dye effluent. Field Samples were not available at the quantity needed for a complete study. Testing the Field Samples was only used to re-affirm and give validity to the results of the laboratory-scale tests run on Acid Dye with Soap and Soda created to mimic the Field Samples.

The laboratory-scale study detailed here used 5 g/L dye mixed with boiled 10 g/L soda, and 3.1 g/L soap in 1-liter tap water which was then acidified to pH 2.5 using hydrochloric acid. Next, hydrogen peroxide was added as an oxidizing agent, and the resulting mixture was poured over 645 cm^2 of rusty scrap iron to a depth of 2.5 cm. The mixture was then left in the sun (in India or the USA) for the appropriate time for full or partial photo-Fenton oxidation to occur. Acid Dye with Soap and Soda partial oxidation times were found via visual observation because separation of Acid Dyes from water is

very noticeable and easy to detect. The partial oxidation time was chosen just before the dye sank to the bottom of solution. Samples were then tested after experiencing three filtration methods (none, sand, sand and carbon). For ease of documentation, the abbreviations listed in Table 6.1 are used for notation of the different sample types and Table 4.2 for notation of the control samples. Methodology of the experimental procedures is detailed in Chapter 3. Field Samples were tested only after full oxidation, full oxidation followed by sand filtration, and full oxidation followed by sand and carbon filtration.

Complete analysis of all samples was completed using UV-visible spectrometry, COD, GC/MS, and ICP. The purpose of this was to determine the organic and inorganic contaminants left in solution. In addition, respirometric analysis was completed to predict the biodegradability of the contaminants left in solution.

Table 6.1: Abbreviations of sample names for acid dyes with soap and soda.

Dye Type	Oxidation Time (Full or Partial)	Filtration Type (None, Sand, Sand and Carbon)	Abbreviation
Acid with Soap and Soda	Full	None	S1
Acid with Soap and Soda	Full	Sand	S2
Acid with Soap and Soda	Full	Sand and Carbon	S3
Acid with Soap and Soda	Partial	None	S4
Acid with Soap and Soda	Partial	Sand	S5
Acid with Soap and Soda	Partial	Sand and Carbon	S6
Field Sample	Full	None	F1
Field Sample	Full	Sand	F2
Field Sample	Full	Sand and Carbon	F3

6.2 UV-visible Spectrometry Results

UV-visible spectrometry was used as an analysis method to determine the optimal time for partial and full oxidation for Acid Dyes with Soap and Soda using photo-Fenton oxidation after optimizing hydrogen peroxide quantity (detailed in Chapter 3). The undiluted samples were analyzed using UV-visible spectrometry to find the location and peak of the color left in solution. C1 spectra displayed indistinguishable peaks because the sample is not diluted. After partial oxidation a peak was present and after full oxidation no visible peak was present.

6.2.1 Partial and Full Oxidation Results

6.2.1.1 Acid Fast Red with Soap and Soda

Table 3.12 lists the wavelengths of the peaks found in the UV-visible spectra for Acid Fast Red with Soap and Soda. Figure A.7 in Appendix A displays diluted samples of the Acid Fast Red with Soap and Soda controls C1-C5. Table A.13 in Appendix A displays calculated actual peak heights for C1-C5 from dilutions. Table A.14 in Appendix A displays peaks for Acid Fast Red with Soap and Soda S1-S6. The results can be viewed in Figure 6.2 which compares (A) S1-S3 and (B) S4-S6 to the diluted control peak C1. Peaks found at 203 nm were only present after acid and hydrogen peroxide were added to solution (C1-C5). Peaks at 214 nm, 280 nm, 317 nm, and 505 nm were also visible in C1.

In general and despite treatment, the peaks at 203 nm and 214 nm stayed much higher than the other peaks. The contaminants displaying UV peaks at 280 nm and 317 nm were

reduced most by full oxidation followed by partial oxidation. Sand and carbon filtration following oxidation greatly decreased the height of the peaks by physically removing the organics out of solution. Occasionally there was a larger peak shown after carbon filtration than after sand filtration, although the increase is very small and stays with the general trend that filtration further degrades oxidized wastewater by removing contaminants from solution.

The visible peak at 505 nm decreased at a faster rate than the peaks in the ultraviolet region but followed the same trends – decreasing more with longer oxidation time. Sand and carbon filtration following full oxidation was more effective at removing the chemicals responsible for the peak at 505 nm (thus making full oxidation followed by sand alone or using both sand and carbon the most effective treatment). As with the UV wavelength peaks, generally sand filtration accomplished more than the carbon filtration due to the physical capture of the solids created by the photo-Fenton oxidation process and the physically removal of them from solution. It should be noted that carbon filtration did no harm to the process.

A 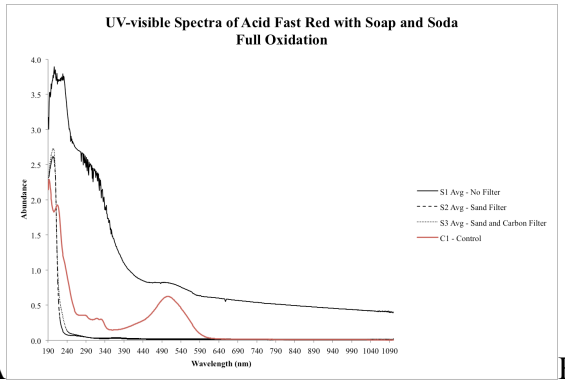

B 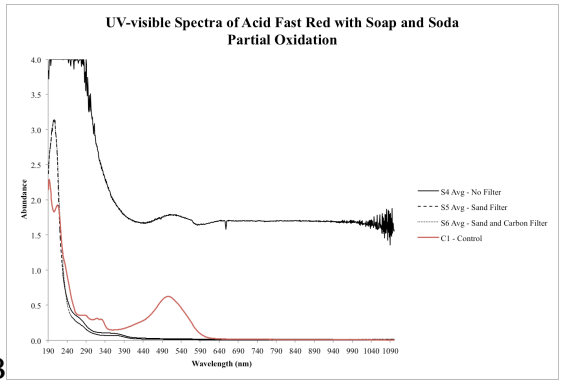

Figure 6.2: Acid Fast Red with Soap and Soda UV-visible spectra of the diluted control C1 compared to (A) S1-S3 and (B) S4-S6.

6.2.1.2 Acid Golden Yellow with Soap and Soda

Table 3.12 lists the peaks found in UV-visible spectra for Acid Golden Yellow with Soap and Soda. Figure A.8 in Appendix A displays diluted samples of the Acid Golden Yellow with Soap and Soda controls C1-C5. Table A.15 in Appendix A lists calculated actual peak heights for C1-C5 from dilutions. Table A.16 in Appendix A displays peaks for Acid Golden Yellow with Soap and Soda S1-S6. These results can also be viewed in Figure 6.3 which compares the UV-visible spectra of the diluted control C1 for Acid Golden Yellow with Soap and Soda to (A) S1-S3 and (B) S4-S6. Peaks found at 205 nm and 360 nm were only present after acid and hydrogen peroxide were added to solution (C1-C5). Peaks at 195 nm, 248 nm, and 403 nm were also present in C1.

In general and despite treatment, the peaks at 195 nm and 205 nm stayed much higher than the other pollutants in solution. The contaminants displaying UV peaks include peaks at 195 nm, 205 nm, 248 nm, 360 nm, and 403 nm. The peak at 403 nm is near the edge of the visible spectrum. However, since this peak acted very similarly to the UV trends, it is taken here as a UV peak. Most listed wavelengths benefit most from full oxidation compared to partial oxidation. Peaks at 360 nm and 403 nm were very slightly lower after partial oxidation. Sand and carbon filtration following oxidation greatly decreased the height of the peaks by physically removing the organics out of solution. Filtration following full oxidation lowered the peak heights more than after partial oxidation thus displaying the increased importance of full oxidation compared with partial. Sand and carbon filtration following oxidation greatly decreased the peaks' heights by physically removing the organics out of solution. The filtration removed more

from solution after longer oxidation time proving oxidation to be necessary as a pretreatment for filtration. Occasionally there is a larger peak shown after carbon filtration than after sand filtration, although the increase is very small and stays with the general trend that filtration further degrades oxidized wastewater by removing contaminants from solution.

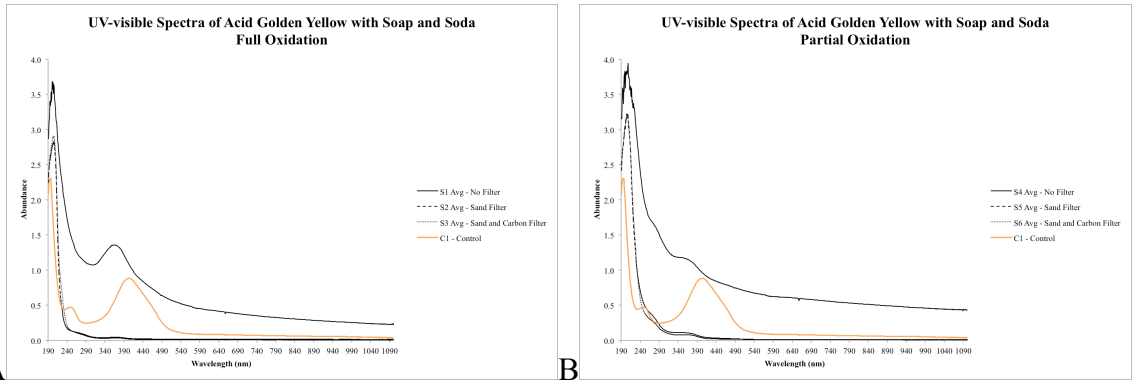

Figure 6.3: Acid Golden Yellow with Soap and Soda UV-visible spectra of the diluted control C1 compared to (A) S1-S3 and (B) S4-S6.

6.2.1.3 Acid Ananda Blue with Soap and Soda

Table 3.12 lists the peaks found in UV-visible spectra for Acid Ananda Blue with Soap and Soda. Figure A.9 in Appendix A displays diluted samples of the Acid Ananda Blue with Soap and Soda controls C1-C5. Table A.17 in Appendix A lists calculated actual peak heights for C1-C5 from dilutions. Table A.18 in Appendix A displays peaks for Acid Ananda Blue with Soap and Soda S1-S6. These results can also be viewed in Figure 6.4 which compares the UV-visible spectra of the diluted control C1 for Acid Ananda Blue with Soap and Soda to (A) S1-S3 and (B) S4-S6. Peaks found at 205 nm, and 360 nm were only present after acid and hydrogen peroxide were added to solution

(C2-C5). Peaks at 196 nm, 259 nm, 311 nm, 411 nm, and 638 nm were also visible in C1.

In general and despite treatment, the peaks at 196 nm and 205 nm stayed much higher than the other peaks. The contaminants at the lower UV peaks including 196 nm, 205 nm, and 259 nm with no filtration were at the peak of the graph after both partial and full oxidation. The contaminants at the higher peaks (both UV and visible) including 311 nm, 360 nm, 411 nm, and 638 nm were reduced more by partial oxidation than full oxidation. Sand and carbon filtration following oxidation greatly decreased the peaks' heights by physically removing the organics out of solution. The filtration removed more from solution after longer oxidation time proving time to be an important factor in the oxidation process. Occasionally there was a larger peak shown after carbon filtration than after sand filtration, although the increase is very small and stays with the general trend that filtration further degraded oxidized wastewater by removing contaminants from solution.

A 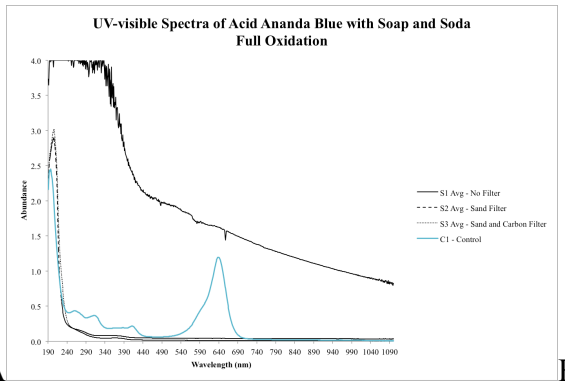

B 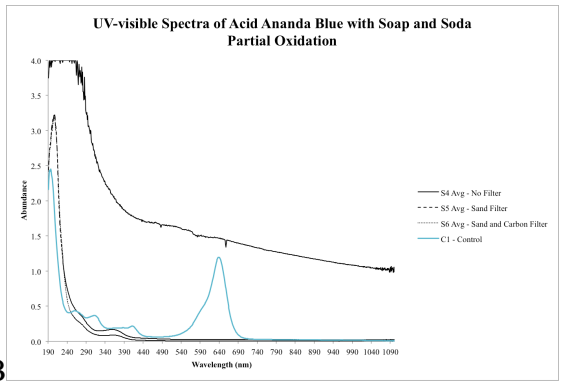

Figure 6.4: Acid Ananda Blue with Soap and Soda UV-visible spectra of the diluted control C1 compared to (A) S1-S3 and (B) S4-S6.

6.2.1.4 Field Samples Green and Maroon

UV-visible spectra for Field Samples Green and Maroon were analyzed to test the decolorization of samples. Figure 6.5 compares the UV-visible spectra of the control C1 to F1-F3 for (A) Green and (B) Maroon.

In general and despite treatment, the peaks in the UV spectra stayed much higher than the visible peaks. The contaminants at the lower UV peaks with no filtration were at the peak of the graph of 4.0 absorbance even after full oxidation. The contaminants at the higher visible range peaks were reduced more by full oxidation. Sand and carbon filtration following oxidation greatly decreased the peaks' heights by physically removing the organics out of solution. Occasionally there was a larger peak shown after carbon filtration than after sand filtration, although sample levels when this is the case were below 0.1 abundance.

A 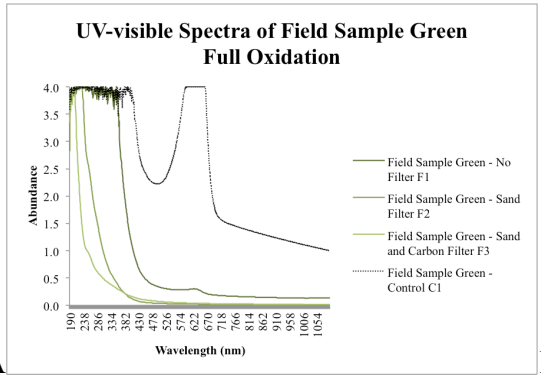

B 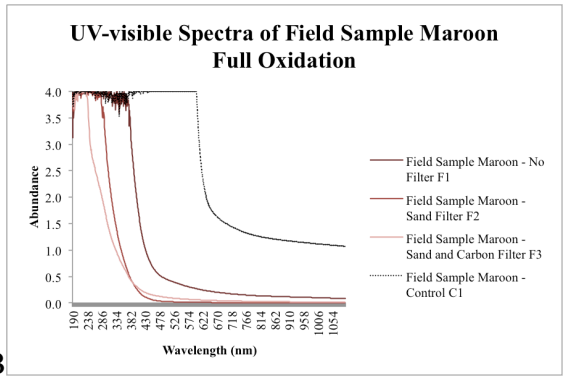

Figure 6.5: Field Samples UV-visible spectra of the control C1 compared to F1-F3 (A) Green and (B) Maroon.

6.3 COD Results

COD is used to analyze organic levels in solution. COD levels showed great variability, even when comparing similar samples. This is because the high level of Acid Dye with Soap and Soda used in this study has an exceptional level of organic material. Photo-Fenton oxidation also forms sludge in solution that is comprised of dye and rust from the iron catalyst. For this reason COD levels that drop below the Karnataka State Pollution Control Board's (KSPCB) allowable 250 ppm limit are particularly noted. The general trend expected for oxidized samples from high COD to low is S4, S1, S5, S6, S2, S3. The fully oxidized sample produces sludge that can keep the COD higher than permissible effluent levels; however, after physical removal of these organics, the sand and carbon filtered samples after full oxidation often brings COD close to negligible. Since partial oxidation does not fully precipitate the organics out of solution, with the shortest partial oxidation times precipitating the least organics, the sand and carbon filtration cannot fully separate them from the water base thus having a higher COD. In the analysis of the data, it is important to also consider ambient temperature, sunlight, and pH during the experiment in order to capture the effects of these variables on the COD reduction caused by the photo-Fenton oxidation process. Chapter 2 contains a discussion of a connection between temperature, sunlight, and COD reduction in dye effluent for studies conducted with dyes at lower concentrations; it is uncertain whether there will be such connections for the photo-Fenton oxidation of the 5 g/L dye effluent.

6.3.1 Acid Fast Red with Soap and Soda

COD results for Acid Fast Red with Soap and Soda as it relates to temperature, pH, iron,

and sunlight can be viewed in Table B.7 in Appendix B. Table 6.2 presents an overview of the average results in India and the USA comparing C1-C5 to S1-S6. Figure 6.6 depicts the general decrease of COD.

The control samples had COD levels that ranged between 608 and 7860 ppm. For India, sample COD in decreasing order was: S1, C1, S4, S5, S6, S2, S3. For the USA, sample COD in decreasing order was: S4, C1, S1, S5, S6, S2, S3. Although the order of decrease was not exactly the same, it was similar. S1 and S4 were very close and surround C1. The filtered samples decreased according to level of filtration (the more filtration the lower COD) and time (the more time the lower COD). Only the USA filtered samples decreased to below the KSPCB permissible level, whereas none of the India samples were low enough to safely dump.

Table 6.2: COD overview of Acid Fast Red with Soap and Soda comparing C1-C5 to S1-S6 in India and the USA.

Acid Fast Red with Soap and Soda	COD India	Avg. COD USA
C1	4380	6340
C2	NA	7860
C3	NA	6100
C4	NA	608
C5	NA	6840
S1	6316	1520
S2	453	15
S3	273	12.5
S4	3168	9000
S5	534	249
S6	498	181.5

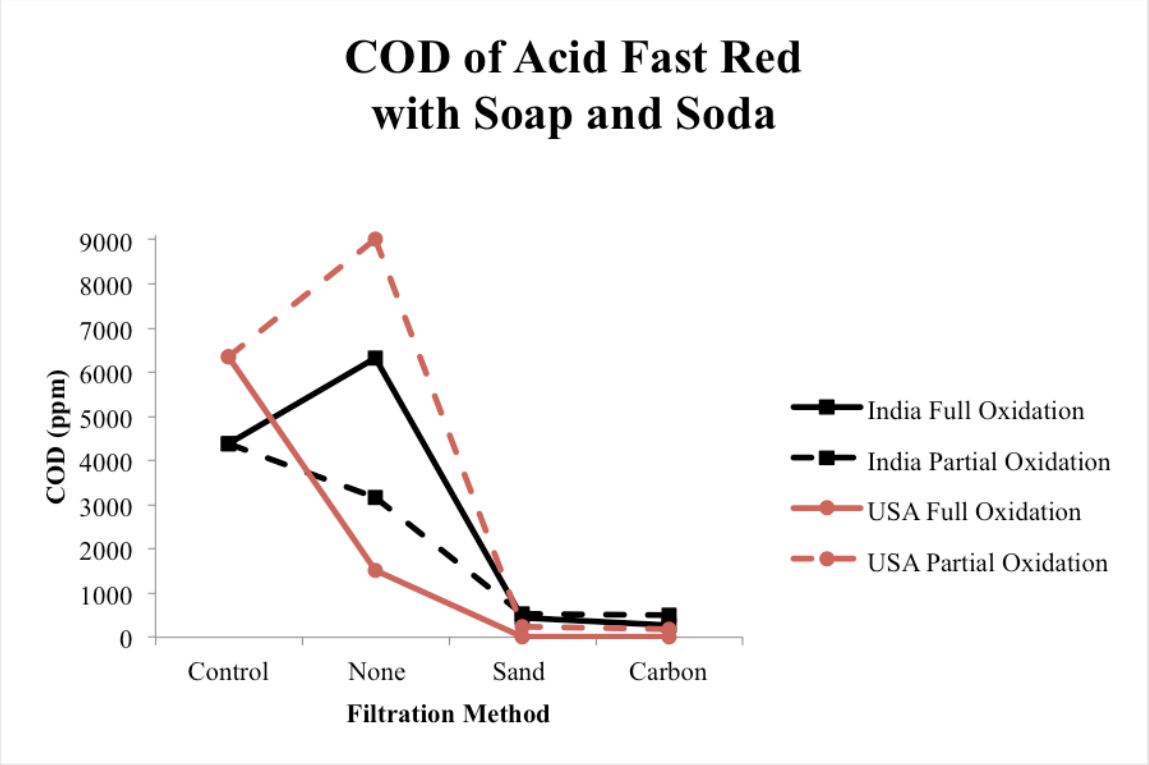

Figure 6.6: COD results comparing Acid Fast Red with Soap and Soda USA and India samples C1 to S1-S6.

6.3.2 Acid Golden Yellow with Soap and Soda

COD results for Acid Golden Yellow with Soap and Soda as it relates to temperature, pH, iron, and sunlight can be viewed in Table B.8 in Appendix B. Table 6.3 presents an overview of the average results in India and the USA comparing C1-C5 to S1-S6. Figure 6.7 depicts the general decrease of COD.

The control samples had COD levels that ranged between 2620 and 9820 ppm. For India, sample COD in decreasing order was as follows: C1, S1, S4, S2, S5, S3, S6. For the USA, sample COD in decreasing order was as follows: C1, S4, S5, S6, S1, S2, S3. Although the order of decrease was not exactly the same, it was similar. S4 was very

close to C1 in both locations. The filtered samples decreased according to level of filtration (the more filtration the lower COD) and time (the more time the lower COD). Outliers existed for both locations. S1 in the USA samples had lower COD than all of the partially oxidized samples, even the filtered samples. In the India samples, S6 had the lowest COD of all, and S5 had a lower COD than S2, which was unexpected. In fact, only S6 in India fell below KSPCB permissible limits, and almost all filtered samples (except S5) were within allowable limits for USA samples.

Table 6.3: COD of Acid Golden Yellow with Soap and Soda comparing C1-C5 to S1-S6 in India and the USA.

Acid Golden Yellow with Soap and Soda	COD India	Avg. COD USA
C1	NA	7580
C2	NA	4180
C3	NA	7740
C4	NA	2620
C5	NA	9820
S1	2436	240
S2	756	63
S3	303	45
S4	2276	1500
S5	648	304
S6	72	244

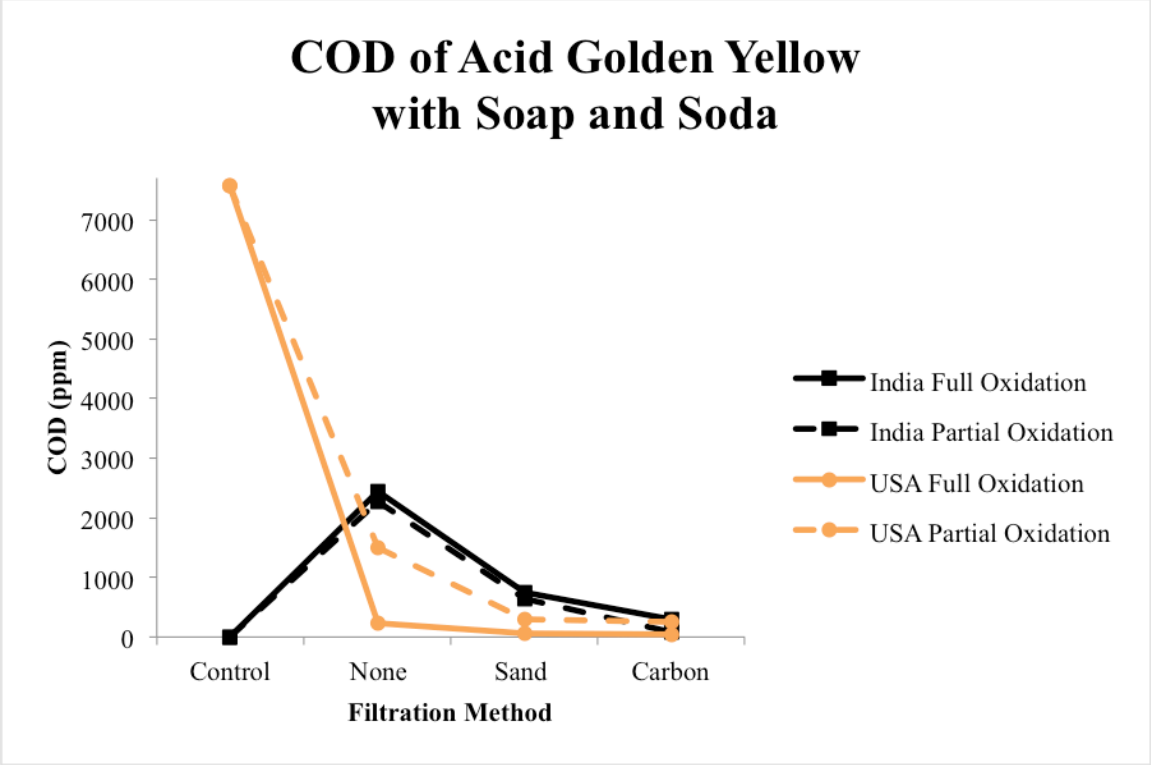

Figure 6.7: COD results comparing Acid Golden Yellow with Soap and Soda USA and India samples C1 to S1-S6.

6.3.3 Acid Ananda Blue with Soap and Soda

COD results for Acid Ananda Blue with Soap and Soda as it relates to temperature, pH, iron, and sunlight can be viewed in Table B.9 in Appendix B. Table 6.4 presents an overview of the average results in India and the USA comparing C1-C5 to S1-S6. Figure 6.8 depicts the general decrease of COD.

The control samples had COD levels that ranged between 3000 and 10880 ppm. For India, sample COD in decreasing order was as follows: C1, S4, S1, S3, S5, S2, S6. For the USA, sample COD in decreasing order was as follows: C1, S4, S1, S5, S6, S3, S2. Although the order of decrease was not exactly the same, it was similar. S1 and S4 were

very close and surround C1. The USA samples followed the general trend where filtered samples decreased according to level of filtration (the more filtration the lower COD) and time (the more time the lower COD) even though S3 and S2 were reversed in actual order, their respective COD levels were extremely similar. In the India samples, S6 had the lowest COD of all, and S5 had a lower COD than S3 which was unexpected but S3 had an unusually high COD. In fact, none of the India samples fell below KSPCB permissible limits, and only S2, S3, and S6 of the India samples were low enough to safely dispose.

Table 6.4: COD of Acid Ananda Blue with Soap and Soda comparing C1-C5 to S1-S6 in India and the USA.

Acid Ananda Blue with Soap and Soda	COD India	Avg. COD USA
C1	3000	8200
C2	NA	6460
C3	NA	9060
C4	NA	8040
C5	NA	10880
S1	1296	2220
S2	549	91
S3	1113	97
S4	1560	3580
S5	738	532
S6	369	201

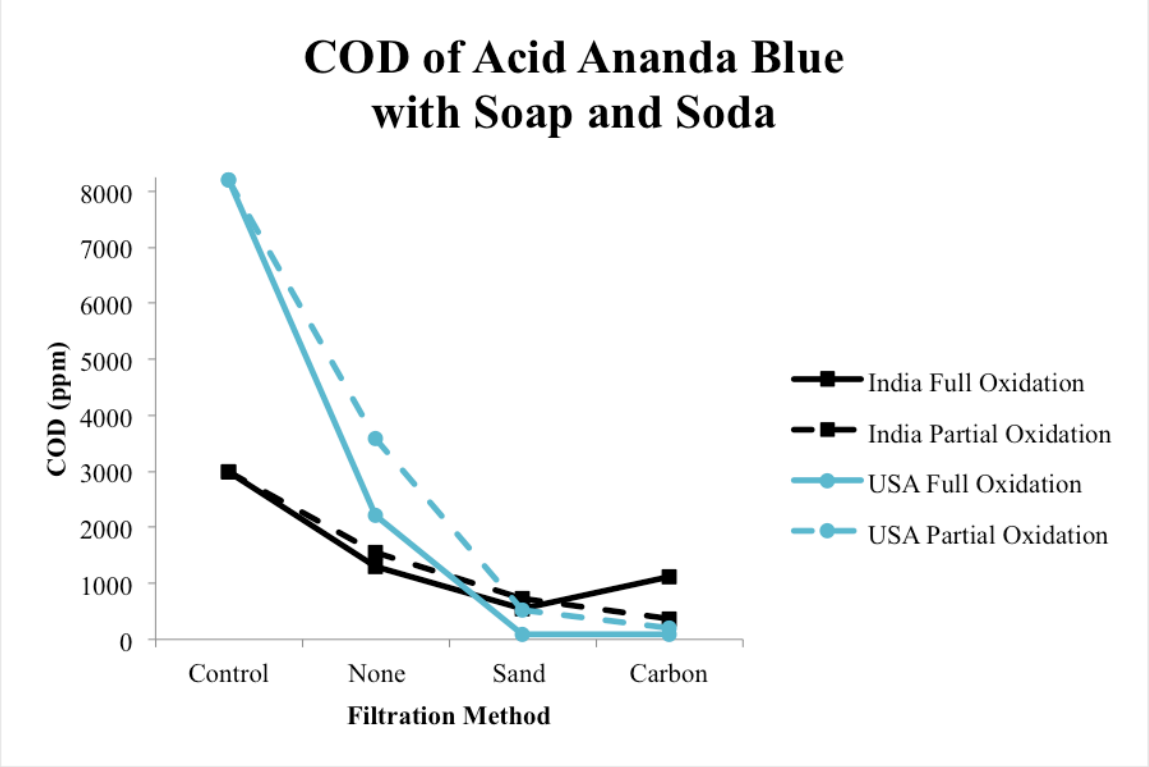

Figure 6.8: COD results comparing Acid Ananda Blue with Soap and Soda USA and India samples C1 to S1-S6.

6.3.4 Field Samples Green and Maroon

Table 6.5 presents an overview of the average COD and pH results in India comparing C1 to F1-F3. Figure 6.9 depicts the general decrease of COD. For both the Green and Maroon Field Samples, sample COD in decreasing order was as follows: F1, F2, F3. The samples followed the general trend where filtered samples decrease according to level of filtration (the more filtration the lower COD) and time (the more time the lower COD).

Table 6.5: COD of Field Samples Green and Maroon comparing C1 to F1-F3 in India.

Field Sample	Green - COD India	Green – pH	Maroon – COD India	Maroon – pH
C1	NA	9.70	NA	9.62
F1	1896	3.98	3456	3.48
F2	1155	5.48	360	4.83
F3	156	8.54	309	5.06

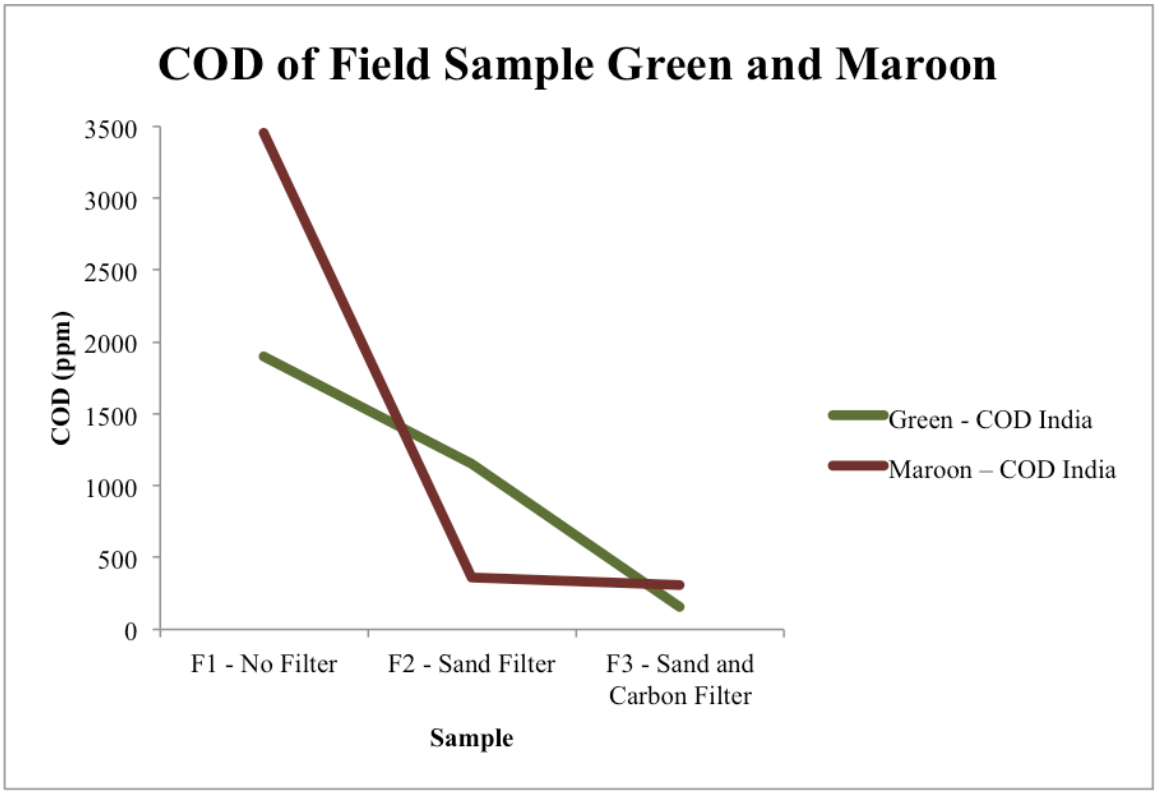

Figure 6.9: COD results comparing Field Samples Green and Maroon F1-F3 in India.

6.3.5 Sludge Production

Sludge production was notable during the photo-Fenton oxidation process with more sludge being produced during longer duration experiments. Sludge volume was quantified for the Acid dye with Soap and Soda studies only during the demonstration

project detailed in Chapter 7. The presence of sludge in non-filtered samples can greatly impact the overall COD level. During an interview with a medium-scale dyer in India, it was learned that sludge production created from biodegradation (customary method of dye wastewater treatment in medium and large-scale textile plants) of their wastewater, was approximately 15% of total solution. Percentage sludge production using sustainable photo-Fenton oxidation is much less.

6.3.6 Solar Irradiance and Temperature

Generally, the solar irradiance in the USA tests was higher than solar irradiance in the India tests since studies in India were completed as the rainy season was beginning. The solar irradiance in India was 152 W/m^2 and in the USA between 412-667 W/m^2. Meanwhile, the USA tests were completed at lower ambient temperatures than the India tests, due to the time of year the studies were performed. The temperature in India was 27.8 ºC and in the USA ranged between 3.47-5.0 ºC. Decolorization and degradation occurred for both test sites, indicating that the process can work for a wide range of temperatures and solar irradiances. COD levels varied more as a result of time and filtration rather than solar irradiance and temperature. The COD levels that resulted from the extreme ends of solar irradiance or temperature were mid-range COD results. It is therefore concluded that while UV irradiance is needed for the reaction to occur, and the temperature must be above the freezing temperature, UV irradiance and temperature are not key factors in producing a successful process. The tests were successful despite the lack of direct sunlight in partly cloudy or partly sunny conditions as long as there was daylight. This is important for eventual field implementation of the

process, as both solar irradiance and temperature are variables that cannot be easily controlled in practice.

6.4 GC/MS Results

GC/MS analysis was used to measure and identify chemical intermediates found in solution before and after oxidation. To qualify, chemical peaks detected by the GC must reach a minimum of 10,000 abundance (based on electrical signal passed through sample) and match the MS library with 80% or more accuracy. In order to verify the quantification of abundance of organics found in solution, a 95% pure sample of Tolylene, 2,4-diisocyanate (also called Benzene, 2,4-diisocyanato-1-methyl) was tested using the same GC/MS methods listed in Chapter 3. This aromatic and cyanate chemical was chosen because of its abundance in the reactive dye solution after treatment. Figure C.46 in Appendix C displays the GC/MS graph of this control. The 95% pure sample absorbed onto the Solid Phase Micro Extraction (SPME) fiber was found to have an abundance of Benzene, 2,4-diisocyanato-1-methyl at 1,800,000; 2H-Benzimidazol-2-one, 1,3-dihydro-5-methyl at 100,000; Bis(2-ethylhexyl) phthalate at 95,000; Squalene at 50,000; 2-Propenoic acid, 3-(4-methoxyphenyl)-, 2-ethylhexyl ester at 40,000; and Dodecanoic Acid, Ethyl Ester at 28,000. The presence of Benzene, 2,4-diisocyanato-1-methyl at 1,800,000 abundance in the pure sample verifies the accuracy of finding a lesser abundance in treated samples tested using the same SPME and GC/MS methodology. The presence of the other organics in the control sample reinforce that the control sample was only 95% pure. The level of Benzene, 2,4-diisocyanato-1-methyl in the 95% pure sample can be described by either fraction of

mass or fraction of ions. GC/MS displays the fraction of mass in its measured level of abundance, here reaching 85% of the total chemicals found; however, the sample is labeled 95% pure based on the fraction of ions in solution.

6.4.1 Acid Fast Red with Soap and Soda

Table C.7 in Appendix C lists all of the GC/MS results as they relate to C1-C5 and S1-S6 for Acid Fast Red with Soap and Soda including when complete degradation had occurred (which resulted in no noticeable peaks). Table 6.6 contains an overview of GC/MS results of all chemicals found in C1-C5 and S1-S6 for Acid Fast Red with Soap and Soda and the types of compounds and their responsible functional groups. Acid Fast Red with Soap and Soda had various organic compounds left in solution after treatment: alkane and aldehyde combined compounds at 64,500 abundance; aromatic and ketone combined compounds at 46,250 abundance; aromatic and aldehyde combined compounds at 45,500 abundance; and alkane and ketone combined compounds at 28,000 abundance. Figures C.31, C.32, C.33, C.34, and C.35 in Appendix C display GC/MS peaks for C1, C2, C3, C4, and C5 respectively for Acid Fast Red with Soap and Soda.

C1 had the most detectable organic chemicals found in solution. Regarding treated samples, fully oxidized samples degrade more than partially oxidized samples. S4 was found to contain the majority of organics detected after treatment. This means that full oxidation followed by filtration provided the greatest reduction in organics, although filtration reduced organics of even the partially oxidized samples. USA samples had more organics than India samples.

Table 6.6: GC/MS overview of Acid Fast Red with Soap and Soda comparing C1-C5 to S1-S6.

Code	Country	Chemical Name	Abundance	Type of Compound	Functional Group
C1	India	Hexadecanoic Acid	42000	Alkane, Carboxylic Acid	Hydrocarbon, Carboxy
C1	India	Octadecanoic Acid	21000	Alkane, Carboxylic Acid	Hydrocarbon, Carboxy
C1	India	Oleic Acid	62000	Alkane, Carboxylic Acid	Hydrocarbon, Carboxy
C4	India	2-Naphthalenol	15000	Aromatic, Alcohol, Bromide	Phenyl, Hydroxy, Bromide
C5	USA	cyclohexasiloxane, dodecamethyl	38000	Organic	Silica
C5	USA	cyclopentasiloxane, decamethyl	21800	Organic	Silica
C5	USA	Hexanal	35000	Alkane, Aldehyde	Hydrocarbon, Carbonyl
S1	India	Hexanal	14500	Alkane, Aldehyde	Hydrocarbon, Carbonyl
S1	USA1	1,4-Naphthalenedione	11000	Aromatic, Ketone	Phenyl, Carbonyl
S2	USA2	Benzaldehyde, 4-methyl	10500	Aromatic, Aldehyde	Phenyl, Carbonyl
S4	USA1	1,4-Naphthalenedione	16000	Aromatic, Ketone	Phenyl, Carbonyl
S4	USA2	1,4-Naphthalenedione	19250	Aromatic, Ketone	Phenyl, Carbonyl
S4	USA1	Nonanal	50000	Alkane, Aldehyde	Hydrocarbon, Carboxy
S4	USA1	Octanal	40000	Alkane, Aldehyde	Hydrocarbon, Carboxy
S4	India	Octanoic Acid	19750	Alkane, Carboxylic Acid	Hydrocarbon, Carboxy
S5	USA2	Benzaldehyde, 3-methyl	12000	Aromatic, Aldehyde	Phenyl, Carbonyl
S5	USA1	Benzaldehyde, 4-methyl	23000	Aromatic, Aldehyde	Phenyl, Carbonyl
S5	USA1	2-Heptanone	42000	Alkane, Ketone	Hydrocarbon, Carbonyl
S5	USA2	2-Heptanone	28000	Alkane, Ketone	Hydrocarbon, Carbonyl

6.4.2 Acid Golden Yellow with Soap and Soda

Table C.8 in Appendix C lists all of the GC/MS results as they relate to C1-C5 and S1-S6 for Acid Golden Yellow with Soap and Soda including when complete degradation had occurred (which resulted in no noticeable peaks). Table 6.7 contains an overview of GC/MS results of all chemicals found in C1-C5 and S1-S6 for Acid Golden Yellow with Soap and Soda and the types of compounds and their responsible functional groups. Acid Golden Yellow with Soap and Soda had various organic compounds left in solution after treatment: alkane and aldehyde combined compounds at 225,000 abundance; alkane and carboxylic acid combined compounds at 26,000 abundance; and aromatic and aldehyde combined compounds at 19,000 abundance. Figures C.36, C.37, C.38, C.39, and C.40 in

Appendix C display GC/MS peaks for C1, C2, C3, C4, and C5 for Acid Golden Yellow with Soap and Soda respectively.

C4 had the most detectable organic chemicals found in solution. Regarding treated samples, fully oxidized samples degraded more than partially oxidized samples. S4 was found to contain the majority of organics detected after treatment. This means that full oxidation followed by filtration still provided the greatest reduction in organics, although filtration reduced organics of even the partially oxidized samples. USA samples had more organics than India samples.

Table 6.7: GC/MS overview of Acid Golden Yellow with Soap and Soda comparing C1-C5 to S1-S6.

Code	Location	Chemical Name	Abundance	Type of Compound	Functional Group
C1	USA	Cyclohexasiloxane, dodecamethyl	24000	Organic	Silica
C1	India	Octanoic Acid	20000	Alkane, Carboxylic Acid	Hydrocarbon, Carboxy
C4	USA	Hexadecanoic Acid	24000	Alkane, Carboxylic Acid	Hydrocarbon, Carboxy
C4	USA	Hexanal	65750	Alkane, Aldehyde	Hydrocarbon, Carbonyl
C4	USA	Oleic Acid	30000	Alkane, Carboxylic Acid	Hydrocarbon, Carboxy
C5	USA	Hexanal	40000	Alkane, Aldehyde	Hydrocarbon, Carbonyl
C5	USA	Benzaldehyde	50000	Aromatic, Aldehyde	Phenyl, Carbonyl
S1	India	Hexanal	48000	Alkane, Aldehyde	Hydrocarbon, Carbonyl
S1	USA2	Hexanal	18000	Alkane, Aldehyde	Hydrocarbon, Carbonyl
S2	USA2	Benzaldehyde, 2-methyl-	19000	Aromatic, Aldehyde	Phenyl, Carbonyl
S4	India	Hexanal	11500	Alkane, Aldehyde	Hydrocarbon, Carbonyl
S4	USA1	Hexanal	31000	Alkane, Aldehyde	Hydrocarbon, Carbonyl
S4	USA2	Hexanal	30500	Alkane, Aldehyde	Hydrocarbon, Carbonyl
S4	USA1	Heptanal	47000	Alkane, Aldehyde	Hydrocarbon, Carboxy
S4	USA1	Octanal	39000	Alkane, Aldehyde	Hydrocarbon, Carboxy
S4	USA1	Octanoic Acid	26000	Alkane, Carboxylic Acid	Hydrocarbon, Carboxy

6.4.3 Acid Ananda Blue with Soap and Soda

Table C.9 in Appendix C lists all of the GC/MS results as they relate to C1-C5 and S1-S6 for Acid Ananda Blue with Soap and Soda including when complete degradation had

occurred (which resulted in no noticeable peaks). Table 6.8 contains an overview of GC/MS results of all chemicals found in C1-C5 and S1-S6 for Acid Ananda Blue with Soap and Soda and the types of compounds and their responsible functional groups. Acid Ananda Blue with Soap and Soda had various organic compounds left in solution after treatment: alkane and carboxylic acid combined compounds at 268,450 abundance; alkane and aldehyde combined compounds at 48,000 abundance; and aromatic and aldehyde combined compounds at 24,750 abundance. Figures C.41, C.42, C.43, C.44, and C.45 in Appendix C display GC/MS peaks for C1, C2, C3, C4, and C5 for Acid Ananda Blue with Soap and Soda respectively.

C4 had the most detectable organic chemicals found in solution. Regarding treated samples, fully oxidized samples degraded more than partially oxidized samples. S4 was found to contain the majority of organics detected after treatment. This means that full oxidation followed by filtration provided the greatest reduction in organics, although filtration reduced organics of even the partially oxidized samples. USA samples had more organics than India samples.

Table 6.8: GC/MS overview of Acid Ananda Blue with Soap and Soda comparing C1-C5 to S1-S6.

Code	Location	Chemical Name	Abundance	Type of Compound	Functional Group
C1	India	Benzaldehyde	220000	Aromatic, Aldehyde	Phenyl, Carbonyl
C1	USA	Benzaldehyde	35000	Aromatic, Aldehyde	Phenyl, Carbonyl
C1	USA	Benzenemethanamine, N-ethyl	41000	Aromatic, Amine	Phenyl, Amino
C1	USA	Cyclohexasiloxane, dodecamethyl	58000	Organic	Silica
C1	USA	Cyclohexasiloxane, dodecamethyl	22000	Organic	Silica
C2	USA	Benzaldehyde	540000	Aromatic, Aldehyde	Phenyl, Carbonyl
C2	USA	Benzenemethanamine, N-ethyl-N-phenyl	60000	Aromatic, Amine	Phenyl, Amino
C2	USA	2-Propenal, 3-pheyl	50000	Aromatic, Aldehyde	Phenyl, Carbonyl
C3	USA	Benzaldehyde	450000	Aromatic, Aldehyde	Phenyl, Carbonyl

C3	USA	Benzaldehyde, 2-hydroxy	140000	Aromatic, Aldehyde	Phenyl, Carbonyl
C4	USA	Benzaldehyde	160000	Aromatic, Aldehyde	Phenyl, Carbonyl
C4	USA	Benzenemethanamine, N-ethyl-N-phenyl	110000	Aromatic, Amine	Phenyl, Amino
C4	USA	Decanoic Acid	93000	Alkane, Carboxylic Acid	Hydrocarbon, Carboxy
C4	USA	Dodecanoic Acid	180000	Alkane, Carboxylic Acid	Hydrocarbon, Carboxy
C4	USA	Hexadecanoic Acid	112000	Alkane, Carboxylic Acid	Hydrocarbon, Carboxy
C4	USA	9,12-Octadecadienoic Acid (Z,Z)	50000	Alkane, Carboxylic Acid	Hydrocarbon, Carboxy
C4	USA	Octadecanoic Acid	68000	Alkane, Carboxylic Acid	Hydrocarbon, Carboxy
C4	USA	Octanoic Acid	60000	Alkane, Carboxylic Acid	Hydrocarbon, Carboxy
C4	USA	Oleic Acid	330000	Alkane, Carboxylic Acid	Hydrocarbon, Carboxy
C4	USA	2-Propenal, 3-pheyl	92000	Aromatic, Aldehyde	Phenyl, Carbonyl
C4	USA	Tetradecanoic Acid	30000	Alkane, Carboxylic Acid	Hydrocarbon, Carboxy
C5	India	Benzaldehyde	26000	Aromatic, Aldehyde	Phenyl, Carbonyl
C5	USA	Benzaldehyde	390000	Aromatic, Aldehyde	Phenyl, Carbonyl
C5	USA	Benzaldehyde, 2-hydroxy	240000	Aromatic, Aldehyde	Phenyl, Carbonyl
C5	USA	Cyclohexasiloxane, dodecamethyl	58000	Organic	Silica
C5	USA	Hexadecanoic Acid	22000	Alkane, Carboxylic Acid	Hydrocarbon, Carboxy
S1	India	Dodecanoic Acid	16700	Alkane, Carboxylic Acid	Hydrocarbon, Carboxy
S1	India	Nonanoic Acid	18750	Alkane, Carboxylic Acid	Hydrocarbon, Carboxy
S1	India	Octanoic Acid	20000	Alkane, Carboxylic Acid	Hydrocarbon, Carboxy
S4	USA1	Hexadecanoic Acid	45000	Alkane, Carboxylic Acid	Hydrocarbon, Carboxy
S4	USA2	Hexadecanoic Acid	53000	Alkane, Carboxylic Acid	Hydrocarbon, Carboxy
S4	India	Heptanal	17000	Alkane, Aldehyde	Hydrocarbon, Carboxy
S4	USA1	Nonanal	18000	Alkane, Aldehyde	Hydrocarbon, Carboxy
S4	India	Nonanoic Acid	46000	Alkane, Carboxylic Acid	Hydrocarbon, Carboxy
S4	India	Octanal	30000	Alkane, Aldehyde	Hydrocarbon, Carboxy
S4	USA1	Octadecanoic Acid	25000	Alkane, Carboxylic Acid	Hydrocarbon, Carboxy
S4	USA2	Octadecanoic Acid	19000	Alkane, Carboxylic Acid	Hydrocarbon, Carboxy
S4	India	Octanoic Acid	25000	Alkane, Carboxylic Acid	Hydrocarbon, Carboxy
S5	USA2	Benzaldehyde	24750	Aromatic, Aldehyde	Phenyl, Carbonyl

6.4.4 Field Studies Green and Maroon

Table C.10 in Appendix C lists all of the GC/MS results as they relate C1 to F1-F3 for Field Samples Green and Maroon including when complete degradation had occurred (which resulted in no noticeable peaks). Table 6.9 contains an overview of GC/MS results of all chemicals found in C1 and F1-F3 for Field Samples and what type of compound each result is and their responsible functional groups. C1 had the most detectable organic chemicals found in solution for Field Sample Maroon to include 90,000 abundance of aromatics. Regarding treated samples, Field Sample Green had only aromatic and alcohol combined compounds at 24,000 abundance. Full oxidation followed by filtration provided the most reduction in organics.

Table 6.9: GC/MS overview of Field Samples Green and Maroon comparing C1 to F1-F3.

Code	Location	Dye	Chemical Name	Abundance	Type of Compound	Functional Group
F2	India	Field Sample Green	Phenol, 2,4-bis(1,1-dimethylethyl)	24,000	Aromatic, Alcohol	Phenyl, Hydroxy
C1	India	Field Sample Maroon	Benzenamine, 4-ethoxy	90,000	Aromatic	Phenyl Group

6.5 ICP Results

ICP testing was used to determine metals left in solution. Although 18 metals were measured, only four were found regularly at high levels: calcium, iron, magnesium, and sodium. Their levels were measured for all samples from C1-C5 and S1-S6 to track when levels decreased below permissible levels. Arsenic, cadmium, lead, and manganese were occasionally found above permissible limits and it is noted when this occurred. Data were taken for all of the samples, including both the India and USA tests. Table

3.10 displays India's permissible effluent standards for wastewater in Dye and Dye Intermediate Industries for disposal in surface waters. India effluent standards do not list calcium, iron, magnesium, and sodium standards in their effluent regulations; therefore levels were compared to drinking water standards shown in Table 3.11. Permissible calcium levels are limited to 75-200 mg/L because calcium causes water hardness between 40-100 mg/L. Permissible magnesium levels are limited to 30-150 mg/L because at 500 mg/L the taste of the water is affected. Permissible iron levels are limited to 0.1-1.0 mg/L because at 0.3 mg/L the taste and aesthetics of the water is affected. Permissible sodium levels are limited to 20 mg/L because at 250 mg/L the taste and aesthetics of the water is affected and can alter natural biological activity. Natural waters have sodium levels between 5-50 mg/L. Permissible manganese levels are limited to 0.1-0.5 mg/L but at 0.05 mg/L the taste and aesthetics of the water is affected. Permissible arsenic levels are 0.01-0.05 mg/L because at 0.05 mg/L arsenic affects human health. Permissible cadmium levels are 0.005-0.01 mg/L but at 0.005 mg/L cadmium is toxic to humans. Permissible lead levels are 0.05-0.1 mg/L because lead causes irreversible neurological damage to humans, especially children (Sengupta, *et al.*, 2008).

The general trend of these ions in solution was an increase of calcium and magnesium after sand filtration. Iron had the opposite trend, as it increased during the oxidation process and decreased to an almost negligible amount after sand filtration. This was a result of the physical capturing of the iron/dye sludge formed in solution during the oxidation process. Sodium increased or remained stable during oxidation and decreased after sand and carbon filtration. Note, the levels of increase or decrease do not fit a

mathematical trend because of the variability in chemical composition of the wastewater at such a high dye concentration. In addition, there is little control as to the sand's contents in India since it was construction sand that had been stored outside open to nature prior to use. Because of the difference in quantitative results between India and the USA, trends are described instead. These trends often match despite these numerical differences.

6.5.1 Acid Fast Red with Soap and Soda

Acid Fast Red with Soap and Soda ICP results are found in Table D.7 in Appendix D. Other than calcium, magnesium, iron, and sodium, for Acid Fast Red with Soap and Soda ICP results, manganese and occasionally arsenic were present in India, whereas arsenic, cadmium, and chromium were present in USA samples at lower levels. Calcium controls ranged from 21.8 to 69.6 ppm with the highest level in C5, magnesium ranged from 1.9 to 15.9 ppm with the highest level in C5, iron from 0.2 to 1.1 ppm with the highest level in C5, and sodium from 524 to 5700 ppm with the highest level in C2.

Calcium content in solution changed as the location of the study changed. For calcium, USA samples and India samples followed the same trend with similar results for the non-filtered samples with increases after filtration. USA filtration increased higher than for India (6-20 times higher). All of the non-filtered samples, S1 and S4, as well as the India samples S5-S6, were below the drinking water permissible limits.

The impact that time had on the magnesium content is very similar to that of calcium; however, very different results came from the sand filtration in the different locations. It was expected that samples would increase after sand filtration, however this was only the case with samples in India. In the USA samples, the sand filtration of each sample decreased magnesium levels to negligible. Carbon filtration changed very little. India samples differed in that magnesium levels all increased after sand filtration by three to four times, and then slightly decreased after carbon filtration. All magnesium levels stayed very low and were well below the permissible drinking water limit.

Regarding the impact that time had on the iron content of solution, it is clear that longer oxidation time produced more iron in solution only to be more easily removed by filtration. The iron levels of all sand filtered samples decreased to negligible (and thus below the permissible drinking water limit) and stayed there after carbon filtration except S5-S6 in India.

Of the metals found in solution, sodium had very similar numbers in both India and USA samples. Filtration greatly decreased sodium levels and had the greatest impact after longer filtration times. No samples were found to be below permissible drinking water limits.

Most India filtered samples found manganese in solution except S4. Arsenic was also found in S3 and S6 in the USA samples and S5 in the India samples. Cadmium was only found in USA samples S4 and S6, while chromium in USA sample S6.

6.5.2 Acid Golden Yellow with Soap and Soda

Acid Golden Yellow with Soap and Soda ICP results are found in Table D.8 in Appendix D. For the samples, there is a consistent presence of calcium, magnesium, iron, and sodium. The India samples occasionally contain manganese and arsenic. Manganese, cadmium, lead, and chromium are present occasionally in both the India and USA samples. Calcium controls ranged from 19.6 to 68.8 ppm with the highest level in C4, magnesium ranged from 2.5 to 19.3 ppm with the highest level in C4, iron from 0.1 to 1 ppm with the highest level in C1, and sodium from 765 to 7020 ppm with the highest level in C4.

To ascertain the impact that time had on the calcium content of solution, it is most clear to compare samples according to location. For calcium, USA samples and India samples followed the same trend with similar results for the non-filtered samples with increases after filtration. USA filtration increased higher than it did for India (6-10 times higher). All of the non-filtered samples (S1 and S4) as well as the India samples S5-S6 were below the drinking water permissible limits.

The impact that time had on the magnesium content is very similar to that of calcium; however, very different results came from the sand filtration in the different locations. It is expected that magnesium levels will increase after sand filtration; however this was only the case with samples in India. In the USA samples, the sand filtration of each sample decreased magnesium levels to negligible. Carbon filtration changed the levels very little. India samples differed in that they all increased after sand filtration by three

to four times, and slightly decreased after carbon filtration. All magnesium levels stayed very low and were well below the permissible drinking water limit.

Regarding the impact that time had on the iron content of solution, it is clear that longer oxidation time produced more iron in solution only to be more easily removed by filtration. The iron in all USA filtered samples decreased to negligible (and thus below the permissible drinking water limit). India samples were slightly higher.

Of the metals found in solution, sodium had very similar numbers in both India and USA samples. Filtration greatly decreased sodium levels and most profoundly after longer filtration times. No samples were found to be below permissible drinking water limits.

Most India filtered samples found a level of manganese in solution except S4. Arsenic was also found in S1 and S4 in the USA samples. Cadmium was only found in USA samples S1 and S5, while chromium in USA sample S5-S6, and lead in USA sample S2 and S5.

6.5.3 Acid Ananda Blue with Soap and Soda

Acid Ananda Blue with Soap and Soda ICP results are found in Table D.9 in Appendix D. For the samples, there is a consistent presence of calcium, magnesium, iron, and sodium. The India samples occasionally find manganese after filtration, and cadmium, and lead only after oxidation with no filtration. USA samples find manganese, arsenic, cadmium, lead, and chromium after no filtration. Calcium controls ranged from 12 to 47

ppm with the highest level in C4, magnesium ranged from 2.9 to 16.7 ppm with the highest level in C2, iron from 0.9 to 3.4 ppm with the highest level in C4, and sodium from 397 to 5620 ppm with the highest level in C4.

To ascertain the impact that time had on the calcium content of solution, it is best to compare samples according to location. For calcium, USA samples and India samples followed the same trend with similar results for the non-filtered samples with increases after filtration. USA filtration increased higher than it did for India (more than 10 times higher). All of the non-filtered samples (S1 and S4) as well as the India samples S5-S6 were below the drinking water permissible limits.

The impact that time had on the magnesium content is very similar to that of calcium; however, very different results came from the sand filtration in the different locations. It is expected that magnesium levels will increase after sand filtration; however this was only the case with samples in India. In the USA samples, the sand filtration of each sample decreased magnesium to negligible levels. Carbon filtration changed the magnesium levels very little. India samples differed in that they all increased after sand filtration by three to four times, and slightly decreased after carbon filtration. All magnesium levels stayed very low and were well below the permissible drinking water limit.

Regarding the impact that time had on the iron content of solution, it is clear that longer oxidation time produced more iron in solution only to be more easily removed by

filtration. All USA filtered samples' iron levels decreased to negligible (and thus below the permissible drinking water limit). India samples were higher.

Of the metals found in solution, sodium had very similar numbers in both India and USA samples. Filtration greatly decreased sodium levels and most profoundly after longer filtration times. No samples were found to be below permissible drinking water limits.

Most India filtered samples found a level of manganese in solution as well as USA sample S1. Arsenic was also found in S2 and S4 in the USA samples. Cadmium was found samples S1 and S4, while lead in samples S1 and S4.

6.5.4 Field Samples Green and Maroon

ICP results for Field Samples Green and Maroon can be viewed in Table 6.10 which compare the control samples C1 with F1-F3.

Field Samples Green show similar results as the Acid Fast Red with Soap and Soda, Acid Golden Yellow with Soap and Soda, and Acid Ananda Blue dye with Soap and Soda results and displayed an increase of iron after oxidation, and a decrease of iron and sodium after sand and carbon filtration. In this case calcium acted slightly differently: increasing from the control to the oxidized sample, halving after sand filtration, and then decreasing more after carbon filtration. Sodium increased after carbon filtration compared to the sand filtered results.

Looking at the Field Samples Maroon, calcium increased after oxidation as did iron and

magnesium. Sodium poses the largest challenge because of its high concentrations but did show promise because it decreased after sand and carbon filtration. Calcium increased slightly after sand filtration and decreased again after carbon filtration. Magnesium levels did not change very much overall staying close to their control level. Iron was the most obviously filterable ion in solution.

Table 6.10: ICP results for photo-Fenton oxidized Field Samples Green and Maroon samples F1-F3 compared with C1.

Dye	Time	Ca	Fe	Mg	Na	Other
Control Field Sample Green	C1	49.3	1	34.6	3882.8	
Field Sample Green	F1	79.6	281.1	41.2	3806.7	Mn: 1.7
Field Sample Green	F2	41.5	1.6	12.4	376.2	Mn: 7.7
Field Sample Green	F3	31	2.7	9.3	437.3	Mn: 4.3
Control Field Sample Maroon	C1	28.8	0.4	15.9	4876.6	
Field Sample Maroon	F1	71.5	356.2	25	4758.9	Mn: 1.5
Field Sample Maroon	F2	72.5	30.2	25.3	1414.1	Mn: 10.2
Field Sample Maroon	F3	61.4	12.6	20.8	1176.9	Mn: 8.6

6.6 Respirometric Results

Respirometric analysis was conducted for partially oxidized samples of differing colors (red, yellow, blue) and of different filtration methods (no filter, sand filter) for India samples. The COD levels for fully oxidized samples were too low to biodegrade further, so respirometric analysis was only completed for partially oxidized samples.

6.6.1 Acid Fast Red with Soap and Soda

Oxygen uptake results can be viewed in Figure E.7 in Appendix E which compare three trials of endogenous and exogenous data describing the oxygen uptake of S4 or S5 for Acid Fast Red with Soap and Soda.

The results of the calculated oxygen uptake based on the data in Figure E.7 in Appendix E are presented in Table 6.11 for Acid Fast Red with Soap and Soda. As can be seen, oxygen uptake was found to be zero for S4 and S5 samples meaning that the bacteria in the CETP sludge sample was not able to consume the pollutants in the substrate.

Table 6.11: Calculated oxygen uptake for Acid Fast Red with Soap and Soda according to partial oxidation time and non-filtered or sand filtered sample results.

Sample	Color	Filter/No Filter	O2 Uptake Value (nMol/min/mg)
S4	Acid Fast Red Soap and Soda	Partial Oxidation - No Filter	0.00
S5	Acid Fast Red Soap and Soda	Partial Oxidation - Sand Filter	0.00

6.6.2 Acid Golden Yellow with Soap and Soda

Oxygen uptake results can be viewed in Figure E.8 in Appendix E which compare three trials of endogenous and exogenous data describing the oxygen uptake of S4 or S5 for Acid Golden Yellow with Soap and Soda.

The results of the calculated oxygen uptake based on the data in Figure E.8 in Appendix E are presented in Table 6.12 for Acid Golden Yellow with Soap and Soda. As can be seen, oxygen uptake was found to be zero for both filtered and non-filtered samples meaning that the bacteria in the CETP sludge sample was not able to consume the pollutants in the substrate.

Table 6.12: Calculated oxygen uptake for Acid Golden Yellow with Soap and Soda according to partial oxidation time and non-filtered or sand filtered sample results.

Sample	Color	Filter/No Filter	O2 Uptake Value (nMol/min/mg)
S4	Acid Golden Yellow Soap and Soda	Partial Oxidation - No Filter	0.00
S5	Acid Golden Yellow Soap and Soda	Partial Oxidation - Sand Filter	0.00

6.6.3 Acid Ananda Blue with Soap and Soda

Oxygen uptake results can be viewed in Figure E.9 in Appendix E which compare three trials of endogenous and exogenous data describing the oxygen uptake of S4 or S5 for Acid Ananda Blue with Soap and Soda.

The results of the calculated oxygen uptake based on the data in Figure E.9 in Appendix E are presented in Table 6.13 for Acid Ananda Blue with Soap and Soda. As can be seen, oxygen uptake was found to be zero for both filtered and non-filtered samples meaning that the bacteria in the CETP sludge sample was not able to consume the pollutants in the substrate.

Table 6.13: Calculated oxygen uptake for Acid Ananda Blue with Soap and Soda according to partial oxidation time and non-filtered or sand filtered sample results.

Sample	Color	Filter/No Filter	O2 Uptake Value (nMol/min/mg)
S4	Acid Ananda Blue Soap and Soda	Partial Oxidation - No Filter	0.00
S5	Acid Ananda Blue Soap and Soda	Partial Oxidation - Sand Filter	0.00

6.6.4 Field Samples Green and Maroon

Oxygen uptake results can be viewed in Figure E.10 in Appendix E which compare three trials of endogenous and exogenous data describing the oxygen uptake of F1 or F2 for Field Samples Green and Maroon.

The results of the calculated oxygen uptake based on the data in Figure E.10 in Appendix E are presented in Table 6.14 for Field Samples Green and Maroon. As can be seen, oxygen uptake was found to be zero for both filtered and non-filtered samples meaning

that the bacteria in the CETP sludge sample was not able to consume the pollutants in the substrate.

Table 6.14: Calculated oxygen uptake for Field Samples Green and Maroon according to partial oxidation time and non-filtered or sand filtered sample results.

Sample	Color	Filter/No Filter	O2 Uptake Value (nMol/min/mg)
F1	Field Sample Green	Partial Oxidation - No Filter	0.00
F2	Field Sample Green	Partial Oxidation - Sand Filter	0.00
F1	Field Sample Maroon	Partial Oxidation - No Filter	0.00
F2	Field Sample Maroon	Partial Oxidation - Sand Filter	0.00

6.7 Discussion of Results

The purpose of the studied photo-Fenton oxidation procedure is to completely degrade organic compounds from an acid dye solution with soap and soda and to bring inorganics to the permissible drinking water level. The level of degradation achieved through various combinations of experimental variables was described above. UV-visible spectrometry can be compared with published data to describe which organics were left after treatment. The COD results can be used to show the total organic load remaining and whether it agrees with the UV-visible spectrometry results. The GC/MS analysis can be used to identify the organics and their respective quantities. The ICP results can be used to describe the inorganic metal ions left in solution. The respirometric analysis allows for the determination of whether the remaining solution is theoretically biodegradable. Finally, the combined results can be used to identify an experimental procedure that will achieve the most effective treatment of the dye effluent in a cost-effective and sustainable manner.

Before recommendations can be made, it is important to understand the actual activities cottage-scale silk dyers perform. By mimicking the cottage-scale silk dyers' wastewater in laboratory-scale studies, the intent was to augment dyers' processes with a low-cost treatment option. For this reason, the following experimental methodology was chosen. (1) Acid dyes at 5 g/L, soap at 3.1 g/L, and soda at 10 g/L concentrations were mixed with household hydrochloric acid; (2) pharmacy-grade hydrogen peroxide was poured into the solution in containers holding rusty metal from old yogurt containers; (3) natural sunlight at ambient temperature were employed; (4) following treatment, sand and carbon filtration of the dye effluent was used. This process was developed to be low-cost and readily available. Since the work was not completed using laboratory-grade supplies, some contamination was expected to be found in the results in the form of outliers in the analysis. That being said, organic and inorganic chemicals found before (in the controls), during (after partial oxidation and followed by filtration), and after (after full oxidation, and followed by filtration) the sustainable photo-Fenton oxidation process, agreed with the literature as described in Chapter 2. And since this study has a practical application because of the need for low-cost decolorization and dye wastewater treatment, the goal of the results is to prioritize the importance of certain variables over others in order to create a viable treatment unit to be used by small-scale silk dyers worldwide. The overall intention is to make sure that the color degrades and the chemical composition oxidizes to a simpler form before reusing the treated water for a second batch of dye, or before dumping it as is normally done.

The variables used for the sustainable photo-Fenton process (including dye color, dye concentration, hydrochloric acid, hydrogen peroxide, iron surface area, solar irradiation, temperature, oxidation time, filtration method) all contribute to the degradation of the chemical dyes in solution. Each variable impacts the outcome of the sustainable photo-Fenton oxidation experiments detailed here. However, the importance of each variable differed from what was expected and previously documented by other research (see Chapter 2). Not all variables were tested in these studies—most were kept constant for all experiments. Time and filtration were tested for each color to measure their impact on the photo-Fenton oxidation process. Dye concentration, iron surface area, acidification using hydrochloric acid, and the quantity of hydrogen peroxide were held constant, and will impact the photo-Fenton oxidation process. Solar irradiation and temperature are also variables that impact photo-Fenton oxidation, but were not controlled in this work. The values of these were recorded, and so it was possible to determine if they significantly impacted the results.

Dye, soap, and soda concentrations were constant for all tests at 5 g/L, 3.1 g/L, and 10 g/L respectively, which is similar to that in the small-scale industry. Acidification with hydrochloric acid did not use a specific volume per solution, but instead always brought solution pH to 2.5. Each dye color required a different volume of 6% hydrogen peroxide, as was decided according to the optimization tests, but then the volume was not altered within each color set. In the case of temperature and solar irradiation, location is noted as India or USA. It is evident that temperature variation is less important than solar irradiation variation. Temperature did not seem to impact oxidation provided that the

sample remained above the freezing temperature. UV light is incredibly important for the reaction to take place, but direct sunlight is not necessary. Each location varies greatly for temperature and solar irradiation, but since the process worked in both places their various levels do not prevent the chemical reaction from taking place.

The results here do not compare dye color but rather test the degradation of three colors that are typically used in the field. Knowing that red, yellow, and blue can form all colors in the rainbow, if their separate degradation using sustainable photo-Fenton oxidation is successful, their mixture, although slightly more complicated, should also be able to be oxidized. High COD levels are found in control samples due to the high concentration of dye, soap, and soda in solution. UV-visible spectra of the control samples also reach well beyond the graph maximum thus denoting very high organic levels in solution. The high concentration of dye, soap, and soda also offered great variation in the measured COD and GC/MS degradation results before filtration. Through UV-visible spectrometry, GC/MS, and COD, it is found that full oxidation followed by sand filtration (or sand and carbon filtration) lowers the amount of organics in solution to near negligible in many cases. The hazard quality of the chemicals remaining in solution is listed according to the Globally Harmonized System of Classification and Labeling of Chemicals (GHS) where each chemical receives an H label for being hazardous followed by a number. 200 level labels distinguish they are physically hazardous, 300 level labels are hazardous to health, and 400 level labels are hazardous to the environment.

Bilgi and Demir (2005) state that while sulphonated azo dyes cannot be analyzed using GC/MS because they are non-volatile, their degradation products and intermediates can be detected, as can other types of dyes such as the non-azo ones tested here; this was also the case in this study. The most prevalent intermediate found using GC/MS analysis differed for each Acid Dye with Soap and Soda. The different chemical groups present their respective hazard as listed in Table 6.15. Many organics decreased during oxidation; however, the organics remaining all increased to their final levels. Acid Fast Red with Soap and Soda was found to contain mostly alkane and aldehyde functional groups, as well as levels of aromatics connected to aldehydes, aromatics connected to ketones, and alkanes connected to ketones. The organic chemicals containing alkanes and aldehydes here are combustible, cause skin and serious eye irritation, and may cause respiratory irritation. Acid Golden Yellow with Soap and Soda was found to contain mostly alkanes linked with aldehydes that increase during oxidation. They also contain less alkanes linked with carboxylic acids, and aromatics linked with aldehydes. The organics comprised of alkanes and carboxylic acids here cause severe skin burns and eye damage and are harmful to aquatic life. Acid Ananda Blue was found to contain mostly alkane and carboxylic acid linked organics although it also contains aromatics connected to aldehydes and alkanes connected with aldehydes. Compounds that contain aromatic and aldehyde functional groups are combustible, harmful if swallowed, causes skin irritation, may cause allergy or asthma if inhaled, and are toxic to aquatic life.

The biodegradability of these organics found in solution was measured using respirometric analysis. The oxygen uptake measure during this procedure showed

positive activity in none of the samples. Considering that the UV-visible spectrometry peaks, COD levels, and GC/MS peaks show aromatics and other functional groups left in solution, it can be concluded that the quantity of pollutants in solution are very low and may not be sufficient for the CETP sludge to react in a short time.

Since full oxidation followed by filtration left the least amount of organics in solution, it can be concluded that longer photo-Fenton oxidation time allows for the chemical reaction to separate more of the dissolved dye from the water in solution. More reaction time results in more sludge created by the separation of dye and iron rust from the aqueous solution. The creation of sludge occurs due to the chemical reaction between hydrochloric acid, iron, UV light, and hydrogen peroxide that frees hydroxyl radicals to attack the pollutants. Dye and rust sludge is easily removed from solution but is also easily remixed into solution. This explains why the organic level of the non-filtered fully oxidized samples, in some cases, can be comparable or higher than the non-filtered partially oxidized samples. The fully oxidized sample may have contained re-dissolved pollutants while the partially oxidized sample still contained dissolved chemicals. Although care was taken to not mix the settled non-filtered sample before testing, this inadvertent mixing can explain any unexpected spikes in COD or peak height of UV-visible spectra. This also explains why the filtration of the sludge out of the fully oxidized sample results in lower organics than filtering the partially oxidized sample which still contains dissolved pollutants.

Iron/dye sludge is very fine and dissolution of sludge particulates is possible. This is a concern and should be studied further. Field studies detailed in Chapter 7 describe two methods that prevent the dissolution of the organic sludge content (that upon dissolution would be un-filterable and render the filtered-water colored) and prevent the inorganic content from clogging the sand filter. The first is to remove the organic sludge that is present in the form of foam from the top of solution before filtration but after photo-Fenton oxidation has taken place. Future studies should create a method that more efficiently utilizes labor time for removing the sludge foam. A third type of filtration in the form of cotton fabric located just before the sand filter is suggested to prevent the inorganic iron rust from clogging the sand. The cotton fabric is more easily washed as compared to the sand and is a finer filter to capture the particulates preventing their reentrance into solution. Future studies should detail a method of separating iron and dye from the sludge. Preliminary work has begun to dissolve the dye from the iron in the sludge thus proving that in fact there are separate organic and inorganic elements within the sludge. It would help decrease costs of photo-Fenton oxidation treatment if iron can be reused; and it would decrease costs for dyers if dye, depending on the extent of its oxidation, can be extracted and reused in future batches.

Using hydrochloric acid results in increased levels of chloride and sodium as measured using ICP. Chapter 3 describes the strong attraction between chloride and sodium ions and also describes that sodium chloride is very soluble in water which makes it un-filterable through sand or carbon. The ICP results agree with this conclusion. Other photo-Fenton oxidation studies detailed in Chapter 2 use sulfuric acid preventing these

high levels, but producing high levels of sulfates in their effluent. Future studies should investigate ways of removing sodium and chloride from treated effluent or compare the results from other acids and their impact on treated water quality.

Iron metal ions that are added to solution during the photo-Fenton oxidation process, via the iron scrap catalyst, are completely removed from solution after filtration. Calcium and magnesium increased during the filtration process but most often stayed below the permissible limits, especially for fully oxidized samples. Cadmium, lead, arsenic, and manganese ions are noted if they are above the permissible limits for drinking water which is sometimes the case, and they most often decrease to permissible levels after full treatment. All of these ions, and especially lead, are often the ingredients in chemical dyes to give them their vibrant color. As discussed in the results, calcium, magnesium, and iron decrease to permissible levels after full oxidation followed by sand and carbon filtration most successfully. Although the sodium in solution decreased substantially after full oxidation followed by filtration, treatment rarely brought the sample to below drinking water permissible limit of 20 mg/L. Further sodium removal will be needed for the success of future studies.

The impact that iron surface area (rather than dissolved iron (II) ferrous salt) has on the photo-Fenton oxidation process is tested in these experiments as 645 cm^2 surface area under 2.5 cm of solution above the iron. Iron rust is used in the sustainable photo-Fenton oxidation process in place of the laboratory-grade chemical iron (II) ferrous salt. Most photo-Fenton oxidation studies, as detailed in Chapter 2, describe optimal iron salt

concentrations in mg/L iron to solution volume. This study uses scrap iron according to how its surface reacts when it is struck by UV radiation after it passes through the dye effluent. There are few previous studies that utilize scrap iron in their research and they quantify iron ion production according to iron weight. These studies utilized iron scrap in the form of shavings which have very high and immeasurable surface area. The role of iron as a catalyst in the photo-Fenton oxidation chemical reaction is detailed in Chapter 2. The amount of iron must be high enough for free iron ions to react in the photo-Fenton oxidation process in order to oxidize the pollutants, but not so high that there are extra ions in solution attracting hydroxyl radicals away from the chemical dye pollutant towards the iron. It can be concluded that despite possible scavenging, it is more beneficial for the degradation process that more iron be present, thus enabling the oxidation to occur, as compared to less iron, which may prevent it from starting. Any iron in solution after degradation is in the form of sludge and is easily filterable thus decreasing iron levels to negligible proven through the ICP results. It was found that higher surface areas of iron resulted in lower full oxidation times. This information can be used for future studies to utilize rusty metal containers for pilot-scale treatment unit construction.

Combining the UV-visible spectra data, COD levels, and the GC/MS labels gives specific detail regarding which organics remain in solution after sustainable photo-Fenton oxidation. The first thing worth mentioning is that UV-visible spectra peaks cannot be simply defined or labeled since a peak at a certain wavelength can be present for many different compounds depending on the color of that compound. Table 3.12, in Chapter 3,

lists the labels for the peaks found in Acid Fast Red with Soap and Soda, Acid Golden Yellow with Soap and Soda, and Acid Ananda Blue with Soap and Soda samples according to past studies detailed in Chapter 2. There are similarities between many peaks found in the UV spectra that may be categorized according to other studies. Visible peaks that are responsible for the color in the dye are already well labeled by previous studies. Many UV and visible peaks remain unlabeled. GC/MS results assist in the labeling, but do not match the location of a UV-visible spectra peak to a specific organic. The UV peaks found in the spectra show high-level peaks as well, thus concluding that the solution contains a variety of organics at different abundances.

A confirmation that the photo-Fenton oxidation reaction is changing the chemical composition of solution can be seen by the presence of different peaks in the UV-visible spectrometry results with oxidation. As can be seen in the analysis of the control samples, UV peaks other than those shown in the control sample C1 were evident after the addition of acid and oxidant. He and Lei (2004) also discuss the presence of new peaks coming on the UV-visible spectra after oxidation.

UV peaks degrade much slower than visible peaks. The peak at 203 nm and 205 nm found for all three acid dyes with soap and soda in this study is at the approximate location of phenol as described by He and Lei (2004) as listed in Table 3.12. Although this cannot be completely confirmed, many organics containing the same phenyl ring were identified by GC/MS as described in Tables 6.6, 6.7, and 6.8. The peaks close to 206 nm is by far the highest of the peaks present in the controls even after partial and full

oxidation and sand and carbon filtration. This is expected because it is difficult to degrade the phenyl or benzene ring.

Visible peaks degrade very quickly. Chapter 2 reveals the theory that the chromophores located in the chemical composition of dyes degrade very quickly. The peaks responsible for dye color in this study also degrade quickly and are completely degraded after full oxidation. Other visible peaks that have not been clearly identified as coming from the color composition also fully degrade; this identification is beyond the scope of this study.

Table 6.15: Hazardous effects of the definable chemicals that remain in solution after photo-Fenton oxidation of acid dyes with soap and soda listed according to the Globally Harmonized System of Classification and Labeling of Chemicals (GHS).

Type of Compound	Hazard Statement
Alkane & Aldehyde	H227 Combustible liquid. H315 Causes skin irritation. H319 Causes serious eye irritation. H335 May cause respiratory irritation.
Alkane & Carboxylic Acid	H314 Causes severe skin burns and eye damage. H402 Harmful to aquatic life.
Aromatic & Aldehyde	H227 Combustible liquid. H302 + H312 Harmful if swallowed or in contact with skin. H315 Causes skin irritation. H317 May cause an allergic skin reaction. H334 May cause allergy or asthma symptons or breathing difficulties if inhaled. H401 Toxic to aquatic life.

6.8 Summary

In summary, laboratory-scale research using sustainable photo-Fenton oxidation to degrade 5 g/L Acid Dyes with Soap and Soda using pharmacy-grade 6% hydrogen peroxide, household hydrochloric acid, scrap iron sheets, and sunlight is best done using full oxidation time followed by sand and carbon filtration to remove sludge.

There are many variables in the photo-Fenton oxidation process that impact the success of dye degradation. These include chemical composition of dyes, concentration of dye, acidified pH of solution, quantity of hydrogen peroxide used, solar irradiation, oxidation time, iron surface area, and filtration method. This study uses a cottage-scale industry dye concentration that is higher than any previous photo-Fenton oxidation study. This study also compares data taken in different locations whose solar irradiation varies greatly. Despite these differences from previous studies, complete color degradation occurred, as other organic and inorganic chemicals in solution also decreased to below permissible effluent levels. Degradation benefited from longer oxidation time and using iron with a greater surface area requires less time for full oxidation. High sodium and chloride levels after full treatment are a concern because of the choice to use readily available hydrochloric acid to acidify the solution.

Overall, the sustainable photo-Fenton oxidation process using scrap metal as the iron catalyst coupled with sand and carbon filtration shows great promise for the decolorization and chemical degradation of Acid Fast Red with Soap and Soda, Acid Golden Yellow with Soap and Soda, Acid Ananda Blue with Soap and Soda, and Field Samples Green and Maroon. The process does not need biodegradation after complete oxidation and filtration, as little additional benefit is seen with biodegradation. Future studies should focus on the remaining treated effluent after filtration including ways to lower sodium and chloride levels as well as how to separate and reuse iron and dye present in solid sludge that settles out of solution or is captured by sand filtration.

When considering that a cottage-scale dyer uses a very high concentration of dye in their dye batch, there is an opportunity for education and system improvement. Speaking with a medium-scale silk dyer in India, it was discovered that small process changes can decrease the impacts that dye effluent has on the environment. However, there are many reasons that interplay and cause a dyer to apply the methodology s/he uses. This work's focus was engineering an option for the current methodology of a cottage-scale silk dyer in rural Bangalore. It is worth mentioning here that there is a need for discussion and upgrading of the current small-scale dyer methodology in order to preserve and protect the natural environment. Despite treatment of the high concentration of dye wastewater, starting with a high level of chemical in an industry results in a high level of chemical waste. This project has successfully contained and modified the chemical waste to a form that is less dangerous and more manageable. However, using a lower concentration of dye or using natural dyes would lessen the impact of the dyeing process on the natural environment.

CHAPTER 7 – DEMONSTRATION PROJECT: SUSTAINABLE PHOTO-FENTON OXIDATION OF COTTAGE-SCALE SILK DYE WASTEWATER IN KARNATAKA, INDIA

7.1 Introduction

A primary goal of this research is to build a pilot project to implement the sustainable photo-Fenton oxidation research at cottage-scale silk dyeing operations in Karnataka, India. To do this is to create a decolorization unit that also decreases toxicity of wastewater at a low cost to the small-scale dye operations knowing that they cannot afford to pay for wastewater treatment. This demonstration-scale project costs $1.30 per 50-liter batch.

7.2 Background and Set-up

Three major locations were visited near Bangalore, India to observed small-scale silk dyeing operations. There are more known locations, but these were selected due to their willingness to accommodate visitors. The typical homespun silk dyer in Karnataka, where dyeing silk is a major source of income, makes 20-150 liter batches of dye at very strong concentrations.

Silk yarn needs to be washed before it can be dyed. Cottage-scale silk dyers currently mix their silk washing solution (soap and soda) with their dye bath. Medium and large-scale dyers separate the processes. Combining the dye and wash activities offers a less expensive option for dyeing because it reduces the need for equipment, fuel resources for

water heating, and demand for water (which may have limited availability). However, less of the dye in solution is absorbed into the yarn when there is soap and soda in solution. In a simple dye bath made of only dye and water, the dye is absorbed into the textile at a higher volume than the water, and color darkness of the fiber increases with dyeing time. This allows the dyer to use a lower concentration of dye in solution and simply leave the yarn in a dye bath for a longer time to obtain a darker color. However, when soap and soda are combined in the bath, the dye is competing with the soap and soda to absorb into the fiber. More dye must be used when less is absorbed, thus resulting in a darker chemical dye effluent. Furthermore, considering the small size of cottage-scale industries and their low income, it is understandable that they cannot afford to treat their mixed color, soap, and soda wastewater. After the effluent is dumped directly onto the soil, it moves through the ground and inevitably contaminates the ground water or overland resources (streams, farm fields, children's play areas).

After dyeing takes place, two fabric rinse cycles are completed—one to remove surface color and the second to ensure color fastness using a small amount of kerosene. After rinsing, concentrations of chemicals in solution are approximately 5 g/L dye, 10g/L soda, and 3.1 g/L soap. Since this is a very dark concentration of color, and sunlight penetration of dye solution is key for the Photo-Fenton oxidation reaction to occur, the dye wastewater must be poured into shallow containers. Hydrogen peroxide and hydrochloric acid are also required for the sustainable photo-Fenton oxidation process. Due to cost constraints of small-scale dyeing units in rural communities in developing

countries, the research focus here is given to create a system with the lowest possible cost.

Upon arrival to India, materials for the reaction unit (container), sand and carbon filter, dye, soap and soda, acid, and hydrogen peroxide were obtained. Ease of procurement and cost determined quality and type of materials used and chemical concentration of acid and peroxide. Acid Dye, soap, and soda were purchased from the same vendor that rural silk dyers use in Bangalore. The concentration mimicked the everyday silk dyeing protocol described in Chapter 3. The pilot project needs to handle 50-150 liters of dye effluent. Originally, the containers constructed at the University of Wisconsin-Milwaukee were used with a plethora of iron scrap covering the bottom of the container. After arrival in India, it became clear that scrap metal was readily available at a low cost. Therefore a rusty iron reactor was made at a local metal market. The container sides were bent to be 15 cm deep creating an open rectangle 1.25 m wide by 2.5 m long, and the corners were gas-welded closed. Appendix H describes the construction of the reactor unit. 32% hydrochloric acid was available at a low cost as was 50% hydrogen peroxide. Two sand filters were built—one using river sand, the other using ocean sand to compare the effectiveness of each sand. A 120-L rain barrel was chosen and filled with 100 kg of sand and covered with a full layer of wood charcoal. Appendix I describes the construction of the sand and carbon filters.

The proposal for the demonstration project described above asked for support from the Karnataka State Pollution Control Board (KSPCB) in finding a textile dye industry

willing to allow a mobile photo-Fenton oxidation and filtration unit to be built at their industry and treat 50-150 liter batches of colored effluent. The KSPCB, specifically the Chairman, Member Secretary, Chief Environmental Officer, Senior Environmental Officers, Environmental Officers, and other staff, agreed to support the demonstration project by connecting the study with a dyer in Peenya, Bangalore. Mr. A. Ramesh, Senior Environmental Officer of the KSPCB, and Mr. Anilkumar, Environmental Officer Peenya Region of the KSPCB, identified a suitable industry for carrying out the demonstration project between April and June 2014. Swan Silk Limited, a medium-scale silk dye industry in Peenya, Bangalore, agreed to house the demonstration project for its duration under supervision of Director Mr. K.S. Radhusa and Dye Manager Mr. Prakash Mangalagatti with complete support from them for space, work assistance, and all chemical needs.

Swan Silk Limited is a medium-scale silk dyer and although they were open to accepting the demonstration project to be built within its industry, they use a much lower dye concentration because they separate their soap and soda wash cycle from the batch dyeing. For that reason, the demonstration project utilized the facilities at Swan Silk Limited for fabricating dye batches that mimicked the cottage-scale operations.

7.2.1 Cottage-Scale Dye Industry Questionnaire

In preparation for the demonstration project, the practice and impact of dumping untreated dye effluent over land was seen during visits to cottage-scale dye operations in villages around Bangalore. During these visits dye protocol and wastewater treatment

was discussed using a questionnaire developed to document various site visits. The questionnaire can be seen in Fig. 7.1.

Every dyer visited expressed their wishes for effluent treatment but worried about their lack of funds to carry out treatment. Most dyers are family based, although the larger cottage-scale dyeing operations hire outside help (most often neighbors who also know the industry). The quantity of dye batches made is completely dependent on the time of year. The wedding and festival seasons create a high demand for silk saris and therefore increase their workload and wastewater effluent. Other times of the year there is a much lower work load. The formula for each dye bath depends on the intensity and brightness of color but was found to range between 5-12 g/L Acid Dye with 10 g/L soda, and 3.1 g/L soap. The supplies including dye, soap, and soda are found at local stores and within major markets in Bangalore.

There are cooperatives within and around the silk dyeing operations that greatly assist in connecting each step in the silk manufacturing process (egg hatchers, mulberry growers, silkworm rearers, cocoon harvesters, silk spinners, silk dyers, silk weavers). The cooperative creates open markets where people from each phase of the operation may go to obtain their needed materials, sell their supplies, find work, and connect with government officials to assist in improved technologies. For instance, dyers may travel to the cooperative to find weavers looking for someone to dye their silk before it gets woven into a sari. Dyeing contracts are often found using word-of-mouth and reputations. Once relationships are made, silk weavers who are connected to buyers

often know dyers that they prefer to work with. The weavers will contract out the dyeing work to these cottage-scale operations.

Some of the dyers entered the industry because their fathers were also dyers; some entered because of the newly formed cooperatives that offered some security through technology and contract assistance. Since the dyer is only a small portion of the complete silk fabric manufacturing operation, the dyer does not make a very high wage. For that reason, only the dyers located close to a larger municipality were found to have access to wastewater decolorization and treatment facilities that were run by the larger government. In the case of the dyers 80 km from Bangalore, there is no municipal or affordable option for treatment despite their lucid awareness of the dangers of dumping chemical dyes into the natural environment. There is, however, a general fear that visits from an outside researcher could get them into trouble with the KSPCB due to the dyers' lack of wastewater treatment before disposal. Dyers agreed that if an affordable wastewater treatment option could be subsidized by the government, it would have the potential to protect their natural environment and their families' health.

Questionnaire for Cottage-Scale Silk Dyer

1. What is the name of your Village, Region, and Country?_____
2. What is your name and your business's name?
3. How many years of formal education have you completed?
4. Are you a part of any local silk industry cooperative that helps you find clients?
5. How many people are working there with you?
    a. Are they family members or hired workers from the community/outside the community?
6. How many years have you been in the dyeing industry?
7. How many batches of dye do you produce in a day/week/month/year?
    a. How much do you earn?
    b. How much do you pay your employees?
    c. Do you have any idea about the profit in the other sectors of sari production?
8. What is your current formula for dyeing (batch mixture)?
    a. Size of batch in liters
    b. Quantity of soap used
    c. Quantity of soda used
    d. Quantity of dye used (range ok)
    e. Quantity of petroleum/kerosene in rinse for color fastness
    f. Quantity of rinse water used
9. Where do you purchase your supplies (dye, soap, soda, etc.)?
10. What is your current method of effluent treatment?
    a. If none, what prevents you from using treatment?
        i. If money, would you be willing to try a method that is either low-cost or subsidized by the Indian government?
11. How do you dispose of your waste?
12. What are your criteria for safe disposal?
13. What kind of money do you want to spend if the techniques are available?
    a. What can you afford?
14. What kind of support do you have from KSPCB?
15. Is there any treatment method that you have heard of that you would be interested in trying?
16. Is there anything that you are afraid of in sharing your industry information with me?
17. Do you have any questions for me?

Figure 7.1: Questionnaire completed for of each cottage-scale dyer visited.

7.3 Apparatus and Methodology

Appendix G contains the educational brochure documenting the methodology used in

the demonstration-scale sustainable photo-Fenton oxidation and slow-sand filtration project. Appendix H contains an educational brochure detailing instructions for the construction of a rusty iron reactor to be used for sustainable photo-Fenton oxidation. Appendix I contains an educational brochure developed in order to explain the construction of a slow-sand, carbon, and cotton filter to be used after photo-Fenton oxidation of textile dye wastewater.

7.4 Results

The following trials were performed on site at Swan Silk Limited in Peenya, Bangalore to see how the experimental details functioned and impacted a typical cottage-scale industry wastewater. Parameters of trials of 5 g/L Acid Fast Red Dye with 10 g/L soda, and 1 bar soap per 10 L solution (3.1 g/L) are listed in Table 7.1. Changes in volume of solution, quantity of 34% hydrochloric acid, quantity of 50% hydrogen peroxide, solar irradiation, solution depth, oxidation time, and type of filtration used are listed according to trial. Degradation results are listed in Tables 7.2-7.9 including changes in pH, conductivity, Total Dissolved Solids (TDS), residual sodium carbonate, sulfates, COD, chloride, chromium, boron, and percent color removal. All tested parameters whose levels were above the KSPCB permissible limits are listed in red in the tables. Parameters for the trial using Swan Silk Limited effluent is listed in Table 7.10 and results are listed in Table 7.11. FTIR was also used to test the Acid Fast Red Dye with Soap and Soda in t_0 samples and compare it to the remaining sludge in solution. FTIR results can be found in Fig. F.1-F.10 in Appendix F.

Table 7.1: Parameters of sustainable photo-Fenton oxidation trials.

Effluent Parameter	Sample	Trial 1	Trial 2	Trial 3	Trial 4	Trial 5	Trial 6	Trial 7	Trial 8
Solution Volume (L) (50-150 L capacity container)	t_0	100	50	50	50	50	50	50	50
Quantity 34% HCl (L) to lower pH to 2.5-4.2	t_0	3.0	1.0	1.0	1.0	1.0	1.1	1.0	1.0
Quantity 50% H2O2 (L) (optimized at 200 mL/ L dye solution)	t_0	2.4	1.2	1.2	1.2	1.2	1.2	1.2	1.2
Solar Energy (Btu/(ft2*hr)	t_0, t_F	Over-load	Over-load	73	Overload	130	80	80	100
Solar Energy (W/m2)	t_0, t_F	Over-load	Over-load	Overlo ad	Overload	Overloa d	Overloa d	Overloa d	Overload
Solution Depth (cm) (optimal 2.5-5 cm)	t_0	5	2.5	2.5	2.5	2.5	2.5	2.5	2.5
Running Time (hr)	t_F	2.5	4	5	5	4.5	6	5	3.5
Filtration Method (sand, charcoal, cotton cloth)	t_F	100 kg Ocean Sand	100 kg River Sand	Cotton Fabric	2 layers Cotton Fabric, 100 kg River Sand	2 layers Cotton Fabric, 100 kg River Sand	2 layers Cotton Fabric, 100 kg River Sand	2 layers Cotton Fabric, 100 kg River Sand	2 layers Cotton Fabric, 100 kg River Sand, 5 cm Charcoal

Note, Solar Energy Overload is greater than 634 Btu/ft2*hr or 1999 W/m2.

Trial 1, whose results are listed in Table 7.2, used a 100L batch at a depth of 5 cm which resulted in almost complete decolorization. Starting with pH 1.7 however proved too acidic since sand filtration did not raise the pH to neutral as was expected and seen in laboratory-scale results described in Chapter 6. The oxidized solution has 3 layers—foam, decolorized solution, iron/dye sludge. All three layers here were poured through filtration. Conductivity, COD, and chloride were above the permissible limits with decreasing values as treatment followed by filtration was completed. In the case of conductivity, values initially increased after oxidation (due to the added chemicals to

solution) but then lowered to below the initial value. Chloride levels acted similarly except that filtration did not cause them to lower below initial concentration due to the added hydrochloric acid in solution.

Table 7.2: Results of sustainable photo-Fenton oxidation of Trial 1.

Effluent Parameter	t0	tF oxidized	tF filtered
pH	10.8 to 1.7	2.04	3.5
Conductivity (µS/cm)	26600	34500	22000
TDS (mg/L)	NA	NA	1140
Residual Sodium Carbonate (meq/L)	NA	0	0
Sulphate (mg/L)	NA	160	89
COD (mg/L)	NA	1246	494
Chloride (mg/L)	6106	15918	10318
Chromium (mg/L)	0.039	0.314	0.010
Boron (mg/L)	0.000	0.296	0.060
% Color Removal based on UV-vis Spectra (505 nm)	0	99.7	100

Trial 2, whose results are listed in Table 7.3, used 50 L at a depth of 2.5 cm which decolorized the sample as sufficiently as 5 cm. Starting with pH 2.2, the pH ended at 5.9 after sand filtration, which is near neutral. New river sand in the filter released many particles into solution. Sludge was thick and clogged flow through the sand since all three layers here were poured through the filter. Conductivity, COD, and chloride are shown here to be above the permissible limits with decreasing values as oxidation followed by filtration was completed. This also follows the same trends as Trial 1.

Table 7.3: Results of sustainable photo-Fenton oxidation of Trial 2.

Effluent Parameter	t0	tF oxidized	tF filtered
pH	10.8 to 2.2	4.4	5.9
Conductivity (µS/cm)	26600	30000	22000
TDS (mg/L)	NA	NA	4520
Residual Sodium Carbonate (meq/L)	NA	39	117
Sulphate (mg/L)	NA	147	134
COD (mg/L)	NA	1052	584
Chloride (mg/L)	6106	15106	11271
Chromium (mg/L)	0.039	0.001	0.001
Boron (mg/L)	0.000	0.000	0.000
% Color Removal based on UV-vis Spectra (505 nm)	0	99.7	99.7

Trial 3, whose results are listed in Table 7.4, started with a pH 2.75 and ended with a pH of 5.4 after cotton fabric filtration, which is near neutral. Cotton fabric alone was chosen since the sand filter in Trial 2 released particulates into solution. Color remained in solution after using only cotton fabric filtration thus communicating that cotton filtration alone was insufficient for decolorization. Again, all three layers of solution were poured through filtration. Conductivity, COD, and chloride are shown here to be above the permissible limits with decreasing values as oxidation followed by filtration was completed. Cotton filtration did not lower COD or chloride values as much as sand filtration as was seen in Trial 1 and 2. Conductivity is slightly lower due to the change in filtration. Sand particles from filtration seem to cause higher conductivity in solution.

Table 7.4: Results of sustainable photo-Fenton oxidation of Trial 3.

Effluent Parameter	t_0	tF oxidized	tF filtered
pH	10.8 to 2.75	4.62	5.4
Conductivity (µS/cm)	14600	15960	15320
TDS (mg/L)	NA	4530	2050
Residual Sodium Carbonate (meq/L)	NA	30	125
Sulphate (mg/L)	NA	128	136
COD (mg/L)	NA	1158	1054
Chloride (mg/L)	6106	15989	15577
Chromium (mg/L)	0.039	0.000	0.000
Boron (mg/L)	0.000	0.000	0.000
% Color Removal based on UV-vis Spectra (505 nm)	0	99.4	99.7

Trial 4, whose results are listed in Table 7.5, used two cotton fabric layers placed over the sand filter for filtration. Starting at a pH of 2.5, the pH rose to 5.54 after filtration. The sludge was still very dense but was easier to handle on the cotton filter, and the cotton is easier to clean than the sand in the sand filter. Flow through cotton was slow because all three layers of solution were poured through filtration, but pH and TDS resulted within allowable range. Conductivity, COD, and chloride are shown here to be above the permissible limits with decreasing values as treatment followed by filtration was completed. Levels are very similar to Trial 1 and 2 following sand filtration.

Table 7.5: Results of sustainable photo-Fenton oxidation of Trial 4.

Effluent Parameter	t0	tF oxidized	tF filtered
pH	10.8 to 2.5	3.2	5.54
Conductivity (µS/cm)	26600	29400	21600
TDS (mg/L)	1730	1960	1930
Residual Sodium Carbonate (meq/L)	NA	62	102
Sulphate (mg/L)	NA	30	62
COD (mg/L)	NA	942	452
Chloride (mg/L)	6106	15812	11636
Chromium (mg/L)	0.039	0.007	0.005
Boron (mg/L)	0.000	0.000	0.000
% Color Removal based on UV-vis Spectra (505 nm)	0	100	100

Trial 5, whose results are listed in Table 7.6, used two cotton fabric layers placed over the sand filter just as with Trial 4. A higher starting pH was chosen to find an upper limit. Starting at a value of 4.2, the pH increased to pH 5.5 after filtration. During this trial, the foam was separated which sped up the cotton filtration process. Conductivity, COD, and chloride are shown here to be above the permissible limits with decreasing values as treatment followed by filtration was completed acting very similarly to all previous trials. Chloride levels increased slightly after filtration, but were still in the same range as previous trials and were well above the limit after oxidation.

Table 7.6: Results of sustainable photo-Fenton oxidation of Trial 5.

Effluent Parameter	t0	tF oxidized	tF filtered
pH	10.8 to 4.15	4.15	5.5
Conductivity (µS/cm)	26600	28900	28100
TDS (mg/L)	6570	3360	2190
Residual Sodium Carbonate (meq/L)	NA	121	33
Sulphate (mg/L)	NA	96	70
COD (mg/L)	NA	1026	918
Chloride (mg/L)	6106	14553	15377
Chromium (mg/L)	0.039	0.004	0.000
Boron (mg/L)	0.000	0.000	0.000
% Color Removal based on UV-vis Spectra (505 nm)	0	99.7	99.7

Trial 6, whose results are listed in Table 7.7, was very similar to Trial 5 but with a slightly lower starting pH of 3.2. Here foam was also separated from solution resulting in very similar results. Conductivity, COD, and chloride are shown here to be above the permissible limits with decreasing values as treatment followed by filtration was

completed acting very similarly to all previous trials. Here COD and chloride levels increase slightly after filtration, but are still in the same range as previous trials and are above the limit after oxidation.

Table 7.7: Results of sustainable photo-Fenton oxidation of Trial 6.

Effluent Parameter	t0	tF oxidized	tF filtered
pH	10.8 to 3.2	5.7	5.74
Conductivity (µS/cm)	26600	29600	29400
TDS (mg/L)	2840	3360	2120
Residual Sodium Carbonate (meq/L)	NA	160	78
Sulphate (mg/L)	NA	106	110
COD (mg/L)	NA	996	1036
Chloride (mg/L)	6106	15824	18247
Chromium (mg/L)	0.039	0.007	0.000
Boron (mg/L)	0.000	0.000	0.000
% Color Removal based on UV-vis Spectra (505 nm)	0	96.9	99.7

Trial 7, whose results are listed in Table 7.8, was very similar to Trial 6 but with a slightly lower starting pH of 2.7. Here foam was separated from solution again resulting in very similar results. TDS of solution after 2 layers of cotton fabric and sand filtration registered that some color came through the sand filter. These results may indicate that after three 50L batches, the cotton filter needs to be cleaned. Conductivity, COD, and chloride are shown here to be above the permissible limits acting very similarly to all previous trials. COD and conductivity levels increased slightly after filtration, but were still in the same range as previous trials and were above the limit after oxidation.

Table 7.8: Results of sustainable photo-Fenton oxidation of Trial 7.

Effluent Parameter	t0	tF oxidized	tF filtered
pH	10.8 to 2.7	2.9	5.3
Conductivity (µS/cm)	26600	28400	28900
TDS (mg/L)	3270	3360	3390
Residual Sodium Carbonate (meq/L)	NA	67	40
Sulphate (mg/L)	NA	19	87
COD (mg/L)	NA	894	972
Chloride (mg/L)	6106	16800	15953
Chromium (mg/L)	0.039	0.000	0.013
Boron (mg/L)	0.000	0.000	0.000
% Color Removal based on UV-vis Spectra (505 nm)	0	100	100

Trial 8, whose results are listed in Table 7.9, started with only 1L of hydrochloric acid and 1L hydrogen peroxide with the intention of lowering the cost and simplifying the protocol. In this case, the hydrochloric acid may have been older and therefore 1 L of acid only acidified the solution to pH 5.8 which was not low enough to completely degrade color. The acidity after sand filtration rose to neutral. Wood charcoal was also added as third form of filtration in hopes of absorbing more color from solution. Conductivity, COD, and chloride are shown here to be above the permissible limits with decreasing values as treatment followed by filtration was completed; this is very similar to all previous trials. Wood charcoal filtration greatly reduced the levels of COD, chloride, and conductivity, but they were still above permissible limits.

Table 7.9: Results of sustainable photo-Fenton oxidation of Trial 8.

Effluent Parameter	t0	tF oxidized	tF sand filtered	tF filtered charcoal
pH	10.8 to 5.8	7.75	6.48	5.6
Conductivity (µS/cm)	26600	29300	28900	23800
TDS (mg/L)	4370	3290	3710	NA
Residual Sodium Carbonate (meq/L)	NA	380	251	164
Sulphate (mg/L)	NA	177	170	276
COD (mg/L)	NA	1080	1026	650
Chloride (mg/L)	6106	17930	15648	12471
Chromium (mg/L)	0.039	0.010	0.045	0.007
Boron (mg/L)	0.000	0.000	0.000	0.000
% Color Removal based on UV-vis Spectra (505 nm)	0	99.4	100	100

Trial 9, whose results are listed in Table 7.11, used 150 liters of Swan Silk Limited Effluent followed by an ocean sand filter. Considering that the medium-scale industry effluent had a much lower dye concentration, the results reflect the lower organic and ion load in solution. Here conductivity and chloride levels remained above permissible limits even after filtration, but were much lower than the 5 g/L Acid Fast Red with Soap and Soda solution described in Trials 1-8.

Table 7.10: Parameters of sustainable photo-Fenton oxidation tested.

Effluent Parameter	Sample	150 liters of Swan Silk Limited Effluent
Solution Volume (L) (50-150 L capacity container)	t_0	150
Quantity 34% HCl (L) to lower pH to 2.5-4.2	t_0	3.00
Quantity 50% H2O2 (L) (optimized at 200 mL/ L dye solution)	t_0	0.072
Solar Energy (Btu/(ft2*hr)	t_0, t_F	NA but sunny
Solar Energy (W/m2)	t_0, t_F	NA but sunny
Solution Depth (cm) (optimal 2.5-5 cm)	t_0	7
Running Time (hr)	t_F	2.5
Filtration Method (sand, charcoal, cotton cloth)	t_F	100 kg Ocean Sand

Table 7.11: Results of sustainable photo-Fenton oxidation of Swan Silk Limited effluent.

Effluent Parameter	t_0	$t_{F\ filtered}$
pH	10.8 to 3.0	3.8
Conductivity (µS/cm)	26600	4640
TDS (mg/L)	1710	1980
Residual Sodium Carbonate (meq/L)	NA	90
Sulphate (mg/L)	NA	216
COD (mg/L)	NA	282
Chloride (mg/L)	6106	4471
Chromium (mg/L)	0.039	0.004
Boron (mg/L)	0.000	0.000
% Color Removal based on UV-vis Spectra (505 nm)	203 nm	3.0

7.4.1 Karnataka State Pollution Control Board Standards

Treated textile effluent standards can be compared to the KSPCB standard requirements for treated textile effluent which is as follows:

- pH between 5.5-9.0
- TDS ≤ 2100 ppm
- TSS ≤ 200 ppm (unable to complete this test at time of study)
- COD ≤ 250 ppm
- BOD3 ≤ 100 ppm (did not complete this test because only chemical oxidation treatment was completed and no biological treatment was used for effluent)
- Conductivity ≤ 2250 µS/cm
- Oil & Grease ≤ 10 ppm (did not complete this test because there is no heavy machinery utilized in treatment)

- Residual Sodium Carbonate ≤ 5.0 meq/L
- Chloride ≤ 600 ppm
- Sulphate ≤ 1000 ppm
- Total Chromium ≤ 2.0 ppm
- Cyanide ≤ 0.2 ppm (did not complete this test because cyanide levels are link to water source, not treatment)
- Boron ≤ 2.0 ppm

The permissible levels listed in red were exceeded by some of the samples during this study.

7.5 Discussion of Results

Conductivity, COD, and chloride levels were generally higher than the KSPCB standard limits for textile industry effluent. Some TDS levels were also found to be above effluent standards. Due to the formation of sludge that prevented sand filtration (without the addition of other filtration types) from efficiently filtering samples as in laboratory studies detailed in Chapter 6, sludge solids were analyzed to view the azo dye bond breakage expected to be responsible for the color removal.

It was found that an initial pH between 2.2 and 4.2 resulted in successful oxidation of the Acid Dye with Soap and Soda in solution. Samples with this pH range experienced almost complete decolorization and left effluent with acceptable TDS and neutral pH after sand and cotton filtration.

Conductivity was very high before and after oxidation and also after sand filtration. It was always above 14600 μS/cm with the highest frequency above 21000 μS/cm. It is clear that the ions in solution that are the dye, soap, and soda that become oxidized and leave the solution through the oxidation and filtration processes are replaced with ions from the addition of chlorides during the acidification process and from ions in the sand filter.

Chloride levels increased 2.6-3.0 times after acidification with little to no change after sand filtration. Chloride levels are very high for two main reasons: (1) presence of chloride atoms in the dye composition; (2) the addition of hydrochloric acid for the acidification of the sample before photo-Fenton oxidation can occur. Other acids can be added instead of hydrochloric acid such as sulfuric acid, nitric acid, or acetic acid. The pros and cons of using different acids and the possible outcomes of this choice are described in Chapter 3. Sun *et al.* (2009) show that chloride ions are also scavenged and thus protected by hydroxyl radicals in the chemical Equations 7.1 and 7.2.

$$Cl^- + {}^*OH \rightarrow ClOH^{*-} \qquad (7.1)$$

$$ClOH^{*-} + Fe^{2+} \rightarrow Cl^- + OH^- + Fe^{3+} \qquad (7.2)$$

COD ranged from 500-1200 mg/L with the lower number usually occurring after filtration. Levels were still above effluent allowance, although sludge build-up on sand and cotton filters raised COD closer to the value just after oxidation. These high COD levels dictate that organics were left in solution—most likely in the form of aromatic compounds and amines such as benzene or naphthalene derivatives with broken azo

double nitrogen bond as was shown in the GC/MS data of multiple repeated 1-liter studies in Chapter 6.

Sludge was also produced during the photo-Fenton oxidation process in two forms: foam floating on top of solution, and heavier iron rust sludge that sank to the bottom of solution. The volume of foam was calculated from the top of the reactor and also the volume of sludge captured from the top of the filter. Sludge was calculated to be less than 5% of the effluent. This can be compared with the 15% that comes during biodegradation processes at a medium-sized textile wastewater treatment plant (information taken during an interview with the medium-scale textile industry manager).

For 4 of the 8 trials using 5 g/L Acid Fast Red with Soap and Soda, foam was separated from solution after the oxidation process was complete. Foam volume varied from 5,670 to 9,640 cm^3 with a 29,000 cm^3 outlier that occurred after 5 hours of oxidation. Overall time varied from 3.5 to 6 hours. The greatest amount of sludge did not occur at the largest amount of time or with an increased amount of sunlight. Sunlight when the 29,000 cm^3 volume of foam was produced was 80 Btu/(ft^2*hr) (Overload W/m^2), whereas the irradiance ranged from 80 Btu/(ft^2*hr) to 130 Btu/(ft^2*hr) during the trials when the foam was separated. Foam quantity seemed to be dependent on an unknown, unpredictable variable. The outlier's high volume could be due to a high quantity of liquid collected at the same time of the foam collection. Sludge collected on the cotton filter and/or sand filter had generally a similar volume for each of the trials and equated to less than 5% of solution.

Fukushina and Tatsumi (2001) describe the range of 3700-3200 cm^{-1} on FTIR as the range for phenolic O-H stretching that might actually represent binding sites for iron. They expand further to show that 1250-1200 and 1100-1000 cm^{-1} corresponding to C-O antisymmetric and symmetric stretching of ether bonds. Karadag *et al.* (2006) concur that 3620, 3430, and 1635 cm^{-1} correspond to natural zeolite thus indicating aluminum-silicon bonds and zeolitic water whereas 2922 and 2851 cm^{-1} correspond to organozeolite and CTAB. Jozwiak *et al*. (2007) list organic bonds studied by FTIR that cannot unfortunately be specified to exactly which molecule they come as detailed in Table 7.13.

Table 7.13: Peak location and identification of respective organic molecule (Jozwiak *et al*., 2007).

Peak location (cm^{-1})	**Organic Molecule**
3620-2800	hydrogen bonded OH and NH stretching
1660-1520	C=C and C=N
1500-1400	C=C
1380	C-CH3
1360-1260	C-C
1160-1120	C-H
1080-1040	S,O,N
720-480	'out of plane' H deformation
550-400	Co-O, C-S, C-N

Sludge analysis was completed by FTIR. FTIR was used to determine the composition of sludge as far as iron and dye composition. The results can be seen in Figures F.1-F.10 in Appendix F. The azo double nitrogen bond peak can be found at approximately 1456 cm^{-1}. The peak in the control t_0 non-oxidized sample was compared with the sludge captured on the cotton filter and also the foam sample. Very large peaks at t_0 ranging from 50-58% transmittance can be seen. For foam, transmittance is 70% with a large azo dye peak concluding that azo dye is in the foam. The sludge from sand and cotton filtration finds transmittance of the azo bond ranging from 75-95% with an average of 85% meaning that the azo bond has broken with less of a peak in the heavier rust sludge that

sinks out of solution than in the foam—finding that this sludge is more rust than dye chromophore.

FTIR analysis of the azo peak found in the sludge samples was taken from the fully oxidized solution after cotton filtration was completed. The sludge that sunk in solution was found to have 95% transmittance, or a low azo peak. The sludge captured on the cotton was tested and found to show 75-95% transmittance ranging from a high to low azo peak. The sludge captured by the sand filter was tested and found to have a 75% transmittance, or a high azo peak. The foam sample taken from the top of solution after photo-Fenton oxidation was completed and found to have a 70% transmittance or a higher azo peak.

FTIR analysis of the azo peak found in the dye sample before photo-Fenton oxidation was completed at t_0 found 50-57.5% transmittance with a high azo peak.

A dried sludge sample was also tested for organic/inorganic composition by mixing with ethanol to test whether sludge dissolved in solution. The dissolution showed the presence of organics and inorganics in sludge and gives the idea that it is possible to separate the dye from the iron in the sludge making reuse of rust and dye from solution possible.

7.6 Estimated Cost of Treatment in Mobile Unit

The total cost to build a sustainable photo-Fenton oxidation unit for 50-liters of dye solution is broken down into chemical and equipment costs listed in Tables 7.14 and

7.15. Table 7.14 details materials and costs required for initial set-up of the oxidation and filtration treatment unit. Table 7.15 details materials and costs needed for each 50-liter treatment process.

The initial set-up of the reactor and filtration unit requires $51.83. Running sustainable photo-Fenton oxidation of 50-liters of 5 g/L acid dye with soap and soda totals $1.30. These low costs will be proposed to the local government and the dye houses as an affordable cost to improve the health of the area and something that could potentially be subsidized by the local government.

Table 7.14: Materials and services costs for initial set-up of 50-liter sustainable photo-Fenton oxidation treatment unit.

Material / Service	Cost (Rupees/INR)	Cost (USD/$)
2.5 m x 1.25 m sheet of rusty iron scrap	1125	18.75
Bending sheet iron into Box	150	2.50
Gas-Welding Corners	60	1.00
Transport to Site	800	13.33
120-L Barrel for Sand Filter	350	5.84
100 kg Construction Sand	200	3.33
Plastic Tap/Faucet	50	0.83
Plastic Screen/Mesh	15	0.25
Epoxy	360	6.00
Used Cotton Fabric/Filter	Free	Free
Wood Charcoal for Carbon Filter	Free	Free
TOTAL	3110	51.83

Table 7.15: Materials costs for 50-liter sustainable photo-Fenton oxidation treatment process.

Material	Cost (Rupees/INR)	Cost (USD/$)
1-1.1 Liter 32% Hydrochloric Acid to bring to pH 2.5-4.2	13.2	0.22
1.2 Liters 50% Hydrogen Peroxide	64	1.08
TOTAL	78	1.30

7.7 Recommendations for continuation of project and construction of 150-liter pilot project June 2015:

1. *Acidification* of solution should range between 2.2 – 4.2 pH; above 5, decolorization is not complete.
2. *Depth of solution* should range between 2.5 – 5 cm average with some places as deep as 6 cm.
3. *Oxidation time* can vary but should be longer than 2 hours for large volumes of solution. The demonstration project solution was left to oxidize over lunch sometimes as long as 6 hours. Although 6 hours is not necessary, oxidation can be seen with heavy bubbling during the first 2 hours of reaction time.
4. *Foam sludge volume* varies greatly during oxidation. There seems to be a threshold linked to time in regards to foam creation—if oxidation time increases, foam begins to expand and overall volume decreases. Considering the ease of the rapid expansion of the foam sludge with time, this should not be a limiting variable for reaction time, however, is worth noting.
5. *Separation of rust* from solution should be studied as the **next step** toward optimizing this research work. Sludge production is found to be 5% of total effluent, which is 10% lower than the medium-sized textile effluent that is biodegraded. However, a portion of this 5% can be separated and reused for future dye batches making sustainable photo-Fenton oxidation a powerful treatment method for textile industries.
6. *High COD, chloride, and conductivity levels* need to be dealt with. It should be remembered that non-treated dye effluent from small-scale dyers is currently

being discharged directly onto land and into water resources. After photo-Fenton oxidation and filtration, the levels of organics and metals have greatly decreased in solution; however, there are still issues with the effluent. Rinse water could dilute effluent by approximately 66% considering that there are generally 2 rinses of equal volume to the dyeing process after dyeing is complete.

7. *Hydrogen Peroxide* addition can be minimized with a further pilot-study in order to decrease costs for cottage-scale industries.

7.8 Summary

In summary, the demonstration project has displayed that the sustainable photo-Fenton oxidation followed by cotton, carbon, and sand filtration costs approximately $52 for initial set-up and $1.30 for each 50-liter batch. This is to treat the cottage-scale silk industry effluent comprised of 5 g/L Acid Dye with 10 g/L soda and 3.1 g/L soap in a shallow rusty metal container manufactured at a local market coupled with a cotton, carbon, and sand filtration unit also constructed of locally sourced materials. pH and TDS, which are two concerns for textile industry dyers, were often well within the allowable range after using this treatment. The largest concerns are with COD, conductivity, and chloride levels. Future work with sustainable photo-Fenton oxidation and filtration should include further study (1) to reduce COD, conductivity, and chloride, as well as (2) to separate the iron and dye in the sludge formed in order to recycle each component for reuse.

CHAPTER 8 – CONCLUSIONS AND RECOMMENDATIONS FOR FUTURE WORK

8.1 Conclusions

There is a tremendous need to provide rural textile dye operations with an effective and low-cost method to clean dye wastewater. The unsustainable and unhealthy disposal methods currently practiced at rural silk dying industries in the developing world can be shocking to people in the developed world. This work has demonstrated that the photo-Fenton oxidation process is able to clean dye wastewater from textile industries all over the world, ultimately improving the health and quality of life for potentially millions of people. Furthermore, the low-cost and simplicity of the sustainable photo-Fenton oxidation reactors makes it possible for residents to implement this system quickly and easily in their own communities. Once the process is perfected for the small-scale dye units, there is great potential to scale up the system for larger units and commercial applications.

There are many variables in the photo-Fenton oxidation process that impact the success of dye degradation. These include chemical composition of dyes, concentration of dye, acidified pH of solution, quantity of hydrogen peroxide used, solar irradiation, oxidation time, surface area of the scrap iron catalyst, and filtration method. This study uses a cottage-scale industry dye concentration that is higher than any previous photo-Fenton oxidation study. This study also compares data taken in different locations whose solar irradiations vary greatly. Despite these differences from previous studies, complete color

degradation occurred in all three dye types, as other organic and inorganic chemicals in solution also decreased to below permissible effluent levels. Degradation benefited from longer oxidation time, although using iron with a greater surface area resulted in less time required for full oxidation. High sodium and chloride levels after full treatment are a concern because of the choice to use readily available hydrochloric acid to acidify the solution.

In summary, laboratory-scale research using sustainable photo-Fenton oxidation to degrade 5 g/L dyes using pharmacy-grade 6% hydrogen peroxide, household hydrochloric acid, scrap iron sheets, and sunlight is best done for Reactive dyes using an intermediate amount of iron surface area (323 cm^2) as the iron catalyst, while allowing for full oxidation time followed by sand and carbon filtration to remove sludge. For Acid dyes, there was less dependence on iron surface area, but it is still necessary to use full oxidation time followed by sand and carbon filtration to remove sludge; this is also the best scenario for Acid dyes with Soap and Soda. Overall, the sustainable photo-Fenton oxidation process using scrap metal as the iron catalyst coupled with sand and carbon filtration shows great promise for the decolorization and chemical degradation of red, yellow, and blue colors in Reactive dyes, Acid dyes, and Acid with Soap and Soda dye baths. The process may not need biodegradation after complete oxidation and filtration, as little additional benefit was seen with biodegradation.

A demonstration project was constructed to treat 50-liters of dye wastewater. The rusty metal reactor and sand and carbon filters cost $51.83. The photo-Fenton oxidation

process of 50-liters of solution costs $1.30 for hydrochloric acid and hydrogen peroxide. With regards to the development and implementation of a 150-liter pilot-scale project, recommendations for the sustainable photo-Fenton oxidation process include (1) acidifying solution to 2.2-4.2, (2) creating a solution depth between 2.5-6 cm, (3) allowing 2 hours for oxidation, (4) separating foam from the top of the treated solution, (5) using cotton fabric as a pre-filter to sand and carbon filtration.

When considering that a cottage-scale dyer uses a very high concentration of dye in their dye batch, there is an opportunity for education and system improvement. Speaking with a medium-scale silk dyer in India, it was discovered that small process changes could decrease the impacts that dye effluent has on the environment. However, there are many cultural and economic motives that interplay and cause a dyer to apply the methodology s/he uses. This work's focus was engineering an option for the current methodology of a cottage-scale silk dyer in rural Bangalore. It is worth mentioning here that there is a need for discussion and upgrading of the current small-scale dyer methodology in order to preserve and protect the natural environment. Despite treatment of the high concentration of dye wastewater, starting with a high level of chemical in an industry results in a high level of chemical waste. This project has successfully contained and modified the chemical waste to a form that is less dangerous and more manageable. However, using a lower concentration of dye or using natural dyes would lessen the impact of the dyeing process on the natural environment.

8.2 Recommendations for Future Work

This work has shown the results of oxidizing and filtering 5 g/L Reactive, Acid, and Acid with Soap and Soda Dyes in 1-liter laboratory and 50 to 100-liter field studies. Future studies should focus on further analysis of that which remains in solution after sustainable photo-Fenton oxidation and sand and carbon filtration is completed.

Sodium and chloride levels remained high as measured by ICP and described in Chapter 4, 5, 6, and 7. Multiple methods could be researched to decrease these high levels by starting the oxidation process with higher pH (3.5-4.2), thus lowering the quantity of hydrochloric acid added. This lower quantity of chloride in solution (because of the higher pH) will not attract as much sodium and thereby will not create such high levels of soluble sodium chloride in the filtered samples. Another method could include a comparison between using hydrochloric acid and sulfuric acid. As stated in Chapter 3, sulfuric acid is available at higher concentrations than hydrochloric acid thereby requiring a lower volume of sulfuric acid to acidify the dye solution in preparation for photo-Fenton oxidation. Using a lower concentration of acid may result in fewer chemical reactions within the solution and allow more pollutants to be filtered.

Benzene and naphthalene derivatives and other aromatics were found at high levels in solution using GC/MS in Chapters 4, 5, and 6, just as COD levels remained high despite treatment in the demonstration project described in Chapter 7. Organic chemicals originate from the high concentration of dye used. Complete oxidation followed by sand and carbon filtration decrease organics the most. Continued study regarding improved

cleaning of the carbon filter to increase its efficiency in removing all remaining organics out of solution is suggested. Increasing the quantity of charcoal to the sand filter may also increase organic removal from solution.

The testing of the oxidized and filtered samples was completed here. However, this study could benefit from further research into how reusing photo-Fenton oxidized and filtered treated water affects future dye batches. This future work should specifically study whether dye added to treated water chemically reacts the same as when it is added to municipal water. Further study should include treating the subsequent dye batches using sustainable photo-Fenton oxidation and filtration to measure decolorization and chemical degradation of the successive samples.

Conductivity levels remained high despite full oxidation and filtration due to the use of natural sand in the sand filter. The benefit of using natural sand is that the silicon and calcium present will increase the pH of the filtrate. Further study into increased charcoal quantity may decrease conductivity by removing more ions from solution. The use of a more standardized sand may also benefit this work. This standardization could involve using a better cleaning system to remove particulates that are normally released during filtration. Standardization could also involve clean storage of the sand and using an export quality of sand whose material profile is well documented.

Sludge production is something that keeps photo-Fenton oxidation from increasing in popularity in the wastewater treatment industry. Although this study has shown that

sludge production was only 5% of total solution volume (as compared to the more readily used biodegradation sludge production of 15%), future studies to find more ways to lower the quantity of sludge production would benefit this field of work.

Finally, regarding sludge formation, this study was the first of its kind to detail the formation of foam as a second type of sludge produced during the sustainable photo-Fenton oxidation process described in the demonstration project detailed in Chapter 7. There should be further study with regards to the cause of foam formation by monitoring temperatures and by completing a more thorough analysis of how broad spectrum solar irradiation affects the formation of foam. According to the FTIR analysis, the foam was comprised mostly of dye, whereas the heavier sunken sludge was an iron/dye mixture. Future research can improve the understanding, and therefore improve the handling of the foam and iron sludges, and increase the efficiency of their removal before filtration. Lastly, the separation and reuse of the components of the heavier iron sludge may benefit the future operation costs of this work. Separating the iron from the dye in the heavier sludge may enable reuse of the iron as the catalyst in future treatment, and even possibly reuse of the dye, depending on the extent of its chemical oxidation, in future dye batches.

REFERENCES

Alaton, I., and Teksoy, S. (2005). Acid dyebath effluent pretreatment using Fenton's reagent: Process optimization, reaction kinetics and effects on acute toxicity. *Dyes and Pigments 73,* 31-39.

Al-Kdasi, A., Idris, A., Saed, K., and Guan, C.T. (2004). Treatment of Textile Wastewater by Advanced Oxidation Processes – A Review. *Global Nest: the Int. J. 6(3)*, 222-230.

Andonian, K., Hierro, J., Khetsuriani, L., Becerra, P., Janoyan, G., Villarreal, D., Cavieres, L., Fox, L., Callaway, R., and Wright, J. (2011). Range-Expanding Populations of a Globally Introduced Weed Experience Negative Plant-Soil Feedbacks. *PLoS ONE,* E20117.

Aplin, R., and Waite, T.D. (2000). Comparison of three advanced oxidation processes for degradation of textile dyes. *Water Science and Technology 42(5),* 345-354.

Arslan-Alaton, I., Gursoy, B.H., and Schmidt, J-E. (2008). Advanced oxidation of acid and reactive dyes: Effect of Fenton treatment on aerobic, anoxic and anaerobic processes. *Dyes and Pigments 78*, 117-130.

Arslan, I. and Balcioglu, I.S. (2001). Advanced oxidation of raw and biotreated textile industry wastewater with O_3, H_2O_2/UV-C and their sequential application. *Journal of Chemical Technology and Biotechnology 76,* 53-60.

Ashby, M. (2009). Ch. 12 Material Profiles. In *Materials and the environment: Eco-informed material choice*. Amsterdam: Butterworth-Heinemann/Elsevier.

Austoria, A, Lakshmi, C., Srinivas, C., Anand, C., and Mathew, A. (2010). Irritancy Potential of 17 Detergents used commonly by the Indian Household. *Indian Journal of Dermatology, Venereology, and Leprology 76*(3), 249-53.

Basic Overview of ICP-AES. (2000). Ocean Drilling Program: Science Operator Retrieved from http://www-odp.tamu.edu/publications/tnotes/tn29/technot2.htm

Bauer, R., and Fallmann, H. (1997). The Photo-Fenton Oxidation – A Cheap and Efficient Wastewater Treatment Method. *Research on Chemical Intermediates 23(4)*, 341-354.

Bavas, J. (2014, May 28). Carcinogenic 'azo' dyes: Federal Government considers banning chemicals found in some clothing. Retrieved on October 1, 2014 from http://www.abc.net.au/news/2014-05-28/govt-considers-banning-carcinogenic-dyes-more-found-in-clothing/5482040

Behnajady, M.A., Modirshahla, N., and Ghanbary, F. (2007). A kinetic model for the decolorization of C.I. Acid Yellow 23 by Fenton Process. *Journal of Hazardous Materials 148*(1-2), 98-102.

Bilgi, S., and Demir, C. (2005). Identification of photooxidation degradation products of C.I. Reactive Orange 16 dye by gas chromatography-mass spectrometry. *Dyes and Pigments* 66, 69-76.

Bobu, M., Yediler, A., Siminiceanu, I., and Shulte-Hostede, S. (2008). Degradation studies of ciprofloxacin on a pillared iron catalyst. *Applied Catalysis B: Environmental 83(1-2)*, 15-23.

Boyles, W. (1997). The Science of Chemical Oxygen Demand. Technical Information Series Booklet No. 9, Hach Company.

CBI: Ministry of Foreign Affairs of the Netherlands (2012). EU legislation: Azo dyes in textile and leather products. Retrieved on October 1, 2014 from http://www.cbi.eu/system/files/marketintel/2012_eu_legislation_azo_dyes_2_ta_adb_0.pdf

CEM Instruments (2012). Solar Power Meter DT-1307. Retrieved on June 15, 2012 from http://www.cem-instruments.com/en/pro/pro-424.html

Chacon, J.M., Leal, M.T., Sanchez, M., and Bandala, E.R. (2006). Solar photochatalytic degradation of azo-dyes by photo-Fenton process. *Dyes and Pigments 69*, 144-150.

Chamarro, E., Marco, A., and Esplugas, S. (2001). Use of fenton reagent to improve organic chemical biodegradability. *Water Research 35*, 1047-1051.

Chang, S.-H., Chuang, S.-H., Li, H.-C., Liang, H.-H., and Huang, L.-C. (2009). Comparative study on the degradation of I.C. Remazol Brilliant Blue R and I.C. Acid Black 1 by Fenton Oxidation and Fe^0/air process and toxicity evaluation. *Journal of Hazardous Materials 166(2–3),* 1279–1288.

Chapman, P.F. and Roberts, F. (1983). *Metal resources and energy, Butterworth's Monographs in Materials.* London: Butterworths and Co., ISBN 0-408-10801-0.

Chemical Education Digital Library (2014). Bicarbonate Ion HCO3-. Retrieved on October 11, 2014 from http://www.chemeddl.org/alfresco/service/org/chemeddl/ttoc/ttoc_results/?id=20917&num_results=3&guest=true.

Chen, R.W., Navin-Chandra, D., and Prinz, F.B. (1993). Product design for recyclability: a cost/benefit analysis. Proceedings of the *IEEE International Symposium on Electronics and the Environment*, Vol. 10-12, 178-183, ISEE.1993.302813.

Conte, L.O., Farias, J., Albizzati, E.D., and Alfano, O.M. (2012). Photo-Fenton Degradation of the Herbicide 2,4-Dichlorophenoxyacetic Acid in Laboratory and Solar Pilot-Plant Reactors. *Industrial and Engineering Chemistry Research 51*, 4181-4191.

Curtronics (2013). Curt Blank's Milwaukee Weather Report September – October 2013 Archives: Solar Radiation Average per Hour (24 Hours). Retrieved on November 5, 2013 from http://www.curtronics.com/Weather/grSolar.html

Dash, D., Venkateswarlu, G., Thangavel, S., Rao, S.V., and Chaurasia, S.C. (2011). Ultraviolet photolysis assisted mineralization and determination of trace levels of Cr, Cd, Cu, Sn, and Pb in isosulfan blue by ICP-MS. *Microchemical Journal 98*, 312-316.

Datta, R.K., and Nanavaty M., (2005). *Global Silk Industry: A Complete Source Book*. Boca Raton, FL, USA: Universal Publishers. ISBN: 1-58112-493-7

Daud, N.K., Ahmad, M., and Hameed, B.H., (2010). Decolorization of Acid Red 1 dye solution by Fenton-like process using Fe–Montmorillonite K10 catalyst. *Chemical Engineering Journal 165(1),* 111–6.

Daud, N.K., and Hameed, B.H., (2010). Decolorization of Acid Red 1 by Fenton-like process using rice husk ash-based catalyst. *Journal of Hazardous Materials, 176(1-3)*, 938-44.

Dhuale, A.D., and Mahajani, V.V. (1999). Reactive Dye House Wastewater Treatment Use of Hybrid Technology: Membrane, Sonication Followed by Wet Oxidation. *Industrial and Engineering Chemistry Research 38*, 2058-2064.

Duesterberg, C. and Waite, T.D. (2006). Process optimization of Fenton oxidation using kinetic modeling. *Environmental Science and Technology 40* (13), 4189 -4195.

Duesterberg, C.K. and Waite, T.D. (2007). Kinetic modeling of the oxidation of *p*-hydroxybenzoic acid by Fenton's reagent: Implications of the role of quinones in the redox cycling of iron. *Environmental Science and Technology 41*(11), 4103-4110.

Duesterberg, C., Mylon, S.E. and Waite, T.D. (2008). pH effects on iron-catalyzed oxidation using Fenton's reagent. *Environmental Science and Technology 42*, 8522-8527.

Eaton, A.D., Clesceri, L.S., Greenberg, A.E., and Franson, M.A.H. (1995). Inductively Coupled Plasma. In *Standard methods for the examination of water and wastewater* (19th ed., pp. 3-33). New York: American Public Health Association.

Eclectic Products (2012). Shoe GOO Adhesive. Retrieved on September 1, 2012 from http://www.eclecticproducts.com/shoegoo.htm

Entropy Resins (2011). Super Sap CLR MSDS CLF (Fast) Hardener, Version No. 02, revised Sept. 9, 2011. Retrieved on September 1, 2012 from http://www.entropyresins.com/products.

Essential Chemical Industry Online (2013a). Colorants. Retrieved on September 15, 2014 from http://www.essentialchemicalindustry.org/materials-and-applications/colorants.html

Essential Chemical Industry Online (2013b). Surfactants. Retrieved on September 15, 2014 from http://www.essentialchemicalindustry.org/materials-and-applications/surfactants.html

Farias, J., Albizzati, D., and Alfano, O.M. (2010). New Pilot-Plant Photo-Fenton Solar Reactor for Water Decontamination. *Industrial and Engineering Chemistry Research 49*, 1265-1273.

Feng, W., Nansheng, D., and Helin, H. (2000). Degradation mechanism of azo dye C.I. reactive red 2 by iron powder reduction and photooxidation in aqueous solutions. *Chemosphere 41*, 1233-1238.

Fu, F., Wang, Q., and Tang, B. (2010). Effective degradation of C.I. Acid Red 73 by advanced Fenton process. *Journal of Hazardous Materials 174*, 17-22.

Fukushima M., Tatsumi, K., and Nagao, S. (2001). Degradation Characteristics of Humic Acid during Photo-Fenton Processes. *Environmental Science and Technology 35*, 3683-3690.

Ganesan, R., and Thanasekaran, K. (2011). Decolourisation of textile dyeing wastewater by modified solar photo-Fenton oxidation. *International Journal of Environmental Science 1*(6), 1168-1176.

Ganesan, R., Latha, A., and Thanasekaram, K. (2014). Treatment of Textile Dyeing Wastewater by Modified UV Photo-Fenton Process Using a New Composite Steel Scrap / H2O2. *International Journal of Emerging Technology and Advanced Engineering 4*(4), 108-113.

García-Montaño, J., Torrades, F., Perez-Estrada, L.A., Oller, I., Malato, S., Maldonado, M.I., and Peral, J. (2008). Degradation Pathways of the Commercial Reactive Azo Dye Procion Red H-E7B under Solar-Assisted Photo-Fenton Reaction. *Environment Science and Technology 42*, 6663-6670.

Garrigos, M.C., Reche, F., Marin, M.L., and Jimenez, A., 2002. Determination of aromatic amines formed from azo colorants in toy products. *Journal of Chromatography A, 976*, 309-317.

Georgiou, D., Melidis, P., Aivasidis, A., and Gimouhopoulos, K. (2001). Degradation of azo-reactive dyes by ultraviolet radiation in the presence of hydrogen peroxide. *Dyes and Pigments 52*, 69-78.

Guidice, F., La Rosa, G. and Risitano, A. (2001). Optimisation and Cost-Benefit Analysis of Product Recovery Cycles. ICED01 13th International Conference on Engineering Design, Glasgow, Scotland, UK, 629-636.

Guidice, F., La Rosa, G., and Risitano, A. (2006). Product Design for the Environment: *A Life Cycle Approach*. Boca Raton: CRC Press, Taylor and Francis Group. ISBN 0-8493-2722-9.

Gutowska, A., Kaluzna-Czaplinska, and Jozwiak, W.K. (2007). Degradation mechanism of Reactive Orange 113 dye by H_2O_2/Fe^{2+} and ozone in aqueous solution. *Dyes and Pigments 74*, 41-46.

Hai, F.I., Yamamoto, K., and Fukushi, K. (2007). Hybrid Treatment Systems for Dye Wastewater. *Critical Reviews in Environmental Science and Technology 37*, 315-377.

Hasan, R. (2014, May 7). Ministry of Environment and Forests Notification. *The Gazette of India: Extraordinary*. Retrieved on November 1, 2014 from http://www.cpcb.nic.in/Industry-Specific-Standards/Effluent/DyeandDye_Inter_Indus.pdf

He, F., and Lei, L. (2004). Degradation kinetics and mechanisms of phenol in photo-Fenton process. *Journal of Zhejiang University Science 5*(2), 198-205.

Hsing, H.-J., Chiang, P.-C., Chang, E.-E., and Chen, M.-Y., (2007). The decolorization and mineralization of Acid Orange 6 azo dye in aqueous solution by advanced oxidation processes: A comparative study. *Journal of Hazardous Materials 141*, 8-16.

Hsueh, C.L., Huang, Y.H., Wang, C.C., and Chen, C.Y. (2004). Degradation of azo dyes using low iron concentration of Fenton and Fenton-like system. *Chemosphere 58*, 1409-1414.

Huang Y-H., Huang, G-H., Chou, S-S., You, H-S., and Perng, S-H. (2000). Process for Chemically Oxidizing Wastewater with Reduced Sludge Production. United States Patent No. 6,143,182.

Idel-aouad, R., Valiente, M., Yaacoubi, A., Tanouti, B., and Lopez-Mesas, M. (2011). Rapid decolorization and mineralization of azo dye C.I. Acid Red 14 by heterogeneous fenton reaction. *Journal of Hazardous Materials 186*(1), 745-750.

Jozwiak, W.K., Mitros, M., Kaluzna-Czaplinska, J., and Tosik, R. (2007). Oxidative decomposition of Acid Brown 159 dye in aqueous solution by H_2O_2/Fe^{2+} and ozone with GC/MS analysis. *Dyes and Pigments 74*, 9-16.

Kang, S-F., Liao, C-H., and Po, S-T. (2000). Decolorization of textile wastewater by photo-Fenton oxidation technology. *Chemosphere 41*, 1287-1294.

Karadag, D., Tok, S., Akgul, E., Ulucan, K., Evden, H., and Kaya, M.A. (2006). Combining Adsorption and Coagulation for the Treatment of Azo and Anthraquinone Dyes from Aqueous Solution. *Industrial and Engineering Chemistry Research 45*, 3969-3973.

Khataee, A.R., Vatanpour, V., and Amani Ghadim, A.R. (2009). Decolorization of C.I. Acid Blue 9 solution by UV/Nano-TiO_2, Fenton, Fenton-like, electro-Fenton, electrocoagulation: A comparative study. *Journal of Hazardous Materials 161*, 1225-1233.

Kim, T-H., Park, C., Yang, J., and Kim, S. (2004). Comparison of disperse and reactive dye removals by chemical coagulation and Fenton oxidation. *Journal of Hazardous Materials B112*, 95-103.

Kumar, A.M., and Puri, A. (2012). Review of Permissible Limits of Drinking Water. *Indian Journal Occupational Environmental Medicine 16(1)*: 40–44.

Kumar, D., and Ameta, R. (2013). Use of Photo-Fenton reagent for the degradation of Basic Orange 2 in aqueous medium. *Journal of Chemical and Pharmaceutical Research 5*(1), 68-74.

Lin, J-J., Zhao, X-S., Liu, D., Yu, Z-G., Zhange, Y., and Xu, H. (2008). Decolorization and Mineralization of Azo Dye C.I. Acid Red 14 by Sonochemical Process: Rate Improvement via Fenton's Reactions. *Journal of Hazardous Materials 157*, 541-546.

Liu, R., Chiu, H.M., Shiau, C.-S., Yeh, R.Y.-L., and Hung, Y.-T. (2007). Degradation and sludge production of textile dyes by Fenton and photo-Fenton processes. *Dyes and Pigments 73(1)*, 1-6.

Liu, Q.Y., Liu, Y.X., and Lu, X.J. (2012). Combined Photo-Fenton and Biological Oxidation for the Treatment of Aniline Wastewater. *Procedia Environmental Sciences 12(A)*, 341-348.

Lodha, B., and Chaudhari, S. (2007). Optimization of Fenton-biological treatment scheme for the treatment of aqueous dye solutions. *Journal of Hazardous Materials 148*, 459-466.

Lucas, M.S., and Peres, J.A. (2006). Decolorization of the azo dye Reactive Black 5 by Fenton and photo-Fenton oxidation. *Dyes and Pigments 71*, 236-244.

Lucas, M.S., Mosteo, R., Maldonado, M.I., Malato, S., and Peres, J.A. (2009). Solar Photochemical Treatment of Winery Wastewater in a CPC Reactor. *Journal of Agricultural and Food Chemistry 57*, 11242-11248.

Modirshahla, N., Behnajady, M.A., and Ghanbary, F. (2007). Decolorization and mineralization of C.I. Acid Yellow 23 by Fenton and photo-Fenton processes. *Dyes and Pigments 73(3)*, 305-310.

MP Biomedicals (2014). Reactive Blue 4. Retrieved on October 11, 2014 from http://www.mpbio.com/product.php?pid=02152016&country=223

Muruganandham, M., & Swaminathan, M. (2006). Photocatalytic decolourisation and degradation of Reactive Orange 4 by TiO2-UV process. *Dyes and Pigments, 68*, 133-142.

Muthuvel, I., and Swaminatham, M. (2008). Highly solar active Fe (III) immobilized alumina for the degradation of Acid Violet 7. Solar *Energy Materials and Solar Cells 92*, 857-863.

Narde, G.K., Kapley, A., and Purohit, H.J. (2004). Isolation and characterization of Citrobacter strain HPC255 for broad-range substrate specificity for chlorophenols. *Current Microbiology 48(6)*, 419-423.

Neamtu, M., Yediler, A., Siminiceanu, I., and Kettrup, A. (2003). Oxidation of commercial reactive azo dye aqueous solutions by the photo-Fenton and Fenton-like processes. *Journal of Photochemistry and Photobiology A: Chemistry 161*, 87-93.

Oller, I., Malato, S., Sanchez-Perez, J.A., Maldonado, M.I., Gernjak, W., Perez-Estrada, L.A., Munoz, J.A., Ramos, C., and Pulgarin, C. (2007). Pre-industrial-scale Combined Solar Photo-Fenton and Immobilized Biomass Activated-Sludge Biotreatment. *Industrial and Engineering Chemistry Research 46*, 7467-7475.

Papic, S., Vujevic, D., Koprivanac, N., and Sinko, D. (2009). Decolourization and mineralization of commercial reactive dyes by using homogeneous and heterogeneous Fenton and UV/Fenton processes. *Journal of Hazardous Materials 164*, 1137-1145.

Paul, S., Chaven, S., and Khambe, S. (2012). Studies on Characterization of Textile Industrial Waste Water in Solapur City. *International Journal of Chemical Sciences, 10*(2), 635-642.

Pielesz, A., Baranowska, I., Rybak, A., and Wlochowicz, A. (2002). Detection and Determination of Aromatic Amines as Products of Reductive Splitting from Selected Azo Dyes. *Ecotoxicology and Environmental Safety 53*(1), 42-47.

Pinheiro, H.M., Touraud, E., and Thomas, O. (2004). Aromatic amines from azo dye reduction: status review with emphasis on direct UV spectrophotometric detection in textile industry wastewaters. *Dyes and Pigments 61*, 121-139.

Puntener, A., and Page, C. (2004). European Ban on Certain Azo Dyes. Retrieved on October 11, 2014 from http://www.tfl.com/web/files/eubanazodyes.pdf

Rodriguez, M., Sarria, V., Esplgas, S., and Pulgarin, C. (2002). Photo-Fenton treatment of a biorecalcitrant wastewater generated in textile activities: biodegradability of the photo-treated solution. *Journal of Photochemistry A 151*, 129-135.

Ruppert, G., Bauer, R., and Heisler, G. (1992). The photo-Fenton reaction – an effective photochemical wastewater treatment process. *Journal of Photochemistry and Photobiology A: Chemistry 73,* 75-78.

Sahunin, C., Kaewboran, J., and Hunsom, M., (2004). Treatment of Textile Dyeing Wastewater by Photo Oxidation using UV/H_2O_2/Fe^{2+} Reagents. *Science Asia 32*, 181-186.

Santa Cruz Biotechnology (2014). Reactive Red 120. Retrieved on October 11, 2014 from http://www.scbt.com/datasheet-215799-reactive-red-120.html

dos Santos, A.B., Cervantes, F.J., and van Lier, J.B. (2007). Review paper on current technologies for decolourisation of textile wastewaters: Perspectives for anaerobic biotechnology. *Bioresource Technology 98*, 2369-2385.

Sengupta, B., Verma, N., Basu, D., Ansari, P., Kumar, P., Thirumurthy, G. Sharma, A., and H.V., G. (2008). Status of Water Treatment Plants in India. Retrieved on November 1, 2014 from http://www.cpcb.nic.in/upload/NewItems/NewItem_103_statusofwaterqualitypackage.pdf

Sigma-Aldrich (2014a). Anthraquinone. Retrieved on October 11, 2014 from http://www.sigmaaldrich.com/catalog/product/aldrich/a90004?lang=en&region=US

Sigma Aldrich (2014b). Triphenylmethane. Retrieved on October 11, 2014 from http://www.sigmaaldrich.com/catalog/product/aldrich/101303?lang=en&region=US

Skoog, D., and Holler, F. (2007). Principles of instrumental analysis (6th ed., pp. 254-259, 608-613). Belmont, CA: Thomson Brooks/Cole.

Sun, J.-H., Sun, S.-P., Wang, G.-L., and Qiao, L.-P. (2007). Degradation of azo dye Amido black 10B in aqueous solution by Fenton oxidation process. *Dyes and Pigments 74*, 647-652.

Sun, S.-P., Li, C.-J., Sun, J.-H., Shi, S.-H., Fan, M.-H., and Zhou, Q. (2009). Decolorization of an azo dye Orange G in aqueous solution by Fenton oxidation process: Effect of system parameters and kinetic study. *Journal of Hazardous Materials 161*, 1052-1057.

Tantak, N.P., and Chaudhari, S. (2006). Degradation of azo dyes by sequential Fenton's oxidation and aerobit biological treatment. *Journal of Hazardous Materials B 136*, 698-705.

Uddin, K., and Hossain, S. (2010). A Comparative Study on Silk Dyeing with Acid Dye and Reactive Dye. *International Journal of Engineering and Technology 10*(6), 22-27.

Vermilyea, A.W., and Voelker, B.M. (2009). Photo-Fenton Reaction in Near Neutral pH. *Environmental Science and Technology 43*, 6927-6933.

World Dye Variety (2012, May 8). Reactive Yellow 81. Retrieved on October 11, 2014 from http://www.worlddyevariety.com/reactive-dyes/reactive-yellow-81.html

Zhang, H., Zhang, J., Zhang, C., Liu, F., and Zhang, D. (2009). Degradation of C.I. Acid Orange 7 by Advanced Fenton Processes in Combination with Ultrasonic Irradiation. *Ultrasonics Sonochemistry 16*, 325-330.

Zheng, H., Pan, Y., and Xiang, X. (2007). Oxidation of acidic dye Eosin Y by the solar photo-Fenton processes. *Journal of Hazardous Materials 141*(3), 457-64.

Appendix A – UV-visible Spectrometry

This appendix contains data of the UV-visible tests. The data is presented as figures of the UV-visible spectra of the dye controls C1-C5 (Figures A.1-A.9), and tables of the peak heights found in the figures for the control samples C1-C5 for Reactive Red 120 (Table A.1), Reactive Yellow 81 (Table A.3), Reactive Blue 4 (Table A.5), Acid Fast Red (Table A.7), Acid Golden Yellow (Table A.9), Acid Ananda Blue (Table A.11), Acid Fast Red with Soap and Soda (Table A.13), Acid Golden Yellow with Soap and Soda (Table A.15), Acid Ananda Blue with Soap and Soda (Table A.17). This appendix also contains tables of the peak heights found in the control samples for all oxidized and filtered samples for Reactive Red 120 (Table A.2), Reactive Yellow 81 (Table A.4), and Reactive Blue 4 (Table A.6) samples R1H-R6H, R1M-R6M, and R1L-R6L; Acid Fast Red (Table A.8), Acid Golden Yellow (Table A.10), and Acid Ananda Blue (Table A.12) samples A1-A12; Acid Fast Red with Soap and Soda (Table A.14), Acid Golden Yellow with Soap and Soda (Table A.16), and Acid Ananda Blue with Soap and Soda (Table A.18) samples S1-S6.

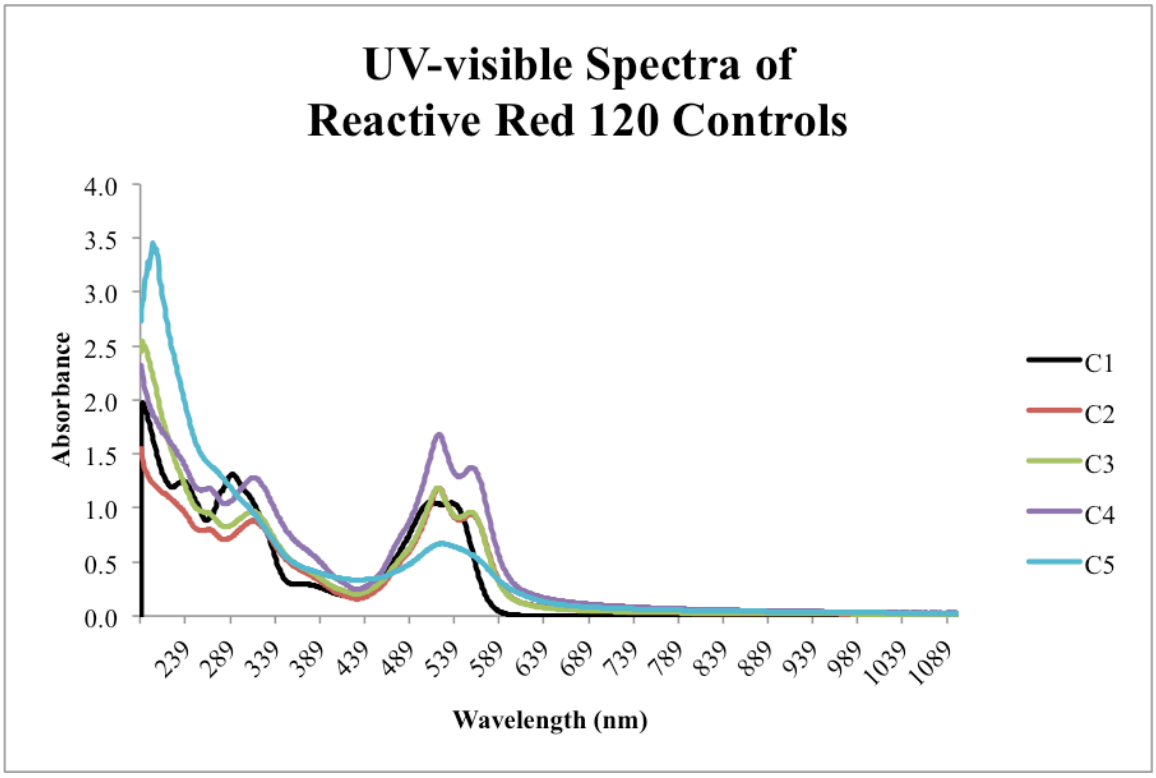

Figure A.1: UV-visible absorption spectra comparing 5g/l Reactive Red 120 dye C1 (black), C2 (red), C3 (green), C4 (purple), and C5 (teal).

Table A.1: UV-visible absorption spectra data calculated control peaks of Reactive Red 120 C1-C5.

	Reactive Red 120 None Control C1	**Reactive Red 120 HCl t_0 Control C2**	**Reactive Red 120 H2O2 t_0 Control C3**	**Reactive Red 120 HCl t_F Control C4**	**Reactive Red 120 H2O2 t_F Control C5**
Wavelength (nm)	**Absorbance (AU)**	**Absorbance (AU)**	**Absorbance (AU)**	**Absorbance (AU)**	**Absorbance (AU)**
206	153	121	214	183	169
237	125	97.8	125	143	103
291	131	73.1	84.0	107	59.2
371	29.6	41.4	44.6	63.6	22.5
512	105	101	104	144	31.3
536	105	96.2	96.6	139	32.7

Table A.2: UV-visible absorption spectra data points comparing peaks of degradation of 5g/l Reactive Red 120 dye samples for R1H-R6H, R1M-R6M, and R1L-R6L. Black values are comparison of peaks found in C1, and red values are those extra peaks found on the spectra after acid or peroxide were added (C2-C5).

Dye	Oxidation Time	Peak Wavelength (nm)	Average Absorbance (AU) of USA Samples using High Iron	Average Absorbance (AU) of USA Samples using Medium Iron	Average Absorbance (AU) of USA Samples using Low Iron
Reactive Red 120	R1	206	3.91	2.95	4.00
		237	3.02	1.66	4.00
		291	2.48	0.771	3.90
		371	2.12	0.752	3.66
		512	0.960	0.671	1.92
		536	0.923	0.655	1.84
Reactive Red 120	R2	206	3.24	0.327	0.691
		237	1.02	0.045	0.102
		291	0.038	0.022	0.038
		371	0.005	0.007	0.018
		512	0.003	0.006	0.010
		536	0.003	0.007	0.010
Reactive Red 120	R3	206	1.24	1.13	1.72
		237	0.137	0.044	0.327
		291	0.017	0.015	0.064
		371	0.002	0.006	0.017
		512	0.001	0.007	0.004
		536	0.001	0.007	0.003
Reactive Red 120	R4	206	3.96	3.58	3.78
		237	4.00	3.89	3.64
		291	3.63	2.66	3.36
		371	2.79	1.09	1.63
		512	0.772	0.382	0.468
		536	0.731	0.350	0.439
Reactive Red 120	R5	206	3.51	3.37	3.76
		237	3.51	3.50	3.75
		291	0.432	0.272	1.07
		371	0.037	0.038	0.719
		512	0.010	0.012	0.542
		536	0.010	0.011	0.518
Reactive Red 120	R6	206	3.06	2.86	3.34
		237	0.715	0.548	2.24
		291	0.260	0.092	1.83
		371	0.057	0.025	1.19
		512	0.020	0.010	0.572
		536	0.019	0.009	0.571

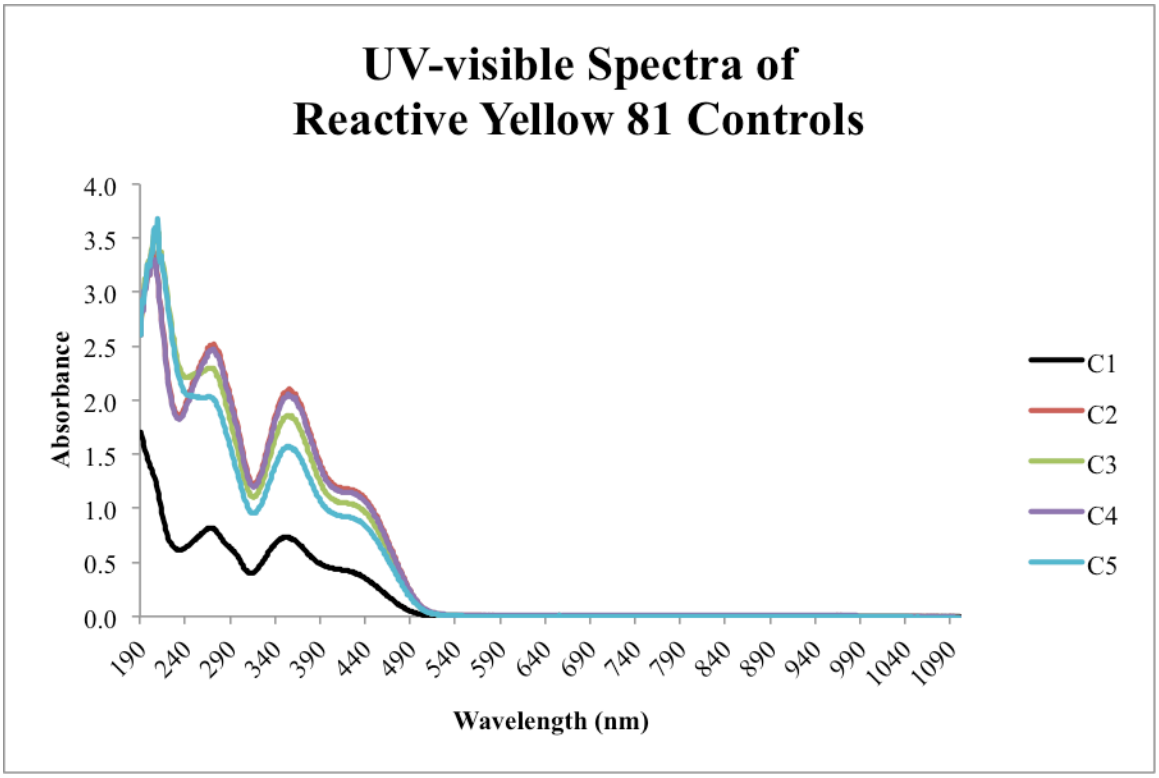

Figure A.2: UV-visible absorption spectra comparing the 5g/l Reactive Yellow 81 dye control samples at C1 t_0 with no added chemicals (black), C2 t_0 acidified to pH 2.5 (red), C3 t_0 acidified with added Hydrogen peroxide (green), C4 t_F acidified (purple), and C5 t_F acidified with hydrogen peroxide but no iron (teal).

Table A.3: UV-visible absorption spectra data points comparing peaks of 5g/l Reactive Yellow 81 dye control samples at t_0 with no added chemicals (black), with peaks of all other control samples (red) t_0 acidified to pH 2.5, t_0 acidified with added hydrogen peroxide, t_F acidified, and t_F acidified with hydrogen peroxide but no iron.

	Reactive Yellow 81 None Control (C1)	**Reactive Yellow 81 HCl t_0 Control (C2)**	**Reactive Yellow 81 H2O2 t_0 Control (C3)**	**Reactive Yellow 81 HCl t_F Control (C4)**	**Reactive Yellow 81 H2O2 t_F Control (C5)**
Wavelength (nm)	**Absorbance (AU)**	**Absorbance (AU)**	**Absorbance (AU)**	**Absorbance (AU)**	**Absorbance (AU)**
206	128	110	116	110	120
229	62.8	62.9	81.5	61.9	78.9
243	65.3	67.3	73.7	66.2	68.3
268	81.8	83.4	76.6	81.9	67.7
352	73.3	69.3	61.8	67.7	52.0
410	43.6	39.7	35.3	38.7	31.1
520	0.482	0.742	0.601	0.827	0.588

Table A.4: UV-visible absorption spectra data points comparing peaks of degradation of 5g/l Reactive Yellow 81 dye samples for R1H-R6H, R1M-R6M, and R1L-R6L. Black values are comparison of peaks found in C1, and red values are those extra peaks found on the spectra after acid or peroxide were added (C2-C5).

Dye	Oxidation Time	Peak Wavelength (nm)	Average Absorbance (AU) of USA Samples using High Iron	Average Absorbance (AU) of USA Samples using Medium Iron	Average Absorbance (AU) of USA Samples using Low Iron
Reactive Yellow 81	R1	206	4.00	4.00	3.90
		229	4.00	3.90	3.81
		243	4.00	3.21	3.69
		268	4.00	2.90	3.75
		352	3.86	2.36	3.32
		410	4.00	1.89	1.46
		520	3.33	1.40	0.515
Reactive Yellow 81	R2	206	3.56	1.89	2.47
		229	3.40	0.621	0.551
		243	2.21	0.300	0.255
		268	0.640	0.138	0.138
		352	0.029	0.016	0.013
		410	0.014	0.009	0.005
		520	0.011	0.010	0.002
Reactive Yellow 81	R3	206	2.06	0.771	1.32
		229	0.535	0.132	0.380
		243	0.261	0.048	0.152
		268	0.138	0.034	0.086
		352	0.018	0.008	0.010
		410	0.011	0.004	0.003
		520	0.009	0.007	0.000
Reactive Yellow 81	R4	206	4.00	3.45	3.60
		229	4.00	3.64	3.67
		243	4.00	3.47	3.37
		268	4.00	3.36	3.36
		352	3.44	0.398	0.572
		410	3.45	0.073	0.116
		520	2.73	0.022	0.028
Reactive Yellow 81	R5	206	3.58	3.79	3.54
		229	3.54	3.90	3.65
		243	2.98	3.90	3.07
		268	1.28	3.81	1.82
		352	0.072	2.33	0.197
		410	0.025	1.42	0.087
		520	0.013	1.61	0.043
Reactive Yellow 81	R6	206	3.13	3.92	2.34
		229	1.24	3.54	0.668
		243	0.465	3.17	0.327
		268	0.268	2.96	0.233
		352	0.041	1.49	0.026
		410	0.018	0.873	0.015
		520	0.013	1.22	0.010

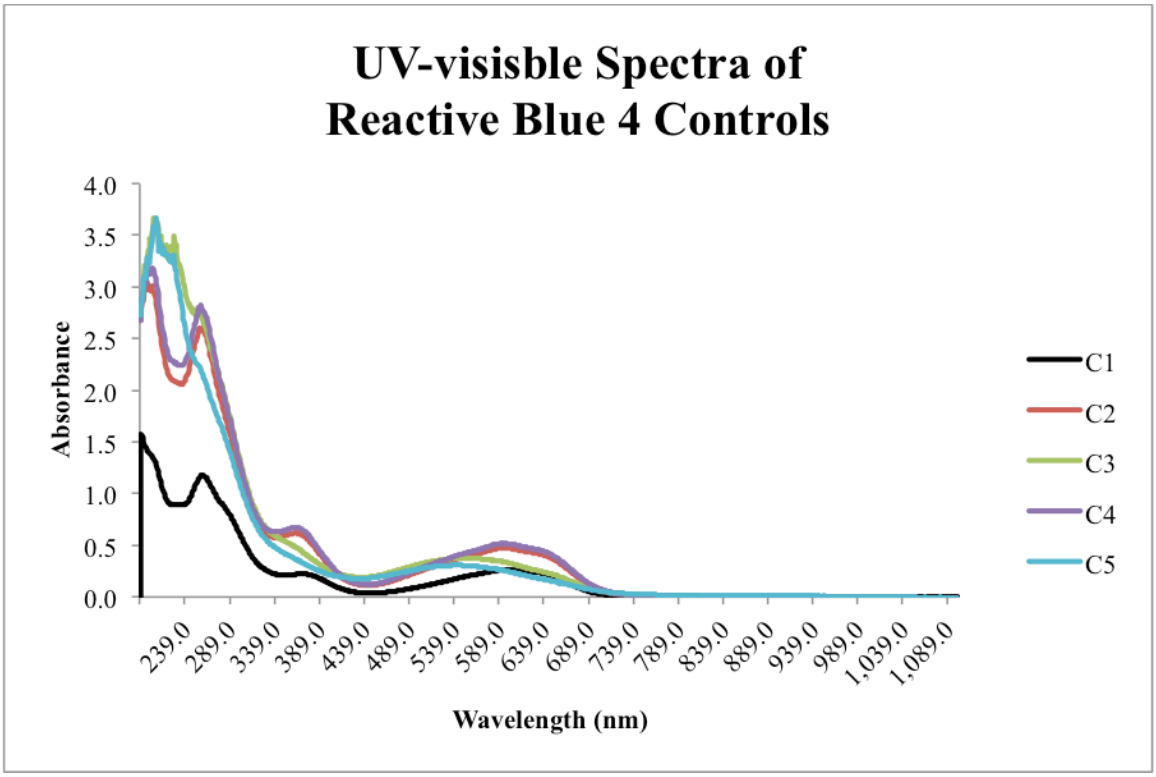

Figure A.3: UV-visible absorption spectra comparing 5g/l Reactive Blue 4 dye control samples at t_0 with no added chemicals (black), t_0 acidified to pH 2.5 (red), t_0 acidified with added Hydrogen peroxide (green), t_F acidified (purple), and t_F acidified with hydrogen peroxide but no iron (teal).

Table A.5: UV-visible absorption spectra data points comparing peaks of 5g/l Reactive Blue 4 dye control samples at t_0 with no added chemicals (black), with peaks of all other control samples (red) t_0 acidified to pH 2.5, t_0 acidified with added Hydrogen peroxide, t_F acidified, and t_F acidified with hydrogen peroxide but no iron.

	Reactive Blue 4 None Control (C1)	**Reactive Blue 4 HCl t_0 Control (C2)**	**Reactive Blue 4 H_2O_2 t_0 Control (C3)**	**Reactive Blue 4 HCl t_F Control (C4)**	**Reactive Blue 4 H_2O_2 t_F Control (C5)**
Wavelength (nm)	**Absorbance (AU)**	**Absorbance (AU)**	**Absorbance (AU)**	**Absorbance (AU)**	**Absorbance (AU)**
206	130	146	119	156	89.1
230	89.2	104	113	113	78.8
253	113	125	91.8	136	56.5
258	118	129	91.6	141	54.8
369	22.4	30.4	15.0	33.0	8.48
520	13.4	15.2	11.7	16.6	7.41
597	26.3	23.7	11.2	25.9	6.32

Table A.6: UV-visible absorption spectra data points comparing peaks of degradation of 5g/l Reactive Blue 4 dye samples for R1H-R6H, R1M-R6M, and R1L-R6L. Black values are comparison of peaks found in C1, and red values are those extra peaks found on the spectra after acid or peroxide were added (C2-C5).

Dye	Oxidation Time	Peak Wavelength (nm)	Average Absorbance (AU) of USA Samples using High Iron	Average Absorbance (AU) of USA Samples using Medium Iron	Average Absorbance (AU) of USA Samples using Low Iron
Reactive Blue 4	R1	206	3.78	4.00	3.67
		230	3.68	4.00	3.74
		258	2.65	3.97	3.53
		369	0.376	2.16	1.92
		520	0.055	1.31	0.198
		597	0.043	1.17	0.181
Reactive Blue 4	R2	206	0.885	3.53	3.419
		230	0.204	3.09	2.41
		258	0.074	1.57	1.17
		369	0.002	0.022	0.014
		520	0.002	0.012	0.001
		597	0.002	0.010	0.000
Reactive Blue 4	R3	206	1.28	1.95	1.76
		230	0.157	0.484	0.502
		258	0.033	0.197	0.181
		369	0.001	0.014	0.010
		520	0.002	0.009	0.003
		597	0.002	0.007	0.002
Reactive Blue 4	R4	206	3.78	3.73	3.82
		230	3.87	3.71	3.72
		258	3.52	3.31	2.71
		369	0.738	0.310	1.22
		520	0.141	0.132	0.851
		597	0.136	0.114	0.587
Reactive Blue 4	R5	206	3.626	3.99	3.96
		230	3.74	3.96	3.68
		258	3.16	3.6164	3.58
		369	0.369	3.4614	3.08
		520	0.088	2.1336	3.24
		597	0.061	0.7693	1.37
Reactive Blue 4	R6	206	3.47	3.9495	3.80
		230	2.04	3.8645	3.68
		258	1.35	3.4828	3.54
		369	0.220	3.0140	2.29
		520	0.067	1.6701	2.07
		597	0.056	0.5550	0.584

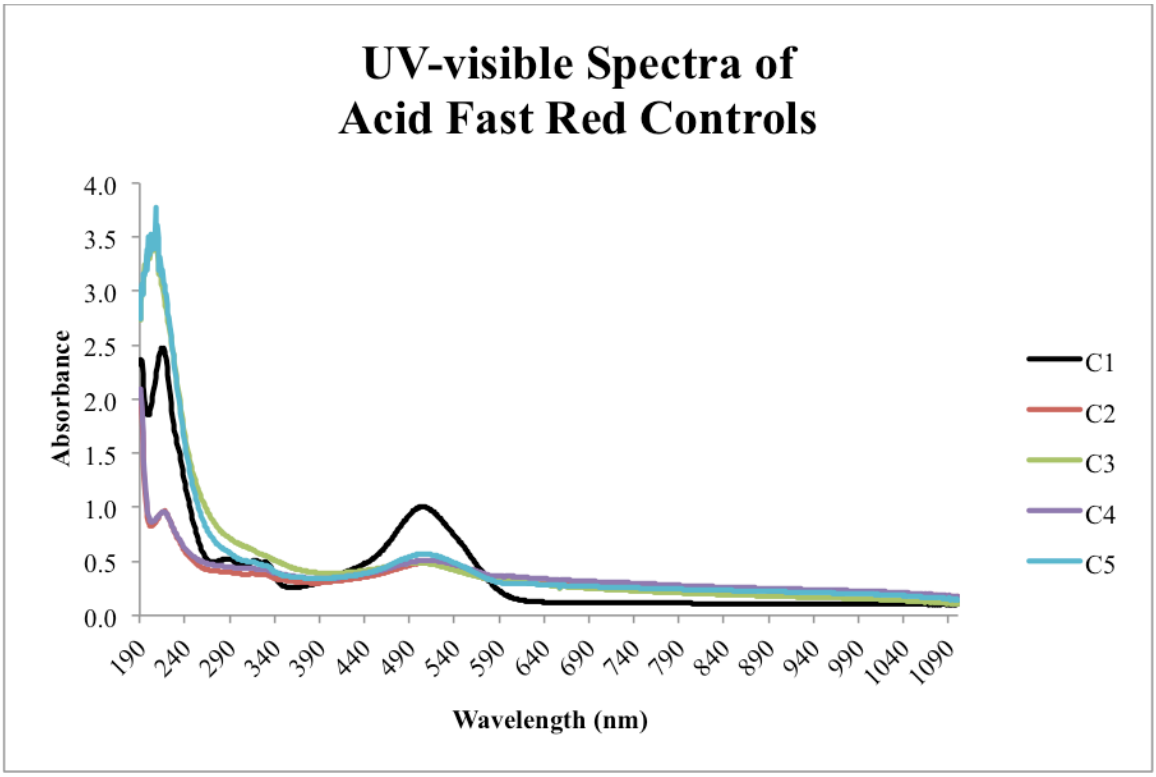

Figure A.4: UV-visible absorption spectra comparing 5g/l Acid Fast Red dye control samples at t_0 with no added chemicals (black), t_0 acidified to pH 2.5 (red), t_0 acidified with added Hydrogen peroxide (green), t_F acidified (purple), and t_F acidified with hydrogen peroxide but no iron (teal).

Table A.7: UV-visible absorption spectra data points comparing peaks of 5g/l Acid Fast Red control samples at t_0 with no added chemicals (black), with peaks of all other control samples (red) t_0 acidified to pH 2.5, t_0 acidified with added Hydrogen peroxide, t_F acidified, and t_F acidified with hydrogen peroxide but no iron.

	Acid Fast Red None Control	Acid Fast Red HCl t0 Control	Acid Fast Red H2O2 t0 Control	Acid Fast Red HCl tF Control	Acid Fast Red H2O2 tF Control
Wavelength (nm)	Absorbance (AU)	Absorbance (AU)	Absorbance (AU)	Absorbance (AU)	Absorbance (AU)
206	53.39075	21.275175	86.431	21.935725	84.7995
214	61.754	23.812325	76.49525	23.7432	78.5935
289	13.136425	10.0579	17.968125	11.278125	14.5625
318	12.677275	9.609525	14.842525	10.782775	12.2537
330	12.319125	9.45245	13.79615	10.613625	11.56955
505	25.184	12.204825	12.141875	12.7349	14.242475
610	3.7307	7.656825	7.9392	8.9838	7.4279

Table A.8: UV-visible absorption spectra data points comparing peaks of degradation of 5g/l Acid Fast Red dye samples (A) for Control Sample C1, (B) for A1-A12. Black values are comparison of peaks found in C1, and red values are those extra peaks found on the spectra after acid or peroxide were added (C2-C5).

A

Dye	Oxidation Time	Peak Wavelength	Absorbance (AU)	Dilution Factor	Actual No.
Acid Fast Red	Control	206	2.14	24	51.3
		214	2.47	24	59.2
		289	0.525	24	12.6
		318	0.507	24	12.2
		330	0.493	24	11.8
		505	1.01	24	24.2
		610	0.149	24	3.58

B

Dye	Oxidation Time	Peak Wavelength	Average Absorbance (AU) or USA	Absorbance (AU) or USA1 Sample	Absorbance of USA2 Sample
Acid Fast Red	A1	206	3.86	3.72	4.00
		214	3.51	3.51	3.52
		289	1.74	1.69	1.80
		318	1.33	1.27	1.38
		330	1.19	1.13	1.24
		505	0.757	0.713	0.803
		610	0.311	0.284	0.339
Acid Fast Red	A2	206	2.47	2.35	2.59
		214	0.790	0.566	1.01
		289	0.052	0.030	0.075
		318	0.039	0.018	0.061
		330	0.039	0.017	0.060
		505	0.031	0.011	0.050
		610	0.025	0.007	0.043
Acid Fast Red	A3	206	2.27	1.65	2.88
		214	1.41	1.17	1.66
		289	0.092	0.043	0.142
		318	0.059	0.029	0.090
		330	0.051	0.027	0.076
		505	0.015	0.005	0.025
		610	0.007	0.000	0.015
Acid Fast Red	A4	206	4.00	4.00	4.00
		214	4.00	4.00	4.00
		289	3.95	3.90	4.00
		318	3.02	2.90	3.15
		330	2.74	2.64	2.84
		505	2.00	1.99	2.02
		610	1.90	1.85	1.94
Acid Fast Red	A5	206	3.19	3.21	3.18
		214	2.60	2.58	2.61
		289	0.191	0.180	0.203
		318	0.133	0.126	0.140
		330	0.143	0.135	0.152
		505	0.021	0.027	0.014
		610	0.012	0.019	0.005
Acid Fast Red	A6	206	3.23	3.24	3.23
		214	2.72	2.72	2.72
		289	0.200	0.195	0.205
		318	0.103	0.102	0.105
		330	0.089	0.088	0.091
		505	0.004	0.005	0.003

		610	0.000	0.000	0.000
Acid Fast Red	A7	206	4.00	4.00	4.00
		214	4.00	4.00	4.00
		289	2.97	2.56	3.37
		318	2.24	1.87	2.61
		330	2.06	1.70	2.41
		505	1.50	1.07	1.94
		610	1.42	1.02	1.81
Acid Fast Red	A8	206	3.50	3.50	3.50
		214	3.32	3.34	3.31
		289	1.16	1.16	1.16
		318	0.924	0.930	0.919
		330	0.925	0.935	0.914
		505	0.045	0.048	0.042
		610	0.007	0.010	0.004
Acid Fast Red	A9	206	3.47	3.45	3.49
		214	3.16	3.16	3.15
		289	0.570	0.563	0.576
		318	0.402	0.400	0.405
		330	0.378	0.377	0.380
		505	0.013	0.013	0.013
		610	0.000	0.000	0.000
Acid Fast Red	A10	206	4.00	4.00	4.00
		214	3.92	4.00	3.84
		289	2.15	2.33	1.97
		318	1.72	1.97	1.47
		330	1.62	1.88	1.35
		505	1.41	1.78	1.04
		610	1.30	1.67	0.934
Acid Fast Red	A11	206	3.60	3.51	3.68
		214	3.40	3.46	3.34
		289	1.74	1.83	1.64
		318	1.30	1.38	1.22
		330	1.23	1.30	1.15
		505	0.081	0.108	0.054
		610	0.027	0.047	0.007
Acid Fast Red	A12	206	3.58	3.53	3.64
		214	3.28	3.28	3.29
		289	0.920	0.923	0.918
		318	0.635	0.639	0.631
		330	0.568	0.572	0.564
		505	0.026	0.027	0.025
		610	0.005	0.005	0.004

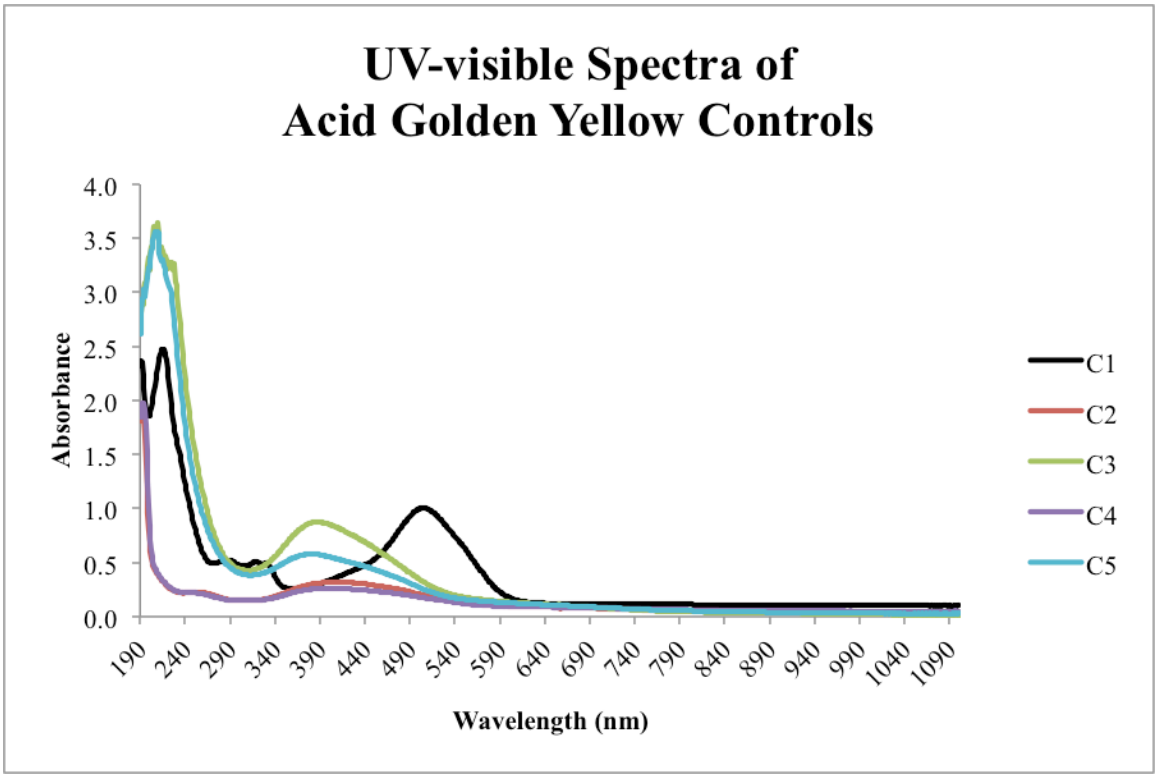

Figure A.5: UV-visible absorption spectra comparing 5g/l Acid Golden Yellow dye control samples at t_0 with no added chemicals (black), t_0 acidified to pH 2.5 (red), t_0 acidified with added Hydrogen peroxide (green), t_F acidified (purple), and t_F acidified with hydrogen peroxide but no iron (teal).

Table A.9: UV-visible absorption spectra data points comparing peaks of 5g/l Acid Golden Yellow dye control samples at t_0 with no added chemicals (black), with peaks of all other control samples (red) t_0 acidified to pH 2.5, t_0 acidified with added Hydrogen peroxide, t_F acidified, and t_F acidified with hydrogen peroxide but no iron.

	Acid Golden Yellow None Control	Acid Golden Yellow HCl t0 Control	Acid Golden Yellow H2O2 t0 Control	Acid Golden Yellow HCl tF Control	Acid Golden Yellow H2O2 tF Control
Wavelength (nm)	Absorbance (AU)	Absorbance (AU)	Absorbance (AU)	Absorbance (AU)	Absorbance (AU)
203	49.4975	4.155742097	28.70076859	2.76756	42.5375
255	17.204525	1.877274906	10.97614427	1.081265	13.3165
350	6.732375	1.816802325	5.477730882	0.996935	6.2418
399	8.287	2.634661276	7.120823489	1.314875	6.9481375

Table A.10: UV-visible absorption spectra data points comparing peaks of degradation of 5g/l Acid Golden Yellow dye samples (A) for Control Sample C1, (B) for A1-A12. Black values are comparison of peaks found in C1, and red values are those extra peaks found on the spectra after acid or peroxide were added (C2-C5).

A

Dye	Oxidation Time	Peak Wavelength	Absorbance (AU)	Dilution Factor	Actual No.
Acid Golden Yellow	Control	203	1.34	7.33	9.82
		255	0.688	7.33	5.04
		350	0.747	7.33	5.48
		399	1.20	7.33	8.81

B

Dye	Oxidation Time	Peak Wavelength	Average Absorbance (AU) or USA	Absorbance (AU) or USA1 Sample	Absorbance of USA2 Sample
Acid Golden Yellow	A1	203	3.13	3.91	2.34
		255	1.46	2.57	0.339
		350	1.10	1.83	0.380
		399	0.960	1.59	0.328
Acid Golden Yellow	A2	203	2.70	2.65	2.75
		255	0.058	0.053	0.063
		350	0.018	0.017	0.018
		399	0.011	0.012	0.011
Acid Golden Yellow	A3	203	3.03	3.01	3.06
		255	0.307	0.273	0.342
		350	0.042	0.030	0.053
		399	0.022	0.014	0.031
Acid Golden Yellow	A4	203	3.71	3.68	3.74
		255	1.80	1.80	1.81
		350	1.26	1.25	1.26
		399	1.09	1.11	1.07
Acid Golden Yellow	A5	203	3.06	3.00	3.12
		255	0.321	0.195	0.448
		350	0.068	0.079	0.058
		399	0.038	0.047	0.028
Acid Golden Yellow	A6	203	3.15	3.17	3.12
		255	0.373	0.475	0.272
		350	0.095	0.061	0.129
		399	0.054	0.028	0.080
Acid Golden Yellow	A7	203	3.84	3.69	4.00
		255	2.25	1.86	2.64
		350	1.31	0.899	1.73
		399	1.05	0.675	1.42
Acid Golden Yellow	A8	203	3.33	3.28	3.37
		255	1.06	0.756	1.36
		350	0.455	0.312	0.598
		399	0.181	0.122	0.241
Acid Golden Yellow	A9	203	3.24	3.19	3.29
		255	0.659	0.534	0.784
		350	0.194	0.143	0.245
		399	0.078	0.060	0.096
Acid Golden Yellow	A10	203	3.67	3.65	3.69
		255	2.89	2.35	3.44
		350	1.01	0.840	1.17
		399	0.605	0.521	0.689
Acid Golden Yellow	A11	203	3.38	3.36	3.39
		255	2.15	1.85	2.44
		350	0.829	0.730	0.927
		399	0.351	0.311	0.391

Acid Golden Yellow	A12	203	3.40	3.36	3.43
		255	1.25	1.04	1.45
		350	0.376	0.309	0.443
		399	0.153	0.126	0.180

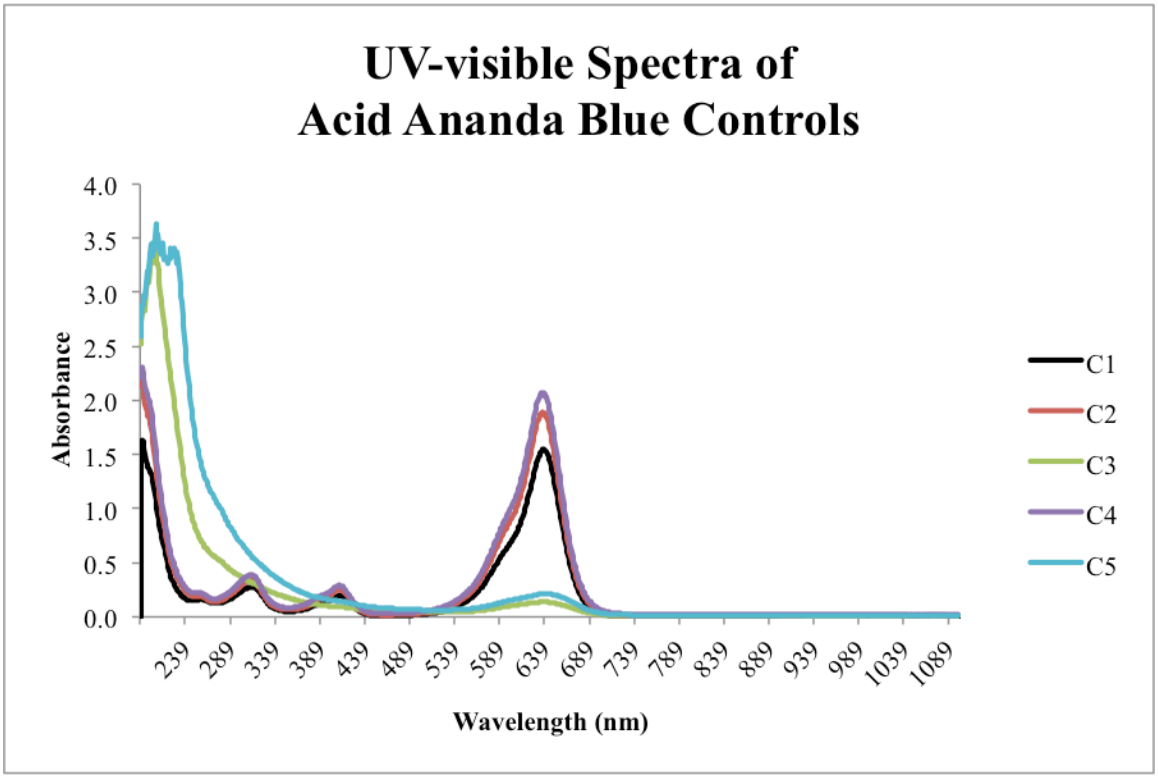

Figure A.6: UV-visible absorption spectra comparing 5g/l Acid Ananda Blue dye control samples at t_0 with no added chemicals (black), t_0 acidified to pH 2.5 (red), t_0 acidified with added Hydrogen peroxide (green), t_F acidified (purple), and t_F acidified with hydrogen peroxide but no iron (teal).

Table A.11: UV-visible absorption spectra data points comparing peaks of 5g/l Acid Ananda Blue dye control samples at t_0 with no added chemicals (black), with peaks of all other control samples (red) t_0 acidified to pH 2.5, t_0 acidified with added Hydrogen peroxide, t_F acidified, and t_F acidified with hydrogen peroxide but no iron.

	Acid Ananda Blue None Control	Acid Ananda Blue HCl t_0 Control	Acid Ananda Blue H2O2 t_0 Control	Acid Ananda Blue HCl t_F Control	Acid Ananda Blue H2O2 t_F Control
Wavelength (nm)	Absorbance (AU)	Absorbance (AU)	Absorbance (AU)	Absorbance (AU)	Absorbance (AU)
206	107.131	145.874	85.02475	160.776	29.10516908
257	16.0487	18.9651	17.7787	22.0543	11.88244135
313	27.7985	34.0536	7.9489	38.7566	4.729285821
340	7.14E+00	9.13E+00	5.395175	11.3492	3.05912763
411	19.7316	25.2292	2.34E+00	28.985	1.210043263
637	154.666	188.679	3.42955	207.468	1.762312838

Table A.12: UV-visible absorption spectra data points comparing peaks of degradation of 5g/l Acid Ananda Blue dye samples (A) for Control Sample C1, (B) for A1-A12. Black values are comparison of peaks found in C1, and red values are those extra peaks found on the spectra after acid or peroxide were added (C2-C5).

A

Dye	Oxidation Time	Peak Wavelength (nm)	Absorbance (AU)	Dilution Factor	Actual No.
Acid Ananda Blue	Control	206	1.07	99	106
		257	0.160	99	15.9
		313	0.278	99	27.5
		340	0.71	99	7.07
		411	0.197	99	19.5
		637	1.55	99	153

B

Dye	Oxidation Time	Peak Wavelength (nm)	Average Absorbance (AU) of USA Samples	Absorbance (AU) of USA1 Sample	Absorbance (AU) of USA2 Sample
Acid Ananda Blue	A1	206	3.75	3.56	3.94
		257	3.32	3.29	3.35
		313	3.11	2.71	3.52
		340	2.12	1.70	2.54
		411	0.465	0.340	0.591
		637	0.167	0.076	0.258
Acid Ananda Blue	A2	206	2.91	2.88	2.95
		257	0.109	0.096	0.123
		313	0.0345	0.030	0.040
		340	0.033	0.027	0.040
		411	0.016	0.014	0.017
		637	0.007	0.006	0.009
Acid Ananda Blue	A3	206	3.28	3.29	3.26
		257	0.529	0.561	0.496
		313	0.134	0.164	0.104
		340	0.083	0.109	0.057
		411	0.037	0.057	0.018
		637	0.014	0.022	0.005
Acid Ananda Blue	A4	206	3.55	3.50	3.59
		257	3.27	3.25	3.29
		313	2.47	2.61	2.33
		340	1.31	1.38	1.24
		411	0.178	0.182	0.175
		637	0.012	0.009	0.015
Acid Ananda Blue	A5	206	3.214	3.21	3.21
		257	0.414	0.375	0.453
		313	0.173	0.151	0.196
		340	0.189	0.170	0.208
		411	0.053	0.049	0.058
		637	0.002	0.004	0.000
Acid Ananda Blue	A6	206	3.20	3.22	3.19
		257	0.406	0.392	0.421
		313	0.118	0.111	0.124
		340	0.092	0.087	0.097
		411	0.023	0.023	0.023
		637	0.000	0.000	0.000
Acid Ananda Blue	A7	206	3.52	3.56	3.48
		257	3.33	3.29	3.36
		313	2.12	2.01	2.23
		340	1.17	1.13	1.21
		411	0.183	0.183	0.182
		637	0.023	0.025	0.021

Acid Ananda Blue	A8	206	3.51	3.51	3.51
		257	1.49	1.53	1.46
		313	0.725	0.753	0.697
		340	0.690	0.724	0.656
		411	0.222	0.224	0.220
		637	0.011	0.000	0.022
Acid Ananda Blue	A9	206	3.42	3.44	3.41
		257	0.846	0.862	0.830
		313	0.351	0.356	0.346
		340	0.295	0.302	0.289
		411	0.086	0.088	0.083
		637	0.000	0.000	0.000
Acid Ananda Blue	A10	206	3.68	3.70	3.66
		257	3.37	3.40	3.33
		313	2.76	2.77	2.76
		340	1.65	1.67	1.63
		411	0.439	0.451	0.428
		637	0.428	0.446	0.411
Acid Ananda Blue	A11	206	3.57	3.51	3.62
		257	2.112	2.13	2.09
		313	1.03	1.03	1.02
		340	0.880	0.872	0.887
		411	0.333	0.309	0.356
		637	0.071	0.037	0.106
Acid Ananda Blue	A12	206	3.47	3.42	3.53
		257	1.15	1.17	1.13
		313	0.478	0.485	0.471
		340	0.364	0.366	0.361
		411	0.108	0.106	0.111
		637	0.007	0.002	0.013

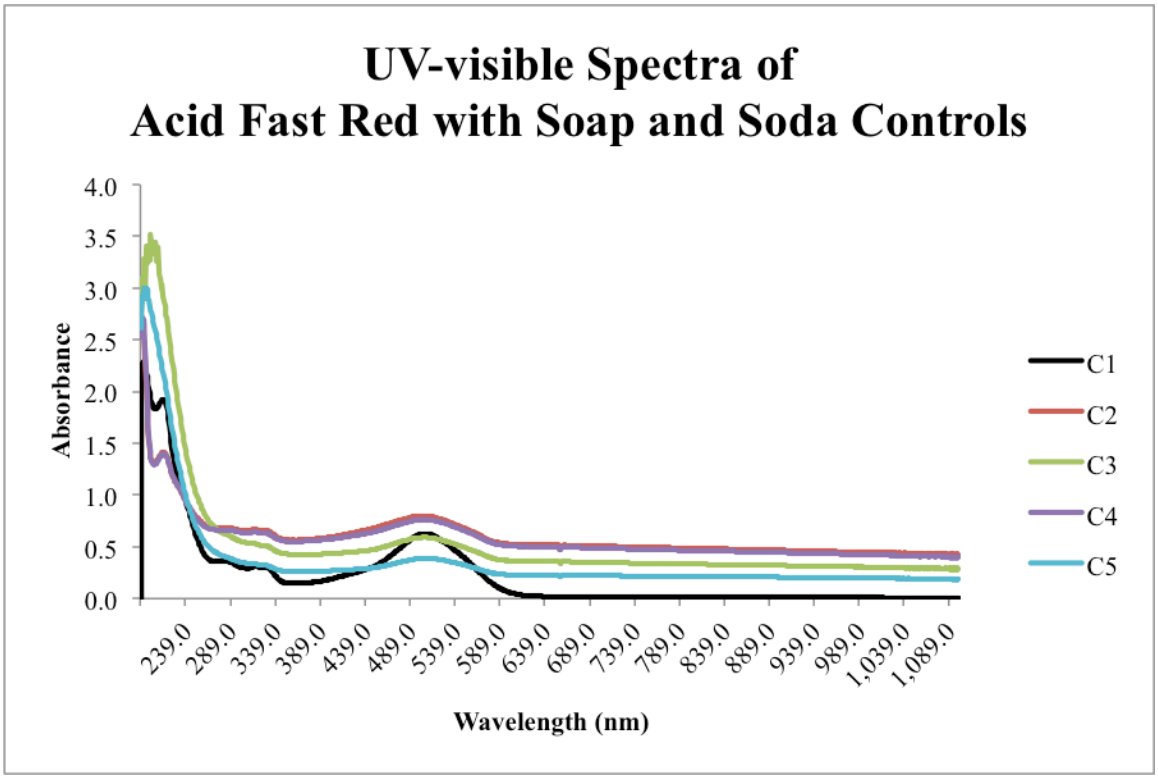

Figure A.7: UV-visible absorption spectra comparing 5g/l Acid Fast Red with Soap and Soda dye control samples at t_0 with no added chemicals (black), t_0 acidified to pH 2.5 (red), t_0 acidified with added Hydrogen peroxide (green), t_F acidified (purple), and t_F acidified with hydrogen peroxide but no iron (teal).

Table A.13: UV-visible absorption spectra data points comparing peaks of 5g/l Acid Fast Red with Soap and Soda dye control samples at t_0 with no added chemicals (black), with peaks of all other control samples (red) t_0 acidified to pH 2.5, t_0 acidified with added Hydrogen peroxide, t_F acidified, and t_F acidified with hydrogen peroxide but no iron.

	Acid Fast Red with Soap and Soda None Control	Acid Fast Red with Soap and Soda HCl t0 Control	Acid Fast Red with Soap and Soda H2O2 t0 Control	Acid Fast Red with Soap and Soda HCl tF Control	Acid Fast Red with Soap and Soda H2O2 tF Control
Wavelength (nm)	Absorbance (AU)	Absorbance (AU)	Absorbance (AU)	Absorbance (AU)	Absorbance (AU)
203	185	32.9	83.6	32.7	136
214	192	35.3	75.9	34.8	111
280	35.9	17.0	16.0	16.6	20.9
317	31.2	16.7	13.3	16.1	16.8
329	29.9	16.4387	12.7	15.8	16.0
505	62.6	20.0	14.8	19.1	19.5

Table A.14: UV-visible absorption spectra data points comparing peaks of degradation of 5g/l Acid Fast Red with Soap and Soda dye samples (A) for Control Sample C1, (B) for A1-A6. Black values are comparison of peaks found in C1, and red values are those extra peaks found on the spectra after acid or peroxide were added (C2-C5).

A

Dye	Oxidation Time	Peak Wavelength	Absorbance (AU)	Dilution Factor	Actual No.
Acid Fast Red with Soap and Soda	Control	203	1.85	99	183
		214	1.92	99	191
		280	0.359	99	35.6
		317	0.312	99	30.9
		505	0.626	99	62.0

B

Dye	Oxidation Time	Peak Wavelength	Average Absorbance (AU) or USA	Absorbance (AU) or USA1 Sample	Absorbance of USA2 Sample
Acid Fast Red with Soap and Soda	S1	203	3.77	4.00	3.54
		214	3.65	3.84	3.45
		280	2.66	3.99	1.33
		317	2.35	3.89	0.806
		505	0.819	1.33	0.307
Acid Fast Red with Soap and Soda	S2	203	2.62	2.59	2.65
		214	1.03	0.950	1.11
		280	0.053	0.059	0.047
		317	0.031	0.041	0.022
		505	0.022	0.031	0.012
Acid Fast Red with Soap and Soda	S3	203	2.73	2.68	2.77
		214	1.14	0.978	1.31
		280	0.058	0.053	0.064
		317	0.026	0.027	0.026
		505	0.011	0.012	0.010
Acid Fast Red with Soap and Soda	S4	203	4.00	4.00	4.00
		214	4.00	4.00	4.00
		280	3.93	3.87	4.00
		317	2.76	2.51	3.01
		505	1.78	1.72	1.84
Acid Fast Red with Soap and Soda	S5	203	3.10	3.06	3.15
		214	2.54	2.41	2.66
		280	0.27	0.24	0.309
		317	0.115	0.103	0.127
		505	0.022	0.023	0.021
Acid Fast Red with Soap and Soda	S6	203	3.10	3.06	3.14
		214	2.63	2.57	2.69
		280	0.204	0.185	0.224
		317	0.083	0.076	0.091
		505	0.012	0.011	0.013

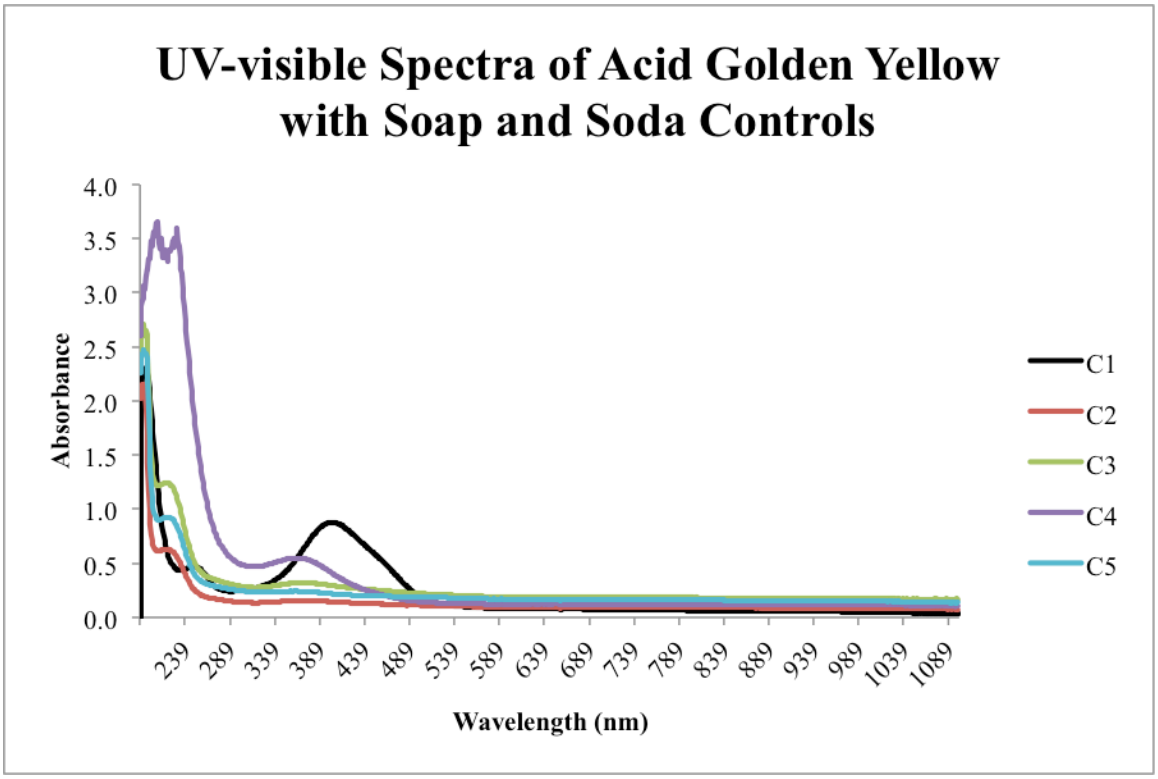

Figure A.8: UV-visible absorption spectra comparing 5g/l Acid Golden Yellow with Soap and Soda dye control samples at t_0 with no added chemicals (black), t_0 acidified to pH 2.5 (red), t_0 acidified with added Hydrogen peroxide (green), t_F acidified (purple), and t_F acidified with hydrogen peroxide but no iron (teal).

Table A.15: UV-visible absorption spectra data points comparing peaks of 5g/l Acid Golden Yellow with Soap and Soda dye control samples at t_0 with no added chemicals (black), with peaks of all other control samples (red) t_0 acidified to pH 2.5, t_0 acidified with added Hydrogen peroxide, t_F acidified, and t_F acidified with hydrogen peroxide but no iron.

	Acid Golden Yellow with Soap and Soda None Control	Acid Golden Yellow with Soap and Soda HCl t0 Control	Acid Golden Yellow with Soap and Soda H2O2 t0 Control	Acid Golden Yellow with Soap and Soda HCL tF Control	Acid Golden Yellow with Soap and Soda H2O2 tF Control
Wavelength (nm)	Absorbance (AU)	Absorbance (AU)	Absorbance (AU)	Absorbance (AU)	Absorbance (AU)
195	115	26.1	16.3	18.9	15.2
205	75.5	8.10	7.96	22.3	6.09
248	23.5	3.45	3.45	12.6	2.70
360	25.5	1.94	1.97	3.42	1.51
403	44.1	1.82	1.84	2.57	1.37

Table A.16: UV-visible absorption spectra data points comparing peaks of degradation of 5g/l Acid Golden Yellow with Soap and Soda dye samples (A) for Control Sample C1, (B) for A1-A6. Black values are comparison of peaks found in C1, and red values are those extra peaks found on the spectra after acid or peroxide were added (C2-C5).

A

Dye	Oxidation Time	Peak Wavelength (nm)	Absorbance (AU)	Dilution Factor	Actual No.
Acid Golden Yellow Soap and Soda	Control	195	2.30	49	113
		205	1.51	49	74.0
		248	0.471	49	23.1
		360	0.511	49	25.0
		403	0.881	49	43.2

B

Dye	Oxidation Time	Peak Wavelength (nm)	Average Absorbance (AU) of USA Samples	Absorbance (AU) of USA1 Sample	Absorbance (AU) of USA2 Sample
Acid Golden Yellow Soap and Soda	S1	195	3.34	3.52	3.16
		205	3.64	3.96	3.32
		248	1.52	1.88	1.16
		360	1.35	1.70	1.01
		403	1.08	1.31	0.843
Acid Golden Yellow Soap and Soda	S2	195	2.59	2.56	2.61
		205	2.83	2.77	2.89
		248	0.138	0.121	0.156
		360	0.043	0.043	0.043
		403	0.027	0.029	0.025
Acid Golden Yellow Soap and Soda	S3	195	2.64	2.63	2.65
		205	2.91	2.88	2.93
		248	0.144	0.134	0.155
		360	0.032	0.032	0.033
		403	0.018	0.018	0.017
Acid Golden Yellow Soap and Soda	S4	195	3.37	3.45	3.28
		205	3.79	4.00	3.58
		248	2.06	2.28	1.84
		360	1.16	1.34	0.987
		403	0.962	1.15	0.771
Acid Golden Yellow Soap and Soda	S5	195	2.79	2.81	2.76
		205	3.18	3.17	3.20
		248	0.537	0.524	0.550
		360	0.107	0.096	0.119
		403	0.050	0.037	0.063
Acid Golden Yellow Soap and Soda	S6	195	2.81	2.81	2.81
		205	3.17	3.13	3.22
		248	0.422	0.422	0.422
		360	0.078	0.076	0.080
		403	0.035	0.032	0.037

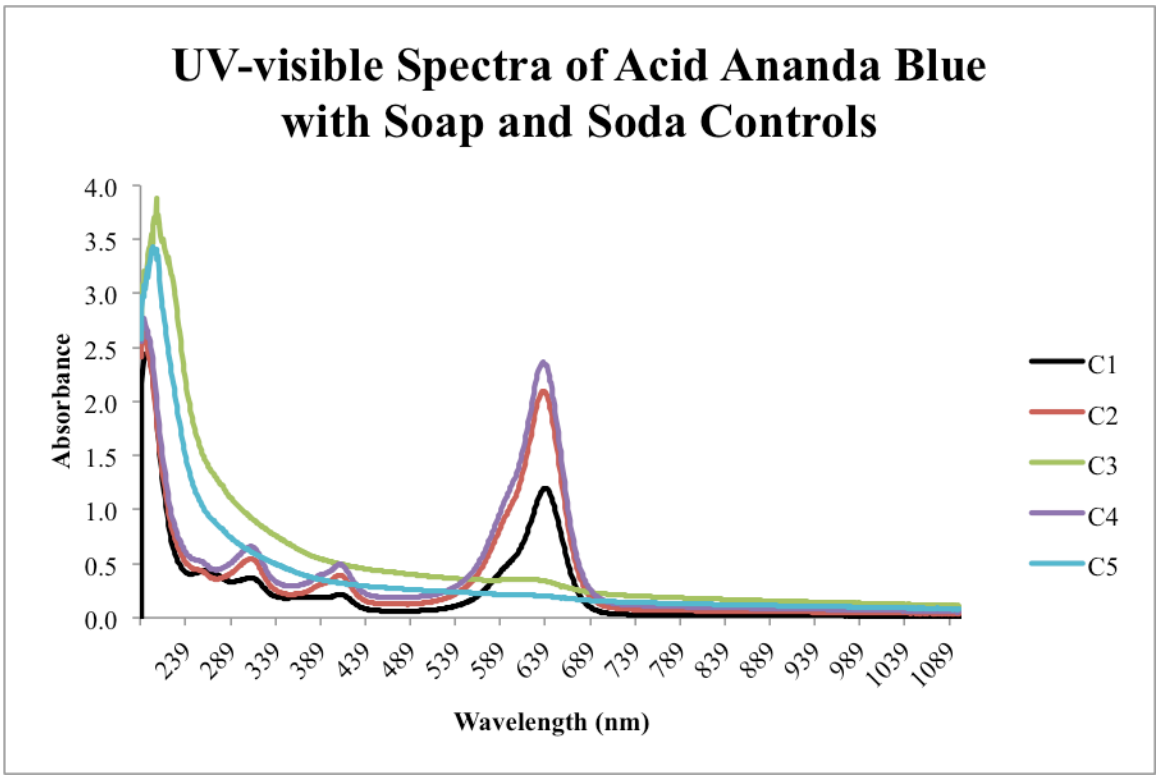

Figure A.9: UV-visible absorption spectra comparing 5g/l Acid Ananda Blue with Soap and Soda dye control samples at t_0 with no added chemicals (black), t_0 acidified to pH 2.5 (red), t_0 acidified with added Hydrogen peroxide (green), t_F acidified (purple), and t_F acidified with hydrogen peroxide but no iron (teal).

Table A.17: UV-visible absorption spectra data points comparing peaks of 5g/l Acid Ananda Blue with Soap and Soda dye control samples at t_0 with no added chemicals (black), with peaks of all other control samples (red) t_0 acidified to pH 2.5, t_0 acidified with added Hydrogen peroxide, t_F acidified, and t_F acidified with hydrogen peroxide but no iron.

	Acid Ananda Blue with Soap and Soda None Control	Acid Ananda Blue with Soap and Soda HCl t0 Control	Acid Ananda Blue with Soap and Soda H2O2 t0 Control	Acid Ananda Blue with Soap and Soda HCl tF Control	Acid Ananda Blue with Soap and Soda H2O2 tF Control
Wavelength (nm)	Absorbance (AU)	Absorbance (AU)	Absorbance (AU)	Absorbance (AU)	Absorbance (AU)
196	245	254	80.3	267	158
205	199	205	92.7	223	170
259	43.6	42.8	37.7	51.5	51.3
311	36.6	54.2	23.4	65.6	30.9
360	18.7	21.8	16.4	29.4	21.4
411	21.6	39.4	12.5	49.3	16.1
638	120	210	8.56	236	10.1

Table A.18: UV-visible absorption spectra data points comparing peaks of degradation of 5g/l Acid Ananda Blue with Soap and Soda dye samples (A) for Control Sample C1, (B) for A1-A6. Black values are comparison of peaks found in C1, and red values are those extra peaks found on the spectra after acid or peroxide were added (C2-C5).

A

Dye	Oxidation Time	Peak Wavelength	Absorbance (AU)	Dilution Factor	Actual No.
Acid Ananda Blue with Soap and Soda	Control	196	2.45	99	243
		205	1.99	99	197
		259	0.436	99	43.2
		311	0.366	99	36.3
		360	0.187	99	18.5
		411	0.216	99	21.4
		638	1.20	99	119

B

Dye	Oxidation Time	Peak Wavelength	Average Absorbance (AU) or USA	Absorbance (AU) or USA1 Sample	Absorbance of USA2 Sample
Acid Ananda Blue with Soap and Soda	S1	196	3.98	3.98	3.98
		205	4.00	4.00	4.00
		259	4.00	3.99	4.00
		311	3.89	3.78	4.00
		360	3.64	4.00	3.28
		411	2.42	2.60	2.24
		638	1.62	1.72	1.53
Acid Ananda Blue with Soap and Soda	S2	196	2.69	2.63	2.75
		205	2.90	2.84	2.96
		259	0.178	0.117	0.240
		311	0.085	0.033	0.137
		360	0.083	0.033	0.132
		411	0.054	0.009	0.098
		638	0.041	0.002	0.081
Acid Ananda Blue with Soap and Soda	S3	196	2.74	2.73	2.74
		205	3.02	3.02	3.01
		259	0.175	0.190	0.160
		311	0.057	0.066	0.049
		360	0.047	0.054	0.040
		411	0.023	0.030	0.015
		638	0.012	0.019	0.004
Acid Ananda Blue with Soap and Soda	S4	196	4.00	3.99	4.00
		205	4.00	4.00	3.99
		259	4.00	4.00	4.00
		311	2.70	2.92	2.49
		360	2.08	2.34	1.82
		411	1.78	2.03	1.53
		638	1.47	1.67	1.27
Acid Ananda Blue with Soap and Soda	S5	196	2.88	2.82	2.93
		205	3.22	3.14	3.30
		259	0.472	0.383	0.561
		311	0.161	0.115	0.206
		360	0.167	0.087	0.247
		411	0.057	0.026	0.088
		638	0.027	0.005	0.048
Acid Ananda Blue with Soap and Soda	S6	196	2.81	2.803	2.82
		205	3.14	3.168	3.12
		259	0.334	0.309	0.360
		311	0.102	0.085	0.118
		360	0.088	0.061	0.115

		411	0.023	0.015	0.030
		638	0.004	0.000	0.008

Appendix B – COD

This appendix contains results of measurements of the temperature (˚C), Sunlight (W/m^2), pH, total iron, and COD (ppm) of all experiments. Each table is separated according to the location of test. Tables describing results from India include the control sample C1 data; tables describing results from the USA include control samples C1-C5. Tables are presented for Reactive Red 120 (Table B.1), Reactive Yellow 81 (Table B.2), and Reactive Blue 4 (Table B.3) samples R1H-R6H, R1M-R6M, and R1L-R6L; Acid Fast Red (Table B.4), Acid Golden Yellow (Table B.5), and Acid Ananda Blue (Table B.6) samples A1-A12; Acid Fast Red with Soap and Soda (Table B.7), Acid Golden Yellow with Soap and Soda (Table B.8), and Acid Ananda Blue with Soap and Soda (Table B.9) samples S1-S6.

Table B.1: COD of Reactive Red 120 with Temperature (deg C), Sunlight (W/m^2), pH, listed for (A) India Samples R1H-R6H compared with C1, (B) USA Samples R1H-R6H compared with C1-C5, (C) India Samples R1M-R6M compared with C1, (D) USA Samples R1M-R6M compared with C1-C5, (E) India Samples R1L-R6L compared with C1, (F) USA Samples R1L-R6L compared with C1-C5.

A

India - Reactive Red 120	Time Sample	Temperature ˚C	Sunlight W/m^2 VAR	pH after oxidation	Total Iron in Solution (Dry Wt per L, Wet Vol)	COD (ppm)
Reactive Red 120	C1H	-	-	3.16	NA	2388
Reactive Red 120	R1H	27.8	386	3.88	0.14g Inorg; 9.23 g Org; 10/1030	558
Reactive Red 120	R2H	27.8	386	8.2	NA	24, 8
Reactive Red 120	R3H	27.8	386	7.96	NA	10, 186
Reactive Red 120	R4H	28.9	485	8.73	NA	798, 456
Reactive Red 120	R5H	28.9	485	7.54	NA	670
Reactive Red 120	R6H	28.9	485	4.45	NA	na

B

USA - Reactive Red 120	Time Sample	Temperature ˚C	Sunlight W/m^2 VAR	pH after oxidation	Total Iron in Solution (Dry Wt per L, Wet Vol)	COD (ppm)
Reactive Red 120	C1	-	-	7.63	NA	3000
Reactive Red 120	C2	-	-	2.57	NA	3140 (0.1ml); 2594 (1ml)
Reactive Red 120	C3	-	-	2.57	NA	6920
Reactive Red 120	C4	0.41	720	2.25	NA	2392
Reactive Red 120	C5	0.97	498	2.22	NA	7320

Reactive Red 120	R1H	16.3	619	3.95, 3.77	Max (>330), max (>330)	200, 1200
Reactive Red 120	R2H	16.3	619	8.61, 8.29	0, 0.08	17, 34
Reactive Red 120	R3H	16.3	619	7.41, 7.48	0.05, 0	0, 6
Reactive Red 120	R4H	23.3	383	2.03, 1.94	max (>330), 119	7680, 11880
Reactive Red 120	R5H	23.3	383	7.03, 6.85	0.05, 0.08	122, 150
Reactive Red 120	R6H	23.3	383	7.51, 7.41	0.01, 0.02	142, 65

C

India - Reactive Red 120	Time Sample	Temperature ˚C	Sunlight W/m^2 VAR	pH after oxidation	Total Iron in Solution (Dry Wt per L, Wet Vol)	COD (ppm)
Reactive Red 120	C1	-	-	3.16	NA	3084
Reactive Red 120	R1M	26.7	304	2.6	1.16; 9.32; 60/890	1350, 150
Reactive Red 120	R2M	26.7	304	7.58	NA	24, 86
Reactive Red 120	R3M	26.7	304	7.55	NA	4, 144
Reactive Red 120	R4M	26.1	81.1	3.98	NA	1758, 660
Reactive Red 120	R5M	26.1	81.1	7.96	NA	302
Reactive Red 120	R6M	26.1	81.1	7.85	NA	88

D

USA - Reactive Red 120	Time Sample	Temperature ˚C	Sunlight W/m^2 VAR	pH after oxidation	Total Iron in Solution (Dry Wt per L, Wet Vol)	COD (ppm)
Reactive Red 120	C1	-	-	7.63	NA	3000
Reactive Red 120	C2	-	-	2.57	NA	3140 (0.1ml); 2594 (1ml)
Reactive Red 120	C3	-	-	2.57	NA	6920
Reactive Red 120	C4	0.41	720	2.25	NA	2392
Reactive Red 120	C5	0.97	498	2.22	NA	7320
Reactive Red 120	R1M	18.9	701	4.26, 4.3	Max (>330), max (>330)	132, 148.8
Reactive Red 120	R2M	18.9	701	8.23, 8.51	0.46, 0.15	0, 0
Reactive Red 120	R3M	18.9	701	7.33, 7.21	0.12, 0.08	0, 0
Reactive Red 120	R4M	15.1	586	1.84, 1.85	91, 82	1100, 600
Reactive Red 120	R5M	15.1	586	6.99, 6.67	0.04, 0.04	0, 0.02
Reactive Red 120	R6M	15.1	586	7.46, 7.6	0, 0.04	0, 0.05

E

India - Reactive Red 120	Time Sample	Temperature ˚C	Sunlight W/m^2 VAR	pH after oxidation	Total Iron in Solution (Dry Wt per L, Wet Vol)	COD (ppm)
Reactive Red 120	C1	-	-	3.16	NA	2334
Reactive Red 120	R1L	27.8	132	2.8	1.03; 9.5; 60/930	288
Reactive Red 120	R2L	27.8	132	8.15	NA	0
Reactive Red 120	R3L	27.8	132	8.06	NA	0
Reactive Red 120	R4L	25.6	81.1	8.59	NA	1716, 5928
Reactive Red 120	R5L	25.6	81.1	3.48	NA	924
Reactive Red 120	R6L	25.6	81.1	5.6	NA	756

F

USA - Reactive Red 120	Time Sample	Temperature ˚C	Sunlight W/m^2 VAR	pH after oxidation	Total Iron in Solution (Dry Wt per L, Wet Vol)	COD (ppm)
Reactive Red 120	C1	-	-	7.63	NA	3000
Reactive Red 120	C2	-	-	2.57	NA	3140 (0.1ml); 2594 (1ml)
Reactive Red 120	C3	-	-	2.57	NA	6920
Reactive Red 120	C4	0.41	720	2.25	NA	2392
Reactive Red 120	C5	0.97	498	2.22	NA	7320
Reactive Red 120	R1L	23.9	713	2.39, 4.75	209, 155	1840, 1220

Reactive Red 120	R2L	23.9	713	8.2, 7.39	2.4, 1.4	0, 0
Reactive Red 120	R3L	23.9	713	8.3, 8.41	0.88, 0	1, 1
Reactive Red 120	R4L	21.5	610	2.18, 2.12	22, 20	9960, 7680
Reactive Red 120	R5L	21.5	610	6.06, 5.76	0.87, 1	600, 360
Reactive Red 120	R6L	21.5	610	7.76, 7.55	1.76, 1.2	103, 800

Table B.2: COD of Reactive Yellow 81 with Temperature (deg C), Sunlight (W/m^2), pH, listed for (A) India Samples R1H-R6H compared with C1, (B) USA Samples R1H-R6H compared with C1-C5, (C) India Samples R1M-R6M compared with C1, (D) USA Samples R1M-R6M compared with C1-C5, (E) India Samples R1L-R6L compared with C1, (F) USA Samples R1L-R6L compared with C1-C5.

A

India - Reactive Yellow 81	**Time Sample**	**Temperature ˚C**	**Sunlight W/m^2 VAR**	**pH after oxidation**	**Total Iron in Solution (Dry Wt per L, Wet Vol)**	**COD (ppm)**
Reactive Yellow 81	C1	-	-	3.19	NA	1794
Reactive Yellow 81	R1H	27.8	386	3.82	0.28; 9.18; 10/1040	270
Reactive Yellow 81	R2H	27.8	386	8.03	NA	278, 0
Reactive Yellow 81	R3H	27.8	386	8.19	NA	16, 186
Reactive Yellow 81	R4H	28.9	485	8.73	NA	1206, 330
Reactive Yellow 81	R5H	28.9	485	7.44	NA	0
Reactive Yellow 81	R6H	28.9	485	4.40	NA	na

B

USA - Reactive Yellow 81	**Time Sample**	**Temperature ˚C**	**Sunlight W/m^2 VAR**	**pH after oxidation**	**Total Iron in Solution (Dry Wt per L, Wet Vol)**	**COD (ppm)**
Reactive Yellow 81	C1	-	-	6.35	NA	5540
Reactive Yellow 81	C2	-	-	2.58	NA	3700
Reactive Yellow 81	C3	-	-	2.58	NA	8180
Reactive Yellow 81	C4	0.41	720	2.27	NA	4000
Reactive Yellow 81	C5	0.97	498	2.24	NA	9760
Reactive Yellow 81	R1H	16.3	619	4.36, 4.56	72, 84	840, 186
Reactive Yellow 81	R2H	16.3	619	7.89, 8.06	0.02, 0	26, 41
Reactive Yellow 81	R3H	16.3	619	7.38, 7.81	0.01, 0	14, 12
Reactive Yellow 81	R4H	23.3	402	2.8, 3.57	237, 64	9000, 9480
Reactive Yellow 81	R5H	23.3	402	7.6, 7.27	0.05, 0.09	81, 88
Reactive Yellow 81	R6H	23.3	402	7.14, 7.65	0.02, 0.05	15, 52

C

India - Reactive Yellow 81	**Time Sample**	**Temperature ˚C**	**Sunlight W/m^2 VAR**	**pH after oxidation**	**Total Iron in Solution (Dry Wt per L, Wet Vol)**	**COD (ppm)**
Reactive Yellow 81	C1	-	-	3.19	NA	2070
Reactive Yellow 81	R1M	26.7	304	8.85	1.58; 9.44; 63/860	486, 312
Reactive Yellow 81	R2M	26.7	304	4.85	NA	92, 32
Reactive Yellow 81	R3M	26.7	304	7.54	NA	46, 18
Reactive Yellow 81	R4M	26.1	81.1	9.34	NA	900,

						300
Reactive Yellow 81	R5M	26.1	81.1	8.1	NA	142
Reactive Yellow 81	R6M	26.1	81.1	7.9	NA	112

D

USA - Reactive Yellow 81	Time Sample	Temperature ˚C	Sunlight W/m^2 VAR	pH after oxidation	Total Iron in Solution (Dry Wt per L, Wet Vol)	COD (ppm)
Reactive Yellow 81	C1	-	-	6.35	NA	5540
Reactive Yellow 81	C2	-	-	2.58	NA	3700
Reactive Yellow 81	C3	-	-	2.58	NA	8180
Reactive Yellow 81	C4	0.41	720	2.27	NA	4000
Reactive Yellow 81	C5	0.97	498	2.24	NA	9760
Reactive Yellow 81	R1M	18.9	701	2.15, 2.09	max (>330), max (>330)	117.6, 124.8
Reactive Yellow 81	R2M	18.9	701	8.57, 8.33	0.25, 0.06	0.02, 0.01
Reactive Yellow 81	R3M	18.9	701	7.31, 7.2	0.07, 0.06	0.02, 0.06
Reactive Yellow 81	R4M	15.3	570	2.04, 2.05	73, 76	1300, 1500
Reactive Yellow 81	R5M	15.3	570	6.98, 6.48	0.84, 2.5	0.14, 0.56
Reactive Yellow 81	R6M	15.3	570	7.25, 7.07	0.72, 1.74	0.14, 0.0

E

India - Reactive Yellow 81	Time Sample	Temperature ˚C	Sunlight W/m^2 VAR	pH after oxidation	Total Iron in Solution (Dry Wt per L, Wet Vol)	COD (ppm)
Reactive Yellow 81	C1	-	-	3.19	NA	2328
Reactive Yellow 81	R1L	27.8	132	3.6	0.88; 18.47; 38.5/890	246
Reactive Yellow 81	R2L	27.8	132	8	NA	28
Reactive Yellow 81	R3L	27.8	132	7.96	NA	8
Reactive Yellow 81	R4L	25.6	81.1	8.78	NA	900, 1008
Reactive Yellow 81	R5L	25.6	81.1	8.1	NA	108
Reactive Yellow 81	R6L	25.6	81.1	7.96	NA	50

F

USA – Reactive Yellow 81	Time Sample	Temperature ˚C	Sunlight W/m^2 VAR	pH after oxidation potentially differ	Total Fe in Solution	COD
Reactive Yellow 81	C1	-	-	6.35	NA	5540
Reactive Yellow 81	C2	-	-	2.58	NA	3700
Reactive Yellow 81	C3	-	-	2.58	NA	8180
Reactive Yellow 81	C4	0.41	720	2.27	NA	4000
Reactive Yellow 81	C5	0.97	497.5	2.24	NA	9760
Reactive Yellow 81	R1L	23.9	713.23	3.74	630, 600	40, 1060
Reactive Yellow 81	R2L	23.9	713.23	7.46, 7.24	0.15, 0.07	0, 0
Reactive Yellow 81	R3L	23.9	713.23	8.46, 8.31	0, 0	0, 2
Reactive Yellow 81	R4L	21.5	609.5	2.15, 2.19	195, 27	2520, 6240
Reactive Yellow 81	R5L	21.5	609.5	7.0, 6.63	0.19, 0.09	148, 226
Reactive Yellow 81	R6L	21.5	609.5	8.29, 7.86	0.34, 0.39	104, 107

Table B.3: COD of Reactive Blue 4 with Temperature (˚C), Sunlight (W/m^2), pH, listed for (A) India Samples R1H-R6H compared with C1, (B) USA Samples R1H-R6H compared with C1-C5, (C) India Samples R1M-R6M compared with C1, (D) USA Samples R1M-R6M compared with C1-C5, (E) India Samples R1L-R6L compared with C1, (F) USA Samples R1L-R6L compared with C1-C5.

A

India - Reactive Blue 4	Time Sample	Temperature ˚C	Sunlight W/m^2 VAR	pH after oxidation	Total Iron in Solution (Dry Wt per L, Wet Vol)	COD (ppm)
Reactive Blue 4	C1	-	-	2.79	NA	4590
Reactive Blue 4	R1H	27.8	386.27	3.85	0.5; 9.13; 40/1200	1404
Reactive Blue 4	R2H	27.8	386	8.08	NA	44, 34
Reactive Blue 4	R3H	27.8	386	8.21	NA	24, 24
Reactive Blue 4	R4H	28.9	485	8.38	NA	2166, 828
Reactive Blue 4	R5H	28.9	485	8.19	NA	82
Reactive Blue 4	R6H	28.9	485	4.91	NA	na

B

USA - Reactive Blue 4	Time Sample	Temperature ˚C	Sunlight W/m^2 VAR	pH after oxidation	Total Iron in Solution (Dry Wt per L, Wet Vol)	COD (ppm)
Reactive Blue 4	C1	-	-	6.34	NA	2360
Reactive Blue 4	C2	-	-	2.58	NA	2700
Reactive Blue 4	C3	-	-	2.58	NA	5620
Reactive Blue 4	C4	0.41	720	2.00	NA	2262
Reactive Blue 4	C5	0.97	498	1.98	NA	7240
Reactive Blue 4	R1H	16.3	619	3.24, 3.02	147, 74	150, 82
Reactive Blue 4	R2H	16.3	619	9.2, 9.05	0.02, 0	4, 13
Reactive Blue 4	R3H	16.3	619	7.2, 7.55	0.02, 0.01	0, 1
Reactive Blue 4	R4H	22.8	291	2.2, 2.14	80, 61	8040, 5400
Reactive Blue 4	R5H	22.8	291	6.65, 6.45	0.27, 1.29	140, 420
Reactive Blue 4	R6H	22.8	291	7.38, 7.2	0.02, 0.1	72, 104

C

India - Reactive Blue 4	Time Sample	Temperature ˚C	Sunlight W/m^2 VAR	pH after oxidation	Total Iron in Solution (Dry Wt per L, Wet Vol)	COD (ppm)
Reactive Blue 4	C1	-	-	2.79	NA	4170
Reactive Blue 4	R1M	26. 7	304	9.12	NA	336, 228
Reactive Blue 4	R2M	26.7	304	4.46	1.61; 9.67; 78/980	350, 88
Reactive Blue 4	R3M	26. 7	304	6.42	NA	48, 16
Reactive Blue 4	R4M	26.1	81.1	8.5	NA	2148, 684
Reactive Blue 4	R5M	26.1	81.1	4.87	NA	216
Reactive Blue 4	R6M	26.1	81.1	7.73	NA	124

D

USA - Reactive Blue 4	Time Sample	Temperature ˚C	Sunlight W/m^2 VAR	pH after oxidation	Total Iron in Solution (Dry Wt per L, Wet Vol)	COD (ppm)
Reactive Blue 4	C1	-	-	6.34	NA	2360
Reactive Blue 4	C2	-	-	2.58	NA	2700
Reactive Blue 4	C3	-	-	2.58	NA	5620
Reactive Blue 4	C4	0.41	720	2.00	NA	2262
Reactive Blue 4	C5	0.97	498	1.98	NA	7240
Reactive Blue 4	R1M	18.9	701	2.4, 2.68	250, 246	159, 165
Reactive Blue 4	R2M	18.9	701	8.07. 7.51	0.16, 0.1	0, 0
Reactive Blue 4	R3M	18.9	701	7.37, 7.44	0.05, 0.02	0, 0
Reactive Blue 4	R4M	15.6	507	2.16, 2.16	38, 2.1	0, 420

Reactive Blue 4	R5M	15.6	507	6.65, 6.67	2.1, 4	0.54, 0.9
Reactive Blue 4	R6M	15.6	507	7.0, 7.17	2.7, 3.7	0.42, 0.06

E

India - Reactive Blue 4	**Time Sample**	**Temperature ˚C**	**Sunlight W/m^2 VAR**	**pH after oxidation**	**Total Iron in Solution (Dry Wt per L, Wet Vol)**	**COD (ppm)**
Reactive Blue 4	C1	-	-	2.79	NA	3396
Reactive Blue 4	R1L	27.8	132	3.3	1.21; 9.55; 50/920	228
Reactive Blue 4	R2L	27.8	132	7.68	NA	62
Reactive Blue 4	R3L	27.8	132	8.01	NA	30
Reactive Blue 4	R4L	25.6	81.1	8.31	NA	1536
Reactive Blue 4	R5L	25.6	81.1	3.64	NA	1422, 6288
Reactive Blue 4	R6L	25.6	81.1	5.64	NA	190

F

USA - Reactive Blue 4	**Time Sample**	**Temperature ˚C**	**Sunlight W/m^2 VAR**	**pH after oxidation**	**Total Iron in Solution (Dry Wt per L, Wet Vol)**	**COD (ppm)**
Reactive Blue 4	C1	-	-	6.34	NA	2360
Reactive Blue 4	C2	-	-	2.58	NA	2700
Reactive Blue 4	C3	-	-	2.58	NA	5620
Reactive Blue 4	C4	0.41	720	2.00	NA	2262
Reactive Blue 4	C5	0.97	498	1.98	NA	7240
Reactive Blue 4	R1L	23.9	713	2.59, 2.38	108, 108	5160, 3960
Reactive Blue 4	R2L	23. 9	713	6.9, 6.63	0.06, 0.7	67, 89
Reactive Blue 4	R3L	23. 9	713	8.0, 8.07	0.04, 0.51	0, 21
Reactive Blue 4	R4L	21.9	596	2.59, 2.35	32, 47	14640, 13320
Reactive Blue 4	R5L	21.9	596	6.24, 6.73	5.4, 0.58	3720, 2280
Reactive Blue 4	R6L	21.9	596	7.85, 7.45	3.8, 2.22	1840, 110

Table B.4: COD of Acid Fast Red with Temperature (deg C), Sunlight (W/m^2), pH, listed for (A) India Samples A1-A12 compared with C1 and C5, (B) USA Samples A1-A12 compared with C1-C5.

A

Dye	Time Sample	Temperature ˚C	Sunlight W/m^2 VAR	pH after oxidation	Total Iron in Solution (Dry Wt per L, Wet Vol)	COD (ppm)
Acid Fast Red	C1	-	-	3.27	NA	1614
Acid Fast Red	C5	NA	NA	NA	7.79; 1.83; 0.07	NA
Acid Fast Red	A1	27.78	630.8	NA	NA	108
Acid Fast Red	A2	27.78	630.8	4.82	NA	58
Acid Fast Red	A3	27.78	630.8	4.35	NA	na
Acid Fast Red	A4	25	260.05	7.93	NA	474
Acid Fast Red	A5	25	260.05	7.96	NA	0
Acid Fast Red	A6	25	260.05	7.84	NA	214
Acid Fast Red	A7	25.56	101	6.82	NA	1308
Acid Fast Red	A8	25.56	101	6.98	NA	322
Acid Fast Red	A9	25.56	101	7.32	NA	16
Acid Fast Red	A10	25.56	101	4.62	NA	1506
Acid Fast Red	A11	25.56	101	5.83	NA	828
Acid Fast Red	A12	25.56	101	7	NA	250

B

Dye	Time Sample	Temperature ˚C	Sunlight W/m^2 VAR	pH after oxidation	Total Iron in Solution (Dry Wt per L, Wet Vol)	COD (ppm)
Acid Fast Red	C1	-	-	8.01-9.10	NA	1762
Acid Fast Red	C2	-	-	2.50	NA	1586
Acid Fast Red	C3	-	-	2.50	NA	5900
Acid Fast Red	C4	3.5	667	2.15	NA	1460 (0.1ml), 270 (1ml)
Acid Fast Red	C5	3.1	412	2.15	NA	6880
Acid Fast Red	A1	14.4	856	6.0; 5.75	3, 6	340, 620
Acid Fast Red	A2	14.4	856	11.84; 12.04	0.04, 0.64	13, 15
Acid Fast Red	A3	14.4	856	8.93; 11.50	0.02, 0.01	13, 24
Acid Fast Red	A4	10.0	296	2.54, 2.74	121, 60	160, 400
Acid Fast Red	A5	10.0	296	11.60, 11.62	0.16, 0	87, 92
Acid Fast Red	A6	10.0	296	11.60, 11.61	0, 0	86, 90
Acid Fast Red	A7	11.7	415	2.38; 2.55	72, 50	80, 2980
Acid Fast Red	A8	11.7	415	11.51; 11.85	0.12, 0.06	232, 236
Acid Fast Red	A9	11.7	415	11.8; 11.87	0.08, 0.05	160, 162
Acid Fast Red	A10	7.2	410	3.32; 2.81	max (>33), max(>33)	2420, 2660
Acid Fast Red	A11	7.2	410	11.65; 11.71	0.09, 0.1	408, 308
Acid Fast Red	A12	7.2	410	11.74; 11.79	0.09, 0.1	224, 234

Table B.5: COD of Acid Golden Yellow with Temperature (deg C), Sunlight (W/m^2), pH, listed for (A) India Samples A1-A12 compared with C1, (B) USA Samples A1-A12 compared with C1-C5.

A

Dye	Time Sample	Temperature ˚C	Sunlight W/m^2 VAR	pH after oxidation	Total Iron in Solution (Dry Wt per L, Wet Vol)	COD (ppm)
Acid Golden Yellow	C1	-	-	3.18	NA	618
Acid Golden Yellow	A1	27.78	630.8	NA	7.99; 1.7; 0.09	216
Acid Golden Yellow	A2	27.78	630.8	6	NA	68
Acid Golden Yellow	A3	27.78	630.8	6.12	NA	na
Acid Golden Yellow	A4	25	260.47	5.56	NA	1086
Acid Golden Yellow	A5	25	260.47	4.39	NA	120
Acid Golden Yellow	A6	25	260.47	6.88	NA	2
Acid Golden Yellow	A7	25.56	101	5.52	NA	900
Acid Golden Yellow	A8	25.56	101	7.58	NA	24
Acid Golden Yellow	A9	25.56	101	7.72	NA	0
Acid Golden Yellow	A10	25.56	101	6.2	NA	1584
Acid Golden Yellow	A11	25.56	101	7.2	NA	172
Acid Golden Yellow	A12	25.56	101	7.33	NA	26

B

Dye	Time Sample	Temperature ˚C	Sunlight W/m^2 VAR	pH after oxidation	Total Iron in Solution (Dry Wt per L, Wet Vol)	COD (ppm)
Acid Golden Yellow	C1	-	-	10.49-10.64	NA	730
Acid Golden Yellow	C2	-	-	2.55	NA	482
Acid Golden Yellow	C3	-	-	2.55	NA	6120
Acid Golden Yellow	C4	3.5	667	2.00	NA	660 (0.1ml); 182(1ml)
Acid Golden Yellow	C5	3.1	412	2.02	NA	6220
Acid Golden Yellow	A1	14.4	856	9.87; 7.76	22, 14	20, 60
Acid Golden Yellow	A2	14.4	856	11.85, 11.77	0.02, 0	7, 18
Acid Golden Yellow	A3	14.4	856	11.33, 11.41	0.04, 0.02	29, 26
Acid Golden Yellow	A4	10.0	296	4.18, 3.59	max(>33), max(>33)	100, 0
Acid Golden Yellow	A5	10.0	296	11.74, 11.71	0.27, 0.02	42, 68
Acid Golden Yellow	A6	10.0	296	11.53, 11.58	0, 0	75, 84
Acid Golden Yellow	A7	11.4	398	3.77; 3.52	30, 64	0, 0
Acid Golden Yellow	A8	11.4	398	11.93; 11.98	0.03, 0	107, 132
Acid Golden Yellow	A9	11.4	398	12.02; 12.02	0.01, 0.05	85, 122
Acid Golden Yellow	A10	6.9	349	2.99; 3.04	max(>33), 26.6	4920, 3840
Acid Golden Yellow	A11	6.9	349	11.64; 11.67	0.05, 0.06	210, 252
Acid Golden Yellow	A12	6.9	349	11.66; 11.7	0.08, 0.04	164, 196

Table B.6: COD of Acid Ananda Blue with Temperature (deg C), Sunlight (W/m^2), pH, listed for (A) India Samples A1-A12 compared with C1, (B) USA Samples A1-A12 compared with C1-C5.

A

Dye	Time Sample	Temperature °C	Sunlight W/m^2 VAR	pH after oxidation	Total Iron in Solution (Dry Wt per L, Wet Vol)	COD (ppm)
Acid Ananda Blue	C1	-	-	3.4	NA	1728
Acid Ananda Blue	A1	27.78	630.8	NA	8.60; 0.58; 0.01	258
Acid Ananda Blue	A2	27.78	630.8	7.22	NA	4
Acid Ananda Blue	A3	27.78	630.8	6.61	NA	na
Acid Ananda Blue	A4	25	260.47	8.75	NA	756
Acid Ananda Blue	A5	25	260.47	7.92	NA	50
Acid Ananda Blue	A6	25	260.47	7.89	NA	12
Acid Ananda Blue	A7	25.56	101	NA	NA	1188
Acid Ananda Blue	A8	25.56	101	7.86	NA	92
Acid Ananda Blue	A9	25.56	101	7.78	NA	528
Acid Ananda Blue	A10	25.56	101	8.46	NA	398
Acid Ananda Blue	A11	25.56	101	7.57	NA	1440
Acid Ananda Blue	A12	25.56	101	7.67	NA	114

B

Dye	Time Sample	Temperature °C	Sunlight W/m^2 VAR	pH after oxidation	Total Iron in Solution (Dry Wt per L, Wet Vol)	COD (ppm)
Acid Ananda Blue	C1	-	-	7.59-7.62	NA	2402
Acid Ananda Blue	C2	-	-	2.56	NA	2544
Acid Ananda Blue	C3	-	-	2.56	NA	6720
Acid Ananda Blue	C4	3.5	667	1.95	NA	2700 (0.1ml); 2632 (1ml)
Acid Ananda Blue	C5	3.1	412	1.92	NA	5980
Acid Ananda Blue	A1	14.4	856	4.43; 4.06	190, max(>330)	100, 0
Acid Ananda Blue	A2	14.4	856	11.76, 11.77	0.06, 0.02	26, 19
Acid Ananda Blue	A3	14.4	856	11.55, 11.57	0.04, 0.02	62, 70
Acid Ananda Blue	A4	10.0	296	2.52, 2.50	114, 132	1320, 200
Acid Ananda Blue	A5	10.0	296	11.63	0, 0.01	93, 94
Acid Ananda Blue	A6	10.0	296	11.65	0, 0	90, 81
Acid Ananda Blue	A7	11.7	412	2.57; 2.51	53, 60	2020, 1480
Acid Ananda Blue	A8	11.7	412	11.93; 11.92	0.04, 1.2	128, 204
Acid Ananda Blue	A9	11.7	412	11.91; 11.90	0.08, 0.09	143, 129
Acid Ananda Blue	A10	7.1	410	2.99; 3.04	44, 57	4300, 3400
Acid Ananda Blue	A11	7.1	410	11.64; 11.67	0.06, 0.06	220, 196
Acid Ananda Blue	A12	7.1	410	11.70; 11.66	0.05, 0.11	172, 152

Table B.7: COD of Acid Fast Red with with Soap and Soda Temperature (deg C), Sunlight (W/m^2), pH, listed for (A) India Samples S1-S6 compared with C1, (B) USA Samples S1-S6 compared with C1-C5.

A

Dye	Time Sample	Temperature ˚C	Sunlight W/m^2 VAR	pH after oxidation	Total Iron in Solution (Dry Wt per L, Wet Vol)	COD (ppm)
Acid Fast Red with Soap and Soda	C1	-	-	2.27	NA	4380
Acid Fast Red with Soap and Soda	S1	27.78	151.67	2.68	NA	6316
Acid Fast Red with Soap and Soda	S2	27.78	151.67	6.31	NA	453
Acid Fast Red with Soap and Soda	S3	27.78	151.67	7.38	NA	273
Acid Fast Red with Soap and Soda	S4	27.78	151.67	2.44	NA	3168
Acid Fast Red with Soap and Soda	S5	27.78	151.67	3.19	NA	534
Acid Fast Red with Soap and Soda	S6	27.78	151.67	6.11	NA	498

B

Dye	Time Sample	Temperature ˚C	Sunlight W/m^2 VAR	pH after oxidation	Total Iron in Solution (Dry Wt per L, Wet Vol)	COD (ppm)
Acid Fast Red with Soap and Soda	C1	-	-	12.21	NA	6340
Acid Fast Red with Soap and Soda	C2	-	-	2.30	NA	7860
Acid Fast Red with Soap and Soda	C3	-	-	2.36	NA	6100
Acid Fast Red with Soap and Soda	C4	3.47	667	2.23	NA	608
Acid Fast Red with Soap and Soda	C5	3.06	412	2.30	NA	6840
Acid Fast Red with Soap and Soda	S1	**4.61**	**577.4**	**2.80; 2.90**	**61, 29**	**2040, 1000**
Acid Fast Red with Soap and Soda	S2	4.61	577.4	12.33; 12.14	0.02, 0.14	12, 18
Acid Fast Red with Soap and Soda	S3	4.61	577.4	12.40; 12.23	0.01, 0.15	0, 25
Acid Fast Red with Soap and Soda	S4	**5**	**536.25**	**2.99; 2.93**	**6, 84**	**9360, 8640**
Acid Fast Red with Soap and Soda	S5	5	536.25	12.34; 12.32	0.4, 0.24	222, 276
Acid Fast Red with Soap and Soda	S6	5	536.25	12.39; 12.39	0.28, 0.16	161, 202

Table B.8: COD of Acid Golden Yellow with Soap and Soda with Temperature (deg C), Sunlight (W/m^2), pH, listed for (A) India Samples S1-S6 compared with C1, (B) USA Samples S1-S6 compared with C1-C5.

A

Dye	Time Sample	Temperature ˚C	Sunlight W/m^2 VAR	pH after oxidation	Total Iron in Solution (Dry Wt per L, Wet Vol)	COD (ppm)
Acid Golden Yellow with Soap and Soda	C1	NA	NA	2.5	NA	NA
Acid Golden Yellow with Soap and Soda	S1	27.78	151.67	2.76	NA	2436
Acid Golden Yellow with Soap and Soda	S2	27.78	151.67	4.77	NA	756
Acid Golden Yellow with Soap and Soda	S3	27.78	151.67	5.77	NA	303
Acid Golden Yellow with Soap and Soda	S4	27.78	151.67	2.54	NA	2276
Acid Golden Yellow with Soap and Soda	S5	27.78	151.67	3.31	NA	648
Acid Golden Yellow with Soap and Soda	S6	27.78	151.67	6.58	NA	72

B

Dye	Time Sample	Temperature ˚C	Sunlight W/m^2 VAR	pH after oxidation	Total Iron in Solution (Dry Wt per L, Wet Vol)	COD (ppm)
Acid Golden Yellow with Soap and Soda	C1	-	-	12.27	NA	7580
Acid Golden Yellow with Soap and Soda	C2	-	-	2.57	NA	4180
Acid Golden Yellow with Soap and Soda	C3	-	-	2.70	NA	7740
Acid Golden Yellow with Soap and Soda	C4	3.47	667	2.58	NA	2620
Acid Golden Yellow with Soap and Soda	C5	3.06	412	2.68	NA	9820
Acid Golden Yellow with Soap and Soda	S1	4.61	577.4	5.58; 5.68	138, 150	400, 80
Acid Golden Yellow with Soap and Soda	S2	4.61	577.4	12.26; 12.24	0.16, 0	42, 84
Acid Golden Yellow with Soap and Soda	S3	4.61	577.4	12.24; 12.19	0.22, 0	32, 58
Acid Golden Yellow with Soap and Soda	S4	5	536.25	2.96; 2.89	49, 33	2160, 840
Acid Golden Yellow with Soap and Soda	S5	5	536.25	12.34; 12.34	0.17, 0.18	310, 298
Acid Golden Yellow with Soap and Soda	S6	5	536.25	12.41; 12.40	0.4, 0.5	246, 242

Table B.9: COD of Acid Ananda Blue with Soap and Soda with Temperature (deg C), Sunlight (W/m^2), pH, listed for (A) India Samples S1-S6 compared with C1, (B) USA Samples S1-S6 compared with C1-C5.

A

Dye	Time Sample	Temperature ˚C	Sunlight W/m^2 VAR	pH after oxidation	Total Iron in Solution (Dry Wt per L, Wet Vol)	COD (ppm)
Acid Ananda Blue with Soap and Soda	C1	-	-	2.19	NA	3000
Acid Ananda Blue with Soap and Soda	S1	**27.78**	**151.67**	**3.08**	**NA**	**1296**
Acid Ananda Blue with Soap and Soda	S2	27.78	151.67	4.53	NA	549
Acid Ananda Blue with Soap and Soda	S3	27.78	151.67	4.96	NA	1113
Acid Ananda Blue with Soap and Soda	S4	**27.78**	**151.67**	**2.5**	**NA**	**1560**
Acid Ananda Blue with Soap and Soda	S5	27.78	151.67	3.16	NA	738
Acid Ananda Blue with Soap and Soda	S6	27.78	151.67	5.1	NA	369

B

Dye	Time Sample	Temperature ˚C	Sunlight W/m^2 VAR	pH after oxidation	Total Iron in Solution (Dry Wt per L, Wet Vol)	COD (ppm)
Acid Ananda Blue with Soap and Soda	C1	-	-	12.35	NA	8200
Acid Ananda Blue with Soap and Soda	C2	-	-	2.44	NA	6460
Acid Ananda Blue with Soap and Soda	C3	-	-	2.56	NA	9060
Acid Ananda Blue with Soap and Soda	C4	3.47	667	2.36	NA	8040
Acid Ananda Blue with Soap and Soda	C5	3.06	412	2.56	NA	10880
Acid Ananda Blue with Soap and Soda	S1	**4.61**	**577.4**	**2.72; 2.64**	**690, 660**	**2160, 2280**
Acid Ananda Blue with Soap and Soda	S2	4.61	577.4	12.4; 12.42	0.5, 1.14	70, 112
Acid Ananda Blue with Soap and Soda	S3	4.61	577.4	12.33; 12.40	0.26, 0.3	100, 94
Acid Ananda Blue with Soap and Soda	S4	**5.28**	**487.5**	**2.48; 2.42**	**70, 70**	**3880, 3280**
Acid Ananda Blue with Soap and Soda	S5	5.28	487.5	12.31; 12.34	0.12, 0.33	780, 284
Acid Ananda Blue with Soap and Soda	S6	5.28	487.5	12.35; 12.36	0.99, 0.77	208, 194

Appendix C – GC/MS

This appendix contains the results of the GC/MS analyses of the control samples and all oxidized and filtered samples. Tables listing the organics remaining in samples and their abundance found using GC/MS analysis of each of the control samples C1-C5 and for all oxidized and filtered samples are used to present the data. Each table is separated according to location of test. Tables describing results from India include the control sample C1 data; tables describing results from the USA include control samples C1-C5. Tables are made for each dye sample Reactive Red 120 (Table C.1), Reactive Yellow 81 (Table C.2), and Reactive Blue 4 (Table C.3) samples R1H-R6H, R1M-R6M, and R1L-R6L; Acid Fast Red (Table C.4), Acid Golden Yellow (Table C.5), and Acid Ananda Blue (Table C.6) samples A1-A12; Acid Fast Red with Soap and Soda (Table C.7), Acid Golden Yellow with Soap and Soda (Table C.8), Acid Ananda Blue with Soap and Soda (Table C.9) samples S1-S6; Field Sample Green, and Field Sample Maroon F1-F3 (Table C.10). This appendix also includes figures of the GC/MS results of the USA dye control samples C1-C5 (Figures C.1-C.45) and pure Benzene, 2,4-diisocyanato-1-methyl control (Figure C.46).

Table C.1: GC/MS results of 5 g/L Reactive Red 120 samples R1H-R6H, R1M-R6M, and R1L-R6L in (A) India compared with C1, (B) in USA1 compared with C1-C5, and (C) in USA2 compared with C1-C5.

A

Dye	Oxidation Time	Peak Time (min)	Chemical Name	Percentage	Abundance
Reactive Red 120	C1	-	-	-	-
Reactive Red 120	R1H	NA	NA	NA	NA
Reactive Red 120	R2H	14.42	Benzene, 1-methoxy-4-(1-propenyl)-Anethole	96	20000
		17.76	Butylated Hydroxytoluene	96	30000
Reactive Red 120	R3H	14.43	Benzene, 1-methoxy-4-(1-propenyl)-Anethole	98	23000
		17.76	Butylated Hydroxytoluene	95	25000
Reactive Red 120	R4H	15.42	Benzene, 2,4-diisocyanato-1-methyl	94	14000
		16.16	2H-Benzimidaol-2-one,1,2-dihydro-5-methyl	78	10000
Reactive Red 120	R5H	14.43	Benzene, 1-methoxy-4-(1-propenyl)-Anethole	98	25000
		17.77	Butylated Hydroxytoluene	95	25000
Reactive Red 120	R6H	17.66	Phenol, 2,4-bis(1,1-dimethylethyl)	94	80000
Reactive Red 120	R1M	None	None	None	None
Reactive Red 120	R2M	17.66	Phenol, 2,4-bis(1,1-dimethylethyl)	91	11700
Reactive Red 120	R3M	None	None	None	None
Reactive Red 120	R4M	None	None	None	None
Reactive Red 120	R5M	None	None	None	None
Reactive Red 120	R6M	None	None	None	None
Reactive Red 120	R1L	NA	NA	NA	NA
Reactive Red 120	R2L	17.65	Phenol, 2,4-bis(1,1-dimethylethyl)	91	36000
Reactive Red 120	R3L	None	None	None	None
Reactive Red 120	R4L	15.34	Benzene, 2,5-diisocyanato-1-methyl	76	6750
		17.69	Phenol, bis(1,1-dimethylethyl)	76	6750
Reactive Red 120	R5L	None	None	None	None
Reactive Red 120	R6L	None	None	None	None

B

Dye	Fe level	Oxidation Time	Peak Time (min)	Chemical Name	Percentage	Abundance
Reactive Red 120	-	C1	9.39	Cyclotetrasiloxane, octamethyl	83	
			12.31	Cyclopentasiloxane, decamethyl	91	65000
			13.91	Benzene, 1,3-bis (1,1-dimethylethyl)	76	27000
			17.63	Phenol, bis(1,1-dimethylethyl)	91	55000
			18.64	Benzene, (1-ethyloctyl)	84	26500
			19.24	Hexadecane	89	25000
			19.94	Benzene, (1-pentylhexyl)	76	59000
			20.01	Benzene, (1-butylheptyl)	95	66500
			20.2	Benzene, (1-propyloctyl)	86	69000
			20.28	Phosphoric acid tributyl ester	87	66000
			20.62	Benzene, (1-ethylnonyl)	86	80000
			21.23	Heptadecane	94	52000
			21.36	Benzene, (1-methyldecyl)	87	72500
			21.88	Benzene, (1-pentylheptyl)	97	84000
			21.98	Benzene, (1-butyloctyl)	97	76500
			22.22	Benzene , (1-propylnonyl)	95	63000
			22.65	Benzene, (1-ethyldecyl)	95	58000
			23.42	Benzene, (1-methylunecyl)	90	76000
			23.85	Benzene, (1-pentyloctyl)	94	84000
			23.98	Benzene, (1-butylnonyl)	95	72000
			24.23	Benzene, (1-propyldecyl)	86	60500
			24.69	Benzene, (1-ethylnonyl)	86	57000
			27.14	Eicosane	94	41000
			28.99	Heneicosane	86	51000
Reactive Red 120	-	C2	11.06	Benzaldehyde, 4-methyl	91	59000
			15.43	Benzene, 2,4-diisocyanato-1-methyl	96	135000
			15.83	1,3-Benzenediamine, 4-methyl	81	89000
			16.1	2H-Benzimidazol-2-one, 1,3-dihydro-5-methyl	87	67500
			16.15	2H-Benzimidazol-2-one, 1,3-dihydro-5-methyl	72	112000
Reactive Red 120	-	C3	9.42	Cyclotetrasiloxane, octamethyl	90	23000
			11.06	Benzaldehyde, 3-methyl	93	38000
			12.33	Cyclopentasiloxane, decamethyl	78	17500
Reactive Red 120	-	C4	11.05	Benzaldehyde, 2-methyl-	95	75000
			14.79	Benzene, 2,4-diisocyanato-1-methyl	95	60000
			15.41	Benzene, 2,4-diisocyanato-1-methyl	97	51000
Reactive Red 120	-	C5	None	None	None	None
Reactive Red 120	High	R1H	None	None	None	None
Reactive Red 120	High	R2H	None	None	None	None
Reactive Red 120	High	R3H	None	None	None	None
Reactive Red 120	High	R4H	None	None	None	None
Reactive Red 120	High	R5H	None	None	None	None

Reactive Red 120	High	R6H	NA	NA	NA	NA
Reactive Red 120	Medium	R1M	None	None	None	None
Reactive Red 120	Medium	R2M	None	None	None	None
Reactive Red 120	Medium	R3M	NA	NA	NA	NA
Reactive Red 120	Medium	R4M	None	None	None	None
Reactive Red 120	Medium	R5M	None	None	None	None
Reactive Red 120	Medium	R6M	NA	NA	NA	NA
Reactive Red 120	Low	R1L	None	None	None	None
Reactive Red 120	Low	R2L	None	None	None	None
Reactive Red 120	Low	R3L	NA	NA	NA	NA
Reactive Red 120	Low	R4L	None	None	None	None
Reactive Red 120	Low	R5L	None	None	None	None
Reactive Red 120	Low	R6L	NA	NA	NA	NA

C

Dye	Fe level	Oxidation Time	Peak Time (min)	Chemical Name	Percentage	Abundance
Reactive Red 120	High	R1H	None	None	None	None
Reactive Red 120	High	R2H	None	None	None	None
Reactive Red 120	High	R3H	NA	NA	NA	NA
Reactive Red 120	High	R4H	None	None	None	None
Reactive Red 120	High	R5H	11.06	Benzaldehyde, 2-methyl-	95	49000
Reactive Red 120	High	R6H	NA	NA	NA	NA
Reactive Red 120	Medium	R1M	None	None	None	None
Reactive Red 120	Medium	R2M	None	None	None	None
Reactive Red 120	Medium	R3M	NA	NA	NA	NA
Reactive Red 120	Medium	R4M	None	None	None	None
Reactive Red 120	Medium	R5M	None	None	None	None
Reactive Red 120	Medium	R6M	NA	NA	NA	NA
Reactive Red 120	Low	R1L	15.43	Benzene, 2,4-diisocyanato-1-methyl	96	58000
Reactive Red 120	Low	R2L	None	None	None	None
Reactive Red 120	Low	R3L	NA	NA	NA	NA
Reactive Red 120	Low	R4L	12.85-14.66	Benzene, 2,4-diisocyanato-1-methyl	95-97	40000-70000
Reactive Red 120	Low	R5L	5.39	Benzene, chloro-	91	8800
			15.42	Benzene, 2,4-diisocyanato-1-methyl	91	9500
Reactive Red 120	Low	R6L	NA	NA	NA	NA

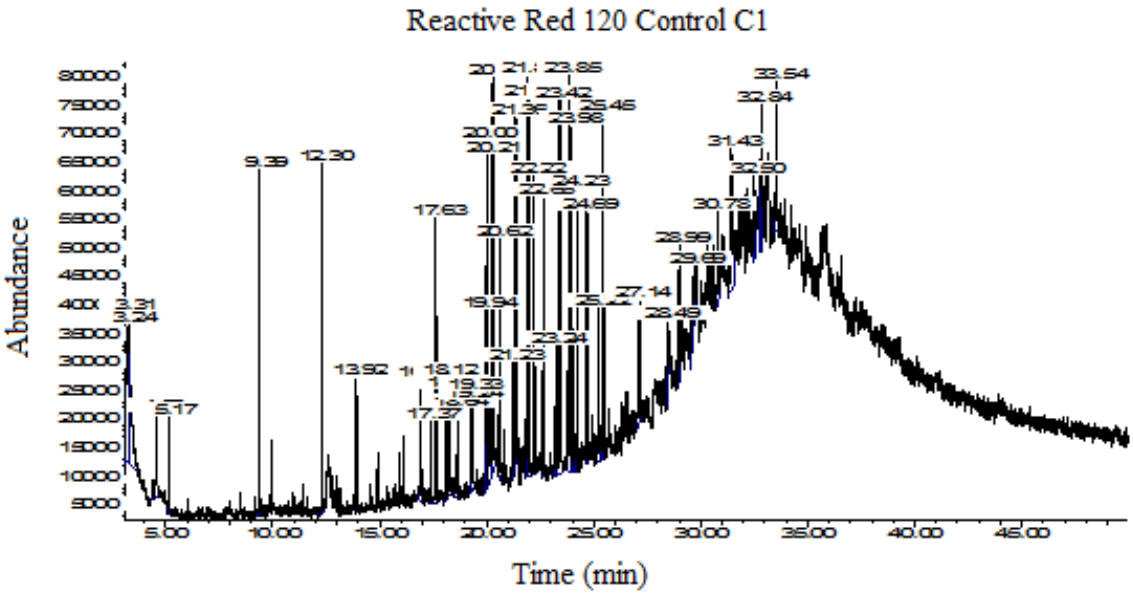

Figure C.1: Total ion GC-MS chromatogram of 5 g/L Reactive Red dye Control C1 in the USA. Major peaks are identified in Table C.1.

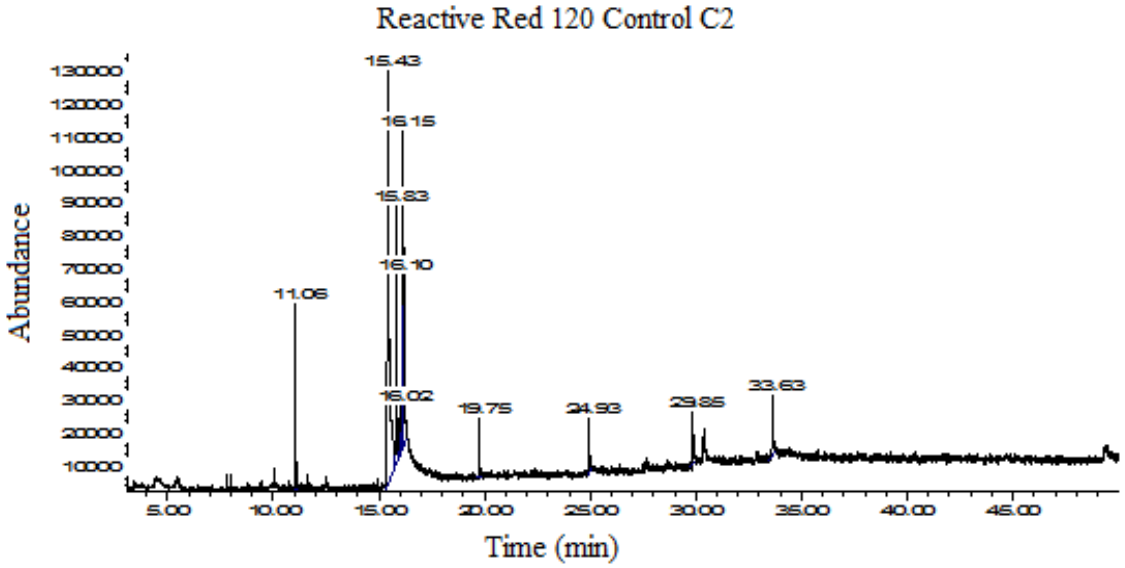

Figure C.2: Total ion GC-MS chromatogram of 5 g/L Reactive Red dye Control C2 in the USA. Major peaks are identified in Table C.1.

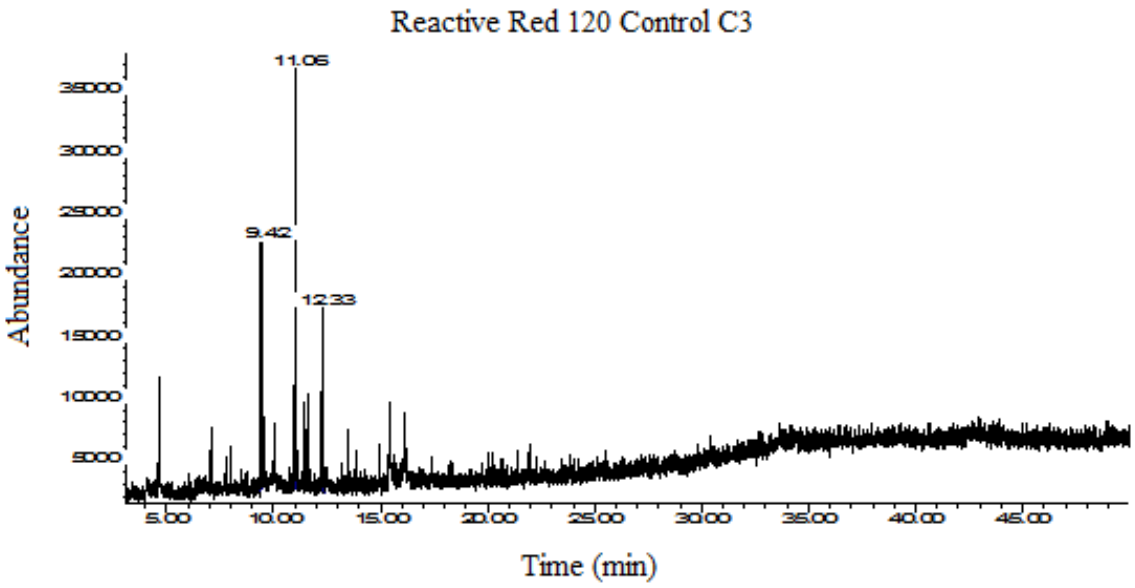

Figure C.3: Total ion GC-MS chromatogram of 5 g/L Reactive Red dye Control C3 in the USA. Major peaks are identified in Table C.1.

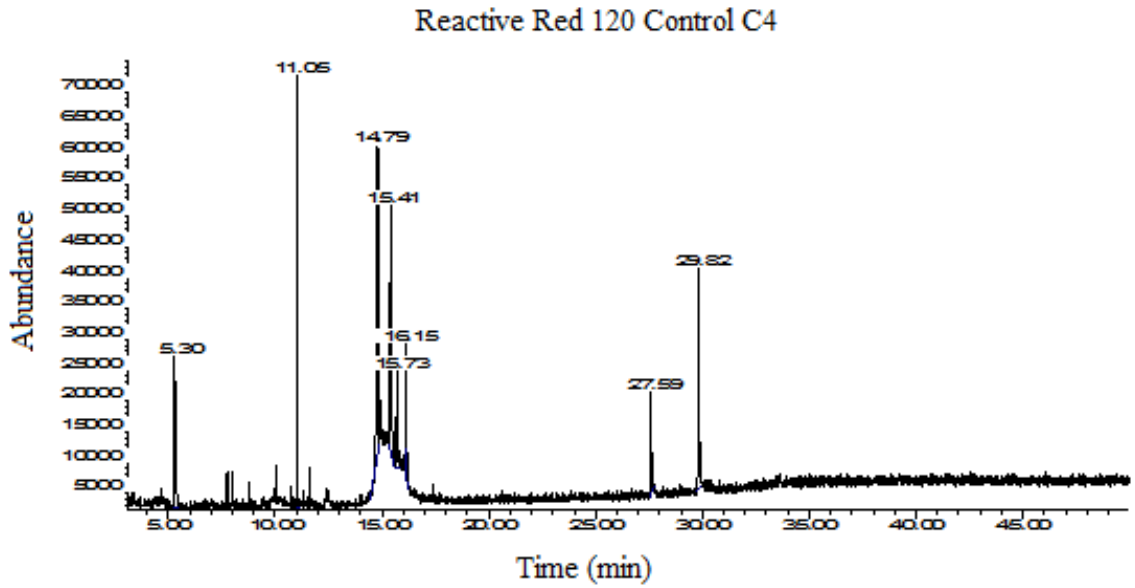

Figure C.4: Total ion GC-MS chromatogram of 5 g/L Reactive Red dye Control C4 in the USA. Major peaks are identified in Table C.1.

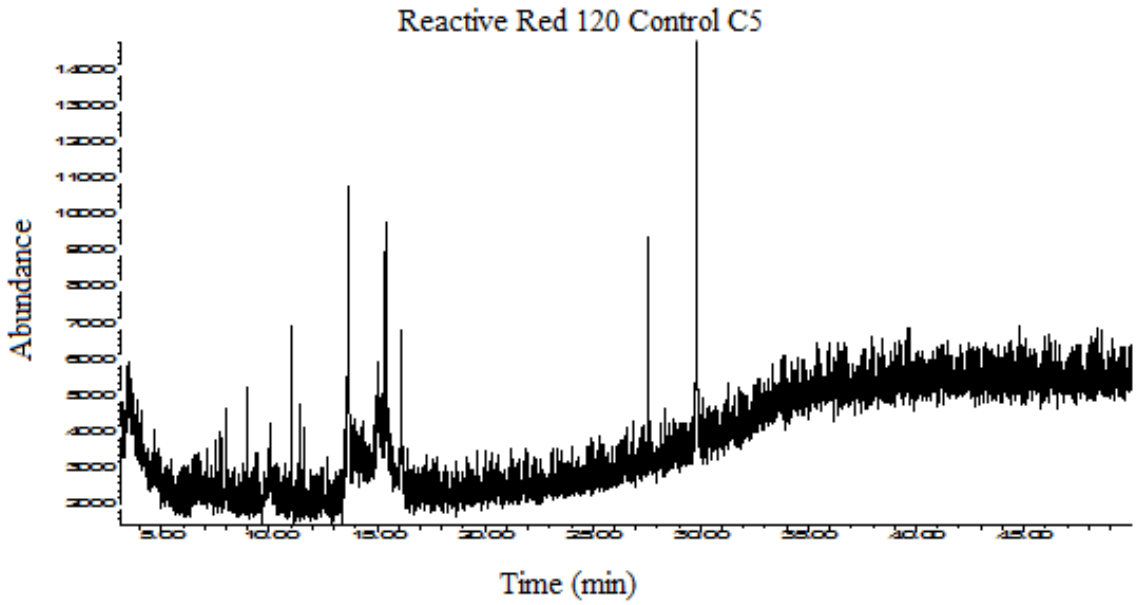

Figure C.5: Total ion GC-MS chromatogram of 5 g/L Reactive Red dye Control C5 in the USA. Major peaks are identified in Table C.1.

Table C.2: GC/MS results of 5 g/L Reactive Yellow 81 samples R1H-R6H, R1M-R6M, and R1L-R6L in (A) India compared with C1, (B) in USA 1 compared with C1-C5, and (C) in USA2 compared with C1-C5.

A

Dye	Fe level	Oxidation Time	Peak Time (min)	Chemical Name	Percentage	Abundance
Reactive Yellow 81	-	C1	-	-	-	-
Reactive Yellow 81	High	R1H	NA	NA	NA	NA
Reactive Yellow 81	High	R2H	15.42	Benzene, 2,4-diisocyanato-1-methyl	93	10000
			16.16	Benzamide, 4-(1-methylethyl)	74	7000
Reactive Yellow 81	High	R3H	15.44	Benzene, 2,4-diisocyanato-1-methyl	95	20000
			16.16	2H-Benzimidazol-2-one, 1,3-dihydro-5-methyl-	95	20000
Reactive Yellow 81	High	R4H	15.34	Benzene, 2,4-diisocyanato-1-methyl	95	18000
			15.43	Benzene, 2,4-diisocyanato-1-methyl	96	20000
Reactive Yellow 81	High	R5H	15.44	Benzene, 2,4-diisocyanato-1-methyl	94	20000
Reactive Yellow 81	High	R6H	15.42	Benzene, 2,4-diisocyanato-1-methyl	90	11500
Reactive Yellow 81	Medium	R1M	None	None	None	None
Reactive Yellow 81	Medium	R2M	16.73	1,3,5-Triazin-2-amine, 4,6-dichloro-	96	20000
			17.66	Phenol, 2,4-bis(1,1-dimethylethyl)	93	115000
Reactive Yellow 81	Medium	R3M	17.66	Phenol, 2,4-bis(1,1-dimethylethyl)	94	115000
Reactive Yellow 81	Medium	R4M	None	None	None	None
Reactive Yellow 81	Medium	R5M	None	None	None	None
Reactive Yellow 81	Medium	R6M	None	None	None	None
Reactive Yellow 81	Low	R1L	NA	NA	NA	NA
Reactive Yellow 81	Low	R2L	None	None	None	None
Reactive Yellow 81	Low	R3L	None	None	None	None
Reactive Yellow 81	Low	R4L	None	None	None	None
Reactive Yellow 81	Low	R5L	17.66	Phenol, 2,4-bis(1,1-dimethylethyl)	93	31000
Reactive Yellow 81	Low	R6L	None	None	None	None

B

Dye	Fe level	Oxidation Time	Peak Time (min)	Chemical Name	Percentage	Abundance
Reactive Yellow 81	-	C1	9.41	Cyclotetrasiloxane, octamethyl	72	20000
			15.42	Benzene, 2,4-diisocyanato-1-methyl	95	185000
			15.67	Benzene, 2,4-diisocyanato-1-methyl	83	35000
			17.66	Phenol, 2,4-bis (1,1-dimethylethyl)	74	29000
			39.12	5-methyl-2-(N-ethyl-p-chlorophenyl amino)-2-thiazoline	93	75000
			44.79	5-methyl-2-(N-ethyl-p-chlorophenyl amino)-2-thiazoline	89	375000
			44.86	5-methyl-2-(N-ethyl-p-chlorophenyl amino)-2-thiazoline	89	360000
Reactive Yellow 81	-	C2	15.23	Benzene, 2,4-diisocyanato-1-methyl	95	44000
Reactive Yellow 81	-	C3	7.99	2-Heptanone, 4-methyl	83	19000
			10.01	1-Hexanol, 2-ethyl	72	43500
			11.04	Benzaldehyde, 3-methyl	95	49000
			11.9	Picloxydine	78	20500
Reactive Yellow 81	-	C4	15.34	Benzene, 2,4-diisocyanato-1-methyl	94	36000
			15.42	Benzene, 2,4-diisocyanato-1-methyl	95	35500

Reactive Yellow 81	-	C5	None	None	None	None
Reactive Yellow 81	High	R1H	None	None	None	None
Reactive Yellow 81	High	R2H	11.06	Benzaldehyde, 4-methyl-	94	22000
Reactive Yellow 81	High	R3H	None	None	None	None
Reactive Yellow 81	High	R4H	None	None	None	None
Reactive Yellow 81	High	R5H	None	None	None	None
Reactive Yellow 81	High	R6H	NA	NA	NA	NA
Reactive Yellow 81	Medium	R1M	6.44	2-Propanone, 1,3-dichloro	86	7000
Reactive Yellow 81	Medium	R2M	None	None	None	None
Reactive Yellow 81	Medium	R3M	NA	NA	NA	NA
Reactive Yellow 81	Medium	R4M	None	None	None	None
Reactive Yellow 81	Medium	R5M	None	None	None	None
Reactive Yellow 81	Medium	R6M	NA	NA	NA	NA
Reactive Yellow 81	Low	R1L	None	None	None	None
Reactive Yellow 81	Low	R2L	NA	NA	NA	NA
Reactive Yellow 81	Low	R3L	NA	NA	NA	NA
Reactive Yellow 81	Low	R4L	6.44	Propanone, 1,3-dichloro	78	3000
Reactive Yellow 81	Low	R5L	None	None	None	None
Reactive Yellow 81	Low	R6L	NA	NA	NA	NA

C

Dye	Fe level	Oxidation Time	Peak Time (min)	Chemical Name	Percentage	Abundance
Reactive Yellow 81	High	R1H	11.92	Picloxydine	83	15500
Reactive Yellow 81	High	R2H	None	None	None	None
Reactive Yellow 81	High	R3H	NA	NA	NA	NA
Reactive Yellow 81	High	R4H	None	None	None	None
Reactive Yellow 81	High	R5H	None	None	None	None
Reactive Yellow 81	High	R6H	NA	NA	NA	NA
Reactive Yellow 81	Medium	R1M	6.48	2-Propanone, 1,3-dichloro0	56	110000
Reactive Yellow 81	Medium	R2M	None	None	None	None
Reactive Yellow 81	Medium	R3M	NA	NA	NA	NA
Reactive Yellow 81	Medium	R4M	15.34	Benzene, 2,4-diisocyanato-1-methyl-	91	7250
Reactive Yellow 81	Medium	R5M	15.34	Benzene, 2,4-diisocyanato-1-methyl-	91	5800
Reactive Yellow 81	Medium	R6M	NA	NA	NA	NA
Reactive Yellow 81	Low	R1L	NA	NA	NA	NA
Reactive Yellow 81	Low	R2L	None	None	None	None
Reactive Yellow 81	Low	R3L	NA	NA	NA	NA
Reactive Yellow 81	Low	R4L	15.42	Benzene, 2,4-diisocyanato-1-methyl	90	8500
			15.43	Benzene, 2,4-diisocyanato-1-methyl	97	20000
Reactive Yellow 81	Low	R5L	16.16	2-methyl-5,6,7,8-tetrahydroquinoxaline	64	3900
Reactive Yellow 81	Low	R6L	NA	NA	NA	NA

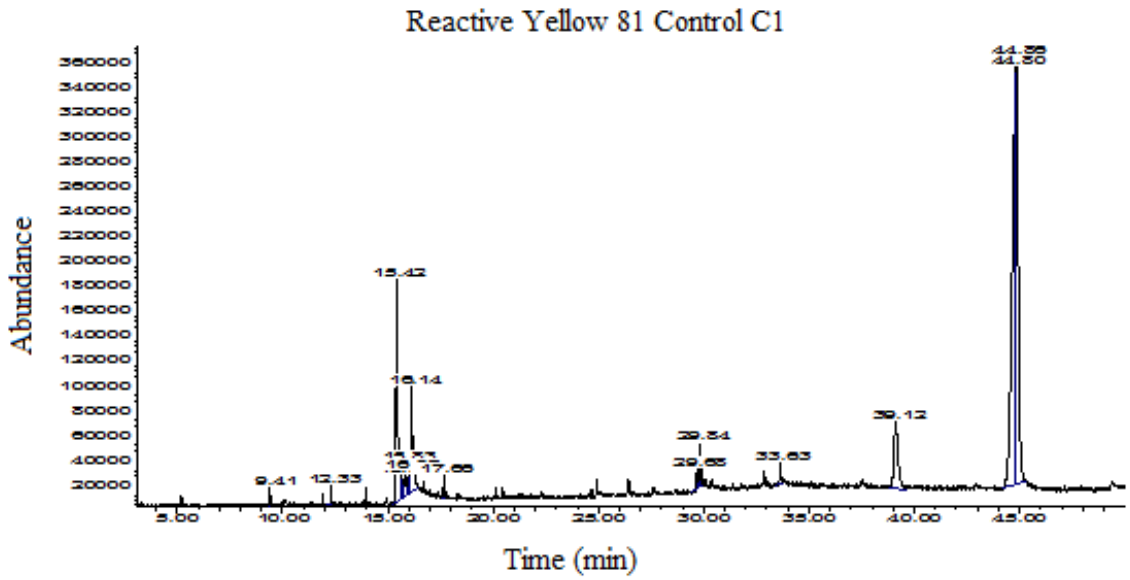

Figure C.6: Total ion GC-MS chromatogram of 5 g/L Reactive Yellow dye Control C1 in the USA. Major peaks are identified in Table C.2.

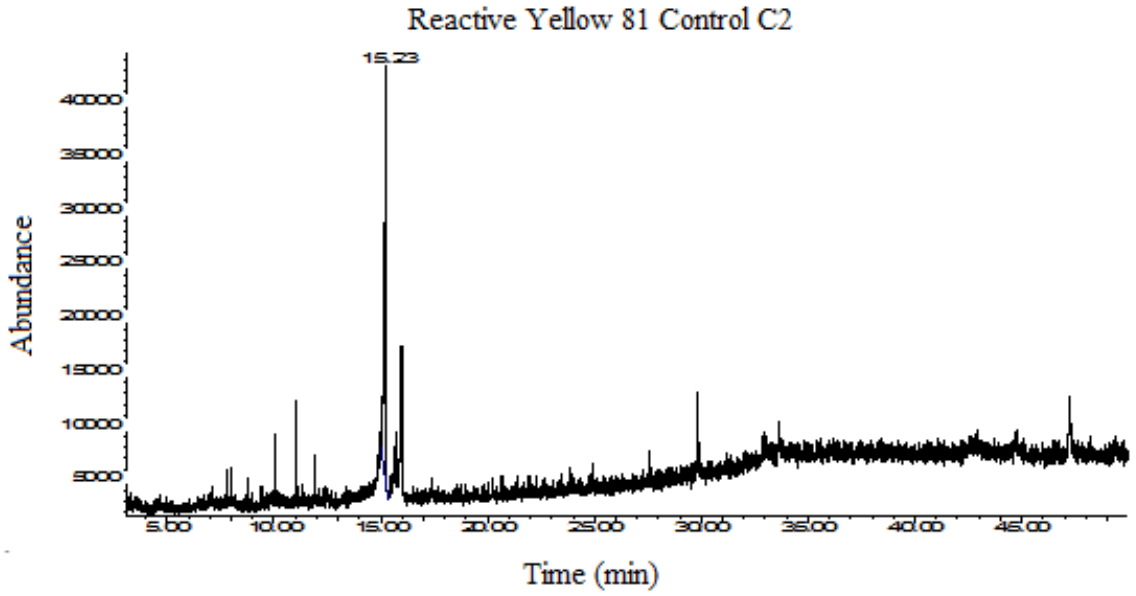

Figure C.7: Total ion GC-MS chromatogram of 5 g/L Reactive Yellow dye Control C2 in the USA. Major peaks are identified in Table C.2.

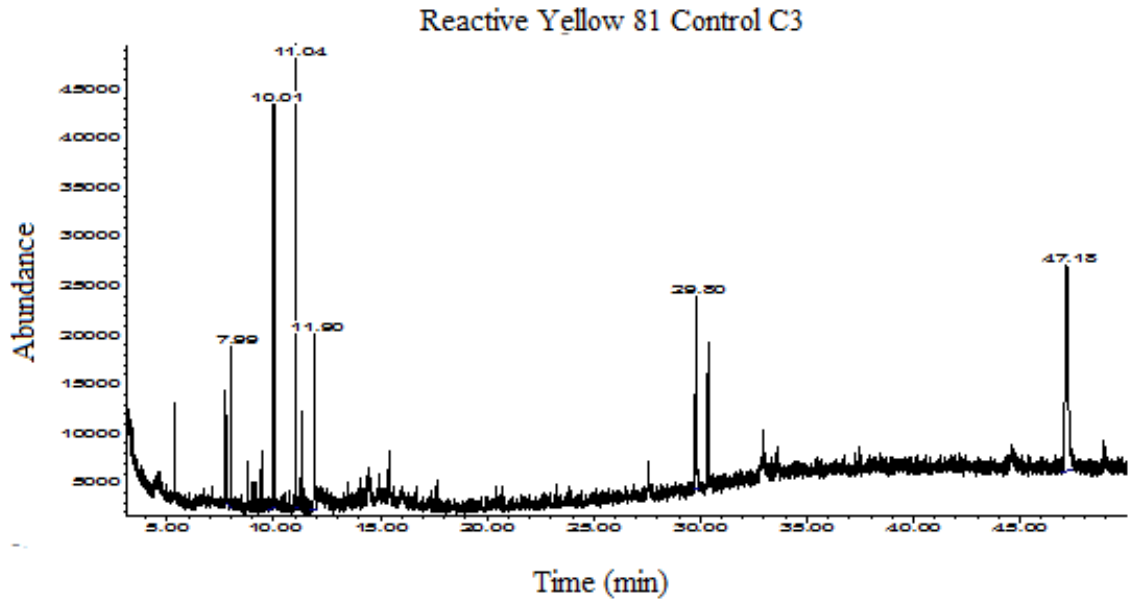

Figure C.8: Total ion GC-MS chromatogram of 5 g/L Reactive Yellow dye Control C3 in the USA. Major peaks are identified in Table C.2.

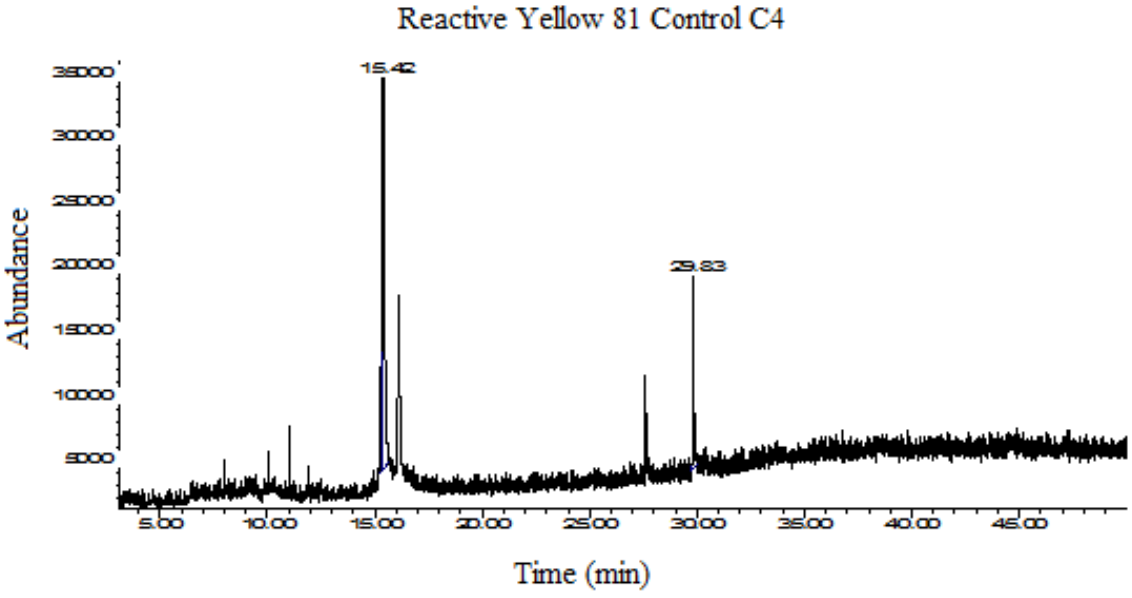

Figure C.9: Total ion GC-MS chromatogram of 5 g/L Reactive Yellow dye Control C4 in the USA. Major peaks are identified in Table C.2.

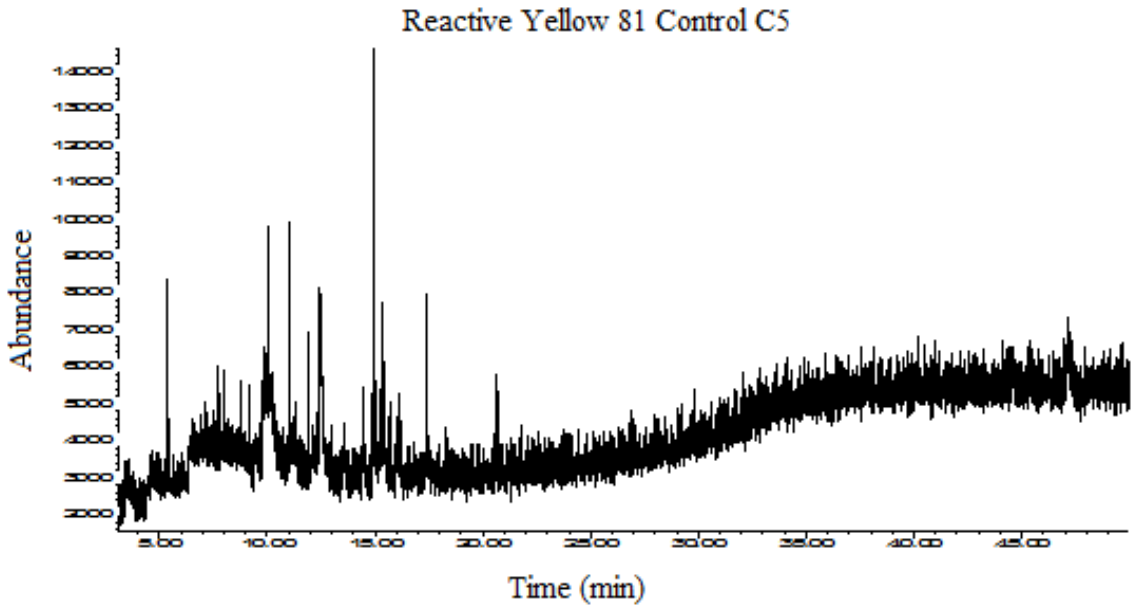

Figure C.10: Total ion GC-MS chromatogram of 5 g/L Reactive Yellow dye Control C5 in the USA. Major peaks are identified in Table C.2.

Table C.3: GC/MS results of 5 g/L Reactive Blue 4 samples R1H-R6H, R1M-R6M, and R1L-R6L in (A) India compared with C1, (B) in USA 1 compared with C1-C5, and (C) in USA2 compared with C1-C5.

A

Dye	Fe level	Oxidation Time	Peak Time (min)	Chemical Name	Percentage	Abundance
Reactive Blue 4	-	C1	-	-	-	-
Reactive Blue 4	High	R1H	NA	NA	NA	NA
Reactive Blue 4	High	R2H	15.42	Benzene, 2,4-diisocyanato-1-methyl	91	7250
Reactive Blue 4	High	R3H	15.43	Benzene, 2,4-diisocyanato-1-methyl	87	9000
			16.16	Methanimidamide, N,N-dimethyl-N'-phenyl-	86	5000
Reactive Blue 4	High	R4H	11.07	Benzaldehyde, 3-methyl-	96	50000
			13.38	Benzaldehyde, 3,4-dimethyl	90	60000
			16.74	1,3,5-Triazin-2-amine, 4,6-dichloro-	95	90000
			17.66	Phenol, 2,4-bis(1,1-dimethylethyl)	94	35000
Reactive Blue 4	High	R5H	17.66	Phenol, 2,4-bis(1,1-dimethylethyl)	91	27000
Reactive Blue 4	High	R6H	13.39	Benzene, 1,3-diisocyanatomethyl-	87	4000
Reactive Blue 4	Medium	R1M	None	None	None	None
Reactive Blue 4	Medium	R2M	None	None	None	None
Reactive Blue 4	Medium	R3M	None	None	None	None
Reactive Blue 4	Medium	R4M	9.44	Cyclotetrasiloxane, octamethyl	64	4600
Reactive Blue 4	Medium	R5M	None	None	None	None
Reactive Blue 4	Medium	R6M	None	None	None	None
Reactive Blue 4	Low	R1L	NA	NA	NA	NA
Reactive Blue 4	Low	R2L	None	None	None	None
Reactive Blue 4	Low	R3L	None	None	None	None
Reactive Blue 4	Low	R4L	None	None	None	None
Reactive Blue 4	Low	R5L	None	None	None	None
Reactive Blue 4	Low	R6L	None	None	None	None

B

Dye	Fe level	Oxidation Time	Peak Time (min)	Chemical Name	Percentage	Abundance
Reactive Blue 4	-	C1	10.4	1-Hexanol, 3,5,5-trimethyl	58	29000
			37.04	1-Amino-4-bromoanthraquinone	62	45000
Reactive Blue 4	-	C2	10.38	1-Hexanol, 3,5,5-trimethyl	90	60000
			11.05	1-Hexanol, 3,5,5-trimethyl	87	19000
			37.02	Benzaldehyde, 3-methyl	72	27000
Reactive Blue 4	-	C3	15.42	4H-3,1-Benzaxazin-4-diisocyanato-1-methyl	96	91000
			16.73	1,3,5-Triazin-2-amine, 4,6-dichloro	95	22500
Reactive Blue 4	-	C4	10.4	1-Hexanol, 3,5,5-trimethyl	86	32000
			15.33	Benzene, 2,4-diisocyanato-1-methyl	86	28500
			15.42	Benzene, 2,4-diisocyanato-1-methyl	94	21000
Reactive Blue 4	-	C5	16.72	1,3-Dichloro-2-fluorobenzene	58	47000
Reactive Blue 4	High	R1H	16.75	1,3,5-Triazin-2-amine,4,6-dichloro-	96	150000
Reactive Blue 4	High	R2H	None	None	None	None
Reactive Blue 4	High	R3H	None	None	None	None
Reactive Blue 4	High	R4H	16.75	1,3,5-Triazin-2-amine,4,6-dichloro-	97	53500
Reactive Blue 4	High	R5H	None	None	None	None
Reactive Blue 4	High	R6H	NA	NA	NA	NA
Reactive Blue 4	Medium	R1M	16.75	1,3,5-Triazin-2-amine, 4,6-dichloro	96	180000
Reactive Blue 4	Medium	R2M	None	None	None	None
Reactive Blue 4	Medium	R3M	NA	NA	NA	NA
Reactive Blue 4	Medium	R4M	16.74	1,3,5-Triazin-2-amine, 4,6-dichloro	97	39000
Reactive Blue 4	Medium	R5M	9.18	Phenol, 2-chloro	83	6500
Reactive Blue 4	Medium	R6M	NA	NA	NA	NA
Reactive Blue 4	Low	R1L	None	None	None	None
Reactive Blue 4	Low	R2L	None	None	None	None
Reactive Blue 4	Low	R3L	NA	NA	NA	NA
Reactive Blue 4	Low	R4L	None	None	None	None
Reactive Blue 4	Low	R5L	9.15	Phenol, 2-chloro0	94	16800
Reactive Blue 4	Low	R6L	NA	NA	NA	NA

C

Dye	Fe level	Oxidation Time	Peak Time (min)	Chemical Name	Percentage	Abundance
Reactive Blue 4	High	R1H	16.74	1,3,5-Triazin-1-amine, 4,6-dichloro-	97	200000
Reactive Blue 4	High	R2H	None	None	None	None
Reactive Blue 4	High	R3H	NA	NA	NA	NA
Reactive Blue 4	High	R4H	16.74	1,3,5-Triazin-2-amine, 4,6-dichloro-	95	22500
Reactive Blue 4	High	R5H	None	None	None	None
Reactive Blue 4	High	R6H	None	None	None	None
Reactive Blue 4	Medium	R1M	None	None	None	None
Reactive Blue 4	Medium	R2M	8.05	2-Heptanone, 4-methyl-	43	5200
Reactive Blue 4	Medium	R3M	NA	NA	NA	NA
Reactive Blue 4	Medium	R4M	16.75	1,3,5-Triazin-2-amine, 4,6-dichloro	93	11000
Reactive Blue 4	Medium	R5M	9.18	Phenol, 2-chloro	91	10600
Reactive Blue 4	Medium	R6M	NA	NA	NA	NA
Reactive Blue 4	Low	R1L	16.73	1,3,5-Triazin-2-amine, 4,6-dichloro-	90	15000
Reactive Blue 4	Low	R2L	15.42	Benzene, 2,4-diisocyanato-1-methyl-	72	4700
			16.16	2H-Benzimidazol-2-one, 1,3-dihydro-5-methyl-	90	3400
Reactive Blue 4	Low	R3L	NA	NA	NA	NA
Reactive Blue 4	Low	R4L	16.72	1,3,5-Triazin-2-amine, 4,6-dichloro-	93	21000
Reactive Blue 4	Low	R5L	15.32	Benzene, 2,4-diisocyanato-1-methyl-	95	19000
Reactive Blue 4	Low	R6L	NA	NA	NA	NA

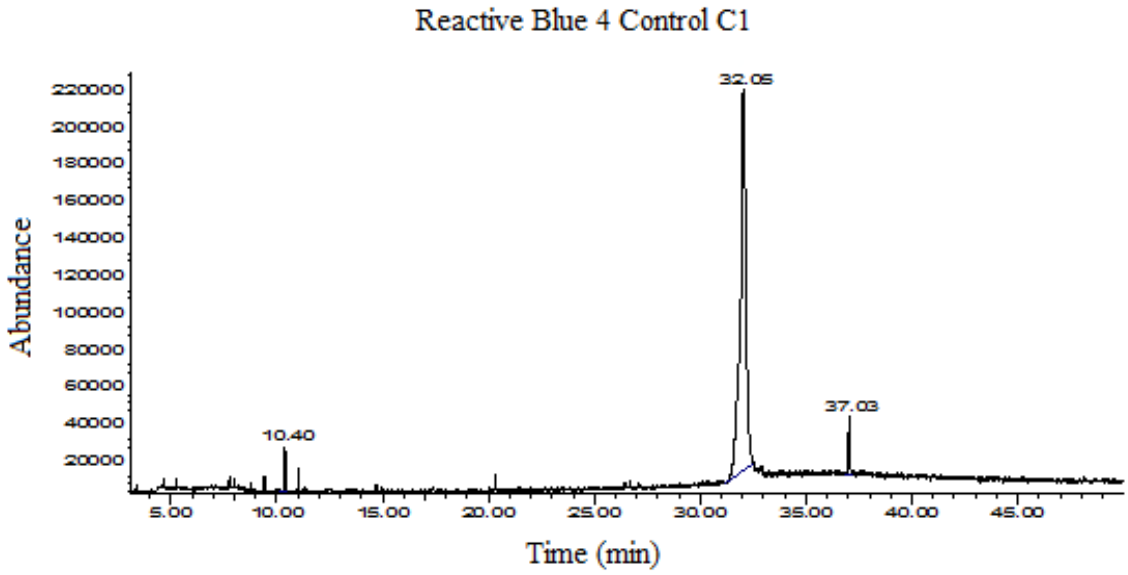

Figure C.11: Total ion GC-MS chromatogram of 5 g/L Reactive Blue dye Control C1 in the USA. Major peaks are identified in Table C.3.

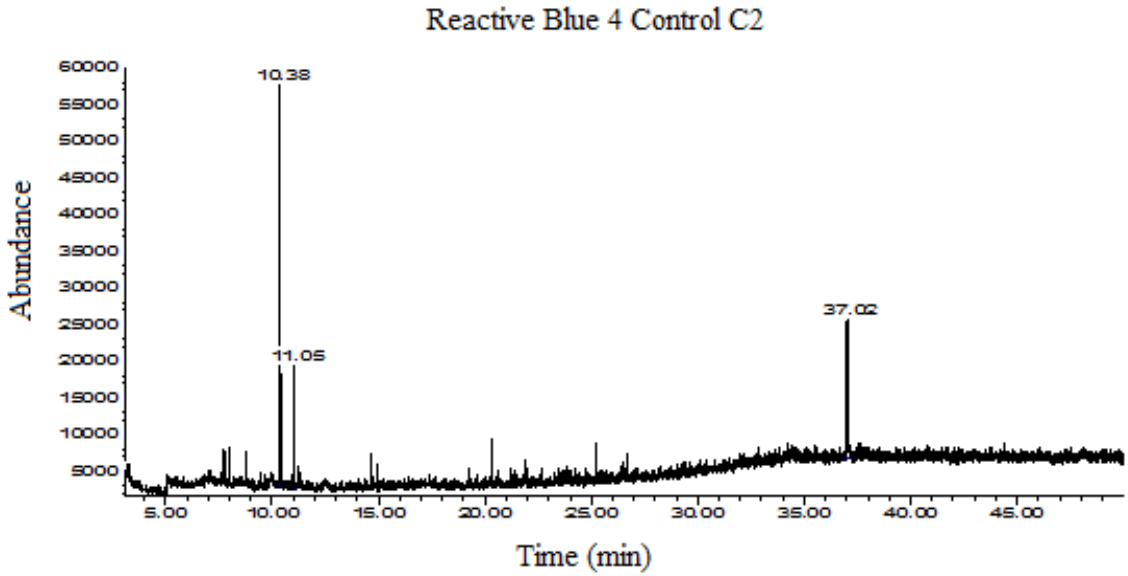

Figure C.12: Total ion GC-MS chromatogram of 5 g/L Reactive Blue dye Control C2 in the USA. Major peaks are identified in Table C.3.

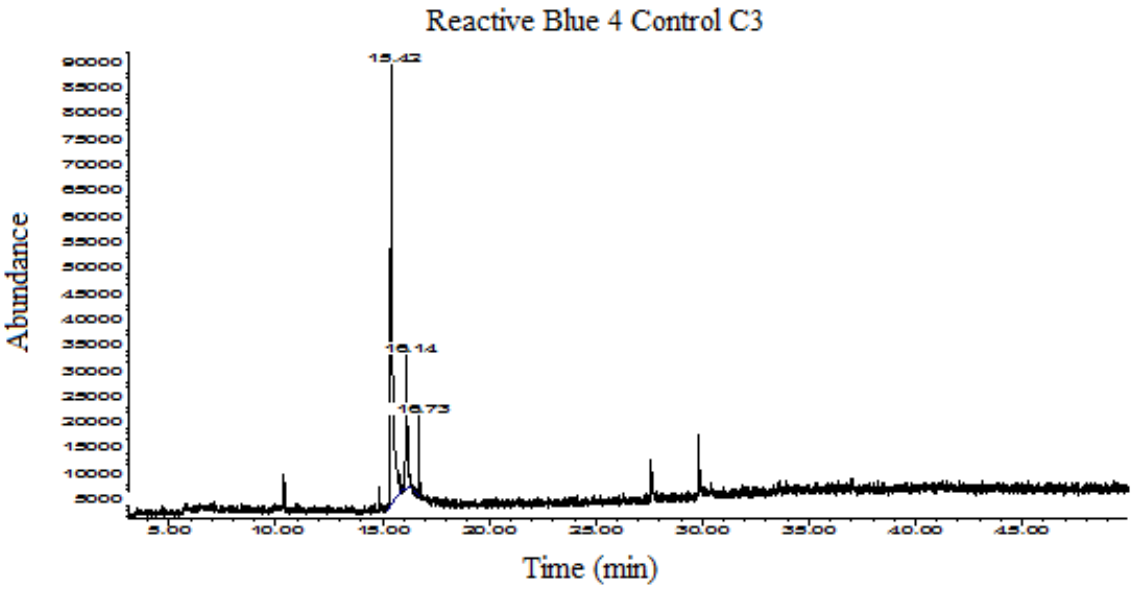

Figure C.13: Total ion GC-MS chromatogram of 5 g/L Reactive Blue 4 dye C3 in the USA. Major peaks are identified in Table C.3

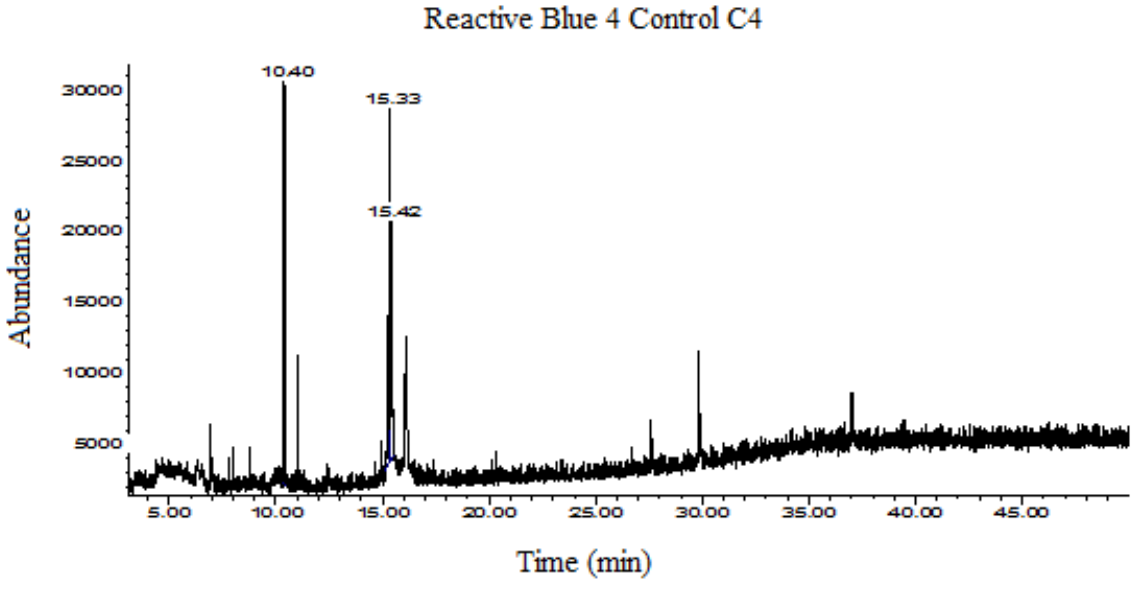

Figure C.14: Total ion GC-MS chromatogram of 5 g/L Reactive Blue dye Control C4. Major peaks are identified in Table C.3.

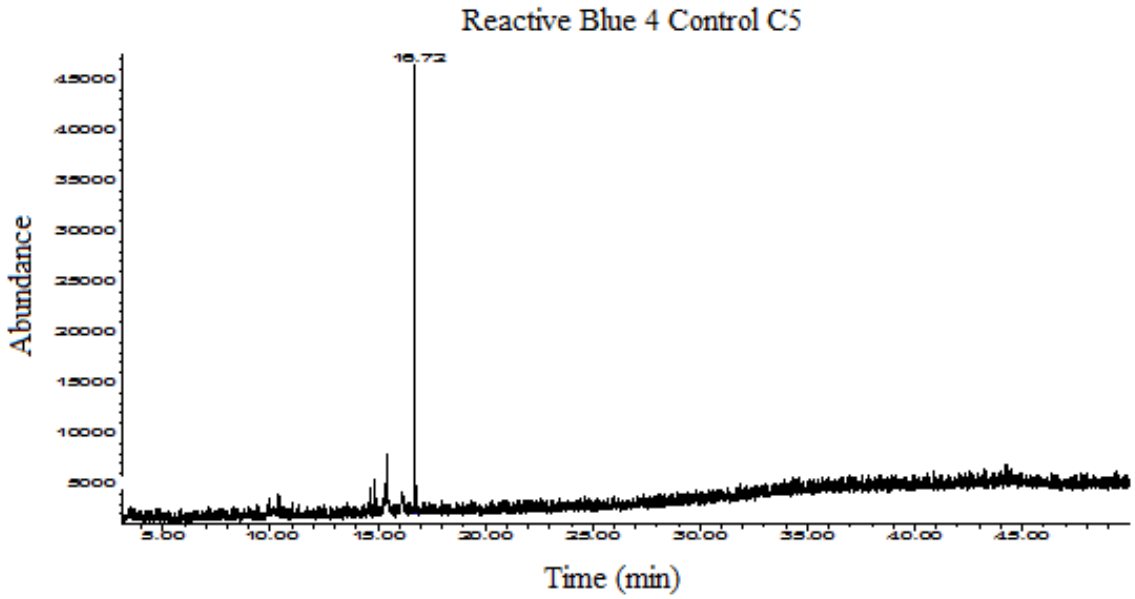

Figure C.15: Total ion GC-MS chromatogram of 5 g/L Reactive Blue dye Control C5 in the USA. Major peaks are identified in Table C.3.

Table C.4: GC/MS results of 5 g/L Acid Fast Red samples A1-A12 in (A) India compared with C1, (B) in USA 1 compared with C1-C5, and (C) in USA2 compared with C1-C5.

A

Dye	Oxidation Time	Peak Time (min)	Chemical Name	Percentage	Abundance
Acid Fast Red	C1	17.85	2-Naphthalenol	91	47000
Acid Fast Red	A1	NA	NA	NA	NA
Acid Fast Red	A2	None	None	None	None
Acid Fast Red	A3	None	None	None	None
Acid Fast Red	A4	32.28	1,1,1,5,7,7,7-Heptamethyl-3,3-bis(trimethylsiloxy)tetrasiloxane	37	6000
Acid Fast Red	A5	NA	NA	NA	NA
Acid Fast Red	A6	17.65	Phenol, 2,4-bis(1,1-dimethylethyl)	90	7250
Acid Fast Red	A7	None	None	None	None
Acid Fast Red	A8	None	None	None	None
Acid Fast Red	A9	17.64	[[4-(1,1-dimethylethyl)phenoxy]methyl]-	86	7800
Acid Fast Red	A10	None	None	None	None
Acid Fast Red	A11	None	None	None	None
Acid Fast Red	A12	None	None	None	None

B

Dye	Oxidation Time	Peak Time (min)	Chemical Name	Percentage	Abundance
Acid Fast Red	C1	11.04	Benzaldehyde, 4-methyl	90	35000
		17.81	2-Naphthalenol	91	375000
Acid Fast Red	C2	11.04	Benzaldehyde, 3-methyl	91	50000
		17.82	2-Naphthalenol	91	1060000
		19.86	bromo	97	70000
		38.9	[1,1'-Binaphthalene]-2,2'-diol	96	25000
Acid Fast Red	C3	17.84	2-Naphthalenol	93	33000
		19.88	bromo	91	17000
Acid Fast Red	C4	17.84	2-Naphthalenol	93	120000
Acid Fast Red	C5	16.19	1,4-Naphthalenedione	96	170000
Acid Fast Red	A1	17.84	2-Naphthalenol	90	2750
Acid Fast Red	A2	None	None	None	None
Acid Fast Red	A3	NA	NA	NA	NA
Acid Fast Red	A4	None	None	None	None
Acid Fast Red	A5	None	None	None	None
Acid Fast Red	A6	NA	NA	NA	NA
Acid Fast Red	A7	None	None	None	None
Acid Fast Red	A8	8.51	Benzaldehyde	83	8250
		11.99	Benzenemethanamine, N-ethyl-	74	2600
Acid Fast Red	A9	NA	NA	NA	NA
Acid Fast Red	A10	None	None	None	None
Acid Fast Red	A11	None	None	None	None
Acid Fast Red	A12	NA	NA	NA	NA

C

Dye	Oxidation Time	Peak Time (min)	Chemical Name	Percentage	Abundance
Acid Fast Red	A1	17.84	2-Naphthalenol	90	18000
Acid Fast Red	A2	10.93	Benzaldehyde, 4-methyl-	83	5000
Acid Fast Red	A3	NA	NA	NA	NA
Acid Fast Red	A4	None	None	None	None
Acid Fast Red	A5	None	None	None	None
Acid Fast Red	A6	NA	NA	NA	NA
Acid Fast Red	A7	None	None	None	None
Acid Fast Red	A8	8.54	Benzaldehyde	91	16000
Acid Fast Red	A9	NA	NA	NA	NA
Acid Fast Red	A10	15.42	Benzene, 2,4-diisocyanato-1-methyl-	64	4200
Acid Fast Red	A11	11.91	Benzenemethanamine, N-ethyl-	93	110000
Acid Fast Red	A12	NA	NA	NA	NA

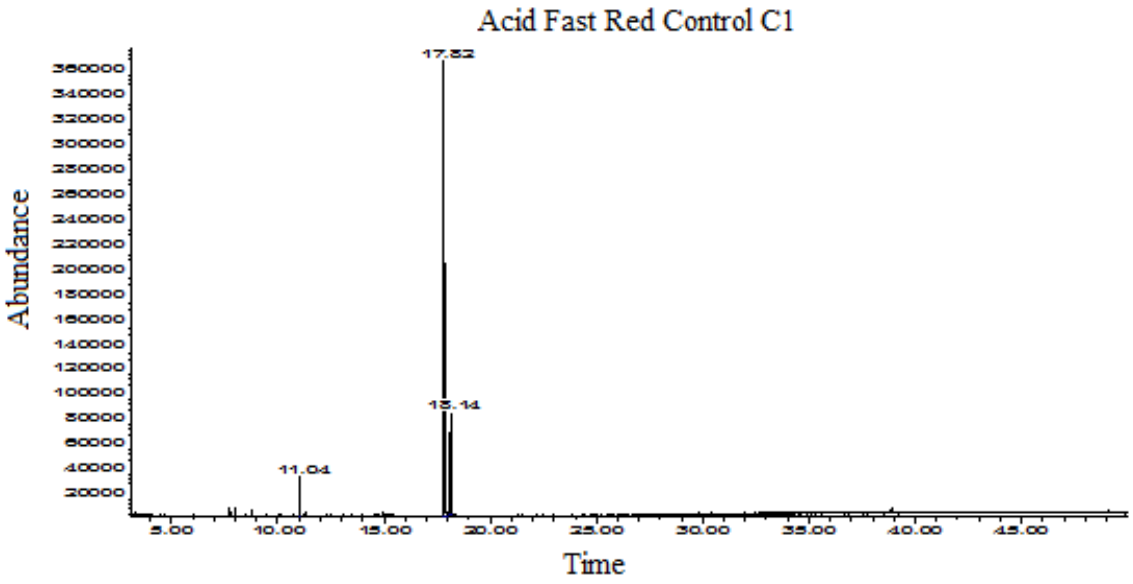

Figure C.16: Total ion GC-MS chromatogram of 5 g/L Acid Fast Red dye Control C1 in the USA. Major peaks are identified in Table C.4.

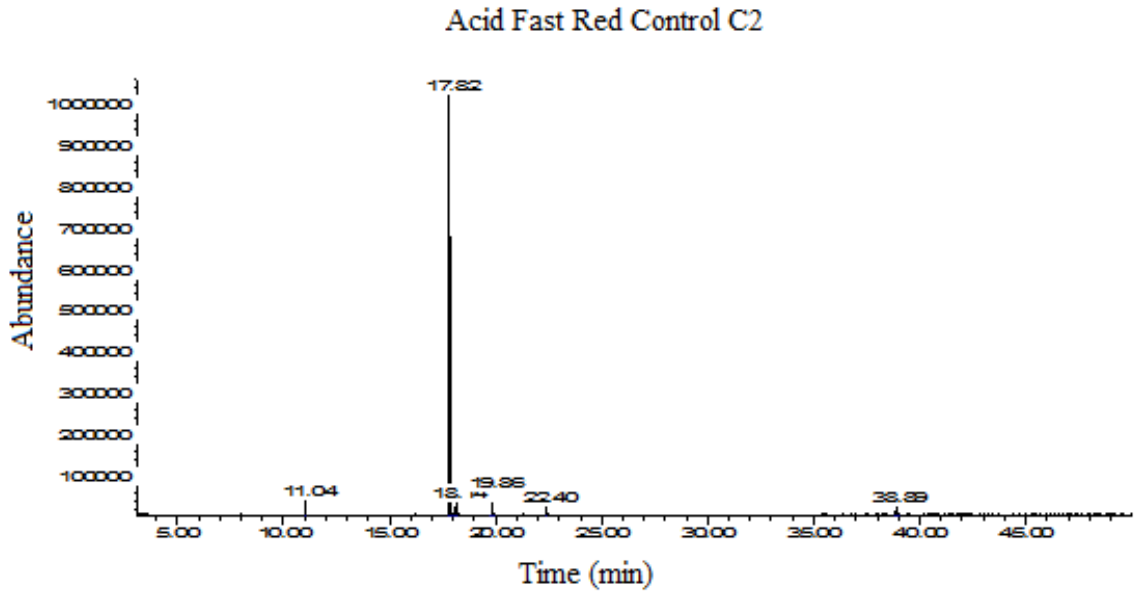

Figure C.17: Total ion GC-MS chromatogram of 5 g/L Acid Fast Red dye Control C2 in the USA. Major peaks are identified in Table C.4.

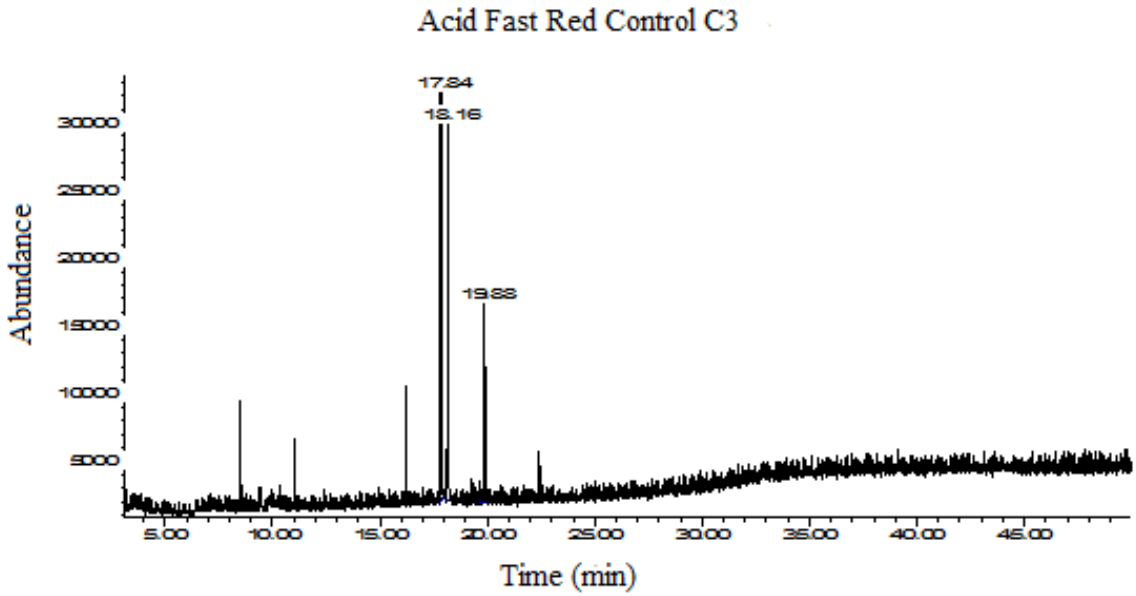

Figure C.18: Total ion GC-MS chromatogram of 5 g/L Acid Fast Red dye Control C3 in the USA. Major peaks are identified in Table C.4.

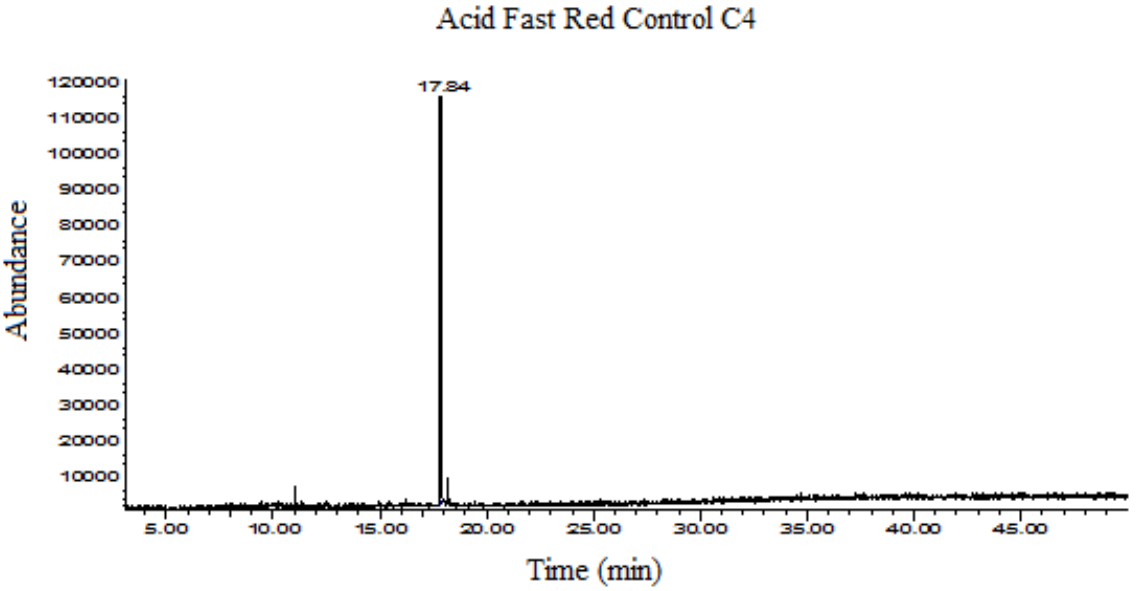

Figure C.19: Total ion GC-MS chromatogram of 5 g/L Acid Fast Red dye Control C4 in the USA. Major peaks are identified in Table C.4.

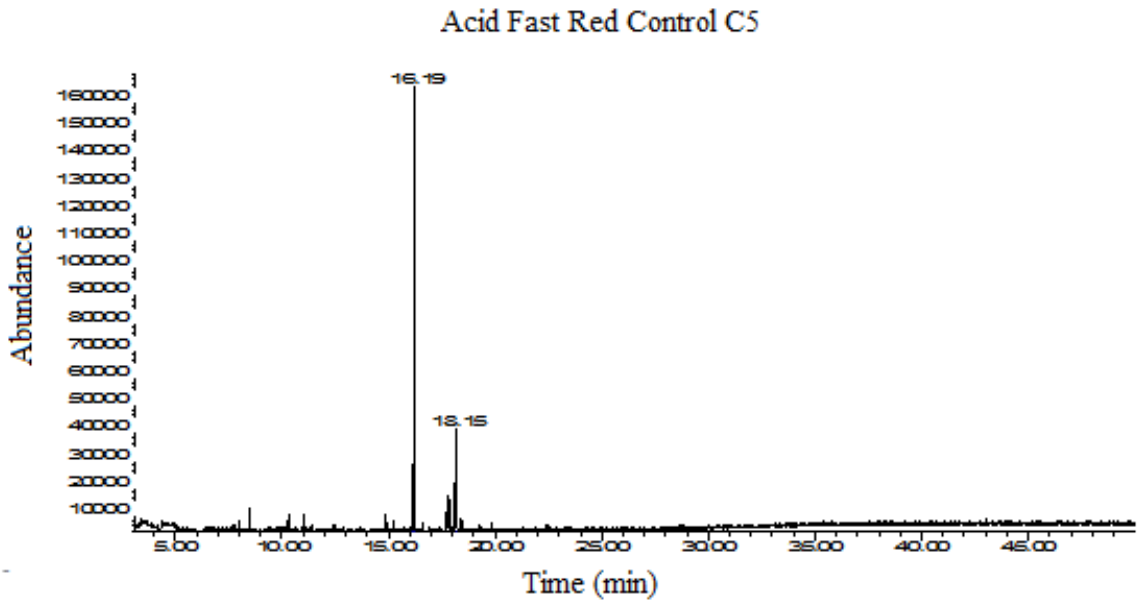

Figure C.20: Total ion GC-MS chromatogram of 5 g/L Acid Fast Red dye Control C5 in the USA. Major peaks are identified in Table C.4.

Table C.5: GC/MS results of 5 g/L Acid Golden Yellow samples A1-A12 in (A) India compared with C1, (B) in USA 1 compared with C1-C5, and (C) in USA2 compared with C1-C5.

A

Dye	Oxidation Time	Peak Time (min)	Chemical Name	Percentage	Abundance
Acid Golden Yellow	C1	None	None	None	None
Acid Golden Yellow	A1	NA	NA	NA	NA
Acid Golden Yellow	A2	17.65	Phenol, bis(1,1-dimethylethyl)-	83	6800
Acid Golden Yellow	A3	None	None	None	None
Acid Golden Yellow	A4	17.65	Phenol, bis(1,1-dimethylethyl)-	90	5300
Acid Golden Yellow	A5	None	None	None	None
Acid Golden Yellow	A6	None	None	None	None
Acid Golden Yellow	A7	None	None	None	None
Acid Golden Yellow	A8	17.65	Oxirane, [[4-(1,1-dimethylethyl)phenoxy]methyl]-	86	8200
Acid Golden Yellow	A9	None	None	None	None
Acid Golden Yellow	A10	None	None	None	None
Acid Golden Yellow	A11	None	None	None	None
Acid Golden Yellow	A12	None	None	None	None

B

Dye	Oxidation Time	Peak Time (min)	Chemical Name	Percentage	Abundance
Acid Golden Yellow	C1	None	None	None	None
Acid Golden Yellow	C2	8.99	Phenol	90	20750
		11.05	Benzaldehyde, 3-methyl	91	24500
Acid Golden Yellow	C3	None	None	None	None
Acid Golden Yellow	C4	None	None	None	None
Acid Golden Yellow	C5	9.24	Benzene, ethoxy	94	127000
		13.01	Parachlorophenol	96	65000
		14.95	Cyclohexasiloxane, dodecamethyl	86	15500
Acid Golden Yellow	A1	17.84	Benzene, 1-cyclopenten-1-yl-	74	2700
Acid Golden Yellow	A2	None	None	None	None
Acid Golden Yellow	A3	NA	NA	NA	NA
Acid Golden Yellow	A4	None	None	None	None
Acid Golden Yellow	A5	None	None	None	None
Acid Golden Yellow	A6	NA	NA	NA	NA
Acid Golden Yellow	A7	None	None	None	None
Acid Golden Yellow	A8	None	None	None	None
Acid Golden Yellow	A9	NA	NA	NA	NA
Acid Golden Yellow	A10	None	None	None	None
Acid Golden Yellow	A11	None	None	None	None
Acid Golden Yellow	A12	NA	NA	NA	NA

C

Dye	Oxidation Time	Peak Time (min)	Chemical Name	Percentage	Abundance
Acid Golden Yellow	A1	None	None	None	None
Acid Golden Yellow	A2	None	None	None	None
Acid Golden Yellow	A3	NA	NA	NA	NA
Acid Golden Yellow	A4	None	None	None	None
Acid Golden Yellow	A5	11.06	Benzaldehyde, 4-methyl-	91	20500
Acid Golden Yellow	A6	NA	NA	NA	NA
Acid Golden Yellow	A7	None	None	None	None
Acid Golden Yellow	A8	8.51	Benzaldehyde	64	12500
Acid Golden Yellow	A9	NA	NA	NA	NA
Acid Golden Yellow	A10	None	None	None	None
Acid Golden Yellow	A11	8.51	Benzaldehyde	91	1100
Acid Golden Yellow	A12	NA	NA	NA	NA

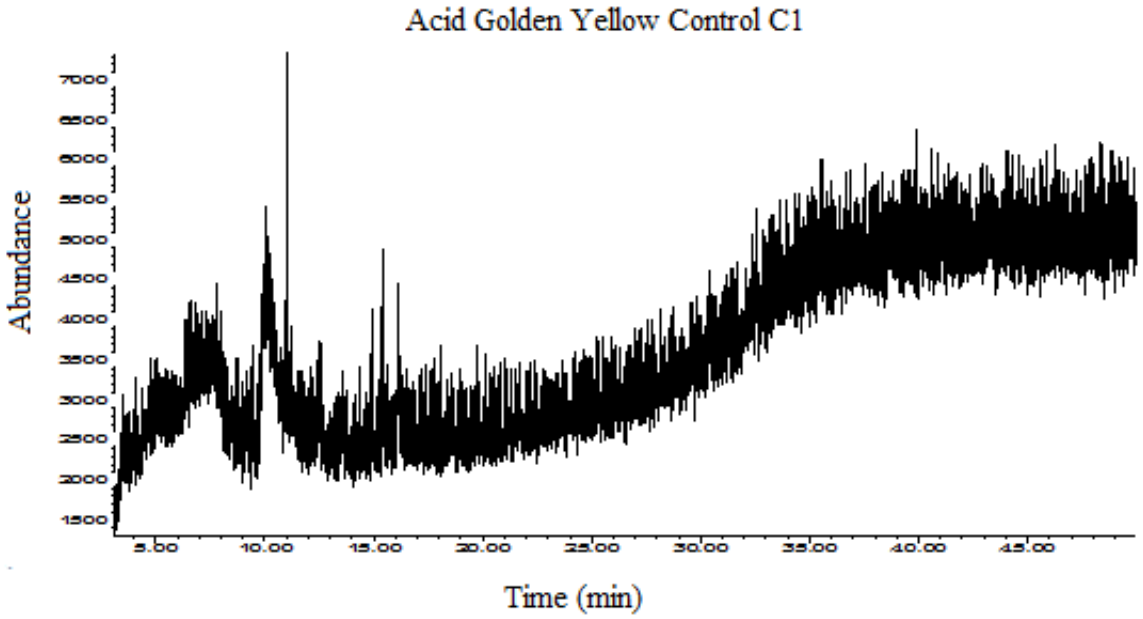

Figure C.21: Total ion GC-MS chromatogram of 5 g/l Acid Golden Yellow dye Control C1 in the USA. Major peaks are identified in Table C.5.

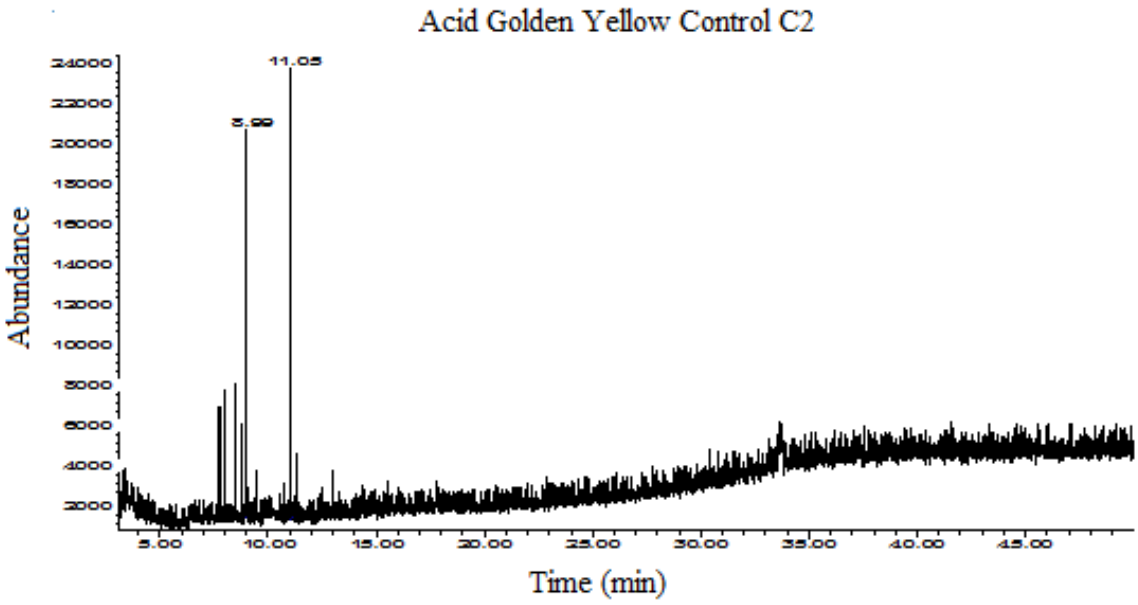

Figure C.22: Total ion GC-MS chromatogram of 5 g/L Acid Golden Yellow dye Control C2 in the USA. Major peaks are identified in Table C.5.

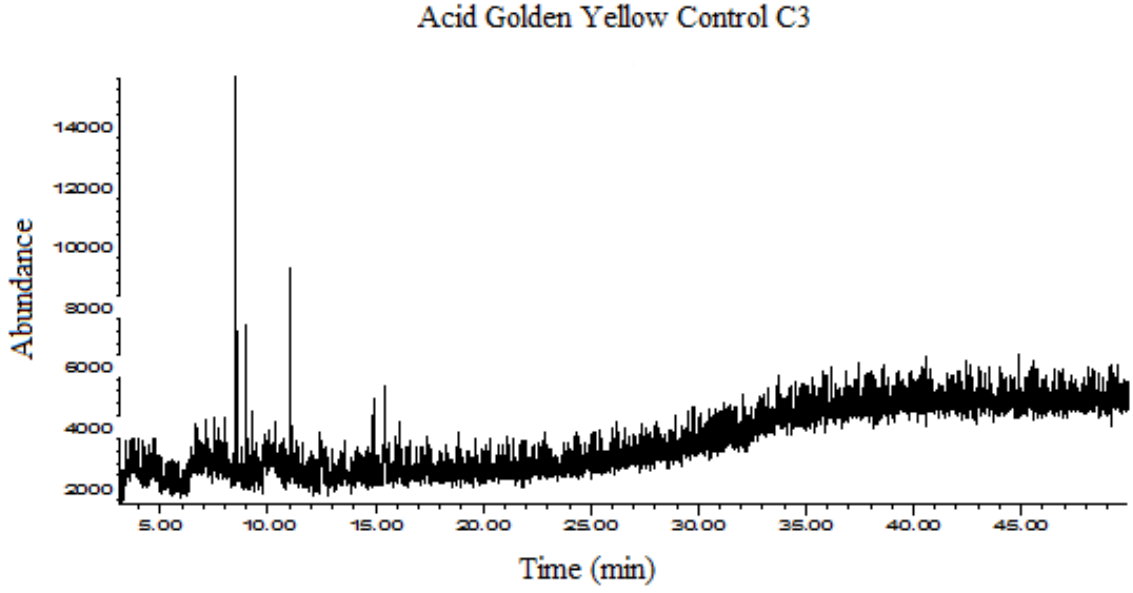

Figure C.23: Total ion GC-MS chromatogram of 5 g/L Acid Golden Yellow dye Control C3 in the USA. Major peaks are identified in Table C.5.

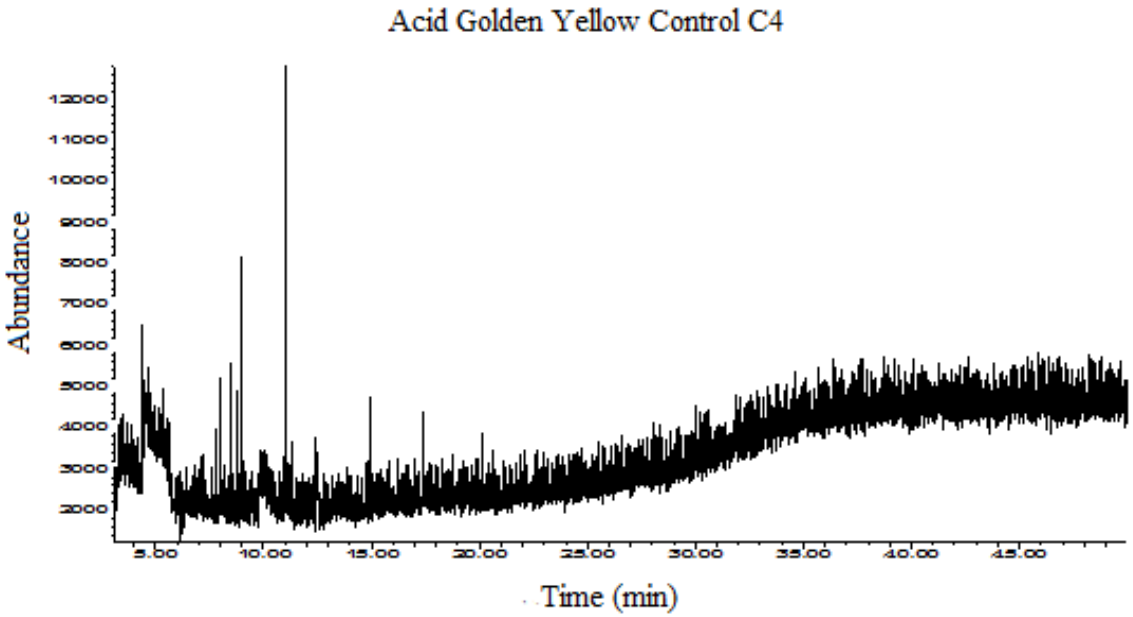

Figure C.24: GC/MS results of 5 g/L Acid Golden Yellow dye Control C4 in the USA. Major peaks are identified in Table C.5.

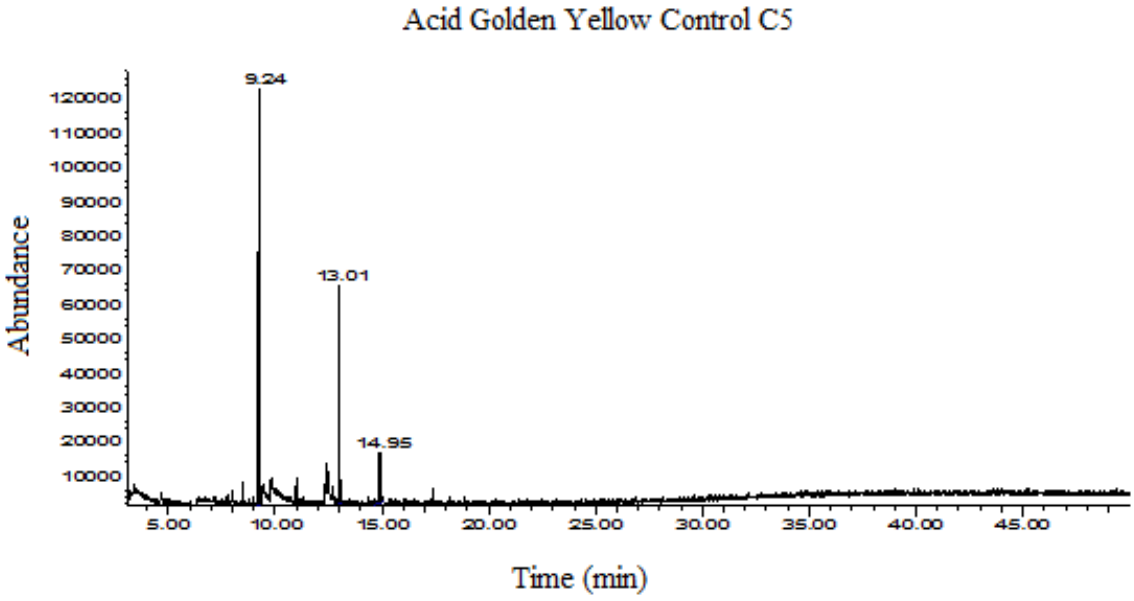

Figure C.25: GC/MS results of 5 g/L Acid Golden Yellow dye Control C5 in the USA. Major peaks are identified in Table C.5.

Table C.6: GC/MS results of 5 g/L Acid Ananda Blue samples A1-A12 in (A) India compared with C1, (B) in USA 1 compared with C1-C5, and (C) in USA2 compared with C1-C5.

A

Dye	Oxidation Time	Peak Time (min)	Chemical Name	Percentage	Abundance
Acid Ananda Blue	C1	22.64	Benzenemethanamine, N-ethyl-N-phenyl-	91	9500
AB	A1	NA	NA	NA	NA
Acid Ananda Blue	A2	None	None	None	None
Acid Ananda Blue	A3	None	None	None	None
Acid Ananda Blue	A4	None	None	None	None
Acid Ananda Blue	A5	None	None	None	None
Acid Ananda Blue	A6	None	None	None	None
Acid Ananda Blue	A7	NA	NA	NA	NA
Acid Ananda Blue	A8	None	None	None	None
Acid Ananda Blue	A9	17.65	Phenol, 2,4-bis(1,1-dimethylethyl)	83	9500
Acid Ananda Blue	A10	None	None	None	None
Acid Ananda Blue	A11	17.64	Phenol, bis(1,1-dimethylethyl)-	83	10750
Acid Ananda Blue	A12	None	None	None	None

B

Dye	Oxidation Time	Peak Time (min)	Chemical Name	Percentage	Abundance
Acid Ananda Blue	C1	None	None	None	None
Acid Ananda Blue	C2	8.5	Benzaldehyde	94	310000
		14.21	2-Propenal, 3-phenyl	90	35000
		22.62	Benzenemethanamine, N-ethyl-N-phenyl	93	20000
Acid Ananda Blue	C3	8.49	Benzaldehyde	94	760000
		9.01	Phenol	87	40000
		10.31	Benzaldehyde, 2-hydroxy	95	280000
Acid Ananda Blue	C4	8.5	Benzaldehyde	94	255000
		14.21	2-Propenal, 3-phenyl	91	40000
		22.63	Benzenemethanamine, N-ethyl-N-phenyl	90	30000
Acid Ananda Blue	C5	8.5	Benzaldehyde	94	170000
		9.01	Phenol	87	22000
		10.31	Benzaldehyde, 2-hydroxyl	94	140000
Acid Ananda Blue	A1	None	None	None	None
Acid Ananda Blue	A2	None	None	None	None
Acid Ananda Blue	A3	NA	NA	NA	NA
Acid Ananda Blue	A4	None	None	None	None
Acid Ananda Blue	A5	None	None	None	None
Acid Ananda Blue	A6	NA	NA	NA	NA
Acid Ananda Blue	A7	None	None	None	None
Acid Ananda Blue	A8	8.55	Benzaldehyde	90	7600
Acid Ananda Blue	A9	NA	NA	NA	NA
Acid Ananda Blue	A10	None	None	None	None
Acid Ananda Blue	A11	6.21	Benzaldehyde	53	3850
		9.83	Cyclotetrasiloxane, oxtamethyl	64	4400
		12.45	Cyclopentasiloxane, decamethyl	64	5900
		14.95	Cyclohexasiloxane, dodecamethyl	78	5800
Acid Ananda Blue	A12	NA	NA	NA	NA

C

Dye	Oxidation Time	Peak Time (min)	Chemical Name	Percentage	Abundance
Acid Ananda Blue	A1	None	None	None	None
Acid Ananda Blue	A2	None	None	None	None
Acid Ananda Blue	A3	NA	NA	NA	NA
Acid Ananda Blue	A4	None	None	None	None
Acid Ananda Blue	A5	None	None	None	None
Acid Ananda Blue	A6	NA	NA	NA	NA
Acid Ananda Blue	A7	None	None	None	None
Acid Ananda Blue	A8	None	None	None	None
Acid Ananda Blue	A9	NA	NA	NA	NA
Acid Ananda Blue	A10	8.51	Benzaldehyde	83	9250
Acid Ananda Blue	A11	8.51	Benzaldehyde	87	20000
		11.9	Benzenemethanamine, N-ethyl-	93	420000
Acid Ananda Blue	A12	NA	NA	NA	NA

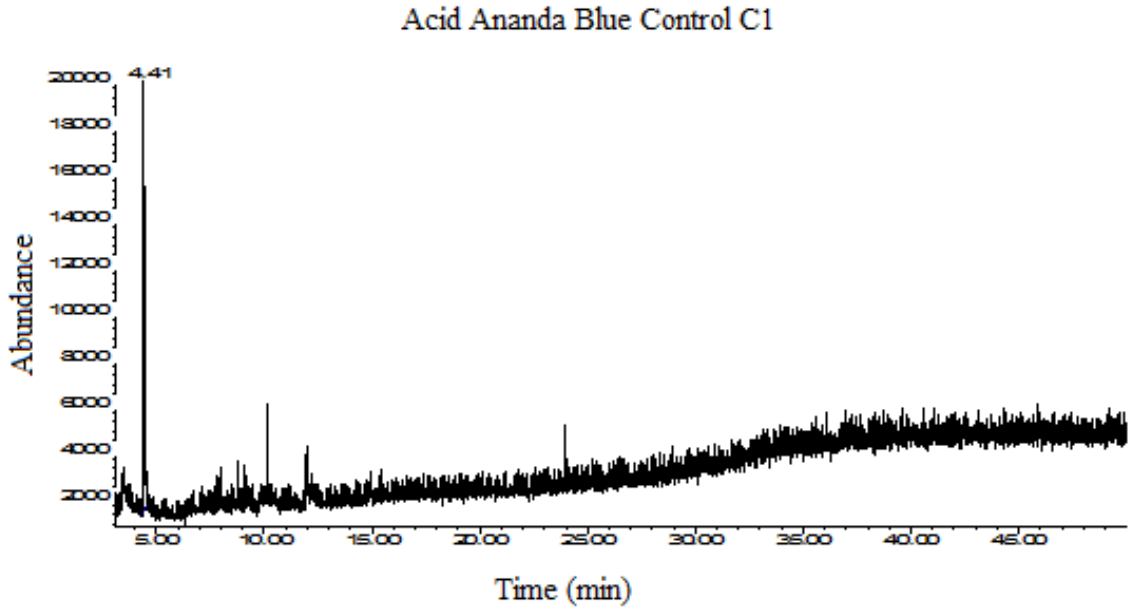

Figure C.26: Total ion GC-MS chromatogram of 5 g/L Acid Ananda Blue dye Control C1 in the USA. Major peaks are identified in Table C.6.

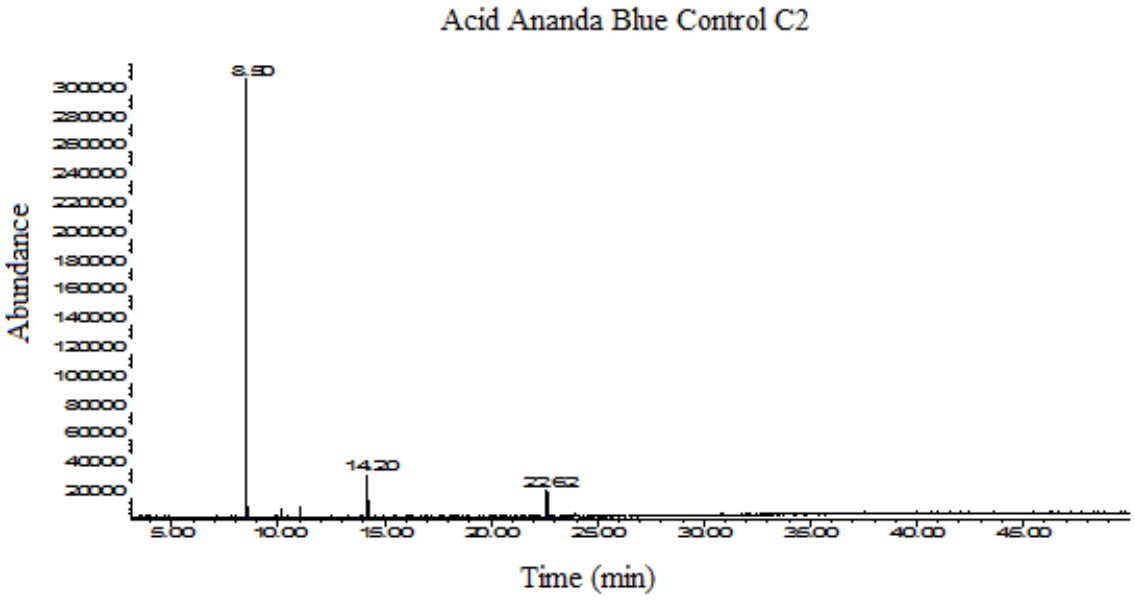

Figure C.27: Total ion GC-MS chromatogram of 5 g/L Acid Ananda Blue dye Control C2 in the USA. Major peaks are identified in Table C.6.

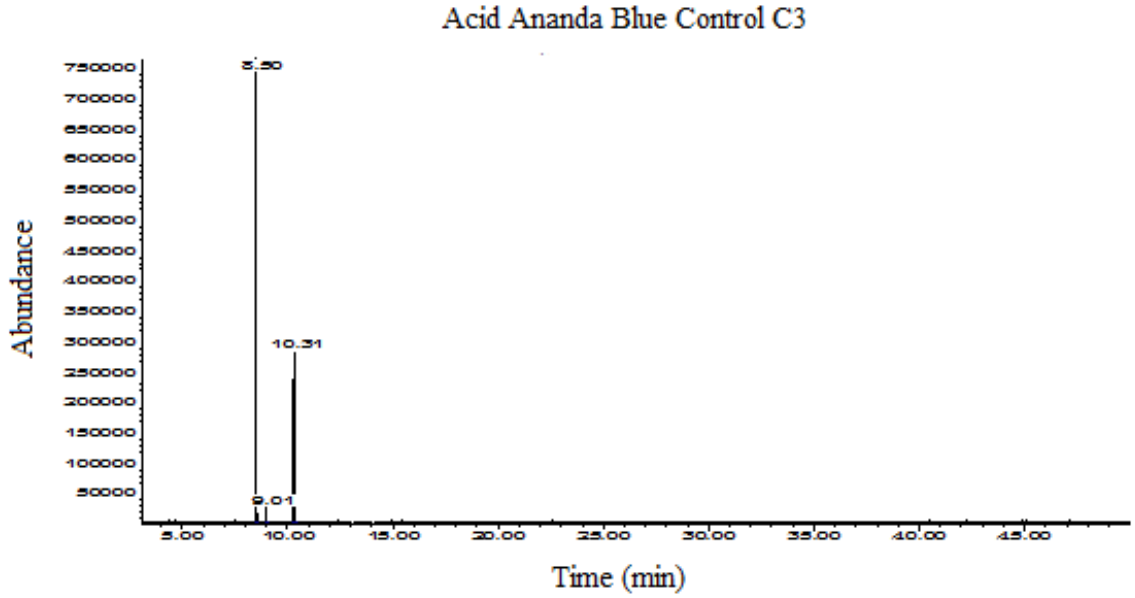

Figure C.28: Total ion GC-MS chromatogram of 5 g/L Acid Ananda Blue dye Control C3 in the USA. Major peaks are identified in Table C.6.

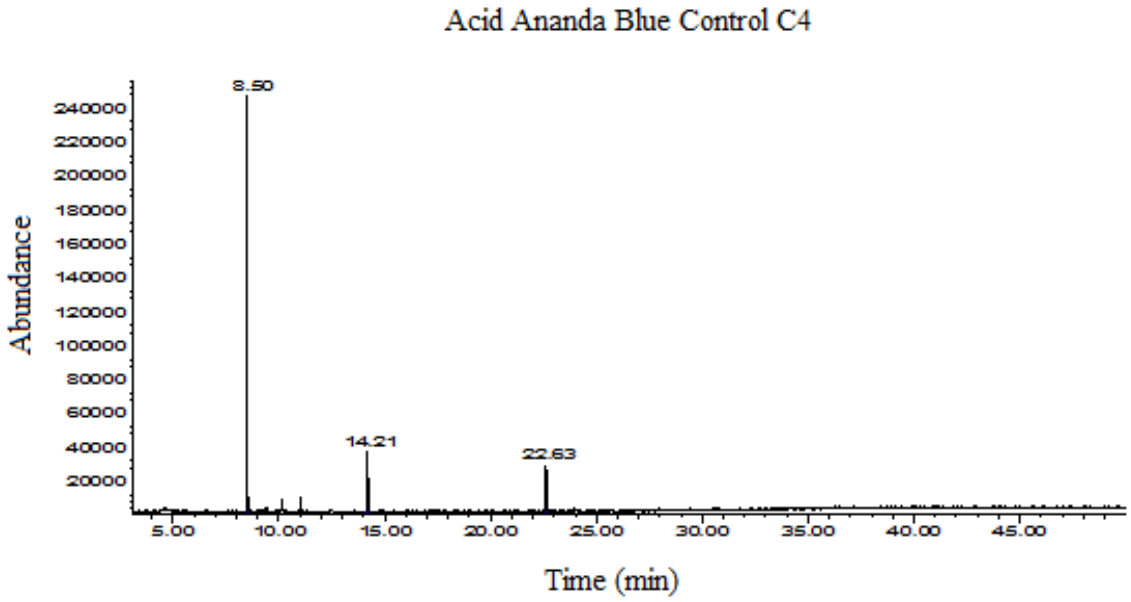

Figure C.29: Total ion GC-MS chromatogram of 5 g/L Acid Ananda Blue dye Control C4 in the USA. Major peaks are identified in Table C.6.

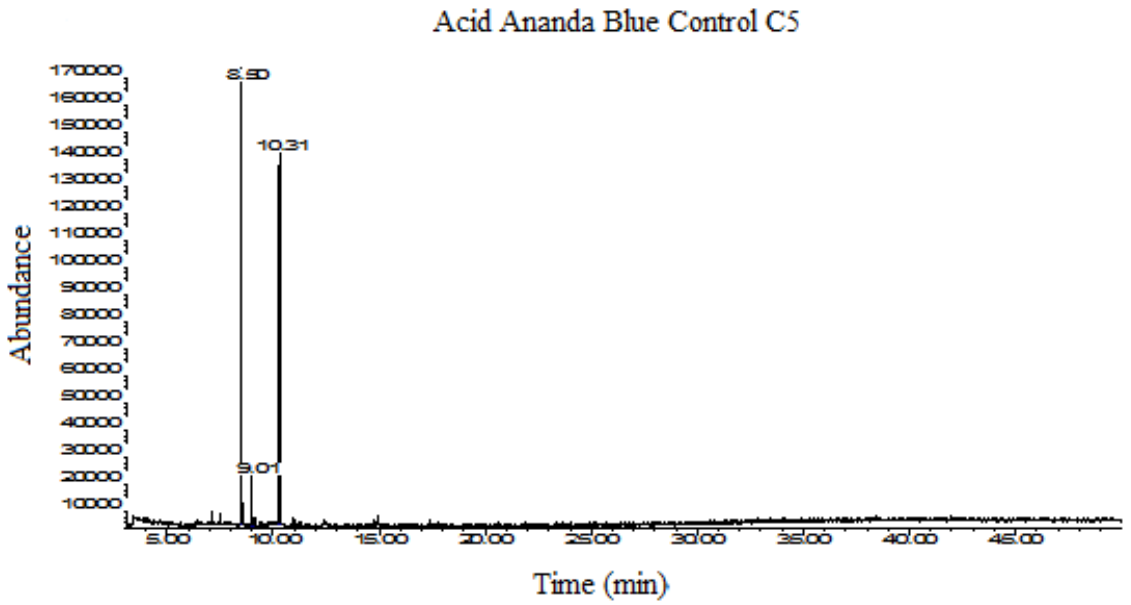

Figure C.30: Total ion GC-MS chromatogram of 5 g/L Acid Ananda Blue dye Control C5 in the USA. Major peaks are identified in Table C.6.

Table C.7: GC/MS results of 5 g/L Acid Fast Red with Soap and Soda samples S1-S6 in (A) India compared with C1, (B) in USA 1 compared with C1-C5, and (C) in USA2 compared with C1-C5.

A

Dye	Oxidation Time	Peak Time (min)	Chemical Name	Percentage	Abundance
Acid Red with Soap and Soda	C1	26.4	Hexadecanoic Acid	99	42000
		29.7	Oleic Acid	99	62000
		30.11	Octadecanoic Acid	98	21000
Acid Red with Soap and Soda	C4	17.84	2-Naphthalenol	90	15000
Acid Red with Soap and Soda	C5	None	None	None	None
Acid Red with Soap and Soda	S1	4.12	Hexanal	90	14500
		8.98	Hexanoic Acid	56	4000
Acid Red with Soap and Soda	S2	None	None	None	None
Acid Red with Soap and Soda	S3	None	None	None	None
Acid Red with Soap and Soda	S4	12.63	Octanoic Acid	83	19750
		14.08	Nonanoic Acid	53	22000
Acid Red with Soap and Soda	S5	None	None	None	None
Acid Red with Soap and Soda	S6	None	None	None	None

B

Dye	Oxidation Time	Peak Time (min)	Chemical Name	Percentage	Abundance
Acid Red with Soap and Soda	C1	29.7	Oleic Acid	64	35000
Acid Red with Soap and Soda	C2	12.57	Octanoic Acid	72	23500
		17.83	Benzofuran, 2-ethenyl	78	19000
		29.69	Oleic Acid	64	29000
Acid Red with Soap and Soda	C3	4.11	Hexanal	59	16700
		29.68	15-Tetracosenoic acid, methyl este	45	17000
Acid Red with Soap and Soda	C4	12.57	Octanoic Acid	64	28000
Acid Red with Soap and Soda	C5	4.09	hexanal	90	35000
		12.42	cyclopentasiloxane, decamethyl	91	21800
		14.94	cyclohexasiloxane, dodecamethyl	91	38000
Acid Red with Soap and Soda	S1	12.57	Octanoic Acid	72	7000
		14.05	Nonanoic Acid	72	14000
		16.2	1,4-Naphthalenedione	86	11000
Acid Red with Soap and Soda	S2	None	None	None	None
Acid Red with Soap and Soda	S3	NA	NA	NA	NA
Acid Red with Soap and Soda	S4	9.48	Octanal	87	40000
		11.46	Nonanal	83	50000
		14.08	Nonanoic Acid	64	26000
		16.2	1,4-Naphthalenedione	91	16000
Acid Red with Soap and Soda	S5	6.79	2-Heptanone	87	42000
		11.06	Benzaldehyde, 4-methyl	94	23000
Acid Red with Soap and Soda	S6	NA	NA	NA	NA

C

Dye	Oxidation Time	Peak Time (min)	Chemical Name	Percentage	Abundance
Acid Red with Soap and Soda	S1	4.11	Hexanal	72	16500
		12.61	Octanoic Acid	72	23000
		14.07	Nonanoic Acid	59	23000
Acid Red with Soap and Soda	S2	11.05	Benzaldehyde, 4-methyl-	91	10500
Acid Red with Soap and Soda	S3	NA	NA	NA	NA
Acid Red with Soap and Soda	S4	9.48	Octanal	74	2100
		14.08	Nonanoic Acid	96	2800
		16.2	1,4-Naphthalenedione	93	19250
		26.35	Tetradecanoic Acid	46	19500
Acid Red with Soap and Soda	S5	6.75	2-Heptanone	87	28000
		11.05	Benzaldehyde, 3-methyl	91	12000
Acid Red with Soap and Soda	S6	NA	NA	NA	NA

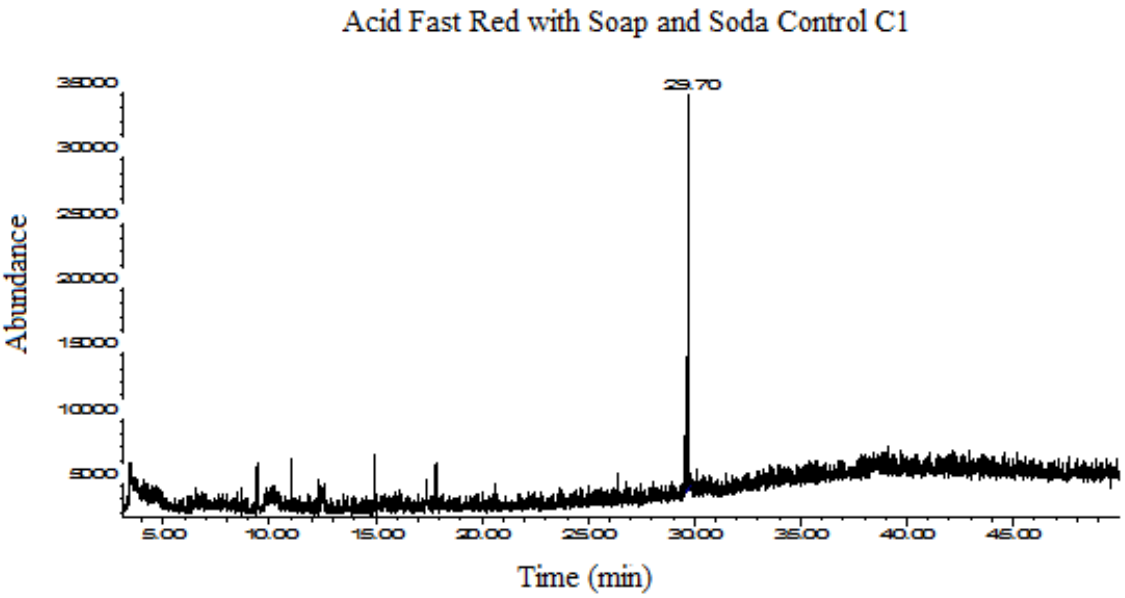

Figure C.31: Total ion GC-MS chromatogram of 5 g/L Acid Fast Red with Soap and Soda dye Control C1 in the USA. Major peaks are identified in Table C.7.

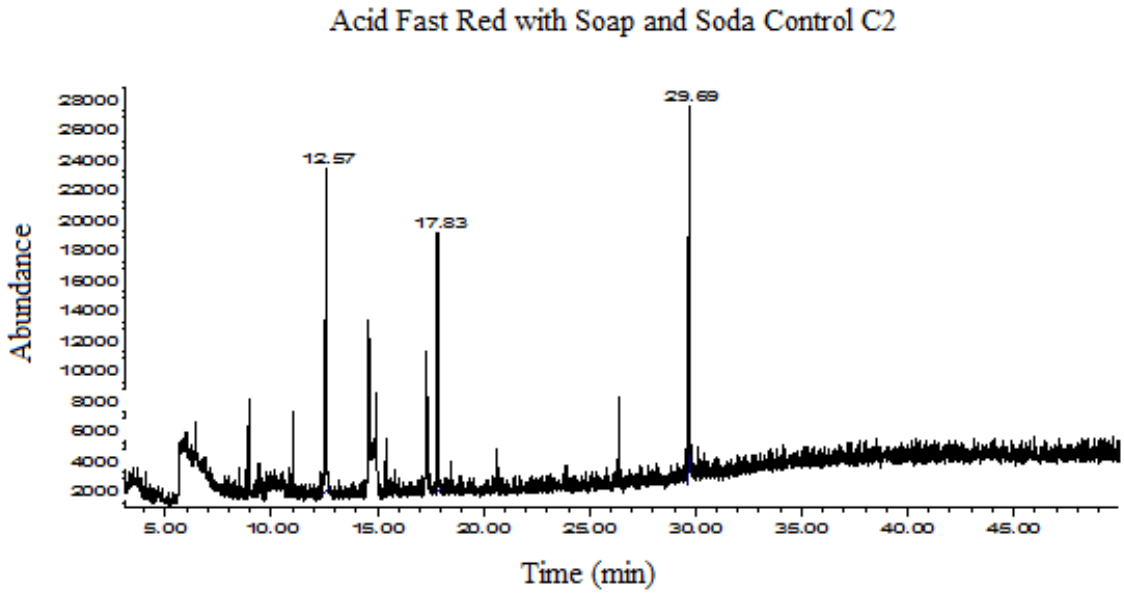

Figure C.32: Total ion GC-MS chromatogram of 5 g/L Acid Fast Red with Soap and Soda dye Control C2 in the USA. Major peaks are identified in Table C.7.

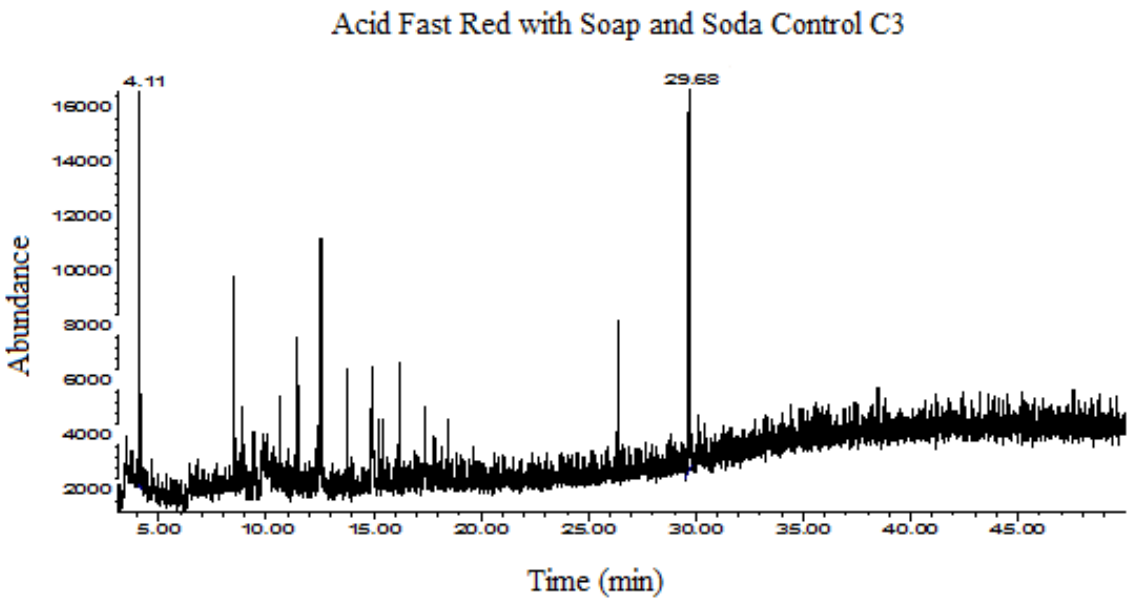

Figure C.33: Total ion GC-MS chromatogram of 5 g/L Acid Fast Red with Soap and Soda dye Control C3 in the USA. Major peaks are identified in Table C.7.

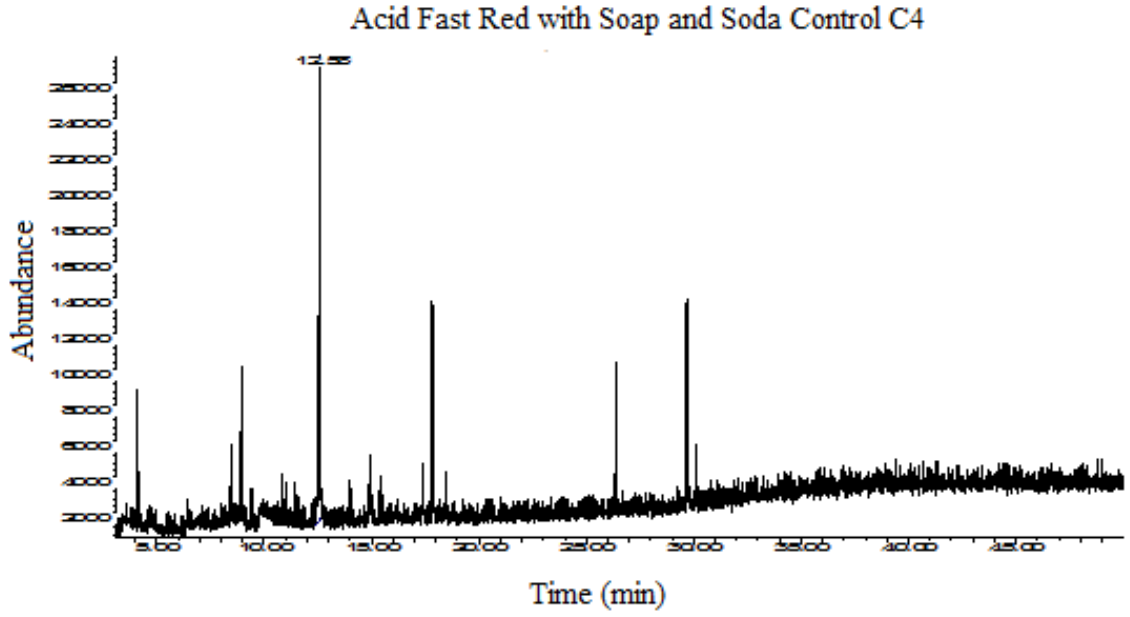

Figure C.34: Total ion GC-MS chromatogram of 5 g/L Acid Fast Red with Soap and Soda dye Control C4 in the USA. Major peaks are identified in Table C.7.

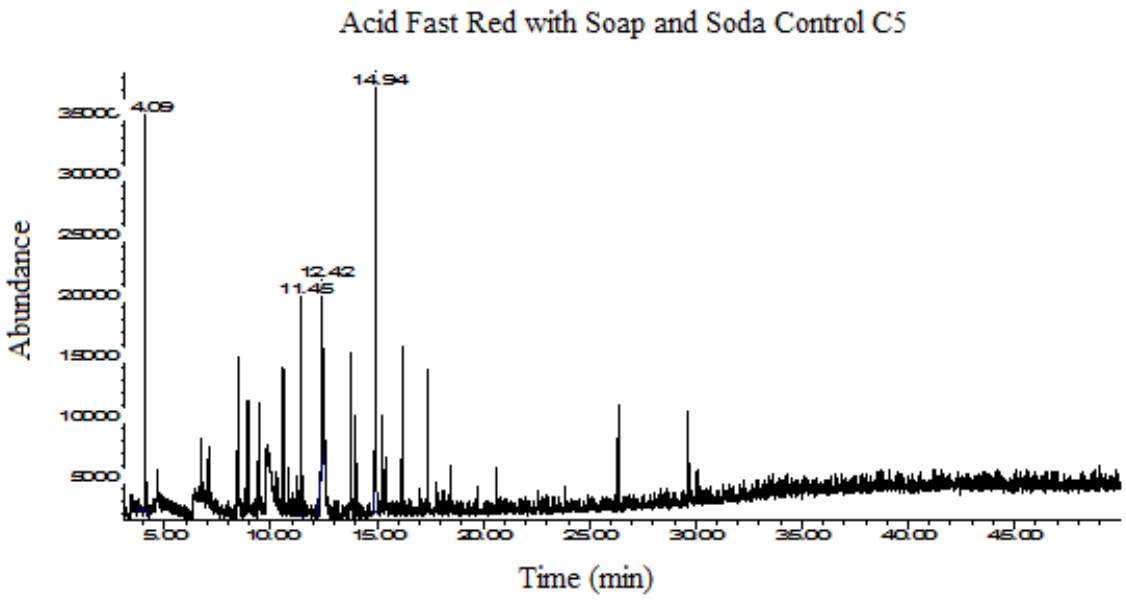

Figure C.35: Total ion GC-MS chromatogram of 5 g/L Acid Fast Red with Soap and Soda dye Control C5 in the USA. Major peaks are identified in Table C.7.

Table C.8: GC/MS results of 5 g/L Acid Golden Yellow with Soap and Soda samples S1-S6 in (A) India compared with C1, (B) in USA 1 compared with C1-C5, and (C) in USA2 compared with C1-C5.

A

Dye	Oxidation Time	Peak Time (min)	Chemical Name	Percentage	Abundance
Acid Yellow with Soap and Soda	C1	9.49	Octanal	64	22000
		12.62	Octanoic Acid	83	20000
		14.03	2-Decenal,(E)-	64	22000
		15.23	2-Cyclohexen-1-ol,3-methyl-6-(1-methylethel)-,cis-	46	22500
Acid Yellow with Soap and Soda	C4	None	None	None	None
Acid Yellow with Soap and Soda	C5	None	None	None	None
Acid Yellow with Soap and Soda	S1	4.12	Hexanal	86	48000
Acid Yellow with Soap and Soda	S2	None	None	None	None
Acid Yellow with Soap and Soda	S3	None	None	None	None
Acid Yellow with Soap and Soda	S4	3.75	Hexanal	90	11500
		12.57	Octanoic Acid	56	7250
Acid Yellow with Soap and Soda	S5	None	None	None	None
Acid Yellow with Soap and Soda	S6	None	None	None	None

B

Dye	Oxidation Time	Peak Time (min)	Chemical Name	Percentage	Abundance
Acid Yellow with Soap and Soda	C1	14.96	Cyclohexasiloxane, dodecamethyl	87	24000
Acid Yellow with Soap and Soda	C2	None	None	None	None
Acid Yellow with Soap and Soda	C3	12.57	Octanoic Acid	78	24500
Acid Yellow with Soap and Soda	C4	4.09	Hexanal	90	65750
		12.57	Octanoic Acid	72	25000
		26.38	Hexadecanoic Acid	90	24000
		29.69	Oleic Acid	80	30000
Acid Yellow with Soap and Soda	C5	4.1	Hexanal	86	40000
		8.51	Benzaldehyde	91	50000
Acid Yellow with Soap and Soda	S1	None	None	None	None
Acid Yellow with Soap and Soda	S2	None	None	None	None
Acid Yellow with Soap and Soda	S3	NA	NA	NA	NA
Acid Yellow with Soap and Soda	S4	4.09	Hexanal	86	31000
		7.02	Hptanal	90	47000
		9.48	Octanal	87	39000
		12.63	Octanoic Acid	83	26000
		14.06	Nonanoic Acid	64	16000
Acid Yellow with Soap and Soda	S5	None	None	None	None
Acid Yellow with Soap and Soda	S6	NA	NA	NA	NA

C

Dye	Oxidation Time	Peak Time (min)	Chemical Name	Percentage	Abundance
Acid Yellow with Soap and Soda	C1	14.96	Cyclohexasiloxane, dodecamethyl	87	24000
Acid Yellow with Soap and Soda	C2	None	None	None	None
Acid Yellow with Soap and Soda	C3	12.57	Octanoic Acid	78	24500
Acid Yellow with Soap and Soda	C4	4.09	Hexanal	90	65750
		12.57	Octanoic Acid	72	25000
		26.38	Hexadecanoic Acid	90	24000
		29.69	Oleic Acid	80	30000
Acid Yellow with Soap and Soda	C5	4.1	Hexanal	86	40000
		8.51	Benzaldehyde	91	50000
Acid Yellow with Soap and Soda	S1	None	None	None	None
Acid Yellow with Soap and Soda	S2	None	None	None	None
Acid Yellow with Soap and Soda	S3	NA	NA	NA	NA
Acid Yellow with Soap and Soda	S4	4.09	Hexanal	86	31000
		7.02	Hptanal	90	47000
		9.48	Octanal	87	39000
		12.63	Octanoic Acid	83	26000
		14.06	Nonanoic Acid	64	16000
Acid Yellow with Soap and Soda	S5	None	None	None	None
Acid Yellow with Soap and Soda	S6	NA	NA	NA	NA

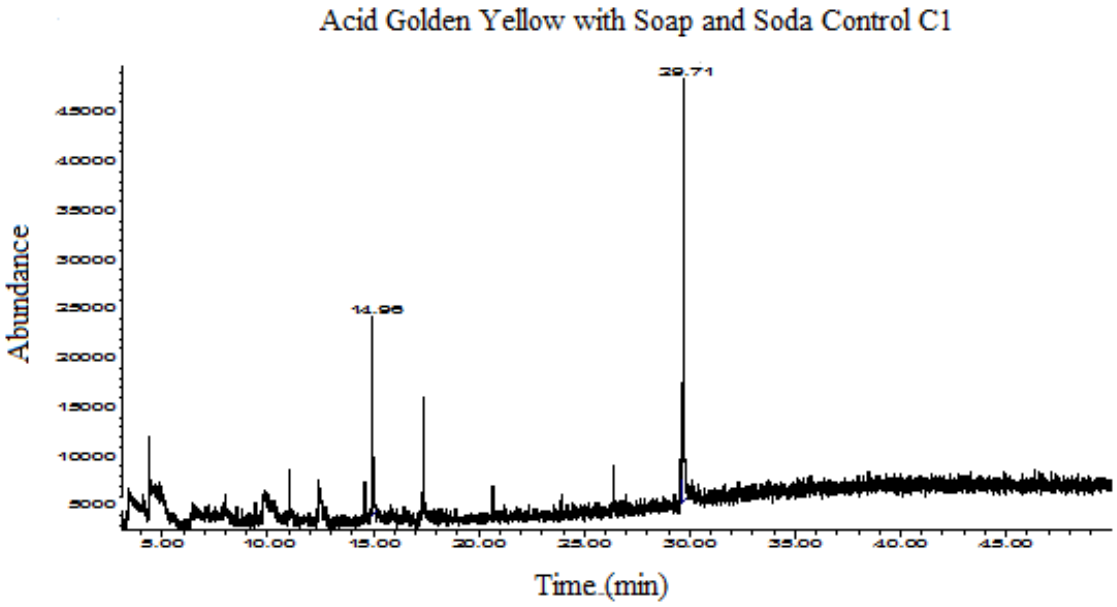

Figure C.36: Total ion GC-MS chromatogram of 5 g/L Acid Golden Yellow with Soap and Soda dye Control C1 in the USA. Major peaks are identified in Table C.8.

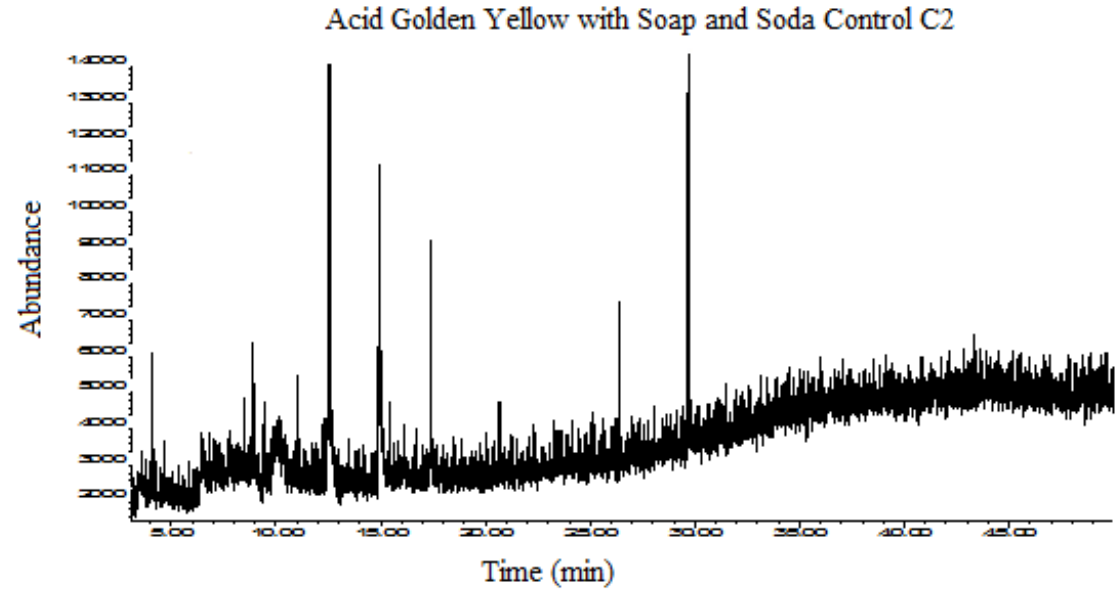

Figure C.37: Total ion GC-MS chromatogram of 5 g/L Acid Golden Yellow with Soap and Soda dye Control C2 in the USA. No major peaks are identified in Table C.8.

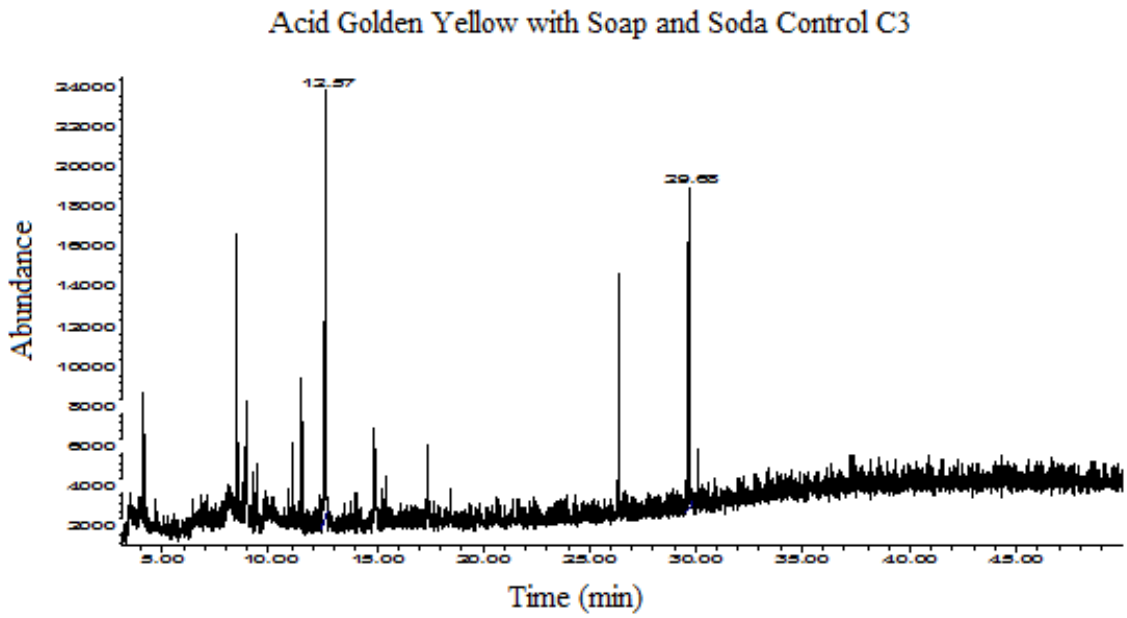

Figure C.38: Total ion GC-MS chromatogram of 5 g/L Acid Golden Yellow with Soap and Soda dye Control C3 in the USA. Major peaks are identified in Table C.8.

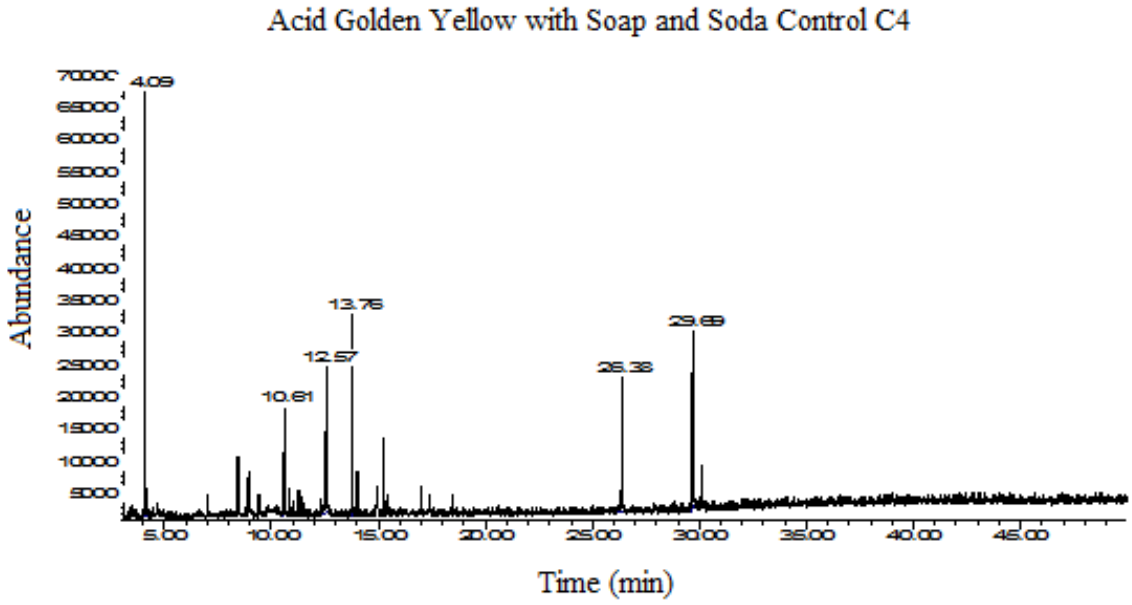

Figure C.39: Total ion GC-MS chromatogram of 5 g/L Acid Golden Yellow with Soap and Soda dye Control C4 in the USA. Major peaks are identified in Table C.8.

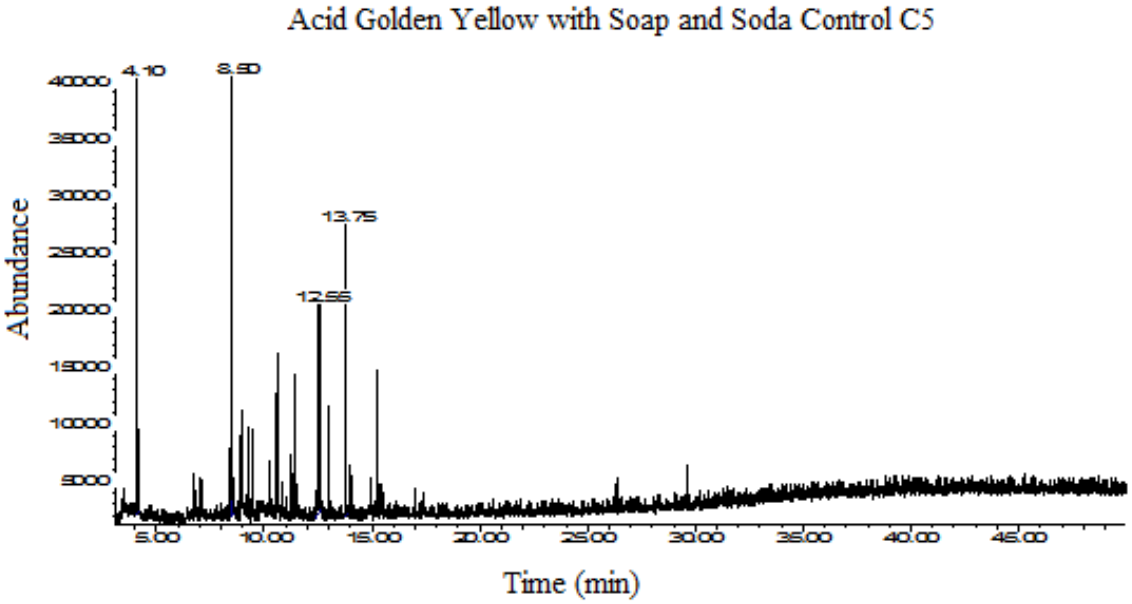

Figure C.40: Total ion GC-MS chromatogram of 5 g/L Acid Golden Yellow with Soap and Soda dye Control C5 in the USA. Major peaks are identified in Table C.8.

Table C.9: GC/MS results of 5 g/L Acid Ananda Blue with Soap and Soda samples S1-S6 in (A) India compared with C1, (B) in USA 1 compared with C1-C5, and (C) in USA2 compared with C1-C5.

A

Dye	**Oxidation Time**	**Peak Time (min)**	**Chemical Name**	**Percentage**	**Abundance**
Acid Blue with Soap and Soda	C1	8.52	Benzaldehyde	96	220000
Acid Blue with Soap and Soda	C4	None	None	None	None
Acid Blue with Soap and Soda	C5	8.54	Benzaldehyde	91	26000
Acid Blue with Soap and Soda	S1	4.12	Hexanal	78	25000
		12.62	Octanoic Acid	83	20000
		14.08	Nonanoic Acid	83	18750
		18.49	Dodecanoic Acid	96	16700
Acid Blue with Soap and Soda	S2	None	None	None	None
Acid Blue with Soap and Soda	S3	None	None	None	None
Acid Blue with Soap and Soda	S4	7.04	Heptanal	86	17000
		9.49	Octanal	83	30000
		12.63	Octanoic Acid	83	25000
		14.11	Nonanoic Acid	93	46000
Acid Blue with Soap and Soda	S5	None	None	None	None
Acid Blue with Soap and Soda	S6	None	None	None	None

B

Dye	Oxidation Time	Peak Time (min)	Chemical Name	Percentage	Abundance
Acid Blue with Soap and Soda	C1	8.51	Benzaldehyde	95	35000
		11.9	Benzenemethanamine, N-ethyl	91	41000
		14.8	Cyclohexasiloxane, dodecamethyl	91	58000
		14.96	Cyclohexasiloxane, dodecamethyl	80	22000
Acid Blue with Soap and Soda	C2	8.5	Benzaldehyde	94	540000
		12.59	Octanoic Acid	72	40000
		14.21	2-Propenal, 3-pheyl	94	50000
		22.62	Benzenemethanamine, N-ethyl-N-phenyl	95	60000
Acid Blue with Soap and Soda	C3	8.49	Benzaldehyde	94	450000
		10.31	Benzaldehyde, 2-hydroxy	96	140000
Acid Blue with Soap and Soda	C4	8.48	Benzaldehyde	94	160000
		12.58	Octanoic Acid	83	60000
		14.18	2-Propenal, 3-pheyl	97	92000
		15.43	Decanoic Acid	98	93000
		18.51	Dodecanoic Acid	96	180000
		22.42	Tetradecanoic Acid	98	30000
		22.59	Benzenemethanamine, N-ethyl-N-phenyl	97	110000
		26.4	Hexadecanoic Acid	99	112000
		29.61	9,12-Octadecadienoic Acid (Z,Z)	99	50000
		29.74	Oleic Acid	99	330000
		30.11	Octadecanoic Acid	95	68000
Acid Blue with Soap and Soda	C5	8.49	Benzaldehyde	94	390000
		10.3	Benzaldehyde, 2-hydroxy	94	240000
		12.42	Cyclohexasiloxane, decamethyl	90	4000
		14.95	Cyclohexasiloxane, dodecamethyl	91	58000
		26.37	Hexadecanoic Acid	89	22000
Acid Blue with Soap and Soda	S1	4.12	Hexanal	78	22250
		12.61	Octanoic Acid	78	17000
		14.08	Nonanoic Acid	78	16250
Acid Blue with Soap and Soda	S2	None	None	None	None
Acid Blue with Soap and Soda	S3	NA	NA	NA	NA
Acid Blue with Soap and Soda	S4	11.47	Nonanal	83	18000
		26.38	Hexadecanoic Acid	99	45000
		30.08	Octadecanoic Acid	99	25000
Acid Blue with Soap and Soda	S5	None	None	None	None
Acid Blue with Soap and Soda	S6	NA	NA	NA	NA

C

Dye	Oxidation Time	Peak Time (min)	Chemical Name	Percentage	Abundance
Acid Blue with Soap and Soda	S1	4.11	Hexanal	72	15000
		14.05	Nonanoic Acid	59	13000
Acid Blue with Soap and Soda	S2	11.05	Benzaldehyde, 4-methyl	43	3300
Acid Blue with Soap and Soda	S3	NA	NA	NA	NA
Acid Blue with Soap and Soda	S4	26.39	Hexadecanoic Acid	97	53000
		30.08	Octadecanoic Acid	98	19000
Acid Blue with Soap and Soda	S5	8.51	Benzaldehyde	91	24750
		11.93	Benzenemethanamine, N-ethyl-	74	28000
Acid Blue with Soap and Soda	S6	NA	NA	NA	NA

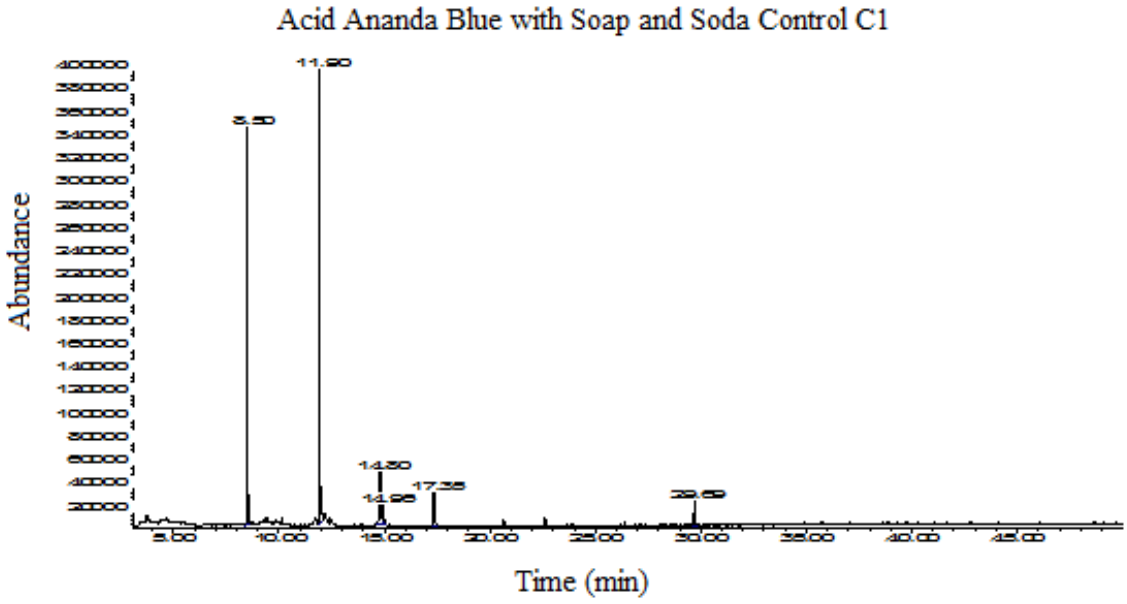

Figure C.41: Total ion GC-MS chromatogram of 5 g/L Acid Ananda Blue with Soap and Soda dye Control C1 in the USA. Major peaks are identified in Table C.9.

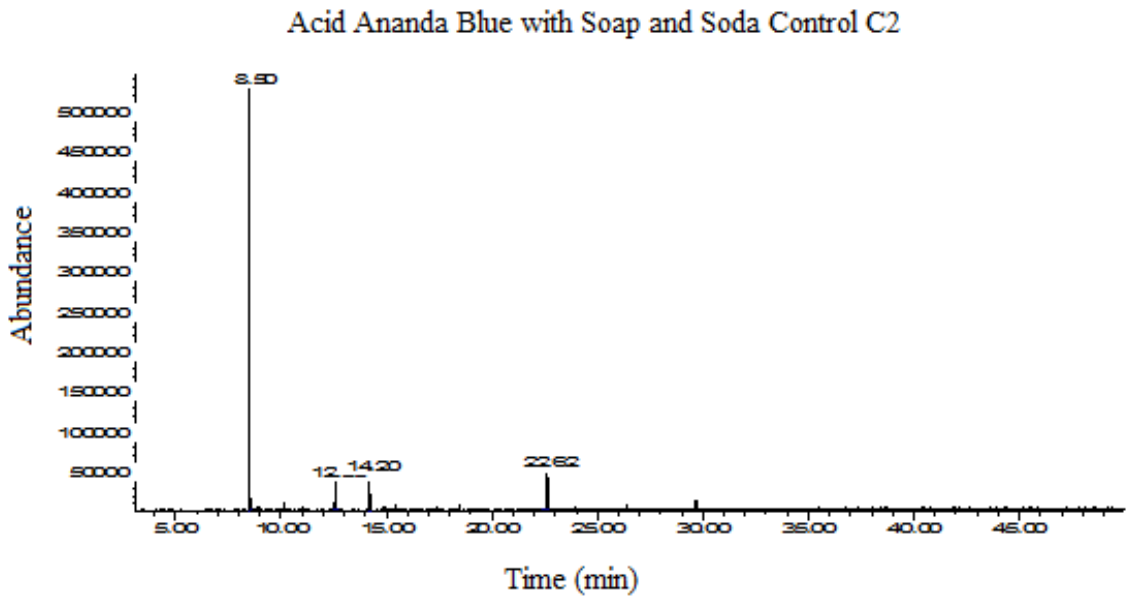

Figure C.42: Total ion GC-MS chromatogram of 5 g/L Acid Ananda Blue with Soap and Soda dye Control C2 in the USA. Major peaks are identified in Table C.9.

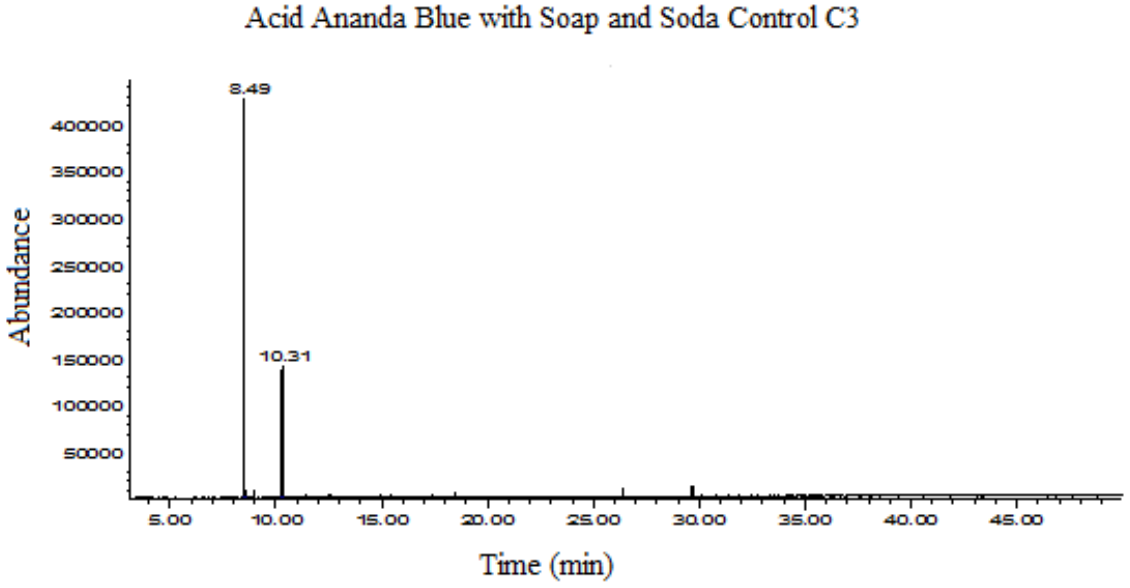

Figure C.43: Total ion GC-MS chromatogram of 5 g/L Acid Ananda Blue with Soap and Soda dye Control C3 in the USA. Major peaks are identified in Table C.9.

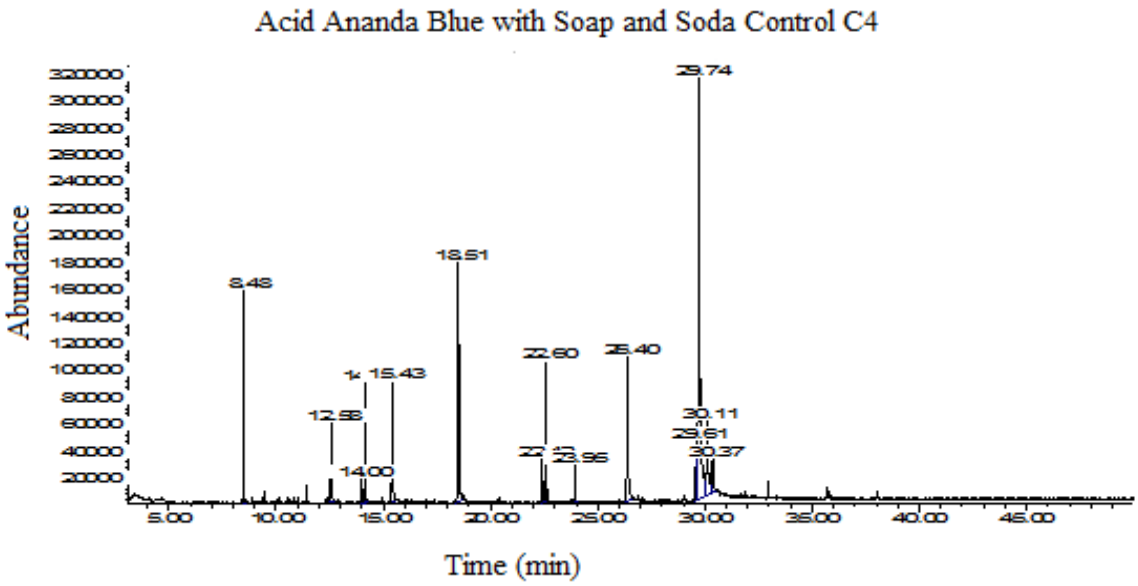

Figure C.44: Total ion GC-MS chromatogram of 5 g/L Acid Ananda Blue with Soap and Soda dye Control C4 in the USA. Major peaks are identified in Table C.9.

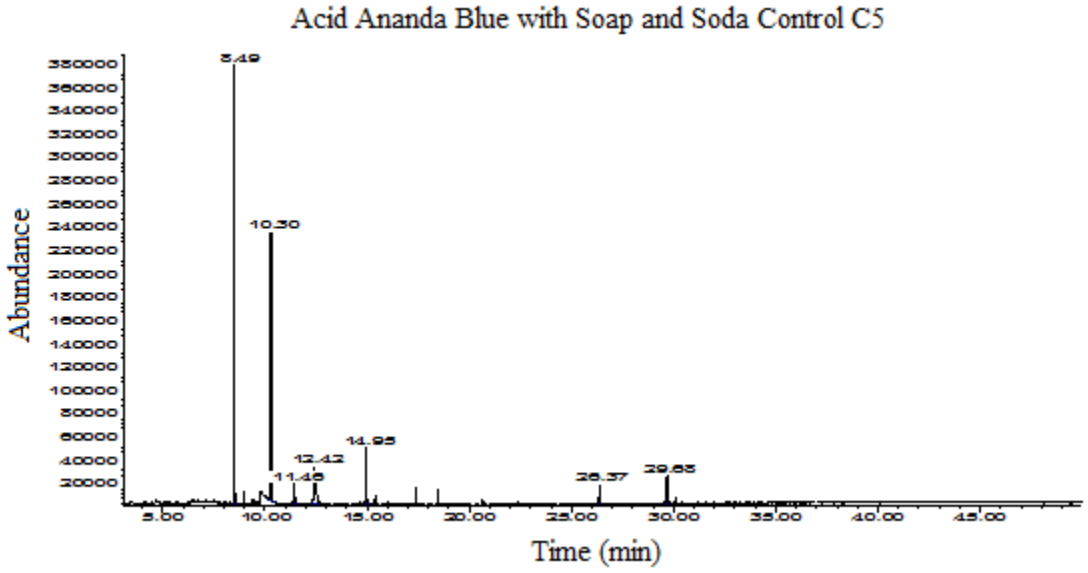

Figure C.45: Total ion GC-MS chromatogram of 5 g/L Acid Ananda Blue with Soap and Soda dye Control C5 in the USA. Major peaks are identified in Table C.9.

Table C.10: GC/MS results of 5 g/L Field Samples Green and Maroon F1-F6 in India compared with C1.

Dye	Oxidation Time	Peak Time (min)	Chemical Name	Percentage	Abundance
Control Green	C1	NA	none	NA	NA
Field Sample Green	F1	NA	none	NA	NA
Field Sample Green	F2	17.65	Phenol, 2,4-bis(1,1-dimethylethyl)	91	24000
Field Sample Green	F3	NA	none	NA	NA
Control Maroon	C1	14.49	Benzenamine, 4-ethoxy	90	90000
Field Sample Maroon	F1	NA	none	NA	NA
Field Sample Maroon	F2	NA	none	NA	NA
Field Sample Maroon	F3	NA	none	NA	NA

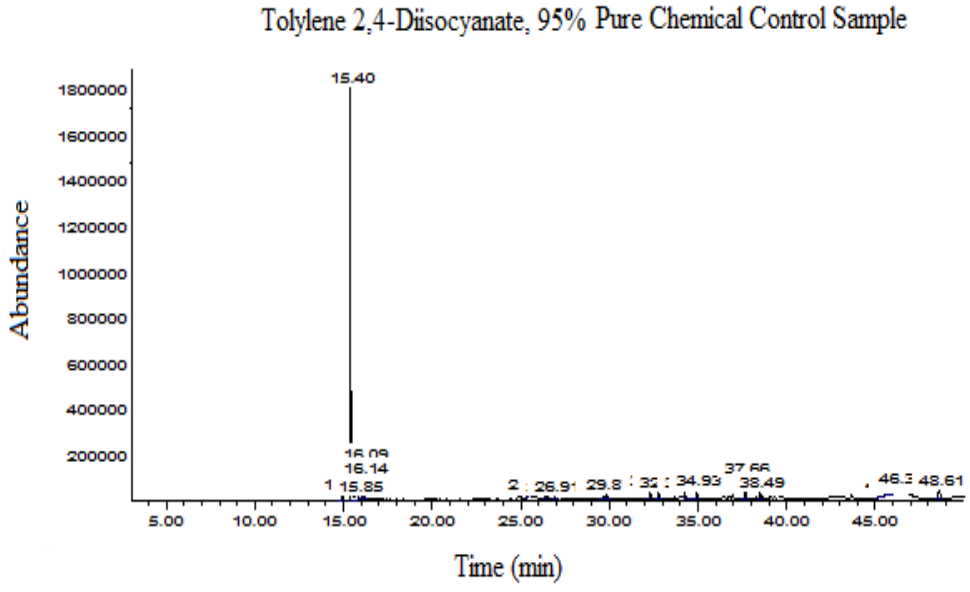

Figure C.46: Total ion GC-MS chromatogram of 5 g/L 95% Tolylene, 2,4-diisocyanate (Benzene, 2,4-diisocyanato-1-methyl). Major peaks are identified in Table C.11.

Table C.11: GC/MS results of 95% Pure Tolylene, 2,4-diisocyanate.

Peak Time (mins)	Chemical Name	Percentage	Abundance
14.95	Dodecanoic Acid, Ethyl Ester	93	28000
15.41	Benzene, 2,4-diisocyanato-1-methyl	95	1800000
16.14	2H-Benzimidazol-2-one, 1,3-dihydro-5-methyl-	86	100000
32.78	2-Propenoic acid, 3-(4-methoxyphenyl)-, 2-ethylhexyl ester	95	40000
37.66	Bis(2-ethylhexyl) phthalate	91	95000
48.61	Squalene	87	50000

Appendix D – ICP

This appendix contains the ICP results specifically listing calcium, magnesium, iron, and sodium, as well as any other metals whose levels were above permissible drinking water limits according to the KSPCB. All metals tested include aluminum, antimony, arsenic, cadmium, calcium, chromium, cobalt, copper, iron, lead, magnesium, manganese, molybdenum, nickel, silver, sodium, tin, zinc. Each table is separated according to the location of test. Tables describing results from India include the control samples C1, C4-C5 data; tables describing results from the USA include control samples C1-C5. Tables are made for Reactive Red 120 (Table D.1), Reactive Yellow 81 (Table D.2), and Reactive Blue 4 (Table D.3) samples R1H-R6H, R1M-R6M, and R1L-R6L; Acid Fast Red (Table D.4), Acid Golden Yellow (Table D.5), and Acid Ananda Blue (Table D.6) samples A1-A12; Acid Fast Red with Soap and Soda (Table D.7), Acid Golden Yellow with Soap and Soda (Table D.8), and Acid Ananda Blue with Soap and Soda (Table D.9) samples S1-S6.

Table D.1: ICP results of 5 g/L Reactive Red 120 samples R1H-R6H, R1M-R6M, and R1L-R6L in (A) India compared with C1, C4, and C5, and (B) in USA average compared with C1-C5.

A

Dye	Sample	Ca	Mg	Fe	Na	Other
Reactive Red 120	C1	21.3	7.8	0.5	1013.3x	
Reactive Red 120	C4	25.7	8.8	1.5	1091.5x	
Reactive Red 120	C5	21.6	6.9	4	605.8x	
Reactive Red 120	R1H	-	-	-	-	No Sample
Reactive Red 120	R2H	105.3	31	0	562.2(x)	
Reactive Red 120	R3H	126.7	35.4	0	663.8(x)	As: 0.9; Mn: 2.0
Reactive Red 120	R4H	3.2	1.6	230.6	2424.1(x)	
Reactive Red 120	R5H	13.1	4.1	70.8	199.6	Mn: 1.6
Reactive Red 120	R6H	16.2	1	1	14.7	Mn: 2.8
Reactive Red 120	R1M	27.9	8.2	220.5	949.1(x)	
Reactive Red 120	R2M	59	14.6	0.6	434.2	Mn: 5.4
Reactive Red 120	R3M	52.9	13.9	0.1	378.6	Mn: 2.4
Reactive Red 120	R4M	7.6	6.1	95.2	1281.5(x)	
Reactive Red 120	R5M	165.7	39.9	3.3	516.6	Mn: 11.4
Reactive Red 120	R6M	131.8	33.6	0.3	440.3	Mn: 10.0
Reactive Red 120	R1L	-	-	-	-	No Sample
Reactive Red 120	R2L	33.5	8.5	0	25.6	
Reactive Red 120	R3L	32.4	8.7	0	27.7	
Reactive Red 120	R4L	15.4	5.1	2.7	969.1(x)	
Reactive Red 120	R5L	61.3	14.1	28.5	349.9	Mn: 10.6
Reactive Red 120	R6L	55.6	12.6	20.5	306.3	Mn: 8.9

B

Reactive Red 120 - USA	Sample	Ca	Mg	Fe	Na	Other
Reactive Red 120	C1	36.6	13.2	0.4	643.8x	
Reactive Red 120	C2	25	9.1	0.1u	628.1x	
Reactive Red 120	C3	20.8	7.6	0.1u	583.4x	
Reactive Red 120	C4	23.4	10	0.7	725.7x	
Reactive Red 120	C5	28.9	10.8	0.7	672.7x	
Reactive Red 120	R1H	43.8	15.1	601.3	824x	Mn: 3.0
Reactive Red 120	R2H	65	32.7	0.25(u)	158.1	
Reactive Red 120	R3H	67.95	28.45	0.05	159.55	
Reactive Red 120	R4H	28.65	8.8	143.3	475.95	As: 0.25uv; Mn: 0.65
Reactive Red 120	R5H	125.15	49.5	0.05(u)	512.15	
Reactive Red 120	R6H	124.3	46.7	0.1(u)	495.4	
Reactive Red 120	R1M	38.75	11.5	274.4	589.55(x)	Mn: 2.1; Pb: 0.55
Reactive Red 120	R2M	13.1	6	0.1	7.2	
Reactive Red 120	R3M	21.8	6.35	0.08(u)	7.2	
Reactive Red 120	R4M	40.15	12	65.5	659.6(x)	
Reactive Red 120	R5M	165	68.1	0.05	390.9	
Reactive Red 120	R6M	143.6	60.3	0.05(u)	347.3	
Reactive Red 120	R1L	97.1, 71.9	42.35, 23.75	45.35, 908.45	1029.35, 1248.35	Mn: 3; Pb: 1.05
Reactive Red 120	R2L	46.05, 30.35	7.75, 2.25	0.35, 0.4	177.2, 18.35	
Reactive Red 120	R3L	37.3, 40.4	8.35, 1.0	0.15, 0	200.6, 21.95	As: 0.35
Reactive Red 120	R4L	25.3	7.3	9.35	388.25	
Reactive Red 120	R5L	175.05	33.85	4.35	488.15	Mn: 1.15
Reactive Red 120	R6L	138.6	27.65	1.25	44.95	

Table D.2: ICP results of 5 g/L Reactive Yellow 81 samples R1H-R6H, R1M-R6M, and R1L-R6L in (A) India compared with C1, C4, and C5, and (B) in USA average compared with C1-C5.

A

Reactive Yellow 81 - India	Sample	Ca	Mg	Fe	Na	Other
Reactive Yellow 81	C1	29.9	8.9	0.2	1095.4x	
Reactive Yellow 81	C4	32.4	9.3	3.3	1137.9x	
Reactive Yellow 81	C5	21	5.7	4	633.8x	
Reactive Yellow 81	R1H	-	-	-	-	No Sample
Reactive Yellow 81	R2H	118.1	33.1	0	778.4(x)	Mn: 1.1
Reactive Yellow 81	R3H	108.9	30.5	0	699.3(x)	
Reactive Yellow 81	R4H	3.4	0.8	113.2	1436.1(x)	
Reactive Yellow 81	R5H	3	1.1	96.2	49.8	
Reactive Yellow 81	R6H	16.6	1.3	1.1	40.2	Mn: 2.7
Reactive Yellow 81	R1M	21.9	6.2	102.5	1186.7(x)	
Reactive Yellow 81	R2M	70.6	17.4	5.2	440.4	Mn: 9.0
Reactive Yellow 81	R3M	67.6	16.7	1.3	382.4	Mn: 7.4
Reactive Yellow 81	R4M	18.4	5.5	51.2	1319.8(x)	
Reactive Yellow 81	R5M	160.2	35.1	0.4	455.3	Mn: 12.5
Reactive Yellow 81	R6M	137.1	33	2.2	442.3	Mn: 11.5
Reactive Yellow 81	R1L	-	-	-	-	No Sample
Reactive Yellow 81	R2L	90.8	20.6	0	210.9	Mn: 2.3
Reactive Yellow 81	R3L	75.1	18	0	174.8	
Reactive Yellow 81	R4L	19	4.7	18.3	1075.6(x)	
Reactive Yellow 81	R5L	57.6	14.4	0	255.3	Mn: 9.4
Reactive Yellow 81	R6L	36.4	12.5	4	215	Mn: 7.7

B

Reactive Yellow 81 - USA	Sample	Ca	Mg	Fe	Na	Other
Reactive Yellow 81	C1	39	13.3	0	983.7x	
Reactive Yellow 81	C2	36.3	12.1	0.1u	937.2x	
Reactive Yellow 81	C3	34.1	10.6	0	893.4x	
Reactive Yellow 81	C4	30.7	12.1	0	900.9x	
Reactive Yellow 81	C5	36.9	11.2	0	799.3x	
Reactive Yellow 81	R1H	35.25	10.8	782.45	566.85(x)	Cd: 0.3; Mn: 6.65
Reactive Yellow 81	R2H	105.75	53.6	0.2	393.1	
Reactive Yellow 81	R3H	88.75	41.2	0.05	314.4	As: 0.4
Reactive Yellow 81	R4H	55.05	21.2	336.75	522.2	Cd: 0.15; Mn: 2.8
Reactive Yellow 81	R5H	152.75	53.2	0.05	466.45	As: 0.4
Reactive Yellow 81	R6H	114.75	39.65	0.1	352	
Reactive Yellow 81	R1M	41.5	11.4	250.8	724.55x	Cd: 0.1; Mn: 1.3
Reactive Yellow 81	R2M	24.55	12.5	0.15	25.75	
Reactive Yellow 81	R3M	22.45	9.45	0.05(u)	20.35	
Reactive Yellow 81	R4M	25.45	7.1	31.7	514.3	As: 0.4
Reactive Yellow 81	R5M	198.2	62.05	3.6	518.85	
Reactive Yellow 81	R6M	179.75	62.35	2.2	506	
Reactive Yellow 81	R1L	55.8, 70.4	15.45, 21.3	193.35, 604.2	764.2x, 152.08x	As: 0, 0.45; Cd: 0.1, 0.3; Mn: 1.15, 2.1
Reactive Yellow 81	R2L	73.4, 48.95	14.4, 8.7	0.25, 0.05	124, 42.8	As: 0.065
Reactive Yellow 81	R3L	46.65, 60.8	12.7, 3.05	0.05, 0.0u	130.5, 38.85	
Reactive Yellow 81	R4L	19	4.7	18.3	1075.6x	
Reactive Yellow 81	R5L	57.6	14.4	0	255.3	Mn: 0.075
Reactive Yellow 81	R6L	36.4	12.5	4	215	As: 0.045uv

Table D.3: ICP results of 5 g/L Reactive Blue 4 samples R1H-R6H, R1M-R6M, and R1L-R6L in (A) India compared with C1, C4, and C5, and (B) in USA average compared with C1-C5.

A

Reactive Blue 4 - India	Sample	Ca	Mg	Fe	Na	Other
Reactive Blue 4	C1	29.1	8.3	0.6	1402.9x	
Reactive Blue 4	C4	29.4	8.1	0.7	1384.6x	
Reactive Blue 4	C5	25.9	6.9	4.7	1019.2x	
Reactive Blue 4	R1H	-	-	-	-	No Sample
Reactive Blue 4	R2H	130.5	35	0	629.7(x)	Mn: 4.5
Reactive Blue 4	R3H	127.3	34.4	0	644.6(x)	Mn: 3.0
Reactive Blue 4	R4H	1.7	0.4	367.2	1000.3(x)	Cd: 0.1; Mn: 1.3
Reactive Blue 4	R5H	27.3	7.4	66.3	412.2	Mn: 3.8
Reactive Blue 4	R6H	12.7	2	5.2	91.8	Mn: 2.0
Reactive Blue 4	R1M	16.8	5	113.5	1371.5(x)	
Reactive Blue 4	R2M	92.4	22	32.5	630.7(x)	Mn: 11
Reactive Blue 4	R3M	21.6	4.9	0.2	24.1	
Reactive Blue 4	R4M	10.6	2.9	60.6	892.3(x)	
Reactive Blue 4	R5M	146.3	29.9	44	534.1	Mn: 16.6
Reactive Blue 4	R6M	121.8	25.2	3.9	436.6	Mn: 12.6
Reactive Blue 4	R1L	-	-	-	-	No Sample
Reactive Blue 4	R2L	86.2	20.4	0.1(u)	381.8	
Reactive Blue 4	R3L	82.6	18.8	0	324.8	Mn: 1.6
Reactive Blue 4	R4L	13	3.8	17.5	1044.2(x)	
Reactive Blue 4	R5L	37	7.7	21.9	202.6	Mn: 7.2
Reactive Blue 4	R6L	102.6	18	0.4	165.6	As: 1.1; Mn: 4.3

B

Reactive Blue 4 - USA	Sample	Ca	Mg	Fe	Na	Other
Reactive Blue 4	C1	39	12.7	0	991.5x	As: 1.0
Reactive Blue 4	C2	38.1	11.5	0	1009.3x	
Reactive Blue 4	C3	34.9	10.8	0.3	789.1x	
Reactive Blue 4	C4	44.2	12.6	0.3	1083.8x	
Reactive Blue 4	C5	39.6	12.3	1.2	1008.2x	
Reactive Blue 4	R1H	39.25	11.6	118.05	95.25x	Cd: 0.05; Mn: 1.05
Reactive Blue 4	R2H	19.95	5.05	0.1x	16.45	
Reactive Blue 4	R3H	28.8	11.05	0.1(u)	43.5	
Reactive Blue 4	R4H	32.15	8.75	31.35	668.65x	As: 0.3
Reactive Blue 4	R5H	125.8	40.15	0.3	481.85	
Reactive Blue 4	R6H	117.4	40.2	0.05	486.8	
Reactive Blue 4	R1M	42.25	10.05	118.75	759.75(x)	Cd: 0.05; Mn: 1.0
Reactive Blue 4	R2M	96.6	42.7	0.1u	165.15	
Reactive Blue 4	R3M	72.65	33.65	0	130.75	
Reactive Blue 4	R4M	27.6	7.55	13.45	573.75x	
Reactive Blue 4	R5M	196.85	44.7	3.05	538.5x	
Reactive Blue 4	R6M	170.6	44.85	1.5	504	
Reactive Blue 4	R1L	38.3, 76.45	9.65, 17.35	35.15, 197.15	516.25, 1414.75	Cd: 0.1; Mn: 1.05
Reactive Blue 4	R2L	195.4, 121.75	40.95, 38.85	1.3, 0.1uv	437.85, 192.65	
Reactive Blue 4	R3L	141.05, 140.8	39.4, 17.15	4.1, 0uv	415.15, 161.4	
Reactive Blue 4	R4L	13	3.8	17.5	1044.2(x)	As: 0.35
Reactive Blue 4	R5L	37	7.7	21.9	202.6	As: 0.5; Mn: 1.95
Reactive Blue 4	R6L	21.1	5.5	3.9	126.2	

Table D.4: ICP results of 5 g/L Acid Fast Red samples A1-A12 in (A) India compared with C1 and (B) in USA average compared with C1-C5.

A

Dye	Sample	Ca	Mg	Fe	Na	Other
Acid Fast Red	C1	24.6	1.7	0.2	946.8	
Acid Fast Red	A1	-	-	-	-	No Sample
Acid Fast Red	A2	38	9.8	4	522.4	Mn: 5.9
Acid Fast Red	A3	10.5	2.7	1	140.3	Mn: 1.6
Acid Fast Red	A4	27.6	2.9	36.6	1201.3	
Acid Fast Red	A5	40.4	9.1	0.8	52.9	
Acid Fast Red	A6	28.7	6.8	0	46.7	As: 0.6u
Acid Fast Red	A7	8.9	1.8	48	1250.1(x)	
Acid Fast Red	A8	60.5	13.6	2.5	270.1	Mn: 4.6
Acid Fast Red	A9	48.5	11	2	215.9	As: 0.5u; Mn: 2.4
Acid Fast Red	A10	43.6	5.6	82.4	887.9(x)	
Acid Fast Red	A11	60.5	9.5	2.3	392.3	Mn: 8.4
Acid Fast Red	A12	42.9	7.6	4.9	309.3	As: 0.6; Mn: 4.2

B

Dye	Sample	Ca	Mg	Fe	Na	Other
Acid Fast Red	C1	42.9	3.4	0	1716.5x	
Acid Fast Red	C2	54.2	6	0.2u	1558.1x	
Acid Fast Red	C3	48.6	6.4	0	1520.1x	
Acid Fast Red	C4	57.3	6.2	0.4	1547.3x	
Acid Fast Red	C5	72.4	17.9	1	1440.1x	
Acid Fast Red	A1	36.9	5.4	54.15	725.8x	Mn: 1.25
Acid Fast Red	A2	235.85	0	20.1	15.8	As: 0.35
Acid Fast Red	A3	108.15	6.9	0	16.6	As: 0.3u
Acid Fast Red	A4	70.1	14.8	96.75	1297.85x	As: 0.5uv; Cd: 0.1uv
Acid Fast Red	A5	499.45	0	0.05u	1422.85x	Cr: 0.55
Acid Fast Red	A6	454.05	0.05	0	1375.3x	Cr: 0.35
Acid Fast Red	A7	69.45	16	54.55	1260.6x	As: 0.6
Acid Fast Red	A8	373.1	0.05	0	1298.15x	
Acid Fast Red	A9	341.05	0.05	0.05u	130.7x	
Acid Fast Red	A10	57.65	10.1	31.05	1237.75x	As: 0.5uv; Cd: 0.05uv
Acid Fast Red	A11	320.95	3.8	0.15	1408.25x	As: 0.85; Cd: 0.05
Acid Fast Red	A12	354.95	0.35	0	1405.4x	

Table D.5: ICP results of 5 g/L Acid Golden Yellow samples A1-A12 in (A) India compared with C1 and (B) in USA average compared with C1-C5.

A

Dye	Sample	Ca	Mg	Fe	Na	Other
Acid Gold Yellow	C1	32.2	5.9	0.2	1380.6	
Acid Gold Yellow	A1	-	-	-	-	No Sample
Acid Gold Yellow	A2	30.5	7.8	4.1	341.3	Mn: 530
Acid Gold Yellow	A3	15.5	4.9	1.1	258.4	Mn: 2.6
Acid Gold Yellow	A4	12.5	8.2	46.8	1266.2(x)	
Acid Gold Yellow	A5	18.2	4.1	1	270.6	Mn: 2.4
Acid Gold Yellow	A6	20.8	4.7	1.1	223.9	Mn: 1.3
Acid Gold Yellow	A7	21.7	6.4	21.1	1263.4(x)	
Acid Gold Yellow	A8	31.8	6.8	1.6	115.6	
Acid Gold Yellow	A9	24.4	5.4	0.1	96.1	
Acid Gold Yellow	A10	13.7	4.7	15	1267.8(x)	
Acid Gold Yellow	A11	12.5	2.3	2.5	59.3	Mn: 1.3
Acid Gold Yellow	A12	13.3	2.5	0.3	56.1	

B

Dye	Sample	Ca	Mg	Fe	Na	Other
Acid Gold Yellow	C1	49.3	14.6	0.1	1933.3x	
Acid Gold Yellow	C2	52.7	10.9	0	1944x	
Acid Gold Yellow	C3	49.6	10.2	0.1u	1654.9x	
Acid Gold Yellow	C4	58.5	13.7	0.4	2076x	
Acid Gold Yellow	C5	54.9	14.7	1.2	1699.3x	
Acid Gold Yellow	A1	242.35	17.1	310.3	1939	As: 2.0uv; Cd: 0.15uv; Mn: 3.15
Acid Gold Yellow	A2	512.85	0.05	0.15	182.4	As: 0.35u
Acid Gold Yellow	A3	233.4	1.85	0.05u	128.35	
Acid Gold Yellow	A4	46.3	15.4	93.1	1442.8x	Cd: 0.05; Cr: 1.15; Mn: 5.15
Acid Gold Yellow	A5	526.05	0.15	0.05	841.9x	Cd: 0.05uv; Pb: 0.8
Acid Gold Yellow	A6	473.9	0.05	0	1079.05X	Cd: 0.1uv
Acid Gold Yellow	A7	42.75	16.65	68.85	1500.9x	Mn: 1.4
Acid Gold Yellow	A8	395.1	0	0.15	1345.35x	
Acid Gold Yellow	A9	386.6	0	0.05	1407.65x	As: 0.6uv; Cd: 0.05uv
Acid Gold Yellow	A10	35.35	13.7	46.4	1537.9	
Acid Gold Yellow	A11	347.95	2	0.05u	1353.75x	As: 1.3uv; Cd: 0.05uv
Acid Gold Yellow	A12	326.95	0.4	0	1312x	As: 0.9

Table D.6: ICP results of 5 g/L Acid Ananda Blue samples A1-A12 in (A) India compared with C1 and (B) in USA average compared with C1-C5.

A

Dye	Sample	Ca	Mg	Fe	Na	Other
Acid Ananda Blue	C1	22.4	5.7	1.6	818.7	
Acid Ananda Blue	A1	-	-	-	-	No Sample
Acid Ananda Blue	A2	11.3	3.2	0	108.1	Mn: 2.2
Acid Ananda Blue	A3	15.8	5.1	1	244.7	Mn: 2.7
Acid Ananda Blue	A4	17.2	4.7	16.3	901.5(x)	
Acid Ananda Blue	A5	79.3	17.3	0.1	190.3	Mn: 1.4
Acid Ananda Blue	A6	50.7	11.5	0.4	168.7	
Acid Ananda Blue	A7	-	-	-	-	No Sample
Acid Ananda Blue	A8	90.1	19.2	0.4	524.6	Mn: 7.3
Acid Ananda Blue	A9	63.4	15.1	1.9	423.7	As: 0.7uv; Mn: 4.5
Acid Ananda Blue	A10	20.2	5.3	19.8	1026.3(x)	
Acid Ananda Blue	A11	66.5	10.3	1.2	537.7	Mn: 10.
Acid Ananda Blue	A12	41.8	7.6	1.7	401.1	Mn: 5.6

B

Dye	Sample	Ca	Mg	Fe	Na	Other
Acid Ananda Blue	C1	35.6	14.4	1.3	1128.3x	Pb: 3.2u
Acid Ananda Blue	C2	32.7	13.3	2.1	1139.4x	Pb: 6.3
Acid Ananda Blue	C3	33.4	12.1	1.9	1018.4x	Pb: 11.1
Acid Ananda Blue	C4	41.8	15.3	3.7	1258.0x	Pb: 6.9
Acid Ananda Blue	C5	38	13.7	2.9	1130.3x	Pb: 3.4
Acid Ananda Blue	A1	89.15	40.6	377.2	1645.7x	As: 0.35uv; Cd: 0.2; Mn: 4.15
Acid Ananda Blue	A2	548.2	0.05	0.15	532.3	As: 0.9
Acid Ananda Blue	A3	391.25	0.2	0	441.35	As: 1.1uv; Cd: 0.05uv; Cr: 0.4uv
Acid Ananda Blue	A4	39.85	13.6	71.5	610.55x	Cd: 0.05; Pb: 0.5uv
Acid Ananda Blue	A5	468.45	0	0.15	1491.15x	Cd: 0.1; Cr: 0.55; Pb: 0.75
Acid Ananda Blue	A6	444.05	0.05	0	1502.65x	As: 1.15uv; Cd: 0.05uv; Cr: 0.45
Acid Ananda Blue	A7	40.35	14.1	56.85	1158.55x	Cd: 0.1uv; Pb: 0.11
Acid Ananda Blue	A8	319.8	0.3	0	1355.15x	
Acid Ananda Blue	A9	352.5	0.1	0	1369.95x	As: 0.4
Acid Ananda Blue	A10	25.9	9.1	20.1	1073.7	As: 0.55; Cd: 0.05uv; Pb: 1.3
Acid Ananda Blue	A11	141.7	1.85	0	1364.05x	As: 1.45
Acid Ananda Blue	A12	301.75	0.35	0.1	1323.15x	As: 0.3; Cd: 0.1uv

Table D.7: ICP results of 5 g/L Acid Fast Red with Soap and Soda samples S1-S6 in (A) India compared with C1, C4, and C5 and (B) in USA average compared with C1-C5.

A

Dye	Sample	Ca	Mg	Fe	Na	Other
Acid Fast Red Soap and Soda	C1	31.7	4.4	0.7	3612.4x	
Acid Fast Red Soap and Soda	C4	21.8	1.9	0.2	746.7x	
Acid Fast Red Soap and Soda	C5	22.8	2.8	0.7	524.4	
Acid Fast Red Soap and Soda	S1	34.9	4.8	84.3	3272.4(x)	Mn: 1.2
Acid Fast Red Soap and Soda	S2	94.1	22.3	0.5	1670.6(x)	Mn: 19
Acid Fast Red Soap and Soda	S3	77.6	18.3	0.1	1336.7(x)	Mn: 15.6
Acid Fast Red Soap and Soda	S4	31	4.3	47.9	2859.8(x)	
Acid Fast Red Soap and Soda	S5	58.7	11.7	27.2	2820.7(x)	As: 0.6; Mn: 8.1
Acid Fast Red Soap and Soda	S6	41.3	9.9	3.1	2363.1(x)	Mn: 6.4

B

Dye	Sample	Ca	Mg	Fe	Na	Other
Acid Fast Red Soap and Soda	C1	61.7	12.8	0.8	5401.8x	Cr: 0.1
Acid Fast Red Soap and Soda	C2	64.4	8.2	0.6	5694.8x	Cr: 0.1
Acid Fast Red Soap and Soda	C3	61.7	14	0.5	4573.3x	
Acid Fast Red Soap and Soda	C4	67.4	12.8	0.8	4673.9x	Cr: 0.1
Acid Fast Red Soap and Soda	C5	69.6	15.9	1.1	4803.7x	Cr: 0.1
Acid Fast Red Soap and Soda	S1	48	10.5	59.8	5177.4x	
Acid Fast Red Soap and Soda	S2	603.35x	0.05	0	286.25	
Acid Fast Red Soap and Soda	S3	392.6	0.4	0	226.05	As: 0.4
Acid Fast Red Soap and Soda	S4	58.7	12.1	15.6	5054.65x	Cd: 0.05u
Acid Fast Red Soap and Soda	S5	983.65x	4822.85x	0.15		
Acid Fast Red Soap and Soda	S6	1015.1x	0.1	0	4445.9x	As: 0.7uv; Cd: 0.05uv; Cr: 0.4

Table D.8: ICP results of 5 g/L Acid Golden Yellow with Soap and Soda samples S1-S6 in (A) India compared with C1, C4, and C5 and (B) in USA average compared with C1-C5.

A

Dye	Sample	Ca	Mg	Fe	Na	Other
Acid Golden Yellow Soap and Soda	C1	23.6	2.5	1	3991.5x	
Acid Golden Yellow Soap and Soda	C4	26.4	5	0.1	1057.2x	
Acid Golden Yellow Soap and Soda	C5	19.6	5.2	0.3	765x	
Acid Golden Yellow Soap and Soda	S1	20.5	5.6	57.9	3191.9(x)	As: 0.7; Mn:
Acid Golden Yellow Soap and Soda	S2	93.1	21.3	6.4	2142.4(x)	Mn: 1663
Acid Golden Yellow Soap and Soda	S3	81.3	18.7	7.3	1843.7(x)	Mn: 14.5
Acid Golden Yellow Soap and Soda	S4	20.7	5.2	32.5	3583.6(x)	As: 1.2uv
Acid Golden Yellow Soap and Soda	S5	66.2	13.4	37.8	2507.7(x)	Mn: 10
Acid Golden Yellow Soap and Soda	S6	80.5	21.6	1.5	3645.2(x)	Mn: 16.3

B

Dye	Sample	Ca	Mg	Fe	Na	Other
Acid Golden Yellow Soap and Soda	C1	46.7	14.2	0.9	6149.8x	Cr: 0.1
Acid Golden Yellow Soap and Soda	C2	54.6	16.8	0.1u	5669.2x	
Acid Golden Yellow Soap and Soda	C3	35.4	14.6	0.2	4361.3x	
Acid Golden Yellow Soap and Soda	C4	68.8	19.1	0.2u	7021.8x	
Acid Golden Yellow Soap and Soda	C5	53.6	17.3	0.2	5603.1x	
Acid Golden Yellow Soap and Soda	S1	37.15	14.95	133.3	5427.15x	Cd: 0.05uv; Mn: 3.1
Acid Golden Yellow Soap and Soda	S2	758.55x	0.05	0.1u	2214.1x	Pb: 0.6
Acid Golden Yellow Soap and Soda	S3	693.35x	0	0.05u	1922.75x	
Acid Golden Yellow Soap and Soda	S4	56.9	14.1	36.2	4147.4x	Mn: 1.1
Acid Golden Yellow Soap and Soda	S5	964.9x	0.05	0	5362.9x	Cd: 0.05uv; Cr: 0.55; Pb: 0.9
Acid Golden Yellow Soap and Soda	S6	994.3x	0.15	0.1u	5171.25x	Cr: 0.45

Table D.9: ICP results of 5 g/L Acid Ananda Blue with Soap and Soda samples S1-S6 in (A) India compared with C1, C4, and C5 and (B) in USA average compared with C1-C5.

A

Dye	Sample	Ca	Mg	Fe	Na	Other
Acid Ananda Blue Soap and Soda	C1	14.1	3.5	2.3	3256.7x	
Acid Ananda Blue Soap and Soda	C4	18.5	4.4	1.2	626.1x	
Acid Ananda Blue Soap and Soda	C5	12	2.9	0.9	397	
Acid Ananda Blue Soap and Soda	S1	19.7	6.1	386.8	4888.9(X)	Cd: 0.1; Mn: 2.5; Pb: 1.4
Acid Ananda Blue Soap and Soda	S2	103	27.3	31.7	3828.7(x)	Mn: 21.2
Acid Ananda Blue Soap and Soda	S3	89.6	23.7	15.1	3281.8(x)	Mn: 18.7
Acid Ananda Blue Soap and Soda	S4	18.9	5.2	147.1	4155.1(x)	Cd: 0.1; Mn: 1.2; Pb: 1.8
Acid Ananda Blue Soap and Soda	S5	72.8	16.1	58.4	4229.6(x)	Mn: 11.1
Acid Ananda Blue Soap and Soda	S6	62.5	13.7	14.9	3390(x)	Mn: 9.5

B

Dye	Sample	Ca	Mg	Fe	Na	Other
Acid Ananda Blue Soap and Soda	C1	34.5	11	2.1	5549.9x	Cr: 2.0; Mn: 1.0; Pb: 11uv
Acid Ananda Blue Soap and Soda	C2	47	16.7	3.2	5308.7x	Cr: 1.0; Mn: 1.0; Pb: 72
Acid Ananda Blue Soap and Soda	C3	36.3	13	2.5	4182.4x	Cr: 1.0; Mn: 1.0; Pb: 54
Acid Ananda Blue Soap and Soda	C4	46.7	16.5	3.4	5617.4x	Cr: 1.0; Mn: 2.0; Pb: 95
Acid Ananda Blue Soap and Soda	C5	39.6	13.9	3.1	4307.9x	Cr: 1.0; Mn: 2.0; Pb: 17uv
Acid Ananda Blue Soap and Soda	S1	32.8	9.45	350.2	5648.3x	Cd: 0.25; Mn: 1.9; Pb: 1.2
Acid Ananda Blue Soap and Soda	S2	1095.1x	0	0.05	3649.45x	As: 0.75
Acid Ananda Blue Soap and Soda	S3	979.35x	0.2	0	3428.9x	
Acid Ananda Blue Soap and Soda	S4	32.5	10.75	54.1	5609.15x	As: 0.55; Cd: 0.1; Pb: 0.6
Acid Ananda Blue Soap and Soda	S5	861.4x	0.05	0.15	5134x	
Acid Ananda Blue Soap and Soda	S6	906x	0	0	5488.15x	

Appendix E – Respirometric Analysis

This appendix contains graphs comparing three trials of endogenous and exogenous data describing the oxygen uptake for each of the color sets. R4H, R4M, R4L or R5H, R5M, R5L for Reactive Red 120 (Figure E.1), Reactive Yellow 81 (Figure E.2), and Reactive Blue 4 (Figure E.3); A4, A5, A7, A8, A10, A11 for Acid Fast Red (Figure E.4), Acid Golden Yellow (Figure E.5), and Acid Ananda Blue (Figure E.6); and S4 and S5 for Acid Fast Red with Soap and Soda (Figure E.7), Acid Golden Yellow with Soap and Soda (Figure E.8), and Acid Ananda Blue with Soap and Soda (Figure E.9); and Field Sample Green and Maroon (Figure E.10).

A

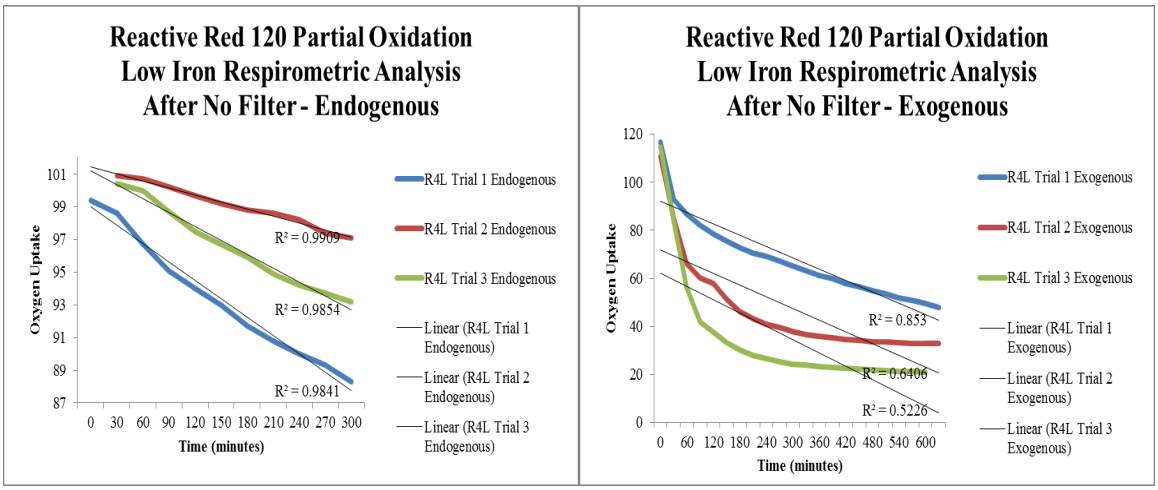
Reactive Red 120 Partial Oxidation
Low Iron Respirometric Analysis
After No Filter - Endogenous
Oxygen Uptake
Time (minutes)
R² = 0.9909
R² = 0.9854
R² = 0.9841
R4L Trial 1 Endogenous
R4L Trial 2 Endogenous
R4L Trial 3 Endogenous
Linear (R4L Trial 1 Endogenous)
Linear (R4L Trial 2 Endogenous)
Linear (R4L Trial 3 Endogenous)
Reactive Red 120 Partial Oxidation
Low Iron Respirometric Analysis
After No Filter - Exogenous
Oxygen Uptake
Time (minutes)
R² = 0.853
R² = 0.6406
R² = 0.5226
R4L Trial 1 Exogenous
R4L Trial 2 Exogenous
R4L Trial 3 Exogenous
Linear (R4L Trial 1 Exogenous)
Linear (R4L Trial 2 Exogenous)
Linear (R4L Trial 3 Exogenous)

B

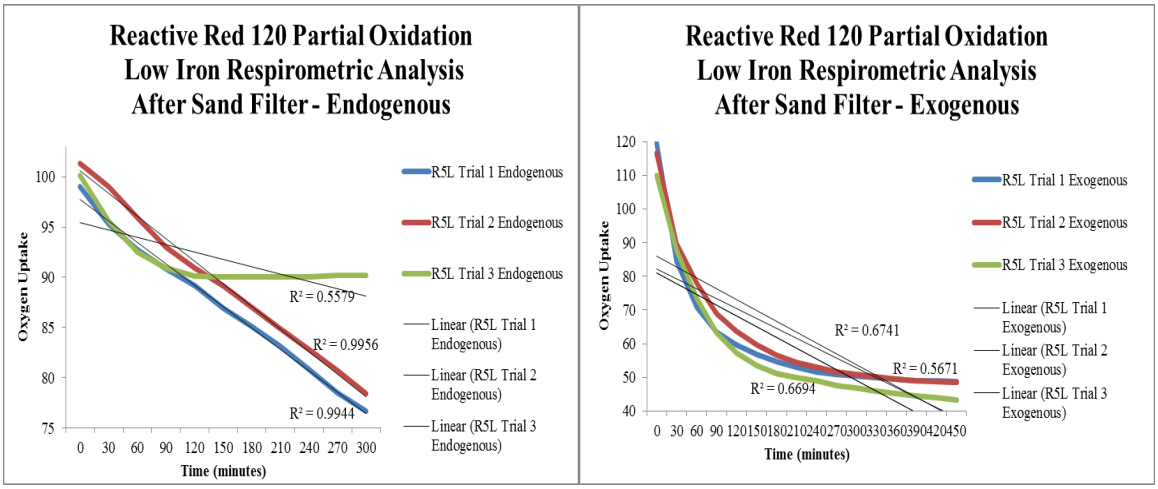
Reactive Red 120 Partial Oxidation
Low Iron Respirometric Analysis
After Sand Filter - Endogenous
Oxygen Uptake
Time (minutes)
R² = 0.5579
R² = 0.9956
R² = 0.9944
R5L Trial 1 Endogenous
R5L Trial 2 Endogenous
R5L Trial 3 Endogenous
Linear (R5L Trial 1 Endogenous)
Linear (R5L Trial 2 Endogenous)
Linear (R5L Trial 3 Endogenous)
Reactive Red 120 Partial Oxidation
Low Iron Respirometric Analysis
After Sand Filter - Exogenous
Oxygen Uptake
Time (minutes)
R² = 0.6741
R² = 0.5671
R² = 0.6694
R5L Trial 1 Exogenous
R5L Trial 2 Exogenous
R5L Trial 3 Exogenous
Linear (R5L Trial 1 Exogenous)
Linear (R5L Trial 2 Exogenous)
Linear (R5L Trial 3 Exogenous)

C

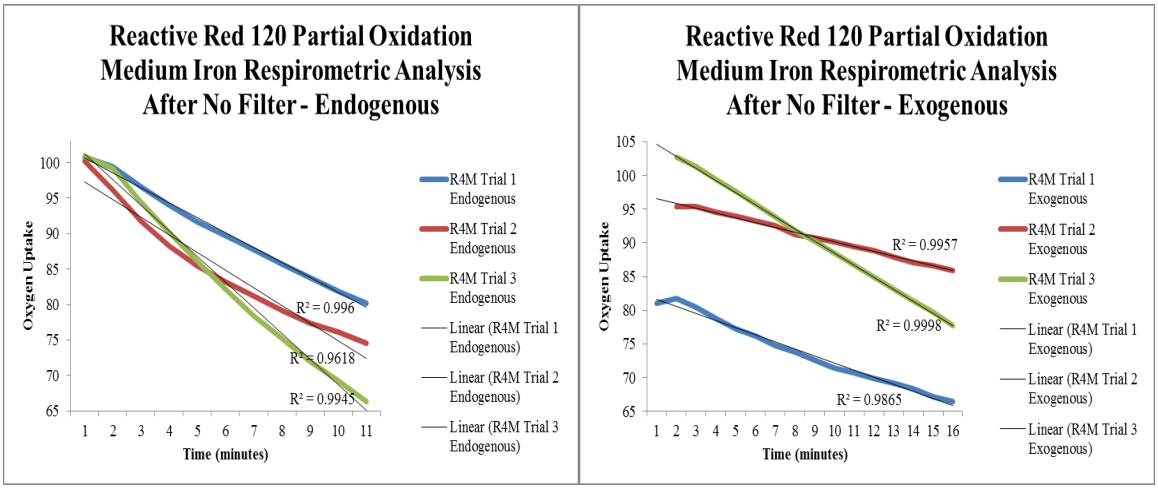
Reactive Red 120 Partial Oxidation
Medium Iron Respirometric Analysis
After No Filter - Endogenous
Oxygen Uptake
Time (minutes)
R² = 0.996
R² = 0.9618
R² = 0.9945
R4M Trial 1 Endogenous
R4M Trial 2 Endogenous
R4M Trial 3 Endogenous
Linear (R4M Trial 1 Endogenous)
Linear (R4M Trial 2 Endogenous)
Linear (R4M Trial 3 Endogenous)
Reactive Red 120 Partial Oxidation
Medium Iron Respirometric Analysis
After No Filter - Exogenous
Oxygen Uptake
Time (minutes)
R² = 0.9957
R² = 0.9998
R² = 0.9865
R4M Trial 1 Exogenous
R4M Trial 2 Exogenous
R4M Trial 3 Exogenous
Linear (R4M Trial 1 Exogenous)
Linear (R4M Trial 2 Exogenous)
Linear (R4M Trial 3 Exogenous)

D

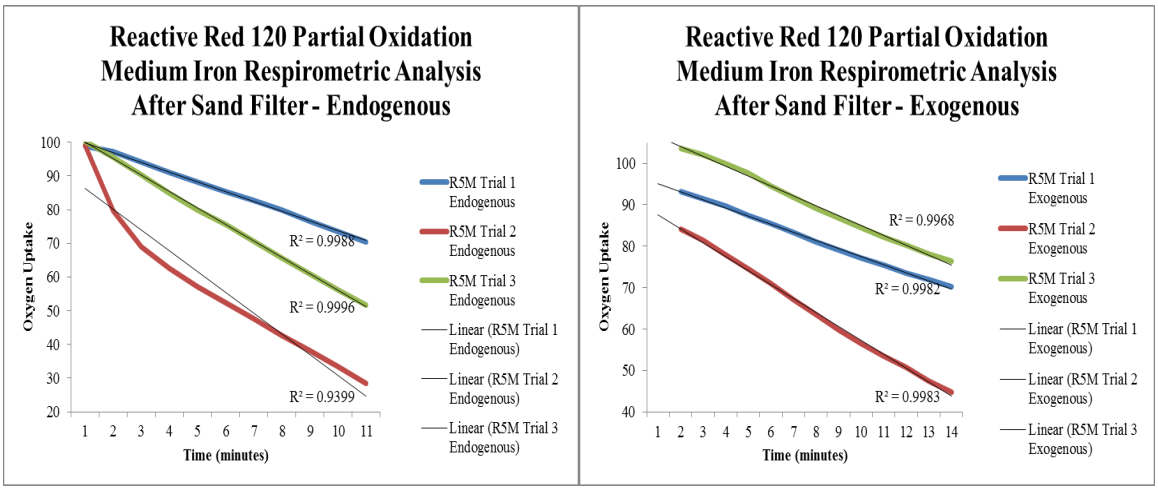

E

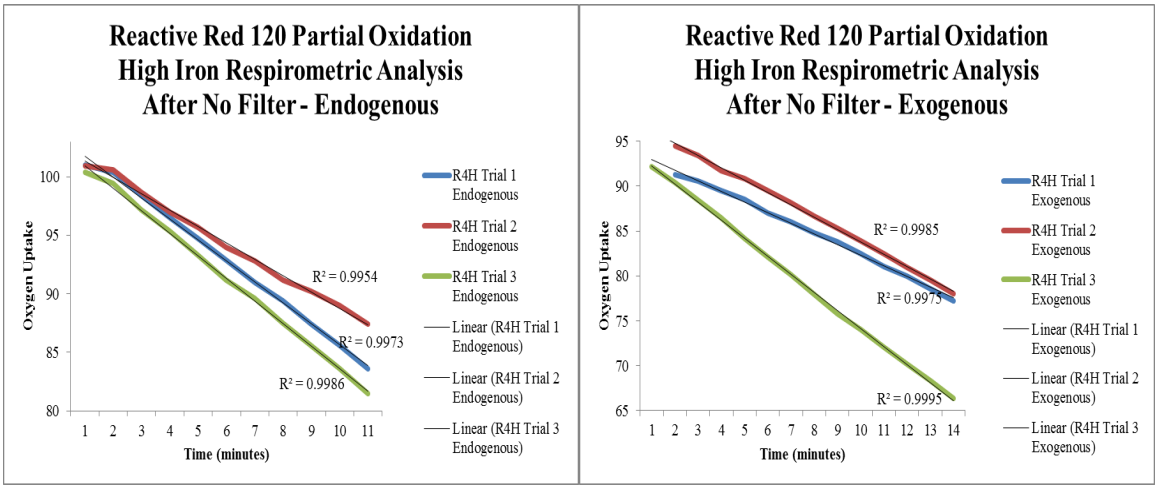

F

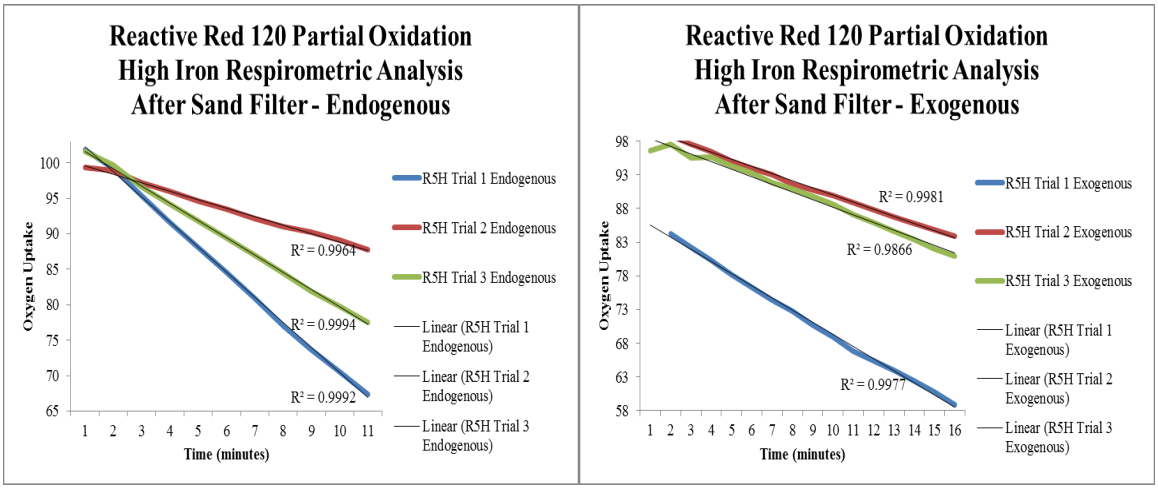

Figure E.1: Reactive Red 120 Respirometric Analysis (A) Low Iron No Filter, (B) Low Iron Sand Filter, (C) Medium Iron No Filter, (D) Medium Iron Sand Filter, (E) High Iron No Filter, (F) High Iron Sand Filter.

A

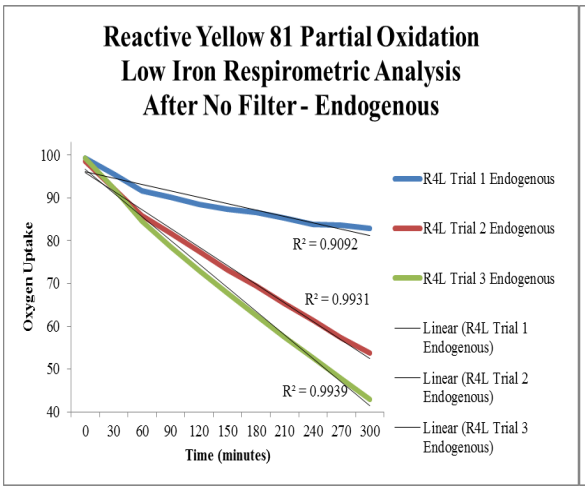
Reactive Yellow 81 Partial Oxidation Low Iron Respirometric Analysis After No Filter - Endogenous
Oxygen Uptake
Time (minutes)
R² = 0.9092
R² = 0.9931
R² = 0.9939
R4L Trial 1 Endogenous
R4L Trial 2 Endogenous
R4L Trial 3 Endogenous
Linear (R4L Trial 1 Endogenous)
Linear (R4L Trial 2 Endogenous)
Linear (R4L Trial 3 Endogenous)

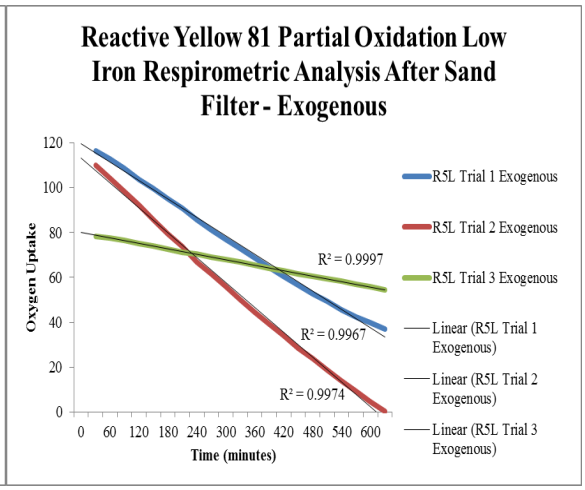
Reactive Yellow 81 Partial Oxidation Low Iron Respirometric Analysis After Sand Filter - Exogenous
Oxygen Uptake
Time (minutes)
R² = 0.9997
R² = 0.9967
R² = 0.9974
R5L Trial 1 Exogenous
R5L Trial 2 Exogenous
R5L Trial 3 Exogenous
Linear (R5L Trial 1 Exogenous)
Linear (R5L Trial 2 Exogenous)
Linear (R5L Trial 3 Exogenous)

B

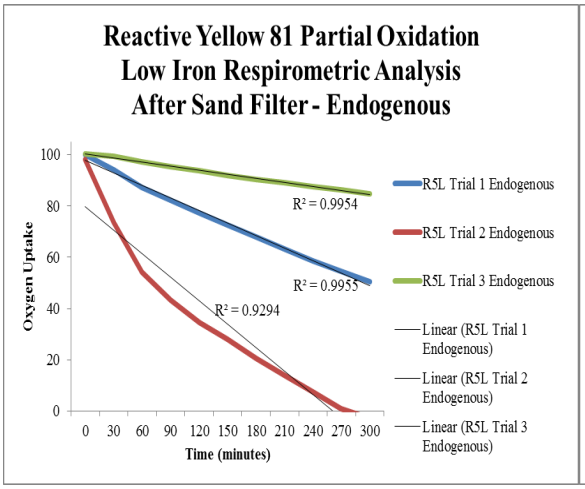
Reactive Yellow 81 Partial Oxidation Low Iron Respirometric Analysis After Sand Filter - Endogenous
Oxygen Uptake
Time (minutes)
R² = 0.9954
R² = 0.9955
R² = 0.9294
R5L Trial 1 Endogenous
R5L Trial 2 Endogenous
R5L Trial 3 Endogenous
Linear (R5L Trial 1 Endogenous)
Linear (R5L Trial 2 Endogenous)
Linear (R5L Trial 3 Endogenous)

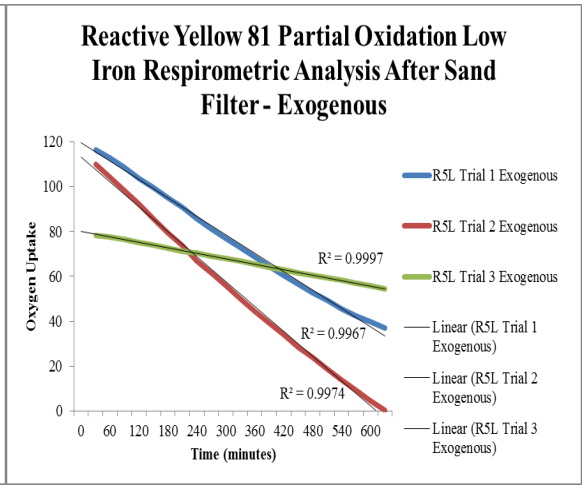
Reactive Yellow 81 Partial Oxidation Low Iron Respirometric Analysis After Sand Filter - Exogenous
Oxygen Uptake
Time (minutes)
R² = 0.9997
R² = 0.9967
R² = 0.9974
R5L Trial 1 Exogenous
R5L Trial 2 Exogenous
R5L Trial 3 Exogenous
Linear (R5L Trial 1 Exogenous)
Linear (R5L Trial 2 Exogenous)
Linear (R5L Trial 3 Exogenous)

C

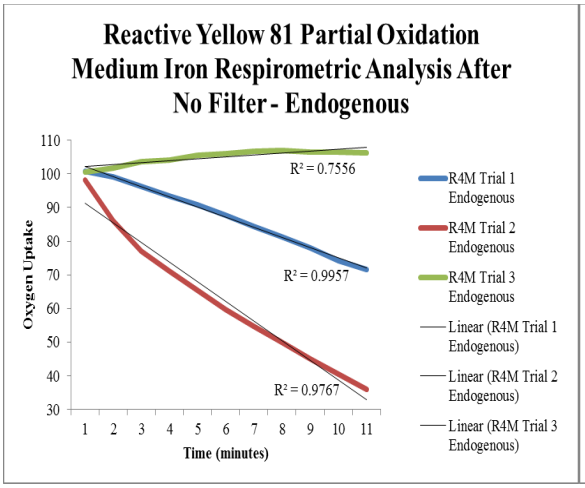
Reactive Yellow 81 Partial Oxidation Medium Iron Respirometric Analysis After No Filter - Endogenous
Oxygen Uptake
Time (minutes)
R² = 0.7556
R² = 0.9957
R² = 0.9767
R4M Trial 1 Endogenous
R4M Trial 2 Endogenous
R4M Trial 3 Endogenous
Linear (R4M Trial 1 Endogenous)
Linear (R4M Trial 2 Endogenous)
Linear (R4M Trial 3 Endogenous)

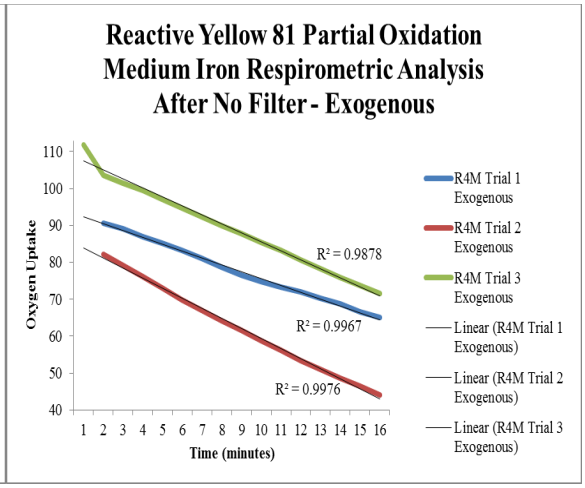
Reactive Yellow 81 Partial Oxidation Medium Iron Respirometric Analysis After No Filter - Exogenous
Oxygen Uptake
Time (minutes)
R² = 0.9878
R² = 0.9967
R² = 0.9976
R4M Trial 1 Exogenous
R4M Trial 2 Exogenous
R4M Trial 3 Exogenous
Linear (R4M Trial 1 Exogenous)
Linear (R4M Trial 2 Exogenous)
Linear (R4M Trial 3 Exogenous)

D

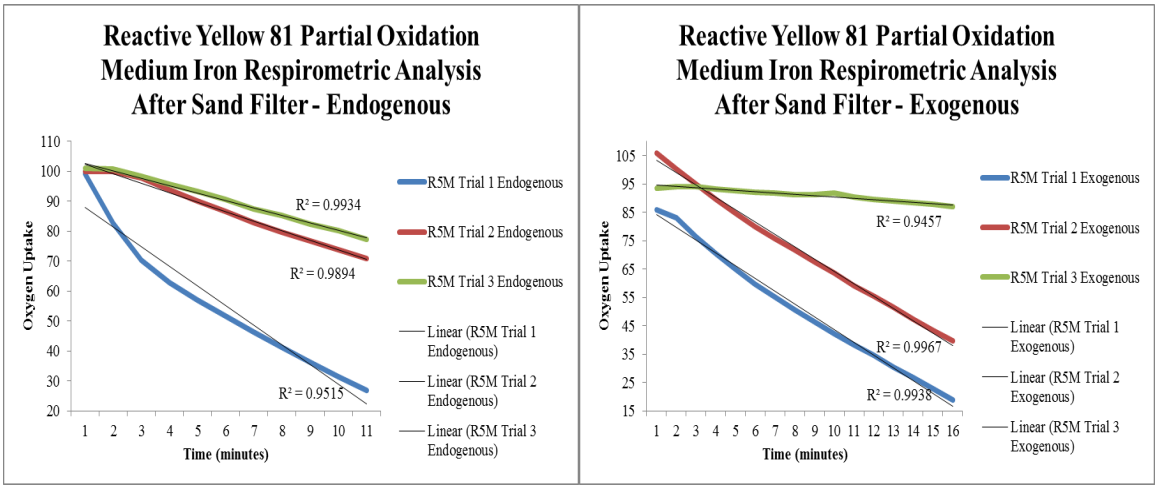

E

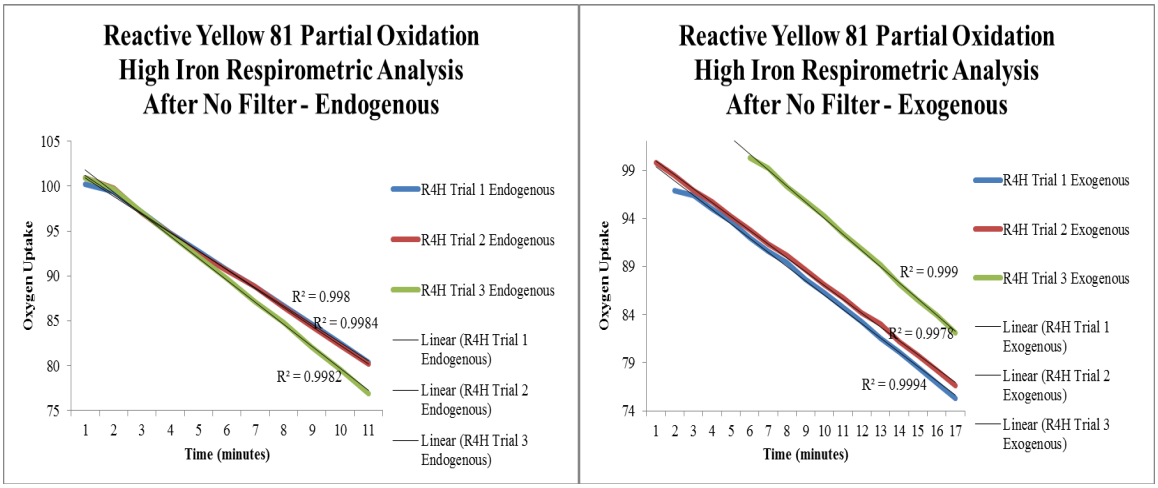

F

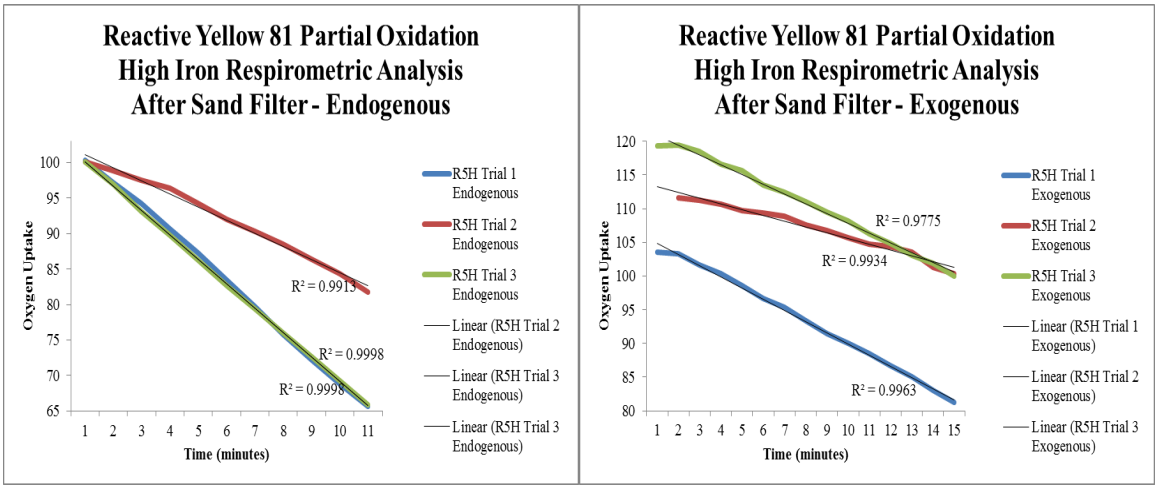

Figure E.2: Reactive Yellow 81 Respirometric Analysis (A) Low Iron No Filter, (B) Low Iron Sand Filter, (C) Medium Iron No Filter, (D) Medium Iron Sand Filter, (E) High Iron No Filter, (F) High Iron Sand Filter.

A

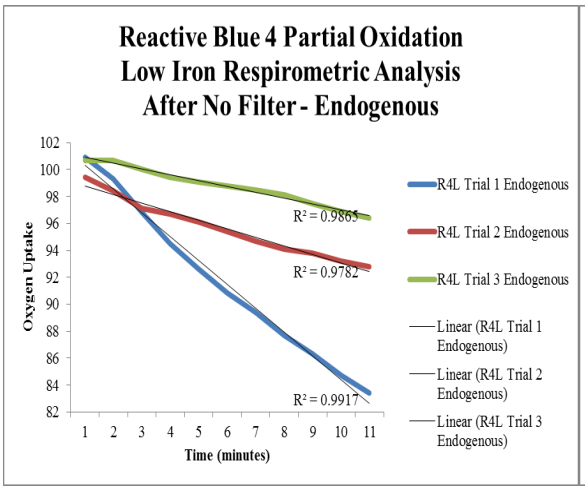
Reactive Blue 4 Partial Oxidation
Low Iron Respirometric Analysis
After No Filter - Endogenous
Oxygen Uptake
Time (minutes)
R² = 0.9865
R² = 0.9782
R² = 0.9917
R4L Trial 1 Endogenous
R4L Trial 2 Endogenous
R4L Trial 3 Endogenous
Linear (R4L Trial 1 Endogenous)
Linear (R4L Trial 2 Endogenous)
Linear (R4L Trial 3 Endogenous)

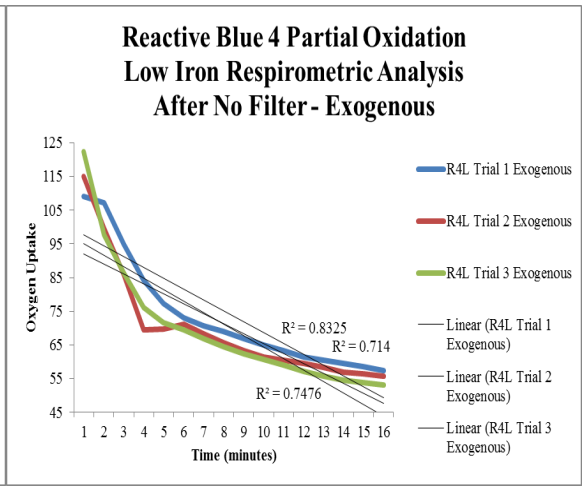
Reactive Blue 4 Partial Oxidation
Low Iron Respirometric Analysis
After No Filter - Exogenous
Oxygen Uptake
Time (minutes)
R² = 0.8325
R² = 0.714
R² = 0.7476
R4L Trial 1 Exogenous
R4L Trial 2 Exogenous
R4L Trial 3 Exogenous
Linear (R4L Trial 1 Exogenous)
Linear (R4L Trial 2 Exogenous)
Linear (R4L Trial 3 Exogenous)

B

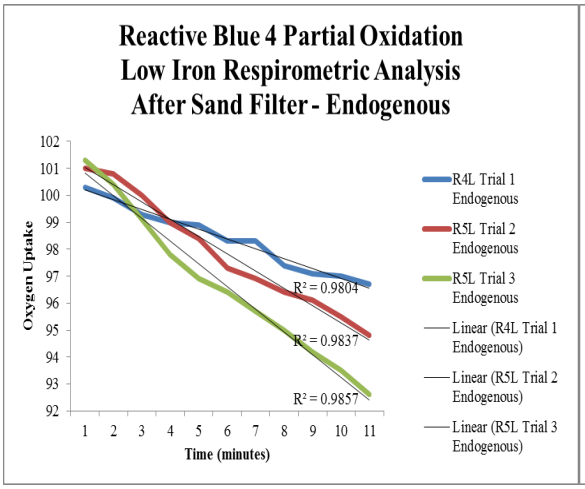
Reactive Blue 4 Partial Oxidation
Low Iron Respirometric Analysis
After Sand Filter - Endogenous
Oxygen Uptake
Time (minutes)
R² = 0.9804
R² = 0.9837
R² = 0.9857
R4L Trial 1 Endogenous
R5L Trial 2 Endogenous
R5L Trial 3 Endogenous
Linear (R4L Trial 1 Endogenous)
Linear (R5L Trial 2 Endogenous)
Linear (R5L Trial 3 Endogenous)

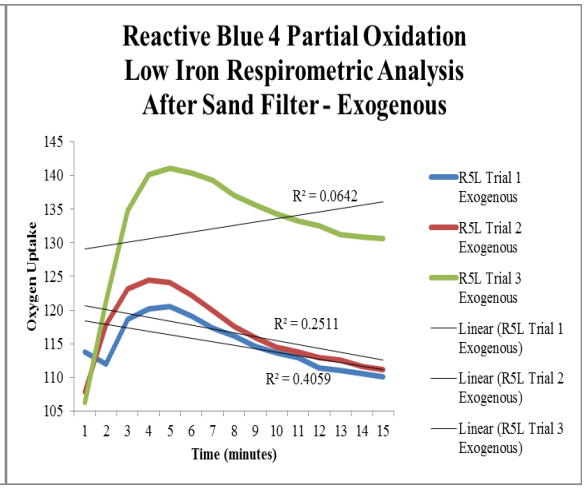
Reactive Blue 4 Partial Oxidation
Low Iron Respirometric Analysis
After Sand Filter - Exogenous
Oxygen Uptake
Time (minutes)
R² = 0.0642
R² = 0.2511
R² = 0.4059
R5L Trial 1 Exogenous
R5L Trial 2 Exogenous
R5L Trial 3 Exogenous
Linear (R5L Trial 1 Exogenous)
Linear (R5L Trial 2 Exogenous)
Linear (R5L Trial 3 Exogenous)

C

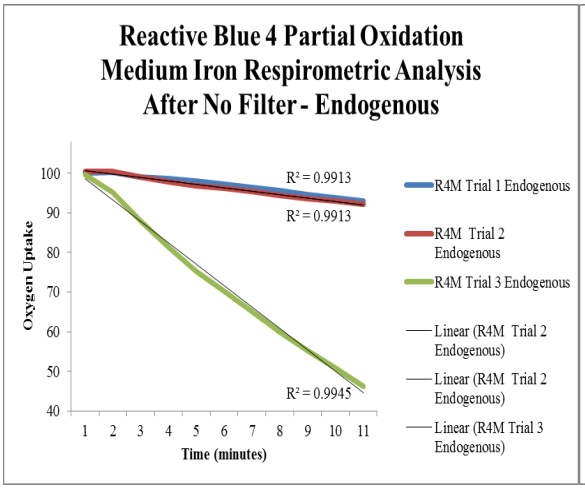
Reactive Blue 4 Partial Oxidation
Medium Iron Respirometric Analysis
After No Filter - Endogenous
Oxygen Uptake
Time (minutes)
R² = 0.9913
R² = 0.9913
R² = 0.9945
R4M Trial 1 Endogenous
R4M Trial 2 Endogenous
R4M Trial 3 Endogenous
Linear (R4M Trial 2 Endogenous)
Linear (R4M Trial 2 Endogenous)
Linear (R4M Trial 3 Endogenous)

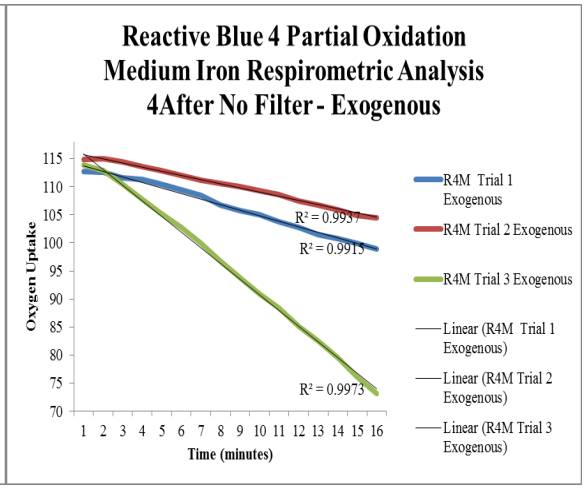
Reactive Blue 4 Partial Oxidation
Medium Iron Respirometric Analysis
4After No Filter - Exogenous
Oxygen Uptake
Time (minutes)
R² = 0.9937
R² = 0.9915
R² = 0.9973
R4M Trial 1 Exogenous
R4M Trial 2 Exogenous
R4M Trial 3 Exogenous
Linear (R4M Trial 1 Exogenous)
Linear (R4M Trial 2 Exogenous)
Linear (R4M Trial 3 Exogenous)

D

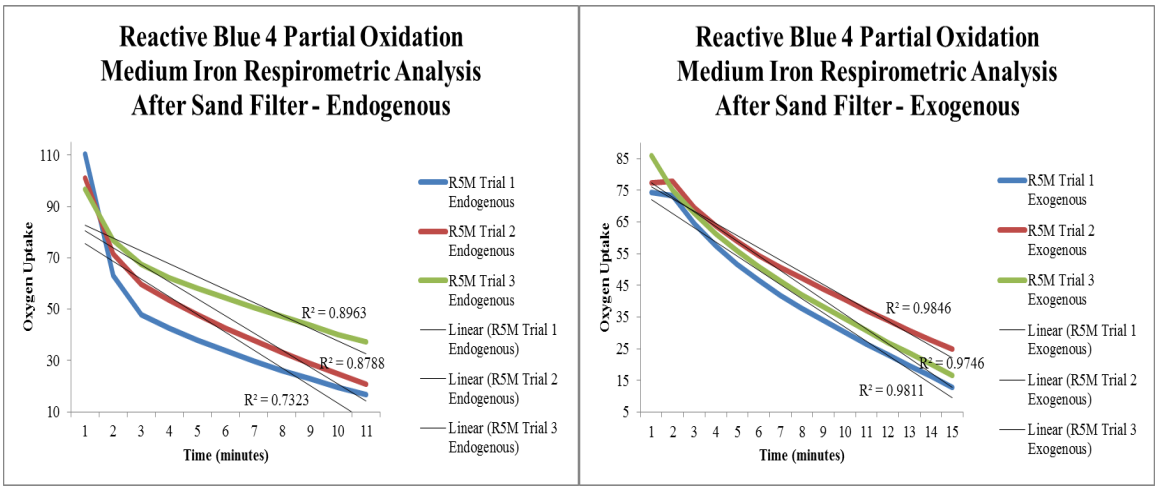

E

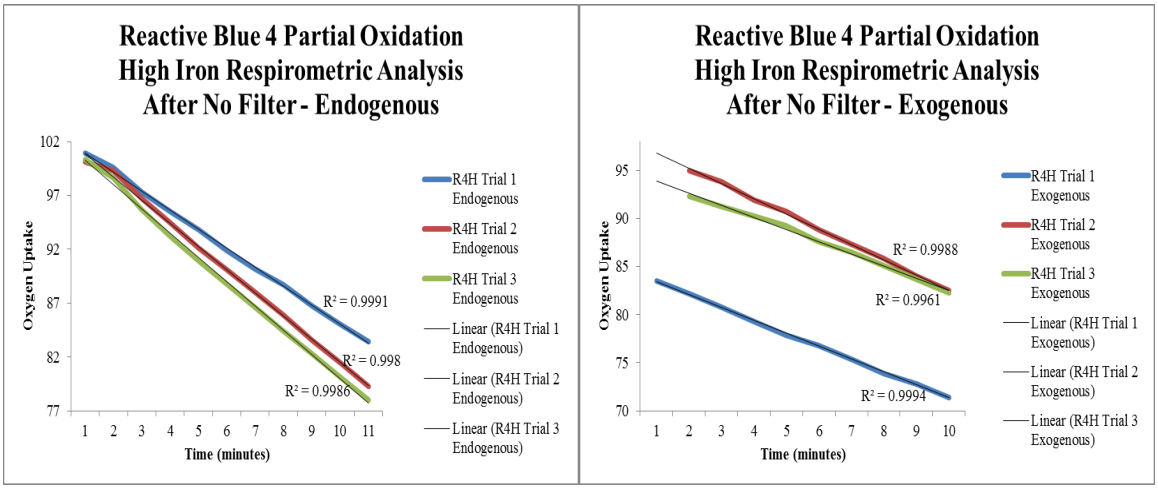

F

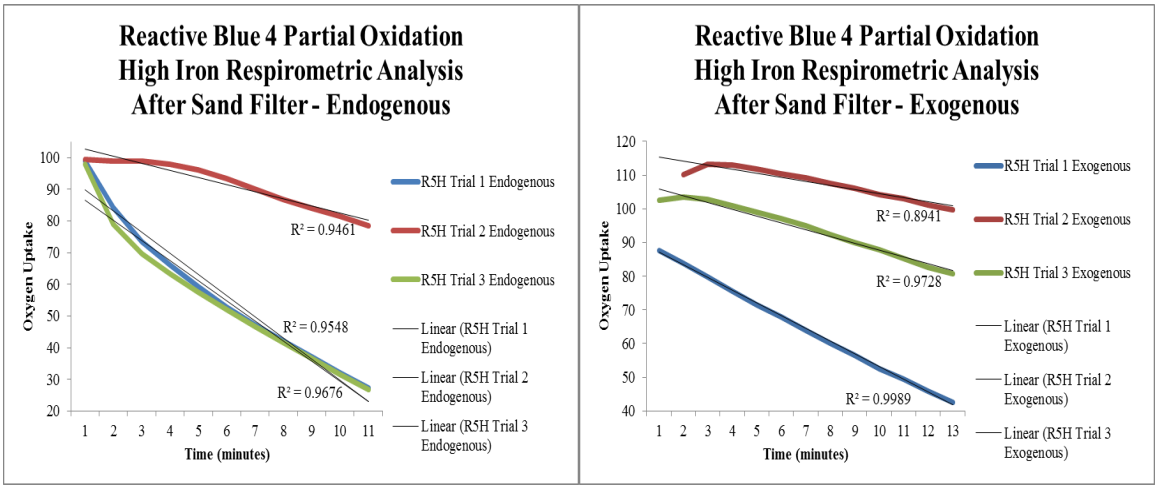

Figure E.3: Reactive Blue 5 Respirometric Analysis (A) Low Iron No Filter, (B) Low Iron Sand Filter, (C) Medium Iron No Filter, (D) Medium Iron Sand Filter, (E) High Iron No Filter, (F) High Iron Sand Filter.

A

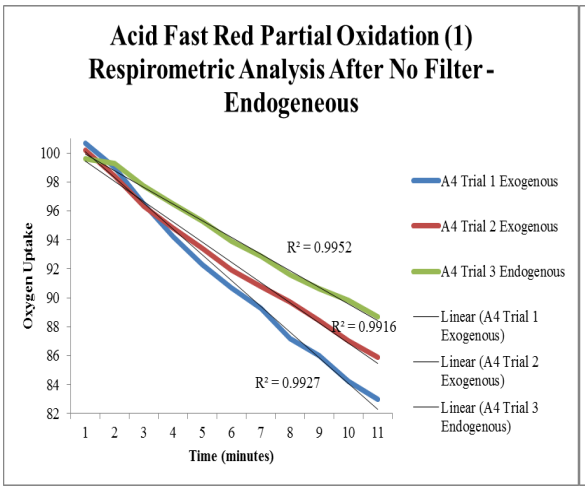
Acid Fast Red Partial Oxidation (1) Respirometric Analysis After No Filter - Endogeneous
Oxygen Uptake
Time (minutes)
R² = 0.9952
R² = 0.9916
R² = 0.9927
A4 Trial 1 Exogenous
A4 Trial 2 Exogenous
A4 Trial 3 Endogenous
Linear (A4 Trial 1 Exogenous)
Linear (A4 Trial 2 Exogenous)
Linear (A4 Trial 3 Endogenous)

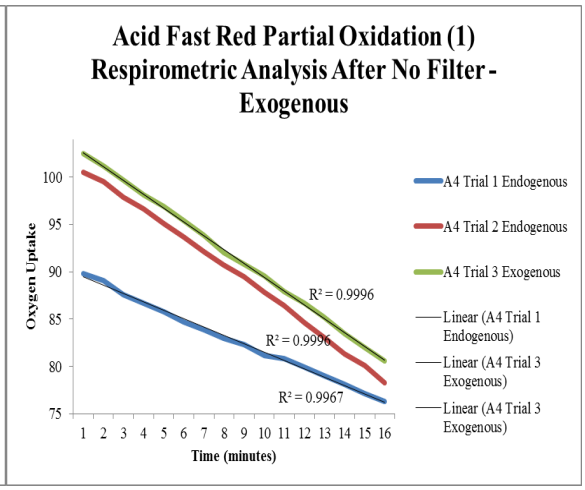
Acid Fast Red Partial Oxidation (1) Respirometric Analysis After No Filter - Exogenous
Oxygen Uptake
Time (minutes)
R² = 0.9996
R² = 0.9996
R² = 0.9967
A4 Trial 1 Endogenous
A4 Trial 2 Endogenous
A4 Trial 3 Exogenous
Linear (A4 Trial 1 Endogenous)
Linear (A4 Trial 3 Exogenous)
Linear (A4 Trial 3 Exogenous)

B

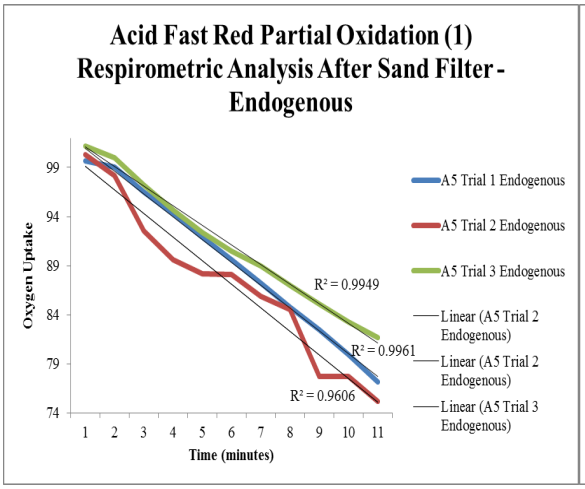
Acid Fast Red Partial Oxidation (1) Respirometric Analysis After Sand Filter - Endogenous
Oxygen Uptake
Time (minutes)
R² = 0.9949
R² = 0.9961
R² = 0.9606
A5 Trial 1 Endogenous
A5 Trial 2 Endogenous
A5 Trial 3 Endogenous
Linear (A5 Trial 2 Endogenous)
Linear (A5 Trial 2 Endogenous)
Linear (A5 Trial 3 Endogenous)

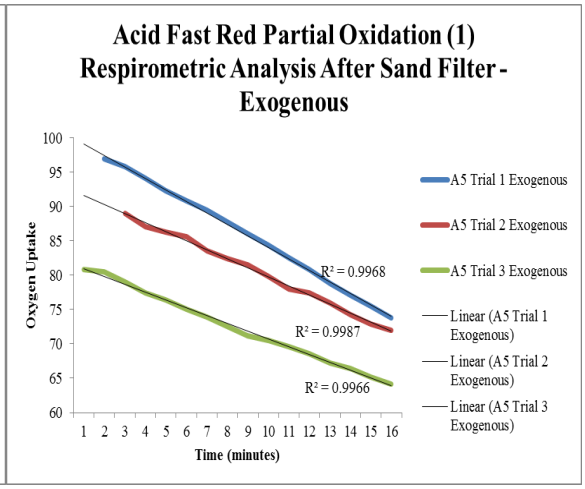
Acid Fast Red Partial Oxidation (1) Respirometric Analysis After Sand Filter - Exogenous
Oxygen Uptake
Time (minutes)
R² = 0.9968
R² = 0.9987
R² = 0.9966
A5 Trial 1 Exogenous
A5 Trial 2 Exogenous
A5 Trial 3 Exogenous
Linear (A5 Trial 1 Exogenous)
Linear (A5 Trial 2 Exogenous)
Linear (A5 Trial 3 Exogenous)

C

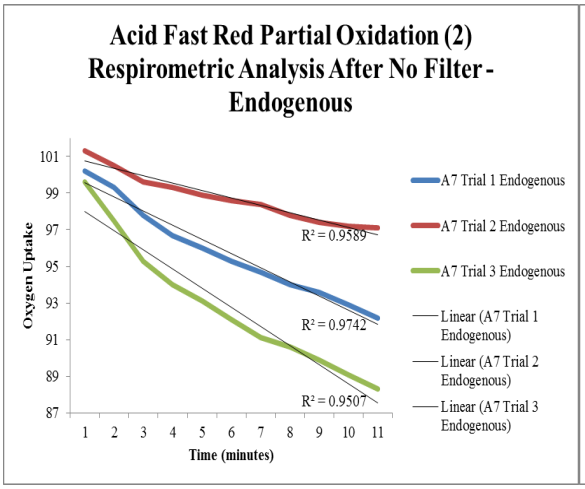
Acid Fast Red Partial Oxidation (2) Respirometric Analysis After No Filter - Endogenous
Oxygen Uptake
Time (minutes)
R² = 0.9589
R² = 0.9742
R² = 0.9507
A7 Trial 1 Endogenous
A7 Trial 2 Endogenous
A7 Trial 3 Endogenous
Linear (A7 Trial 1 Endogenous)
Linear (A7 Trial 2 Endogenous)
Linear (A7 Trial 3 Endogenous)

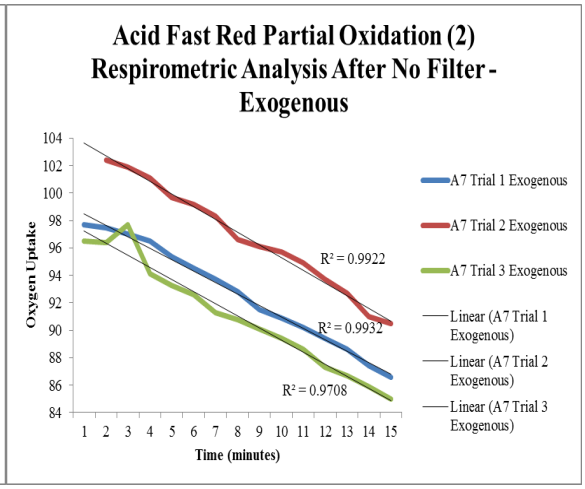
Acid Fast Red Partial Oxidation (2) Respirometric Analysis After No Filter - Exogenous
Oxygen Uptake
Time (minutes)
R² = 0.9922
R² = 0.9932
R² = 0.9708
A7 Trial 1 Exogenous
A7 Trial 2 Exogenous
A7 Trial 3 Exogenous
Linear (A7 Trial 1 Exogenous)
Linear (A7 Trial 2 Exogenous)
Linear (A7 Trial 3 Exogenous)

D

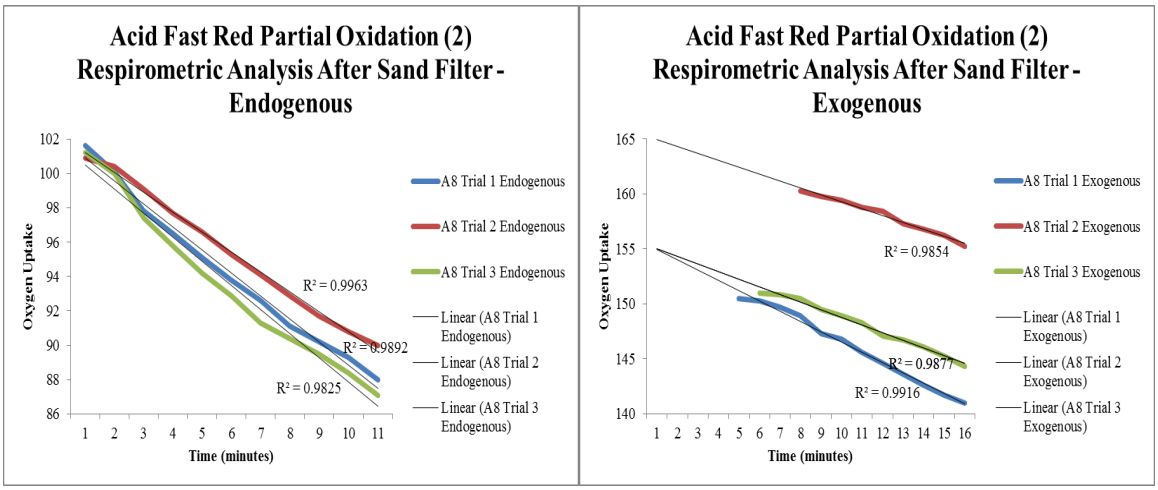

E

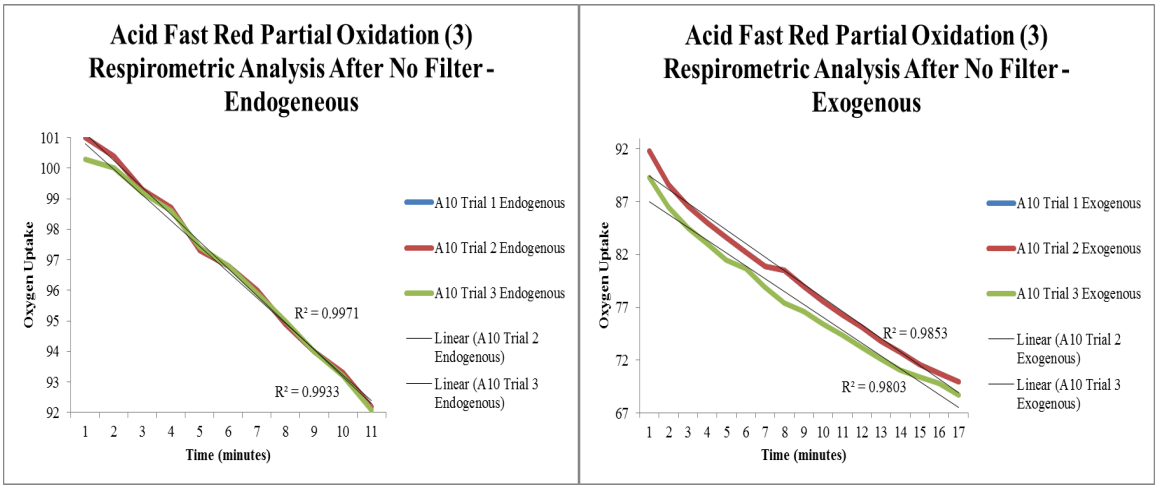

F

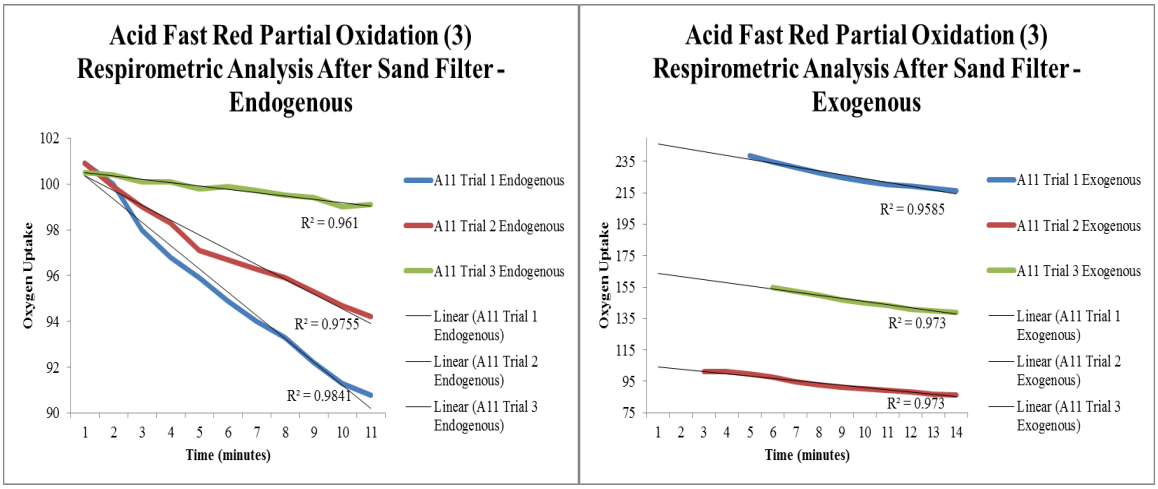

Figure E.4: Acid Fast Red Respirometric Analysis (A) Partial Oxidation 1 No Filter, (B) Partial Oxidation 1 Sand Filter, (C) Partial Oxidation 2 No Filter, (D) Partial Oxidation 2 Sand Filter, (E) Partial Oxidation 3 No Filter, (F) Partial Oxidation 3 Sand Filter

A

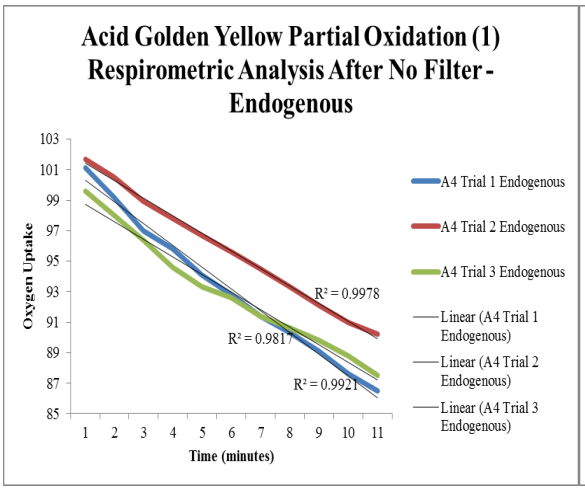
Acid Golden Yellow Partial Oxidation (1) Respirometric Analysis After No Filter - Endogenous
Oxygen Uptake
Time (minutes)
R² = 0.9978
R² = 0.9817
R² = 0.9921
A4 Trial 1 Endogenous
A4 Trial 2 Endogenous
A4 Trial 3 Endogenous
Linear (A4 Trial 1 Endogenous)
Linear (A4 Trial 2 Endogenous)
Linear (A4 Trial 3 Endogenous)

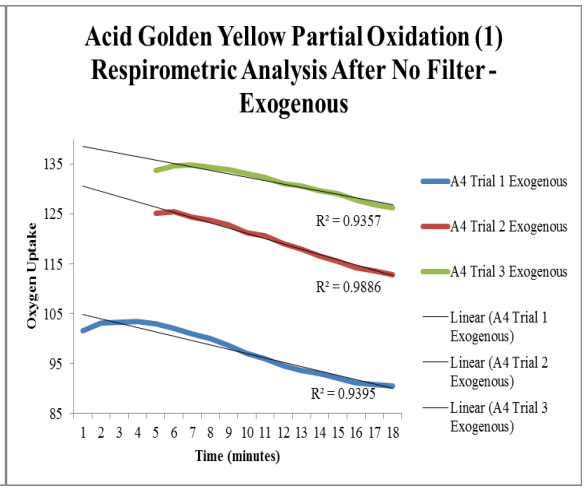
Acid Golden Yellow Partial Oxidation (1) Respirometric Analysis After No Filter - Exogenous
Oxygen Uptake
Time (minutes)
R² = 0.9357
R² = 0.9886
R² = 0.9395
A4 Trial 1 Exogenous
A4 Trial 2 Exogenous
A4 Trial 3 Exogenous
Linear (A4 Trial 1 Exogenous)
Linear (A4 Trial 2 Exogenous)
Linear (A4 Trial 3 Exogenous)

B

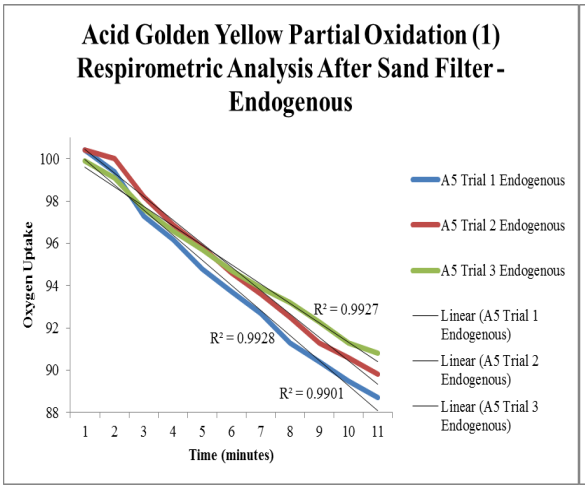
Acid Golden Yellow Partial Oxidation (1) Respirometric Analysis After Sand Filter - Endogenous
Oxygen Uptake
Time (minutes)
R² = 0.9927
R² = 0.9928
R² = 0.9901
A5 Trial 1 Endogenous
A5 Trial 2 Endogenous
A5 Trial 3 Endogenous
Linear (A5 Trial 1 Endogenous)
Linear (A5 Trial 2 Endogenous)
Linear (A5 Trial 3 Endogenous)

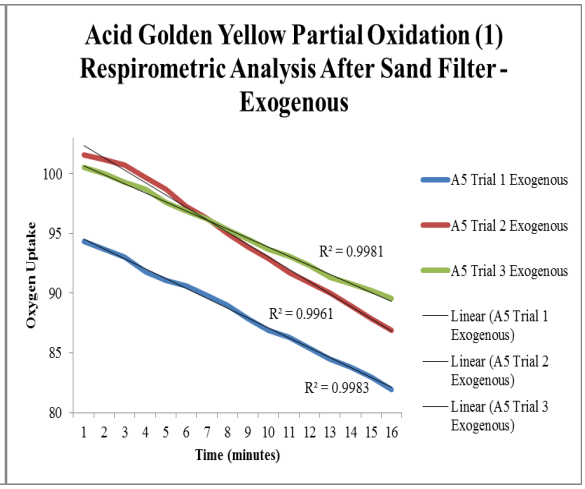
Acid Golden Yellow Partial Oxidation (1) Respirometric Analysis After Sand Filter - Exogenous
Oxygen Uptake
Time (minutes)
R² = 0.9981
R² = 0.9961
R² = 0.9983
A5 Trial 1 Exogenous
A5 Trial 2 Exogenous
A5 Trial 3 Exogenous
Linear (A5 Trial 1 Exogenous)
Linear (A5 Trial 2 Exogenous)
Linear (A5 Trial 3 Exogenous)

C

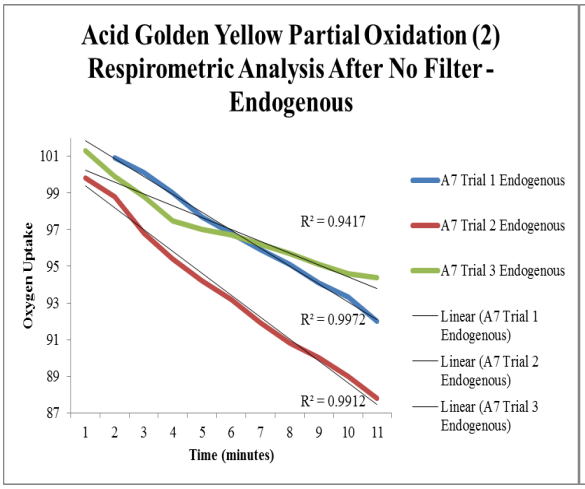
Acid Golden Yellow Partial Oxidation (2) Respirometric Analysis After No Filter - Endogenous
Oxygen Uptake
Time (minutes)
R² = 0.9417
R² = 0.9972
R² = 0.9912
A7 Trial 1 Endogenous
A7 Trial 2 Endogenous
A7 Trial 3 Endogenous
Linear (A7 Trial 1 Endogenous)
Linear (A7 Trial 2 Endogenous)
Linear (A7 Trial 3 Endogenous)

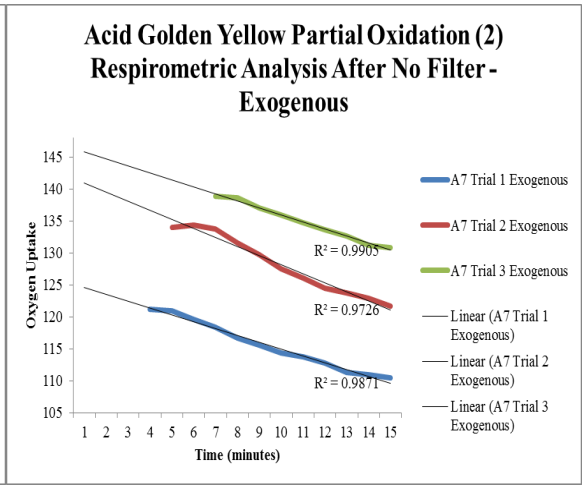
Acid Golden Yellow Partial Oxidation (2) Respirometric Analysis After No Filter - Exogenous
Oxygen Uptake
Time (minutes)
R² = 0.9905
R² = 0.9726
R² = 0.9871
A7 Trial 1 Exogenous
A7 Trial 2 Exogenous
A7 Trial 3 Exogenous
Linear (A7 Trial 1 Exogenous)
Linear (A7 Trial 2 Exogenous)
Linear (A7 Trial 3 Exogenous)

D

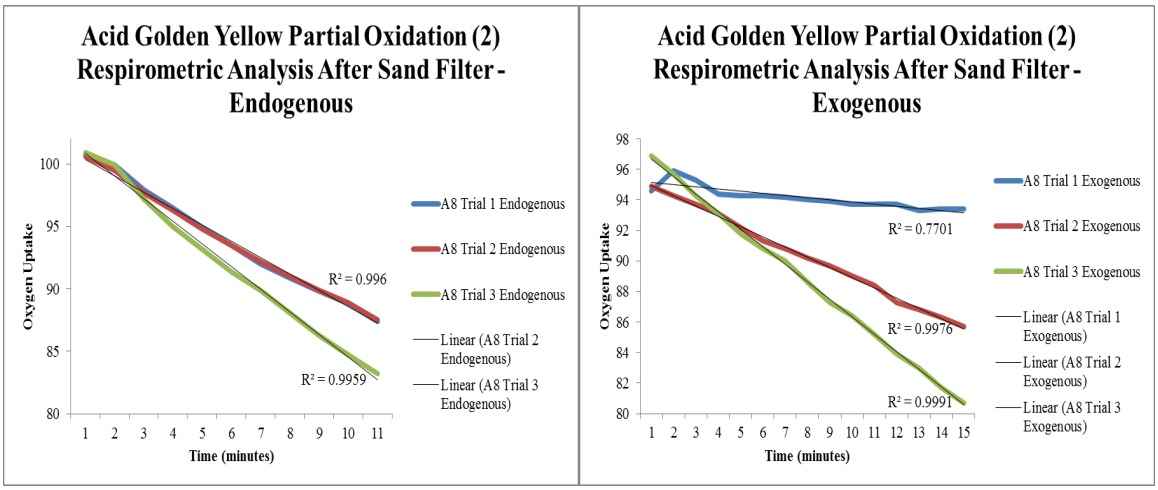

E

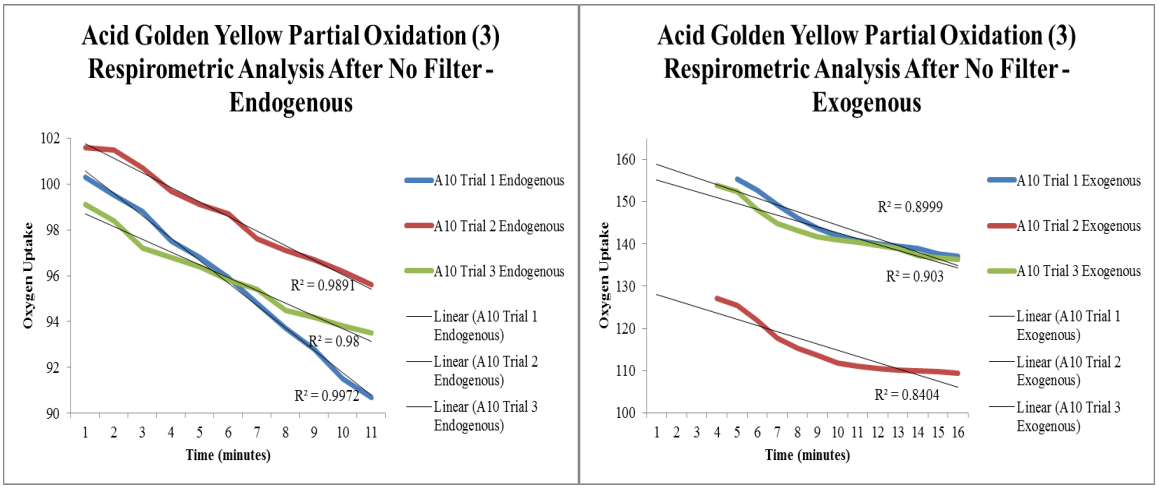

F

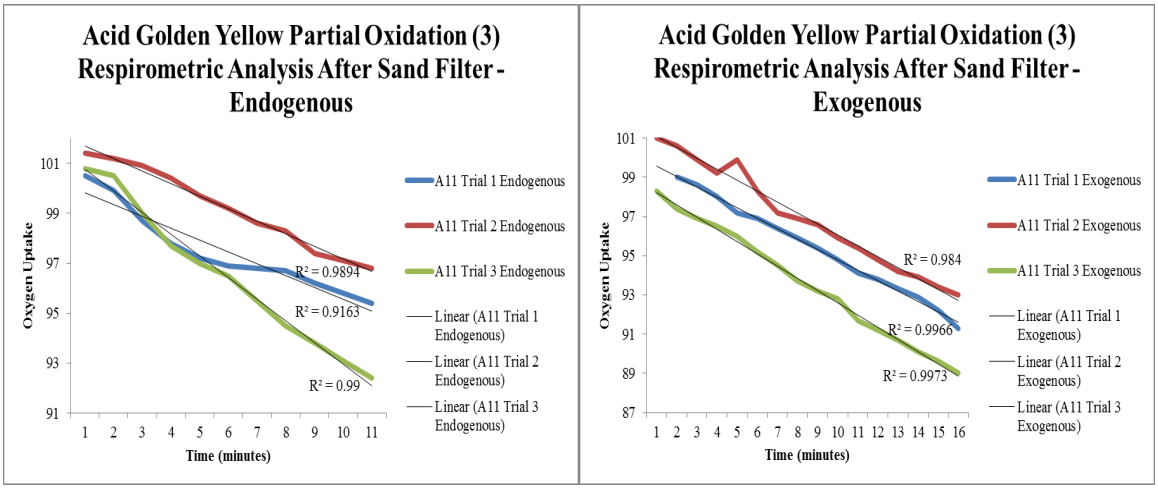

Figure E.5: Acid Golden Yellow Respirometric Analysis (A) Partial Oxidation 1 No Filter, (B) Partial Oxidation 1 Sand Filter, (C) Partial Oxidation 2 No Filter, (D) Partial Oxidation 2 Sand Filter, (E) Partial Oxidation 3 No Filter, (F) Partial Oxidation 3 Sand Filter

A

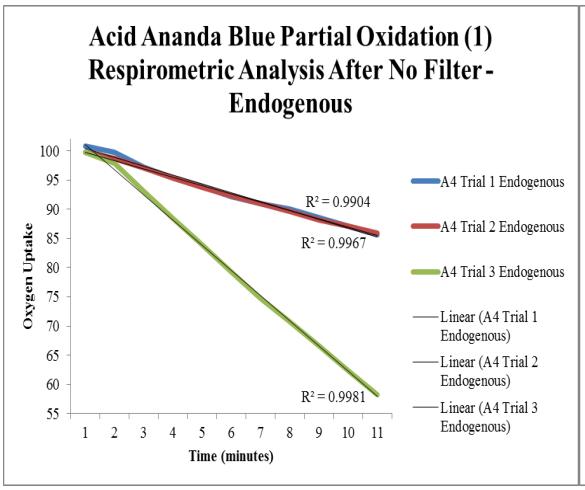
Acid Ananda Blue Partial Oxidation (1) Respirometric Analysis After No Filter - Endogenous
Oxygen Uptake
Time (minutes)
R² = 0.9904
R² = 0.9967
R² = 0.9981
A4 Trial 1 Endogenous
A4 Trial 2 Endogenous
A4 Trial 3 Endogenous
Linear (A4 Trial 1 Endogenous)
Linear (A4 Trial 2 Endogenous)
Linear (A4 Trial 3 Endogenous)

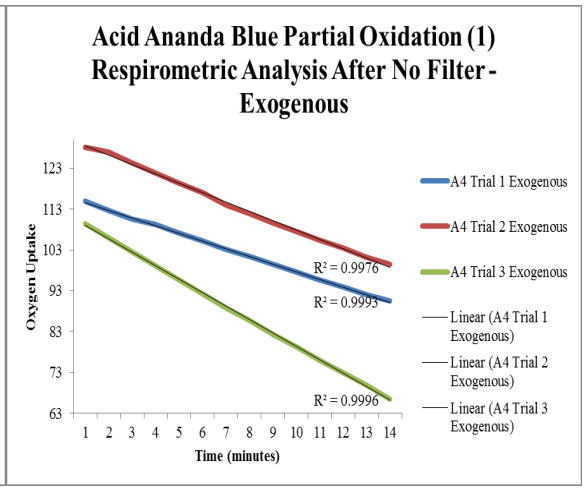
Acid Ananda Blue Partial Oxidation (1) Respirometric Analysis After No Filter - Exogenous
Oxygen Uptake
Time (minutes)
R² = 0.9976
R² = 0.9993
R² = 0.9996
A4 Trial 1 Exogenous
A4 Trial 2 Exogenous
A4 Trial 3 Exogenous
Linear (A4 Trial 1 Exogenous)
Linear (A4 Trial 2 Exogenous)
Linear (A4 Trial 3 Exogenous)

B

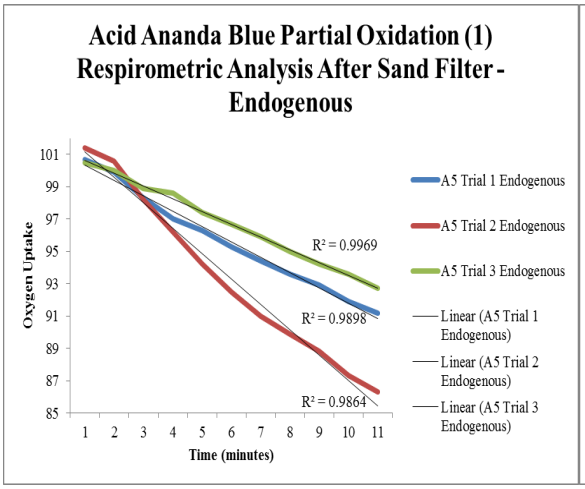
Acid Ananda Blue Partial Oxidation (1) Respirometric Analysis After Sand Filter - Endogenous
Oxygen Uptake
Time (minutes)
R² = 0.9969
R² = 0.9898
R² = 0.9864
A5 Trial 1 Endogenous
A5 Trial 2 Endogenous
A5 Trial 3 Endogenous
Linear (A5 Trial 1 Endogenous)
Linear (A5 Trial 2 Endogenous)
Linear (A5 Trial 3 Endogenous)

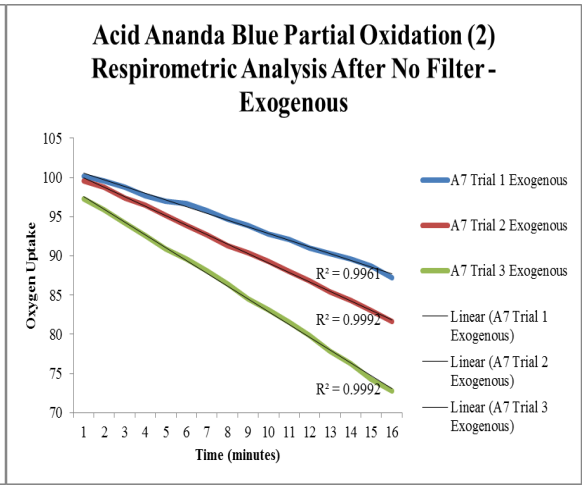
Acid Ananda Blue Partial Oxidation (2) Respirometric Analysis After No Filter - Exogenous
Oxygen Uptake
Time (minutes)
R² = 0.9961
R² = 0.9992
R² = 0.9992
A7 Trial 1 Exogenous
A7 Trial 2 Exogenous
A7 Trial 3 Exogenous
Linear (A7 Trial 1 Exogenous)
Linear (A7 Trial 2 Exogenous)
Linear (A7 Trial 3 Exogenous)

C

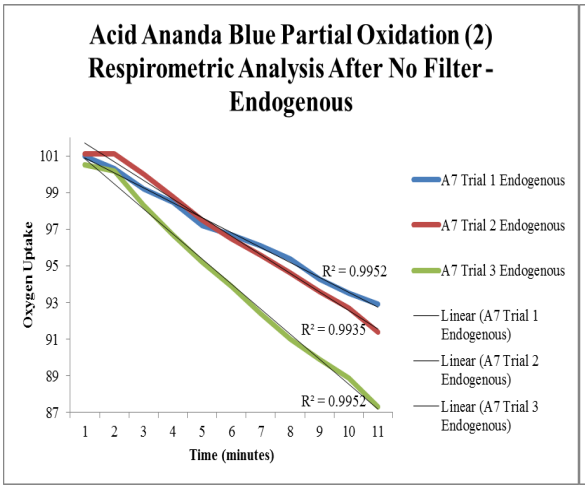
Acid Ananda Blue Partial Oxidation (2) Respirometric Analysis After No Filter - Endogenous
Oxygen Uptake
Time (minutes)
R² = 0.9952
R² = 0.9935
R² = 0.9952
A7 Trial 1 Endogenous
A7 Trial 2 Endogenous
A7 Trial 3 Endogenous
Linear (A7 Trial 1 Endogenous)
Linear (A7 Trial 2 Endogenous)
Linear (A7 Trial 3 Endogenous)

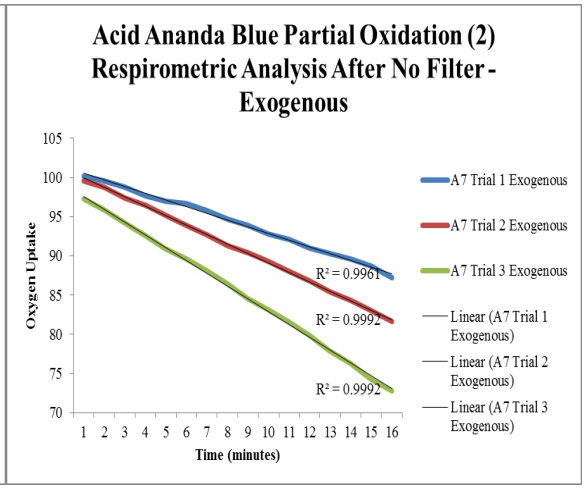
Acid Ananda Blue Partial Oxidation (2) Respirometric Analysis After No Filter - Exogenous
Oxygen Uptake
Time (minutes)
R² = 0.9961
R² = 0.9992
R² = 0.9992
A7 Trial 1 Exogenous
A7 Trial 2 Exogenous
A7 Trial 3 Exogenous
Linear (A7 Trial 1 Exogenous)
Linear (A7 Trial 2 Exogenous)
Linear (A7 Trial 3 Exogenous)

D

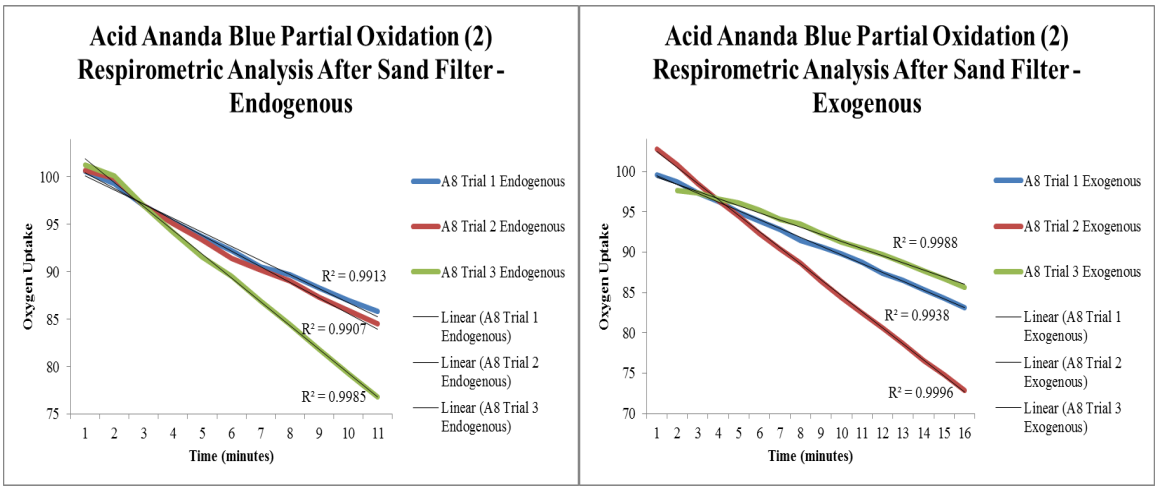

E

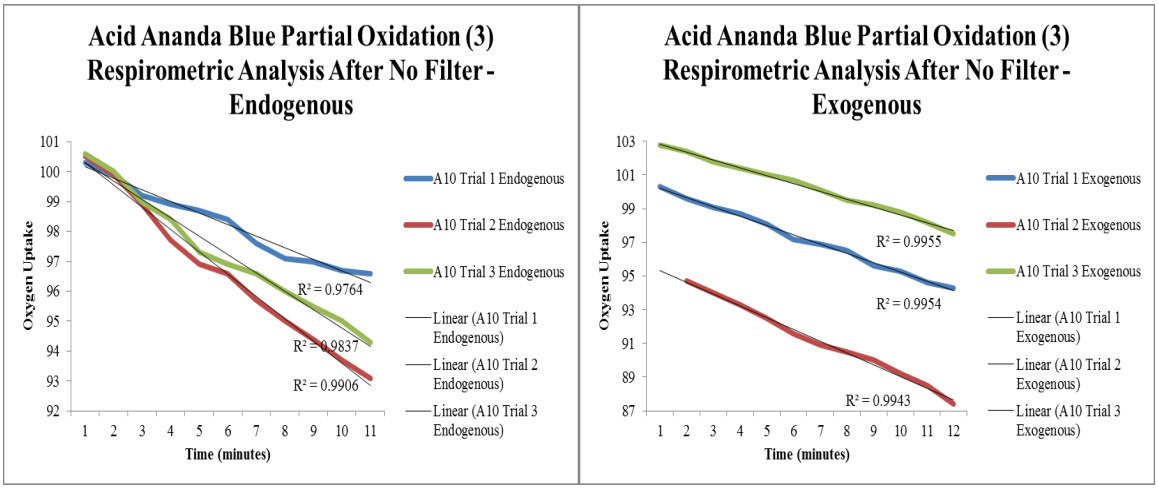

F

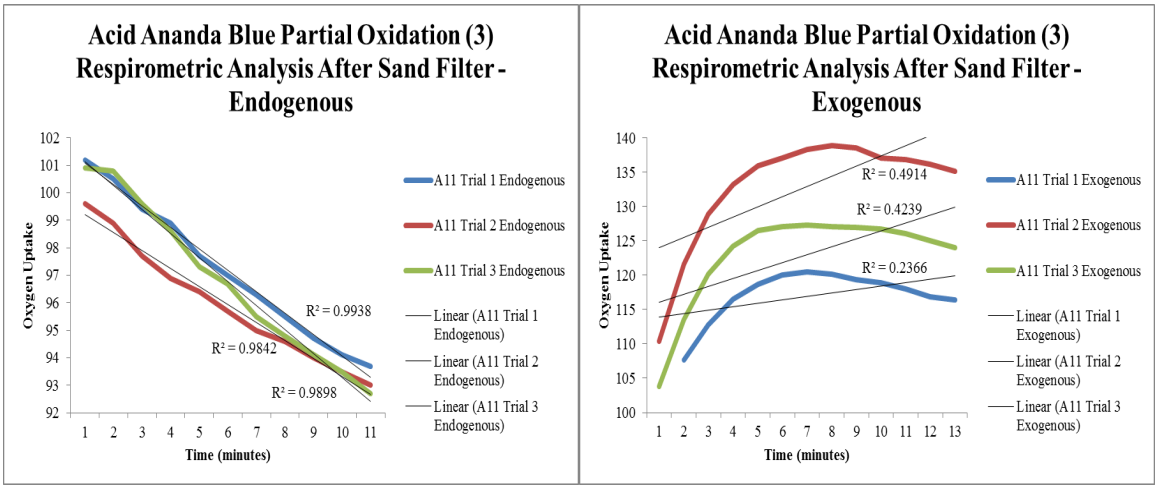

Figure E.6: Acid Ananda Blue Respirometric Analysis (A) Partial Oxidation 1 No Filter, (B) Partial Oxidation 1 Sand Filter, (C) Partial Oxidation 2 No Filter, (D) Partial Oxidation 2 Sand Filter, (E) Partial Oxidation 3 No Filter, (F) Partial Oxidation 3 Sand Filter

A

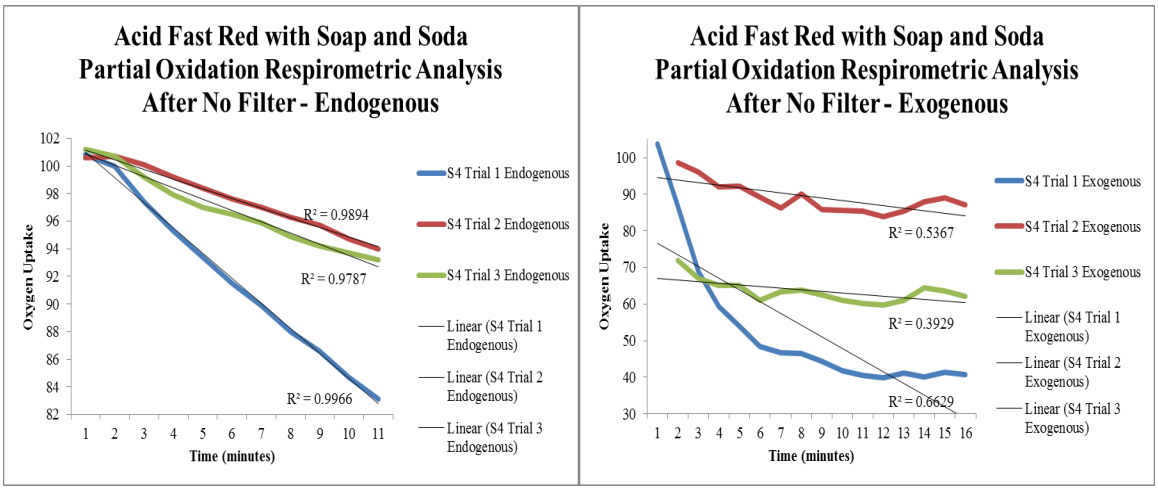

B

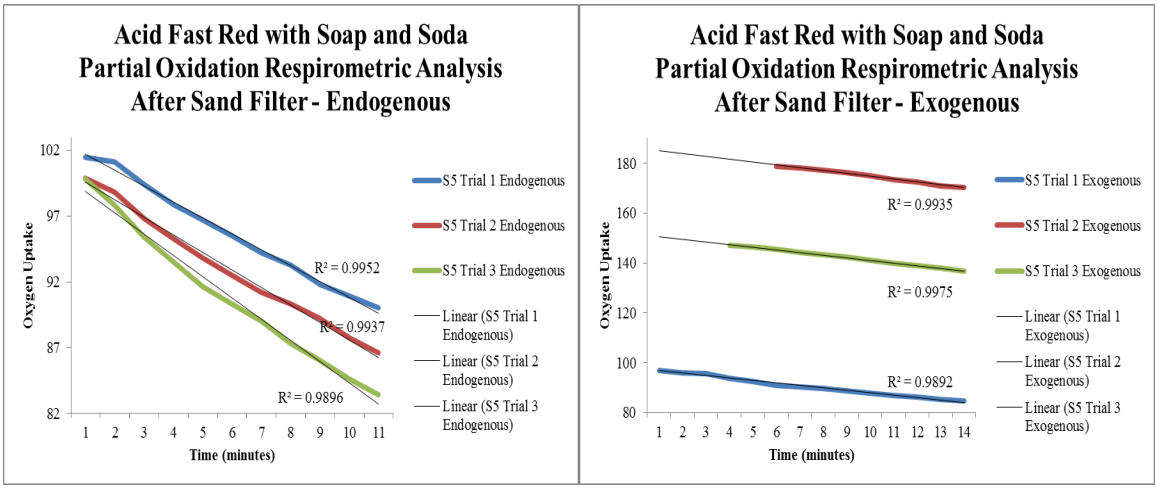

Figure E.7: Acid Fast Red with Soap and Soda Respirometric Analysis (A) No Filter, (B) Sand Filter

A

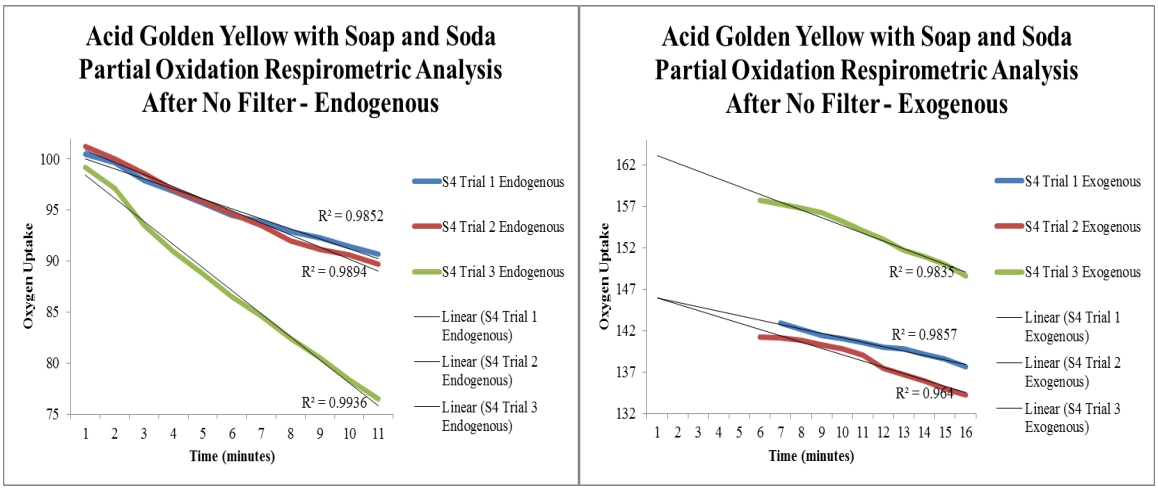

B

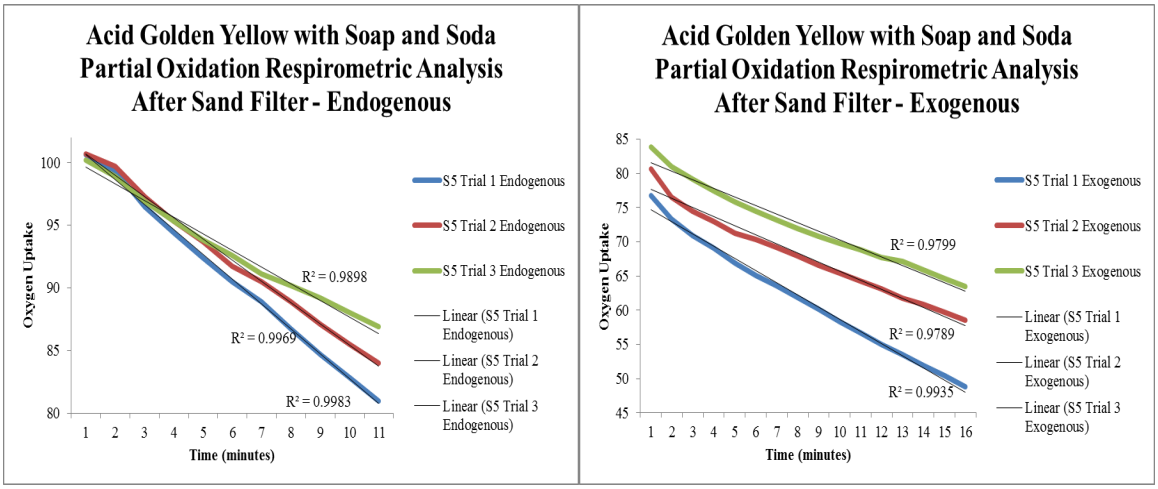

Figure E.8: Acid Golden Yellow with Soap and Soda Respirometric Analysis (A) No Filter, (B) Sand Filter

A

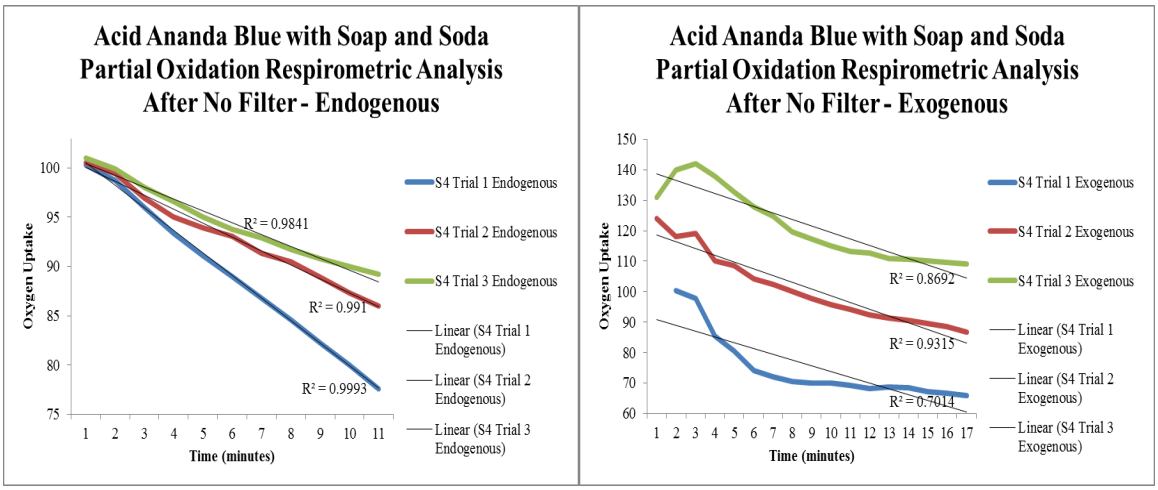

B

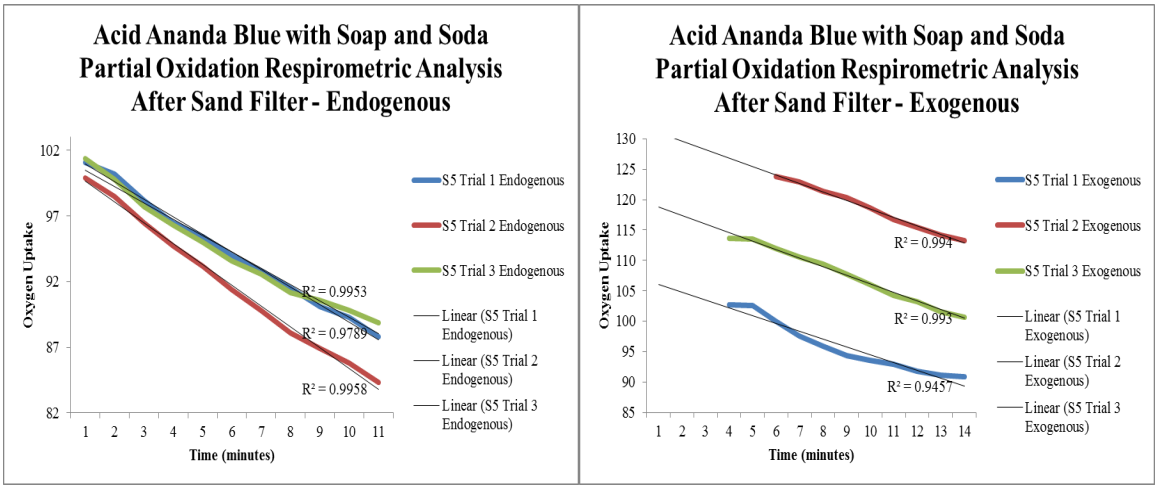

Figure E.9: Acid Ananda Blue with Soap and Soda Respirometric Analysis (A) No Filter, (B) Sand Filter

A

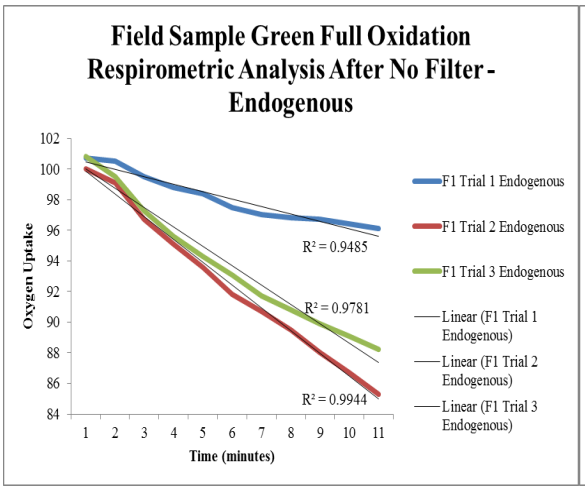
Field Sample Green Full Oxidation Respirometric Analysis After No Filter - Endogenous
Oxygen Uptake
Time (minutes)
R² = 0.9485
R² = 0.9781
R² = 0.9944
F1 Trial 1 Endogenous
F1 Trial 2 Endogenous
F1 Trial 3 Endogenous
Linear (F1 Trial 1 Endogenous)
Linear (F1 Trial 2 Endogenous)
Linear (F1 Trial 3 Endogenous)

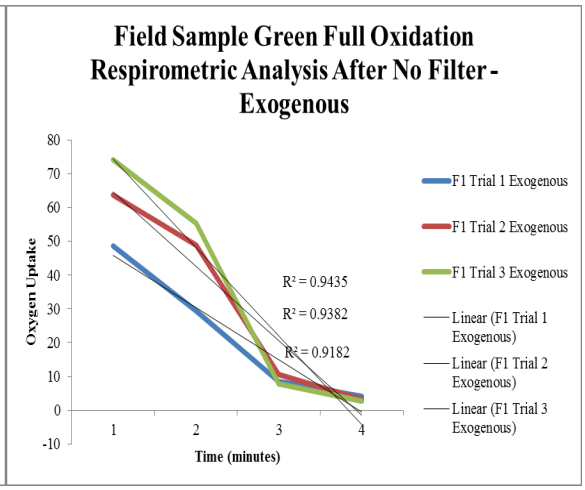
Field Sample Green Full Oxidation Respirometric Analysis After No Filter - Exogenous
Oxygen Uptake
Time (minutes)
R² = 0.9435
R² = 0.9382
R² = 0.9182
F1 Trial 1 Exogenous
F1 Trial 2 Exogenous
F1 Trial 3 Exogenous
Linear (F1 Trial 1 Exogenous)
Linear (F1 Trial 2 Exogenous)
Linear (F1 Trial 3 Exogenous)

B

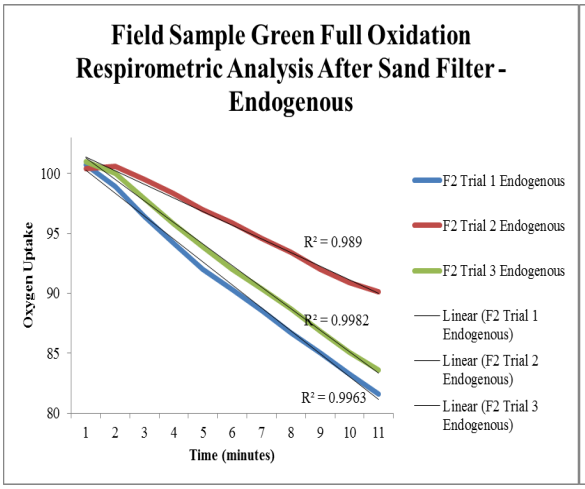
Field Sample Green Full Oxidation Respirometric Analysis After Sand Filter - Endogenous
Oxygen Uptake
Time (minutes)
R² = 0.989
R² = 0.9982
R² = 0.9963
F2 Trial 1 Endogenous
F2 Trial 2 Endogenous
F2 Trial 3 Endogenous
Linear (F2 Trial 1 Endogenous)
Linear (F2 Trial 2 Endogenous)
Linear (F2 Trial 3 Endogenous)

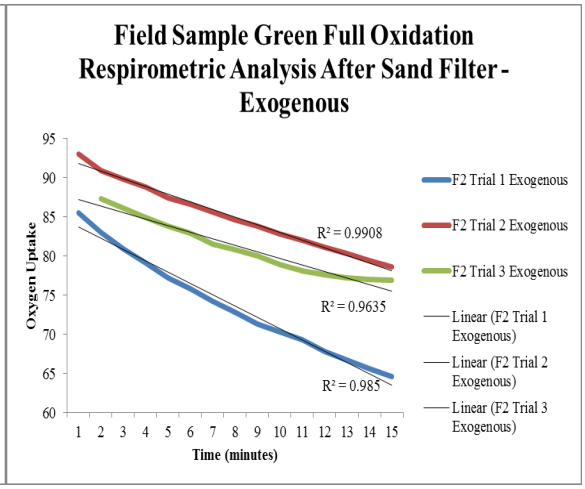
Field Sample Green Full Oxidation Respirometric Analysis After Sand Filter - Exogenous
Oxygen Uptake
Time (minutes)
R² = 0.9908
R² = 0.9635
R² = 0.985
F2 Trial 1 Exogenous
F2 Trial 2 Exogenous
F2 Trial 3 Exogenous
Linear (F2 Trial 1 Exogenous)
Linear (F2 Trial 2 Exogenous)
Linear (F2 Trial 3 Exogenous)

C

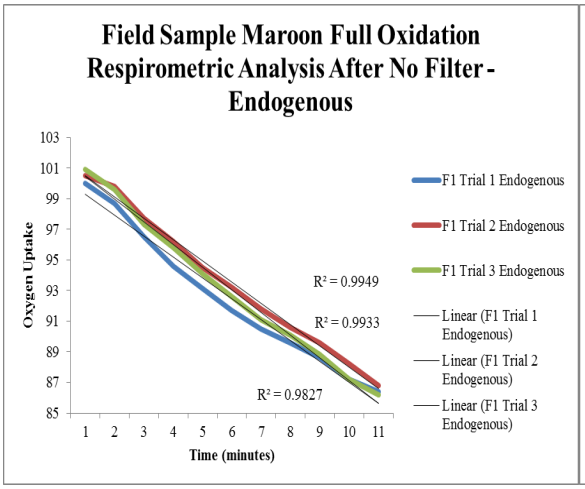
Field Sample Maroon Full Oxidation Respirometric Analysis After No Filter - Endogenous
Oxygen Uptake
Time (minutes)
R² = 0.9949
R² = 0.9933
R² = 0.9827
F1 Trial 1 Endogenous
F1 Trial 2 Endogenous
F1 Trial 3 Endogenous
Linear (F1 Trial 1 Endogenous)
Linear (F1 Trial 2 Endogenous)
Linear (F1 Trial 3 Endogenous)

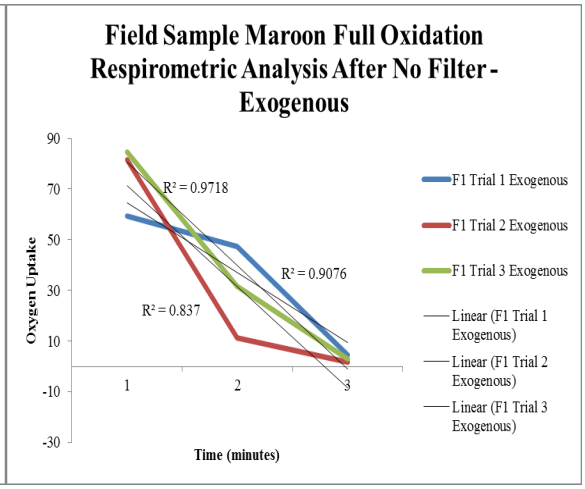
Field Sample Maroon Full Oxidation Respirometric Analysis After No Filter - Exogenous
Oxygen Uptake
Time (minutes)
R² = 0.9718
R² = 0.9076
R² = 0.837
F1 Trial 1 Exogenous
F1 Trial 2 Exogenous
F1 Trial 3 Exogenous
Linear (F1 Trial 1 Exogenous)
Linear (F1 Trial 2 Exogenous)
Linear (F1 Trial 3 Exogenous)

D

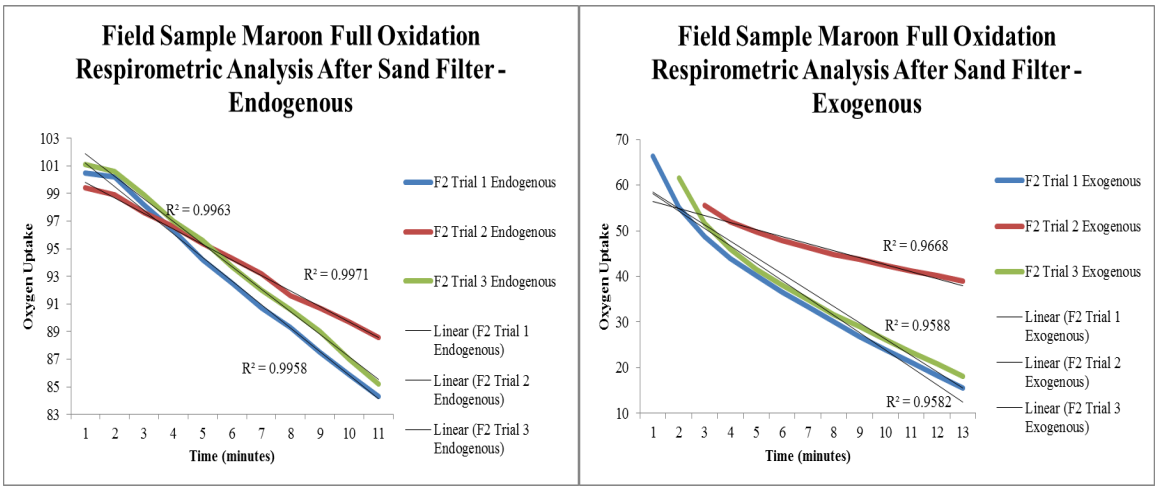

Figure E.10: Field Study Respirometric Analysis (A) Green No Filter, (B) Green Sand Filter, (C) Maroon No Filter, (D) Maroon Sand Filter.

Appendix F – FTIR

This appendix contains figures displaying the azo peaks found in 5g/L of Acid Fast Red with Soap and Soda samples from the demonstration project detailed in Chapter 7. Dye solution before oxidation, sludge after sand and cotton filtration, and foam after filtration were the samples tested. Figure F.1 displays sludge with a 95% transmittance or a low azo peak. Figure F.2 displays sludge from sand filter with a 75% transmittance or a high azo peak. Figure F.3 displays sludge from cotton filter with a 95% transmittance or a low azo peak. Figure F.4 displays sludge after cotton filter with an 88% transmittance or a low azo peak. Figure F.5 displays Acid Fast Red Dye with a 57.5% transmittance or a high azo peak. Figure F.6 displays Acid Fast Red Dye with a 55% transmittance or a high azo peak. Figure F.7 displays Azo Fast Red Dye with a 70% transmittance or a high azo peak. Figure F.8 displays sludge from cotton filter with a 75% transmittance or a high azo peak. Figure F.9 displays foam with a 70% transmittance or a high azo peak. Figure F.10 displays sludge from cotton filter with an 80% transmittance or a mid azo peak.

Figure F.1: Sludge sample #1 found at the bottom of the oxidized sample after 50-liters of 5 g/L Acid Fast Red with Soap and Soda was photo-Fenton oxidized to full oxidation.

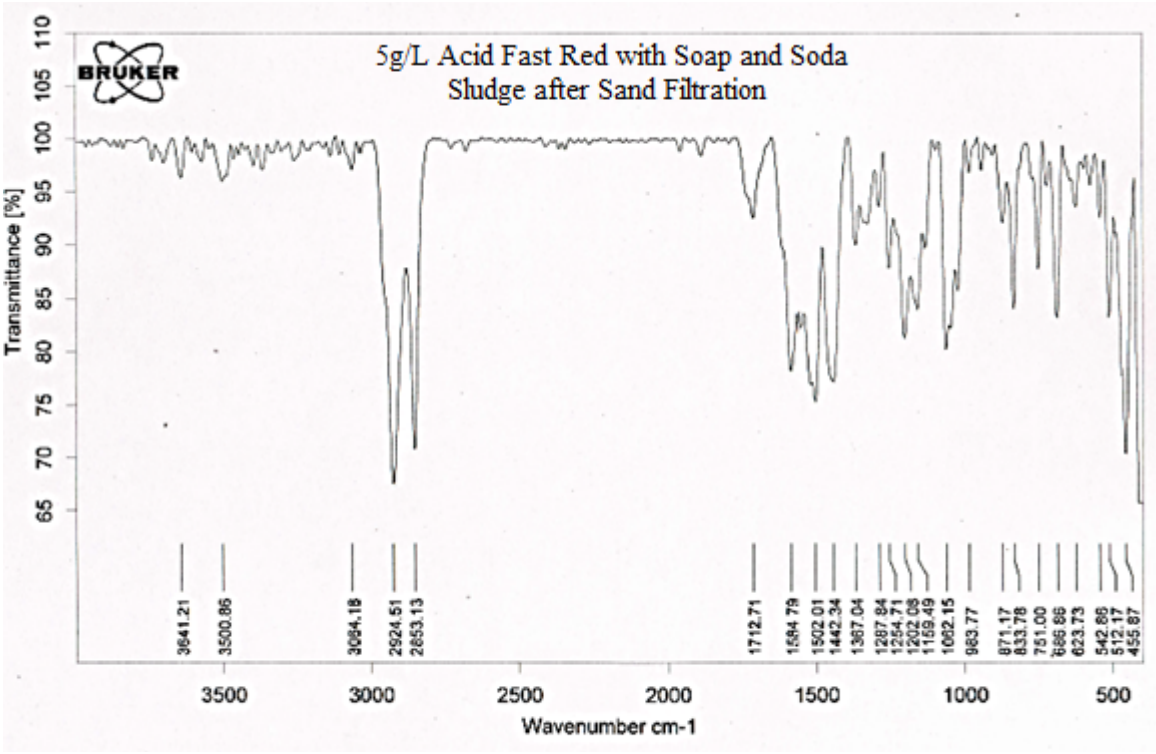

Figure F.2: Sludge sample #2 found on sand filtration after 100-liters of 5 g/L Acid Fast Red with Soap and Soda was photo-Fenton oxidized to full oxidation.

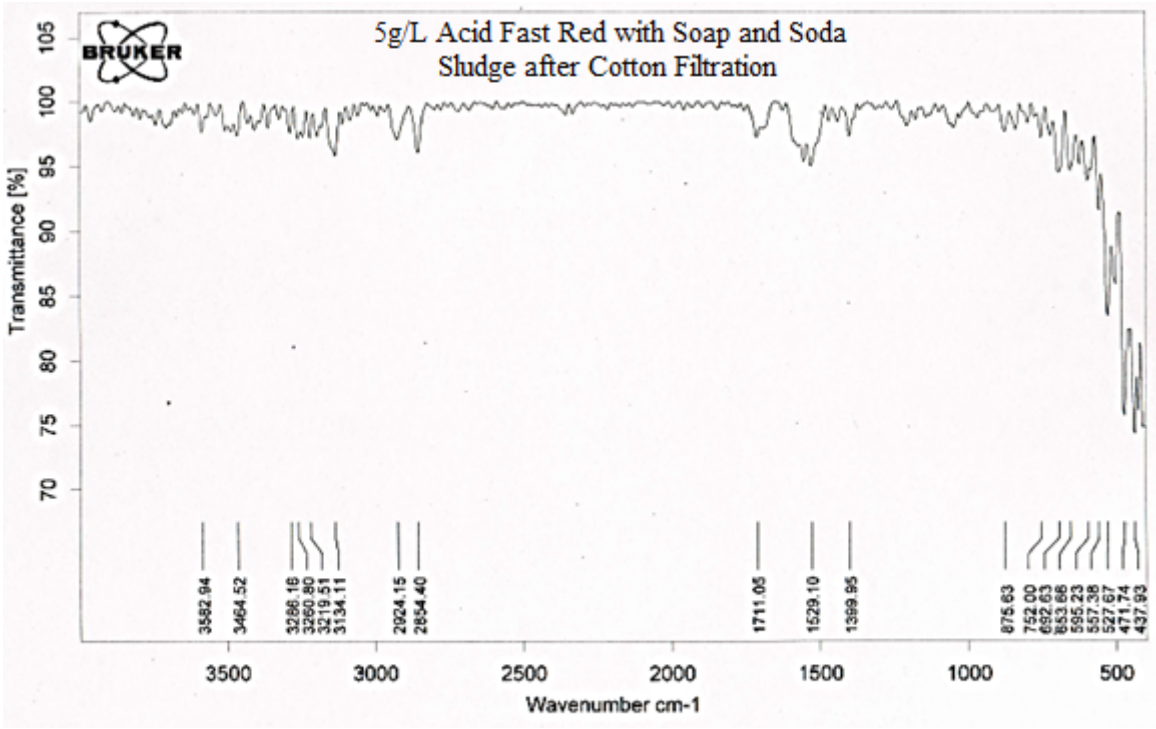

Figure F.3: Sludge sample #3 found on cotton filtration after 50-liters of 5 g/L Acid Fast Red with Soap and Soda was photo-Fenton oxidized to full oxidation.

Figure F.4: Sludge sample #4 found on cotton filtration after 50-liters of 5 g/L Acid Fast Red with Soap and Soda was photo-Fenton oxidized to full oxidation.

Figure F.5: Sludge sample #5 is 5 g/L Acid Fast Red with Soap and Soda at t_0.

Figure F.6: Sludge sample #6 is 5 g/L Acid Fast Red with Soap and Soda at t_0.

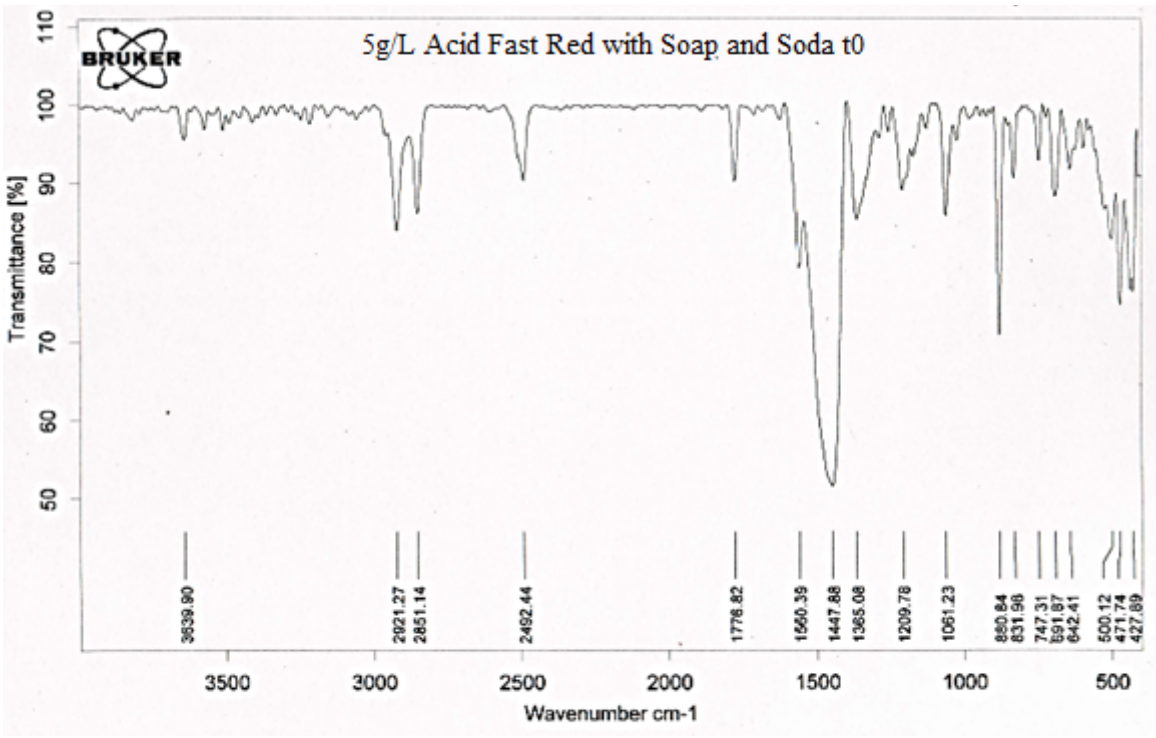

Figure F.7: Sludge sample #7 is 5 g/L Acid Fast Red with Soap and Soda at t_0.

Figure F.8: Sludge sample #8 found on cotton filtration after 50-liters of 5 g/L Acid Fast Red with Soap and Soda was photo-Fenton oxidized to full oxidation.

Figure F.9: Sludge sample #9 found foam floating on top of treated effluent of 50-liters of 5 g/L Acid Fast Red with Soap and Soda was photo-Fenton oxidized to full oxidation.

Figure F.10: Sludge sample #10 found on cotton filtration after 50-liters of 5 g/L Acid Fast Red with Soap and Soda was photo-Fenton oxidized to full oxidation.

Appendix G – Educational Brochure: Sustainable photo-Fenton Oxidation and Slow Sand Filtration of Textile Dye Wastewater

This appendix contains the material list and step-by-step numbered instructions detailing how to execute the sustainable photo-Fenton oxidation followed filtration processes.

Materials Needed:

Rusty Metal Container

Sand Filter (optional wood charcoal over sand)

Cotton Fabric for Filter

Operations:

1. Pour dye into rusty metal container

2. Depth should be 2.5-5.5 cm average

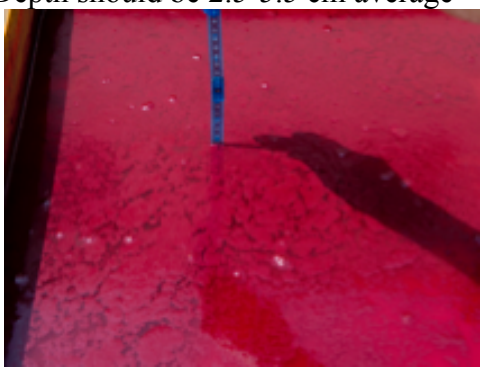

3. Acidify solution to pH 2.2-4.2

4. See reaction bubbles

5. Add Hydrogen Peroxide (1.2 L 50% H2O2 per 50 L 5 g/L dye with 10 g/L soda and 5 bars of soap)

6. Mix well to make homogeneous

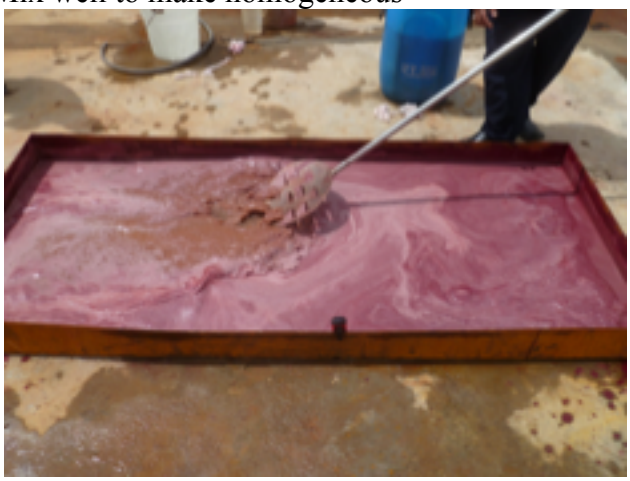

7. Expose solution to open sky— sunlight is best but also functions on cloudy day

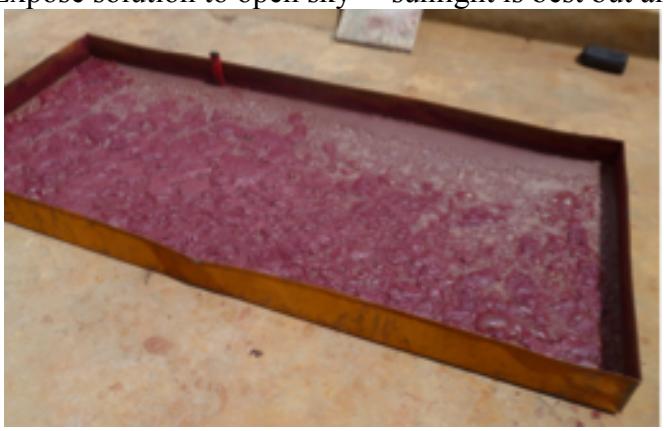

8. When foam forms after approximately 2 hours, reaction is complete

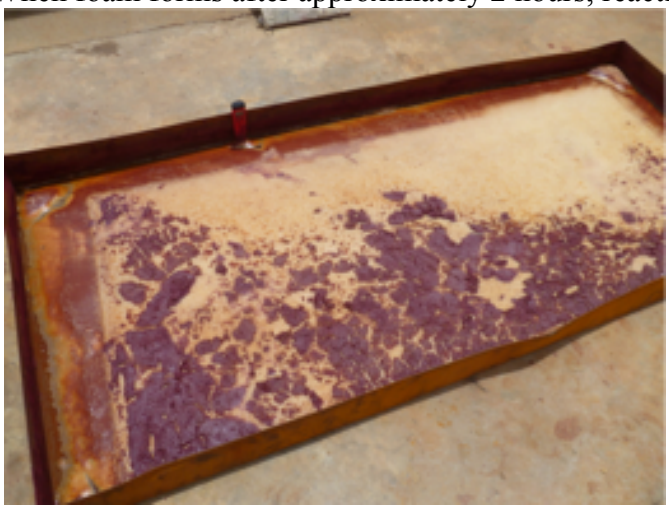

9. Foam can get quite thick if sun is very bright

10. Scoop foam from solution and dispose of safely as it is made of dye, rust, and chemicals

11. Collect remainder of solution for filtration

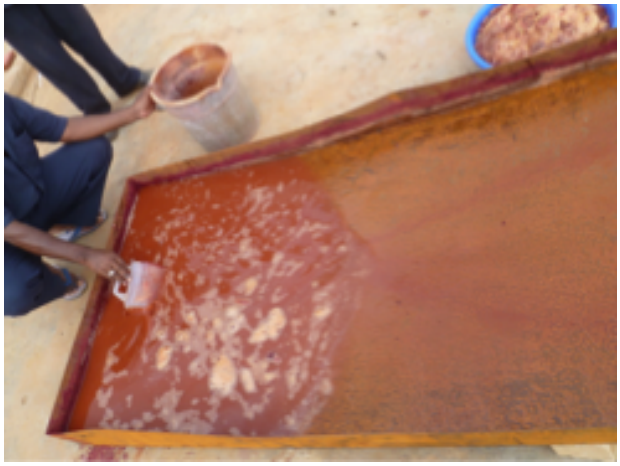

12. Pour through cotton filter and then naturally filtrate through sand filter

13. Sand and cotton are reusable for future batches and can be washed at convenience

14. Sludge on cotton should also be disposed off safely in hazardous waste (future studies will focus on separating iron from dye for chemical reuse)

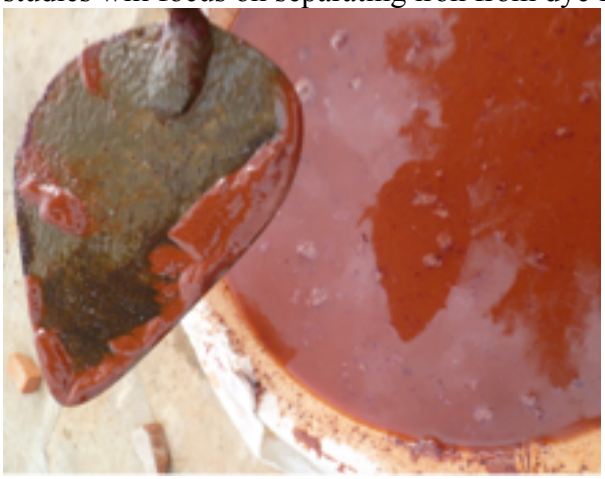

15. Collect for reuse

16. Before / After

Appendix H – Educational Brochure: Making a Rusty Iron Reactor to be used for photo-Fenton Oxidation of Textile Dye Wastewater

This appendix contains the material list and step-by-step numbered instructions detailing how to construct the rusty iron reactor used in the sustainable photo-Fenton oxidation process.

Materials Needed:

Large rusty metal sheet
This one is 250cm x 125cm, 0.8mm thickness (finished box 220cm x 95cm)
This size handles 50-100L of textile wastewater for a depth of 2.5-5cm

Construction:

1. Measure out 15cm square from corners

2. Cut 15cm squares from the corners

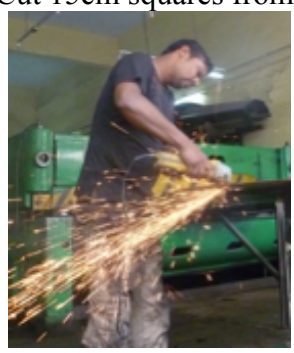

3. Fold over 1cm edge on each side to keep box safe for transporting so as not to cut your skin

4. Fold 14 cm remaining sides so that rust is inside and creates a box

5. Gas weld corners closed

6. Container is ready to use

Appendix I – Educational Brochure: Making a Slow Sand Filter to be used after photo-Fenton Oxidation of Textile Dye Wastewater

This appendix contains the material list and step-by-step numbered instructions detailing how to construct the slow sand, carbon, and cotton filters used after the sustainable photo-Fenton oxidation process.

Materials Needed:

120 L Barrel

Tap

3 small pieces of mesh

Epoxy

100 kg construction sand

Wood Charcoal

Cotton Cloth

Construction:

1. Make hole to fit tap approximately 4 cm from bottom of barrel

2. Mesh keeps sand from leaving the barrel. The holes of the mesh need to be smaller than the sand. In order to use the plastic mesh available in hardware stores in India, the plastic mesh must be stretched to fit around the tap and also layered to create small enough holes.

3. Place mesh over threaded end of tap

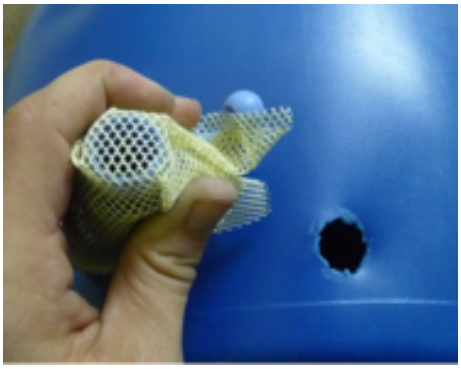

4. Fit into hole and do this for all 3 pieces

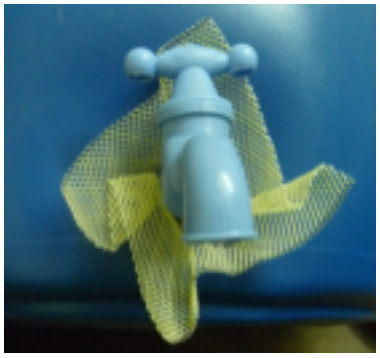

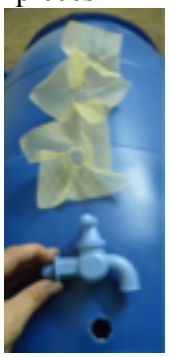

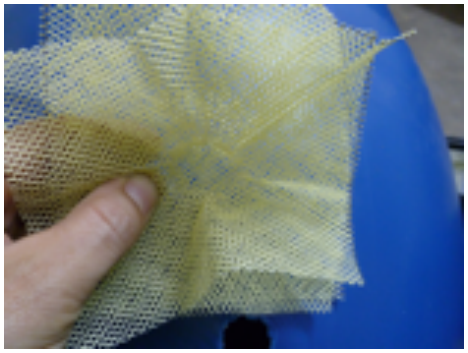

5. Put all 3 pieces on tap together and fit into hole. Be sure to turn each piece of mesh so that the angle changes and the holes on each layer are staggered.

6. Trim mesh around seam

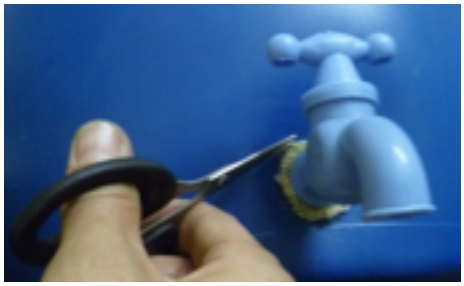

7. Seal seam with epoxy

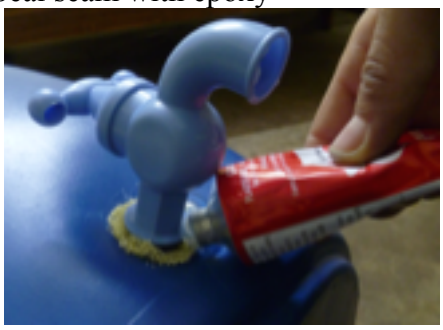

8. Allow to dry overnight

9. Place barrel on ledge to ease water collection

10. Wash 100 kg sand until rinse water is not so muddy

11. Pour into barrel

12. Pour wood charcoal on top of sand

13. Pat in place to ensure charcoal completely covers sand

14. Secure double cotton filter over opening of sand and charcoal filter

CURRICULUM VITA

MARISSA R. JABLONSKI

engineeringforpeople.com

"I met Ms. Jablonski in 2012 and thought I would never see her again. I now see her in front of the Karnataka State Pollution Control Board proposing the project she was discussing; she is one determined woman." –Dr. B.S. Jai Prakash, Vice President ACHMM-India Chapter, Director IEHMM, Member KSPCB, April 2014

EDUCATION

Ph.D. in progress, Civil / Environmental Engineering, September 2009 – May 2015
Department of Civil Engineering and Mechanics, University of Wisconsin – Milwaukee
Dissertation Topic: Sustainable Decolorization of Reactive and Acid Dye Wastewater using Photo-Fenton Oxidation, Biodegradation, and Sand and Carbon Filtration: Laboratory and Field Studies
Advisor: Dr. John Reisel

M.S., Civil / Environmental Engineering, September 2007 - August 2009
Department of Civil Engineering and Mechanics, University of Wisconsin – Milwaukee
Thesis: Comparison of the Role of Ionic Strength and Surface Charge Heterogeneity on the Initial Adhesion and Detachment of Escherichia coli O157:H7 and JM109 in Porous Media *Advisor: Dr. Jin Li*

Post-baccalaureate Study, September 2005 - May 2006: *Statics & Dynamics, Environmental Engineering* **Marquette University, Milwaukee, WI**;
Post-baccalaureate Study, January 2005 - May 2006: *Calculus I, II, III, Differential Equations, Calculus-based Physics* **Milwaukee Area Technical College, Milwaukee, WI**

B.S., Resource Management and Spanish, September 1998 - May 2003
University of Wisconsin - Stevens Point, Stevens Point, WI

RESEARCH EXPERIENCE:

2009-present, **Research Assistant,** College of Engineering and Applied Science, University of Wisconsin – Milwaukee
Topics: Degradation Kinetics of Resorcinol by Enterobacter Cloacae Isolate, Sustainable and Low-Cost Photo-Fenton Oxidation of Reactive and Acid Textile Dye Effluent with and without Biodegradation including the use of Sand and Carbon Filtration for Cottage-Scale Dye Industries

2010-present, **Research Intern,** Environmental Genomics Division at the Council of Scientific and Industrial Research – National Environmental Engineering Research Institute (CSIR-NEERI), Nagpur, India
Topics: Biodegradation of Textile Dye Intermediates, Sustainable photo-Fenton Oxidation Treatment of Chemical Textile Dye for Cottage-Scale Dye Industries, funded by RISE and IUSTFF

2012, **Research Fellow,** NSF East Asia and Pacific Summer Institute, Beijing Normal University
Topics: Sustainable Photo-Fenton oxidation of Reactive Textile Dyes followed by Slow-sand filtration, funded by NSF

2007-2009, **Project Assistant,** Departments of Civil Engineering and Biological Science, University of Wisconsin – Milwaukee
Topics: Gram-Negative Bacteria Transport and Adhesion in Glass Bead Packed Columns

2000-2001, **Research Project Assistant,** Department of Environmental Sciences at Jagiellonian University, Krakow, Poland
Topics: Deposition of Heavy Metals on Different Aspects of Seven Area Forests around Krakow, Poland.

TEACHING EXPERIENCE:

- Spring 2015, Creator and Instructor of new course **Engineering for Developing Communities: Sustainable Methods to Meet Basic Human Needs**, College of Engineering and Applied Science, University of Wisconsin-Milwaukee
  Focus on design options for drinking water supply and treatment, wastewater treatment, solid waste management, indoor air quality, and sustainable energy sources to help the 5 billion people on Earth who make less than $10/day
- 2010-present, Natural Science Instructor, **Environmental Science, Science of Technology**, Milwaukee Area Technical College
- 2006-2007, **Math, Science, and Language Tutor,** Milwaukee Area Technical College
- 2004-2006, **Bilingual Community Educator**, Waukesha Public Health Department
- 2001, **Environmental Educator**, Begich, Boggs Visitor Center in Portage, AK

COMMUNITY DEVELOPMENT AND PROGRAM MANAGEMENT EXPERIENCE:

2010-present, **Fostering Opportunities foR Tomorrow's Engineers Program Coordinator,** College of Engineering and Applied Science at the University of Wisconsin – Milwaukee
Accomplishments: Recruitment and retention of women and minorities to the College of Engineering through STEM programs including Summer Bridge, Peer-led Math Study Groups, High school Girls Engineering Camp, Living-Learning Community, Robotics and Digital Media.

2007-present, **UW-Milwaukee Student Chapter of Engineers Without Borders,** College of Engineering and Applied Science at the University of Wisconsin – Milwaukee
Accomplishments: Design and construction of gravity and pump-fed water distribution systems. Mentor of student groups in all facets of collaborative international development and sustainable engineering. Education for villages about health and sanitation and related construction of hand-washing stations and latrines in war torn communities in Guatemala. Founding member.

2010-present, **La Asociación Medio Ambiental de la Region Ixil,** Nebaj, Guatemala
Accomplishments: Facilitation of the development of the association, communicate its existence and goals to outside groups (funders, engineers, development organizations), and facilitate collaborative work and transition of outside groups to work with new Guatemala Non-profit.

REFEREED PUBLICATIONS

1. **M.R. Jablonski**, H. Ranicke, A. Qureshi, H. Purohit, J.R. Reisel, K.G. Satyanarayana (2015). "Sustainable Decolorization of Reactive Red 120, Reactive Yellow 81, and Reactive Blue 4 using Photo-Fenton Oxidation both with and without Biodegradation." *In preparation*
2. **M.R. Jablonski**, H. Ranicke, A. Qureshi, H. Purohit, J.R. Reisel, K.G. Satyanarayana (2015). "Sustainable Decolorization Comparing Acid Dye Wastewater with and without soap and soda for Acid Fast Red, Acid Golden Yellow, and Acid Ananda Blue using Photo-Fenton Oxidation both with and without Biodegradation." *In preparation*
3. **M.R. Jablonski**, H. Ranicke, A. Qureshi, H. Purohit, J.R. Reisel, K.G. Satyanarayana (2015). "Pilot Project: Sustainable Photo-Fenton Oxidation of Cottage-Scale Acid Fast Red Silk Dye Wastewater with Soap and Soda in Karnataka, India." *In preparation*
4. **M.R. Jablonski**, H. Ranicke, A. Qureshi, H. Purohit, J.R. Reisel, K.G. Satyanarayana (2015). "Review of Sustainable Photo-Fenton Oxidation both with and without Biodegradation of Reactive and Acid Silk Dyes." *In preparation*
5. J.R. Reisel, **M. Jablonski**, E. Munson, and H. Hosseini (2014). "Peer-led Team Learning in Mathematics Courses for Freshman Engineering Students." *Journal of STEM Education* (Vol 15 issue 2, pg 7-15).

REFEREED PUBLICATIONS CONT.

6. J.R. Reisel, **M. Jablonski**, A. Kialashaki, E. Munson, and H. Hosseini (2014). "Analysis of the Impact of Participation in a Summer Bridge Program on Mathematics Course Performance by First-Semester Engineering Students." *Proceedings of the 2014 American Society for Engineering Education Annual Conference & Exposition*. Paper No. 8492, Indianapolis, IN.
7. **M.R. Jablonski**, S. Shaligram, A. Qureshi, H. Purohit, J. Reisel, and R. El-Hajjar. (2013). "Degradation Kinetics of Resorcinol by Enterobacter Cloacae Isolate." *African Journal of Microbiology Research 7: 3632-3640*.
8. **M. Jablonski**, J.R. Reisel (2013). "The Importance of Native In-Country Coordinators for Predictive Awareness of Cultural and Design Details for International Sustainable Engineering Projects." *Proceedings of the 2013 ASCE World Environmental & Water Resources Congress.* Paper No. 707, Cincinnati, OH.
9. **M. Jablonski**, J.R. Reisel (2012). "Sustainable International Development as a Process." *2012 American Society for Engineering Education Annual Conference & Exposition,* Paper No. AC 2012-4985, Session M645B.
10. J.R. Reisel, **M. Jablonski**, E. Munson, and H. Hosseini (2012). "Analysis of the Impact of Formal Peer-led Study Groups on First-year Student Math Performance." *2012 American Society for Engineering Education Annual Conference & Exposition,* Paper No. AC 2012-2983, Session M550.
11. J.R. Reisel, **M. Jablonski**, L. Rineck (2012). "Analysis of Math Course Placement Improvement and Sustainability Achieved through a Summer Bridge Program." *2012 American Society for Engineering Education Annual Conference & Exposition,* Paper No. AC 2012-2984, Session M356.
12. J.R. Reisel, **M. Jablonski**, H. Hosseini, and E. Munson (2012). "Assessment of Factors Impacting Success for Incoming College Engineering Students in a Summer Bridge Program." *Int. J. of Mathematical Education in Science & Technology*, 43: 421-433.
13. J.R. Reisel, L. Rineck, **M. Jablonski**, E. Munson, and H. Hosseini (2011). "Evaluation of the Impacts of Math Course Placement Improvement Achieved Through a Summer Bridge Program." *2011 American Society for Engineering Education Annual Conference & Exposition,* Paper No. AC 2011-51, Session M548.
14. **M. Jablonski**, J.R. Reisel, H. Hosseini, E. Munson, and L. Rineck (2011). "Initial Evaluation of the Impacts of Math Study Groups on First-Year Student Course Success." *2011 American Society for Engineering Education Annual Conference & Exposition,* Paper No. AC 2011-243, Session M354.
15. J.R. Reisel, **M. Jablonski**, H. Hosseini, and E. Munson (2010). "Evaluation of Factors Affecting the Success of Improving Math Course Placement for Incoming Freshmen in a Summer Bridge Program." *2010 American Society for Engineering Education Annual Conference & Exposition,* Paper No. AC 2010-231, Session 1376, 9 pages.
16. Soehartono, **M. Jablonski** (2010). "Clean Water for Villages in Guatemala Requires Appropriate Technology." *Water Conditioning and Purification* Vol. 52 (10), 38-41. (Available online: http://www.wcponline.com/pdf/October%20Soehartono_Jablonski.pdf)
17. **M. Jablonski**, C. Papadopoulos, and J.R. Reisel (2009). "Building Trust During International Development Work: A Case Study of a Recent EWB Project." *2009 American Society for Engineering Education Annual Conference & Exposition*, Paper No. AC2009-1089, Session 1360, 6 pages.

CONFERENCE PRESENTATIONS

1. **M. Jablonski** (2015). "Necessities for Sustainability: Water, Food, Health, Education." *Sustainability Summit and Expo Breakout Session: Helping Developing Countries in Central America Address Water Challenges*, Milwaukee, WI, March 4-6, 2015.
2. **M. Jablonski**, D. Ramirez (2013). "The Importance of In-Country Coordination: A Discussion with Local and Global Leaders." *Engineers Without Borders Midwest Regional Conference* 2013, University of Kansas.
3. **M. Jablonski** (2011). "Potable Water Distribution Systems in Guatemala by a Student Chapter of Engineers Without Borders." *Sustainability Summit and Expo Breakout Session Chair: Water-Energy Nexus: Efficient Use of Water*, Milwaukee, WI, March 7-9, 2011.
4. **M. Jablonski** (2011). "Sustainable Development as a Long-term Process." *Sustainability Summit and Expo Breakout Session: Sustainable Manufacturing*, Milwaukee, WI, March 7-9, 2011.
5. **M. Jablonski** (2009). "Gravity-Fed Water Distribution and Sanitation System in La Libertad, Guatemala." *Engineers Without Borders-USA Regional Conference*, Milwaukee, WI, November 2009.
6. **M. Jablonski** (2009). "Gravity-Fed Water Distribution/Sanitation System in La Libertad, Guatemala." *Rotary District Conference*, Elkhart Lake, WI, April 2009.

POSTERS

1. **M. Jablonski**, H. Cleveland (2013). "Slow Sand Filtration in Batzaja, Guatemala: Small-Scale Construction." *University of Wisconsin, Milwaukee, College of Engineering and Applied Science Research Poster Competition 2013*.
2. **M. Jablonski**, H. Cleveland (2012). "Slow Sand Filtration: A Pilot Project in Batzaja, Guatemala." *University of Wisconsin, Milwaukee, College of Engineering and Applied Science Research Poster Competition 2012*.
3. A. Soehartono, D. Cary, J. Spaeth, **M. Jablonski**, A. Engel, M. Smith, C. Hasler, L. Enders, D. Hall, D. Gallegos, G. Guerra, S. Higgins, B. Downs, J. Thede, A. DeBlaey, J.R. Reisel, D. Langhoff, H. Cleveland (2011). "Engineers Without Borders at University of Wisconsin, Milwaukee in Vitostix and Vijolom III, Guatemala: Design and Implemenation of a Joint Gravity-Fed Water Distribution System." *University of Wisconsin, Milwaukee, College of Engineering and Applied Science Research Poster Competition 2011*, 2nd place.
4. J. Hegarty, **M. Jablonski**, C. Hasler, A. Plier, D. Cary, S. Olejnik, I. Hoff, A. Soehartono, J. Curry, J. Spaeth, D. Hall, J.R. Reisel (2010). "Engineers Without Borders at University of Wisconsin, Milwaukee: Gravity-Fed Water Distribution and Sanitation System in La Libertad, Guatemala." *University of Wisconsin, Milwaukee, College of Engineering and Applied Science Research Poster Competition 2010*, 3rd place.
5. J. Hegarty, **M. Jablonski**, A. Plier, C. Hasler, A. Stager, J. Schafer, S. Anderson, H. Adelle Stephenson, A. Soehartono, J. Curry, D. Gallegos, K. Kulinski, E. Youngblum, J. Sullivan, A. Franz, D.J. Silkey, J. Effinger, C. Wall (2009). "Engineers Without Borders at University of Wisconsin, Milwaukee: Potable Water Distribution System in Quejchip, Guatemala, Phase II." *University of Wisconsin, Milwaukee, College of Engineering and Applied Science Research Poster Competition 2009*, 2nd place.
6. **M. Jablonski**, K. Sawicka-Kapusta (2001). "Deposition of Heavy Metals on Different Aspects of Seven Area Forests around Krakow, Poland." *University of Wisconsin – Stevens Point, College of Natural Resources Student Research Symposium Poster Presentation*.

INVITED PRESENTATIONS

1. Sevadal Mahila Mahavidyalaya College, Department of Environmental Science. **Significance of Environmental Science and Engineering Across the Globe**. Nagpur, India, April 2014.
2. B.M.S. Engineering College. **Photo-Fenton Oxidation of Textile Dye Wastewater**. Bangalore, India, August 2012.
3. K.G.S. Science College. **Bacteria Transport through Porous Media**. Nagpur, India, August 2010.
4. EWB-USA Conference Welcome. **Water Distribution System in Guatemala**. Milwaukee, WI, March 2009.
5. Women in Science and Engineering Breakfast Lecture, UWM School of Continuing Education. **Professionalism with Purpose**. Milwaukee, WI, March 2012.
6. Discovery World Building the Water Generation event. **Photo-Fenton Oxidation of Textile Dye Wastewater in Developing Communities**. Milwaukee, WI, November 2011, 2012.

LEADERSHIP EXPERIENCE:

- 2007-present, Project Lead, University of Wisconsin – Milwaukee Student Chapter of Engineers Without Borders
- 2010-present, Mentor, University of Wisconsin – Milwaukee Student Chapter of Engineers Without Borders
- 2007-2010, Co-chair, University of Wisconsin – Milwaukee Student Chapter of Engineers Without Borders at the University of Wisconsin – Milwaukee
- 2008-2010, Elected Delegate, Milwaukee County Conservation Congress
- 2006-2007, Intern, Major Construction Project Management, Pieper Electric, Inc., Milwaukee, WI

SKILLS/EXPERTISE:

- Effective in public relations roles including public policy and public speaking experience
- Fluency in English and Spanish languages
- Civil engineering project design, construction, and management experience
- Personable and a fast learner; Inventive and thorough when helping others
- International Experiences in Africa, South and Central America, Western and Eastern Europe, China, and India

AWARDS & HONORS:

- **Philanthropic Education Organization** Scholar Award 2013-2014 **($15,000**)
- **National Science Foundation** EAPSI (East Asia and Pacific Summer Institutes) Fellow, **Beijing, China** 2012 ($6,000 +travel)
- **RISE** (Research Internship in Science and Engineering) and **IUSTFF** (Indo-US Science and Technology Forum) Fellowship to complete 3 months of engineering research in **CSIR-NEERI, Nagpur, India** 2010 ($1200 +travel)
- **Mondialogo** International Student Project Silver Medalist and Presenter in **Stuttgart, Germany**, 2009: Development of a Low-Cost, Low Maintenance and Mobile Bio-Solartech Unit for Water Purification (**2nd place Award of $20,000**)
- **National Science Foundation** Graduate Research Fellowship Honorable Mention 2008
- **Wisconsin Water Association** Scholarship 2008
- UWM's **Chancellor's Graduate Student Award** 2007, 2015

PROFESSIONAL SOCIETY MEMBERSHIPS

- ASEE American Society for Engineering Education
- EWB Engineers Without Borders
- SWE Society of Women Engineers
- ASCE American Society for Civil Engineers

"You are one of the best teachers I've ever had, and by far the best I've had at MATC. You just exude passion for the subject and the work that you do here and overseas is amazing. I really felt inspired after that first class. It was so clear that you were invested in the subject and really wanted us to learn, and the blog idea was exciting to me as well."

–Student of Environmental Science at MATC, November 2014